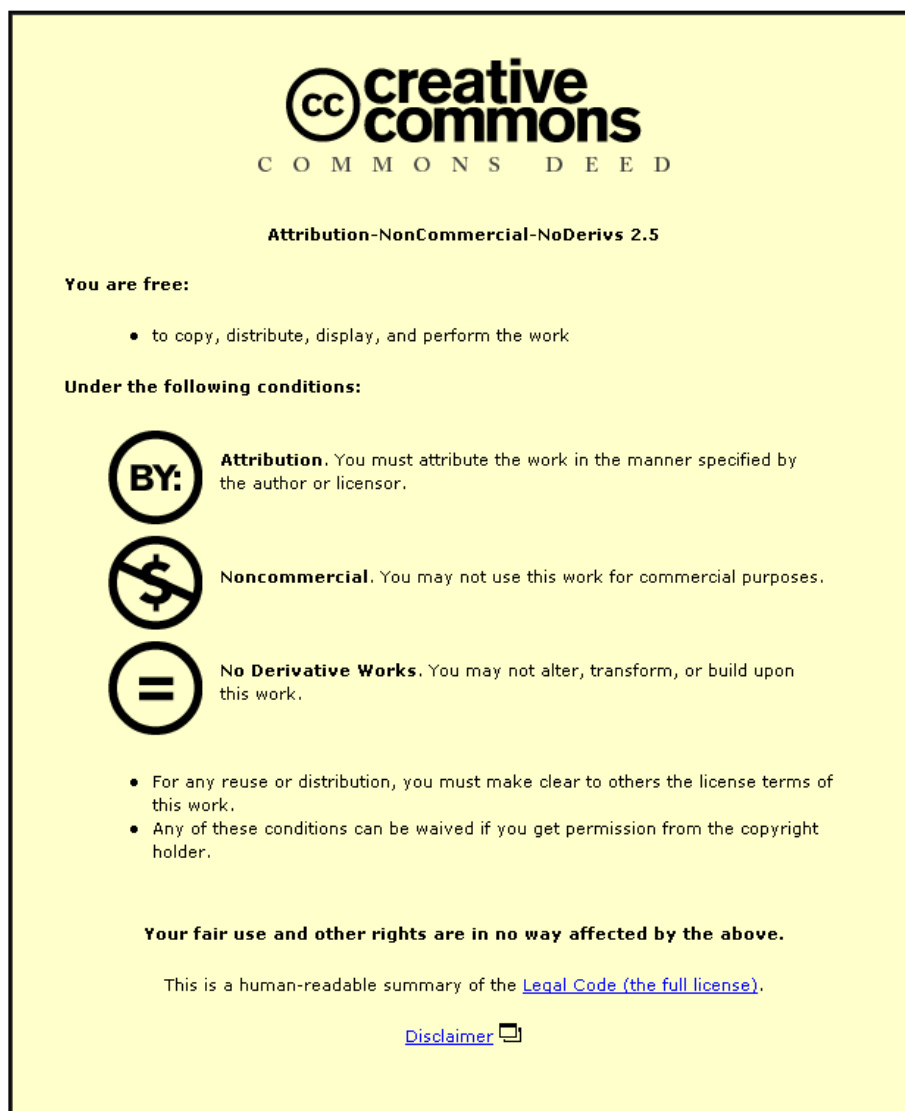


This item was submitted to Loughborough University as a PhD thesis by the author and is made available in the Institutional Repository (<https://dspace.lboro.ac.uk/>) under the following Creative Commons Licence conditions.



For the full text of this licence, please go to:  
<http://creativecommons.org/licenses/by-nc-nd/2.5/>



**Pilkington Library**

Author/Filing Title ..... AL-KINDY, A .....

Accession/Copy No. ....

Vol. No. .... Class Mark ..... T .....

14 JAN 2000

10 MAR 2000

22 MAY 2000

LOAN COPY

0402084942





**Macro and Microclimate Effects on Cover Zone Properties  
of Field Cured Concrete**

By  
Adil Al-Kindy

**A Doctoral Thesis**  
**Submitted in partial fulfilment of the requirements**  
**for the award of**  
**Doctor of Philosophy of the Loughborough University**

**October, 1998**

**© Adil Al-Kindy 1998**

 Loughborough UNIVERSITY LIBRARY
Date <i>June 99</i>
Class
Acc No. <i>040208494</i>

*K0641294*

بِسْمِ اللّٰهِ الرَّحْمٰنِ الرَّحِیْمِ

*In the name of God, Most Merciful, Most Compassionate*

... وما أُوتِيتُمْ من العلم إِلَّا قَلِيلًا ."

"... Of Knowledge it is only a little that is communicated to you (O men!)."

(Holy Quran, S17, v: 85)

*To my son Almoatez and the future generations of Oman*

## ABSTRACT

Three sets of concrete blocks were cast to investigate the effects of natural exposure conditions, at the macro and microclimate scale, and field curing on the performance and durability of OPC and OPC/GGBS concretes. These are termed the Loughborough winter series, the Loughborough summer series and the Muscat summer series.

Three concrete mixes were investigated in the two Loughborough series (30 and 50 MPa OPC concrete mixes and a 30 MPa OPC/GGBS concrete mix) and two in the Muscat weather series (the two 30 MPa concretes). A group of specimens were cast with each mix consisting of 600 × 500 × 150mm concrete blocks plus control cubes and prisms. The samples were cured in-situ and exposed to a range of curing methods and microclimates.

Surface zone properties (up to 50mm depth) were evaluated by air permeability, sorptivity, carbonation, thermogravimetry (TG) and mercury intrusion porosimetry (MIP) tests, conducted after 3 and 12 months of site exposure.

The results revealed distinct variations due to macroclimate, microclimate, curing, concrete type and age.

The air permeability, sorptivity and carbonation of the concrete exposed under moderate and rainy conditions of a Loughborough summer season were lower than identical concrete cast and cured during a very cold and dry Loughborough winter season. Further, the sorptivity of concrete subjected to the hot and dry climatic conditions of Muscat was significantly higher than companion samples subjected to the temperate Loughborough climate.

Significant variations in properties were observed within the two sides of the same concrete element, each subjected to a different microclimate.

The air permeability, sorptivity, carbonation and porosity were reduced with increased hessian curing duration. However, premature drying of wet hessian

during curing had an adverse effect on concrete quality as this produced concrete of higher permeability and carbonation than non-cured concrete. The application of controlled permeability formwork was effective in improving the concrete's sub-surface properties.

The curing affected zone (CAZ) extended to approximately 20mm below the surface of the concrete that was exposed to the Loughborough winter and summer climate, and 40-50mm for the concrete exposed to the Muscat climate, with notable variation in properties due to climate and curing.

The TG and MIP results provided insights into the mechanisms associated with the variations in the three concrete's properties due to natural field exposure.

*Key words:* macroclimate, microclimate, exposure conditions, cover zone, curing, air permeability, sorptivity, carbonation, porosity, hydration.

## ACKNOWLEDGEMENTS

My sincerest thanks and appreciation go to my research supervisor Dr Simon Austin for his advice and assiduous support throughout the duration of this research. Thanks are also due to my director of research Dr Peter Robins.

I would also like to thank Dr Mathew Ball of the Department of Chemistry for his advice during my work at the Chemistry Department. Thanks are also due to Dr Ali Al-Harthy and Mr Suleiman Al-Kindi of the of the Department of Civil Engineering of the Sultan Qaboos University for their assistance with the experimental work in Muscat.

I also wish to thank the technical staff of the following departments for their assistance during my experimental work:

- The Concrete and Soil Laboratories of the Department of Civil Engineering
- The Polymer Laboratory of the Department of Chemistry.
- The Polymer Laboratory of the Institute of Polymer Technology and Materials Engineering of the University.
- The Department of Civil Engineering of the Sultan Qaboos University
- The Meteorological Laboratory of the Department of Geography of the University.
- The Department of Meteorology of the Seeb International Airport, Muscat.

Finally, my special thanks go to The President and Staff of Muscat Municipality for their unfailing support throughout the course of this research.

# CONTENTS

	<b>Page</b>
Abstract	I
Acknowledgements	III
Contents	IV
<b>Chapter 1</b> <b>Introduction</b>	<b>1</b>
1.1    Overview	1
1.2    Aim and objectives of the research	3
1.3    Structure of the thesis	3
<b>Chapter 2</b> <b>Climate, Curing and Concrete Cover</b>	<b>6</b>
2.1    Background	6
2.1.1    Introduction	6
2.1.2    Hydration, microstructure, and strength	6
2.1.3    Permeability and durability	10
2.1.4    Shrinkage	15
2.2    Macroclimate	16
2.2.1    Denotation and significance of cold and hot climate	16
2.2.2    Cold climate concreting	19
2.2.3    Hot climate concreting	21
2.3    Microclimate	38
2.3.1    Denotation and significance of microclimate	38
2.3.2    Microclimate influence on concrete properties	39
2.4    Curing	42
2.4.1    Denotation and significance of curing	42
2.4.2    Curing methods	44
2.4.3    Curing efficiency	46
2.4.4    Curing specification and current practice	47
2.4.5    Influence of curing on engineering properties	50
2.5    Concrete cover	52
2.5.1    Denotation and significance of concrete cover	52
2.5.2    Influence of cover properties on concrete performance	55
2.6    Concluding remarks	57
2.6.1    Macroclimate	57
2.6.2    Microclimate	58
2.6.3    Curing	58
2.6.4    Concrete cover	59
<b>Chapter 3</b> <b>Materials, Mix Details and Site Exposure</b>	<b>60</b>
3.1    Introduction	60

3.2	Philosophy behind choice of specimen size, exposure conditions, curing and materials	61
3.2.1	Specimen size	61
3.2.2	Exposure duration, testing age, macro and microclimate	61
3.2.3	Curing regime	63
3.2.4	Materials	64
3.3	Materials	66
3.3.1	Ordinary Portland cement	66
3.3.2	Ground-granulated blast-furnace slag	66
3.3.3	Aggregates	66
3.3.4	Controlled permeability formwork	67
3.3.5	Curing membrane	67
3.4	Mix details	67
3.5	Site exposure and microclimates	68
3.5.1	Exposure site	68
3.5.2	Microclimates	68
3.6	Curing	69
<b>Chapter 4</b>	<b>Background to the Tests and Methodology</b>	<b>76</b>
4.1	Introduction	76
4.2	Test methods - justification	77
4.2.1	Introduction	77
4.2.2	Absorption	78
4.2.3	Permeation	78
4.2.4	Carbonation	79
4.2.5	Pore structure	80
4.3	Compressive strength	80
4.4	Air permeability	81
4.4.1	Theoretical background	81
4.4.2	Preliminary investigation	82
4.4.3	Apparatus	83
4.4.4	Sample preparation	83
4.4.5	Test procedure	84
4.5	Sorptivity	85
4.5.1	Theoretical background	85
4.5.2	Preliminary investigation	88
4.5.3	Apparatus	91
4.5.4	Sample preparation	91
4.5.5	Test procedure	92
4.6	Carbonation	93
4.6.1	Theoretical background	93
4.6.2	Measurement of carbonation	95
4.6.3	Test procedure	96

4.7	Thermogravimetry	96
4.7.1	Theoretical background	96
4.7.2	Preliminary investigation	98
4.7.3	Apparatus	99
4.7.4	Sample preparation	100
4.7.5	Test procedure	101
4.8	Mercury intrusion porosimetry	102
4.8.1	Theoretical background	102
4.8.2	Preliminary investigation	104
4.8.3	Apparatus	106
4.8.4	Sample preparation	107
4.8.5	Test procedure	108
<b>Chapter 5</b>	<b>Loughborough Winter Climate</b>	<b>118</b>
5.1	Introduction	118
5.2	Weather data	119
5.3	Compressive strength	119
5.4	Air permeability	120
5.4.1	Introduction	120
5.4.2	30 MPa OPC concrete	122
5.4.3	50 MPa OPC concrete	124
5.4.4	30 MPa OPC/GGBS concrete	125
5.5	Sorptivity	127
5.5.1	Introduction	127
5.5.2	30 MPa OPC concrete	128
5.5.3	50 MPa OPC concrete	130
5.5.4	30 MPa OPC/GGBS concrete	131
5.6	Carbonation	133
5.6.1	Introduction	133
5.6.2	30 MPa OPC concrete	133
5.6.3	50 MPa OPC concrete	134
5.6.4	30 MPa OPC/GGBS concrete	135
5.7	Thermogravimetry	137
5.7.1	Introduction	137
5.7.2	30 MPa OPC concrete	139
5.7.3	50 MPa OPC concrete	140
5.7.4	30 MPa OPC/GGBS concrete	140
<b>Chapter 6</b>	<b>Loughborough Summer Climate</b>	<b>173</b>
6.1	Introduction	173
6.2	Weather data	173
6.3	Compressive strength	174
6.4	Air permeability	174

6.4.1	Introduction	174
6.4.2	30 MPa OPC concrete	176
6.4.3	50 MPa OPC concrete	178
6.4.4	30 MPa OPC/GGBS concrete	178
6.5	Sorptivity	179
6.5.1	Introduction	184
6.5.2	30 MPa OPC concrete	184
6.5.3	50 MPa OPC concrete	185
6.5.4	30 MPa OPC/GGBS concrete	186
6.6	Carbonation	188
6.6.1	Introduction	193
6.6.2	30 MPa OPC concrete	193
6.6.3	50 MPa OPC concrete	194
6.6.4	30 MPa OPC/GGBS concrete	195
6.7	Thermogravimetry	198
6.7.1	Introduction	198
6.7.2	30 MPa OPC concrete	198
6.7.3	50 MPa OPC concrete	199
6.8	Mercury intrusion porosimetry	199
6.8.1	Introduction	199
6.8.2	30 MPa OPC concrete	201
6.8.3	50 MPa OPC concrete	202
6.8.4	30 MPa OPC/GGBS concrete	202
<b>Chapter 7</b>	<b>Muscat Summer Climate</b>	<b>264</b>
7.1	Introduction	264
7.2	Weather data	264
7.3	Compressive strength	265
7.4	Sorptivity	265
7.4.1	Introduction	265
7.4.2	30 MPa OPC concrete	266
7.4.3	30 MPa OPC/GGBS concrete	266
<b>Chapter 8</b>	<b>Trends and Discussion</b>	<b>280</b>
8.1	Introduction	280
8.2	Depth and curing affected zone (CAZ)	280
8.2.1	Permeability and sorptivity	280
8.2.2	Carbonation	283
8.2.3	Porosity and hydration	285
8.3	Macroclimate	287
8.3.1	Loughborough winter versus Loughborough summer	287
8.3.2	Loughborough versus Muscat	290
8.4	Microclimate	292

8.4.1	Permeability and sorptivity	292
8.4.2	Carbonation	294
8.5	Duration of hessian curing	296
8.5.1	Permeability and sorptivity	296
8.5.2	Carbonation	298
8.5.3	Porosity and hydration	300
8.6	Curing method	302
8.6.1	Permeability and sorptivity	302
8.6.2	Carbonation	303
8.7	Controlled permeability formwork	303
8.7.1	Permeability and sorptivity	303
8.7.2	Carbonation	305
8.8	Concrete type	306
8.8.1	OPC concretes: 30 MPa versus 50 MPa	306
8.8.2	30 MPa concretes: OPC versus OPC/GGBS	307
8.9	Age: 3 months versus 12 months	310
8.9.1	Permeability and sorptivity	310
8.9.2	Carbonation	312
8.10	Correlation between properties	313
8.10.1	Permeability and sorptivity	313
8.10.2	Carbonation	314
8.10.3	Porosity	315
<b>Chapter 9</b>	<b>Conclusions and Recommendations</b>	<b>331</b>
9.1	Conclusions	331
9.1.1	The curing affected zone	331
9.1.2	Climatic effects	332
9.1.3	Curing methods	333
9.1.4	Microstructural effects	334
9.1.5	Concrete type	335
9.2	Recommendations	336
9.2.1	Depth of cover	336
9.2.2	Curing method	337
9.2.3	Test method	338
9.2.4	Concrete type	338
9.3	Further research	339
Appendix A	Graphs and tables: Chapter 5	359
Appendix B	Graphs and tables: Chapter 6	403
Appendix C	Graphs and tables: Chapter 7	460

# Chapter 1 Introduction

---

## 1.1 OVERVIEW

Concrete's environment plays a central role in its performance, integrity and service life. Most deterioration mechanisms occur as a result of the interaction between the concrete and the environment in which it is located. Specifically, degradation processes are most commonly caused by the ingress into the concrete of substances, which are inexhaustible in the natural environment, yet very harmful to reinforced concrete. Therefore, detailed consideration of the environment and climate, on the macroclimate level generally (the country) and the microclimate level specifically (near the concrete surface), during the inception stage of structures is imperative if durable reinforced concrete is to be achieved.

The full environmental strain, which comprises a profusion of geological and climatic components, is first exerted on concrete's surface layers or cover, i.e., the part of concrete that is in immediate contact with the surrounding environment or microclimate. The transport of aggressive agents from the surrounding environment into concrete takes various forms depending on the conditions of exposure and the transported agent. The conditions of exposure influence the internal moisture condition of concrete upon which the ingress of these agents is essentially dependent. When the concrete pore system is saturated, the transport of fluids at normal pressures occurs mainly by diffusion, whereas under high pressures, fluid permeation predominates. In unsaturated concrete, the relevant transport processes are mainly adsorption, gas diffusion and capillary suction. The rate of transport of the aggressive agents and the consequent corrosive reactions are chiefly dependent on the

porosity and penetrability characteristics of surface layers or concrete's cover. For this reason it increasingly realised and accepted that concrete's durability is largely governed by the quality and performance of its surface layers. The environmental offensive, however, is compounded by the fact that the cover zone is inherently weaker and more permeable than the inner sections of concrete. This inherent weakness is exacerbated by early drying of the surface, as caused by poor curing practice or inadequate curing relative to concrete's natural exposure environment. Curing mainly affects the surface layers of concrete and it is applied solely to enhance the quality of the surface region. Inadequate curing results in restricted hydration in the cover zone and hence greater continuity and volume of pores and higher permeability. Curing, therefore, assumes significant importance for the durability of concrete through its direct effect on the quality of the cover concrete.

The industry's introspective evaluation of concretes poor past performance, and the considerable cost associated, is prompting a change of direction in durability design of concrete, the basis of which is performance specification rather than materials prescription. As a result, emphases are shifting towards concrete's permeability and capillary absorption, particularly that of the cover zone, as being the controlling factor for concrete durability (e.g. RILEM, 1995; prEN 104, 1995). Thus, research work is increasingly being directed towards acquiring a better understanding of the transport processes of species from the environment into concrete and the actuation of degradation mechanisms, and their effect on performance. The specific aim is to develop durability criteria which are based quantitatively on concrete's performance and resistance to degradation processes. However, the concept of performance-based durability specification is hindered by the lack of a suitable test and in-situ test method that can be used routinely to verify compliance.

To be durable, concrete should be designed to achieve predetermined performance targets that enables it to explicitly withstand the full loading that its immediate environment or microclimate is expected to impose during its intended service life.

## **1.2 AIM AND OBJECTIVES OF THE RESEARCH**

The aim of this research work was to study the effects of natural exposure conditions at the macro and microclimate scale, on the penetrability properties of the cover zone layers of OPC and GGBS concretes which had been subjected to a variety of on site curing regimes. More specifically, the objectives were:

- (1) to quantify the effects of macro and microclimates and examine the effectiveness of various curing regimes in improving the penetrability characteristics of concrete's cover zone;
- (2) to examine the suitability of the test methods as indicators of concrete quality and as potential measures for specifying performance; and
- (3) to assess the sensitivity and reliability of each test as a measure of the extent of hydration and therefore curing efficiency.

In this study, concrete's environment denotes the climatic and geological conditions where it is located; concrete cover denotes the cover to reinforcement; and macro and micro climates define the exposure conditions (i.e., the temperature, relative humidity, wind, rain and solar radiation) acting on the regional scale and the location of the concrete element respectively.

## **1.3 STRUCTURE OF THE THESIS**

The thesis can be considered to be in 5 sections: Chapter 2 which gives a background review on the subject; Chapters 3 and 4, which describe the experimental programme and test methods; Chapters 5, 6 and 7 which present the experimental results; Chapter 8 which gives a summary and detailed discussion of all the results; and Chapter 9 which contains the conclusions.

### **1. Background to the Subject**

Chapter 2 gives a general review on the significance and effects of the macro and micro climates, curing and concrete cover on properties and performance

of concrete. The Chapter also contains relevant background information on the chemistry of cement hydration and microstructural development of concrete and its influence on strength, permeability, durability and shrinkage. Particular emphasis is placed on the climatic and geological conditions in the Gulf countries and its influence on concrete's fresh and hardened properties. A brief background is also given to cold weather concreting and the general control measures recommended. The significance of curing is discussed in the later sections of the chapter, with a review of curing methods, curing efficiency, curing specifications, current practice and, effects on engineering properties. The chapter also addresses the importance and influence of cover concrete on the performance and durability of concrete and concludes with a brief summary and remarks.

## **2. Experimental Programme and Test Methodology**

Chapter 3 details the materials, mixture design, site exposure and curing methods adopted in the investigation. A detailed discussion is also given on the rationale behind the choice of materials, specimen size, testing age, curing regimes and conditions of exposure. Chapter 4 gives a detailed description of the test methods and methodology employed in the experimental work and justifications for the choice of the research tests. The chapter also includes a brief theoretical background to the tests and a review of the preparatory research work conducted prior to the execution of the main programme. A full description is given in the chapter of the test apparatus, and sample preparation and conditioning procedures.

## **3. Experimental Results**

Chapters 5, 6 and 7 present the experimental results of the UK winter climate concrete series, the UK summer climate concrete series and Oman summer climate concrete series respectively. The results of the five tests are presented, showing the influence of macro and microclimate, curing, concrete strength and composition, and exposure duration on the cover zone of concrete.

#### **4. Discussion of Experimental Findings**

Chapter 8 gives a brief summary of the results of the three climate series and a detailed discussion of the results and trends. The extent of the curing affected zone within the surface region is evaluated and the influences of the experimental variables i.e. macro and microclimate, curing regime and duration, concrete type and age are discussed.

The relationships between the physical property tests (air permeability and sorptivity) with the microstructural tests (porosity and hydration) are examined and possible correlations between these tests and durability characteristics (carbonation depth) are explored.

#### **5. Conclusions**

Chapter 9 gives the conclusions of the research work and recommendations on the depth of cover to reinforcement, curing, concrete type and test method for performance and durability assessment.

## Chapter 2 Climate, Curing and Concrete Cover

---

### 2.1 BACKGROUND

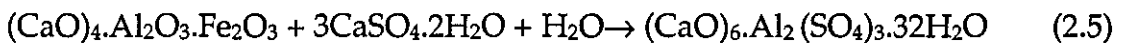
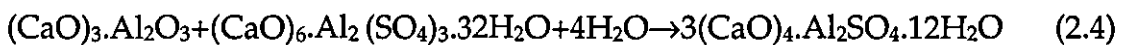
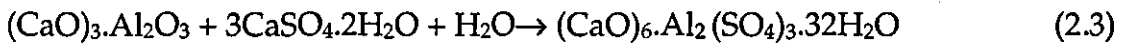
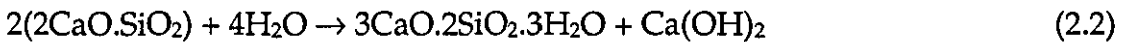
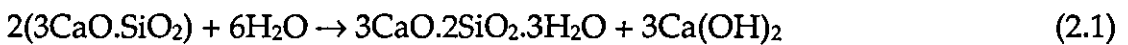
#### 2.1.1 Introduction

Concrete's engineering properties, such as its strength, permeability and durability, are directly related to the processes of cement hydration and pore structure development. These engineering properties are discussed later in this chapter whilst this section is intended to give relevant background information on the chemistry of cement hydration and the influence of the hydration process on the microstructural development of concrete. The influence of pore structure and porosity on strength, permeability and durability is reviewed. Also included is a brief review of the mechanism of shrinkage due to its relevance to thermal and drying shrinkage cracking, which are of a major concern in hot climate concreting.

#### 2.1.2 Hydration, Microstructure and Strength Development

The hydration process of cement and the nature, morphology and microstructure of the hydration products is well documented (e.g. Bogue, 1955; Lea, 1980; Taylor, 1990; Neville, 1995). In this review, a simplified summary of the main stages of hydration reactions of cement paste will be given. It is generally accepted that the hydration reaction advances through five distinct stages (e.g. Jolicoeur and Simard, 1998): (1) initial hydration (approximately 0-15 minutes), (2) induction or dormant period ( $\approx$  15min-4 hrs), (3) acceleration and set ( $\approx$  4-8 hrs), (4) deceleration and hardening ( $\approx$  8-24 hrs), and (5) curing (1-28 days). Amongst the accepted theories is that cement reaction and the formation of the hydration products takes place by an

immediate through solution reactions, topochemical or interfacial reactions and a later, long-term diffusion controlled, core or solid-state reaction (e.g. Jolicoeur and Simard, 1998; Paulini, 1994). During the initial through solution reactions, the reactants dissolve to produce ions in solution, which chemically combine to form the hydrates that precipitate continually from the solution. The topochemical reaction takes place on the surface of the cement grain and the hydration products are deposited outwards to form a dense layer on the surface of the cement. During the early stages of hydration, i.e. up to the onset of the hardening stage or later, both chemical reaction phenomena (through solution and topochemical) are usually involved. Subsequent reactions will be of a topochemical nature and ultimately (over months and years) the slow diffusion-controlled reactions predominate (Scrivener and Pratt, 1984). Typical hydration products of OPC paste are calcium silicate hydrates ( $3\text{CaO}\cdot 2\text{SiO}_2\cdot 3\text{H}_2\text{O}$ ), calcium hydroxide ( $\text{Ca}(\text{OH})_2$ ), ettringite ( $(\text{CaO})_6\cdot \text{Al}_2(\text{SO}_4)_3\cdot 32\text{H}_2\text{O}$ ) and sulfoaluminate ( $3(\text{CaO})_4\cdot \text{Al}_2\text{SO}_4\cdot 12\text{H}_2\text{O}$ ). These hydrates result from the hydration of the 4 major compounds of Portland cement namely tricalcium silicate ( $3\text{CaO}\cdot \text{SiO}_2$ ), dicalcium silicate ( $2\text{CaO}\cdot \text{SiO}_2$ ), tricalcium aluminate ( $(\text{CaO})_3\cdot \text{Al}_2\text{O}_3$ ) and tetracalcium aluminoferrite ( $(\text{CaO})_4\cdot \text{Al}_2\text{O}_3\cdot \text{Fe}_2\text{O}_3$ ), as follows:



The relative reactivity of the above 4 major compound of Portland cement with water is given as  $\text{C}_3\text{A} \rightarrow \text{C}_3\text{S} \rightarrow \text{C}_2\text{S} \cong \text{C}_4\text{AF}$ . The direct reaction of tricalcium aluminate ( $\text{C}_3\text{A}$ ) with water is violent and causes immediate stiffening of the cement matrix or flash set. This is therefore avoided through the added gypsum ( $\text{CaSO}_4\cdot 2\text{H}_2\text{O}$ ), which combines with  $\text{C}_3\text{A}$  to form ettringite as shown in equation (2.3). Calcium aluminate hydrates (C-A-H) are

eventually formed although this stage is preceded by the formation of monosulfoaluminate, as shown in equation (2.4). Like  $C_3A$ ,  $C_4AF$  also acts as a flux and its hydration is similar to  $C_3A$  as shown in equation (2.5).

Due to the early reaction of  $C_3A$  (stage 1), the cement particles become fully coated with aluminate rich layer, which hinders the diffusion of reacting species in and out of the cement surface. This causes a sharp reduction in the rate of reaction, thereby marking the beginning of the dormant or induction period of hydration (stage 2). In the early stages of the dormant period the reaction of the aluminate phases continue to predominate, and later during this stage, the transformation of ettringite (of hexagonal rods morphology) to monosulfoaluminate (hexagonal plates) takes place (equation (2.4)) and the initial aluminates layer becomes thickened with an overlay of C-S-H gel. Towards the end of the dormant stage, the disruption of the protective hydrate layer takes place and the beginning of the acceleration and set stage is started (stage 3). It is thought that the protective layer on the cement grains is broken down by osmotic pressure effects and/or the growth of the C-S-H and CH crystals. Following the acceleration and set stage, the reaction slows down and continues at a slower rate towards the end of the hardening and the beginning of the curing stages (stages 4 and 5).

Evidence from electron microscopy suggests that the outgrowth of calcium silicate hydrates C-S-H (the most abundant phase of the hydrates) from the cement grains adopts a fibrillar and sheet like morphology. Once the cement grains are covered in these fibrils, access of water to the cement grain is hindered and the diffusion controlled reaction then takes place. Under normal temperature conditions, the hydration rate proceeds at a normal rate and the hydration products grow out towards the water-filled space. As the fibrillar outgrowths from the various grains increases, adjacent cement grains become immobile and fixed in some pattern. On continued hydration the network of fibrils become reinforced with sheet-like C-S-H spanning across the interfibrillar spaces. Most of the C-S-H is formed in the vicinity of the cement grains and the remainder of the water present in the matrix becomes occupied

by the calcium hydroxide. With the progression of hydration, a continuous change of porosity takes place and microscopic evidence indicates the presence of typically 4 types of porosity (Bailey and Stewart, 1984): (1) porosity within the C-S-H, typically several Angstroms; (2) porosity between fibrils and foils which is approximately 0.1  $\mu\text{m}$ ; (3) porosity due to packing and W/C ratio which is typically around 1 $\mu\text{m}$ ; (4) porosity on the macro scale such as air voids and cracks and spaces between particles. The later two types of porosity predominate during the initial stages of hydration, with type (1) and (2) appearing at later ages with continued hydration. This pore divisions is analogous of the Powers-Brownyard (Young, 1988) pore size classification of cement paste where pores up to 10nm (0.01 $\mu\text{m}$ ) are classified as gel pores (corresponding to type 1 above), pores between 10-10,000nm are capillary pores (types 2 and 3), and those over 10,000 (10 $\mu\text{m}$ ) are considered air voids (type 4).

The resultant hydrated matrix consists of a complex system of amorphous mass commonly termed cement gel, crystals of various morphology and sizes of calcium hydroxide ( $\text{Ca}(\text{OH})_2$ ) that have been deposited into the original water space (approximately 20% of the solid material), unhydrated cement grains and air or water filled voids. The amorphous mass of the cement gel is formed mainly of calcium silicate hydrates (approximately 70% of the solid material) and smaller amounts of aluminates and alumino-ferrite hydrates (approximately 10%). The hydration reaction, under low temperature and temperate conditions, is reported to be slow enough to permit the hydration products to diffuse slowly and precipitate uniformly to fill the interstitial space between the cement grains throughout the cement paste matrix (Verbeck and Helmuth, 1968; Kjellsen et al, 1990).

The relationship between compressive strength and porosity have been studied extensively and empirical and semi-empirical relationships have been developed (e.g. Taylor, 1990; Rahman, 1984). However, since the development of porosity depends on the conditions of hydration (compaction, curing and

degree of hydration,) and the W/C ratio, concrete strength therefore too is dependent on these factors. Nevertheless, strength was found to depend more on the pore size distribution than the total porosity. Rahman (1984) in his review of the topic cited the work of Birchall and his co-workers who found that the strength of cement pastes varied by a factor of six despite displaying the same total porosity. They also noted that the low tensile properties of cement paste results from the presence of macro pores  $> 10 \mu\text{m}$ . It is generally considered that the volume of pores, their size and continuity are the factors that determine strength, although there appear to be no general consensus on the exact range or type of porosity directly involved (e.g. Taylor, 1990).

### **2.1.3 Permeability and Durability**

Concrete's permeability in this section refers to the ease with which different species, e.g. liquid, gas or ionic species, can penetrate into and through the concrete. Due to its importance to concrete durability (especially in the Gulf environment), the transport processes involved in the penetration of chlorides into concrete are included later in this section whilst background to the various transport processes (permeation, capillary absorption and diffusion) is also given in Chapter 4.

The durability of concrete may be defined as its ability to withstand its environmental and service loading and perform satisfactorily throughout its intended design life. Most degradation mechanisms of reinforced concrete involve the permeability of harmful substances from the environment into concrete. As a result, there is increasing interest in concrete's permeability as a criterion for its durability (e.g. Dhir et al, 1994; RILEM, 1995). Of particular interest is the permeability of the surface region or concrete's cover, which controls the ingress of these substances into the inner sections of concrete (e.g. Krijger, 1984; Dhir et al, 1986). The cover zone of concrete is discussed in Section 2.5.

The permeability of fluids into concrete takes place via its pores and therefore depends largely on the pore structure characteristics of the concrete. Concrete

typically embodies a very large size range of pores, which are considered to be part of the bulk cement paste within the concrete. The cement paste pores, as discussed earlier, are classified into gel pores ( $< 0.01\mu\text{m}$ ), capillary pores ( $0.01\text{-}10\mu\text{m}$ ) and air voids ( $> 10\mu\text{m}$ ). In their study, Powers and Brownyard (1947) suggested that the permeability depends more on the volume of capillary pores than smaller pores. Since then, numerous studies established correlations between permeability and capillary porosity with the conclusion that concrete's permeability is determined by the volume and continuity of the large or capillary pores (e.g. Mehta and Manmohan, 1980; Nyame and Illston, 1980 and 1981; Goto and Roy, 1981).

Additional to the cement paste pores, another area of influence on concrete permeability and durability is thought to be the transition regions where the paste-aggregate interface occurs, which is commonly known as the aggregate-paste interfacial transition zone (ITZ) (e.g. Winslow and Liu, 1990; Scrivener and Nemat, 1996; Alexander et al, 1995; Halamickova et al, 1995). This has been a subject of interest for many years and there are suggestions that this zone influences important concrete properties such as transport properties and permeability, strength and stiffness (e.g. Alexander et al, 1995; Garboczi, 1995). The ITZ is generally considered to be a zone of weakness, which is characterised by higher capillary porosity and larger pores than in the bulk of the cement matrix, and higher concentration of calcium hydroxide than observed in the bulk (Garboczi, 1995). According to Garboczi (1995), this zone of weakness arises from two major causes: (1) poor packing of cement particles against the aggregates due to the flat edge or wall effect, and (2) the one sided growth of cement hydrates against the aggregates (as opposed to the all direction growth of cement hydrates in free space). The width of the ITZ is typically between  $30\text{-}50\ \mu\text{m}$ , although recent studies indicate that it may extend to a width of  $100\mu\text{m}$  into the paste (Scrivener and Nemat, 1996). Winslow and Liu (1990) on investigating the pore size distribution of cement paste in concrete and mortars using mercury intrusion porosimetry concluded that the paste in concrete is more porous than the pure cement

paste, and that additional porosity occurs in pores larger than found in the pure paste. Halamickova et al (1995) found that including relatively impenetrable sand particles resulted in notably higher diffusivities and permeabilities than pure cement pastes. The authors' results are in agreement with the general view that the permeability of concrete is approximately 1-2 orders of magnitude higher than that of pure cement paste (Young, 1988). The contribution of aggregates to the permeability of concrete is not significant ( $\leq 1-2\%$ ) as their pores are mostly discontinuous and are usually coated or enclosed within the cement paste.

Factors that affect concrete permeability are those that influence its porosity and pore size distribution or more specifically, influencing the capillary porosity. Capillary pore volume and continuity are dependant on the W/C ratio and the conditions of hydration (compaction, curing, exposure and age) of the concrete. For the same W/C ratio, the capillary porosity and subsequently permeability, decreased with increased hydration time (e.g. Mehta and Manmohan, 1980; Nyame and Illston, 1980 and 1981). This is mainly due to the progressive production of the hydration products and the continual filling and segmentation of the originally water-filled spaces between the cement grains. Mehta and Manmohan (1980) observed a reduction in the threshold diameter and the volume of pores at any given diameter with increasing hydration age (28 days, 90 days and 1 year). The threshold diameter (or critical pore diameter) was defined as the diameter of the largest pore present at which mercury begins to penetrate into the pores of the specimen. Moreover, the authors noted that the pore size distribution was not uniformly affected i.e. the hydration products tended to follow the paths of least resistant by filling the larger pores ( $> 132\text{nm}$ ) first, while causing little or no change to the volume of smaller pores ( $< 132\text{nm}$ ).

Mehta and Manmohan (1980) and Goto and Roy (1981) similarly observed that under the same hydration conditions, the cumulative pore volume at any given diameter and the threshold diameter increased significantly with

increasing the W/C ratio. Mehta and Manmohan (1980) noted that the increased total porosity due to increasing the W/C ratios manifests itself in the form of large pores only ( $> 132\text{nm}$ ). Since the influence on the permeability of large pores was greater than small pores, the authors concluded that pore size distribution provides a better parameter for assessment of the permeability than the total pore volume. Nyame and Illston (1980) arrived at the same conclusions however, the authors point out that the changes brought about by the variation in the W/C ratios are very different from those resulting from hydration. The lower volume of large pores in the pastes with lower W/C ratios was attributed to the closer initial packing of the cement grains (due to the smaller quantity of water) which facilitates the cross linking of the inter-granular spaces with hydration products. Dinku and Reinhardt (1997) investigated the effect of ten W/C ratios on the penetrability, carbonation and strength of different concrete mixes. The gas permeability, sorptivity and carbonation decreased with decreased W/C ratios. The compressive strength was increased with decreased W/C ratios and was found to be more sensitive to changes in the W/C ratios than variation in curing duration.

The permeability of concrete to chlorides and reinforcement corrosion is the largest cause of durability related problems in the Arabian Gulf (e.g. Rasheeduzzafar, 1984). The transport of chloride ions into concrete is a complex process that involves diffusion, capillary suction and convective flow with flowing water, accompanied by physical and chemical binding (RILEM, 1995). Depending on the condition of exposure, the transport processes involved will be permeation of salt solution, capillary suction of a chloride-containing solution and diffusion of free chloride ions. The permeation of chloride ions in solution is a convective flow controlled by the flow of the liquid and its chloride ion concentration. In this case, flow takes place under the influence of a high hydrostatic pressure and, as such, is only applicable in special applications such as marine structures (submerged) or solution retaining structures. Similarly, the transport of chloride containing solutions

by capillary suction is driven by surface tension and the pore radius of the liquid, its density and viscosity (see Section 4.5.1). Unlike permeation and capillary suction, the transport of chloride ions by pure diffusion is caused by gradients of the chloride concentration. The diffusion rate of chloride ions is therefore dependent on its concentration gradient as well as the water content of the concrete element, which constitutes the medium through which the ions diffuse. These transport processes may be involved singularly, simultaneously or consecutively, depending on the condition of exposure. It is generally assumed that chloride penetration into concrete under normal service exposure would involve a combination of capillary absorption and subsequently diffusion. Bamforth and Pocock (1990) found better correlation between the chloride content profiles and sorptivity profiles than with the apparent diffusion coefficients of large concrete blocks subjected to sea, roadway and industrial exposure. The authors concluded that in the early stages of exposure to chlorides the rate of ingress is largely independent of the chloride diffusion coefficient and that the ingress of chlorides into concrete within the first 6 months of site exposure was controlled by the sorptivity of the concrete.

The penetration of chlorides into concrete depends on concrete's properties and quality i.e. its mixture composition, cement type, W/C ratio, porosity and thickness of the cover, compaction and curing, as well as environmental exposure e.g. chloride concentration, temperature and relative humidity. The critical chloride content required to initiate depassivation of reinforcement depends on a variety of factors including the pH of the pore solution of concrete and cement composition. Most specifications limit the maximum concentration of chlorides from all constituents to 0.1-0.4% by weight of cement content, depending on the type of reinforcement and concrete composition (e.g. BS 8110, 1985).

#### 2.1.4 Shrinkage

The mechanism of shrinkage (volumetric contraction) is a complex phenomenon which is thought to involve a number of mechanisms such as capillary and surface tension (e.g. Bentur et al, 1980; Soroka, 1993). Wittmann (1976) reported that plastic shrinkage or contraction occurs due to the compressive stresses that are induced by capillary tension of the pore water within the fresh concrete. Because these compressive stresses occur when the concrete is still plastic, concrete can be consolidated and contraction or shrinkage occurs. The mechanism of drying shrinkage is thought to take place primarily as a result of the movement or removal of the interlayer water from the cement pastes in concrete upon drying. In a study of hydrated calcium silicate compounds using X-ray diffraction methods, Bernal (1952) suggested that the loss of intra-crystalline water on drying reduce the inter-layer spacing and causes volume decrease or shrinkage.

The extent of drying shrinkage depends primarily on climatic conditions as well as the W/C ratio and aggregate stiffness and content. The effect of climate on the rate evaporation (plastic shrinkage) and drying of concrete is discussed later in Section 2.2.3. The rate of evaporation or drying increases with increased ambient temperature, reduced relative humidity and increased wind velocity. Hence the intensity of drying and, therefore, the amount of shrinkage, are increased under hot and dry conditions. Further, drying shrinkage is said to be affected by the cement content, water content and the W/C ratio. An increase in the cement content increases the paste concentration in the matrix and lead to greater shrinkage. This is because volume contraction is primarily caused by the shrinkage of the paste (removal of water from the paste). Similarly, higher water contents results in increased water loss and therefore, increased shrinkage. Therefore, both parameters i.e. water and cement content as well as the W/C should be kept to a minimum to minimise shrinkage. Higher W/C ratios have been observed to results in greater shrinkage because of its effect on modulus of elasticity and strength (Soroka, 1993). However, Brookes (1989) showed that shrinkage of hydrated

cement paste is directly proportional to the W/C ratios only in the range from 0.2 to 0.6, above which loss of water on drying does not cause shrinkage.

The shrinkage of the aggregate is considerably smaller than that of the cement paste. However, aggregate size and content influence shrinkage indirectly, as larger aggregate size and content results in a leaner mix (lower paste concentration) and, therefore lower shrinkage. Additionally, higher aggregate stiffness has a direct influence on shrinkage and, the greater the stiffness of the aggregates (which imparts greater modulus of elasticity) the greater the resistance to shrinkage in the system. The shrinkage of concrete containing soft sandstone aggregates is said to be more than twice that made with granite, basalt or limestone aggregate (ACI, 1984).

## **2.2 MACROCLIMATE**

### **2.2.1 Denotation and Significance of Cold and Hot Climates**

Climate defines the weather conditions at a particular place over a period of time. The variation of climate over the surface of the Earth is determined by a combination of factors that include (Hutchinson, 1996): (1) the effect of latitude and the Earth's axis tilt to the plane of the orbit around the Sun; (2) the large-scale movements of the various wind belts over the Earth's surface; (3) the temperature difference between land and sea; (4) the contours of the ground; and (5) the location of the area with respect to the ocean currents. The extent of the heat that the Earth receives from the Sun varies in different latitudes and at different times of the year. However, the distribution of the climate is mainly linked to the intricate distribution of land and sea, and the resulting complexity of the general circulation of the atmosphere.

Realisation of the important effects of the environment, i.e. climatic and geological conditions, on concrete construction resulted in the familiar broad classifications of hot and cold climates, which are commonly used in the construction industry. It is generally considered that the climate in European countries is predominantly cold to temperate, whereas that of the Arabian

Gulf countries is classified as ultra hot or very hot and dry (e.g. Al-Abideen, 1998; Summers and Olsen, 1996). As a guide to concreting practice, the terms have been defined by committees such as the American Concrete Institute and RILEM. According to ACI Committee 306 (1990), cold weather is defined as 'a period when for more than 3 successive days, the following conditions exist: (1) the average daily air temperature is less 5 °C (40 °F); and (2) the air temperature is not greater than 10 °C (50 °F) for more than one-half of any 24-hour period'. ACI Committee 305 (1991) defined hot weather as 'any combination of the following conditions that tend to impair the quality of freshly mixed or hardened concrete by accelerating the rate of moisture loss and rate of cement hydration, or otherwise resulting in detrimental results: (a) high ambient temperature; (b) high concrete temperature; (c) low relative humidity; (d) wind velocity; and (e) solar radiation'. However, RILEM TC 94 (1993) provides a more detailed consideration of the climate with sub-classifications such as hot-dry or hot-humid, arid or moderate etc. with special emphasis on the microenvironment that immediately surrounds the structure.

Definitive and detailed specifications are very difficult, if not impossible, to produce, and it is apparent that strict interpretation of the general definitions of climate as given above will not be appropriate nor economical to apply to all construction conditions under these general macroclimates. Independent assessment of the climate specific to the locality of a particular construction scheme is imperative for sound durability design. In the UK, for example, the weather conditions for concreting practice are generally temperate, and extreme climatic conditions occur only occasionally and briefly (Kay and Slater, 1995). Therefore, the application of the stringent specifications of cold weather concreting that may apply to the extreme parts of Europe, for all construction practice and at all times of the year is clearly not practical nor cost effective. To illustrate the extent of the seasonal variation effect that may occur in the same country, Kay and Slater (1995) gave an example where a bridge deck construction in the UK was rejected because of inadequate

compaction due to poor workability (slump loss). This was because the mix trials were conducted in the winter while the actual construction took place during a hot summer.

Similarly, the definition of hot climate as given above is somewhat too simple and vague to describe the vast and environmentally diverse, both climatically and geologically (e.g. Fookes, 1995), area of the Arabian Peninsula. The absolute temperature and temperature gradient variations, the relative humidity cycles, wind velocity and rain fall differences, as well as the extreme variations in geomorphologic formations for concrete making materials are remarkably distinct from one country to another in the Arabian Gulf and in different parts of the same country (Al-Abideen, 1998). It is in these adverse and diverse conditions that accurate definition and close assessment of the micro-environment is most needed.

The variation between the coastal and inland climatic conditions within the same country in the Gulf results in distinct degradation phenomena. In the coastal areas, the climate can be classified as hot-humid to hot-dry due to the large fluctuation in relative humidity, whereas in the inland regions the climate is predominantly hot-dry due to the generally low prevailing diurnal and annual relative humidity (Al-Gahtani et al, 1998). As a result, the fluctuating humidity and high temperature conditions of the coastal areas are most conducive to chemical attack of concrete, which leads to sulphate damage and corrosion of reinforcement (e.g. Rasheeduzzafar et al, 1984). In the hot and dry inland conditions, on the other hand, degradation is often associated with plastic and drying shrinkage, cessation of hydration, insufficient strength gain, and general lack of durability (Rasheeduzzafar et al, 1985, Al-Amoudi et al, 1993).

The large fluctuation in the temperature in the hot climate countries, which can fall drastically in some parts during the winter, and the occasional heat wave that may occur in temperate climate countries during the summer, calls for a prudent interpretation of climate classifications. The essence is to follow

cautiously the necessary concreting precautions based on the environmental variables (climatic and geological) obtaining at a particular location and during a specific period of time.

## **2.2.2 Cold Climate Concreting – A Brief Review**

### *Introduction*

For completeness, a brief review of the effects of cold weather on concrete and concreting practice have been included.

Concreting during low temperatures constitutes three major concerns due to delayed setting time: increased risk of concrete freezing and subsequent physical damage at early age before the concrete attains compressive strength of at least 3.5 MPa; low strength development for removal of formwork or handling of structural loads at a given age; and damage due to thermal stresses as a result of rapid surface cooling and the formation of large temperature gradients between the surface and the inner sections of concrete (e.g. Nmai, 1998; Turton, 1995; Senbetta, 1994). However, it is generally considered that cold weather is ideal for concrete construction provided that proper planning is performed ahead of construction, and adequate control and protection against freezing provided during execution (e.g. Scanlon, 1992 and 1997). Cold weather concreting is covered in a number of guides and standards e.g. BS 8110 (1985) and ACI 306 (1990), which recommend appropriate measures to control the various effects of cold weather on concrete properties. Requirements for adverse weather concreting in the UK are relatively forthright since the conditions are generally not as severe as in other cold climate countries (Kay and Slater, 1995).

### *Recommendations for cold weather concreting*

Based on the general definition of cold weather given earlier, most specifications stipulate a concrete temperature limit of 5 °C, above which concrete placement is not recommend. The concrete must be protected from freezing for at least 24 hours after placement and water curing should not be applied to avoid concrete saturation until sufficient strength gain has been

achieved. Placement against frozen ground should not be permitted and the formwork should be pre-heated where possible. Further, most specifications require that concrete making material, e.g. aggregates and water, and all surfaces likely to come into contact with fresh concrete to be free from snow, ice and frost.

Measures to control the mix temperature include: heating the water or aggregates or both; the use of rich mixes with low W/C ratio; the use of high early strength cements (high in C<sub>3</sub>S and C<sub>3</sub>A contents); the use of finer cement; reduction of proportion of cement replacement materials in thin sections; the use of chemical admixtures to accelerate concrete setting and early age strength development; the use of anti-freeze admixtures to depress the freezing point of mix water; the use insulation material to protect the freshly placed concrete surface; delaying formwork striking time; and enclosing and heating the area in which the concrete is to be placed.

To avoid the risk of flash set, the mix water should not be heated to exceed 60-80 °C (Neville, 1995). Similarly, where heating of aggregate is required, it is inadvisable that the aggregate temperature exceeds 52 °C. Further, removal of insulation from the concrete should be carried out in such a manner so as to ensure that sudden cooling of the surface and the consequent development of temperature gradients within the concrete does not take place.

Concrete curing is generally aided with the application of some of the described control measures e.g. insulation curing, admixtures and heating concrete materials and the space enclosure where concrete is to be placed. However, other curing methods that involve application of external heating may be employed where necessary. These methods include one of or a combination of the following (Scanlon, 1997): Electrode or electric heating; heating with infrared lamps; steam curing; heating with hot air or natural gas combustion products.

The presented control measures for cold weather concreting give a wide range of options that may be employed in various ways to achieve the

intended purpose. Although the main criteria for the selection of a suitable option or a combination of options are normally concrete set and strength development, the choice of appropriate measures should be made after consideration of the type of control measures contemplated in relation to the type of construction and the subsequent cost involved.

### **2.2.3 Hot Climate Concreting**

#### *Introduction*

The majority of durability problems in the Arabian Gulf are initiated and subsequently actuated by external elements from the surrounding environment of concrete (e.g. Rasheeduzzafar and Al-Kurdi, 1992). The unification of the (1) ultra hot climate and (2) geologically aggressive medium, combined with (3) poor concreting practice in some instances and (4) inappropriate materials and design approach in others, resulted in drastic reductions in concrete's service life with huge cost implications. Nevertheless, numerous examples illustrate that durable concrete can be produced routinely in these adverse conditions provided that adequate measures are taken (e.g. White, 1997; Al-Abideen, 1998). It is apparent that the key to durability in the Gulf lies in the precise understanding of the effects of the first two factors (hot climate and geological conditions) and their various components on concrete properties, and consequently in the formulation of appropriate design and concreting approaches (the last two factors) to suit these conditions.

#### *Climatic components*

The characteristic ultra hot climate of the Arabian Peninsula emanates from the interplay of the various climatic components namely: the air temperature, relative humidity, wind velocity and solar radiation; the typical features of which is as follow:

### (a) Air temperature

The ambient temperature in the Gulf countries rises rapidly, and repeatedly reach and remain sustained at 45-50 °C during the summer months (e.g. Rasheeduzzafar et al, 1984). Furthermore, the rapid temperature gain during the day is often accompanied by large and sudden drops in temperature at night, the resultant day-night variation in temperature during a typical summer's days can be as high as 20-30 °C (FIP, 1986; Al-Amoudi et al, 1993). The rate of hydration is almost doubled for every 10 °C increase in temperature and according to ACI Committee Report 305 (1991), a limit that is most favourable for concreting in hot weather exists between about 24-38 °C.

### (b) Relative humidity

The relative humidity at a particular location is mainly determined by the conditions of wind and proximity from the sea. The relative humidity is generally low in the inland regions of the Gulf and fluctuate substantially in the coastal areas from around 100% to as low as 5-10% within 24 hours. Further, dew points occur at sunrise and often again in the afternoon period. The precipitation is generally very low i.e. ranging from 3.5 to 13 cm/year, with an average of around 8 cm/year for the area (Rasheeduzzafar et al, 1984; CIRIA, 1984; Walker, 1996).

### (c) Wind velocity

High wind contributes significantly to the problems of hot weather concreting. Although the intensity of wind generally compares with that experienced in parts of western Europe, the number of instances when the wind velocity exceeds 17 km/h is 25% more (CIRIA, 1984). The rate of evaporation can reach serious proportions if wind speed exceeds 15 km/hr (FIP, 1986). According to the ACI Committee Report 305 (1991), for example, the evaporation rate of a concrete placed at 21 °C with a relative humidity of 50% and a wind speed of 16 km/hr, will have 6 times the evaporation rate of the same concrete when there is no wind. The evaporation rate in some parts of the Arabian Peninsula is 124 cm/year (e.g. Rasheeduzzafar et al, 1984;

Fookes, 1993). Further, the effect is exasperated by the wind transportation of sand and silt which can be contaminated with salts (e.g. Fookes, 1993; Walker, 1996).

#### (d) Solar radiation

This is a distinguishing feature of hot climate countries in general and the Gulf countries in particular. The mean total solar radiation level typical of the Gulf region, measured in terms of power per area, is in excess of 350 W/m<sup>2</sup>. This level of radiation is the highest in the world and exceeds that of the Death Valley and Phoenix in north America which have a solar radiation range of 320-350 W/m<sup>2</sup> (Summers and Olsen, 1996). Such level of radiation was found to elevate the already high air temperature in the Gulf by an additional 40 °C on unshaded black surfaces, however more remarkably, this was achieved within a space of just 3 hours (Summers and Olsen, 1996). The duration of daily sunshine is typically in excess of 12 hours during the summer months.

#### *Geological components*

Geology affect concrete's performance in two ways: (1) by the conditions of the construction ground and (2) as a source of the concrete making materials. A brief description of typical conditions in the Arabian Peninsula is given below, however, it should be noted that the conditions will vary from one region to another and detailed consideration of the microenvironment must be given for different locations independently.

#### (a) Ground conditions

Most of the area is of recent geological formation consisting of weak sedimentary rock, older igneous and metamorphic rocks occurring predominantly in the remote mountains of Oman (CIRIA, 1984; Fookes, 1995). The coastal regions, where a lot of the development has taken place in the Gulf, are mostly low-lying flats that are normally bordered by shallow and highly saline seas along one side and 'sabkhas' along the other side. The coastline sediments are typically salty gravel and sands, shelly sands with

thin carbonate silts, and clays. The ground water table near the sea is commonly highly rich in chlorides and sulphates. In the inland regions, the same kind of sedimentary, weak sandstone and limestone formations and clay and marls occur in broad and gently inclined area, with local salinity in some parts. Furthermore, the Gulf waters are the hottest (average 30 °C) and most saline in the world due to the semi-enclosed nature of the Gulf, which restricts tidal movements and interchange of water with the Gulf of Oman and Arabian sea (Walker, 1996). The salinity concentration of the Gulf Sea is more than 40,000 ppm, compared for example, with 25,000 ppm with the Atlantic Ocean off the coast of Miami (Summers and Olsen, 1996). As a result, the coastal seawater adjacent to dry land has high salinity, which affects both the ground water and the air-borne moisture. In addition, wind-blown sea spray can be spread over large inland areas, contaminating it with salt as it evaporates.

#### (b) Source of materials (aggregates)

With the exception of some parts of northern Oman where old igneous and metamorphic rocks occur, most rocks in the region are predominantly young limestone of varying quality and constitute the only source of aggregates for some regions. Some of these rocks yield aggregate material that is porous, absorptive, weak and excessively dusty on degradation (CIRIA, 1984; e.g. Rasheeduzzafar et al, 1984). However, an important characteristic of these rocks is their high variability, with the result that different quality aggregates can be obtained from the same source. The contamination of some limestone rocks with salts, carbonates, chert and flint results in the production of highly reactive aggregates which are unsuitable for concrete construction. Sand is normally obtained from mountain quarries, which can produce a reasonable quality of fine and coarse aggregates. Sand is also obtained from desert sand dunes, which normally has a fine single-sized grading and is usually free from contaminants like chlorides and sulphates. This is normally mixed with other sand to obtain the required grading. Other sources of sand include

beaches, this however, is often prone to contamination with chlorides and sulphates.

#### *Effect of hot climate on fresh concrete properties*

The effect of hot climate on the properties of concrete are well documented (e.g. CIRIA, 1984; BS 8110, 1985; FIP, 1986; ACI, 1991, RILEM, 1993) and are now well realised. Detailed discussion about these effects will not be reproduced in this review, however a summary of important findings will be given. It is noteworthy that although the effect of hot climate as a whole on the properties of concrete have been extensively investigated, there are few detailed studies on the effect of the individual climatic components on the various properties. The combined effect of the climatic components, i.e. high temperature, low relative humidity, high wind and solar radiation, on fresh concrete may result in increased water demand, slump loss and premature setting, insufficient compaction and enhanced tendency for plastic shrinkage cracking.

#### (a) Water demand, slump loss and setting time

Setting, or stiffening as described by BS 5075 (1982), governs the time up to which the concrete can be sufficiently compacted (FIP, 1986). Setting is affected by the initial slump or workability of the concrete and can only occur after the loss of the later (e.g. Egan, 1995). These effects are mainly caused by the excessive evaporation of water from the mix and by the hydration reaction between the cement and water, which are typically accelerated by high temperature. The rate and amount of evaporation depends on the conditions of the climate as a whole, i.e. temperature, relative humidity, wind and solar radiation, but appears to be especially more sensitive to the relative humidity conditions (ACI, 1991). Shalon and Ravina (1960) found the rate of evaporation to be considerably higher at a temperature of 30 °C and R.H. of 20% than at 40 °C and 70% R.H. This was reflected in considerable loss of workability (measured by the slump and V.B time) at these conditions and lesser loss at R.H. above 45%, with the effect of temperature on the

workability being less significant. On the other hand, Klieger (1958) found that an increase in concrete temperature of 11 °C may decrease the slump by 25mm. Berhane (1984) found that the evaporation in a hot-humid climate was 3.5 lower than in a hot-moderate climate and 7.5 time lower than in a hot-dry climate. In the same study, the total amount and rate of water evaporated was found to be higher with increased W/C ratio at the end of 24 hours after casting.

Removal of water from the mix also occurs during cement hydration. This is mainly due to the fact that some mix water becomes chemically bound as the formation of hydrates progresses while other water becomes physically adsorbed on the surface of these hydration products (Ravina and Soroka, 1992). Furthermore, high temperatures lead to increased rate of hydration and heat evolution, which increases the rate of setting and leads to insufficient compaction (e.g. Soroka and Ravina, 1998).

#### (b) Early volume changes and cracking

Volume change in fresh concrete or plastic shrinkage (pre-hardening volumetric contraction) is also a function of water removal from the mix due to evaporation, cement hydration, absorption of water by dry aggregates and the bleeding of free water. This gives rise to various types of cracking in the young concrete which occur within a few hours of placement.

It is generally believed that plastic shrinkage cracking occurs when the rate of evaporation of the freshly placed concrete is greater than the rate at which water rises to the surface (Neville, 1998; ACI, 1991). According to ACI Committee 305 (1991), the risk of plastic shrinkage cracking increases when: the evaporation rate approaches 1.0 kg/m<sup>2</sup> per hour, when slow setting cement is used, excessive amount of retarding admixtures are used, when fly ash is used as a cement replacement or when the concrete is over cooled. However, some researchers reported that plastic shrinkage cracking is not a direct function of evaporation and shrinkage but is more directly dependent on the stress/strength ratio, i.e. plastic cracking occurs when the concrete

strength is less than shrinkage stresses (Kovler, 1995). Ravina and Shalon (1968) showed that due to its higher tensile strength, plastic cracking did not occur in semi-plastic mortars exposed to severe evaporation conditions while plastic and wet mortar cracked under the same conditions. Soroka (1993) identified various distinct stages of plastic shrinkage. The first stages of shrinkage occur as the rate of evaporation becomes higher than the rate of bleeding. At this stage shrinkage starts but no cracking occurs because the concrete is still plastic enough to accommodate the resulting volume changes. As the concrete becomes brittle on continued drying (drying and shrinkage up to this stage proceeded at the same rate), restraint of shrinkage induces tensile stresses in the concrete which cracks when its tensile strength is lower than the induced tensile stresses. Thus, exposure to higher rates of evaporation when the concrete is not strong enough to resist the tensile stresses caused by the restrained shrinkage results in plastic shrinkage cracking. The possibility of plastic shrinkage cracking occurring is therefore dependent on the intensity of evaporation or drying and the climatic factors that affects it as well as the rate of stiffening and strength development of the fresh concrete. Hence, the risk of this type of cracking occurring can be minimised through adequate protection of the concrete surface when the concrete is most vulnerable i.e. during the first few hours after placement and through appropriate mix design. Plastic shrinkage cracks affects the concrete surface but can be very deep with variable widths ranging from 0.1 to 3mm, which may be short or as long as 1m (FIP, 1986; ACI, 1984).

Plastic settlement cracking occurs due the loss of water from the fresh concrete through bleeding and the obstruction of the subsequent settlement of concrete (ACI, 1984; ACA Bulletin, 1995). The concrete settlement may be obstructed by aggregate particles or reinforcement bars thereby causing differential settlement of the concrete which, in turn, causes cracking if the concrete is not strong enough to resist the associated movement. The cracks can be deep and are orientated i.e. they follow the cause of obstruction such

as the reinforcement bars or aggregates or the geometry of the element involved.

#### *Effect of hot climate on hardened concrete properties*

For hardened concrete, hot climate may result in inadequate hydration, thermal and drying shrinkage cracking, reduced later strength, increased permeability, enhanced tendency for chemical reaction and reduced durability (e.g. ACI, 1991; Al-Amoudi et al, 1993; Al-Ghatani et al, 1998).

#### (a) Hydration, microstructure and strength

It is well known that hot weather conditions have an accelerating effect on the rate of cement hydration. Soroka and Ravina (1998) suggest that a rise in the hydration temperature from 20 to 40 °C increases the hydration rate by a factor of 2.4 in the first few hours. Consequently, the formation of the cement gel during the hydration process of concrete in hot conditions is accelerated. Based on evidence from X-ray diffraction and heat of hydration measurement, Verbeck and Helmuth (1968) proposed that the rate of cement reaction at high temperatures is much faster than the rate of diffusion of the hydrates. As a result, the hydration products are not able to diffuse to a significant distance and end up being deposited immediately around (encapsulating) the cement grains. Accordingly, the hydration products cannot disperse uniformly to fill the interstitial space among the cement grains before the paste hardens. This was later verified by Kjellsen et al (1990) who obtained direct evidence to support the theory using backscattered electron imaging. In this work, the authors found that the hydration products of the samples hydrated at 5 °C are much more evenly distributed than that hydrated at 50 °C. Moreover, unlike the samples hydrated at 5 °C, the samples hydrated at 50 °C had two different densities of the C-S-H phase, which represents the relatively dense “shells” around the cement grains and the less dense structure between the grains as was originally envisioned by Verbeck and Helmuth. Furthermore, the authors point out that although the C-S-H near the cement grains is much denser and

stronger in the samples hydrated at 50 °C than at 5 °C, the strength is controlled by the porous C-S-H in the interstices between the cement grains.

Although there are views to the contrary, it is generally accepted that high temperature (up to 100 °C) affects the morphology and pore structure of the hydration products but does not alter the stoichiometry of hydration i.e. the chemical composition of the hydration products remain the same as those produced under moderate temperatures (e.g. Taylor, 1990; Soroka, 1993). This, however, has significant implications for concretes produced in hot climate since concrete's strength, stiffness, shrinkage and creep as well as permeability and durability are largely determined by its porosity and pore size distribution (e.g. Rahman, 1984; Young, 1988; Taylor, 1990).

Although there are some contradictory findings (e.g. Martin, 1992; Malvin and Odd, 1992; Arafah et al, 1996), it is widely reported that due to the accelerating influence of high curing temperature on the initial rate of hydration, the early age strength (up to 7 days) of concrete is increased, however, its later-age (28 days and later) strength is adversely affected (e.g. Price, 1951; Klieger, 1958; Verbeck and Helmuth, 1968; Barnes et al, 1977; Gaynor et al, 1983; Ramezaniapour and Malhotra, 1995; Mouret et al, 1997). Ramezaniapour and Malhotra (1995) compared the compressive strength at different ages of samples that had been cured under standard moist curing conditions, and samples that were cured at 38 °C and 65% relative humidity immediately after demoulding (no other curing measure). The authors found that the samples cured at higher temperatures achieved higher early age strength (3 days) than the moist cured samples, however, their compressive strength after 180 days was significantly lower than the moist cured samples. Haque (1990) investigated the combined effect of temperature and relative humidity on concrete performance. The author found that the warm-wet conditioning regime (water tank stored at 45 °C) enhanced the 7 days strength compared to fog cured samples, but adversely affected the strength (over 30% drop in strength) at 91 days.

The rationale behind the lower later-age strength of concrete is often explained in the light of the Verbeck and Helmuth, (1968) theory on the influence of temperature on the pore structure characteristics of the cement paste (e.g. see Taylor, 1990). Accordingly, the dense layer of the hydration products that encapsulate the cement grains retards further hydration and therefore influences later hydration and strength development. In addition, the uneven distribution of the hydration products results in a lower gel/space ratio in the interstices among the cement grains, which is thought to control the strength of the cement paste. It follows that cement paste strength is thought to emanate from the interlocking mechanism of the fibrillar and foil-like hydration products produced from the neighbouring cement grains, i.e. the initial packing, density and nature of the interfacial bond of the hydrates controls the strength characteristics of the matrix (Bailey and Stewart, 1984).

The detrimental effect of high temperature on the porosity and therefore, strength, was verified by numerous workers (e.g. Goto and Roy, 1981; Kjellsen et al, 1990a). Kjellsen et al, (1990a) investigated the pore structure of cement pastes hydrated at 5, 20 and 50 °C, using mercury intrusion porosimetry and backscattered electron image analysis. The authors found that for the same W/C ratio and degree of hydration, the higher the curing temperature the greater the total porosity and volume of larger or capillary pores (> 0.1 µm).

#### (b) Thermal and drying shrinkage

Thermal and drying shrinkage cracking are a common feature of concrete damage in the Arabian Gulf (Rasheeduzzafar and Al-Kurdi, 1992). Thermal cracking is caused by temperature gradients between the concrete surface and its inner sections, which results in differential volume changes and subsequently, thermal cracking if the tensile strain due to these changes is greater than the tensile strength of the concrete element. In large concrete elements, temperature gradients are intensified by excessive heat of hydration, resulting in higher internal temperature while the surface layers

tend to cool. Restraint of contraction therefore will result in tensile stresses and consequently cracking when the strain capacity of the element is exceeded. The larger the difference in temperature between the inner concrete mass and the outer layers, the higher the restraint of thermal movement and therefore the higher the possibility of thermal cracking occurring. However, the adverse effects of hot climate are often the dominant cause of thermal as well as drying shrinkage cracking in the Arabian Gulf. The commonly experienced large daily temperature and relative humidity variations may induce sustained expansion and contraction cycles that generate tensile stresses far beyond the tensile strength of concrete, thus resulting in cracking (Rasheeduzzafar and Al-Kurdi, 1992). Thermal movements are further aggravated by the thermal incompatibility of concrete materials i.e. aggregates and cement paste. The most widely used aggregate in the region, limestone aggregate, has a wide range of coefficient of thermal expansion ranging from 1 to  $10 \times 10^{-6}/^{\circ}\text{C}$ , while that of hardened cement paste is much higher ranging from 10 to  $20 \times 10^{-6}/^{\circ}\text{C}$  (Rasheeduzzafar and Al-Kurdi, 1992; Al-Amoudi et al, 1993). This results in differential thermal movement which gives rise to micro cracking especially at the aggregate-paste interface.

### (c) Permeability and durability

As outlined before, most deterioration problems of reinforced concrete emanate from the ingress of substances such as moisture, carbon dioxide, oxygen and chlorides and sulphates salts from concrete's surrounding environment. This is especially the case in the Arabian Gulf, where as described earlier, the environmental conditions, i.e. the conditions of the ground and climate, are particularly conducive to accelerated degradation. Most studies and condition surveys of deteriorated structures in the region show that the prime causes of degradation results from the immediate interaction between concrete and its environment. This is manifested in the following features of deterioration, given in decreasing order of importance: reinforcement corrosion, sulphate attack, salt weathering and cracking due to drying and thermal stresses (e.g. Rasheeduzzafar et al, 1984; Al-Amoudi et al,

1993; Al-Abideen, 1998; Al-Ghatani et al, 1998). It is evident that concrete's permeability plays a dominant role in these deterioration processes, particularly the most serious and widespread amongst those listed namely, reinforcement corrosion and sulphate attack.

Additional to W/C ratio and hydration (discussed in Section 2.1.3), exposure temperatures play an important role on the pore structure characteristics and permeability of concrete. The effect of temperature on the porosity was discussed earlier but will be addressed briefly in the context of permeability. Numerous investigators found that higher concrete curing temperatures induce a coarser pore system and result in increased permeability (Goto and Roy, 1981; Mangat and El-Khatib, 1992; Owens, 1985). Mangat and El-Khatib (1992) investigated the effect of curing temperature in the range 20 to 45 °C and different relative humidities (25, 55 and 100%) on the pore structure characteristics and absorption of cement pastes and concrete. The results showed that samples cured under dry or high temperature regimes exhibited higher pore volume, larger pore sizes (1000-10,000nm) and higher absorption values than companion samples cured under wet or lower temperature conditions. Similarly, Goto and Roy (1981) found the total porosity, volume of large pores and permeability of the cement paste samples cured at 60 °C were higher than the samples cured at 20 °C. Winslow and Liu (1990), however, observed that for the same W/C ratio, the pore volume and pore size distribution of cement paste, mortar and concrete samples were similar regardless of curing temperature (10-30 °C).

#### (d) Corrosion of reinforcement and sulphate attack

These are the two most widespread degradation phenomena in the Arabian Gulf (e.g. Rasheeduzzafar et al, 1985). Corrosion of reinforcement and the associated expansion due to rust formation leads to cracking, spalling and subsequent acceleration of deterioration and the eventual disintegration of the section under attack. Corrosion of steel reinforcement is normally inhibited due to the high alkalinity (pH of approximately 12.6) of the concrete and the

formation of a stable oxide film on the steel bars, thereby protecting it against attack. Corrosion of reinforcement may occur when the protective layer is destroyed or disrupted as a result of carbonation, leaching or chloride ion ingress (e.g. Taylor, 1990). The carbonation mechanism and its effect on the alkalinity of concrete are discussed in Section 4.6.1, and the transport of chloride into concrete was addressed earlier in section 2.1.3. Chloride ions may be introduced into concrete through contaminated materials such as aggregates or admixtures or from the environment. In the Arabian Peninsula, chlorides are the main cause of reinforcement corrosion (e.g. Rasheeduzzafar et al, 1985). Sources of chlorides in the region include contaminated aggregates, sea water and sea spray, contaminated ground water and by wind transport of salt-contaminated sand and dust.

The rate of reinforcement corrosion is increased significantly under high temperature and humidity conditions. Rasheeduzzafar et al (1984) cited data indicating that the rate of corrosion is accelerated sharply within the temperature range of 20-40 °C and relative humidity range of 50-70%. The effect of temperature, cement type, W/C ratio and concrete cover on chloride diffusion and corrosion of reinforcement have been widely reported (e.g. Rasheeduzzafar et al, 1985; Rasheeduzzafar and Ali, 1992a, Page et al, 1980; Bamforth and Pocock, 1990; Dhir et al, 1993). Page et al (1981) found that the diffusion rate of chloride ions increased with increasing temperature and W/C ratio. In the same study, the authors confirmed that the diffusion of chloride ions is strongly influenced by cement composition. Blended cement pastes containing GGBS or PFA sustained lower diffusion rates than OPC pastes of the same W/C ratio. A similar study confirmed that the addition of 5% silica fume and 30% slag replacement (by weight) of OPC concrete significantly improved chloride permeability and was more effective than lowering the W/C ratio (Detwiler et al, 1994). The authors found no evidence to suggest that lower C<sub>3</sub>A content of the cement significantly affected chloride diffusion kinetics. However, Dhir et al in a series of recent investigations (e.g. 1996, 1996a and 1997) on the effect of binder type on chloride ingress found

that the chloride binding capacity of concretes increases with increased levels of ground granulated blast-furnace slag (GGBS) and pulverised-fuel ash (PFA) replacement (up to 50% PFA replacement). Thermal analysis measurements implied that the improvement in chloride binding capacity is a result of the high aluminate contents in GGBS, which led to an increase in the quantities of Friedel's salt produced. The authors confirmed that both the intrinsic permeability and binder type have a significant effect on chloride durability of concrete, the effect of the later being the most significant. Rasheeduzzafar and Ali (1992) investigated the effect of temperature on two sets of reinforced concrete samples maintained at 25 and 60 °C. The authors found that corrosion activity of the reinforcing steel cured at 60 °C was notably higher than that at lower temperature. In a comprehensive study on reinforcement corrosion in the Gulf, Rasheeduzzafar and his co-workers (1985) found that chloride content, cover to reinforcement, concrete composition and electrical resistivity have a significant effect on reinforcement corrosion. Based on the results of their study, Bamforth and Pocock (1990) suggested that an ideal concrete mix for salt exposure would be designed to have low sorptivity, low chloride diffusion and high resistivity.

Sulphate attack is the second cause of deterioration in the Gulf. The source of sulphates in the Gulf is contaminated soil, aggregates, ground water especially near the sea and seawater. The mechanism of sulphate attack is complex involving reactions of different forms of sulphates such as calcium and magnesium sulphates with the cement paste (Taylor, 1990). It generally involves a reaction between the sulphate ions and the alumina-bearing phases of the hydrated cement to form a high sulphate form of calcium aluminate (ettringite), as given in equation (2.3) in Section 2.1.2. The formation of ettringite, in severe cases, involves expansion and subsequent cracking and reduction in strength. The penetration of sulphate ions into concrete involves the same transport processes discussed earlier for chlorides (Section 2.1.3). Factors affecting sulphate resistance includes cement composition, cement content and W/C ratio, concrete permeability and temperature. Most current

specifications stipulate a maximum limit of sulphates in concretes in terms of total water-soluble sulphate content in the concrete mix; the maximum sulphate content ( $\text{SO}_3$ ) limit being 4% by weight of the cement (BS, 1985; CIRIA, 1984).

Rasheeduzzafar and co-workers (1984) conducted a field investigation to assess the main features and extent of the problem in the eastern part of Saudi Arabia. The authors found two distinct features of damage due to sulphate attack. The first type is a complete disintegration of the cement matrix and its transformation into a non-cohesive granular mass with exposed aggregates, which is said to be typical of the reaction of magnesium sulphates with calcium silicate hydrates. The second type is characterised by concrete expansion and cracking, which is typical of the formation of ettringite. The role of permeability in sulphate attack has been investigated in a recent study (Khatri and Sirivivatnanon, 1997). The authors found that the permeability and the chemical resistance of the binder both have a significant influence on sulphate resistance. McCarthy et al (1997) in a study on a wide range of pulverised-fuel ash (PFA) mortars reported that expansion due to exposure to sulphates was reduced with increased PFA content especially when used in conjunction with sulphate resisting cement.

#### *Recommendations for hot climate concreting*

Recommendations and control measures for hot climate concreting are covered in great detail in many International Standards and special Committee Recommendations (e.g. FIP, 1986, CIRIA, 1984, ACI, 1991, BS 8110, 1986). Recommendations are also given in many local publications in the Gulf region (e.g. Al-Amoudi et al, 1993; Ramezaniyanpour, 1993).

A brief review and summary of the most important guidelines and recommendations for hot weather concreting is given below.

#### (a) Concrete mix design

Concrete is commonly designed to meet strength, workability and durability requirements. In hot weather, workability and durability essentially require

extra attention. The variables involved are cement content, cement type, W/C ratio, aggregate proportioning and use of admixtures.

Optimum cement content to meet functional requirements is essential. Rich mixes generate higher heat of hydration with increased risk of drying shrinkage cracking and high thermal stresses in thicker sections. Cement content should be limited to the range 340-420 kg/m<sup>3</sup>, depending on the requirements, with attendant changes in the W/C ration so as not to compromise durability. The type of cement plays a significant role in durability design and the choice of adequate cement to suit the conditions of exposure is essential. Research in the Gulf has shown that OPC performed 1.7 times better than SRPC in terms of initiation of corrosion. Modification of the phase contents (e.g. C<sub>3</sub>S/C<sub>2</sub>S and C<sub>3</sub>A content) of cements may be necessary in certain situation where both chlorides and sulphates are operative. Cements with relatively low heat of hydration are preferable.

Most degradation phenomena in the Gulf are permeability-orientated and adequate selection of W/C ratio therefore is imperative from durability considerations. Numerous research work have found that the permeability of concrete is markedly decreased below 0.40 W/C ratio. The water content should be kept to the minimum possible with the maximum limit for the W/C ratio being around 0.4. Further, mixes should be designed with optimum coarse to fine aggregates ratio, taking into account workability, durability and strength as regards to grading and aggregates quality. Over-sanded mixes result in reduced workability whereas under-sanded mixes have tendency to segregation. Moreover, the use of admixtures is encouraged to overcome hot weather problems, such as reduced slump and rapid loss of workability and reduced density and strength. However, appropriate selection of approved types is essential with checks for compatibility with the cement used. Application of the admixtures and dosage must be followed according to specifications.

Constituent materials (aggregates, water and cement) as well as the materials involved in the production (formwork and steel reinforcement) should be free from impurities and contaminants. Special attention should be given to coarse aggregates, which may contain dust and heavy materials that are contaminated with chlorides and sulphates. Due care must also be given to selection of fine aggregates as these may also be heavily contaminated with chlorides and sulphates. Thorough washing of aggregates is mandatory to ensure contaminants-free concrete.

#### (b) Mixing, transportation, placement and compaction

Adequate planning prior to starting these activities is considered to be an integral part of the whole process. Mixing should be continued till all the materials are homogeneously distributed and the required workability is achieved. Over-mixing should be avoided to guard against segregation and loss of workability. The haul distance and waiting time to unload should be as short as possible. Placement should be carried out during the coldest part of the day and, together with compaction, should be performed as rapidly as possible. Highly permeable concrete is often in the Gulf is often associated with poor placement and, more importantly, poor compaction practice. Full compaction is typically marked with non-appearance of entrapped air and the appearance of a thin film of cement paste on the surface of concrete.

#### (c) Curing

This is the most crucial stage of the concreting activities in hot climate. Prior planning is of considerable importance to ensure that curing is performed properly throughout the prescribed period. Water curing methods are preferred and considered to be most effective. Where water retention method of curing are to be used, use of white pigmented curing materials and membranes is preferable. The employment of combination of curing methods may prove most effective. Screening and shading, where possible, are preferred at the early stages of curing.

## **2.3 MICROCLIMATE**

### **2.3.1 Denotation and Significance of Microclimate**

There are very few precise definitions of the microclimate in the literature. Fookes (1995) defined macro, meso and micro climates as the climates on the scale of the country, the site and the particular element of the structure respectively. Accordingly, the microclimate around a structure results from the interaction of the meso climate with the characteristic geometry and location of the structure. Nillson (1996) defined the microclimate as being the climatic conditions very close to, or at the concrete surface. In a similar manner, Al-Abideen (1998) refers to the microenvironment to indicate the climate and environment conditions that surrounds the structure directly. Wood (1995), on the other hand, referred to the microclimate as being the internal microclimate within the concrete, i.e. the cyclic patterns of temperature and humidity inside the concrete element that results from the interaction with the meteorological conditions surrounding the element.

A distinction between the meso and micro climates is that the former is not affected by the precise location, orientation and detailing of the structure concerned. Thus, the microclimate constitutes the external boundary conditions for the processes occurring inside the concrete, and therefore has the most influential effect on the internal properties and functionality than any other external parameter. Consequently, adequate understanding of the effects of microclimate at the start of the design process (i.e. prior to structural design considerations, materials, mixes and construction specification) is essential if durability design is to be achieved.

The role and significance of the microclimate is increasingly been acknowledged. The quantification of the effect of micro, meso and macro climates is considered to be a necessary part of the concept of service life design, and is one of the R & D items in the current work of the Architectural Institute of Japan (AIJ) towards producing a service life design guide on the

basis of the previous guide, *Principal Guide for Service Life Planning of Buildings* (Nireki, 1996).

### **2.3.2 Microclimate Influence on Concrete Properties**

There are very few detailed studies in the literature on the effect of microclimate on concrete's engineering properties. Some studies made on the influence of exposure conditions on concrete quality have occasionally referred to changes in properties of elements due to microclimate effects (e.g. Parrott, 1992; Petersson, 1996). The reported influence of the microclimate on concrete properties such as porosity, permeability, curing, carbonation and strength is presented below.

Parrott (1992a) investigated the effect of 4 exposure conditions on the porosity, absorption and carbonation of concrete and cement pastes samples made with different cement types. The specimens were stored for 4 years under: (1) controlled temperature and relative humidity laboratory conditions (20 °C and 58 ± 3% RH), (2) uncontrolled relative humidity office exposure (temperature 15-25 °C), (3) outside sheltered from rain, (4) outside exposed to rain (6-21°C, 58-90 RH and 40-70mm/month rainfall). The exposure conditions caused variation in the long-term trends of relative humidity within a 15mm surface layer of the concrete samples. The laboratory stored samples maintained an internal RH of 58%; the office stored samples maintained an RH of 45%; the RH of the outside sheltered samples fluctuated between 70-85%; the RH of the outside vertical exposed surfaces fluctuated between 80-95%; and the RH of outside horizontal exposed surfaces fluctuated between 85-100%. The author found that the capillary porosity and rate of water absorption within the cover zone was greater for the outside sheltered and laboratory stored samples than the outside exposed samples. The office exposure samples exhibited the highest absorption rate, followed by the laboratory and outside sheltered samples respectively. Furthermore, the horizontal exposed surfaces (outside exposure) displayed a notably lower absorption than the similarly exposed samples stored in a vertical orientation.

The variation in absorption was attributed to differences in capillary porosity arising from drying as well as limitation in cement hydration as a result of the drier exposure conditions (lower relative humidity). The beneficial effect of rain on the exposed surfaces was reflected in higher internal relative humidity, better hydration, lower capillary porosity and absorption especially for the horizontally orientated samples. Similarly, the carbonation of the laboratory and offices exposed samples was significantly higher than the outside sheltered and exposed concretes due to the influence of internal moisture on the CO<sub>2</sub> diffusion (slower diffusion with higher internal RH).

Osborne (1989) studied the effect of environmental conditions and microclimate on the carbonation, permeability (gas and water) and compressive strength of different existing reinforced concrete structures. The proposed coring and testing techniques of the existing structures were evaluated on a series of 300mm concrete blocks of similar mix design, which were site-stored for 2-3 years. The in-situ concrete structures were made with 50-70% blast-furnace slag cement and had a total binder content of 360-380 kg/m<sup>3</sup>. The author found that the depth of carbonation was greater with: drier internal exposure conditions, sheltered outside exposure locations and higher (70% slag) cement replacement. Further, the carbonation (for concretes with similar cement contents) was lower for: damp environments inside buildings, unsheltered external structures subject to driving rain and lower (50% slag) cement replacement or with plain OPC. The gas and water permeability measurements revealed that specimens from the inner sections of the structures were more permeable than the outer sections. In another detailed study on the effect of microclimate, Osborne (1994) concluded that the microclimate had a significant influence on the rate of carbonation, but had far less effect on the permeability or compressive strength. The carbonation was greater for high slag cement concrete in the warmer, drier conditions than in moist environments.

In a similar study on the effect of exposure conditions, Ewerston and Petersson (1993) subjected concrete samples to 3 different climates: outdoors exposed to rain, outdoors protected from rain and indoors. Water permeability (including depth of water penetration) and carbonation tests were performed after one year of field exposure. The water penetration depth and rate of carbonation were highest for the concrete samples stored under laboratory conditions (20 °C and 65% RH), and lowest for the outdoor samples exposed to rain. Similarly, Petersson (1996) investigated the effect of curing and exposure conditions on the strength and durability of concrete. The author found that the compressive strength gain of concrete between 28 days and 3 years was 30-35% for the specimens stored outdoors exposed to rain, 25-35% for the specimens stored outdoors protected from rain and only 5-10% for the specimens stored indoors under relatively dry laboratory conditions. The carbonation rate was similarly found to increase as the exposure conditions become drier, with the outdoors exposed to rain and indoor samples (laboratory storage at 20 °C and 65% RH) giving the lowest and highest carbonation rates respectively.

Ho et al (1989) reported the findings of a study on the influence of directional rain on curing of exposed concrete. The authors found that after one year of exposure, the rainfall received by the vertical surfaces facing north was much less than that received by south-facing inclined surfaces. The differences in rainfall were due to the variation in the two microclimates as a result of the different orientation of the concrete elements. The author concluded that the position and orientation of the specimens influenced the improvement in the quality of exposed surfaces.

Whereas most of the above studies highlight the microclimate influence largely in terms of dry/wet exposure conditions, the microclimates that may ensue around real life structures can be remarkably diverse. Al-Abideen (1996) cited an example of a pier in a causeway that was subjected to 5 microclimates, each with a distinct level of exposure. These levels of exposure,

from the foundation of the pier to the bridge deck were: underwater, tidal zone, splash zone, spray zone and atmospheric zone of exposure. Hence, the processes occurring internally within these different parts of the pier are clearly governed by the conditions obtaining at their surface. Nilsson (1996) similarly showed significant variation in the chlorides concentration around a bridge deck high above sea level. The chloride concentrations on the surface around the bridge deck varied from 0.3 to 4.0% depending on the microclimate involved.

## **2.4 CURING**

### **2.4.1 Denotation and Significance of Curing**

Curing has received many definitions over the years. Amongst the better definitions is its description as “the process of maintaining a satisfactory moisture content and favourable temperature in concrete during the period immediately following placement so that hydration may continue until the desired properties are developed to a sufficient degree to meet the requirements of service” (HRB, 1952).

The above definition stems from the basic fact that the development of concrete’s microstructure with time following placement is essentially dependent on the continuation of the hydration process. The role of cement hydration in the development of the concrete’s pore structure and capillary porosity, and the effect of the latter on the development of strength, permeability and durability has been discussed earlier. The continuation of hydration is governed by the availability of moisture, which, in turn, is determined by the initial W/C ratio of the concrete mix and the extent of moisture loss during the early stages of placement and curing. Since the W/C ratio is normally more than sufficient for the available cement to attain complete hydration (e.g. Cather, 1994; Jolicoeur and Simard, 1998), then the criterion of importance is prevention of moisture loss from the young concrete. The loss of moisture in concrete occurs through self-desiccation (lower W/C ratio), bleeding (higher W/C ratios and inconsistent mixes),

evaporation (early stages) and natural drying (later stages), which are essentially influenced by the natural exposure conditions of concrete. The efficiency of curing, therefore, fundamentally lies in its ability to sustain an appropriate level of moisture in the concrete by protection against the natural drying processes and prevention of moisture loss for a prescribed duration.

Numerous efforts have been made to quantify the critical level of internal moisture that influence the hydration process. These efforts were inspired by the early work of Powers (1947) who found that the internal vapour pressure (moisture content) within the concrete mass must be maintained at a value over 80% if hydration is to proceed at an appreciable rate. Using modern techniques and on modern cement, Patel and Parrott and their co-workers through a series of publications (1985, 1986, 1988 and 1989) demonstrated experimentally by three independent measures of hydration (TGA, XRD and methanol adsorption) that the rate of cement hydration was reduced sharply with a drop in the relative humidity of the curing environment from 100 to 70%. The authors further noted that the hydration reaction virtually ceases below 70% RH. The results suggested that the rate of cement hydration is related to the amounts of water in the larger capillary pores rather than the porous hydrate coatings on the cement grains. The studies concluded that premature drying of concrete results in higher capillary porosity at the surface and less protection to the underlying concrete and steel reinforcement. In a similar study, Ho et al (1989) investigated the effectiveness of curing under various relative humidities and constant temperature of 23 °C. The authors found that concrete quality (assessed by sorptivity) remained almost unchanged at storage conditions of 50, 65 and 75%, and improved marginally at 84% RH. In their conclusion, the authors reaffirmed the general view that hydration of cement is negligible at humidity levels below 80%. The consensus conclusion from all these investigations is that even a small drop (5-10%) in the relative humidity below 100% significantly limited cement hydration.

The magnitude of quality improvement due to curing depends mainly on the curing method, curing time and the climatic conditions involved. Moisture loss through evaporation and drying is one of main problems of concreting in hot climate countries. Achieving adequate curing in the severe drying environments of the Gulf countries is a major challenge. The environmental factors that influence curing are temperature, relative humidity, solar radiation and wind speed. These parameters together with the accelerating effect of high ambient and concrete temperatures on the hydration have been discussed in Section 2.2.3. Although concrete temperature is normally controlled through addition of ice in the mix water, the ultra high ambient temperature increases the surface temperature of concrete and promotes evaporation and drying even at high relative humidity. The effectiveness of curing in the Arabian Gulf countries is therefore governed directly by the ability of the selected curing methods to overcome the combined operative drying parameters of the environment mentioned above and offer the required level of protection throughout the required time.

#### **2.4.2 Curing Methods**

On site curing methods are commonly classified into two main categories: (1) water addition, and (2) water retention techniques. Both techniques have evolved from principle of moisture preservation and temperature control of the concrete. The choice of an appropriate curing method depends on the concrete type, the orientation and location of the structural members, and the climatic conditions during the curing period (Senbetta, 1994). Appropriate choice should consider the economics of the selected curing method since this is likely to be influenced by the availability of water, labour and curing materials on site (ACI, 1991).

Detailed descriptions of the water addition and retention curing methods are available in many references such as the ACI Committee 308 Report, ACI 308-81 (1991) and the FIP Guide to good practice (1986). A brief listing and discussion of various methods under these categories is given below.

### *Water addition techniques*

Typical site curing methods adopted under this technique include: (a) covering with wet burlap or hessian, (b) ponding or complete immersion in water, (c) water spraying or sprinkling, (d) covering wet sand, earth, hay, straw or sawdust evenly spread on the surface.

The water curing methods are known to provide excellent curing. These methods provide cooling to the concrete surface and additional water that can benefit hydration. However, these curing methods should be applied continuously to avoid drying out of the concrete surface. The water used should be clear from any deleterious materials and should comply with the permissible levels of chlorides, sulphates and organic matter. Further, the temperature of the curing water should not be much colder than the concrete temperature so as not to cause thermal shock or large thermal gradients between the concrete surface and the inner sections. Curing with wet sand or earth and ponding are particularly effective on large flat surfaces (FIP, 1986).

### *Water retention techniques*

Curing methods under this technique include: (a) covering the concrete surface with plastic sheeting or reinforced waterproof paper, (b) application of liquid membrane-forming compounds.

Covering with sheeting such as polythene or waterproof paper provides an effective barrier against evaporation and surface drying. These should be securely fitted with adequate overlap to prevent evaporation. Membrane-forming liquid compounds can be either water or solvent-based and are designed to form a continuous film that is intended to seal the concrete surface and prevent evaporation. These compounds can be applied, after the bleed water has stopped, by spraying, rolling or brushing on the concrete surface. The water-retaining methods are generally considered to be not as effective as the continuous water curing methods, however, they are advantageous in situations where water is scarce or uneconomical to use for curing purposes. The advantages of the curing membrane-forming

compounds include ease and speed of application, economy, maintenance-free, and practical in situations where conventional curing is difficult or not possible to perform.

### 2.4.3 Curing Efficiency

Concrete curing is directly related to the degree of hydration, and a measure of the latter immediately following curing provides a quantitative measure of the efficiency of the curing method employed.

The efficiency of a curing method ( $E_t$ ) is therefore given by (Kern et al, 1995):

$$E_{(t)} = \frac{\alpha_m(t)}{\alpha_u(t=7d)} \quad (2.6)$$

where  $\alpha_m$  is the degree of hydration after curing time ( $t$ ) by a curing method  $m$ , and  $\alpha_u$  the degree of hydration after 7 days moist curing at 20 °C.

Cabrera et al (1989) measured the curing efficiency ( $E$ ) of a particular curing method in terms of the coefficient of intrinsic oxygen permeability  $k$  ( $m^2$ ):

$$E = \frac{k_1 - k_2}{k_1 - k_3} \quad (2.7)$$

where  $k_1$ ,  $k_2$  and  $k_3$  are the intrinsic permeability ( $m^2$ ) of a non cured specimen, a specimen cured by the method being evaluated and the water-cured specimen respectively.

There is limited information in the literature on the true curing efficiency of the different site-curing methods under the various conditions of exposure, i.e. as determined directly by the degree of hydration of concrete at the end of the curing period. Tests that are related to concrete performance, such as permeability and sorptivity, are increasingly being employed to assess concrete curing especially in the surface zone (e.g. Dhir et al, 1987; Dinku and Reinhardt, 1997). Most studies (compressive strength, water and gas permeability, absorption and carbonation) generally indicate that the water-adding methods, e.g. continuous moist curing, fog curing, wet hessian or burlap are more effective than the water-retaining methods, e.g. covering

with polythene and curing membranes, (see Senbetta, 1984; Haque, 1990; Mangat and El-Khatib, 1992; Petersson, 1996; Khatri et al, 1997).

Finally, concrete curing efficiency as whole is not a simple function of the curing materials employed, but depends on a combination of factors. These are: (1) the characteristics of the concrete mix, (2) the suitability and efficiency of the curing material adopted, (3) the timing of initial application of curing after the finishing stage, (4) the length of curing time, (5) and the efficiency of the workforce to maintain curing from the starting time to the time curing is discontinued.

#### **2.4.4 Curing Specification and Current Practice**

##### *Curing specification*

The selection of an appropriate curing time depends largely on the conditions and requirements pertaining to the particular structure concerned. Curing requirements vary substantially depending on a variety of factors, such as, the severity of exposure conditions, construction type and intended use, strength and durability prerequisites. However, guides for minimum curing times for various exposure conditions are given in most standard specifications and codes of practice. British Standard recommendations BS 8110 (1985) lists minimum curing times depending on the type of cement, ambient conditions and the temperature of the concrete. The given curing times vary from no special requirements to 10 days depending on the conditions involved. The European Standard ENV 206 (1992) minimum curing times vary from 1 to 10 days depending on the rate of strength gain of concrete, ambient conditions during curing, the temperature of concrete and the exposure condition to which the concrete will be subjected. The ACI Committee 308 (1991) recommends various curing times for different construction, e.g. pavements and ground slabs, structures and building, mass concrete and other construction types. The main criteria for curing duration specifications are ambient temperature and strength gain. Typical curing duration specified range from a minimum of 7 days or the time taken to attain 70% strength

when the ambient temperature is above 5 °C, to 28 days for high strength structural members (columns) when placed at temperatures lower than 5 °C. For hot weather construction, a minimum period of seven days continuous curing is generally specified (e.g. ACI, 1991; FIP, 1986). The importance of the early period of curing (first 3 days) and the necessity for continuous, uninterrupted curing throughout the prescribed time are stressed.

There are generally no standard specifications for the water-adding curing materials or methods. There are, however, standard specifications for the water-retaining curing materials such as sheet materials and membrane-forming compounds. ASTM C171 (1991) specifications for sheet materials include minimum tensile strength, minimum elongation, minimum water retention and reflectance for white materials. The ASTM C156-93 (1993) recommends a test method 'Test Method for Water Retention by Concrete Curing Materials' for the laboratory determination of the efficiency of liquid membrane-forming compounds and sheet materials. The moisture retention requirement is limited (in ASTM C171 and C306) to evaporation loss of no more than 0.55 kg/m<sup>2</sup> when tested according to ASTM C156 test method. However, the ASTM C156 moisture retention test method has been criticised for lack of precision and reproducibility (Cabrera, 1989; Senbetta, 1994).

#### *Current practice*

It has often been reiterated that the limitation in the current curing specifications, in most standards and codes of practice, is that they specify curing methods, curing materials and length of curing without reference to the quality or performance of the cured concrete. Curing is a surface phenomenon, as it is exclusively applied to the concrete surface, and affects and modifies the properties of surface region alone, i.e. the first 50mm or so from the exposed surface. It is generally accepted that the durability of concrete is largely dependent on the integrity of its surface region. It is this region of concrete, therefore, that can provide verification of curing efficiency or otherwise. This important aspect is not addressed in most current curing

efficiency tests, which are solely concerned with the assessment of curing materials, and through tests on cement mortar samples stored under controlled laboratory-simulated environmental conditions (for example the previously discussed ASTM C 156-93 and BS 7542: 92). An exception to this is the ASTM C1151 (1991) test for the evaluation of the efficiency of sheet materials and membrane-forming curing compounds based on the sorptivity of mortar test samples, which is intended to ultimately replace the C156 test. Carrier (1983) pointed out at the time that there was no test available for the measurement of shrinkage cracking or microcracking associated with inadequate curing. This is still believed to be the situation to-date (e.g. see Geiker and Edvardsen, 1997). Research work to develop curing efficiency tests based on the measurement of performance properties, such as the intrinsic gas permeability test (equation 2.7), is a step in the right direction. Another important effort in this respect is that made by Dhir and co-workers (e.g. 1987, 1995) for the development of a sensitive in-situ test that can verify the quality of the near surface region of concrete. Research effort in this direction will no doubt ultimately lead to the development of an accepted, performance-based curing efficiency test that can be applied in-situ.

In terms of new developments in curing practice, no significant progress has been noted with regard to curing methods and materials. With regards to curing materials, a notable development is the introduction of controlled permeability formwork systems to aid curing and improve the near surface porosity and permeability of concrete. In terms of curing methods, a number of alternative curing approaches have been explored. Xueqan et al (1987) found that microwave curing could be applied, without adversely affecting later-age strength, with significant advantages such as shorter curing duration, reduced porosity and permeability compared to conventionally cured samples. Dhir et al (1994a) explored the concept of self-cure concrete by addition of water-soluble chemicals during mixing. The authors found that one of the chemicals investigated was successful in achieving self-cure concrete through improved water retention and hence enhanced hydration,

increased strength and improved surface quality (significantly low ISAT results). Further work on this chemical admixture revealed that the magnitude of quality improvement depends on the applied dosage and confirmed its beneficial effects on the microstructural development (enhanced morphology of the hydrates) and durability properties (surface quality, chloride diffusion, carbonation, corrosion potential and freeze/thaw resistance) of concrete (Dhir et al, 1995a, 1996b and 1998).

#### **2.4.5 Influence of Curing on Engineering Properties**

The effects of curing on various important engineering properties have been widely reported. The effect of curing in promoting the hydration of cement and pore structure development and the effect of the porosity on the strength and durability (permeability) of concrete have been discussed earlier in this chapter (Sections 2.1 and 2.4.1). Experimental results have shown that adequate curing increases strength development, abrasion resistance, corrosion resistance, pozzolanic activity and weatherability, and decrease permeability, shrinkage cracking and carbonation. A brief review of the effect of curing on important concrete properties is given below.

##### *Strength development*

Ramezaniapour and Malhotra (1995) investigated the effect of curing on compressive strength of concrete. The authors found that lack of curing resulted in a reduced rate of strength development from 1 to 180 days compared to moist cured samples. After 180 days, there was a 28% reduction in strength relative to cured, companion samples. Petersson (1996) observed that taking no curing measure resulted in a drop in strength of 50-60% at 28 days, compared to similar samples that had been wet cured

##### *Abrasion resistance*

Dhir et al (1991) conducted a detailed investigation on the effects of W/C ratio, curing regime, workability and mix constituents on the surface abrasion resistance of concrete using an accelerated test machine. The specimens were subjected to a range of simulated in-situ curing methods. The authors found

that by promoting hydration through proper curing, the abrasion resistance of the samples was significantly improved over that of the air-cured samples. The abrasion depth of the 4 days wet hessian cured samples (then air at 20 °C and 55% RH) was more than 100% lower than the samples that were air cured at 20 °C and 55% RH.

### *Permeability*

As discussed earlier in this chapter, concrete permeability is directly dependent on the volume and continuity of the capillary porosity of the cement paste, which is governed mainly by the extent the hydration process of cement is allowed to progress and the W/C ratio of the mix. Adequate curing of concrete promotes hydration and leads to decreased permeability.

Ballim (1993) investigated the effect of different durations of moist curing on the air permeability and sorptivity of concrete. The results showed that lack of adequate curing caused an increase in the air permeability of the concrete surface of up to 50 times, relative to the moist cured samples. Similarly, although less marked than the air permeability results, the water sorptivity results of the air cured (23 °C and 65% RH for 27 days) samples were significantly higher than similar samples that were moist-cured for the same duration. The author concluded that greater influence on the durability could be effected by extending the duration of early-age moist curing rather than decreasing the W/C ratio. Similarly, Dinku and Reinhardt (1997) found that extending moist curing time from 1 to 7 days resulted in a notable reduction in the air permeability (up to 50%) and sorptivity of concrete, although the results of the latter test appeared to be less sensitive to curing than the former.

### *Carbonation*

Loo et al (1994) investigated the effect of water curing duration (3, 7, 14 and 28 days) on the carbonation of concrete using an accelerated carbonation test. The authors concluded that longer water curing times help to reduce the carbonation, but beyond 14 days of curing the reduction more gradual. Similar conclusions were reached by Dhir et al (1989a) who noted that

extending the water curing period beyond 14 days has much less effect on the carbonation rate than the early-age curing.

## **2.5 CONCRETE COVER**

### **2.5.1 Denotation and Significance of Concrete Cover**

Concrete cover denotes the layer of concrete which extends from the exposed outermost surface layer to the depth at which the steel reinforcement is located inside the concrete. The depth of concrete cover is typically specified by the structural design engineer to mainly provide adequate protection to the steel reinforcement and, in certain situations, protection against fire and abrasion. The factors that are taken into account when specifying concrete cover typically include severity of the exposure environment, concrete type and maximum diameter and type of steel reinforcement. In practice, the cover region of concrete is usually limited to a thickness of 80-100mm to avoid the possibility of cracking.

By definition, therefore, the function of concrete cover is to provide protection to concrete's interior against external influences. These external influences include the ingress of chlorides, carbon dioxide, oxygen and moisture through the cover into the inner sections of concrete, which results in the loss of protection to steel reinforcement and the onset of corrosion. Also, the ingress of sulphate salts and subsequent reactions with the cement hydrates, resulting in damage due to cracking and expansion. Finally, the ingress of moisture may lead to freeze-thaw and frost damage, and enhances alkali-silica reaction. The aforementioned forms of degradation constitute the main problems of reinforced concrete today with the resultant premature damage ensuing in huge repair and maintenance costs worldwide. The significant protective role of the cover region of concrete has, of late, led to the accepted conclusion that the performance of concrete's cover is the principal factor governing concrete deterioration (e.g. RILEM, 1995).

Despite this importance, however, failure to achieve the specified cover is said to be the single most significant factor in the premature deterioration of reinforced and pre-stressed concrete structures (Sharp, 1997; Clark et al, 1997). Coupled with this is the fact that the cover region is innately of a different quality to the inner sections of concrete. This difference in quality originates from an aggregation of factors, which can be classified as intrinsic and extrinsic factors. The intrinsic factors include:

(a) The typical migration of a proportion of the mix water towards the formwork surface during vibration and compaction accompanied by sedimentation and settlement of coarse aggregates due to gravity effects, which increases the W/C at the concrete-formwork interface with a subsequent increase in the porosity in that surface region.

(b) The poor packing capability of cement particles against flat edges, as compared to free space, results in lower cement content and higher porosity at the formwork-concrete interface.

The extrinsic factors include:

(a) The temperature, solar radiation, relative humidity and wind conditions of concrete's microclimate enhances loss of water from the cover region through evaporation at early ages and creates moisture gradients within the concrete, which leads to restricted hydration and increased capillary porosity with increased proximity to the exposed surface.

(b) The later age drying have an additional coarsening effect on the pores in the cover region as a result of the driving off of moisture.

The influence of the extrinsic factors diminishes with increasing depth from the exposed surface up to a distant point inside the concrete where these influences have virtually no effect. The zone extending from the exposed concrete surface to this internal point is known as the curing affected zone (CAZ). The depth of the curing affected zone depends on a combination of factors including the severity of the exposure environment, curing and

concrete composition and quality. The magnitude of the CAZ has been considered to be in the band of 20-50mm, based on the estimates of numerous workers (Cather, 1994).

The negative effects of the intrinsic factors on the quality of the concrete cover are worsened by inadequate mix design and poor concreting practice. The extrinsic factors are exacerbated by the misapprehension of, or the failure to account for, the role of exposure conditions in the surrounding environment of concrete (microclimate). This results in the production of concrete with insufficient cover depth or inadequate quality to suit its service conditions. This is verified by recent reports that inferior cover quality along with failure to achieve the specified cover depth at site are the principal causes of concrete's poor performance (Sharp, 1997; Clark et al, 1997, Harrison, 1996).

Selection of appropriate cover depth and improvement of the quality of concrete cover are of considerable importance to concrete durability. However, it is now accepted that durability is not assured through the specification of cover (and curing or mix constituents), rather, through specifying its required performance. The lack of durability of past and current structures, the increased awareness of the different degradation mechanisms and the transport processes involved and the appreciated protective role of concrete cover have all contributed to the introduction of the concept of performance-based durability design. It has been suggested that such a durability design may be based on the established relationship between durability characteristics and the resistance of the cover region of concrete to the penetration of hostile liquids and gases by capillary absorption, diffusion and permeation process (e.g. Dhir et al, 1994; RILEM, 1995). The aim being that the measured parameters of these transport processes, i.e. coefficient of air/water permeability, sorptivity and diffusion coefficients are used as criteria for durability specification.

However, as pointed out by Dhir et al (1994), specifying durability by performance requires, besides durability measurement through permeation

transport parameters, a simple and reliable test, and a test method that is suitable for site use. Amongst the favoured transport parameters are coefficient of gas permeability and capillary suction rate (RILEM, 1995). Gas permeability has a close correlation with the diffusion coefficient for gases, the diffusion of aggressive ions in the liquid phase as well as with the permeability for water or diluted solutions (RILEM, 1995). Capillary suction is regarded as a decisive mechanism for the uptake of water and salt solutions, therefore directly affecting the resistance of concrete against frost attack, corrosion of reinforcement and sulphate attack (RILEM, 1995). The recommended tests are the Cembureau test for the measurement of coefficient of gas permeability and the sorptivity for the measurement of capillary suction rate of the cover concrete (RILEM, 1995). A draw back of the tests is that they are laboratory-based, although drilled cored from site concrete can be tested. A number of site tests for absorption measurements of the surface/near-surface zone have been critically reviewed and practical limitations and disadvantages discussed (e.g. Dhir et al, 1987; Basheer, 1993). The notable ones amongst these surface tests are the initial surface absorption test (ISAT), Figg hypodermic methods, the Covercrete absorption test and the Autoclam test. A version of the British Standard ISAT, modified at Dundee University, has been found to have good correlation with certain durability characteristics (Dhir et al, 1994). The authors suggested that the test have good potential for quality verification and durability performance assessment.

## **2.5.2 Influence of Cover Properties on Concrete Performance**

### *Porosity of concrete cover*

Tsukinaga et al (1995) conducted a detailed investigation into the effects of permeable formwork on the porosity and properties of the cover concrete. The authors found that decreased total pore volume (in all pore size ranges especially volume of larger pores) of the cover region (20-30mm) resulted in marked improvement in strength and durability. In terms of strength characteristics, lower pore volume resulted in improved pull-off tensile

strength, rebound number, pulse velocity and pin penetration resistance. For durability, lower pore volume lead to improved freeze/thaw resistance and lower carbonation, chloride ion penetration and water permeability. Similar findings were reported by Long et al (1995).

#### *Depth of concrete cover*

The required depth of concrete cover depends primarily on the porosity and permeability of concrete (W/C ratio and degree of hydration). For example, minimum cover depths of 50, 75 and 100-mm were found to be necessary to protect reinforcing steel for concretes with W/C ratios of 0.4, 0.5, and 0.6 respectively (Cady, 1978). Accordingly, for the same quality concrete, corrosive action are expected to be abated by larger covers.

Rasheeduzzafar et al (1985) found that increased depth of cover lead to sharp reduction in corrosion, especially in the depth range of 12-25 mm. Corrosion due to chlorides ingress was found to be substantially mitigated by covers larger than 38mm. This was attributed to the fact that larger covers provided an effective physical barrier against the diffusion of reactants, especially oxygen. Parrott (1996) investigated the effect of depth of cover on the corrosion of reinforcement. 100mm diameter concrete cube samples were fitted with four 6.4mm diameter mild steel reinforcing rods at 4, 8, 12 and 20 mm from the exposed vertical surface. The steel rods were marked, cleaned and weighed before being fitted in the moulds so that the corrosion loss after 6 months of dry exposure and 4 weeks of chloride exposure could be determined. After the 6 months of drying exposure at 20 °C and 60% RH, the exposed surfaces of the samples were immersed to a depth of 1mm in a 10% sodium chloride solution for 6 hours. The exposed surfaces were then supported above a water surface for 28 days to maintain a relative humidity close to 100%. The loss of corrosion was determined by weighing the reinforcing steel bar after cleaning.

The results indicated that the corrosion levels of the reinforcing bars decreased with increasing cover depth; the highest corrosion levels being for

the steel reinforcement with the least cover depth (4mm), while the steel bars with 20mm cover exhibited the lowest corrosion levels. The author found that a corrosion rate of 30 kg/m<sup>2</sup> in 28 days, if sustained, might be expected to cause visible cracking of cover concrete in 2 years. The highest corrosion rates were observed for concretes containing 75% ground granulated blast-furnace slag.

## 2.6 CONCLUDING REMARKS

### 2.6.1 Macroclimate

The significance and influence of the macroclimate have been reviewed and the important effects on concrete properties presented, with particular emphasis given to hot climate. Most of the local research work is carried out in the eastern parts of Saudi Arabia, with very little contribution from the rest of the other Gulf Countries. Numerous research works have been published since the mid-1980s, which appears to be mostly channelled towards understanding the effects of hot climate and the environment on concrete properties. The situation today, as assessed by current publications, still remains largely the same. A lot of the work appears to be of limited objectives, as no positive reflection, of any notable magnitude, on the concreting practice have yet been realised. An important example of this is the fact that international design guides which have been developed for different climatic and environmental exposure conditions are still being used (with some modifications) for concrete design in most Gulf countries. This is partly attributable to the absence of planned and co-ordinated research programmes, as well as the failure to make full use of the past and current research findings.

The effects of the macroclimate and the macro-environment of the Gulf are well documented and understood. The current state of knowledge warrants the departure from diagnostic research into finding the cure. Current knowledge as well as future research efforts, therefore, should be directed towards the formulation of a credible, local, tailor-made durability design

guide with detailed specifications to suit the local conditions. The research efforts should be in-line with the current European work that aims to develop performance-based durability design and specifications.

### **2.6.2 Microclimate**

The significance of microclimate and its influence on concrete properties have been reviewed and presented. Research work into the effects of microclimate is scarce and microclimate influences generally do not constitute part of current design considerations. It has been shown that considerable quality gradients could ensue within the same structure due microclimate variations around it. However, interest in the microclimate influence and its role in concrete durability is increasing. It has been pointed out that quantification of the microclimate has been considered in the preparation of some service life design guides.

### **2.6.3 Curing**

The significance of curing, and the influence of current curing methods and curing efficiency on relevant concrete properties have been reviewed and presented. The importance of curing is well understood, but there are some obstacles that hinder good curing application in practice. The chief amongst these is the absence of performance specifications and the lack of a reliable and practical curing efficiency test that can be used to assess concrete quality in-situ and verify compliance with predetermined performance specifications. Therefore, the level of curing required to achieve certain durability-related quality targets of in-situ concrete is not currently known nor can it be accurately specified or routinely verified at site. Curing should essentially be included as a pay item in contract specifications, although ideally curing should be made part of the design and acceptance process, however, it has been said that what cannot be proved cannot be specified.

#### **2.6.4 Concrete Cover**

The significance of the cover concrete and the influence of its properties on the performance of the bulk concrete have been reviewed and discussed. The properties and quality of the cover concrete assumes significant importance for concrete's performance and service life. Concrete's cover is the main protective barrier against the penetration of corrosive agents from the surrounding environment into inner sections of concrete. Therefore, concrete durability is largely dependent on the permeation characteristics of the cover region of concrete.

## Chapter 3 Materials, Mix Details and Site Exposure

---

### 3.1 INTRODUCTION

Three weather series were cast to investigate the effect of curing, macro and microclimate on the durability of OPC and OPC/GGBS concretes. These are termed the Loughborough winter series, the Loughborough summer series and the Muscat summer series. Three concrete mixes were investigated in the two Loughborough weather series (30 and 50 MPa OPC concrete mixes and a 30 MPa OPC/GGBS concrete mix) and two in the Muscat weather series (30 MPa OPC mix and 30 MPa OPC/GGBS concrete mix).

A group of specimens were cast with each mix consisting of a number of large concrete blocks of the size 600 × 500 × 150 mm, 500 × 100 × 100 mm beams, and three 100 mm control cubes. The samples were cured in-situ where on each occasion, the concretes were exposed to a range of curing methods (two per block) and microclimates (created by changing block orientations at site). The Muscat series was cast and cured in Loughborough, using the same materials and under the same conditions as the two Loughborough series, and was air freighted immediately after curing to Muscat for exposure.

This chapter discusses the philosophy behind the choice of specimen size, testing age, macro and microclimate exposure, curing methods and materials. A detailed description is then given of the concrete materials, mixture design, the site exposure conditions and curing methods that have been adopted in the above work.

## **3.2 PHILOSOPHY BEHIND CHOICE OF SPECIMEN SIZE, EXPOSURE CONDITIONS, CURING AND MATERIALS**

### **3.2.1 Specimen Size**

Recent research findings indicated that measurements of concrete properties on small size specimens do not provide reliable indication of the properties and durability of in-situ concrete (Marsh and Ali, 1994; Hollinshead et al, 1997). Small specimens with large surface area to volume ratio interact and respond differently to external influences. Further, the effect of weather conditions etc. is often observed to be exaggerated in these specimens and the curing affected zone is considerably different than is in real life structures. Large size specimens are, therefore, necessary if reliable prediction of the performance of concrete under service conditions is to be obtained. Therefore, large concrete blocks of various sizes were evaluated, and blocks of the size 600 x 500 x 150mm were considered suitable for purpose of this investigation. Larger size samples proved difficult to manage in terms of handling and transporting from laboratory to the exposure site and vice versa.

### **3.2.2 Exposure Duration, Testing Age, Macro and Microclimate**

#### *Exposure duration and testing age*

Studies made on new concrete, or that which has been exposed to natural or simulated exposure conditions for a short duration cannot reflect or detect changes in the properties of real structures that had been in service for years. Therefore, these cannot be relied on for the prediction of the long-term durability of concrete (e.g. Olsen and Summers, 1997). For this reason, it was decided to expose the specimens to natural conditions for as long as possible, bearing in mind the time constraints of the programme. An open site at the University was considered ideal and was subsequently used for exposure. Exposure duration of one year was considered practicable and was adopted. Early age testing, however, was also considered, as this is relevant to the quality control of real structures and will help the elucidation of the change in

properties with time, which aids the prediction of long time performance. Testing after the initial exposure of three months was preferred to the conventional 28 day testing as the former allows longer interaction with the exposure environment and therefore facilitates the detection of any change in the properties of the concrete. A third testing age was also contemplated but was not possible due to the scale and extent of the testing programme involved.

### *Macro and microclimate*

The effects of macroclimate on concrete performance have been studied extensively. This resulted in the familiar broad classification of climates such as, temperate and hot climates. The adverse effect of hot climate, in particular, has been receiving considerable attention especially in the Gulf countries where the macroclimate is one of the most hostile climates to concrete construction in the world (e.g. Al-Abideen, 1998; Walker, 1996). Comparing the performance of concrete in different environments, such as hot with temperate, has helped in understanding the extent of the influence of hot climates on concrete durability. However, the basis of comparisons have not always been sound. The large differences in materials, labour, construction practice as well as the climatic conditions, between temperate and hot climate countries, raises questions on the extent the climate, per se, contributes to concrete's bad performance in hot climate. Studies that are based on simulation of hot weather under laboratory conditions are often based on idealised assumptions and are divorced from real life conditions.

The above complications instigated a different investigative approach in this research where most of these variables (differences in materials, labour etc.) were eliminated and, at the same time, exposure of the same concrete to the two climates was achieved. This was accomplished by air freighting concrete blocks, immediately after curing, from Loughborough to Muscat for exposure under local weather conditions there. These blocks were cast together with the concrete blocks that were stored for exposure at Loughborough, i.e. using

the same materials and under the same mixing and curing conditions. The blocks were flown at night and were taken within hours of arrival in Muscat to a suitable exposure site at Sultan Qaboos University where they were, at the correct age, tested.

It is apparent that most of the serious deterioration processes, such as reinforcement corrosion and sulphate attack, occur as a result of the direct interaction between the concrete and its surrounding environment. Although there have been numerous studies on the effect of natural exposure conditions on concrete' properties, little attention has been given to the potential effect of microclimate on these properties. Furthermore, most of these studies were based on laboratory simulated exposure and on concrete that does not represent real structures. In his study, Osborne (1989) reminded that more research work is needed on representative concrete, with particular attention being given to the effect of the local microclimate involved. Wood (1994) further stressed that quantification of the effect of microclimate is imperative if durability design is to be achieved. For these reasons, it was considered important to investigate the possible effects of microclimate on the durability characteristics of concrete.

The microclimate in this study denotes the climate immediately and directly around a structural element, which results from the interaction between the site climate (mesoclimate) with its specific geometry and location. To this end, the concrete blocks were arranged in different orientations according to the site climate conditions, in order to permit different interaction between each side of the blocks and the site climate (see Section 3.5.2).

### **3.2.3 Curing Regimes**

Different site curing regimes were considered. Hessian curing is the most common method of curing in Oman and was, therefore, the main method in the investigation. Three hessian curing durations were examined: 2, 4 and 6 days (plus one day in the mould). Longer curing periods are not economical

and are not adopted under normal conditions in practice and, therefore, were not studied. Hessian was sprayed with water once in 24 hours to represent poor and commonly encountered site practice. Polythene curing is widely used with and without hessian, and was evaluated on a selection of specimens in the investigation. Further, the use of curing membranes is reported to be simple, economical, and practical in situations where conventional curing methods are difficult to apply (e.g. Senbetta, 1994). The utilisation of curing membranes can especially be convenient in hot weather countries where curing is expensive and is seldom practiced efficiently. However, the efficiency of curing membranes as a credible alternative to other curing methods has been open to question (e.g. Mangat and El-Khatib, 1992). For these reasons, it was decided to examine the effectiveness of a widely used curing membrane on a selection of specimens in the investigation. Further, the benefits or otherwise of each curing method was evaluated by comparison with the non-cured concrete blocks (air cured) that were included with each concrete mix.

#### **3.2.4 Materials**

##### *Ground granulated blast-furnace slag*

The beneficial effects of using cementitious materials as cement replacement in improving the durability of concrete is widely reported (e.g. Khatri et al, 1997; Bamforth, 1995). The use of pozzolanic materials and slag is known to produce dense and impermeable concrete resulting in lower susceptibility to durability related attacks. The use of these materials is also attractive because of their reduced cost and the lower energy requirements associated with their production. The role of slag cement, in particular, in improving durability related properties of concrete, especially in hot environments has been the subject of many investigations (e.g. Bamforth, 1986 and 1997a). The use of slag cement with high replacement levels in concrete is reported to have many advantages including lower heat of hydration, reduced shrinkage cracking,

lower permeability and improved resistance to chloride penetration (e.g. Bijen, 1985; Hollinshead et al, 1997; Dhir et al, 1996b). However, the longer curing duration required for pozzolanic cement concrete compared to OPC concrete still raises questions on its suitability for hot weather countries (Osborne, 1986; Mangat and El-Khatib, 1992; Parrott, 1995). Many investigators believe that a period of 28 to 90 days is required for pozzolanic cement concrete to attain similar properties to that of plain cement concrete due to its slower rate of reaction (Parrott, 1992; Marsh et al, 1985; Nagataki and Ujike, 1986; Ho et al, 1986). Much of the information available on the effect of curing on blended cements relates to ideal concretes or pastes that had been cured in laboratories using methods which allow maximum hydration to take place (Hughes, 1985; Shigun and Roy, 1986). Studies that represent real life structures under realistic service conditions in this area are scarce. The use of GGBS and other cement replacements to improve durability in hot weather countries is increasing (e.g. Saricimen et al, 1995) and it was, therefore, considered important to study the various effects of slag concrete and its durability characteristics as influenced by climate and field curing.

#### *Controlled permeability formwork systems (CPF)*

Concrete durability is governed by the properties of the surface concrete or "covercrete", which controls the ease or difficulty with which aggressive substances from the environment can permeate through it into the inner sections of concrete. Recognising this, issues relating to the permeation properties of the surface concrete and measures that help improve its quality, and subsequently concrete's durability, are currently receiving world wide attention (e.g. Rilem, 1995). Amongst these measures are: ensuring adequate curing, the use of cement replacement materials to produce denser and less permeable concrete, and the application of controlled permeability formwork (CPF) to improve the surface properties of concrete (Sha'at, 1997). Since these issues constitute the core of this investigation, it was considered necessary to evaluate the influence of CPF systems on the surface properties and durability

of concrete. A commercially available CPF liner was, therefore, included in the investigation on a selection of specimens.

### **3.3 MATERIALS**

#### **3.3.1 Portland Cement**

Portland cement (PC) supplied by Castle Cement, conforming to the requirements of BS 12: 1991 Class 42.5 N, was used throughout the programme. The term OPC has been adopted throughout this study because this is the standard terminology in Oman. The chemical composition of the principal oxides of the cement is given in Table 3.1.

#### **3.3.2 Ground Granulated Blast-Furnace Slag**

The ground granulated blast-furnace slag was supplied by the Frodingham Cement Company, Scunthorpe. The GGBS fineness range is 375-425 m<sup>2</sup>/kg, its bulk density range is 1000-1100 kg/m<sup>3</sup> and its specific gravity is approximately 2.90. The chemical composition of the principal oxides of the GGBS cement is given in Table 3.1.

#### **3.3.3 Aggregates**

The fine aggregate was a river sand conforming to the zone M requirements of BS 882 (1992). The coarse aggregate was 10mm diorite, which belongs to the Gabbro group of aggregates (igneous rock) according to BS 812: Part 1: 1975 classification of natural aggregates. Mix water was tap water at laboratory temperatures.

Diorite was preferred to river gravel because of its lower porosity and absorption (absorption less than 0.7% compared to 1.8% for river gravel) which was desirable in view of the investigation tests (permeation and microstructure tests). Further, the length of the test specimens (55mm diameter × 20mm long discs) dictated the choice of the single 10mm size coarse aggregates.

### **3.3.4 Controlled Permeability Formwork System (CPF)**

A Zemdrain controlled permeability formwork (CPF) liner was used in a selection (see Table 3.3) of OPC/GGBS concrete summer series samples. The liner was stretched and fixed onto the timber formwork according to the manufacturer's specifications. The fresh concrete was then placed and vibrated as usual.

### **3.3.5 Curing Membrane**

A widely used curing membrane supplied by Sika Products, UK, was applied to a selection of OPC/GGBS concrete summer series samples (see Table 3.3). The membrane was sprayed onto the concrete surface using a spray gun immediately after removing the moulds. The application of the membrane was done in compliance with the manufacturer's specification.

## **3.4 MIX DETAILS**

Three concrete mixes were investigated. These are 30 and 50 MPa plain OPC concrete mixes and 30 MPa OPC/GGBS concrete. The 30 and 50 MPa mixes were investigated as being representative of concretes specified for 'mild' and 'most severe' conditions of exposure, in accordance with BS 5328: Part 1: 1997 specifications. The design of the concrete mixes was carried out according to the "Design of Normal Concrete Mixes" (Teychenne et al, 1975). The target workability was  $75 \pm 25$  mm. To assess the effect of concrete grade, the two OPC concrete mixes were designed to have 28 days strengths of 30 and 50 N/mm<sup>2</sup>. The OPC/GGBS mix was designed to have the same workability and 28 days strength as the 30 N/mm<sup>2</sup> OPC concrete to provide a sound basis for comparison between them. The mix proportions and other design details of the three mixes are given in Table 3.2.

The dry materials were weighed, placed in the mixer, the water was then added and the materials were mixed for 2-3 minutes. Once the mixing was complete, the concrete was placed into the moulds on a vibrating table, and

each mould was half filled before vibration started. The moulds were then filled and struck off using a float. The concrete in the moulds was then covered with wet hessian and polythene sheets and left to harden for 24 hours. The specimens were subsequently demoulded, marked with their mix identification and transported to the exposure site.

### **3.5 SITE EXPOSURE AND MICROCLIMATES**

#### **3.5.1 Exposure Site**

The concrete blocks were cured and stored for exposure at the meteorological site of the Department of Geography of the University. The site was ideal because it is situated in an open area; unobstructed from wind, sun radiation and rain fall. Furthermore, facilities were available for the automatic recording of local weather parameters such as temperature, relative humidity, wind direction and rain fall. This enabled the monitoring and recording of all weather conditions on a daily basis, throughout the exposure duration. The Muscat series samples were air freighted to Muscat immediately after curing for exposure under the local weather conditions. They were stored at an appropriate exposure site at Sultan Qaboos University. The weather parameters were recorded at a weather station near the exposure site. The Loughborough exposure site is shown in Figure 3.1.

#### **3.5.2 Microclimates**

Four microclimates were created by arranging pairs of concrete blocks in different orientations such that different interaction takes place between each side of the blocks and the site climate (meso climate). The blocks were arranged in pairs where the horizontal blocks (slabs) were placed on the vertical blocks (representing wall units), which were placed along the north-south plane. This created two microclimates one either side of the vertical blocks and two on either side of the slabs. This arrangement is shown in Figure 3.2.

The west facing sides of the vertical blocks were exposed to the prevailing wind, rain and sunshine (west microclimate) whereas the east facing sides of the blocks were partly sheltered from rain, the prevailing wind and sunshine (east microclimate). Similarly, the upper faces of the slabs were open to rain and sunshine, while the bottom faces were sheltered from rain and sunshine. The two microclimates on either side of the slabs (top and bottom microclimates) were different from the east and west microclimates of the vertical blocks in that both these faces were not as susceptible to direct wind, due to their horizontal orientation. The four microclimates are designed to provide insight into how the interplay of the weather elements (temperature, wind, rain and solar radiation) affects concrete's performance. The weather conditions in the 4 microclimates can, therefore, be summarised as follow:

1. West microclimate: exposed to direct wind, rain and sunshine
2. East microclimate: partly exposed to wind, rain and sunshine (prone to cyclic wetting and drying condition)
3. Top microclimate: exposed to rain and sunshine (not susceptible to direct wind)
4. Bottom microclimate: sheltered from rain and sunshine (not susceptible to direct wind).

### **3.6 CURING**

Table 3.3 outlines the curing methods and durations for the three weather series. Curing was performed at the exposure site where each concrete block was subjected to two types of curing, one on each half of the face, as shown in Figure 3.3. This arrangement reduced the number of blocks required to cover the full range of curing durations and minimised the sample-to-sample variability. The curing methods were air curing (no curing), hessian curing, covering with plastic polythene sheeting for six days and application of curing membrane. The two later methods were applied on a selection of the OPC/GGBS concrete blocks of the summer series only (see Table 3.3). The

hessian curing durations ranged from 2 to 6 days and it was kept wet during the curing period by spraying it with water once every 24 hours. All samples were cured in the mould during the first 24 hours.

**Table 3.1** Principal oxide composition

Oxides	Weight (%)	
	OPC	GGBS
CaO <sub>2</sub>	65	40
SiO <sub>2</sub>	20	37
Al <sub>2</sub> O	6	11
Fe <sub>2</sub> O <sub>3</sub>	2.5	0.2

**Table 3.2** Concrete mix details

Concrete group	Design strength (MPa)	Binder type	Binder content (kg/m <sup>3</sup> )	Free water content (liter)	Coarse aggregate (kg/m <sup>3</sup> )	Fine aggregate (kg/m <sup>3</sup> )
A	30	OPC	330	230	819	1001
B	50	OPC	420	230	865	865
C	30	OPC+GGBS	370	230	819	1001

**Key:**

Concrete: A = 30 MPa OPC, B = 50 MPa OPC, C = 30 MPa OPC/GGBS

**Table 3.3 Curing method and mix type**

Concrete series	Concrete group	Curing method					
		none	+2dH	+4dH	+6dH	+6dP	C/M
UK winter	A	T	T	T	T		
	B	T	T	T	T		
	C	T	T	T	T		
UK summer	A	T	T	T	T		
	B	T	T	T	T		
	C	T/C	T/C	T	T	T/C	T/C
Muscat summer	A	T	T	T	T	T	T
	C	T	T	T	T	T	T

**Key:**

Curing: H = hessian, P = polythene, CM = curing membrane

Concrete: A = 30 MPa OPC, B = 50 MPa OPC, C = 30 MPa OPC/GGBS

Formwork: T = timber, C = controlled permeability formwork (CPF)

+2 days H = 2 days curing with hessian plus one days in the mould.



Fig. 3.1 General views of the Loughborough exposure site



Fig. 3.2 Microclimate exposure arrangement of the blocks at the exposure site



Fig. 3.3 Site curing arrangement of the blocks (2 curing methods per block)

## Chapter 4 Background to the Tests and Methodology

---

### 4.1 INTRODUCTION

Five test methods were employed in this investigation, namely: air permeability, sorptivity, carbonation, thermogravimetry (TG) and mercury intrusion porosimetry (MIP). In addition, a standard 28 days compressive strength test was conducted on the control cubes cast with each mix for quality verification and control. A detailed justification and description of the test methods, as well as the sample preparation and conditioning for each test, is given in this chapter.

The three climate series i.e. the Loughborough winter, Loughborough summer and the Muscat summer series, were each tested after 3 and 12 months of site exposure. The air permeability and sorptivity tests were performed after 3 and 12 months exposure. The carbonation test was conducted after 6 and 12 months of site exposure and both the TG and MIP tests were conducted after 12 months of exposure. Only the sorptivity test was performed for the Muscat weather series, after 3 and 12 months of local site exposure. At the correct testing age, the large concrete blocks were transported from the exposure site to the laboratory where they were cored and specimens were prepared for each test. Figure 3.1 shows the concrete blocks at the exposure site in Loughborough. After coring, the blocks were returned to the exposure site.

## 4.2 TEST METHODS - JUSTIFICATION

### 4.2.1 Introduction

It is now widely accepted that the permeation characteristics of the surface concrete or covercrete, determines its durability (e.g. RILEM, 1995; Clark et al, 1997). As a result, efforts have gathered momentum to try to understand the properties of both the transport processes and the surface concrete, and their influence on concrete durability. A review of the literature indicated that efforts in this respect, although neither planned nor co-ordinated, are being channelled into three directions. The first direction is towards better understanding of the transport processes namely, absorption, permeation and diffusion, and the extent each process contributes to the transport of harmful substances from the environment into concrete during its service. The second direction is towards studying the properties of the concrete in the surface region and finding measures to improve its quality and hence concrete durability. Finally, there are investigations of the effects of the microclimate i.e. the immediate environment that surrounds concrete structures, and the role it plays during the service life of these structures. However, suitable test methods and methodology that represent these transport processes as they occur in real life are far from being decided. Further, views are often conflicting on the measures that are proposed to improve the durability of the surface concrete. Studies aimed at improving understanding of the role of microclimate in real life structures have been scarce, despite recognition its importance.

The three issues discussed above form the basis of this work, and different test methods to investigate the transport processes were evaluated. In searching for suitable test methods, the selection criteria were: the relevance of the test methods and their measured parameters to the transport processes occurring in concrete under service conditions; the soundness of their theoretical basis; the simplicity of the test methodology; and finally their reliability and practicality.

#### **4.2.2 Absorption**

On this basis, the sorptivity (the rate of water up-take due to capillary suction) and air permeability tests were selected for the measurement of the water absorption rate and coefficient of air permeability of the investigated concrete. Capillary suction is an important transport process that plays a significant role in most deterioration mechanisms of concrete, depending on the condition of exposure (RILEM, 1995). The ingress of chlorides as well as sulphate attack in concretes that are subjected to intermittent wetting and drying conditions involves the transport of chloride and sulphate ion containing liquids by capillary suction. Frost damage occurs when concretes pore solution is fully saturated; a condition that can be attained by the capillary absorption of water. Similarly, alkali-silica reaction can be enhanced by the absorption of water and alkali ions into concrete by capillary suction. Moreover, capillary suction is relevant to corrosion of reinforcement since the transport of chloride ions (anodic reaction) and moisture (cathodic reaction) can take place by capillary suction. Further, measurement of water sorptivity was found to be broadly indicative of chloride absorption (Parrott, 1996). Finally, carbonation is indirectly dependent on capillary absorption since the rate of CO<sub>2</sub> diffusion depends, amongst other things, on the moisture state of the concrete.

#### **4.2.3 Permeation (and Diffusion)**

Although the permeation to air or other gases under an applied pressure head is only relevant to degradation mechanisms in special cases, this transport process has been well correlated with concrete performance and is being widely used as a durability indicator of concrete. As with capillary suction, close correlations have been established between permeation to air and other gases with durability characteristics such as carbonation rate, depth of chloride penetration, weight loss and gain due to frost damage and sulphate attack respectively (RILEM, 1995). The advantages of using gas rather than water to assess the permeability are apparent. Apart from its shorter test

duration, an important advantage of gas over water permeability tests is that it does not interfere with the microstructure of the concrete during the test. This enabled the use of the same samples following the test for the sorptivity measurement and without the need for further conditioning (drying). The measurement of air permeability under an applied pressure by the output test method (Dhir et al, 1989) and sorptivity (capillary suction) by shallow immersion (Hall, 1989) have been chosen for the investigation. Apart from their sound theoretical basis, the advantages of the two tests include their simplicity and the relatively short test duration.

The diffusion of gas molecules ( $\text{CO}_2$ ,  $\text{O}_2$ ) and ions (chlorides and sulphates) is a very important transport process for corrosion mechanisms in concrete. However, unlike gas permeability and sorptivity, these transport processes (molecular and ionic diffusion) have not been tested elaborately for a correlation with concrete performance (RILEM, 1995). Furthermore, the diffusion tests often require long test duration and sophisticated testing equipment. Nevertheless, since deterioration mechanisms are very slow and concrete internal characteristics change continually with time, the effectiveness of accelerated diffusion tests in reflecting natural degradation processes is questionable.

#### **4.2.4 Carbonation**

The service life of reinforced concrete can be defined as the time up to the onset of reinforcement corrosion (RILEM, 1995). Carbonation as well as chlorides ingress leads to corrosion of reinforcement, which is one of the major causes of deterioration in reinforced concrete. Therefore, the carbonation of reinforced concrete can severely compromise its service life and it relates quantitatively to its durability. Apart from reduction of concrete's high alkalinity (see Section 4.6), carbonation may exasperate chloride-induced corrosion by releasing some of the aluminates-bound chloride ions (Richardson, 1998). Furthermore, carbonation of concretes continuously alter its microstructure during the course of carbonation and

modify its permeability characteristics (e.g. Patel et al, 1985). Based on this, the carbonation test to measure the depth of carbonation as a measure of concrete durability was considered an important complementary test in the investigation and was included.

#### **4.2.5 Pore Structure**

Most of the important properties of concrete, such as its strength, corrosion resistance, permeability and durability are closely related to its pore structure (Mehta and Manmohan, 1980; Roy, 1989; Halamickova et al, 1995). The emphasis of this work has been on engineering properties, with the aim of relating concrete's permeation properties and curing efficiency to fundamental changes in its microstructure. Thermogravimetric analysis (TGA) and mercury intrusion porosimetry (MIP) were found to be the most prominent tools to achieve this purpose (e.g. Winslow and Diamond 1970; Bagel and Zivica, 1997). These tests provide important information relating to concrete hydration and porosity. The tests were, therefore, included in the test programme. Originally, the tests were planned to be conducted at 3 and 12 months, as with the other tests, however, due to certain difficulties with the instruments during the early stages of the programme (see Sections 4.7.1 and 4.8.1), this was not possible. These tests were therefore conducted at the age of 12 months for the two Loughborough series

### **4.3 COMPRESSIVE STRENGTH**

The compressive strength test was carried out in accordance with BS 1881: Part 116, using 100-mm cubes. Three 100-mm control cubes were cast from each concrete batch for all series. As with the main samples, the cubes were cured with wet hessian and covered with polythene sheeting for the first 24 hours. After de-moulding, the cubes were placed in a curing tank to cure in water at  $20 \pm 2$  °C before being tested at the age of 28 days. Three cubes from each concrete batch were tested and the total average from six tests was then reported for each concrete mix.

## 4.4 AIR PERMEABILITY

### 4.4.1 Theoretical background

The calculation of permeability through a porous material is normally obtained from Darcy's basic flow equation (Bamforth, 1987):

$$V = k \frac{p}{l} \quad (4.1)$$

where  $V$  is the velocity of flow (m/s),  $k$  is the coefficient of permeability (m/s),  $p$  is the pressure head (m) and  $l$  is the thickness of specimen in the direction of flow (m).

The coefficient of permeability ( $k$ ) from equation (4.1) is dependant on the properties of the permeating fluid (i.e. its density  $\rho$  and viscosity  $\eta$ ) as well as the pore structure of the penetrated material. Equation (4.1) is modified to give a more practical permeability coefficient, which is dependent only on the pore structure characteristics of the penetrated medium, i.e. independent of the properties of the penetrating fluid ( $\rho, \eta$ ). This theoretically enables permeability comparisons of different concretes, regardless of the test fluid. The modified expression as presented by the Concrete Society Working Party (1988) is:

$$V = \frac{Q}{A} = \frac{-k}{\eta} \frac{dp}{dl} \quad (4.2)$$

where  $Q$  is the volume flow rate of permeating fluid ( $m^3/s$ ),  $A$  is the cross sectional area through which the fluid permeates ( $m^2$ ),  $\eta$  is the viscosity of the fluid ( $Ns/m^2$ ),  $k$  is coefficient of permeability ( $m^2$ ) and  $dp/dl$  is the pressure gradient across the specimen length.

If the permeating fluid is non-compressible, such as water, the permeability equation is obtained by the direct integration of equation (4.2) to give:

$$k = \eta \frac{Q}{A} \frac{L}{(P_1 - P_2)} \quad (4.3)$$

where  $P_1$  is the inlet pressure ( $\text{N}/\text{m}^2$ ),  $P_2$  is the outlet pressure ( $\text{N}/\text{m}^2$ ) and  $L$  is the length (thickness) of the specimen in the direction of flow (m).

When a compressible fluid, such as air, is used, Darcy's equation (4.2) is further modified to calculate the flow rate at the average pressure within the specimen to give (Cabrera and Lynsdale, 1988; Dhir et al, 1989):

$$k = \eta \frac{Q}{A} \frac{2L P_2}{(P_1^2 - P_2^2)} \quad (4.4)$$

where  $k$  ( $\text{m}^2$ ),  $\eta$ ,  $Q$ ,  $A$ ,  $L$ ,  $P_1$  and  $P_2$  are as defined previously. Equation (4.4) is strictly valid for laminar-viscous flow conditions.

#### 4.4.2 Preliminary investigation

Several trial tests were conducted to establish the most appropriate specimen size, test pressure and test duration. Cylindrical samples of 55mm in diameter with lengths ranging from and 150 to 20mm were tested. The sample size was found to have no significant effect on the air permeability test results providing that the sample length is at least twice the maximum aggregate size. This was in agreement with other published work (e.g. Cabrera and Lynsdale, 1988). The chosen specimen size, the 55mm diameter and 20mm long discs were found to be most suitable for the purpose of this investigation. This size (20mm length) was chosen chiefly to enable closer assessment of the cover zone layers and accurately measure the changes in properties within the this region of concrete. Furthermore, this size allowed larger number of specimens to be extracted from each concrete block, thus reducing the sample-to-sample variability and the total number of blocks required for testing. Another advantage of this sample size is the reduced test duration due to the reduced length (thickness) of the specimen.

Two factors were considered in determining the driving flow pressure of the test. The first was the fact that air flow during the test must be laminar for Darcy's flow conditions to apply, which constitutes the basis of the air permeability calculations (Section 4.4.1). The second consideration was testing

time. Lower flow pressures will satisfy Darcy's laminar flow condition; however, they result in prolonged test duration with increased tendency for gas slippage effects. Inflow test pressures ranging from 20 to 80 psi were evaluated for steady state flow and this revealed an almost linear relationship (insignificant deviation). A 50-psi pressure was eventually selected on the basis of the repeatability of the results at this pressure and test duration. A sealing pressure of 500-psi (10 times the flow pressure) was applied to ensure no leakage took place during the test. Checks were performed regularly to ensure that there was no leakage during the test.

#### **4.4.3 Apparatus**

The air permeability apparatus was based on equipment used by Lovelock (1970) and is similar in principal to that described by the Cembureau method (1989) for the measurement of oxygen permeability of concrete. The apparatus consists of two pressure cells designed to take 55 or 25 mm diameter test specimens. The air supply to the cell comes from a compressor via a pressure regulator. The inlet air pressure was measured by an accurate pressure gauge and the outlet pressure from the specimen was measured either by rotating float flow meters or a bubble flow meter. Sealing the circumferential surface of the specimens was achieved initially by inserting it in a plastic sleeve, which has approximately the same diameter as the specimen (i.e. squeezed against it). Once the specimen and the sleeve were inside the cell, high-pressure sealing was then applied using Nitrogen.

#### **4.4.4 Sample Preparation**

The air permeability test was conducted after 3 and 12 months of field exposure for each series. At the testing age, the concrete blocks were transported from the exposure site to the laboratory for coring. Two pairs of cylindrical cores 55mm diameter and 150mm in length (representing the entire thickness of the blocks) from each concrete block were taken for the test. The cores were cut from the blocks using a diamond tipped core bit. The cores were then sliced using a masonry saw with a diamond tipped blade to

obtain 20mm thick discs. Ten discs were cut from each pair of cores (for the vertical blocks, five discs to test the 50-60 mm of the east face, and five for the west face) so that permeability was measured at average depths of 10, 20, 30, 40, and 50 mm from the surface of the blocks. Figure 4.1 shows the method of slicing the cores to obtain discs at the required depths. The same sequence was repeated for the horizontal blocks (slabs) for the measurement of the air permeability of the top and bottom faces of these slabs. The procedure was followed on the second pair of cores (duplicate samples) from each block and the average values of each pair of samples from the same depth were calculated.

This arrangement was slightly modified for the 12 months tests. Measurements were taken at average depths of 5, 10, 20, 30 and 40 mm from the surface. This change was based on the results obtained from the 3 months tests, which revealed no significant variation in properties at depth beyond 20-40 mm from the surface. As a result, measurement at the new average depth of 5mm from the surface was introduced and the 50mm deep discs were abandoned.

The samples were then dried in a well-ventilated oven at 50 °C to constant weight  $\pm 0.1$ g in 24 hours. Drying at higher temperatures, e.g. the much used 105 °C, was avoided as this may induce changes to the microstructure of the samples (Young, 1988; Lydon and Mahawish, 1991). The time taken to reach constant weight ( $\pm 0.1$  g in 24 hours) was  $14 \pm 2$  days, depending on the samples. The samples were then removed from the oven and placed in a desiccator over fresh silica gel to cool for a further 24 hours before testing.

#### **4.4.5 Test Procedure**

The test procedure followed is generally in agreement with the Cembureau recommendation (1989). The conditioned 55mm diameter  $\times$  20mm thick disc was inserted in the sleeve, which was then placed in the pressure cell. A sealing pressure of 500-psi was applied to seal the circumferential surface. Flows were then measured using a driving pressure of 50-psi (approx. 3.4

bar). Once a flow has stabilised, which took approximately 5-10 minutes from the start of the experiment, flow rates were recorded. The outlet flow was measured using a bubble flow meter and the average of three readings of each disc taken to calculate the coefficient of air permeability ( $k$ ) in  $\text{m}^2$  using equation (4.4). In this work, the gas slippage effect (e.g. see Dhir et al, 1989) was considered negligible (see section 4.4.2). To ensure isothermal flow conditions, the test was conducted at constant laboratory temperature of  $20 \pm 2$  °C and relative humidity of  $65 \pm 5$  %. The procedure was repeated on the duplicate disc from the same block and the average value from the two discs obtained. The duration of the test for each disc was approximately 10 to 15 minutes. Each disc was returned to the desiccator immediately after the test. The test apparatus and sleeve with specimens are shown in Figure 4.2 and 4.3.

## 4.5 SORPTIVITY

### 4.5.1 Theoretical Background

The rate of transport of a fluid in a porous material is a function of two basic factors:

1. The forces acting on each element of volume of the fluid in the pores
2. The resistance to flow offered by the pore space of the material

The forces acting on an element of volume of pore fluid include externally imposed pressure gradients within the material (hydrostatic pressure differences), gravitational force and capillary forces. The resistance to flow by the material depends on the characteristics of its pore structure (e.g. the diameter of the capillary pores and their continuity) and the transported fluid (viscosity, density and surfaces tension).

When the porous medium is saturated, capillary forces are absent and flow is described by the saturated flow theory, where flow can only occur under the influence of externally imposed pressure gradients or gravity (Hall, 1977). If the porous medium is unsaturated or partly saturated, flow is predominantly

caused by capillary forces, the gravitational and hydrostatic pressure effects being often negligible. This has been verified by Kelham (1988) and Hall (1989) who showed that capillary forces are the most dominant driving forces in the water absorption of many building materials and concrete, which are most often partly saturated in practice and are rarely saturated.

Flow under the action of capillary forces depends on the pore structure of the penetrated medium, its local moisture content and the properties of the penetrating fluid (i.e. its viscosity and surface tension). The capillary forces are strongest when the material is dry and decrease progressively with increased saturation (MaCarter et al, 1992). The flow velocity due to capillarity therefore is also determined by the pore structure characteristics of the material and its degree of saturation. Further, the dependence of capillary flow and permeability on both these parameters (pore structure and water content) provided the basis for the application of the unsaturated flow theory, as originally developed for unsaturated flow in soils, to the capillary water absorption properties in concretes.

The physics of the capillary flow is assumed to follow the modified Darcy law (Hall, 1987):

$$v = k(\omega) F_c(\omega) \quad (4.5)$$

where  $v$  is the flow due to capillary suction,  $k$  is the permeability and  $F_c$  is the capillary force; and both  $k$  and  $F_c$  depend on the water content  $\omega$ . The capillary force  $F_c$  is a function of the gradient of the capillary suction  $\Psi$ :

$$F_c = -\frac{d\Psi}{dx}(\omega) \quad (4.6)$$

and capillary suction  $\Psi$  is determined through the Kelvin equation:

$$\Psi = \frac{2\sigma}{r} \quad (4.7)$$

where  $\sigma$  is the surface tension of the liquid and  $r$  is the mean radius of curvature of the liquid meniscus within the pores.

Substituting therefore in equation (4.5) for one-dimensional flow:

$$v = -k(\omega) \frac{d\Psi}{dx} \quad (4.8)$$

Thus the flow ( $v$ ) is proportional to the gradient of capillary suction ( $\Psi$ ).

By a series of solutions to equation (4.8), re-expressed as a diffusion equation, Hall (1977) and Gummerson (1980) showed that unsaturated flow theory (as summarised in equations 4.6 to 4.8) provides theoretical support to the empirical relationship between capillary absorption and time:

$$i = S (t^n) \quad (4.9)$$

where  $S$  is the material constant termed the sorptivity,  $t^n$  is a time function and  $i$  is the cumulative volume of absorbed water per cross sectional area of inflow surface, given by:

$$i = \frac{\Delta w}{\rho A} \quad (4.10)$$

where  $\Delta w$  is the increase in weight (g),  $A$  is the cross sectional area of the flow surface ( $\text{mm}^2$ ) and  $\rho$  is the density of water ( $\text{g}/\text{mm}^3$ ).

The power exponent ( $n$ ) in the time function of equation (4.9) may vary depending on the condition of the sample and exposure. However, experimental work frequently shows the cumulative water absorption  $i$  to increase proportionally to the square root of elapsed time (Kelham, 1988; Hall, 1989; McCarter, 1992; Persson, 1997). Equation (4.9) therefore is re-written as:

$$i = S\sqrt{t} + C \quad (4.11)$$

where  $C$  is a small intercept on the  $t = 0$  axis, arising from the filling of open surface porosity of the inflow surface and the vertical sides or circumference of the specimen, and  $\sqrt{t}$  is the square-root of immersion time ( $\text{min}^{0.5}$ ). The sorptivity ( $S$ ) as determined from equation (4.11) has the unit ( $\text{mm}/\text{min}^{0.5}$ ).

As previously outlined, the water sorptivity of concrete depends on the gradients of capillary suction (capillary pressure) which, in turn, is

determined by the surface tension ( $\sigma$ ) and the radius ( $r$ ) of the meniscus of water (equation 4.7). It is clear from this equation that capillary suction is inversely proportional to  $r$ , i.e., the smaller the radius of curvature of the water menisci (smaller pores), the greater the surface tension and therefore capillary suction. Since the radius of the water meniscus varies with the water content within the different pores in the concrete (depending on the geometry of the pores), the capillary suction gradients and the sorptivity, therefore, are also dependent on the water content of the material.

Furthermore, it has been reported that the sorptivity increases with temperature due to its effect on the viscosity ( $\eta$ ) and surface tension ( $\sigma$ ) of the water (or the test liquid) (Hall, 1989). This was verified experimentally by Gummerson and co-workers (1981) who showed that the sorptivity is proportional to the quantity  $(\sigma \eta)^{0.5}$ .

#### **4.5.2 Preliminary Investigation**

Several factors relating to the test methodology, duration and specimen size were evaluated before the final test set up was established. Water absorption by capillary suction is now recognised as an important transport mechanism that is relevant to deterioration processes, however, there is as yet no established standard test procedure that researcher accept and adhere to. The test methodology, specimen size and conditioning, as well as the measured indices are often different from one work to another, and valuable opportunities are therefore wasted to make full use of the published data. Indeed, simple comparison of results often raises doubt due to these differences, and can at times be scientifically unacceptable.

The size of the specimen was found to be the most important factor in deciding the test duration and time intervals for weight gain measurements. Cylindrical specimens ranging from 100 to 55 mm in diameter and 150 to 20 mm in length were tested during trials. These specimens were cored from large concrete blocks that were cast specifically for test trials, and were cured and exposed under laboratory conditions. Table 4.1 lists typical sorptivity

values obtained from 100 and 55mm diameter discs (20mm thick). The size of the specimen was found to have no significant effect on the sorptivity (coefficient of variation being typically within 10%), which verifies other reports (Kelham, 1988; Hall, 1989). The specimens took between 6 days to 4 hours to reach saturation depending on their size. The calculation of the sorptivity is based on the linear relationship between the cumulative water absorption and the square root of elapsed time. However, this relationship was only found to be linear during the first few hours of the test in most specimens. This is in agreement with McCarter and his co-workers (1992) findings that significant downward curvature occurs (deviation from the linear relationship) when the specimens are tested over extended periods (more than 25 hours). This downward curvature is mainly due to moisture and porosity gradients within the concrete (Hall, 1989; MacCarter et al, 1992). In these cases, sorptivity is calculated using the early time data that corresponds to the straight-line portion of the least squares plot between the cumulative water absorption and square root of time (Kelham, 1988; Hall, 1989). Shorter test durations are therefore preferable to prolonged durations, as far as the calculation of the sorptivity is concerned, providing that adequate number of readings are taken to define a good sorptivity plot. Continuing the test until saturation is usually performed to obtain the effective porosity of the specimen (which is defined as the mass of water required to saturate the concrete), however, sorptivity is still calculated using the early time data (e.g. Kelham, 1988; Reihardt and Aufrecht, 1995).

The early sorptivity tests included measurements of the depth of water penetration into the discs as well as weight gain. Studies on the depth of water penetration found that, like water up-take, it followed a square root-time relationship and is relevant to durability (MacCarter et al, 1992). However, difficulties were encountered in observing the precise water penetration depth on the surface of discs. A water-soluble dye dissolved in the water reservoir was subsequently tried to aid the visual detection of the advancing waterfront onto the discs surface. However, this did not improve

the accuracy of measurement due to the relatively small sample height (20-mm). Depth measurements have been accomplished in previous investigations by splitting the specimens longitudinally to measure the precise depth of penetration (e.g. Ho, 1986, MacCarter et al, 1992). This, however, was not possible in this work as the specimens were to be subsequently re-used for other tests, and depth measurements were therefore abandoned.

The effect of the drying regime on the sorptivity results was evaluated by performing the test 3 times on the same samples before being dried to equilibrium (constant weight  $\pm 0.1$  g in 24 hours) in each occasion at 50 °C. Typical results are given in Table 4.2. The coefficient of variation was largely within 10%. Further, it was interesting to observe that the sorptivity tended to increase with increased drying frequency. This tendency is unlikely to be due to a drying-induced change or damage to the microstructure, as this is more likely to cause a reduction rather than an increase in the sorptivity of the samples (Patel et al, 1988). The increased sorptivity with increased drying frequency is more likely to be due an increase in the porosity as a result of additional weight loss (moisture loss) of the samples after repeated drying. This is confirmed by the initial weight of the samples given in Table 4.3, which shows a reduction in the equilibrium weight after each drying cycle (before the sorptivity test was commenced). These results provide a further insight into the adverse effect of cyclic wetting and drying that site concrete normally undergoes.

The advantages of the adopted specimen size i.e. the 55-mm diameter x 20-mm long discs (the same specimens were used for the air permeability and sorptivity tests) were discussed earlier in section 4.5.1. The variations in the sorptivity when determined using this size and the trial sizes was small (coefficient of variation less than 10%). Further, the effect of removing the top surface skin on the sorptivity was evaluated. The sorptivity test was performed on a large number of discs before and after trimming (sawing approximately 0.5mm from the surface) the skin of their surface. Typical

results are presented in Table 4.4. No notable difference was observed in the sorptivity values between the cast and sawn surfaces of the samples, the coefficient of variation being less than 5% in all cases. Lydon and Mahawish (1991) reached the same conclusion upon investigating the effect of trimming the surface skin of the samples on the air permeability results.

The test specimens took approximately 2 hours to reach saturation. Based on this, the most suitable test duration was found to be 50 minutes. Closer time intervals for the measurement of weight gain, especially at an early stage in the test, and increasing the number of measurements was found to produce excellent results with improved curve fitting (correlation coefficient,  $r \approx 0.99$  in all cases).

The sorptivity test was performed on the same samples that had been used for the air permeability test. Apart from reducing the total number of samples, reusing the same samples enabled a more accurate evaluation of the relationship between the two parameters since both were obtained from the same samples.

#### **4.5.3 Apparatus**

The test method is based on the procedure described by the European Standard prEN 104-837 (1995) and is broadly similar to that recommended by RILEM (1974). The apparatus consists of a water reservoir with stable rigid supports and a perforated flat-based tray that is supported by means of four adjustable screws mounted over the reservoir rim. The test was conducted at laboratory temperature of  $20 \pm 2$  °C and  $65 \pm 5$  % relative humidity. A sensitive scale, weighing to 0.01 g was used to record the weight gain. Figure 4.4 shows the apparatus with specimens being tested.

#### **4.5.4 Sample Preparation**

The sorptivity test was conducted on the same discs used for the air permeability test. After the air permeability test was completed, the discs were returned to the desiccator and remained in it for a further 24 hours

before the sorptivity test was conducted (each disc was only 10-15 minutes out of the desiccator during the air permeability test). The samples were weighed before the test was started and, in almost all cases, no weight change in the samples was observed. For the Muscat samples, the sorptivity test was conducted after 3 and 12 months of local exposure in the Civil Engineering Department laboratory at the Sultan Qaboos University in Oman.

Like the air permeability results, the 3 months tests revealed little change in the sorptivity from approximately 25-50mm deep in most samples, and the 12 months air permeability discs were therefore used for the sorptivity test at 12 months, as before.

#### **4.5.5 Test Procedure**

- The conditioned 55mm diameter x 20mm thick discs were weighed and then placed in the shallow tray such that the depth of immersion up the sides of the discs was between 2-3 mm.
- The weight gain was recorded at 1, 4, 10, 15, 25, 35, and 50 minutes from the start of test. At the above test intervals, the discs were removed from the tray and surface water was mopped off with a damp tissue before the weight gain was recorded. As stated earlier, the test duration and the time intervals for weight gain measurements were based on the actual rate of water uptake of the disks and the time taken to reach full saturation which were determined during trial tests.
- The discs were then returned immediately to the tray. The removal, drying, weighing and weight recording of each specimen were completed within 15 seconds.
- Throughout the test, the water in the reservoir was maintained at a constant level and temperature. Two discs were tested from the same sample and the average sorptivity value was then obtained.

## 4.6 CARBONATION

### 4.6.1 Theoretical Background

The carbonation of concrete involves a chemical reaction within the concrete pores between the dissolved atmospheric carbon dioxide (carbonic acid- $\text{H}_2\text{CO}_3$ ) and the various cementitious phases. Carbon dioxide ( $\text{CO}_2$ ) at the normal atmospheric concentration of about 0.03% reacts most readily with calcium hydroxide ( $\text{Ca}(\text{OH})_2$ ), however, virtually all the hydrated and unhydrated cement phases can react with carbon dioxide (e.g. Loo et al, 1994). Nevertheless, there are conflicting views as to whether the reaction of phases other than  $\text{Ca}(\text{OH})_2$ , e.g. calcium silicate hydrate (C-S-H), takes place simultaneously with, or only after the conversion of  $\text{Ca}(\text{OH})_2$  (Sims, 1994). The main cement hydrates, i.e.  $\text{Ca}(\text{OH})_2$  and C-S-H and the various calcium aluminate or ferro-aluminate hydrates react with  $\text{CO}_2$  to form calcium carbonate ( $\text{CaCO}_3$ ), silica gel and hydrated aluminium and iron oxides (Parrott, 1987, Loo et al, 1994). These reactions are accompanied by a drop in the alkalinity of the pore fluid of concrete from a pH of about 12.6 to below 9 (Richardson, 1998; Parrott, 1987). As a result, the corrosion protection is lost due to the break down of the passive ferrous oxide layer on the steel reinforcement, which was maintained by the high alkalinity of the surroundings.

The rate of carbonation is controlled by the diffusion of  $\text{CO}_2$  or water diffusion into the concrete. This was found to depend on the properties of the concrete i.e. its mixture composition, cement type, compaction and curing, as well as environmental exposure i.e. temperature, relative humidity and  $\text{CO}_2$  concentration in the atmosphere (Nagataki et al, 1986; Parrott, 1987). The rate of carbonation is slow under normal exposure conditions however it increases with an increase in the temperature, porosity and carbon dioxide concentration (Roy et al, 1996, Parrott, 1987). The relative humidity of the surrounding environment plays an important role in controlling the diffusion of  $\text{CO}_2$  into concrete, with the highest rates occurring for concretes that are in

equilibrium with ambient RH of between 50-70% (e.g. Petersson, 1996, Neville, 1995).

Prediction of the rate of carbonation is normally based on Fick's first law of diffusion, which describes the diffusion of carbon dioxide into concrete as follow (RILEM, 1995; Richardson, 1998):

$$m = -DA \frac{c_1 - c_2}{x} t \quad (4.12)$$

where  $m$  is the mass of  $\text{CO}_2$  (g),  $D$  is the diffusion coefficient for  $\text{CO}_2$  through carbonated concrete ( $\text{m}^2/\text{s}$ ),  $A$  is the cross sectional area of the penetrated section ( $\text{m}^2$ ),  $c_1$  and  $c_2$  are the surface and internal concentrations of  $\text{CO}_2$  ( $\text{g}/\text{m}^3$ ),  $t$  is time (s) and  $x$  is the length of the penetrated concrete layer (m).

For the carbonation of a unit volume of alkaline compounds, an amount of  $\text{CO}_2$   $a$  ( $\text{g}/\text{m}^3$ ) is required. Therefore, the mass of  $\text{CO}_2$  required at the carbonation front to increase the depth of carbonation by an increment  $dx$  is given by:

$$m = a A dx \quad (4.13)$$

substitution of equation (4.13) in (4.12) gives:

$$a A dx = -DA \frac{c_1 - c_2}{x} t \quad (4.14)$$

re-arranging equation (4.14) and integrating gives:

$$x^2 = -\frac{2D}{a} (c_1 - c_2) t \quad (4.15)$$

Combining all constant parameters in equation (4.15) into a single constant  $K$  gives:

$$x = K\sqrt{t} \quad (4.16)$$

where  $x$  is depth of carbonation (m) at time  $t$  (s) and  $K$  is constant.

Amongst the simplifications in the application of Fick's law of diffusion and therefore the limitation of the application of equation (4.16) is the assumption

that the diffusion coefficient  $D$  is constant i.e. independent of concrete properties (mix composition, cement type and curing history) and its environmental exposure conditions (e.g. relative humidity and temperature). Furthermore, the amount  $a$  ( $\text{g}/\text{m}^3$ ) of  $\text{CO}_2$  required for the carbonation of the alkaline compounds in a unit volume of cementitious materials is not constant as has been assumed, but will vary depending on the cement type and its  $\text{CaO}$  content (Richardson, 1998; RILEM 1995; Osborne, 1986; Litvan and Meyer; 1986).

#### 4.6.2 Measurement of Carbonation

Concrete carbonation can be monitored by a variety of laboratory test methods including X-ray diffraction, microscopical techniques, chemical extraction and thermogravimetric analysis (Neville, 1995). The X-ray diffraction method measures the reduction of  $\text{Ca}(\text{OH})_2$  and the increase of  $\text{CaCO}_3$ , however, amorphous calcium carbonate will not be detected (Parrott, 1987; Sims, 1994). Microscopical techniques enable the direct observation of calcium carbonate in thin sections of concrete as the fine-grained  $\text{CaCO}_3$  mass appear typically lighter than the non carbonated matrix (Sims, 1994). The chemical methods involve the extraction of dust from drilled samples at various depths and analysing quantitatively the amounts of  $\text{Ca}(\text{OH})_2$  and  $\text{CaCO}_3$  present in the samples (Litvan and Meyer, 1986). The amount of  $\text{CaCO}_3$  can also be determined by thermogravimetry, however, the precision of the technique may be affected by the possible presence of  $\text{CaCO}_3$  in different types of aggregates (Sims, 1994).

The most common method used to measure carbonation is spraying a freshly broken concrete surface with a phenolphthalein, pH indicator solution (e.g. RILEM, 1984). Typical proportion of the indicator range from 50-100 ml alcohol, 50-0 ml water with 1g phenolphthalein (Parrott, 1987). As the indicator is sprayed onto a freshly broken surface, the carbonated areas with pH lower than 9 remain colourless while the uncarbonated areas with a pH of more than 9 turn pink in colour. The test is simple, rapid and gives

reproducible results (e.g. Parrott, 1987). Dunster et al (1996) found a good correlation between carbonation measured by pH indicator and that determined by thin section. However, a draw back of the test is that it merely indicates the presence of  $\text{Ca(OH)}_2$  ( $\text{pH} > 9$ ) but not a complete absence of carbonates, which relatively limits its sensitivity and accuracy (Litvan and Méyer, 1986).

#### **4.6.3 Test Procedure**

The measurement of carbonation depth was carried out in accordance with the recommendations of the RILEM Committee CPC - 18 (1984). The test was conducted at 6 and 12 months and on the surface discs that had been used for the air permeability and sorptivity tests. Figure 4.1 shows the cores and location of the discs used for the tests. The discs were dried in an oven for 24 hours at 50 °C to prevent any possibility of hydration as a result of wetting from the sorptivity test. The carbonation depth was determined by spraying the freshly split surface of the discs with a phenolphthalein indicator with a 1% solution in a 70% ethyl alcohol (Figure 4.5). Measurements were taken at equi-distant points along the edge of the specimens and the average depth of each disc determined. The average carbonation depth of two discs from the same sample was calculated.

### **4.7 THERMOGRAVIMETRY (TG)**

#### **4.7.1 Theoretical Background**

Thermogravimetric analysis (TGA) is a thermal analysis technique for investigating the thermal decomposition of materials and changes in mass as they are heated. The technique yields quantitative information about the heated sample's composition from the percent weight change occurring at various temperature transitions. Thermal analysis methods have been widely used to investigate the progress of hydration in cementitious materials (e.g. Mackenzie, 1972; Bogue, 1955; Taylor, 1990). In these methods, the degree of reaction is indirectly obtained from quantification of the amount of chemically

combined water in the cement paste or from its calcium hydroxide content (e.g. Taylor, 1990; Parrott et al, 1990; Patel et al, 1988).

At any stage of hydration, the hardened cement paste consists primarily of cement gel, crystals of calcium hydroxide, gel pores, capillary pores and unhydrous cement. As samples are heated, a continuous loss of water takes place. At around 100 °C the capillary pore water and most of the water adsorbed in the cement gel is lost (evaporable water). With increasing temperature, the water loss continues until around 400 °C when crystalline  $\text{Ca(OH)}_2$  loses its water as it decomposes into calcium oxide ( $\text{CaO}$ ) and water. It is generally suggested that  $\text{Ca(OH)}_2$  loses its water over a narrow temperature range (e.g. Taylor, 1964), however, conversion of  $\text{Ca(OH)}_2$  can take place over a wide range from 400-600 °C (Bazant and Kalpan, 1996). The loss of water of the heated sample continues at a slower rate up to approximately 850-900 °C where no further loss in weight is observed. The dehydration of the principal silicate and aluminate hydrates takes place over a wide range of temperatures, which may extend from around 105 °C, or less, to approximately 800 °C. The decomposition of the cement gel over such a wide temperature range makes the interpretation of the TG curves of cementitious materials particularly difficult (Taylor, 1984). Further, a weight loss peak in the TG curve at about 750-800 °C may occur which is usually attributed to the loss of  $\text{CO}_2$  due to the decarbonation of calcium carbonate ( $\text{CaCO}_3$ ) (Bazant and Kalpan, 1996).

The amount of evaporable and non-evaporable (chemically combined) water can therefore be calculated from the weight loss of the heated samples (Danielsson, 1972):

$$W_e = \frac{W_{20} - W_{105}}{W_{1050}} \quad (4.17)$$

where  $W_e$  is the quantity of evaporable water,  $W_{20}$  is weight of sample before drying,  $W_{105}$  is the weight of sample after drying or heating up to 105°C and  $W_{1050}$  is the weight of sample after ignition at approximately 1000°C.

The quantity of non-evaporable water  $W_n$  is given by:

$$W_n = \frac{W_{105} - W_{1050}}{W_{1050}} \quad (4.18)$$

The degree of hydration  $\alpha$  at a specific age is given by:

$$\alpha = \frac{W_n}{W_{nc}} \quad (4.19)$$

where  $W_{nc}$  is the non-evaporable water content at complete hydration, and  $W_n$  is the non-evaporable water content at a specific age.

Alternatively, the degree of reaction can be determined quantitatively by calculating the areas under the peaks of the derivative thermogravimetric curves, as these areas are proportional to the amount of reacting material (Murphy, 1958; Mackenzie, 1972). This approach affords a more detailed quantification of the degree of reaction than the simple determination of a single parameter such as the non-evaporable water content.

#### 4.7.2 Preliminary Investigation

Thermal analysis tests were initially planned to be conducted on a selection of concrete samples immediately after the curing period, and at the ages of 3 and 12 months. The aim of the first test was to establish a relationship between concrete curing efficiency and its degree of hydration. This required that the concrete blocks be cored in-situ, as at that stage blocks were being cast while others were curing. A portable corer was required for the job and since this was not available at the time, trials were made to obtain small cores using a large drill with a 20-mm core bit attachment. This, however, was not successful as rigid support was needed to enable correct coring and as a result, performing the test at that age was not possible.

The 3 months tests were preceded by trials, which were conducted on a Stanton Redcroft TG 750 furnace located in the Department of Chemistry of the University. The tests, however, were frequently interrupted by repeated breakdown of the instrument due to faults with the temperature controller and furnace balance, which eventually lead to the abandonment of the test. Work was subsequently resumed on a newer version of the instrument, a Stanton Redcroft TG 760, at the Institute of Polymer Technology and Materials Engineering (IPTME) of the University. Nevertheless, similar problems were encountered with this instrument, which resulted in frequent disruption of work and long periods of delay. As a result, the 3 months tests surpassed their intended testing age and the tests were abandoned. The instruments were relatively old and the problems encountered were mainly due to their generally impractical design, especially that of the balance systems and the sample pan assemblies (balance arm, the hang-down wire and the sample pan). This resulted in its over sensitivity to simple operations, such as the manual loading and unloading of the sample pan on and off the balance.

A decision was finally made to make use of a TGA system at the IPTME, which was mainly reserved for special work at the institute. The new instrument, the TGA 2950 module, was much superior to the two instruments in all respects. The instrument was much easier to operate, faster and produced very reliable results.

#### **4.7.3 Apparatus**

Thermogravimetric analysis (TGA) was carried out using a Hi-Res TGA 2950 system available in the Institute of Polymer Technology and Materials Engineering (IPTME) of the University. The instrument has three modes of operation, a conventional mode, a constant reaction rate Hi-Res mode and a Dynamic rate Hi-Res mode. The latter technique was used in this investigation. It differs from the traditional technique in that the heating rate of the sample is dynamically and continuously modified in response to

changes in the rate of decomposition of the sample so as to maximise weight change resolution. As the derivative of weight change (%/minute) increases, heating rate is decreased. The heating rate is constrained to the range 0.001 °C/minute (minimum) to the maximum specified in the ramp segment (up to 200 °C/minute). The system allows the use of very high maximum heating rates during Hi-Res (high-resolution) ramp segments while avoiding transition temperature overshoot. A mathematical function is used to relate the rate of weight change (%/minute) to the sample heating rate (°C/minute). Because the dynamic rate mode reduces heating rate smoothly and only when necessary, it is the fastest and most reliable of the various techniques. It gives good results with most temperature separable transitions.

The Hi-Res TGA 2950 module consists of five major components: the balance, the sample loading assembly, the furnace, the cabinet and the heat exchanger. The balance, the most important part of the TGA system, provides precise measurement of the sample weight. The sample loading assembly automatically loads and unloads samples from the TGA balance. The furnace controls the sample atmosphere and temperature. The cabinet contains the system electronics and mechanics. The heat exchanger dissipates heat from the furnace. The TGA 2950 system is shown in Figure 4.6.

#### **4.7.4 Sample Preparation**

Samples for the TGA test were taken from 3 surface discs so that measurement was taken at the average depths of 5, 10 and 20 mm from the surface. The analysis were restricted to the first 20mm from the surface based on the air permeability and sorptivity test results which revealed no significant change in properties beyond 20mm depth. Further, the test was performed on a selection of samples (see Chapter 5) due to limited access to the instrument and time constraints. The same discs that had been used for the air permeability and sorptivity tests were utilised for the TG test. The discs were dried immediately after the sorptivity test for 24 hours at 50 °C in a well-ventilated oven. They were then gently broken to remove the coarse and

any unidentifiable particles, and a fraction was then lightly ground using a small pestle and mortar to pass the 150 $\mu$ m sieve (the remainder of the disc was used for the MIP test). This sample preparation procedure is similar to that adopted by Litvan and Mayer (1986) in their TG investigations. The powder was then placed in a ventilated desiccator and left to condition over a sodium chloride solution and solid sodium hydroxide. The salt solution was used to provide a standard relative humidity of around 75 % for all the samples, and the solid calcium hydroxide was used to prevent carbonation of the cement paste (Young, 1967). The samples took approximately 5 to 7 days to reach constant weigh ( $\pm 0.1$  g in 24 hours). During that time, the desiccator was stored in a sheltered location in the laboratory where the ambient temperature was reasonably constant. The salt solution in the desiccator was agitated from time to time. The samples were then taken, in the desiccator, to the IPTME laboratory for testing.

#### **4.7.5 Test Procedure**

Before the test was started, the required operation mode was selected and the sample information and the test parameters were entered to the instrument controller, which was accessed through the instrument control screen. The instrument controller was linked to a PC integrated with the system. The samples were placed in platinum sample pans, which were then positioned on the sample platform. The sample platform can house up to 16 sample pans. Once the samples were in the platform, the Start button on the controller was pressed and each sample was automatically loaded onto the balance and the furnace then automatically moved up around the sample and the experiment was started. The sample loading operation to the starting of the test was done as quickly as possible to avoid any possibility of CO<sub>2</sub> contamination from the atmosphere.

The instrument operates within a temperature range of 25 to 1000 °C with a wide range of heating rates from 0.001 to 200 °C /minute. The maximum heating rate specified for the tests in this investigation was 50 °C per minute

in the dynamic Hi-Res Ramp mode. This means that the heating rate during the test varied from the minimum 0.001 °C/minute to the maximum specified i.e. 50 °C/minute, depending on the rate of weight change of the samples (%/minute). As sample heating was started, changes in the sample weight with temperature and time were recorded. The system operates on a null balance principle. Physically attached to a taut-band meter movement, the balance arm is maintained in a horizontal reference position by an optically actuated servo loop. When the balance is in a null position, a flag located on top of the balance arm blocks an equal amount of light to each of the photodiodes (the light is supplied by a constant current infrared LED). As sample weight is lost, the beam becomes unbalanced, causing an equal amount of light to strike the photodiodes. The unbalanced signal is acted upon by the control circuitry and reduced to zero, or nulled. This is accomplished by an increase or decrease in the current to the meter movement, causing it to rotate back to its original position (null position). The change in current necessary to accomplish this task is directly proportional to the change in mass of the sample. The current is converted to the weight signal. The samples were heated up to 900 °C (maximum allowed) at which most of the weight changes in the sample are expected to have occurred. The test was operated under a Nitrogen atmosphere. Thermogravimetric (TG) and derivative thermogravimetric (DTG) plots of the samples were printed automatically after the test.

## **4.8 MERCURY INTRUSION PROSOMETRY (MIP)**

### **4.8.1 Theoretical Background**

The mercury intrusion technique is based on the principle that a non-wetting liquid, i.e. a liquid forming a contact angle greater than 90° with a given solid, will only intrude the open pores of the solid under applied pressure. The technique was first introduced by Ritter and Drake (1945) for the determination of the distribution of the total pore volume and the total pore

surface area using mercury. The use of mercury as the intruding liquid is particularly advantageous because of its inertness in terms of chemical reactivity, its low vapour pressure and compressibility and the fact that its contact angle with most materials is greater than 90° (Winslow and Diamond, 1970). The technique with various modifications is currently widely used in the construction industry.

The technique involves forcing the mercury into the pores of the evacuated solid under applied pressure. The pressure is applied in single steps, and the pore volume corresponding to each pressure increment is obtained by the volume of mercury intruded. The equivalent pore diameter at each pressure step is calculated from the Washburn (1921) equation:

$$d = -\frac{4 \sigma \cos \theta}{P} \quad (4.20)$$

where  $d$  is the pore diameter corresponding to the applied pressure  $P$ ,  $\sigma$  is the surface tension of mercury and  $\theta$  is the contact angle between mercury and the solid.

A possible source of error in the porosity measurement by this technique is the limitation inherent in the assumption that the intruded pores are cylindrical in geometry, which forms the basis of the porosity calculations. Numerous researchers found that mercury intrusion and extrusion curves do not coincide with each other (e.g. Ritter and Drake, 1945; Winslow and Diamond, 1970). This was attributed to the entrapment of mercury in pores with entryways narrower than the pore itself. These large pores, which are only accessible through their narrow entryways, are intruded at higher pressure and will invariably be classed as smaller diameter pores on the basis of the pore entry pressure applied.

Furthermore, due to pressure limitation, pores with very narrow diameter or entryways cannot be intruded and will not therefore be measured. Similarly, pores that are isolated cannot be measured regardless of the applied pressure.

#### 4.8.2 Preliminary Investigation

Interest in concrete porosity and pore structure increased over the years as a result of its well-established association with concrete's engineering properties such as its strength and durability. With reference to durability, correlation between concrete permeability and its pore structure characteristics was often inferred through the study of neat cement paste systems, commonly investigated by the MIP technique (e.g. Mehta and Manmohan, 1980; Nyame and Illston, 1980). Further work using MIP and other techniques (e.g. optical and imaging techniques) revealed that the pore structure of pure cement pastes is different from that developed in the presence of fine or coarse aggregates (e.g. Winslow and Liu, 1990; Young, 1988; Feldman, 1986). The presence of coarse and fine aggregates was shown to increase the pore volume; change the pore size distribution and the connectivity of the pores (e.g. Winslow et al, 1994; Karen and Kamran, 1996; Marchand et al, 1996). However, despite the reported differences between the cement paste and concrete microstructures, most of the reported MIP investigation work is still carried out on ideal, homogeneous, laboratory made materials like neat cement pastes, with the findings implied to concrete. Work on cement mortar instead of cement pastes is intended to give closer understanding to concrete pore structure, however, the materials, sample sizes, mixing, curing and exposure conditions in these investigations are invariably completely divorced from real life concrete (e.g. Bagel and Zivica, 1997; Halamickova and Detwiler, 1995). The difficulties in investigating pore structure properties of representative concrete are apparent. However, with the current state of knowledge and technology, more effort should have been channelled towards the development of techniques and instruments that enable a more practical assessment of concrete internal structure.

As previously stated, the aim of the pore structure investigation in this work was mainly to try to explain the durability related properties of concrete in light of its porosity and pore size distribution and assess the correlation that may exist between them. In view of the practical considerations discussed

above, and to achieve the aims of the study, it was decided that pore structure investigation on especially made companion cement paste or mortar samples would not be relevant. Limitation with the MIP instrument with regard to the maximum sample size that can be tested meant that no representative sample of concrete could be investigated. Therefore, a sampling technique followed by some workers, e.g. Litvan and Meyer (1986), whereby the coarse aggregates are removed from small concrete samples that have been extracted from site concrete was considered the most practical alternative and was adopted as will be described later.

As with the other tests in this investigation, the original plan was to conduct the MIP test after 3 and 12 months of concrete exposure, on a limited number of samples. However, work on the instrument, which was originally located in the Civil Engineering laboratories, was not possible due to the enforcement of new safety regulations concerning working with, and the handling of mercury. The new regulations required special ventilation arrangement to be made to ensure that poisonous mercury vapour does not accumulate beyond certain levels in the work place. Other safety regulations required adequate measures be made to deal with mercury spillage and the safe storage and disposal of the mercury filled samples after the test. This required elaborate alteration works to be carried out in the Civil Engineering laboratories that were considered not practical and, therefore, a suitable location in the University was sought where these safety regulations could be met. During this time (several months), the proposed 3 months tests could not be carried out. The instrument was eventually located in the Department of Chemistry laboratories where facilities were adequate to meet the required safety standards.

Work on the instrument subsequently showed that the set safety regulations were warranted. Incidents of mercury spillage are unavoidable and did occur, in one occasion, during the tests. Correct safety procedures were followed to initially contain the mercury and then safely dispose of it. The incident was

then reported and safety checks were carried out to ensure that the instrument and the work place were safe.

### 4.8.3 Apparatus

The porosity measurements were determined using a Micromeritics Autopore 9310 located in the Chemistry Department of the University. The instrument has a maximum pressure capacity of 207 MPa and it calculates pores volume and their distributions in the range 300 to 006  $\mu\text{m}$ . The instrument consists of two low pressure and a high pressure station that enables sample analysis of both macro and micro pores. In the low-pressure stations, the samples were pressurised up to 0.17 MPa and the mercury intrusion level was measured. The samples in the third high-pressure station were pressurised up to 207 MPa and the volume of mercury intruded was measured in the same time. The reduction in height of the mercury column in the penetrometer capillary, as mercury is forced into the samples, was measured by means of three pressure capacitance transducers. These measure the change in electrical capacitance of a cylindrical coaxial capacitor formed by an outer metallic film around the penetrometer stem and the inner capillary of mercury. The penetrometer is a dilatometer like sample holder, which houses the samples tested. A typical penetrometer assembly is shown in Figure 4.7.

In the low-pressure test, pressure is increased from vacuum levels up to 0.21 MPa. This is achieved by means of a solenoid valve that allows dry air to be admitted, thus gradually elevating the pressure. Pressure measurement is provided by a 0–0.21 pressure transducer mounted on the low-pressure chamber assembly. The low-pressure tests are done manually. High-pressure measurement is accomplished with a ram generator driven by a ball screw which is, in turn, driven by a small universal type gear motor. The controls allow precise setting of desired pressures with ease. The system is integrated with an IBM compatible computer that logs and saves all the information about the sample, which was entered manually. The high-pressure test is

controlled by the computer and run automatically. Figure 4.8 shows the apparatus.

#### 4.8.4 Sample Preparation

Samples for the pore sizer were small prisms cut from the 3 surface discs that were used for the TG test. The porosity measurements, therefore, were also taken at the average depths of 5, 10 and 20 mm from the surface. As stated earlier, testing was confined within 20mm from the surface based on the air permeability and sorptivity results that revealed no significant change in properties beyond this depth. The 3 surface discs were dried in an oven at 50 °C for 24 hours immediately after the sorptivity test was completed. They were then gently broken and small prisms from the centre of the discs were cut after the removal of the coarse aggregates (a fraction of the disc was taken for the TG test). Similar sample preparation procedures were adopted in recent concrete and mortar MIP investigations (Jacobs and Mayer, 1992; Halmicova and Detwiler, 1995; Marchand et al, 1996). The samples were then placed in a well-ventilated oven to dry at 105 °C for 24 hours. Rigorous drying is necessary to ensure complete emptying of the pores prior to mercury intrusion (Winslow and Diamond, 1970). The samples were then cooled in a desiccator over fresh silica gel for 24 hours before they were taken to the Chemistry Department laboratory for testing.

Although the porosity values are expressed as percentages of sample volume, testing samples of random sizes and shapes and from random locations in the discs produced variable results. This was caused by the ill-defined cement weight in these small samples due to the presence of the fine aggregates. After many trials, increasing the equilibrium time at each intrusion step from 15 to 30 seconds, as well as the sampling procedure adopted, was seen to improve the re-productability of the results.

#### 4.8.5 Test Procedure

Each dried sample was weighed and loaded into the penetrometers, which were sealed and weighed again. The penetrometers were then inserted into the two low-pressure ports. Appropriate data relating to samples' weights, pressure tables, mercury density, contact angle, surface tension etc were entered by the key board for each penetrometer and the low pressure test is started. A mercury contact angle of  $130^\circ$  with a surface tension value of 485 dyne/cm were used as recommended by the manufacturer of the instrument. The instrument evacuates the samples automatically. When the pressure reaches  $50\mu\text{m}$  or has stabilised below that, mercury filling was started. The low-pressure test was then started by increasing the pressure manually in stages and prompting the computer to take record of the intrusion at each stage up to 0.17 MPa. At this stage the penetrometers were removed from the low-pressure chambers and weighed. Additional information was then entered into the computer and the high-pressure test was started. The instrument automatically increased the pressure in increments, as per the specified pressure table, up to 207 MPa. Upon completion of the high-pressure test, data from the low and high-pressure runs were combined and a full report was automatically produced.

**Table 4.1** Effect of sample size on the sorptivity (100 and 55mm values are the average sorptivity values from 3 samples)

Disc diameter x 20mm long	sorptivity (mm/min <sup>0.5</sup> )									
100 mm	0.061	0.087	0.139	0.160	0.151	0.118	0.118	0.173	0.177	0.165
55 mm	0.064	0.073	0.136	0.140	0.153	0.095	0.128	0.149	0.149	0.149
Mean	0.063	0.080	0.138	0.150	0.152	0.106	0.123	0.161	0.163	0.157
STDEV	0.00155	0.007	0.00135	0.0099	0.00085	0.0113	0.00485	0.012	0.01405	0.00795
Coefficient of variation (%)	2.5	8.7	1.0	6.6	0.6	10.6	4.0	7.4	8.6	5.1

**Table 4.2** Effect of drying regime on the sorptivity - approximately 14 days drying at 50 degrees C

Drying	sorptivity (mm/min <sup>0.5</sup> )									
First drying	0.056	0.055	0.124	0.116	0.132	0.032	0.037	0.112	0.117	0.150
Second drying	0.052	0.051	0.147	0.118	0.154	0.033	0.043	0.134	0.124	0.161
Third drying	0.063	0.058	0.176	0.141	0.188	0.039	0.049	0.170	0.158	0.204
Mean	0.057	0.055	0.149	0.125	0.158	0.035	0.043	0.139	0.133	0.172
STDEV	0.0046397	0.0025962	0.0212306	0.0113226	0.0227615	0.0034586	0.0045746	0.0235708	0.0179222	0.0233023
Coefficient of variation (%)	8.1	4.7	14.2	9.1	14.4	10.0	10.6	17.0	13.5	13.6

**Table 4.3** Equilibrium weight after each drying cycle (before the sorptivity test was started)

Drying	sample weight (g)									
First drying	64.64	112.95	108.44	106.81	104.49	72.05	107.72	106.40	106.48	105.27
Second drying	64.68	112.77	108.28	106.55	104.35	71.96	107.51	106.81	106.20	105.06
Third drying	64.37	112.21	107.76	105.95	103.85	71.60	106.98	105.62	105.57	104.43

**Table 4.4** Effect of removal of the top surface (0.5mm) of the samples (discs)

Disc surface	sorptivity (mm/min <sup>0.5</sup> )									
Before sawing surface of disc	0.244	0.135	0.189	0.203	0.145	0.133	0.133	0.107	0.023	0.153
After sawing surface of disc	0.231	0.137	0.176	0.191	0.155	0.144	0.144	0.106	0.026	0.168
Mean	0.238	0.136	0.183	0.197	0.150	0.138	0.138	0.107	0.025	0.161
STDEV	0.0065	0.0012	0.00675	0.006	0.00505	0.00585	0.00595	0.0007	0.0012	0.00755
Coefficient of variation (%)	2.7	0.9	3.7	3.0	3.4	4.2	4.3	0.7	4.9	4.7

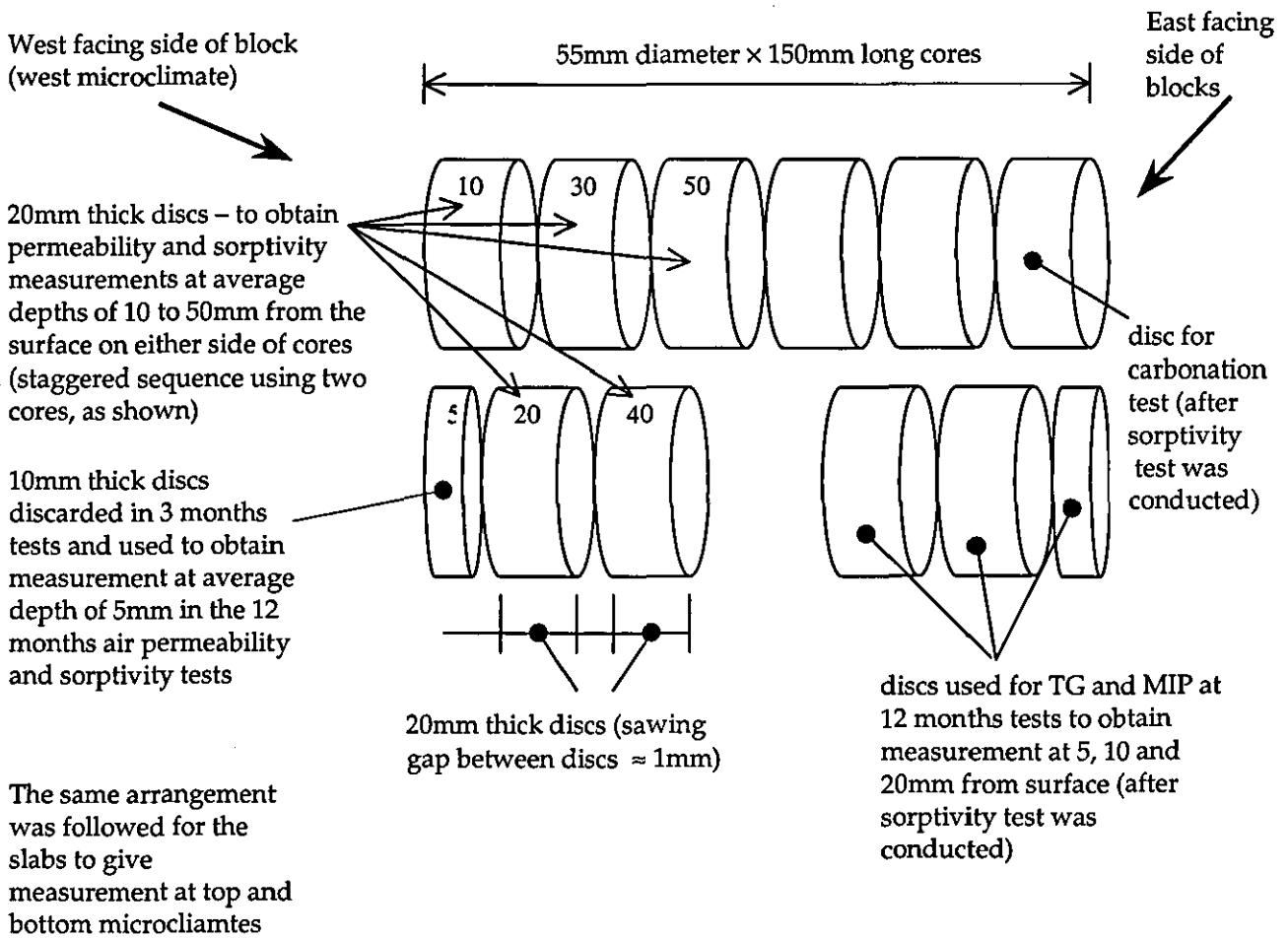


**Fig. 4.1** Method of slicing cores and location of discs for the tests

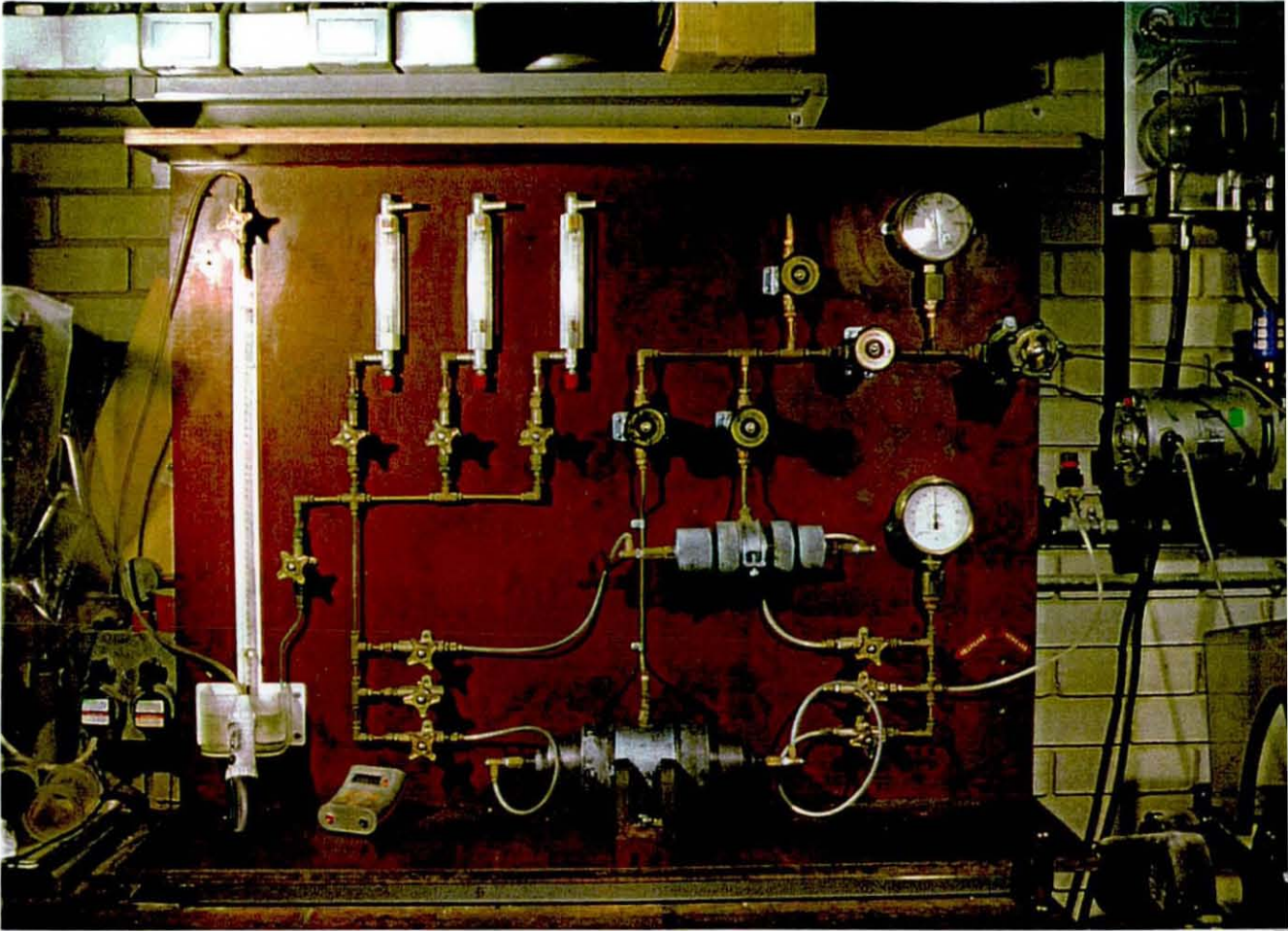


Fig. 4.2 Air permeability test apparatus

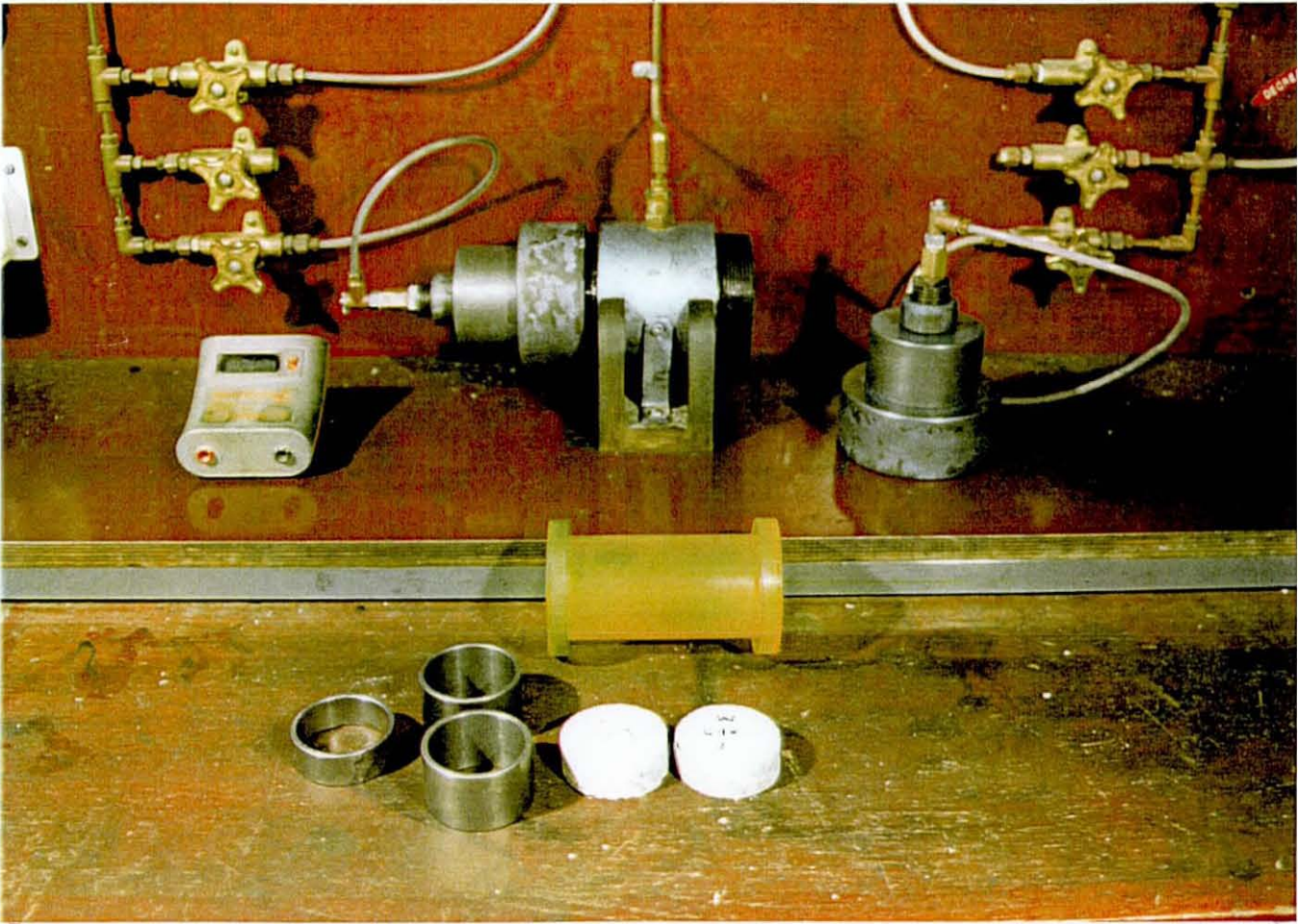


Fig. 4.3 Air permeability test specimen and sleeve



Fig. 4.4 Sorptivity test apparatus



Fig. 4.5 Depth of carbonation by phenolphthalein pH indicator

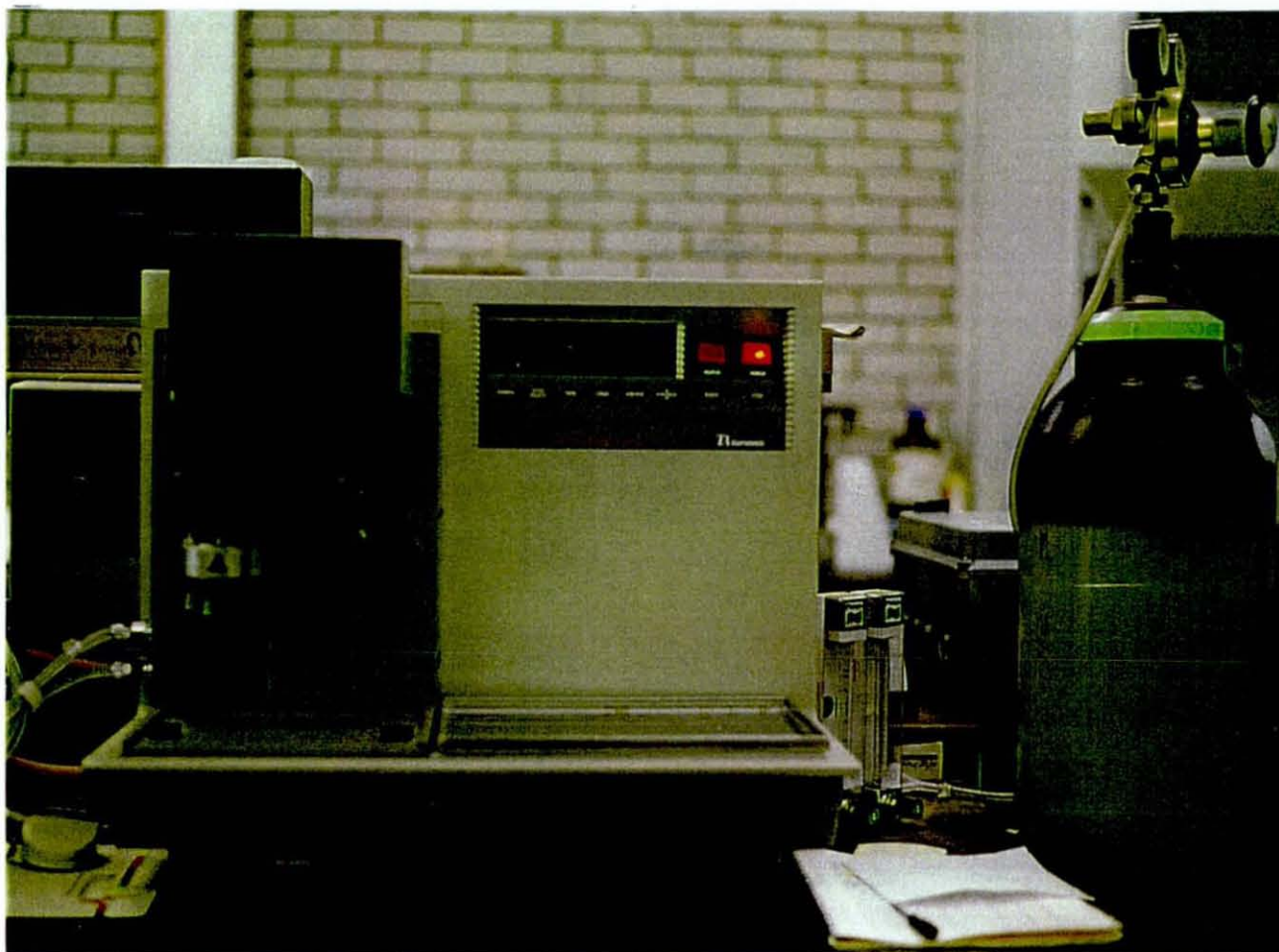


Fig. 4.6 Thermogravimetric analysis system

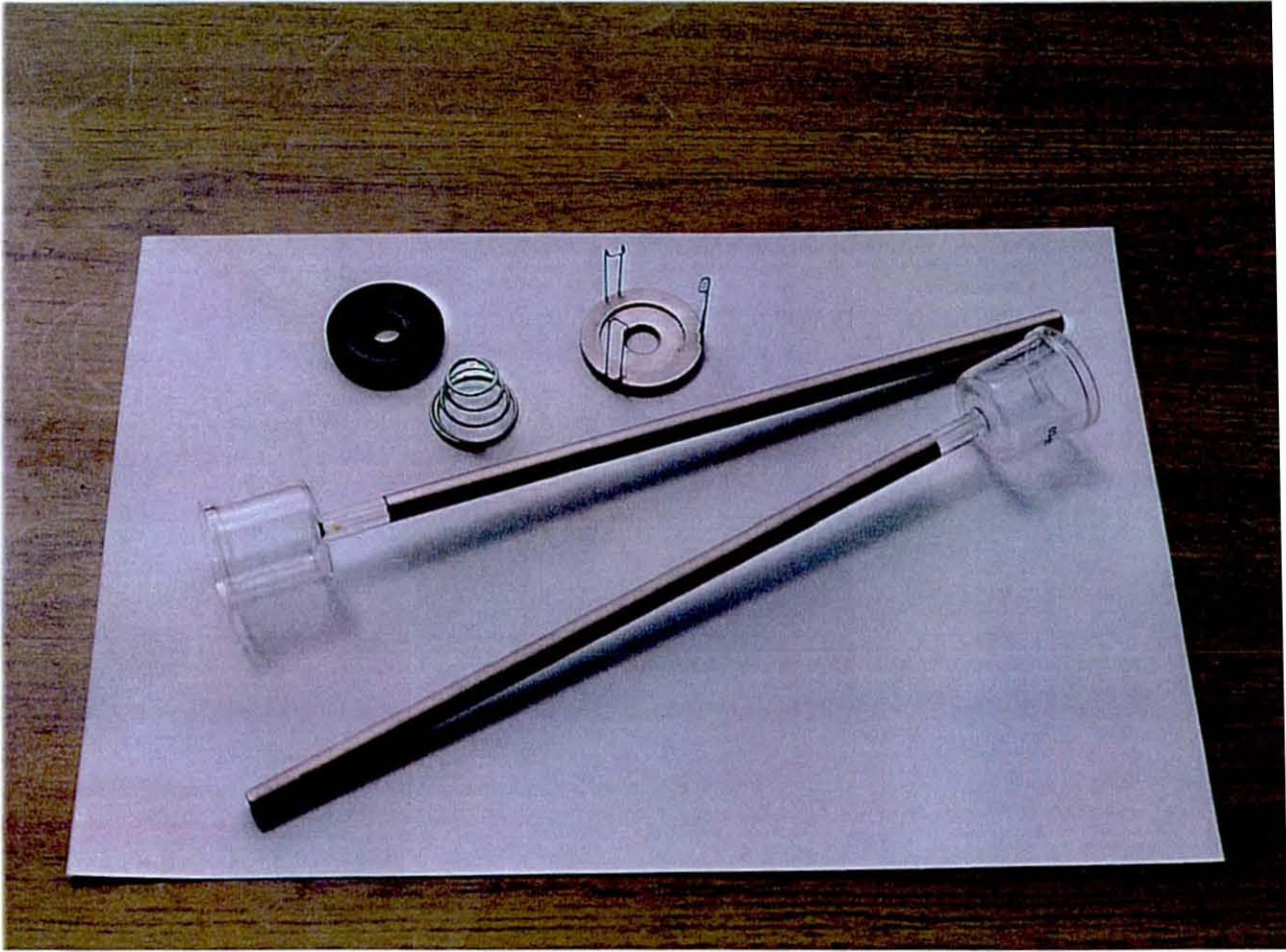


Fig. 4.7 Penetrometer assembly



Fig. 4.8 Mercury intrusion porosimeter

## Chapter 5 Loughborough Winter Climate

---

### 5.1 INTRODUCTION

In this chapter, the results of the four tests adopted in the investigation of the Loughborough winter series are presented. The effect of hessian curing duration, microclimate and exposure time on the three concrete mixes that constitute the winter series (30 and 50 MPa OPC concrete mixes and a 30 MPa OPC/GGBS concrete mix) are reported. A detailed discussion of the results and trends of the winter series is given in Chapter 8. The winter series was tested at the ages of 3 and 12 months. Three main tests were conducted when the concretes were 3 months old and four at 12 months old. These are: air permeability, sorptivity, carbonation depth and thermal analysis by thermogravimetry (TG) (the first 3 were conducted at 3 months and all 4 at 12 months). In addition, standard 28 days compressive strength tests were carried out throughout the investigation for quality verification and control.

The winter tests were conducted on the samples that were extracted (cored) from the concrete blocks that were cast in the winter. At the age of 3 months, the concrete blocks were transported from the exposure site to the laboratory for testing. The blocks were cored, sliced and conditioned as described in detail in chapter 4, before the tests was conducted. Immediately after coring, the blocks were returned to the site for a further exposure period of 9 months. At the age of 12 months, the blocks were transported back to the laboratory for the 12 months tests, and the same preparation and testing procedures were followed.

## 5.2 WEATHER DATA

Tables 5.1 and 5.2 give the average weekly and monthly temperature, relative humidity, wind speed and direction during the curing period and first 3 months of exposure respectively, for the three concrete mixes in the winter series. The quoted average monthly wind direction is an approximation calculated on the basis of the combined daily wind speed and direction.

The average temperature and relative humidity during the initial curing period (first week of exposure) of the 30 MPa OPC and OPC/GGBS concretes were similar (average 5 °C), and notably lower during the curing period of the 50 MPa OPC concrete. The relative humidity during the initial curing and throughout the first 3 months of exposure for the three concretes was similar. The wind speed during the curing period of the mixes was low (average 3 m/s). The prevailing wind direction during the initial curing period was mainly easterly. During the first 2 months of exposure, the prevailing wind direction was easterly to south easterly, changing to south westerly in the third month. The rainfall was negligible during the curing and initial period of exposure. The Loughborough temperature and relative humidity data for the whole exposure year (1996) are plotted in Figure 5.1.

## 5.3 COMPRESSIVE STRENGTH

The compressive strength test results of the Loughborough winter series are given in Tables 5.3. As mentioned earlier, the average of three tests for each concrete batch was taken and the total average for each concrete mix in the three series was then reported (average of six cubes). The compressive strength results for the three concretes showed low mix-to-mix variation, indicating no significant mix differences between blocks. The coefficients of variation for all mixes were within 3-9%.

## 5.4 AIR PERMEABILITY

### 5.4.1 Introduction

The air permeability test method, the apparatus and the sample preparation for the test are described in detail in Chapter 4, Section 4.2.

The coefficient of air permeability  $k$  ( $m^2$ ) was calculated from equation (4.4). The air permeability calculations were based on an average of three flow rate determinations. The repeatability of the test was excellent with coefficients of variation within 2%. The reproducibility of the test was evaluated by testing duplicate samples taken from another pair of cores adjacent to the position of the original cores from the same concrete block. The reproducibility of the test varied in the surface layers (0-20mm) from that taken at depths below. The coefficient of variation of the surface and subsurface samples therefore varied widely as shown in the air permeability tables of the winter series given in Appendix A, Tables A1.1 to A1.6, but was on average within 20% and 10% at the surface and subsurface zones respectively.

It is apparent from the graphs that the air permeability was higher at the layers immediately near the surface than the sub-surface layers. The cover zone, i.e. the area extending from the surface to approximately 50-60mm below, could distinctly be divided into two regions or sub-zones: the surface and sub-surface zones. For brevity, the region extending from the surface down to around 15-20 mm was designated as the surface zone (SZ) and that from 20-50mm from the surface as the sub-surface zone (SSZ).

It was interesting to note that regardless of microclimate (orientation) or hessian curing duration, the curing profiles of the blocks in the sub-surface zone (SSZ) were similar in magnitude (small variation) and often followed identical trends in each orientation, at both ages. The variations in the permeability values at the SZ, on the other hand, were larger and the different curing profiles often followed a distinctly independent trend.

Based on the above, Figures 5.4 and 5.5 were plotted to show the effect of curing duration on the surface and sub-surface zones of the samples. The surface curves were based on the single surface values plotted for each curing duration, from 0 to 6 days. The sub-surface zone curves were plotted by calculating the average values from 20-50mm deep, for each curing duration. A complete listing of the coefficients of air permeability with depth and curing of the winter series is given in Tables A1.1 to A1.6 in Appendix A.

The 3 month air permeability values of the 3 concretes were, on average, 20-25% higher at the SZ (10mm) than the SSZ. The difference in magnitude between SZ and SSZ was more pronounced in the OPC/GGBS concrete and least apparent in the 50 MPa OPC concrete.

The 12 months test results revealed a change in the surface (SZ) and subsurface zones (SSZ) profile trends of the two OPC concretes. Unlike the 3 months results (the samples of which were extracted from the same concrete blocks), the SZ values in the majority of samples were lower than the SSZ values. This effect was prevalent, in particular, at 5-mm depth from the surface of the 30 MPa OPC concrete. The coefficients of air permeability of the 30 MPa OPC concrete, however, were generally higher at the SZ from 10 to 20 mm than the SSZ, despite the slight drop at the 5-mm depth.

The coefficients of air permeability of the 30 MPa OPC concrete at 12 months were 15-30% higher at the SZ than the SSZ (Figures 5.3 & 5.9 (a) and (b)). The difference was much smaller for the top and bottom faces of the slabs (0-15%). The variations between the SZ/SSZ of the 50 MPa OPC concrete were very small.

Contrary to the two OPC concretes, the coefficient of air permeability of the 30 MPa OPC/GGBS concrete remained higher at the SZ (5-20mm) than the SSZ at 12 months. Furthermore, the difference in magnitude between the SZ and SSZ indices increased, since the improvement in SZ indices with age was small. The SZ air permeability indices at 12 months were, on average, 30-50% higher than the SSZ, compared to 20-25% at 3 months.

#### 5.4.2 30 MPa OPC Concrete

##### *Microclimate*

Figures 5.2 and 5.3 show the effect of microclimate on the air permeability profiles of the 30 MPa OPC concrete samples at the ages of 3 and 12 months respectively. The results with statistical analysis are presented in Appendix A, Tables A1.1 and A1.2 (a) & (b), for the 3 and 12 months tests respectively.

The results show that the east facing surfaces (east faces) of the vertical concrete blocks were more permeable than the west facing surfaces (west faces), and the bottom surfaces of the slabs (bottom faces) were more permeable than the top surfaces of the same slabs (top faces).

At 3 months of age, the east faces of the vertical blocks were, on average, 25% more permeable than west faces at the SZ and SSZ.

The bottom faces of the slabs were approximately 50 and 20% more permeable in the SZ and SSZ respectively, than the top faces (Figure 5.2 (c) and (d)).

The influence of microclimate on the samples remained unchanged after 12 months of field exposure. The east faces of the vertical blocks were more permeable than the west faces, as can be seen from the graphs in Figure 5.3 (a) and (b). The coefficients of air permeability in the SZ of the east faces were approximately 50% higher than the west faces. In the SSZ, the permeability indices were, on average, 30% higher in the east than the west faces.

Similarly, from Figure 5.3 (c) and (d), the bottom faces were approximately 40 and 20% more permeable at the SZ and SSZ respectively, than the top faces of the slabs.

The difference in the coefficients of air permeability due to microclimate exposure was higher at the SZ than the SSZ in all samples.

### *Duration of hessian curing*

The relationship between air permeability and curing duration of the 30 MPa OPC concrete at the ages of 3 and 12 is presented in Figures 5.4 and 5.5 (a) and (b), respectively.

Contrary to what might be expected, there generally was no improvement in the air permeability of the samples with increased curing duration at 3 months of age. Further, the air permeability values in some instances increased as hessian-curing duration was increased.

The 12 months tests revealed no significant change in the relationship between air permeability and curing duration. There was generally no clear improvement in the air permeability due to increased hessian curing duration. The coefficients of air permeability in some instances increased with increased curing duration, especially at the SSZ (Figures 5.3 and 5.5 (a) & (b)). This effect was most apparent in the top faces of the slabs where the air permeability at both, the SZ and SSZ, increased with increased hessian curing duration from 0-6 days

### *Age*

Figures 5.6 and 5.7 illustrate the typical relationship between air permeability and age at the SZ and SSZ respectively.

The coefficients of air permeability of the concrete blocks were lower at 12 months than 3 months, at both the SZ and SSZ. At 12 months, there was an average of 45% improvement in the air permeability indices (lower permeability) of the east and west faces of the blocks, and over 55% improvement in the top and bottom faces, compared to the results obtained at 3 months. In general, the coefficients of air permeability of the 12 months old blocks were about two times lower than they were at the age of 3 months. Further, the difference in magnitude between the SZ and the SSZ values (in each microclimate) after 12 months of field exposure was also smaller compared to the 3 months results. The gap between the SZ and SSZ was reduced by approximately 10% in the east and west faces after 12 months of

exposure. The reduction was approximately 20% in the top and bottom faces of the slabs.

### 5.4.3 50 MPa OPC Concrete

#### *Microclimate*

Figures 5.8 and 5.9 show the effect of microclimate on the air permeability profiles of the 50 MPa OPC concrete samples at the ages of 3 and 12 months respectively. The results with statistical analysis are presented in Appendix A, Tables A1.3 and A1.4 (a) & (b), for the 3 and 12 months tests respectively.

There was no significant difference in the air permeability indices between the east and west faces of the vertical blocks at the age of 3 months. However, the bottom faces of the horizontal blocks (slabs) were approximately 35% and 15% more permeable than the top faces at the SZ and SSZ respectively.

At 12 months, the east faces of the blocks were, on average, 30 and 20% more permeable than the west faces, at the SZ and SSZ respectively. This difference, however, is not obvious from the graphs because of the very low permeability indices of the 50 MPa OPC concrete (see Table A1.4 (a)). The results of the 3 concrete mixes in this series (30 MPa OPC, 50 MPa OPC and 30 MPa OPC/GGBS concrete) were drawn on the same scale for ease of comparison.

Similarly, the bottom faces of slabs were approximately 65 and 30% more permeable than the top faces at the SZ and SSZ respectively. Despite the overall improvement in the permeability of the samples in the 4 microclimates with age, the microclimate influence became more distinct with age.

#### *Duration of hessian curing*

The relationship between air permeability and curing duration of the 50 MPa OPC concrete at the ages of 3 and 12 is presented in Figures 5.4 and 5.5 (b) and (c), respectively.

The 3 months results showed no improvement in the coefficients of air permeability of the samples with increased curing duration. Instead, the air permeability indices of the concrete blocks increased at the SZ and SSZ as

curing duration was increased from 0-6 days by more than 50%, in the 4 microclimates.

The effect of curing duration on the air permeability remained similar with age (Tables A1.3 and A1.4, Appendix A). At 12 months of age, the air permeability indices of the non-cured blocks of east and west faces were, on average, 20% lower than the 6 days cured blocks at the SZ and SSZ.

The coefficient of air permeability of the non-cured top and bottom faces of the slabs were, on average, 50% lower than the 6 days cured faces at both, the SZ and SSZ.

#### *Age*

The relationship between air permeability and age of the 50 MPa OPC concrete is shown in Figures A1.1 and A1.2 in Appendix A, for the SZ and SSZ respectively.

The coefficients of air permeability of the 12 months old blocks were, on average, 50 and 60% lower than the 3 months results at the SZ and SSZ respectively, in the 4 microclimates.

#### **5.4.4 30 MPa OPC/GGBS Concrete**

##### *Microclimate*

Figures 5.10 and 5.11 show the effect of microclimate on the air permeability profiles of the 30 MPa OPC/GGBS concrete samples at the ages of 3 and 12 months respectively. The results with statistical analysis are presented in Appendix A, Tables A1.5 and A1.6 (a) & (b), for the 3 and 12 months tests respectively.

The variation in the air permeability due to microclimate on the OPC/GGBS concrete blocks was not clear at 3 months. The microclimate influence after 12 months exposure, however, was much more apparent. The east faces of the vertical blocks were more permeable than the west faces, as shown in Figure 5.11 (a) and (b). The coefficient of air permeability being higher in the east

faces by approximately 30% than the west faces at the SZ. The SSZ indices of the two faces were generally comparable.

Similarly, the bottom faces of the slabs were more permeable than the top faces by approximately 20 and 30% at the SZ and SSZ respectively (Figure 5.11 (c) and (d) and Tables A1.5 & A1.6, Appendix A).

It is worth to note that while the microclimate influence was evident on the 30 and 50 MPa OPC concrete at 3 months, it was not clearly established on the 30MPa OPC/GGBS concrete at this age. However, this influence became distinct with age as seen in the 12 months results.

#### *Duration of hessian curing*

The relationship between air permeability and curing duration of the 30 MPa OPC/GGBS concrete at the ages of 3 and 12 is presented in Figures 5.4 and 5.5 (e) and (f), respectively.

Similar to the two OPC concretes, no improvement in the air permeability was observed with increased hessian curing duration. Further, the increase in the air permeability values with increased hessian curing duration was more pronounced in the slag concrete than was in the two OPC concretes. In virtually the 4 microclimates, the air permeability of the 4 and 6 days blocks were higher by approximately 20-40% compared to the 0 and 2 days cured blocks at the age of 3 months.

Like the 3 months results, the air permeability at 12 months was higher in the 4 and 6 days cured blocks than the 0 and 2 days cured blocks. Unlike OPC concrete, the higher air permeability values with increased duration were more distinct in the SZ than the SSZ. Although there was a slight improvement in the air permeability of the 0 and 2 cured blocks with age at the SZ, the permeability of the 4 and 6 days hessian cured blocks deteriorated further with age. The 4 and 6 days cured blocks being, on average 30-50% more permeable than the 0 and 2 days cured blocks at the SZ.

## Age

The relationship between air permeability and age of the 30 MPa OPC/GGBS concrete is shown in Figures A1.3 and A1.4 in Appendix A, for the SZ and SSZ respectively.

Except for the east facing surfaces of the blocks, the air permeability of the slag concrete reduced with age at both, the SZ and SSZ. The coefficients of air permeability of the east faces at 12 months were 10-50% higher at the SZ, compared to the 3 months results (Figure A1.4 (a)). The air permeability of the west faces were, on average, 20 and 10% lower at the SZ and SSZ respectively compared to 3 months.

Similarly, the SZ and SSZ indices of the slabs were, on average, 20 and 50% lower at 12 months respectively, compared to the 3 months concrete.

## 5.5 SORPTIVITY

### 5.5.1 Introduction

The sorptivity test methodology, the apparatus and the sample preparation for the test are described in detail in Chapter 4, Section 4.3.

The water sorptivity,  $S$ , was calculated in accordance with the procedure described by CEN/TC 104/SC8 (1995) and Hall (1989). Accordingly, the sorptivity was obtained by plotting the cumulative capillary absorption (volume) per unit area of inflow surface results  $i$  (equation (4.10), Chapter 4) against the square root of immersion time. The plot conformed well to equation (4.11). The best-fit lines were linear with correlation coefficients  $r > 0.99$  in all cases. Typical sorptivity plots of samples and their duplicates (reproducibility samples) are shown in Figure 5.12 and 5.13 respectively. A selection of sorptivity plots, showing the sorptivity and intercept values for the 3 concretes are given in Figures A1.5 to A1.8 in Appendix A.

The repeatability of the test was evaluated by repeating the standard sorptivity measurements 3 times on a large selection of discs from different

mixes. The discs were dried to equilibrium (approximately 14 days) after each test in a ventilated oven at 50 °C (the drying regime adopted throughout the investigation). The coefficient of variation was within 10% in most cases (see Table 4.2).

The reproducibility of the test was evaluated by testing duplicate samples taken from another pair of cores adjacent to the position of the original cores from the same concrete block (the same duplicate samples that were initially used for the air permeability test). Figure 5.13 shows typical reproducibility results obtained from duplicate samples taken from the 30 MPa OPC concrete block (compare with Figure 5.12). The coefficient of variation between duplicate samples varied widely with depth from the surface, with it being in most cases within 10%, as shown in the sorptivity results, Tables A1.7 to A1.12 in Appendix A.

At 3 months, the sorptivity indices of the east and bottom faces of the 3 concretes were slightly higher at the SZ (approximately 10%) than SSZ. The sorptivity profiles of the west and top faces of the 3 concretes were generally flat with no notable distinction between the SZ and SSZ sorptivity indices. The variation in the sorptivity in the SSZ was small in all cases.

As with the air permeability results, the 12 months sorptivity results revealed a change in the surface SZ profile' trends of the two OPC concretes, while that of the OPC/GGBS concrete remained unchanged. The sorptivity indices of the two OPC concrete being, on average, more than 50% lower at the SZ (10mm) than the SSZ in all samples. For the OPC/GGBS concrete, however, the sorptivity indices were, on average, 17% higher at the SZ than the SSZ, in the 4 microclimates.

## **5.5.2 30 MPa OPC Concrete**

### *Microclimate*

Figures 5.14 and 5.15 show the effect of microclimate on the sorptivity profiles of the 30 MPa OPC concrete samples at the ages of 3 and 12 months

respectively. The results with statistical analysis are presented in Appendix A, Tables A1.7 and A1.8, for the 3 and 12 months tests respectively.

The 3 months sorptivity indices of east and bottom faces at the SZ were, on average, 20% higher than the west and top faces of the blocks respectively. The differences in the sorptivity indices due to microclimate at the SSZ were marginal.

At 12 months, the sorptivity indices of the east faces were, on average, 30 and 10% higher than the west faces at the SZ and SSZ respectively. The sorptivity of the bottom faces of the slabs were, on average, 15 and 10% higher than the top faces at the SZ and SSZ respectively.

#### *Duration of hessian curing*

The relationship between the sorptivity and curing duration of the 30 MPa OPC concrete at the ages of 3 and 12 is presented in Figures 5.16 and 5.17 (a) and (b), respectively.

The 3 months results showed an average reduction in the sorptivity of 20% with increased curing duration of the east and west faces, at the SZ and SSZ. Similarly, the sorptivity indices of the top faces improved by 15% with increased hessian-curing duration at the SZ. However, the sorptivity indices of the bottom faces of the slabs increased by approximately 20% with increased hessian curing duration (0-6 days) at both, the SZ and SSZ.

After 12 months of field exposure, the sorptivity of the 6 days hessian cured blocks was, on average, 10% lower than the non-cured blocks, in the 4 microclimates.

#### *Age*

The relationship between the sorptivity and age of the 30 MPa OPC is shown in Figures 5.18 and 5.19, for the SZ and SSZ respectively.

The sorptivity indices of the concrete blocks were, on average, 30% lower at 12 months than 3 months at the SZ.

Surprisingly, the sorptivity indices at the SSZ of the east and west faces were slightly higher at 12 months than 3 months (Figure 5.21, (a) and (b)). This is in contradiction with the air permeability results of the same concrete samples, which showed a reduction of almost 50% in the permeability indices after 12 months of field exposure.

### 5.5.3 50 MPa OPC Concrete

#### *Microclimate*

Figures 5.20 and 5.21 show the effect of microclimate on the sorptivity profiles of the 50 MPa OPC concrete samples at the ages of 3 and 12 months respectively. The results with statistical analysis are presented in Appendix A, Tables A1.9 and A1.10 (a) & (b), for the 3 and 12 months tests respectively.

Similar to the air permeability results, the influence of microclimate on the 50 MPa OPC concrete at 3 months of age was not significant. There was no notable difference in the sorptivity indices between the east and west faces of the vertical blocks. The sorptivity indices of the bottom faces were, on average, 10% higher than the top faces of the slabs at the SZ. The difference in the sorptivity indices between the two faces at the SSZ was very small.

The influence of microclimate on the sorptivity was more determined at 12 months. The sorptivity indices of the east faces of the blocks were, on average, 30 and 10% higher than the west faces, at the SZ and SSZ respectively.

Similarly, the sorptivity of the bottom faces of slabs was approximately 15% more permeable than the top faces at the SZ and SSZ.

#### *Duration of hessian curing*

The relationship between the sorptivity and curing duration of the 50 MPa OPC concrete at the ages of 3 and 12 is presented in Figures 5.16 and 5.17 (b) and (c), respectively.

As with the air permeability results, the 3 months sorptivity results showed an increase with increased curing duration. The sorptivity indices of the

concrete blocks increased at the SZ and SSZ as curing duration was increased from 0-6 days by 10-15%, in the 4 microclimates.

The effect of curing duration on the sorptivity of the 50 MPa OPC concrete remained largely similar after 12 months of field exposure. The sorptivity indices of the 4-6 days cured blocks were generally 5-10% higher than the 0-2 days cured blocks.

#### *Age*

The relationship between the sorptivity and age of the 50 MPa OPC concrete is shown in Figures A1.9 and A1.10 in Appendix A, for the SZ and SSZ respectively.

The sorptivity reduced with age at the SZ and SSZ of the concrete blocks, in the four microclimates. At the SZ, the sorptivity indices were, on average, 60% lower after 12 months of exposure. The reduction at the SSZ was smaller, being on average, 25% lower than the 3 months results.

### **5.5.4 30 MPa OPC/GGBS Concrete**

#### *Microclimate*

Figures 5.22 and 5.23 show the effect of microclimate on the sorptivity profiles of the 30 MPa OPC/GGBS concrete samples at the ages of 3 and 12 months respectively. The results with statistical analysis are presented in Appendix A, Tables A1.11 and A1.12 (a) & (b), for the 3 and 12 months tests respectively.

Similar to the air permeability, the variations in sorptivity of the OPC/GGBS concrete blocks due to microclimate were not distinct at 3 months.

The microclimate influence after 12 months exposure was much more evident. The sorptivity of the east and bottom faces of the concrete blocks were higher than the west and top faces respectively. The sorptivity indices of the east faces were, on average, 30 and 10% higher at the SZ and SZ respectively, than the west faces.

Similarly, the sorptivity indices of the bottom faces of the slabs were more approximately 15% higher than the top faces at the SZ and SSZ.

#### *Duration of hessian curing*

The relationship between the sorptivity and curing duration of the 30 MPa OPC/GGBS concrete at the ages of 3 and 12 is presented in Figures 5.16 and 5.17 (e) and (f), respectively.

At 3 months of age, the SZ sorptivity of the east and west faces of the concrete blocks increased by approximately 15% with increased curing duration. At the SSZ of the blocks, the sorptivity showed a small improvement (average of 5%) with increased curing duration. Further, the sorptivity of the top and bottom faces of the slabs improved marginally with increased curing duration. The sorptivity indices of the 6 days cured blocks were, on average, 10% lower than the non-cured slabs, at the SZ and SSZ.

The effect of hessian curing duration on the sorptivity of the east and west faces at 12 months remained largely unchanged from that revealed at the 3 months. The sorptivity indices were generally marginally higher in the 4-6 days cured blocks than the 0-2 cured blocks.

Like the 3 months results, the sorptivity indices slabs were generally reduced with increased curing duration. This was more apparent in the bottom faces of the slabs, the sorptivity indices being approximately 15% lower than the non-cured samples after 6 days of curing.

#### *Age*

The relationship between the sorptivity and age of the 30 MPa OPC/GGBS concrete is shown in Figures A1.11 and A1.12, for the SZ and SSZ respectively.

The sorptivity of the slag concrete reduced with age at both, the SZ and SSZ. The sorptivity indices reduced by 20-25% at the SZ of the concrete blocks, in the 4 microclimates. At the SSZ, the sorptivity indices were, in average, 35% lower than the 3 months indices.

Unlike the 2 OPC concretes, the reduction in the sorptivity of the OPC/GGBS concrete with age was more noticeable in the SSZ than the SZ.

## 5.6 CARBONATION

### 5.6.1 Introduction

The carbonation measurements were conducted after 6 and 12 months of field exposure. The test was performed on the same specimens after they were first used for the air permeability and sorptivity tests. The discs were in contact with water for 50 minutes during the sorptivity tests, and were subsequently dried at 50 °C for 24 hours to prevent any possibility of further hydration due to re-wetting.

The effect of microclimate and duration of hessian curing on the carbonation depth of the three concrete mixes is presented graphically in Figures 5.24 and 5.25 at the ages of 6 and 12 months respectively. The results are also presented in Appendix A, Tables A1.13 and A1.14 for the 6 and 12 months tests respectively.

### 5.6.2 30 MPa OPC Concrete

#### *Microclimate*

The carbonation depth of the blocks in the east and west microclimates were generally comparable after 6 months of field exposure, with it being fractionally lower in the east faces. Equally, the depths of carbonation in the top and bottom microclimates of the slabs were generally similar at 6 months.

The differences in carbonation due to microclimate were more apparent after 12 months of exposure, being generally higher in the drier east and bottom microclimates. The average carbonation depth of the east faces was 6-mm compared to 5-mm in the west faces (17% higher), and 3-mm in the top compared to 6-mm in the bottom faces (100% higher).

### *Duration of hessian curing*

As can be seen from the 6 months results, carbonation decreased as curing duration was increased from 2 to 6 days in the east and west faces of the vertical blocks. The relationship between carbonation and curing duration was not clear in the top and bottom faces, as the 4 and 6 days cured blocks exhibited higher carbonation depths than 0 and 2 days cured blocks.

Surprisingly, the 4 and 6 days cured blocks showed higher carbonation than 0 and 2 days cured blocks at 12 months. This implies that the carbonation rate was higher in these samples, since at 6 months their carbonation was lower than the 0-2 days cured samples. Generally, the 12 months data showed an increase in carbonation with increased curing duration in the 4 microclimates. This relationship is in agreement with the winter air permeability and sorptivity results.

### *Age*

Figure 5.26 presents the carbonation results of the 30 MPa OPC concrete after 6 and 12 months of exposure.

As shown, the carbonation depth increased with age in all the samples with it being more significant in the east and bottom microclimates. At 12 months, the average carbonation depth increased from 3-mm at 6 months, to 6-mm in the east faces and from 3.5 to 5-mm in the west faces (100 and 40% increase in the two faces respectively). The average carbonation depth of the top faces increased from 2.5 at 6 months, to 3.5-mm at 12 months (40% increase); and from 2.5 to 6-mm for the bottom faces (more than 100% increase).

### **5.6.3 50 MPa OPC Concrete**

#### *Microclimate*

The 50 MPa OPC concrete showed no sign of carbonation in the 4 microclimates after 6 months of exposure. After 12 months, the average carbonation depth of east faces was 1.5-mm compared to 1-mm in the west faces (50% higher than west). Apart from the 4 days hessian cured blocks, the

top faces revealed no sign of carbonation after 12 months of exposure. The bottom faces, on the other hand, carbonated to slightly higher depths than the east faces of the vertical blocks, the average depth of carbonation being 2mm.

#### *Duration of hessian curing*

The 6 months tests revealed no sign of carbonation in the blocks in the 4 microclimates. At 12 months, the progress of carbonation appeared similar in all blocks regardless of curing regime, the carbonation depth of the 4-6 days cured blocks being generally either higher or similar to the 0-2 days cured blocks.

#### *Age*

Figure 5.27 presents the carbonation results of the 50 MPa OPC concrete after 6 and 12 months of exposure.

As can be seen from the graphs, no carbonation was detected at 6 months. After 12 months of exposure, the progress of carbonation in the 50 MPa concrete was slow; the average carbonation depth being, 1.5, 1.0 and 2.0 mm in the east, west and bottom faces of the blocks. Apart from the 4 days hessian cured slabs (1.3-mm carbonation depth), the top faces showed no sign of carbonation after 12 months of exposure.

### **5.6.4 30 MPa OPC/GGBS Concrete**

#### *Microclimate*

The carbonation depth of the concrete in the east and west microclimates were generally similar at 6 months. Similarly, there was no significant difference in the depth of carbonation between the top and bottom faces of the slabs at this age.

However, the differences in carbonation depth due to microclimate were more distinct after 12 months of field exposure. The average carbonation depth of the east and bottom faces respectively being, 13.5 and 8-mm compared to 10 and 7.5mm for the west and top faces respectively, i.e.

approximately 30% and 5% higher than the west and bottom faces respectively.

#### *Duration of hessian curing*

Contrary to the 6 months results, the carbonation depth at 12 months was generally higher with increased hessian curing duration. As with the other mixes, the rate of carbonation was higher in the samples that received longer curing duration. The carbonation of the 4-6 days cured blocks was, on average, 10% higher than the 0-2 days cured blocks. Like the OPC concrete, this trend is in agreement with the winter air permeability and sorptivity results.

#### *Age*

Figure 5.28 presents the carbonation results of the 30 MPa OPC/GGBS concrete after 6 and 12 months of exposure. As shown, the increase in carbonation with age was more notable in the vertical blocks than the slabs. Further, the rate of carbonation was higher in the 4-6 days cured blocks, as these blocks showed lower carbonation at 6 months than the 0-2 days cured blocks.

The average carbonation depth in the east faces increased from approximately 5-mm at 6 months, to 13.5-mm at 12 months (an increase of more than 100%). In the west faces, the carbonation depth increased from 5-mm at 6 months, to approximately 10-mm at 12 months (100% increase).

The carbonation rate varied widely in the top and bottom faces of the slabs. In the top faces, the increase in carbonation from 6 to 12 months varied from 8% for the non-cured blocks to 100% for the 6 days cured blocks, with an average increase of 60% for the 2-4 days cured blocks. In the bottom faces, the carbonation increased by, on average, 30% for the 2-4 days cured blocks and 66 and 400% for the non-cured and 6 days cured blocks respectively.

## 5.7 THERMOGRAVIMETRY

### 5.7.1 Introduction

The thermogravimetry test methodology, apparatus and sample preparation procedure for the test are described in detail in Section 4.7.

The repeatability of the test was good with coefficients of variation less than 5% in all cases. The reproducibility of the test was evaluated by testing duplicate samples taken from other cores adjacent to the position of the original cores from the same concrete block. The coefficient of variation was typically within 15%.

The thermogravimetric analysis curves (TG) and their derivatives (DTG) are given in Appendix A, Figures A1.13 to A1.17. Five weight loss parameters were identified from the peaks of the DTG curves as shown typically in Figure 5.29. The weight loss processes occurred typically within the following temperature ranges for most samples:

1. Below 95 °C: The loss of evaporable water from capillary pores and adsorbed gel water
2. 95-200 °C: The loss of hydrates water from calcium silicate hydrates (C-S-H) and calcium aluminate hydrates (C-A-H)
3. 400-470 °C: The loss of water from calcium hydroxide ( $\text{Ca(OH)}_2$ )
4. 550-630 °C: The loss of water from calcium ferrite hydrates (C-F-H) and decomposition of carbonates other than calcite
5. 630-730 °C: The loss due to the decomposition of  $\text{CaCO}_3$

The weight losses over the given temperature ranges are assumed (and generally accepted) to be due to the decomposition of the phases described above (e.g. Bazant and Kaplan, 1996; Atlassi, 1995). The weight losses were determined by integrating the areas under the peaks of the DTG curves (Mackenzie, 1972, Litvan and Meyor, 1986). These are presented in Table A1.15 in Appendix A.

The detailed consideration of the thermogravimetric results as given in steps 1-5 reveal an intricate make-up of the hydrated matrix, which clearly illustrates that single or bulk parameters (e.g. loss on ignition) cannot be relied on if a reliable assessment of concrete's hydration characteristics is to be made. Thermogravimetric analysis performed on samples that are representative of field concrete are scarce. Such tests, as found from the results of this work, yield results that provide a useful insight into the hydration characteristics of site concrete. However, such results are difficult to compare with those normally published in the literature, as the latter are often performed on ideal samples (pure cement paste or its single phases) that are regularly prepared, cured and stored under ideal conditions.

The results were generally difficult to interpret and distinct trends could not be established. The loss above the calcium hydroxide step, which is generally assumed to be due to carbon dioxide, was particularly difficult to explicate. The weight loss above the calcium hydroxide step (above  $\approx 500$  °C) in a number of samples was higher than the combined losses due to hydrate water and the water from lime. Taylor (1990) reported that losses above 550 °C of more than 3% (referred to the ignited weight) indicate serious carbonation. Losses significantly larger than 3% were evident in a number of samples (see Table A1.15). However, it is not clear why such losses were undetected in other samples that were conditioned and tested under the same standard conditions. Although some carbonation of powdered samples is unavoidable, it is unlikely that this would have such a significant contribution. A possible explanation of weight losses of this magnitude is that phases such as, C-S-H, C-A-H, C-F-H, CH or other phases present, may have not decomposed fully at the assumed temperatures and therefore could have contributed to the total weight loss at this temperature region. On the other hand, higher weight losses were reported at temperatures of about 600-700 °C of 6% for concrete samples made with quartzite and basalt aggregates and 15% for limestone aggregates (Bazant and Kaplan, 1996). At this temperature range, 3% of the weight loss in the quartzite and basalt aggregates concretes was attributed to

the decomposition and transformation (from  $\alpha$ -quartz to  $\beta$ -quartz) of the aggregates. For the limestone aggregates concretes, 9% of the loss was due to the decarbonation of the aggregates at approximately 600 °C. Therefore, the presence of fine aggregates as well as the possibility of contamination with residues from the coarse aggregates in the powdered samples is a probable cause for the higher weight losses observed above 500 °C in some samples. This, however, cannot be established from the TG results alone, and other complimentary methods are clearly needed to enable a more accurate evaluation of the results.

The hydrates water and calcium hydroxide (lime) content profiles of the 3 concrete mixes were distinct (see Figure 5.30). The 30 MPa OPC concrete showed an increase in the hydrates water and lime content up to 10mm from the surface with the 20mm values being invariably lower than the 10mm values. This effect was not observed in the 50 MPa concrete, as the two parameters generally increased with depth from the exposed surface. However, the increase in the two parameters with depth in the two concretes was not significant, being typically between 1.5 to 2%. Contrary to the two OPC concretes, the hydrate water and calcium hydroxide content of the OPC/GGBS concrete exhibited a reduction with increased depth from the exposed surface. The difference between the surface (10mm) and sub-surface zone (10-20mm) values was generally small, being more pronounced in the hydrate water profiles than the lime content profiles.

### 5.7.2 30 MPa OPC Concrete

#### *Duration of hessian curing*

The effect of hessian curing duration on the hydrate water and lime contents is presented graphically in Figure 5.31 (a) and (b) respectively.

The hydrate water increased with increased hessian curing duration at the surface (10mm) and subsurface zone (20mm). The increase however was small, the hydrate water of the 6 days hessian cured samples being approximately 1% higher than the non-cured samples.

Similarly, the lime content of the samples increased with increased curing duration at the SZ and SSZ. Like the hydrate water, the average increase in lime content with curing duration from 0-6 days was approximately 1 to 1.5%.

### **5.7.3 50 MPa OPC Concrete**

#### *Duration of hessian curing*

The effect of hessian curing duration (only the non-cured and 2 days hessian cured samples were investigated for the 50 MPa OPC concrete) on the hydrate water and lime contents of the 50 MPa OPC concrete is given in Table A1.15, Appendix A.

Similar to the 30 MPa OPC concrete, there was a small increase (1%) in the hydrate water and lime contents with increased hessian curing duration.

### **5.7.4 30 MPa OPC/GGBS Concrete**

#### *Duration of hessian curing*

The effect of hessian curing duration on the hydrate water and lime contents is presented graphically in Figure 5.31 (c) and (d) respectively.

Contrary to the two OPC concretes, the hydrate water of the blast-furnace slag concrete decreased by approximately 1% as curing duration was increased from 0-6 days, at the SZ and SSZ.

Similarly, the lime content decreased fractionally with increased hessian curing duration at both, the SZ and SSZ.

**Table 5.1** Weather data during curing period (curing environment)

Concrete reference	Mean weekly temperature (°C)	Mean weekly relative humidity (%)	Mean wind speed (m/s)	Wind direction
A	8.5	76	2.9	south
	5.0	78	1.9	east
B	-0.3	74	3.9	east
	0.35	78	2.2	east
C	2.8	75	3.3	east
	3.5	74	3.5	south east

Concrete: A = 30 MPa OPC, B = 50 MPa OPC, C = 30 MPa OPC/GGBS

**Table 5.2** Weather data during the first three months of exposure

Month (1996)	Average air temperature(°C)	Average monthly relative humidity (%)	Wind direction
January	4.1	76.6	east
February	2.4	75.8	south east
March	3.7	74.7	west / south west

**Table 5.3** Compressive strength results

Concrete reference	Design Strength (MPa)	Actual strength* (MPa)
A	30	29-33
B	50	48-53
C	30	28-33

Concrete: A = 30 MPa OPC, B = 50 MPa OPC, C = 30 MPa OPC/GGBS

\* Average of six tests

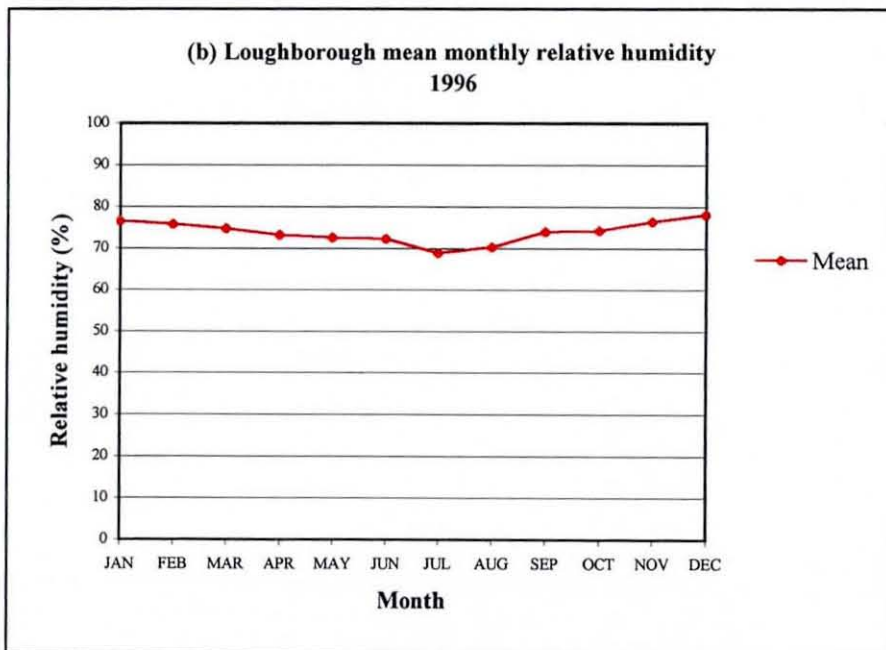
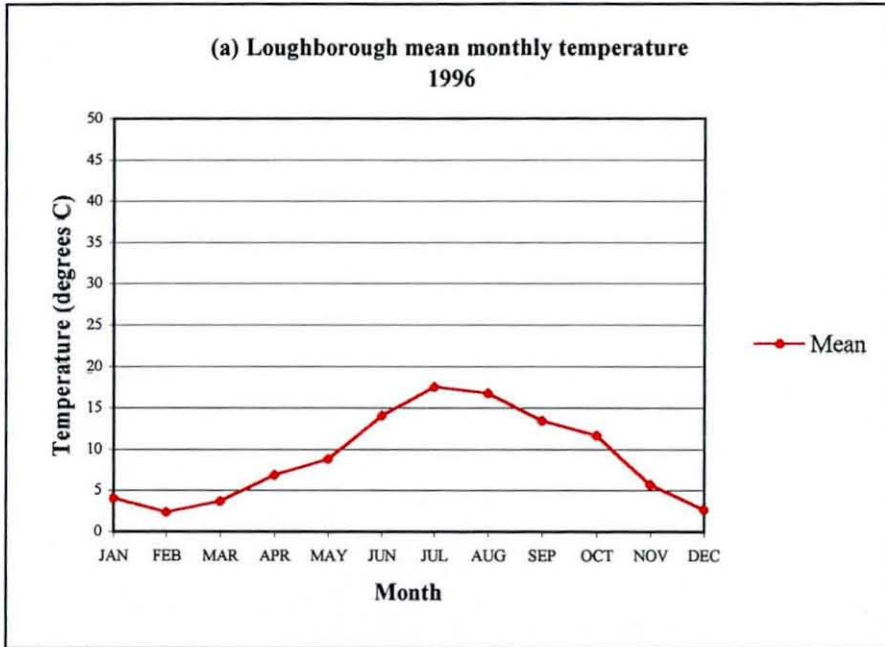
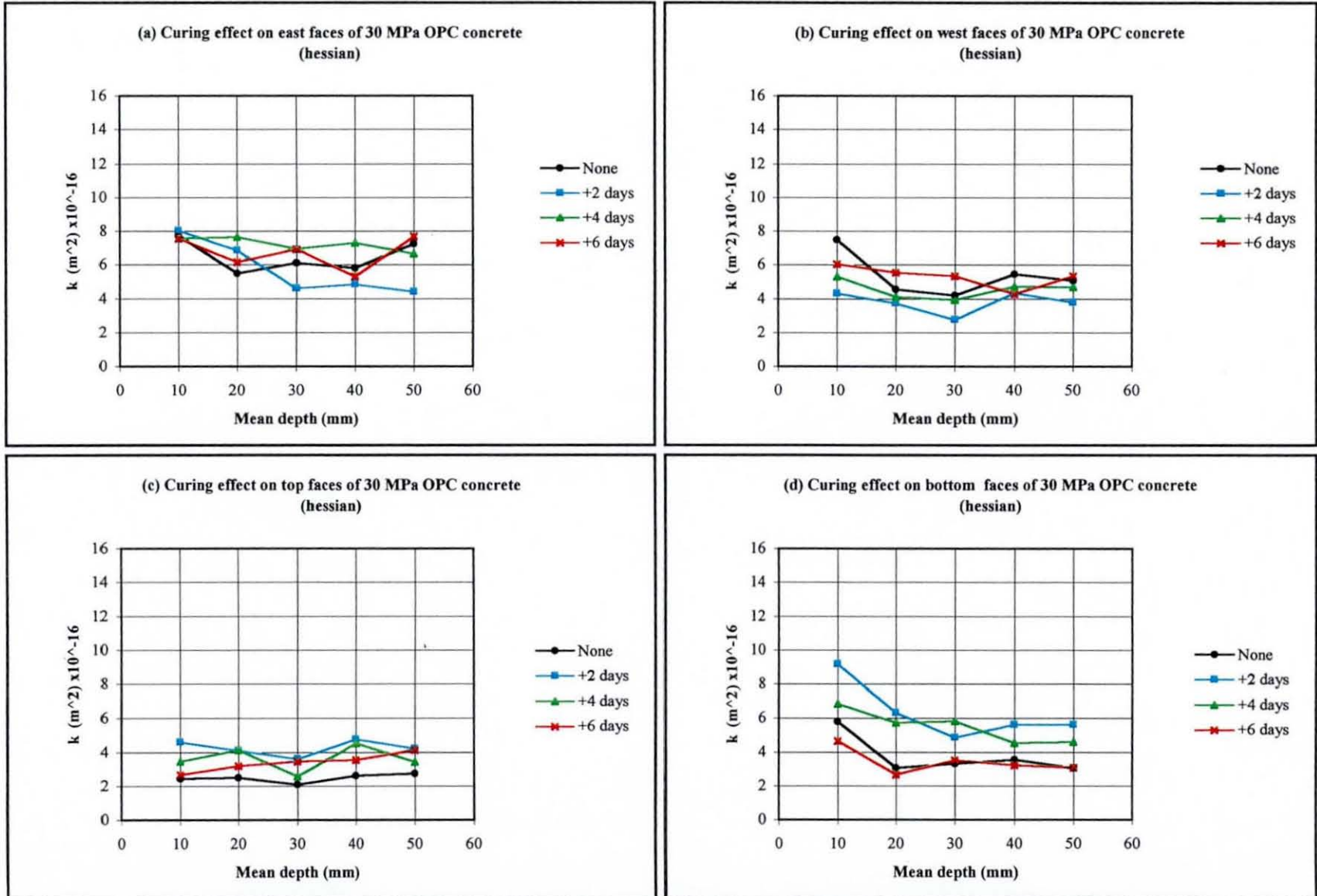


Fig. 5.1 Mean monthly temperature and relative humidity - Loughborough 1996



**Fig. 5.2.** Effect of curing regime on the air permeability profiles of 30 MPa OPC concrete - 3 months winter series

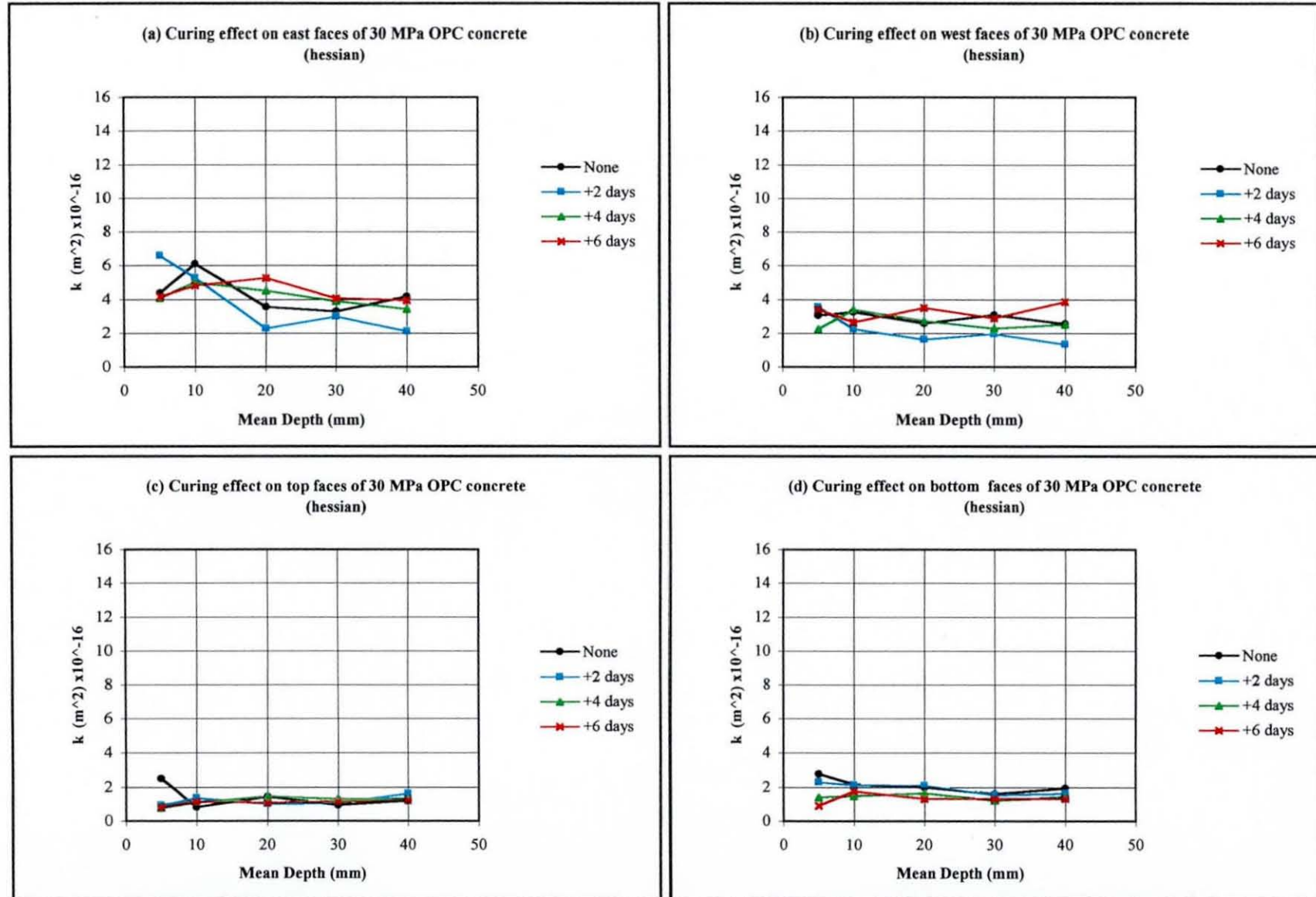


Fig. 5.3. Effect of curing regime on the air permeability profiles for the 30 MPa OPC concrete - 12 months winter series

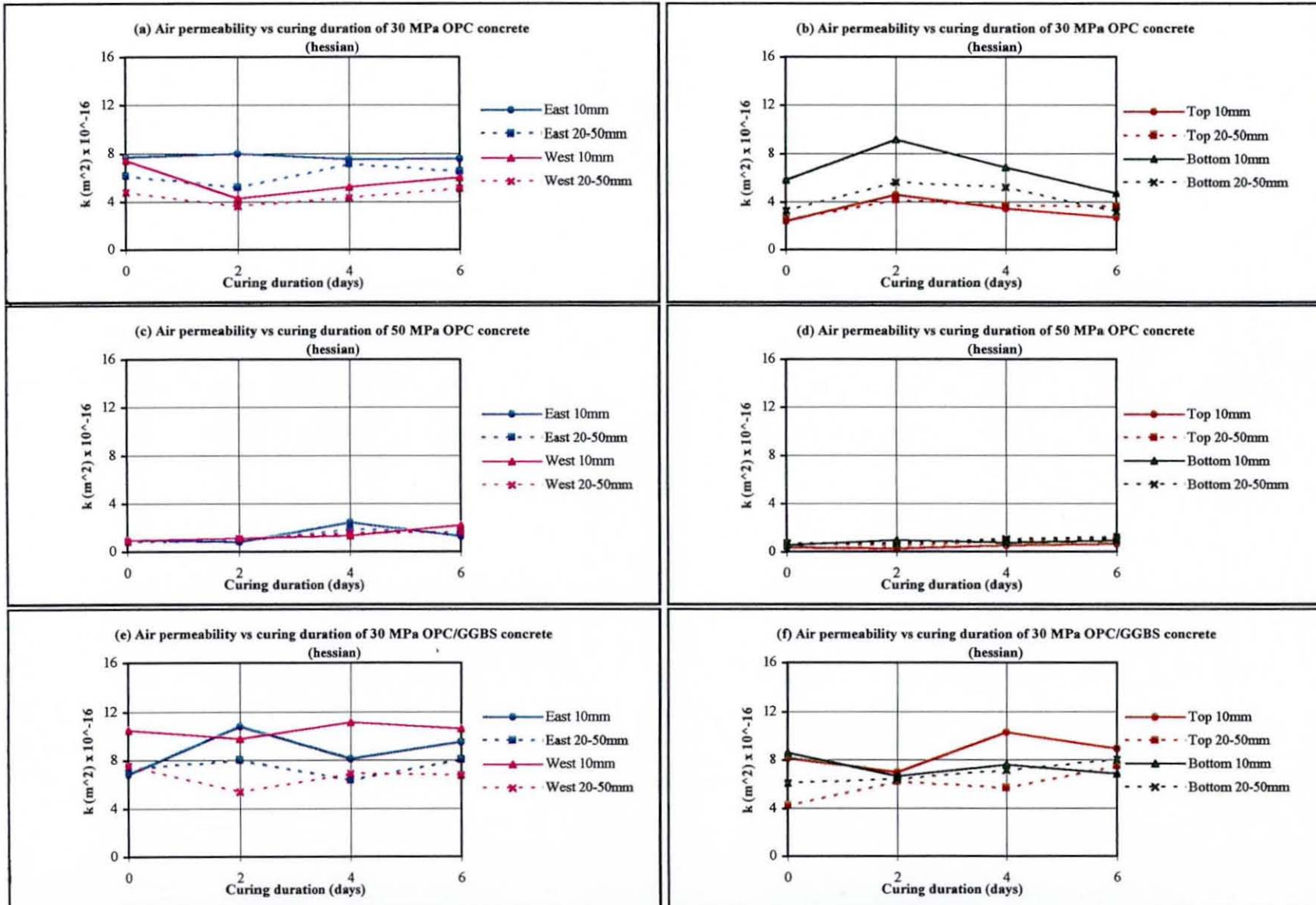


Fig. 5.4. Effect of curing duration on the air permeability of OPC and OPC/GGBS concrete - 3 months winter series

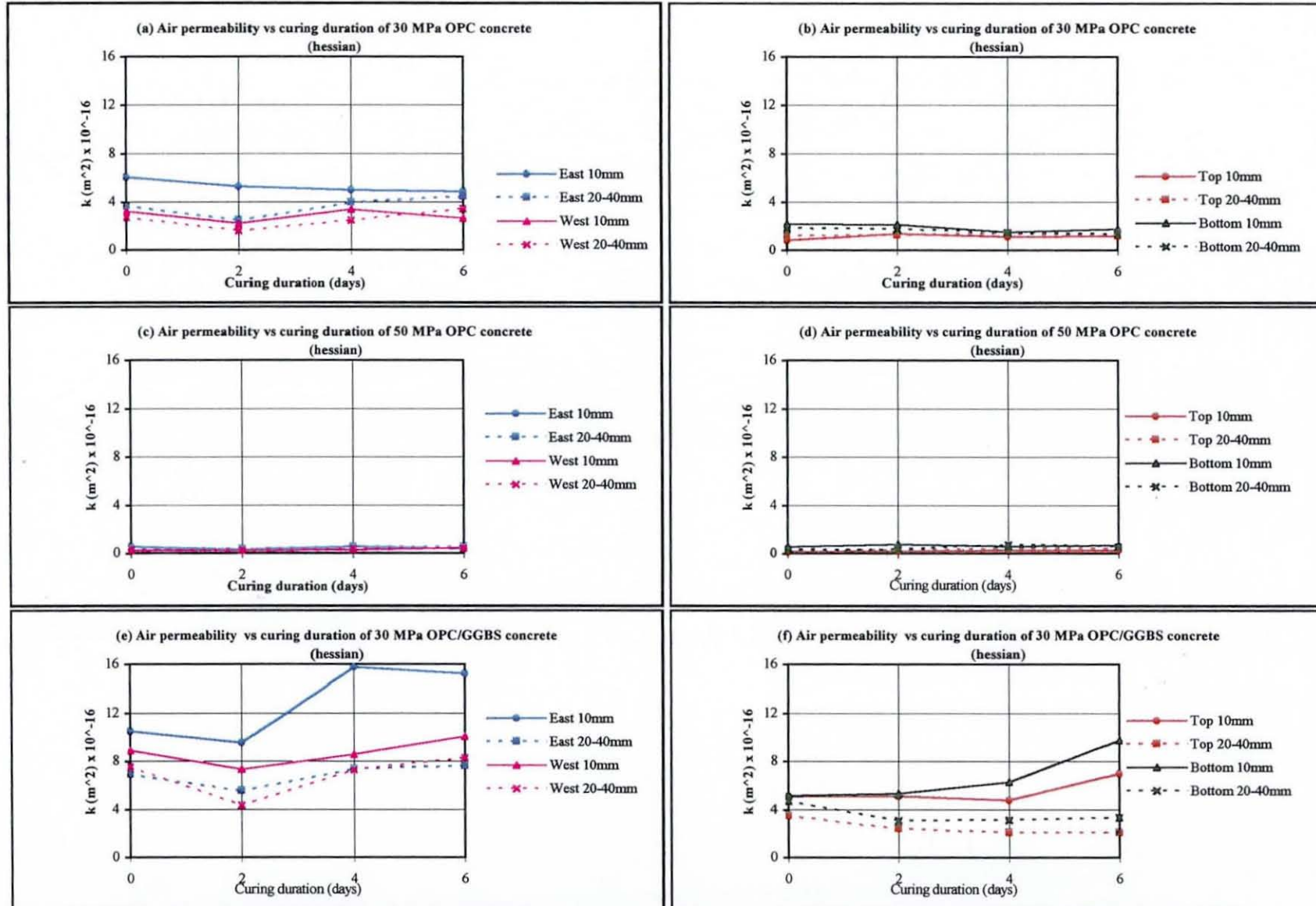


Fig. 5.5. Effect of curing duration on the air permeability for the OPC and OPC/GGBS concrete - 12 months winter series

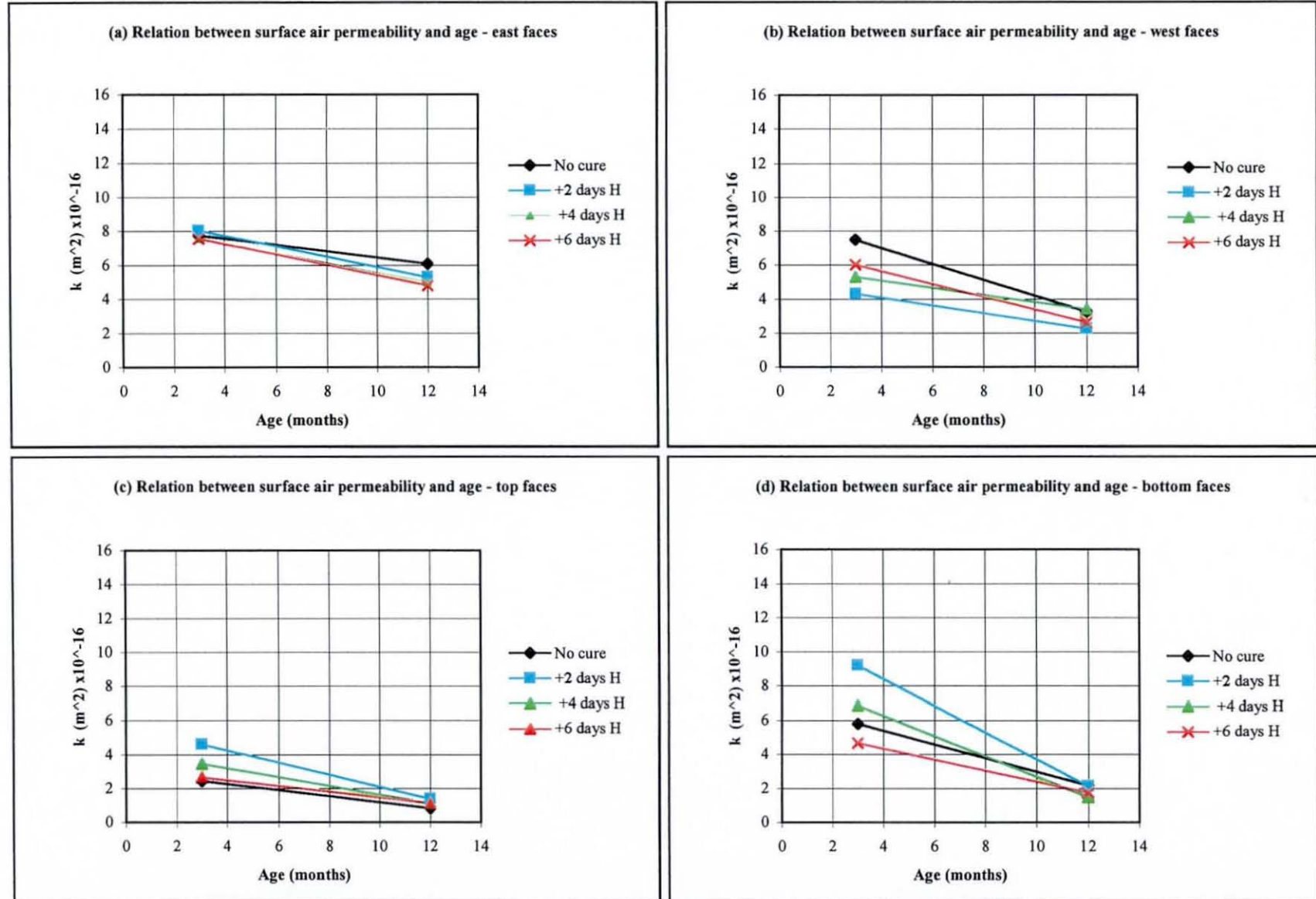


Fig. 5.6. Relationship between surface air permeability and age of the 30 MPa OPC concrete - UK winter

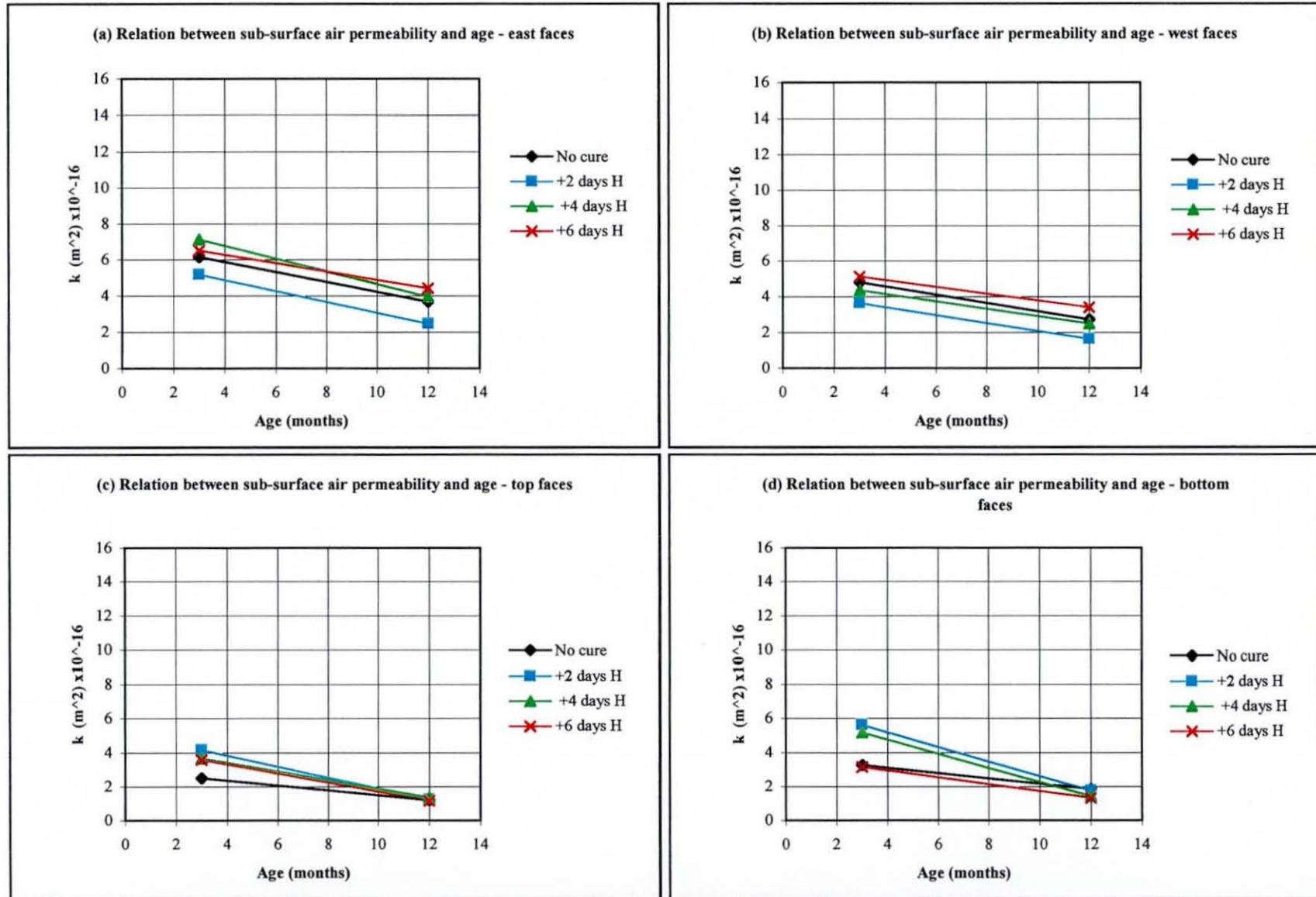


Fig. 5.7 Relationship between sub-surface air permeability and age of the 20 MPa OPC concrete at 28 days

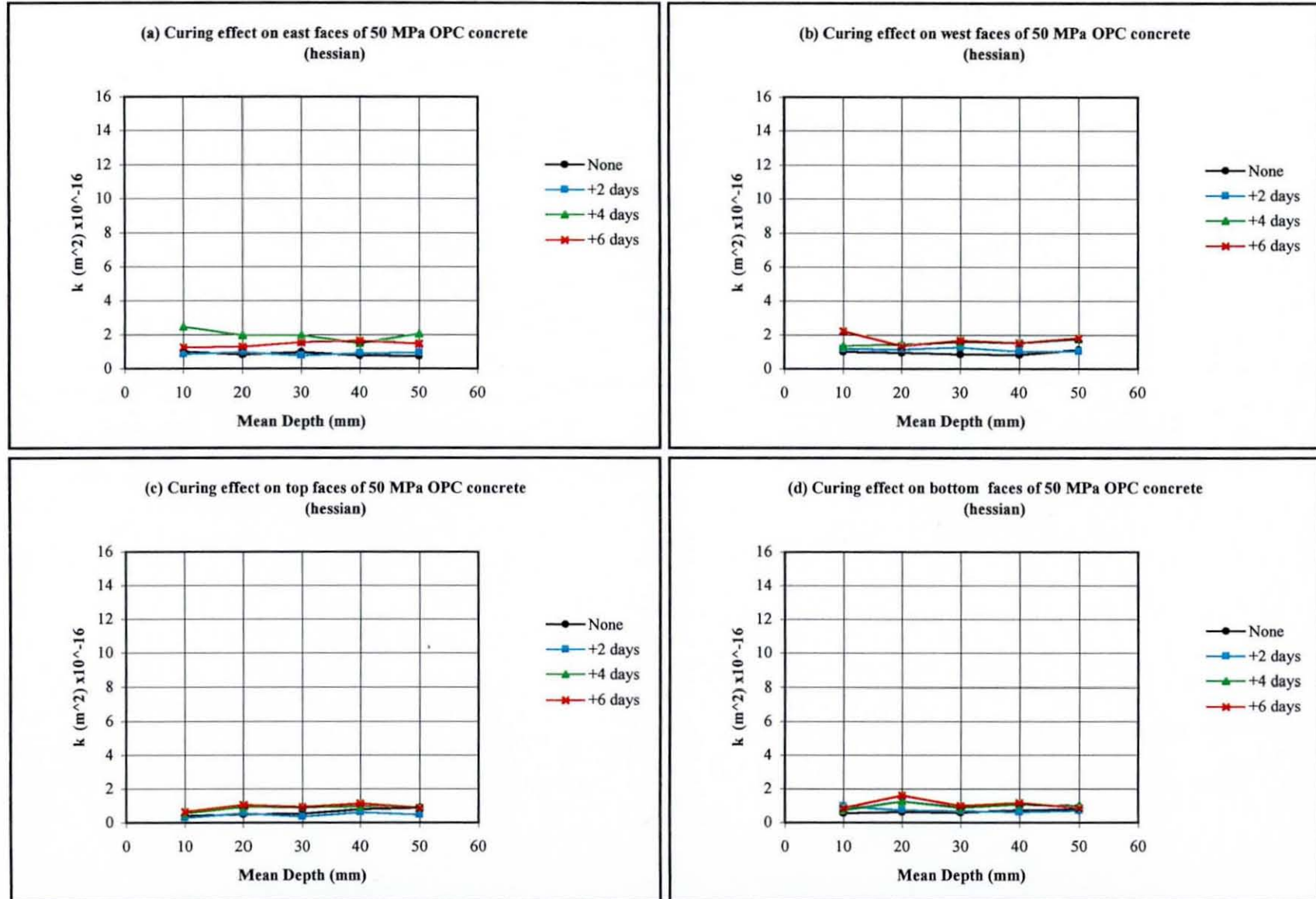


Fig. 5.8. Effect of curing regime on the air permeability for the 50 MPa OPC concrete - 3 months winter series

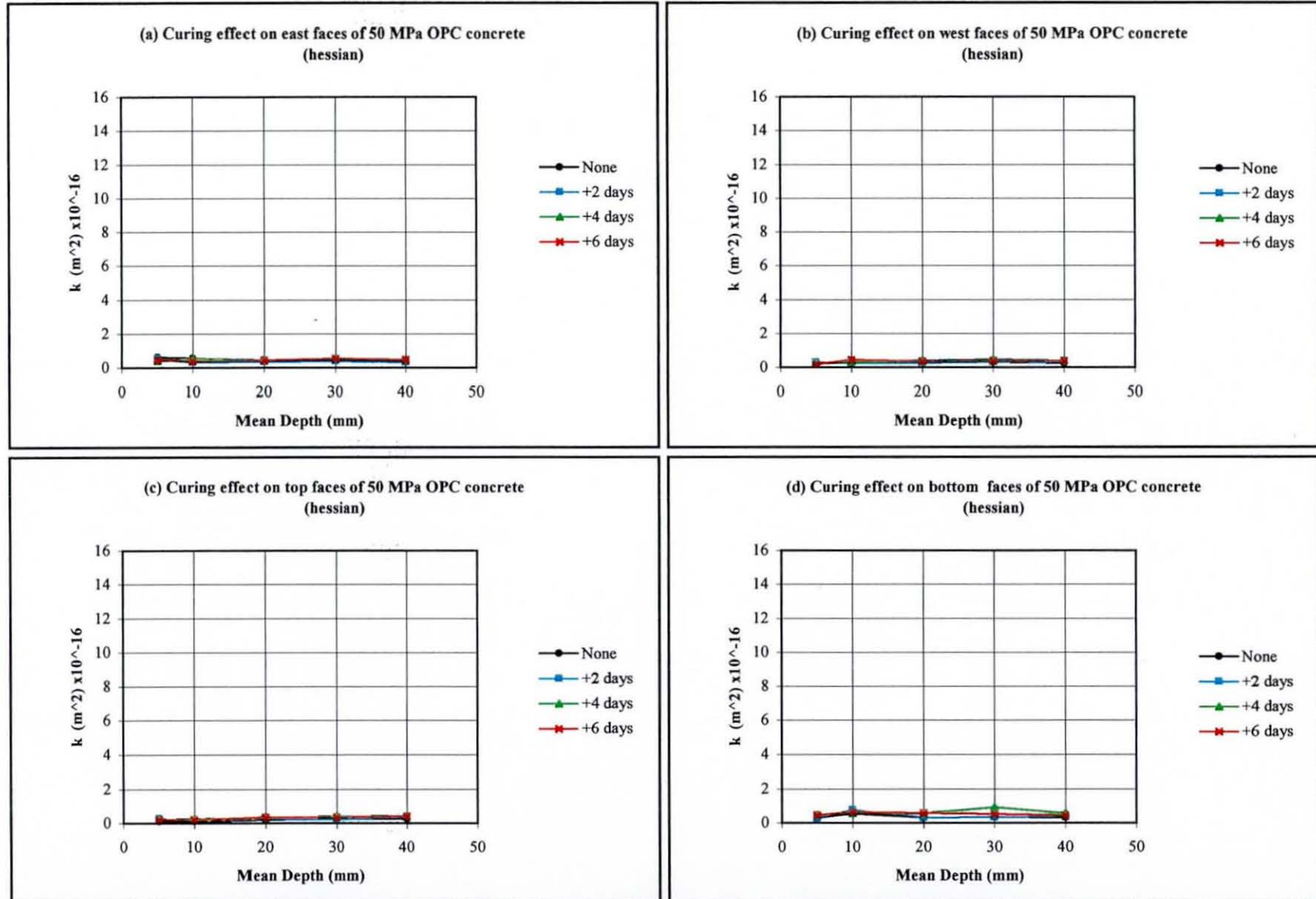


Fig. 5.9. Effect of curing regime on the air permeability profiles for the 50 MPa OPC concrete - 12 months winter series

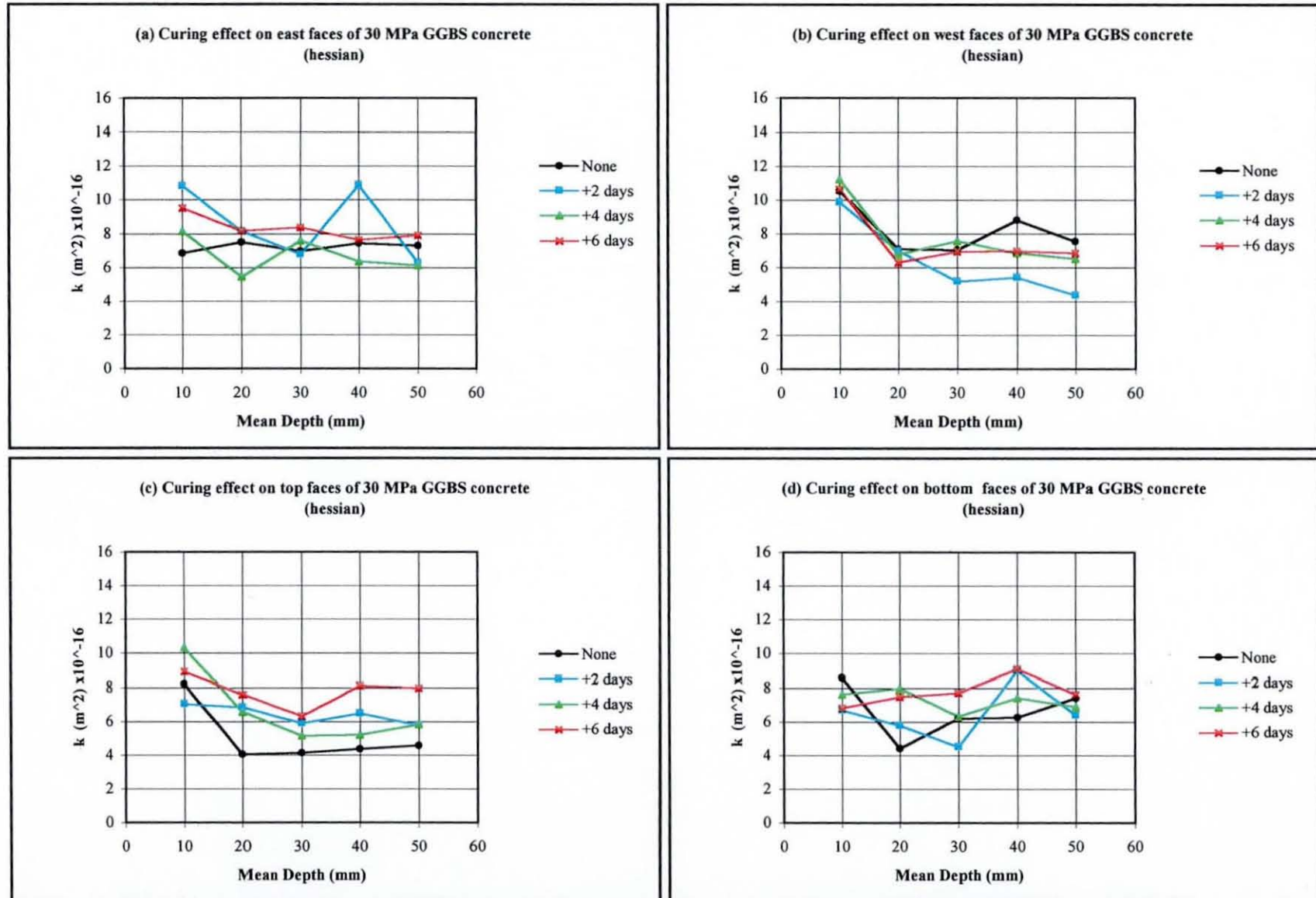


Fig. 5.10. Effect of curing regime on the air permeability for the 30 MPa OPC/GGBS concrete - 3 months winter series

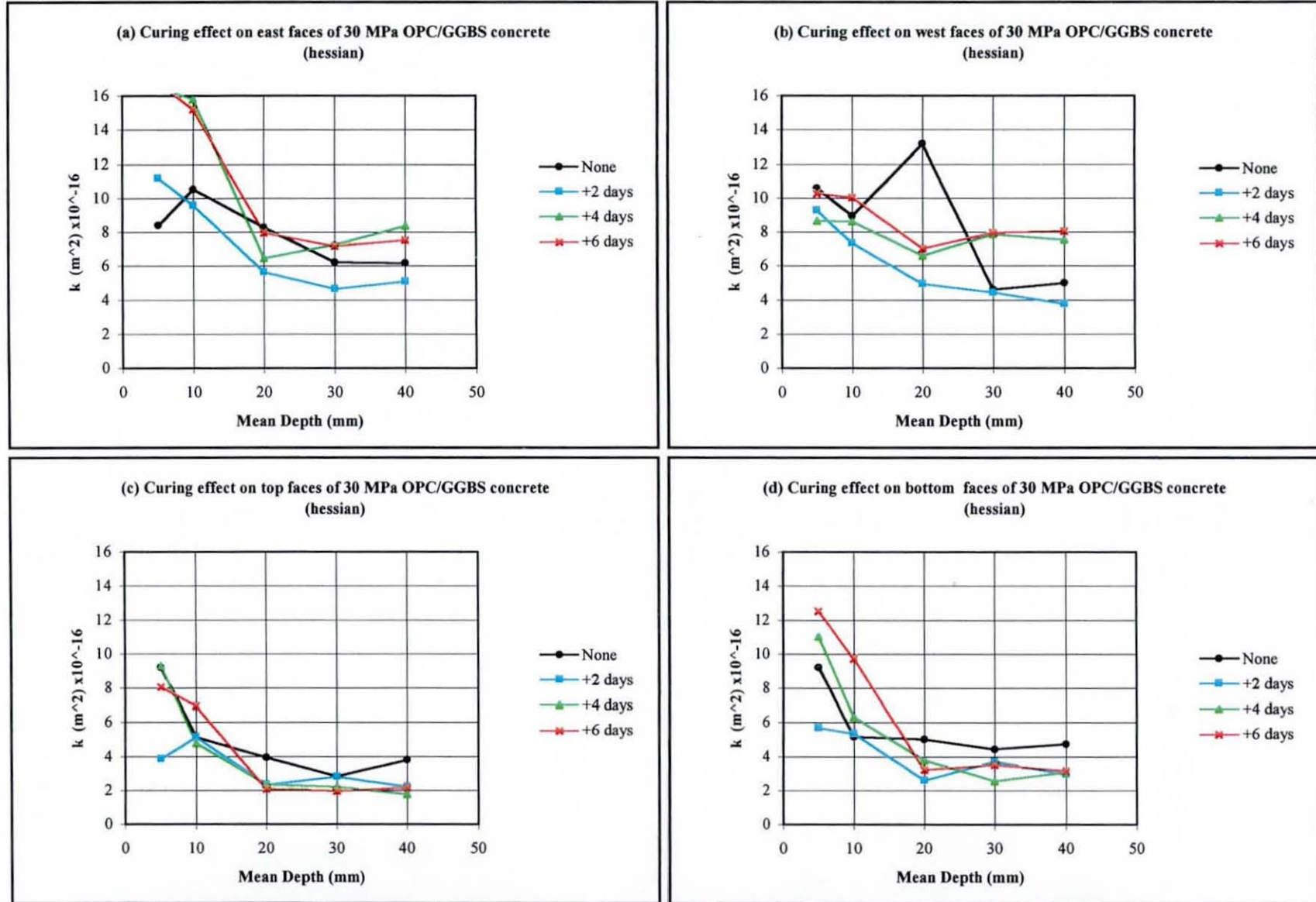


Fig. 5.11. Effect of curing regime on the air permeability profiles for the 30 MPa OPC/GGBS concrete - 12 months winter series

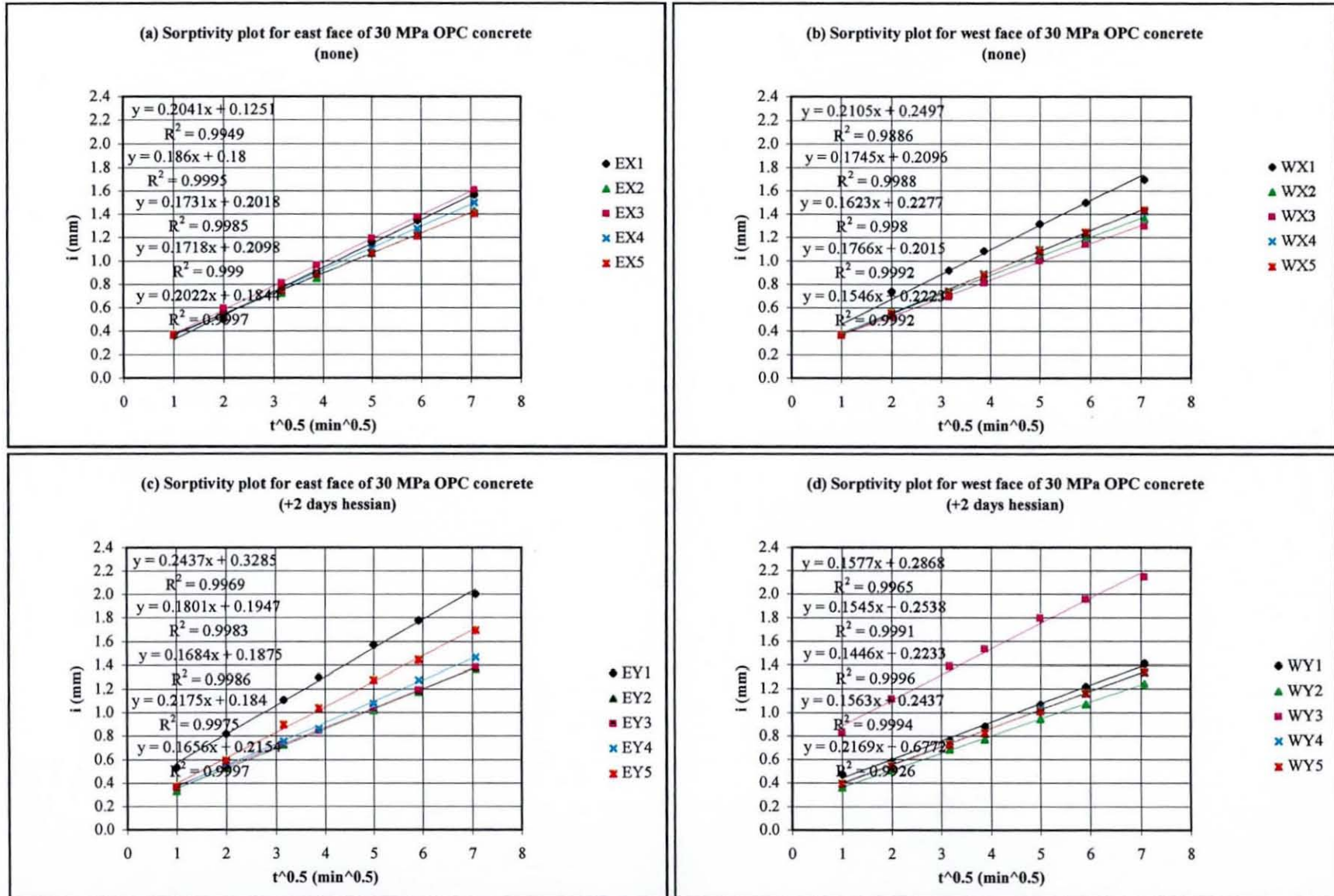


Fig. 5.12. Sorptivity plots for the 30 MPa OPC concrete - 3 months winter series (Table A1.7)

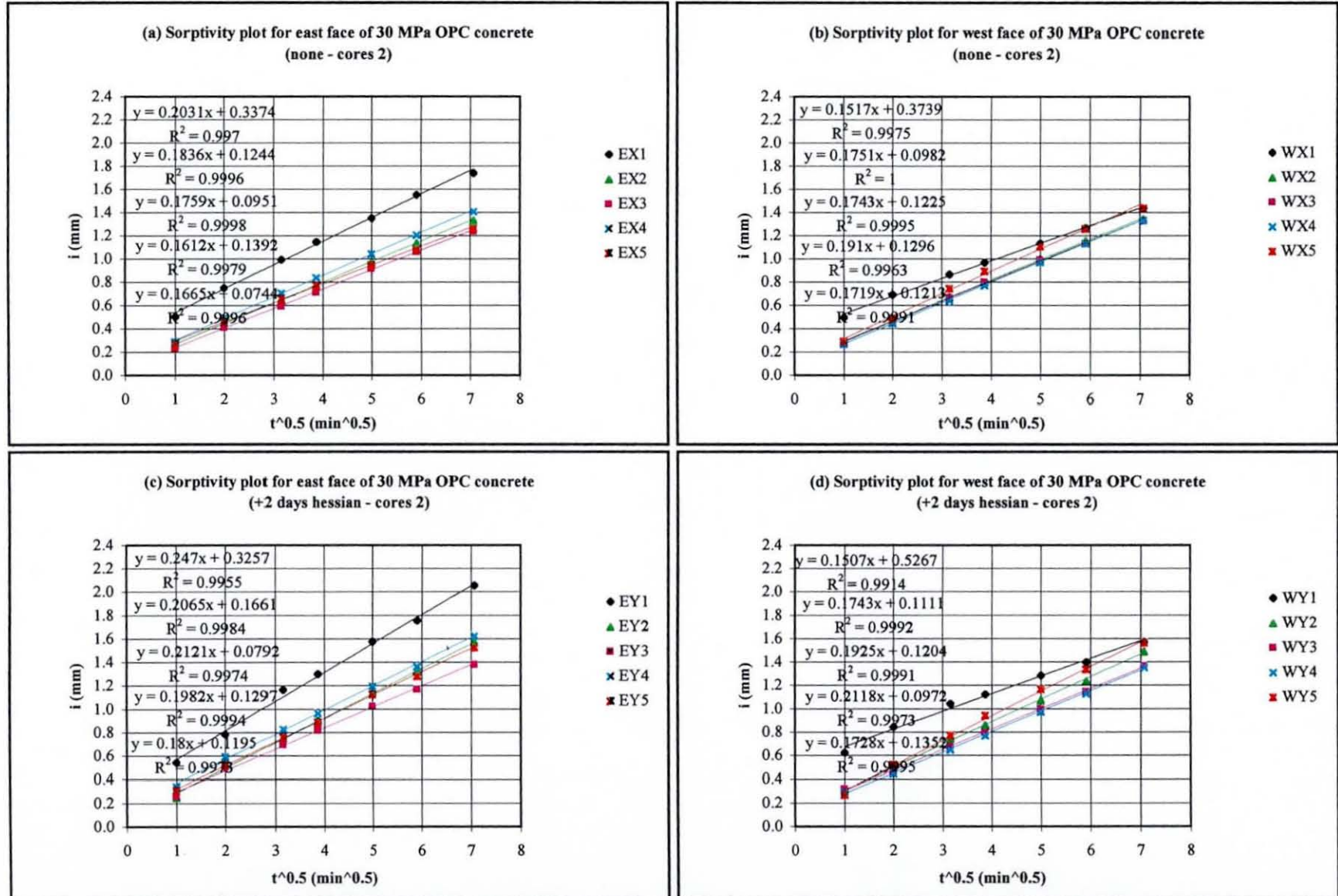


Fig. 5.13. Reproducibility of sorptivity plots for the 30 MPa OPC concrete - 3 months winter series (compare with Fig. 5.12)

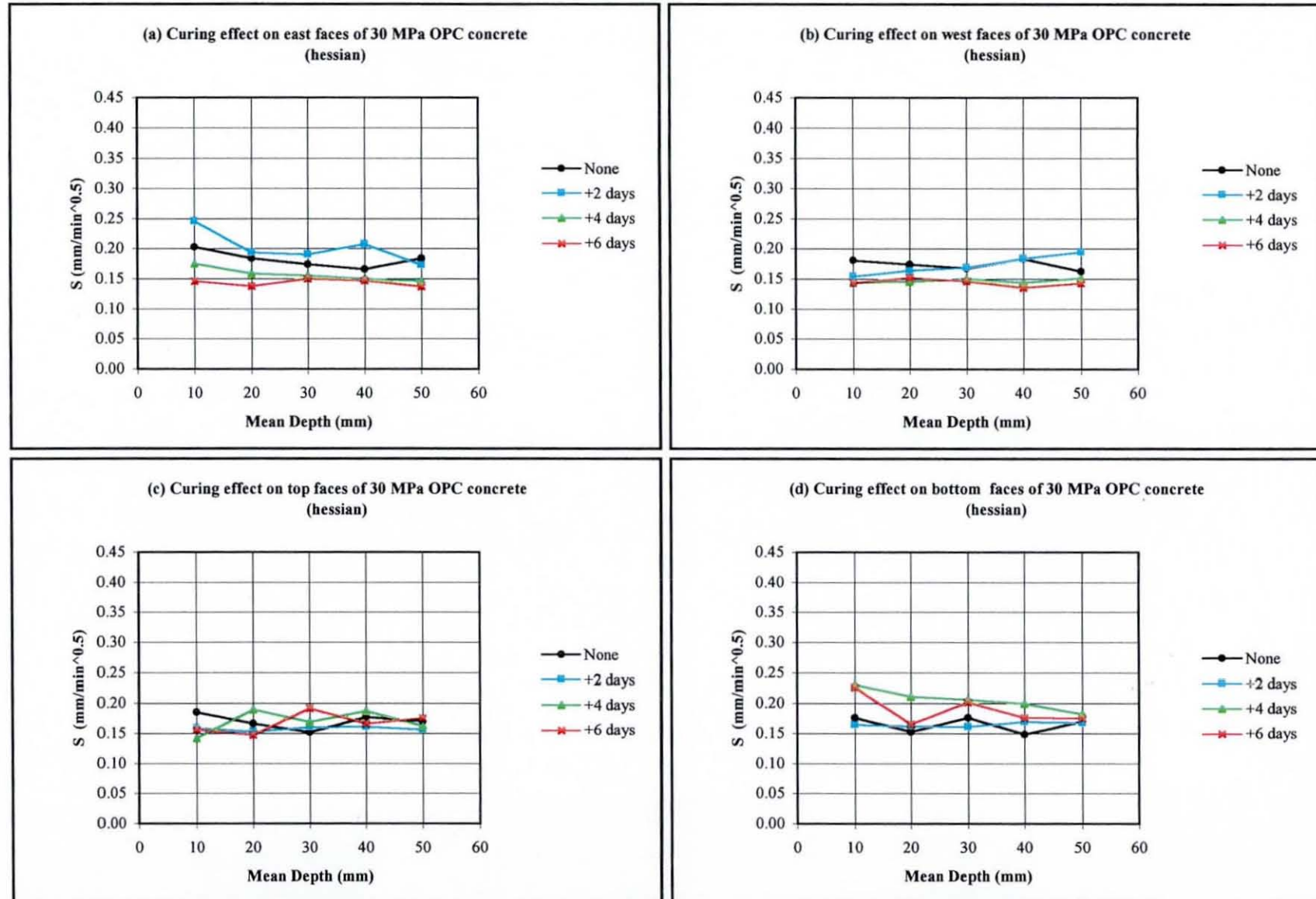


Fig. 5.14. Effect of curing regime on the sorptivity of 30 MPa OPC concrete - 3 months winter series

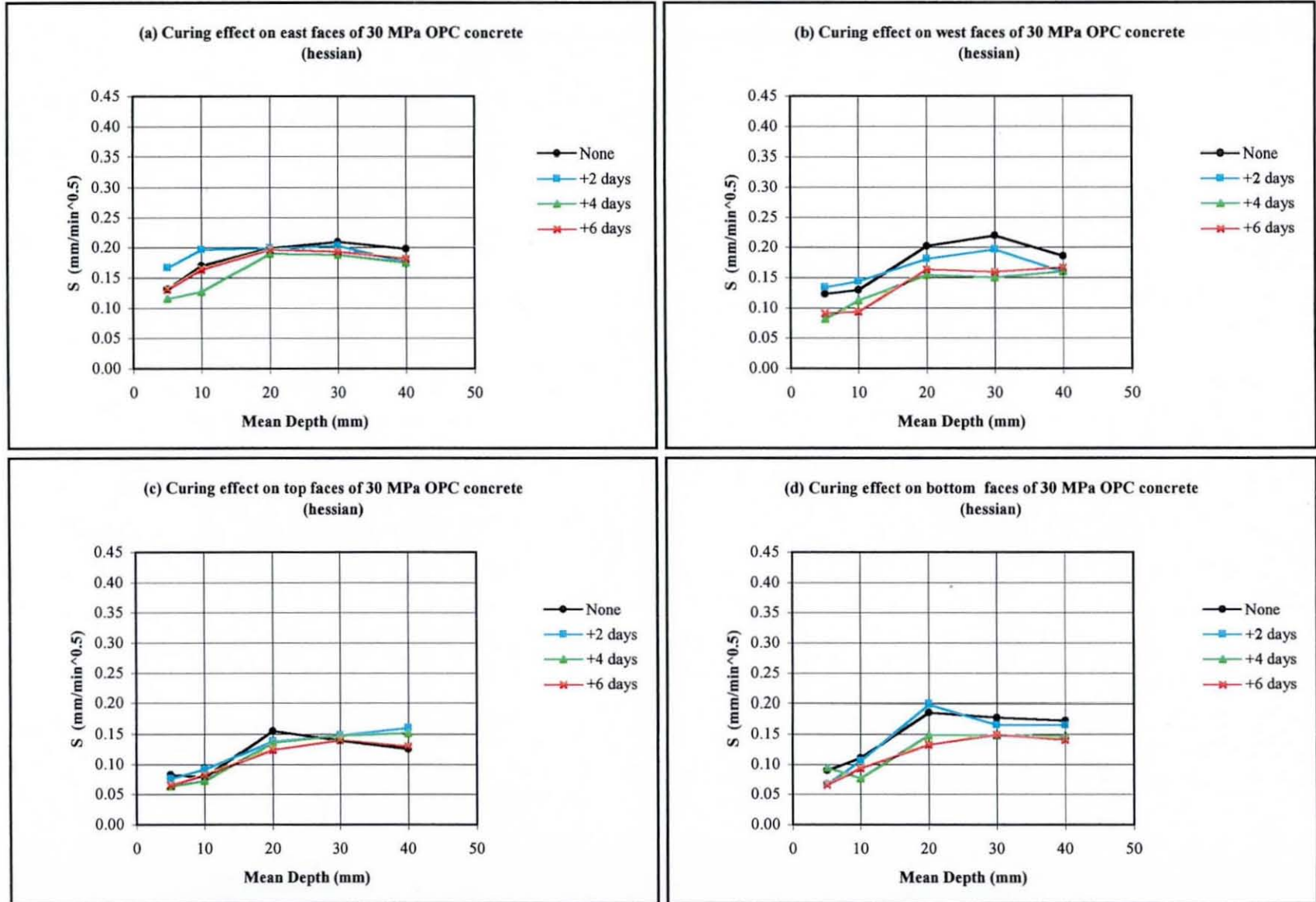


Fig. 5.15 Effect of curing regime on the sorptivity of 30 MPa OPC concrete - 12 months winter series

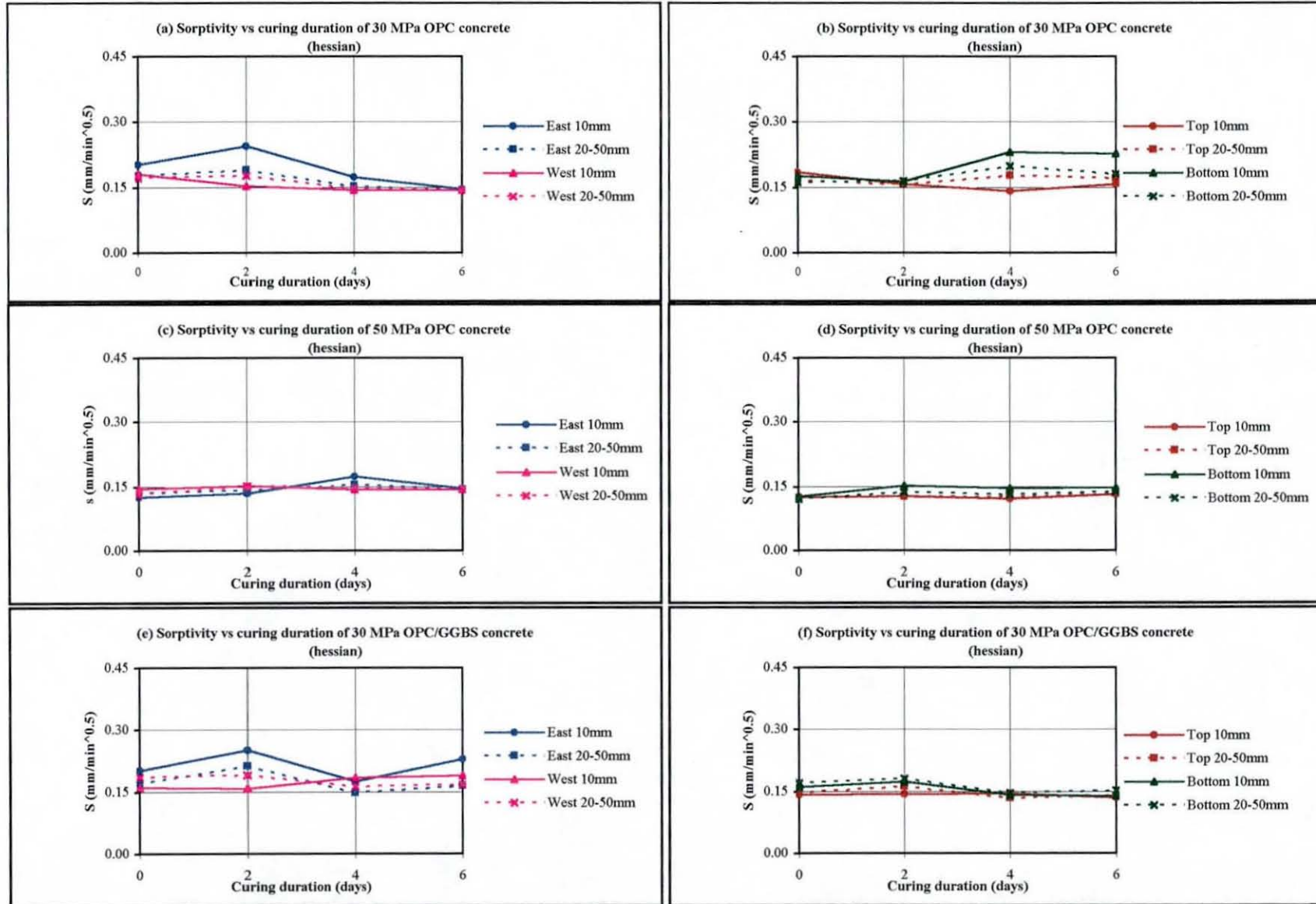


Fig. 5.16. Effect of curing duration on the sorptivity of OPC and GGBS concrete - 3 months winter series

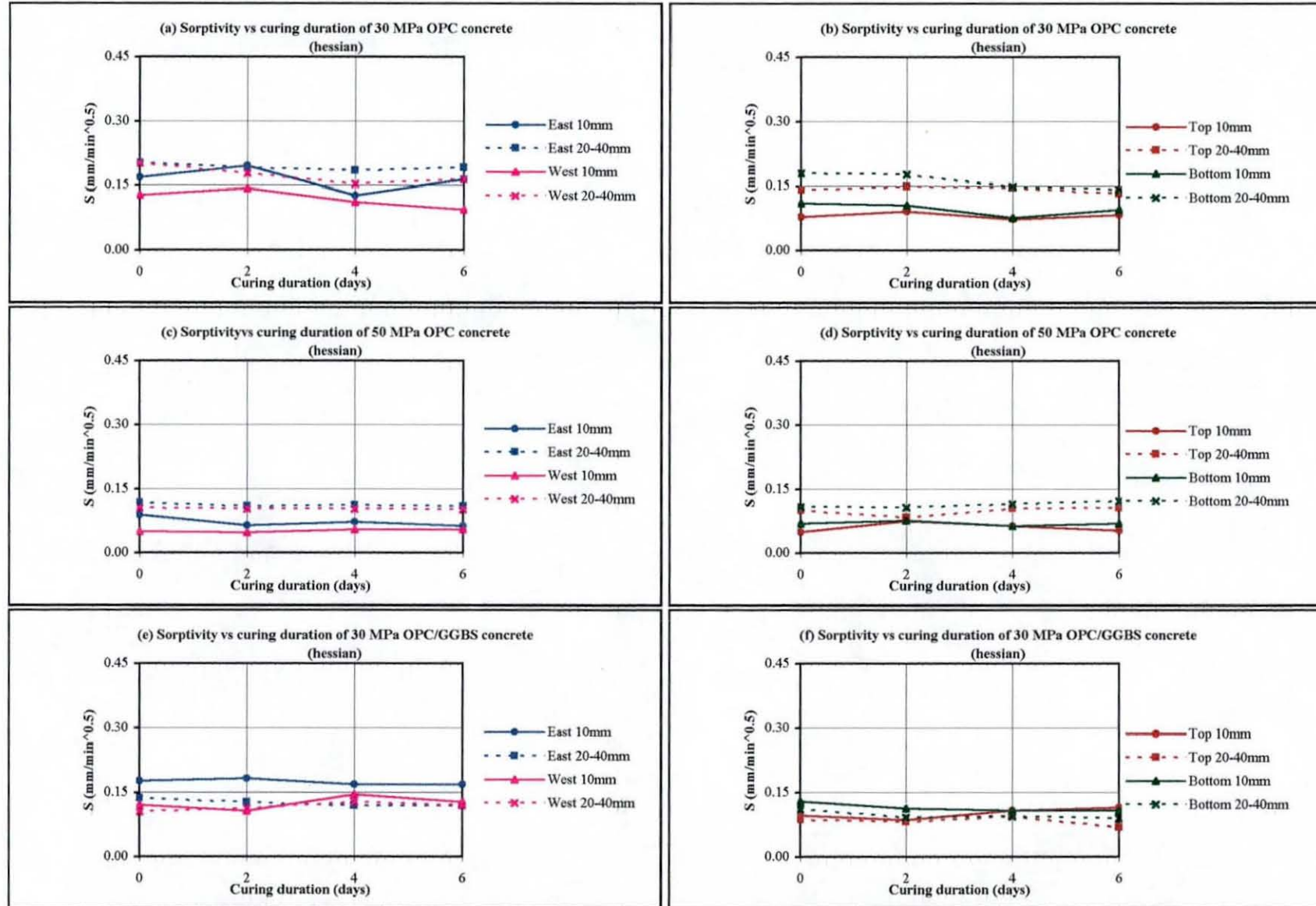


Fig. 5.17 Effect of curing duration on the sorptivity of OPC and OPC/GGBS concrete - 12 months winter series

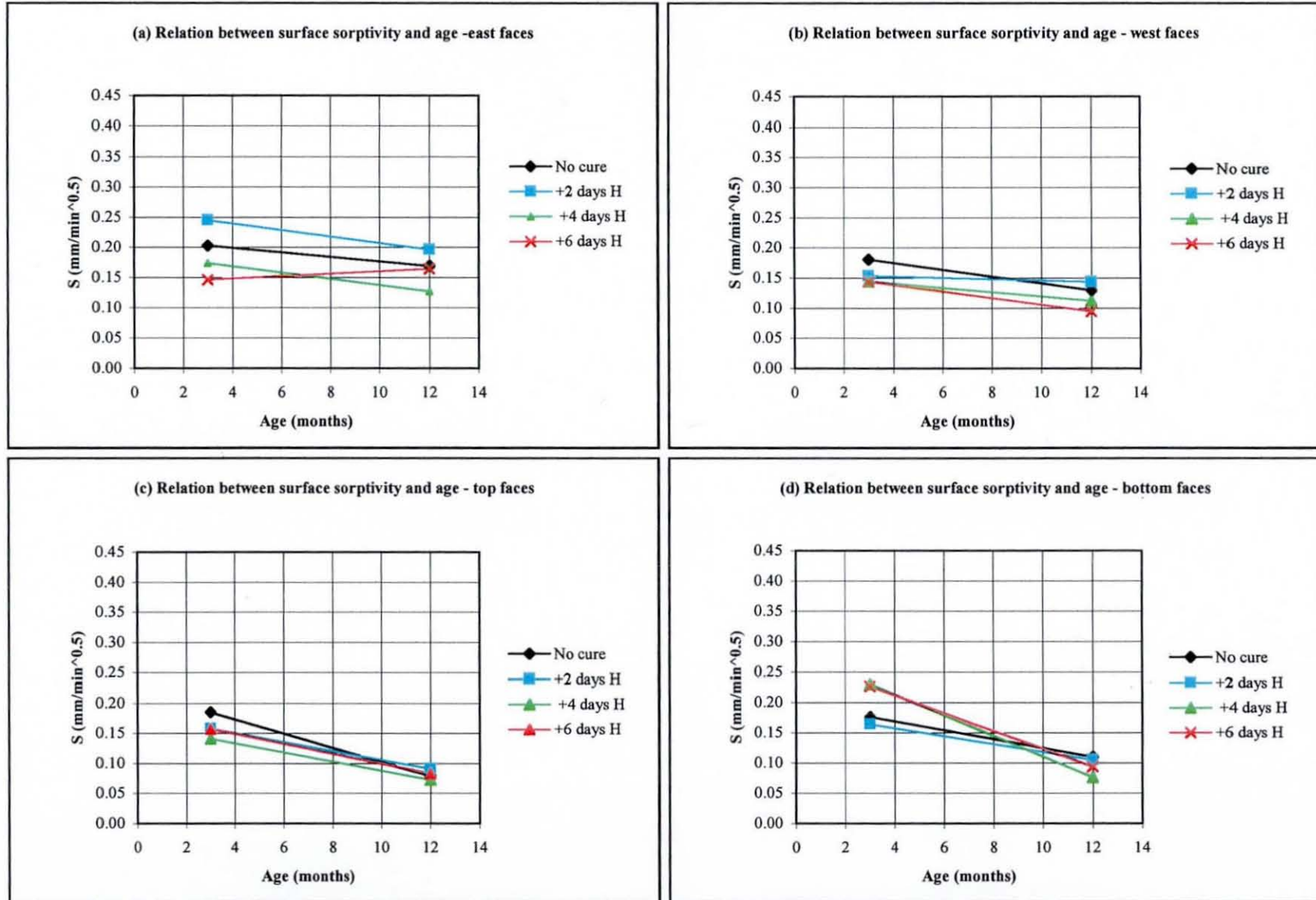


Fig. 5.18 Relationship between surface sorptivity and age of the 30 MPa OPC concrete - UK winter

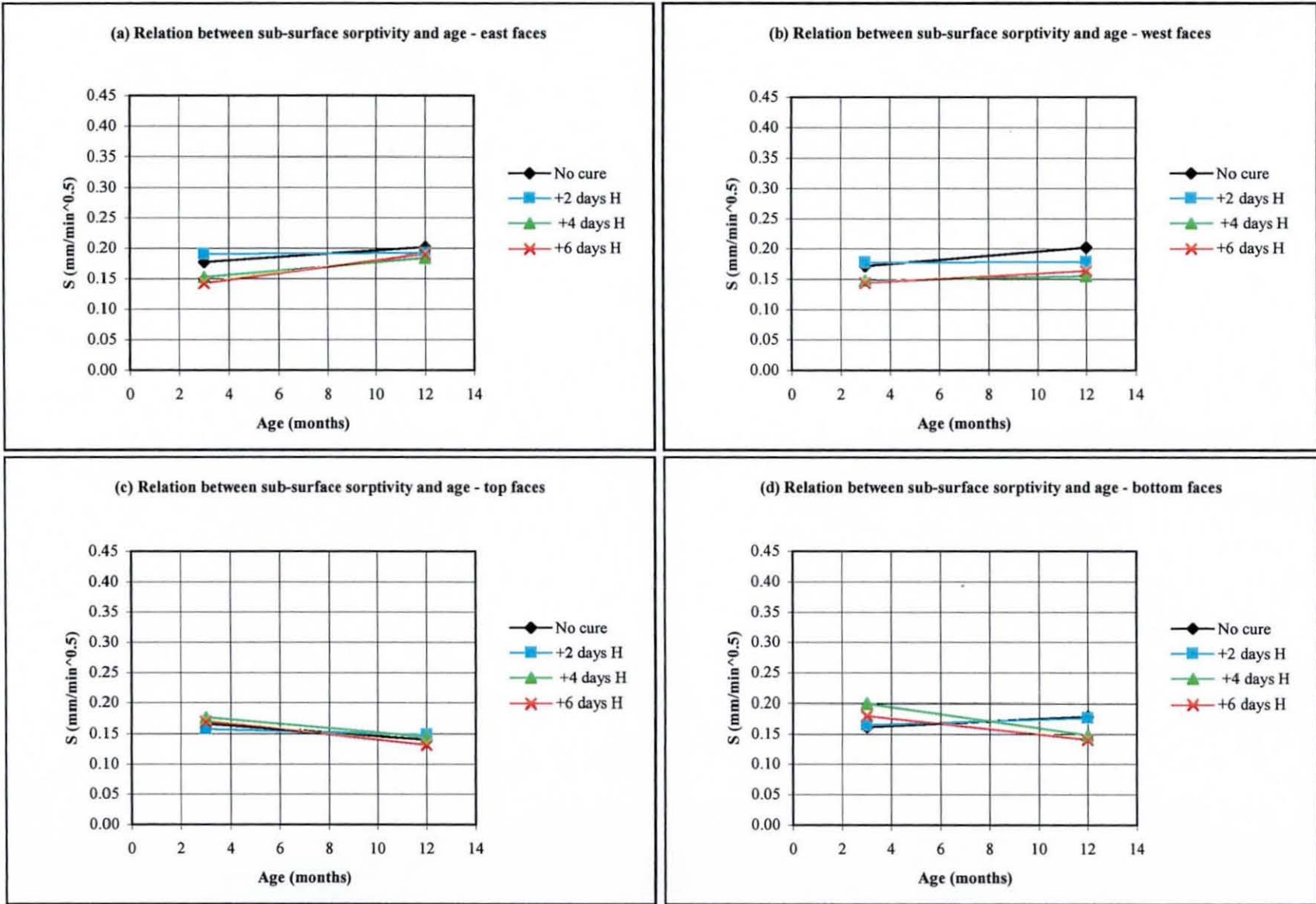


Fig. 5.19 Relationship between sub-surface sorptivity and age of the 30 MPa OPC concrete - UK winter

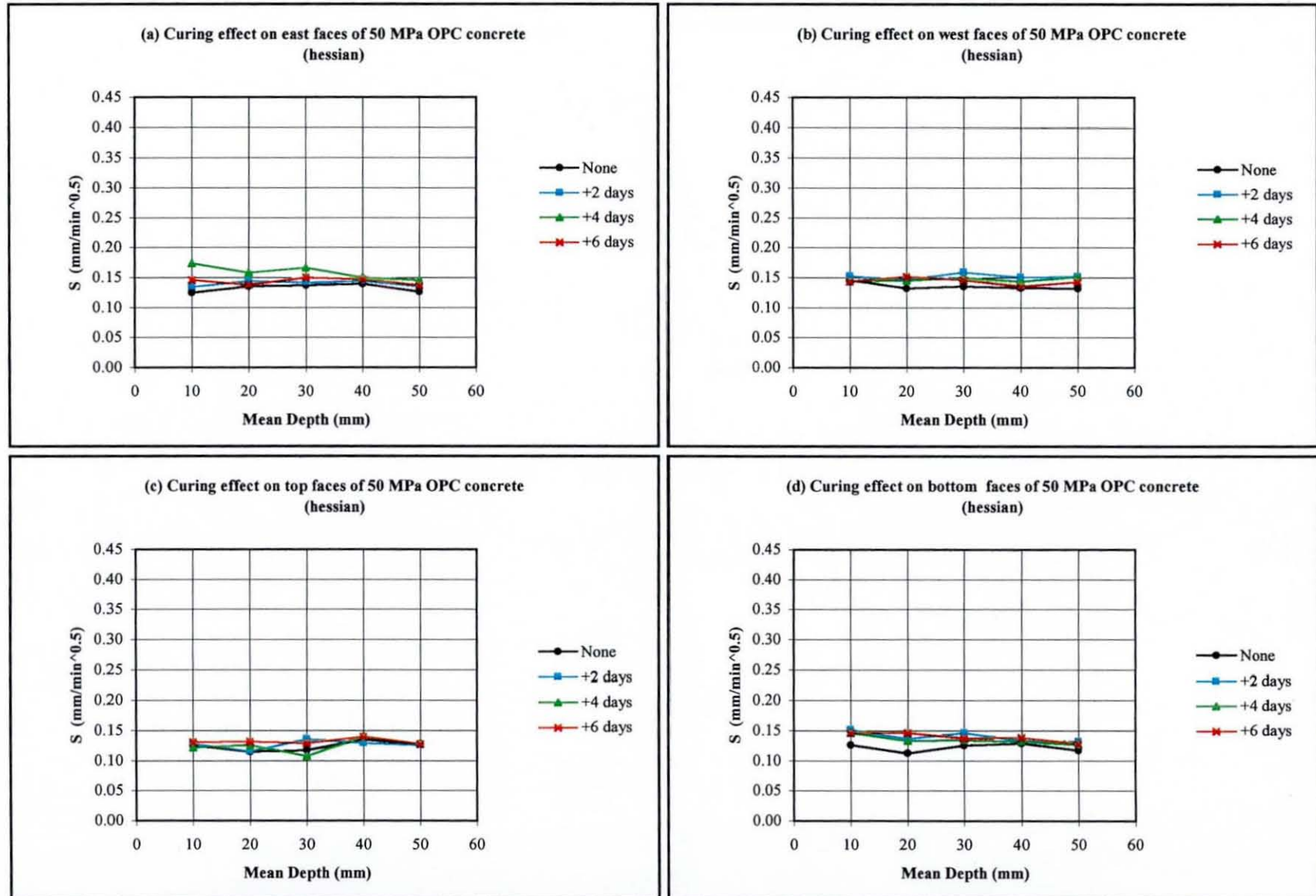
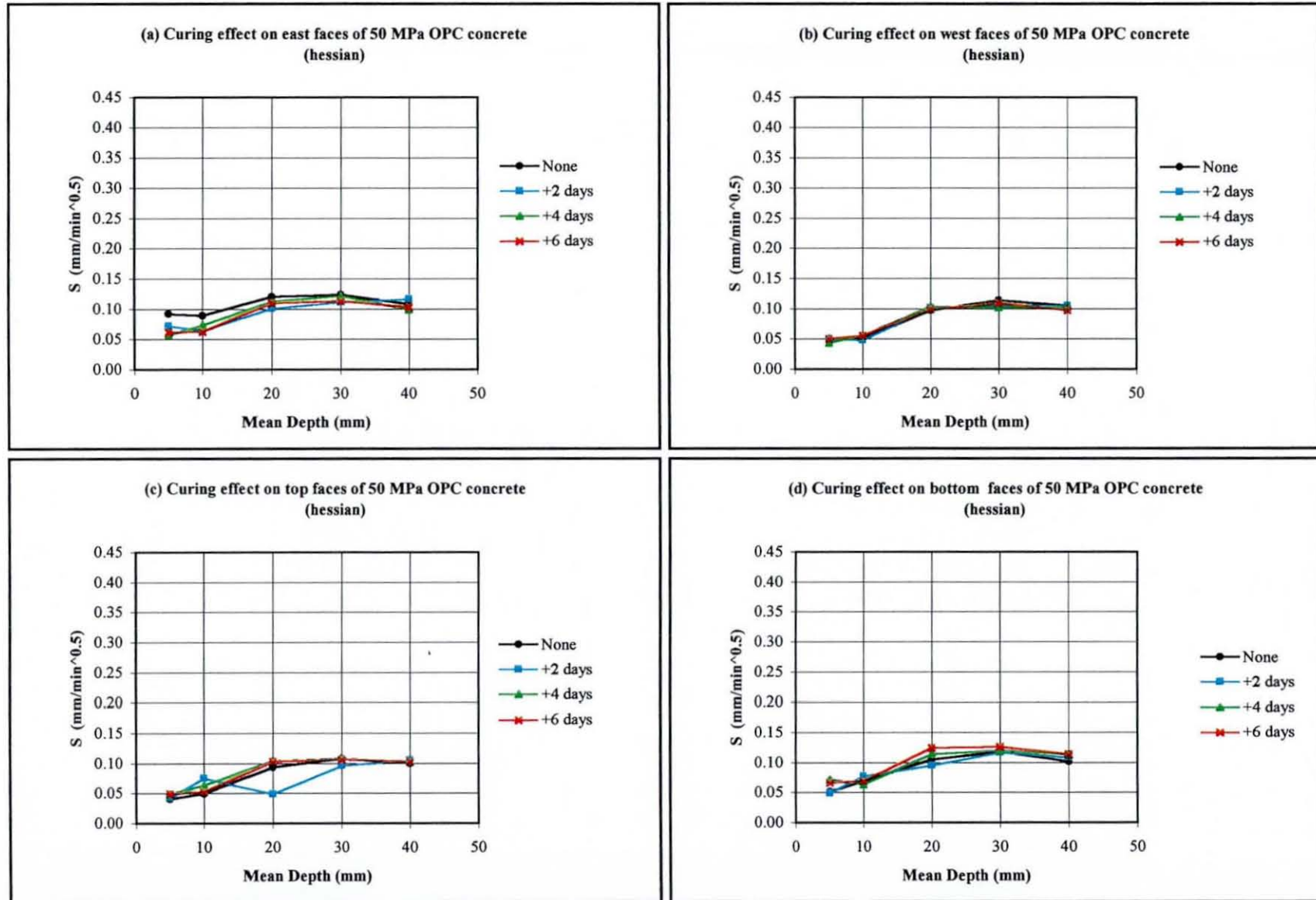


Fig. 5.20. Effect of curing regime on the sorptivity of 50 MPa OPC concrete - 3 months winter series



**Fig. 5.21** Effect of curing regime on the sorptivity of 50 MPa OPC concrete - 12 months winter series

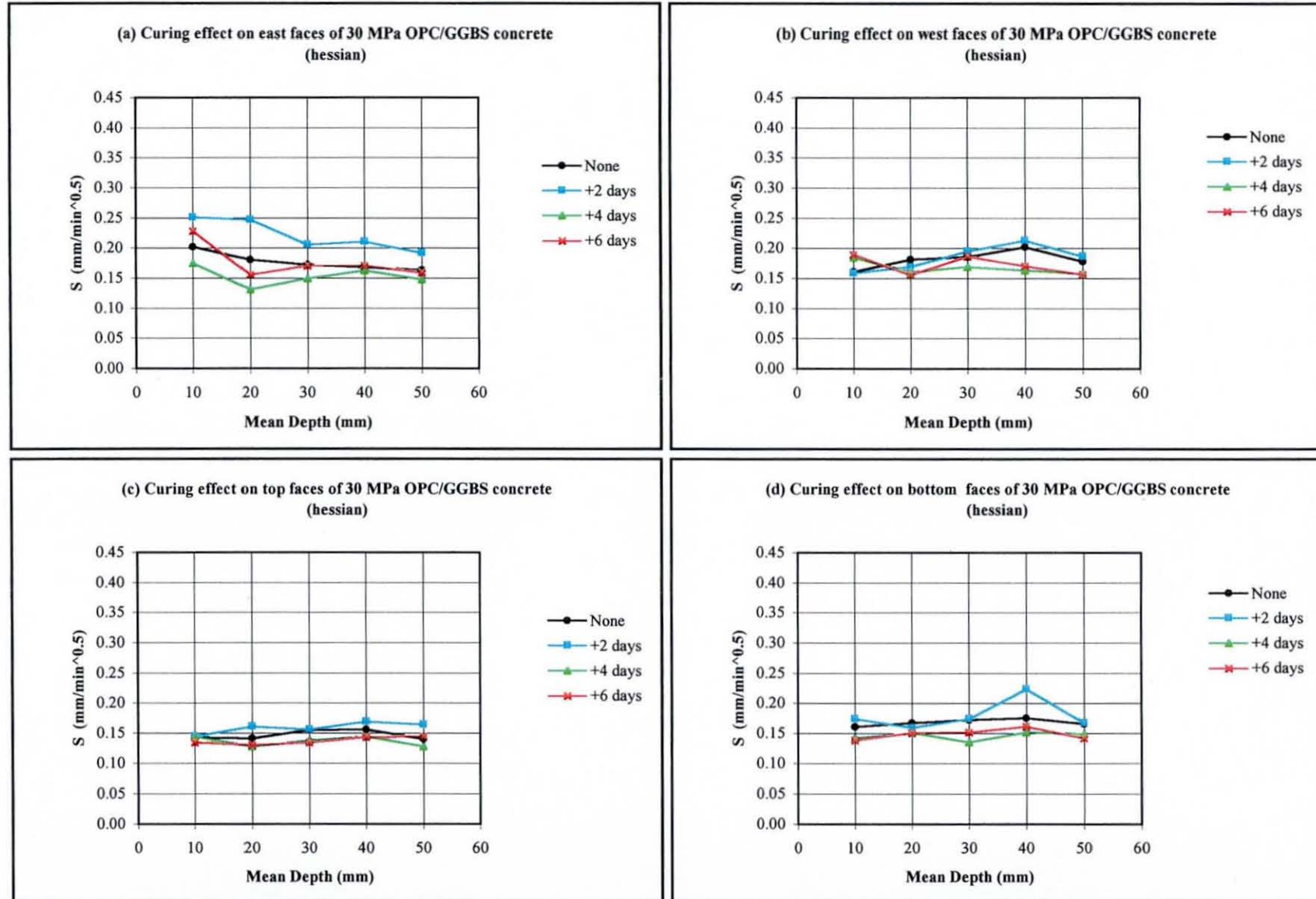


Fig. 5.22. Effect of curing regime on the sorptivity of 30 MPa OPC/GGBS concrete - 3 months winter series

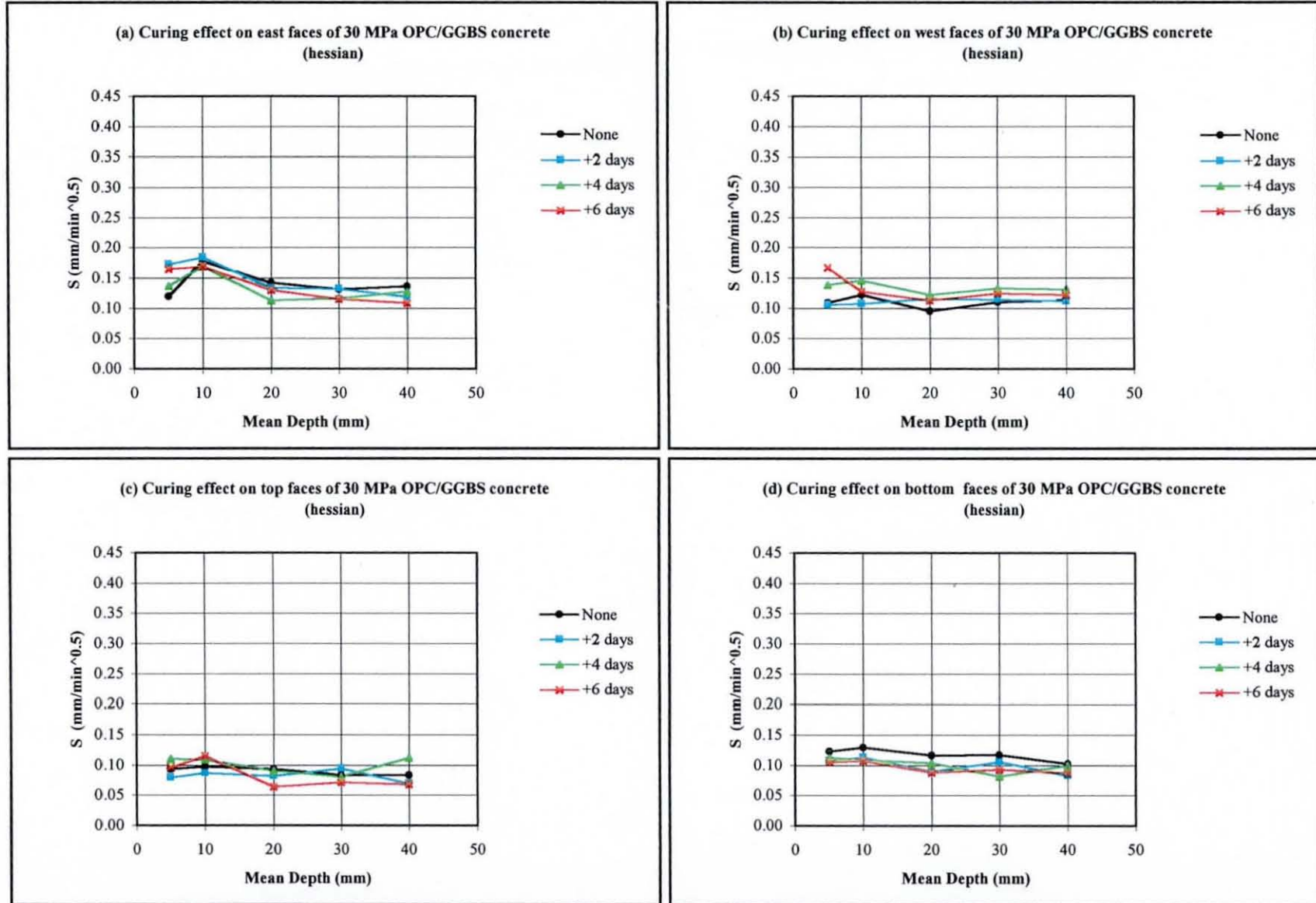


Fig. 5.23 Effect of curing regime on the sorptivity of 30 MPa OPC/GGBS concrete - 12 months winter series

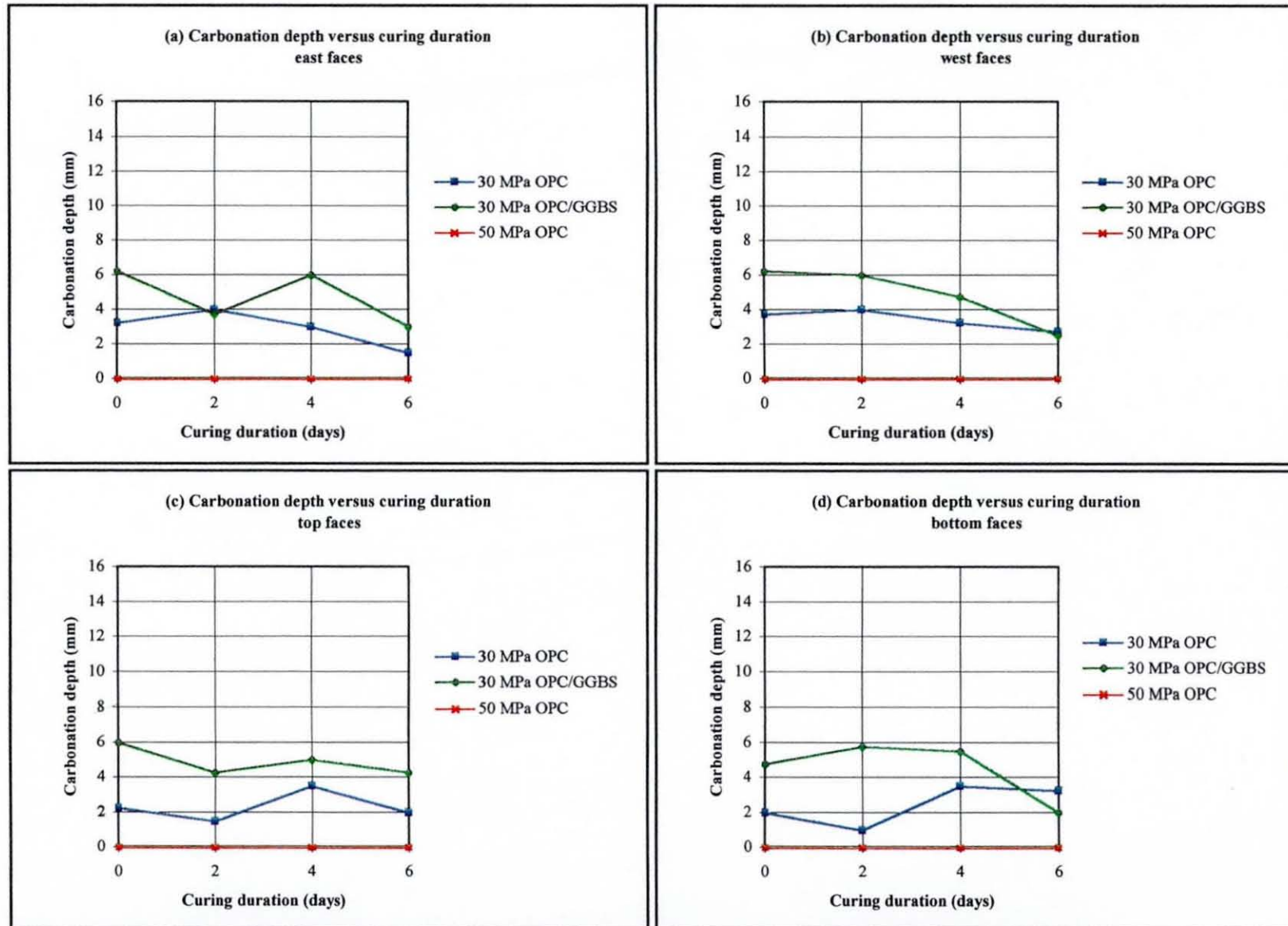


Fig. 5.24 Effect of hessian curing duration on carbonation depth - 6 months winter series (from Tables A1.13)

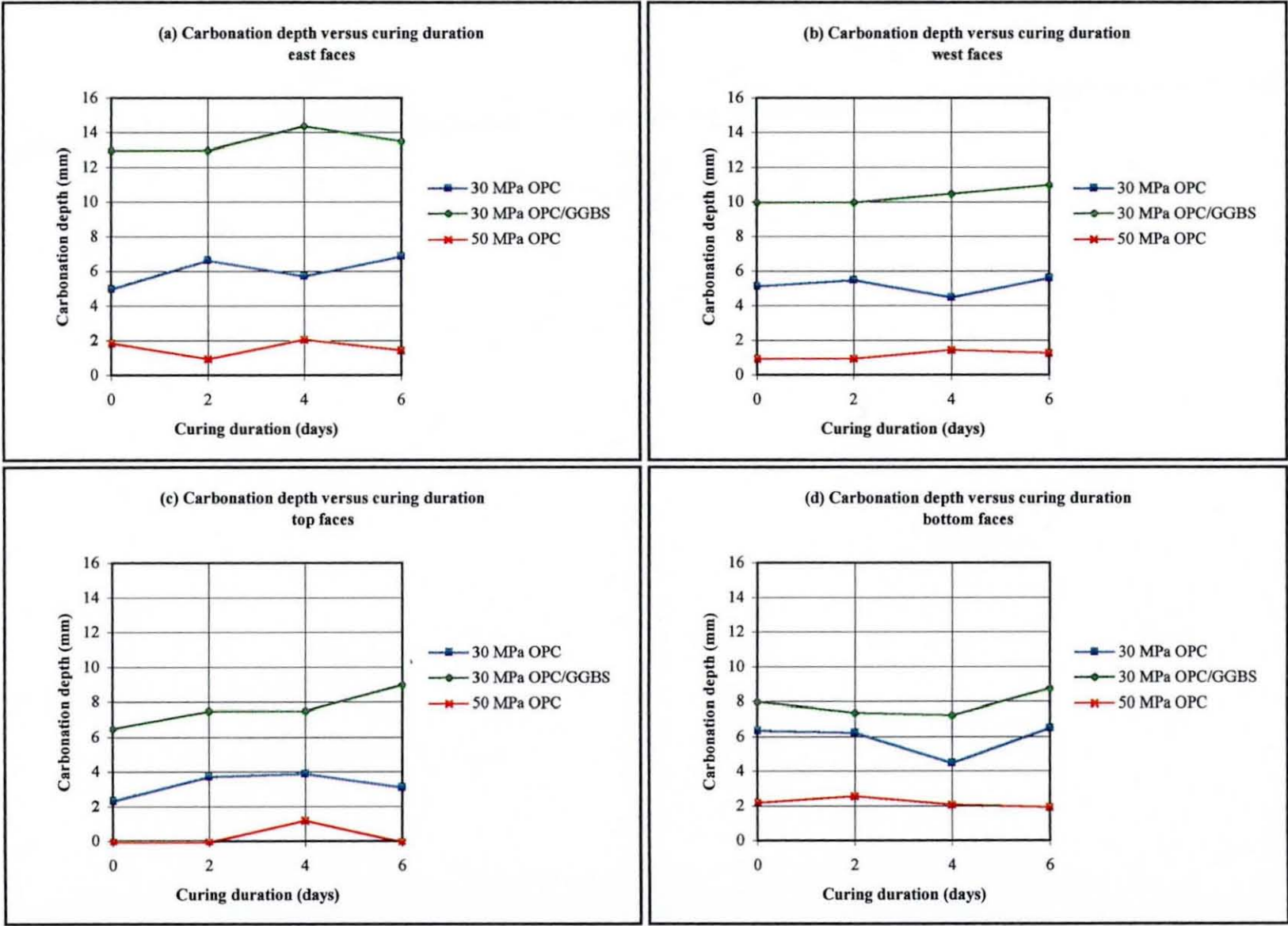


Fig. 5.25 Effect of microclimate, curing and concrete type on carbonation depth - 12 months winter series (from Tables A1.14)

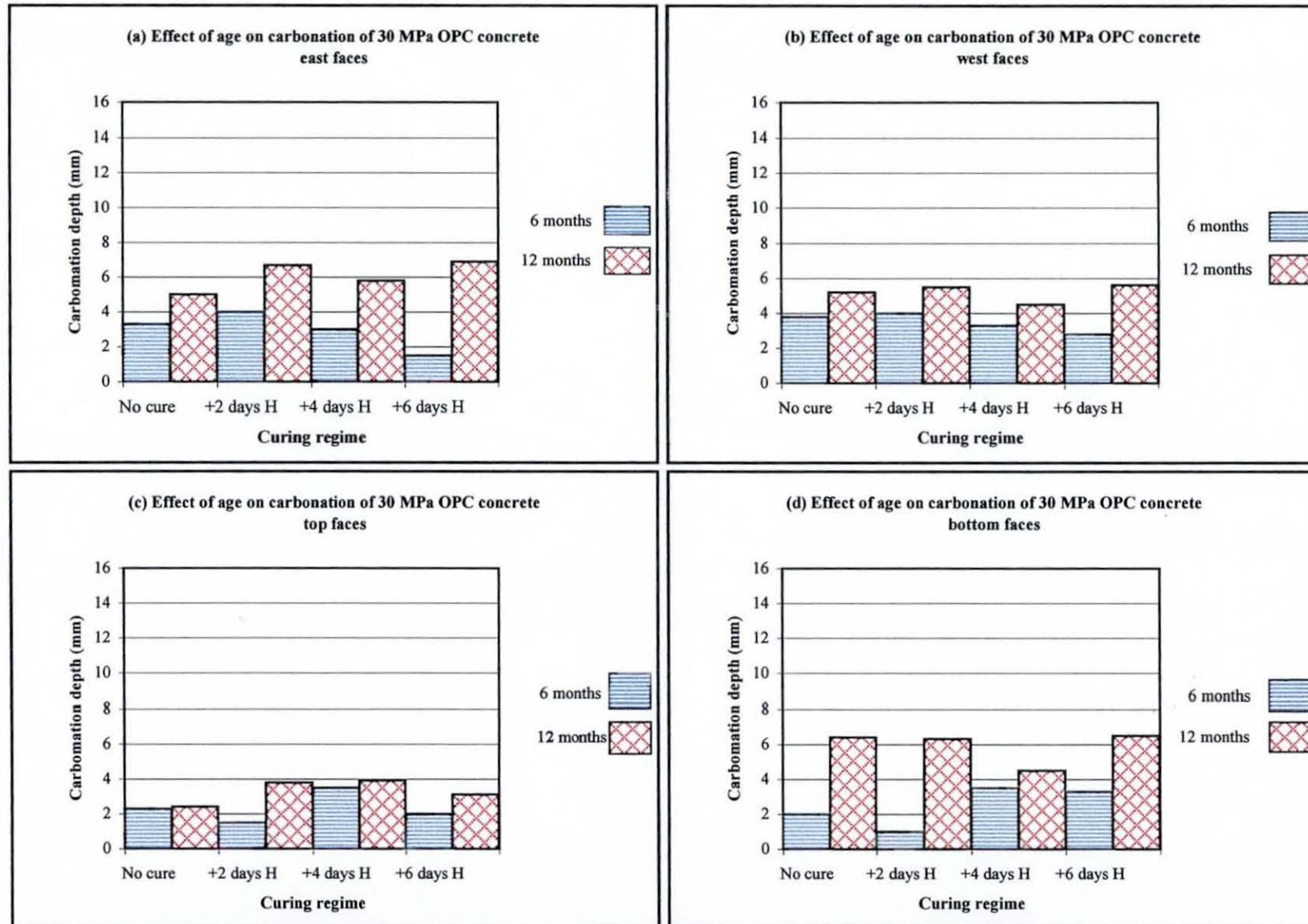


Fig. 5.26 Effect of age on carbonation depth of the 30 MPa OPC concrete - winter series

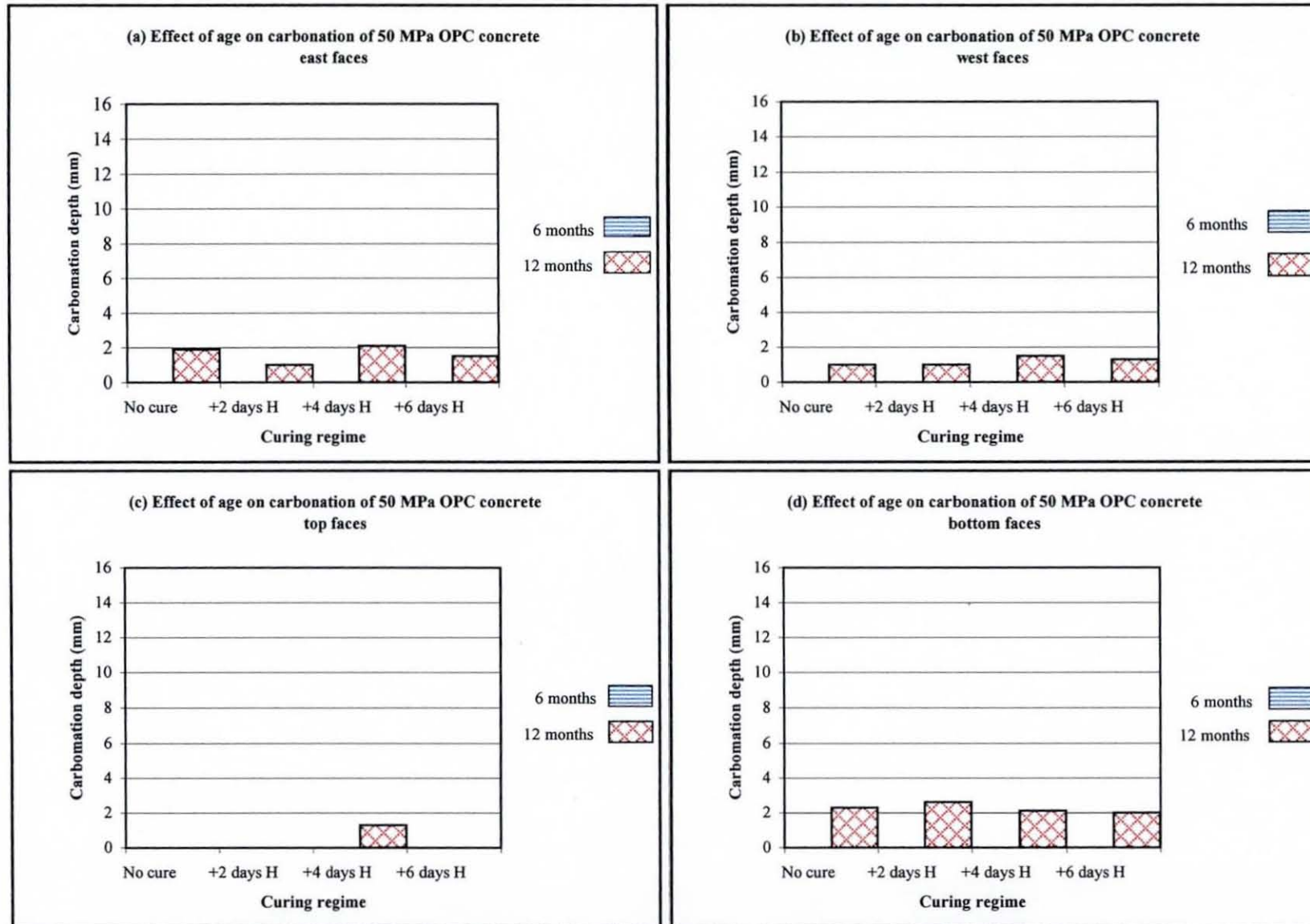


Fig. 5.27 Effect of age on carbonation depth of the 50 MPa OPC concrete - winter series

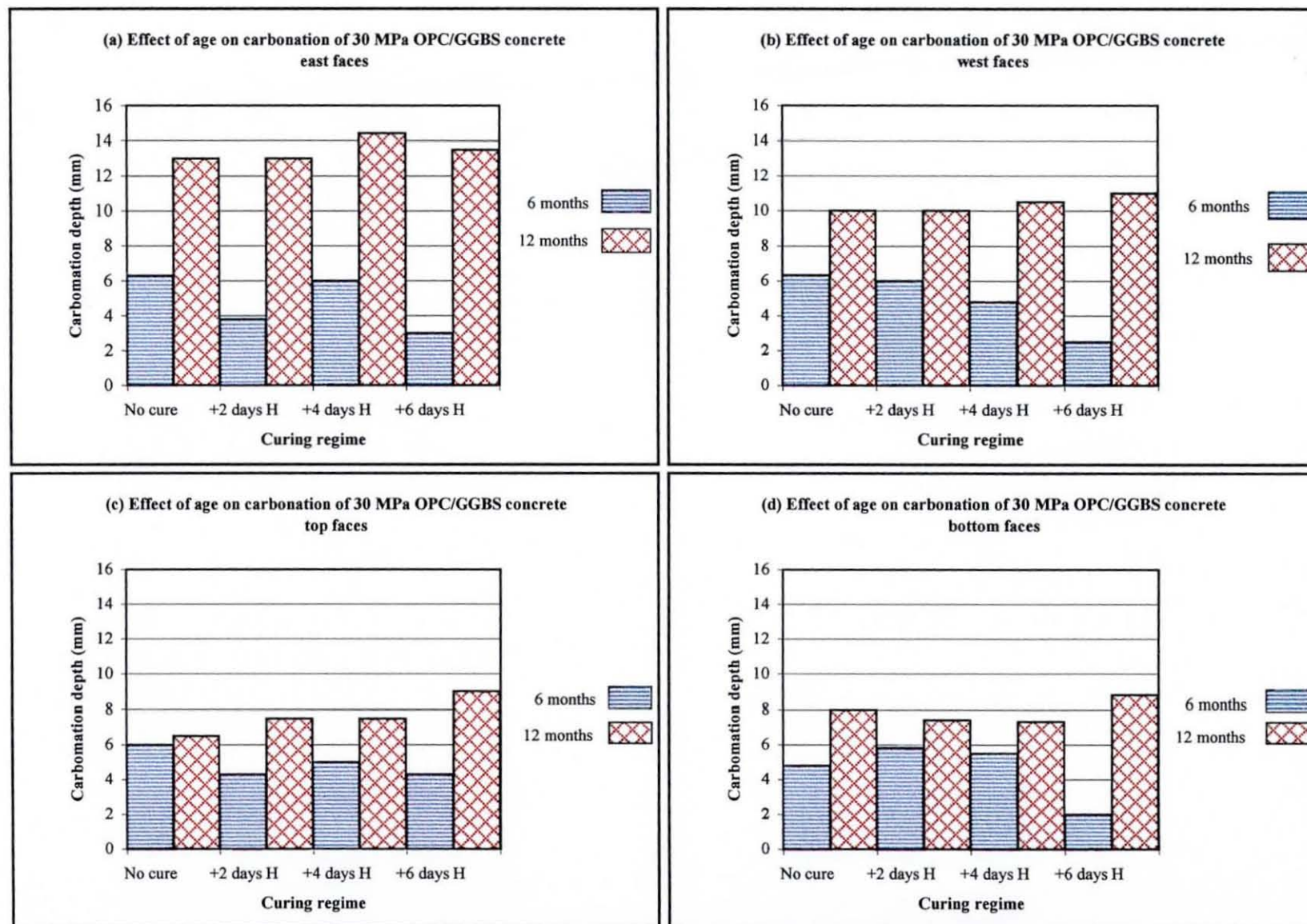


Fig. 5.28 Effect of age on carbonation depth of the 30 MPa OPC/GGBS concrete - winter series

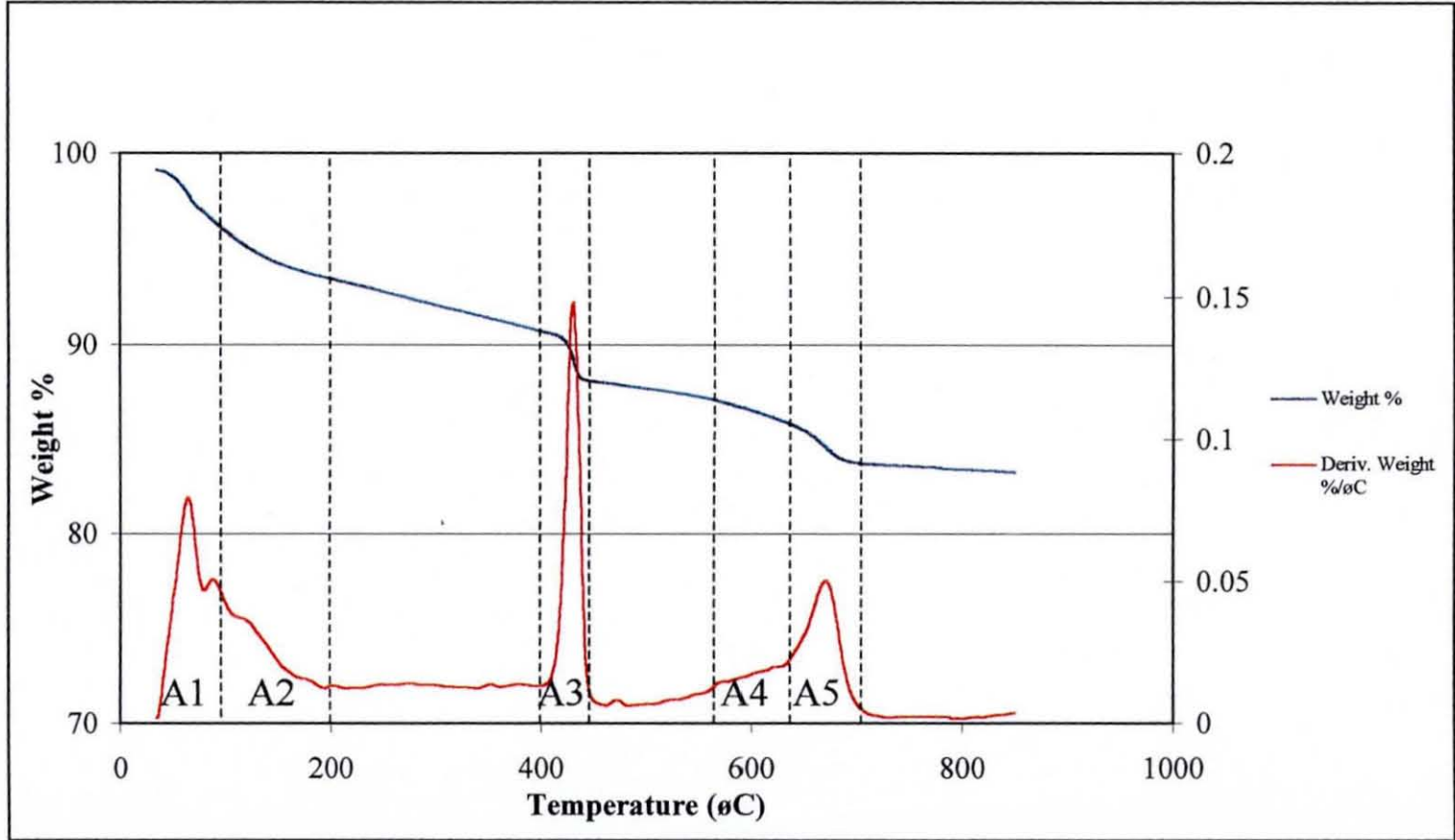


Fig. 5.29 Typical temperature boundaries for the calculation of weight loss of phases from the areas under the DTG peaks (Tables A1.15 and B1.23)

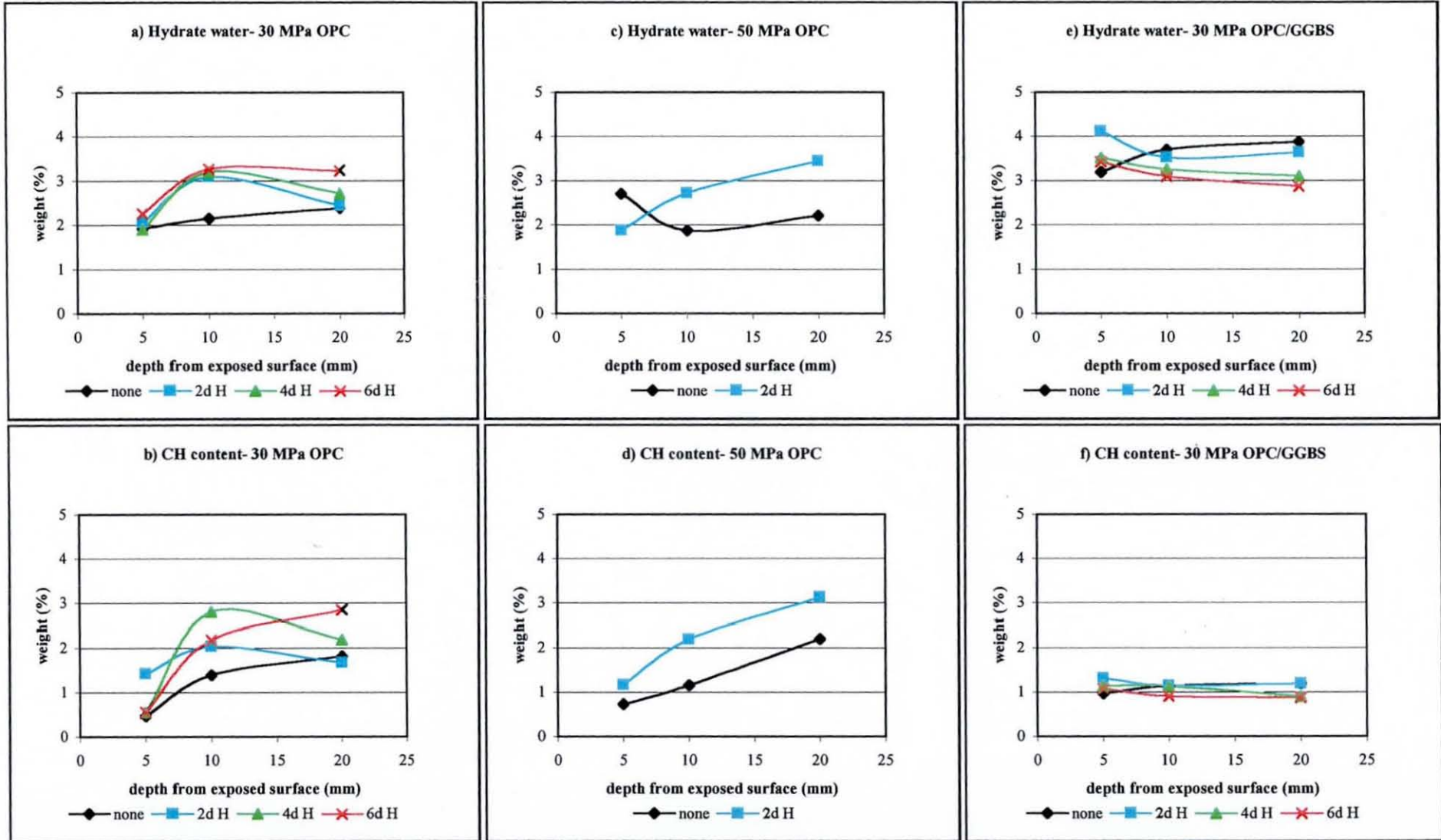


Fig. 5.30 Hydrates water and lime content profiles of the 3 concretes - 12 months winter (from Table A1.15)

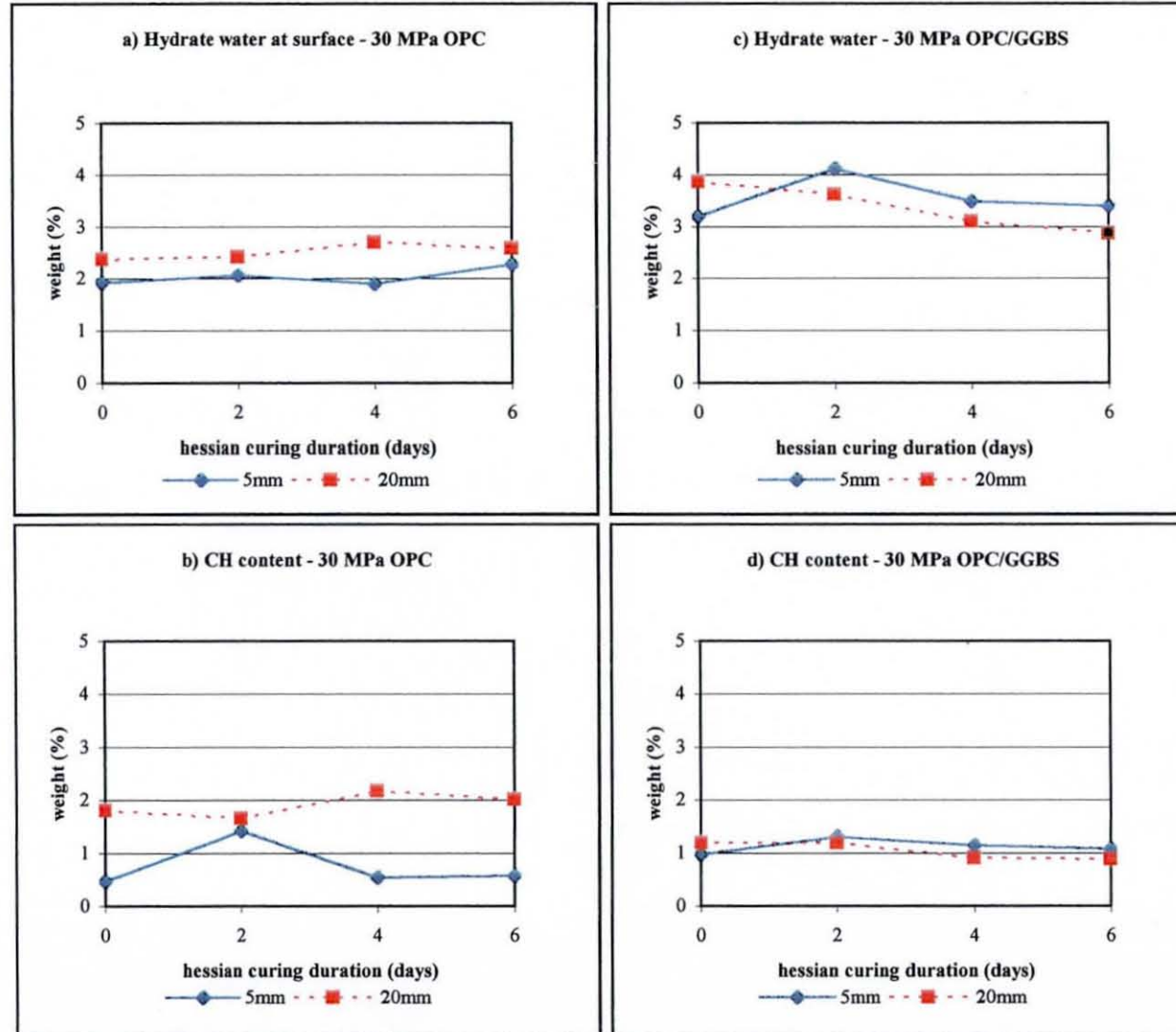


Fig. 5.31 Hydrates water and lime content at the surface (5mm) and subsurface (20mm) layers of concrete - 12 months winter

## Chapter 6 Loughborough Summer Climate

---

### 6.1 INTRODUCTION

This chapter presents the results of the five tests performed in the investigation of the Loughborough summer series. The effects of alternative curing methods and duration, microclimate, the application of controlled permeability formwork liner and exposure time on the three concrete mixes in this series (30 and 50 MPa OPC concrete mixes and a 30 MPa OPC/GGBS concrete mix) are reported.

The concrete blocks were tested at the ages of 3 and 12 months. The air permeability and sorptivity tests were conducted when the concretes were 3 months old, and the carbonation test at 6 months old. These tests, as well as thermal analysis by thermogravimetry (TG) and mercury intrusion porosimetry (MIP) were conducted at 12 months. As with the winter series, standard 28 days compressive strength tests were carried out throughout the investigation for quality verification and control. A detailed discussion of the results and trends of the summer series results is given in Chapter 8.

The procedures adopted during the sample preparation and conditioning of the winter series were followed for the summer series tests (Chapter 4).

### 6.2 WEATHER DATA

Tables 6.1 and 6.2 give the average weekly and monthly temperature, relative humidity and wind direction for the three concrete mixes in the summer series, during the initial curing period and the first 3 months of exposure

respectively. The temperature and relative humidity were generally similar during both the initial curing and exposure periods for all the mixes. The prevailing wind direction was largely westerly to north westerly during the first two months of exposure, changing to south easterly in the third month. There was 35 days of rain during the initial curing and exposure periods. These were 9 days in August; 14 days in September and 12 days in October, the average rainfall being 6.2, 1 and 5.4 mm respectively. The wind direction during these days was mainly south to south westerly.

### **6.3 COMPRESSIVE STRENGTH**

The compressive strength test results are given in Tables 6.3. The variation in the compressive strength results between the mixes was small, indicating no significant mix-to-mix differences between the blocks. The coefficient of variation of the compressive strength test results between nominally identical specimens was within 10%.

### **6.4 AIR PERMEABILITY**

#### **6.4.1 Introduction**

The sample preparation procedures and test methodology were discussed earlier in Chapters 4 and 5. Additional curing methods (polythene and a curing compound) and a controlled permeability formwork system (CPF) were evaluated on the slag concrete mix. These were not included in the OPC concrete mixes because of time and resources constraints.

The repeatability and reproducibility of the air permeability test were discussed earlier in Section 5.4.1.

Similar to the winter series results, the air permeability of the two OPC concretes were higher at the surface zone (SZ) than the sub-surface zone (SSZ) at 3 months. The variations in the air permeability values were small at the SSZ of the blocks, in the 4 microclimates. The SZ values of the east and west faces of the 30 MPa OPC concretes were approximately 50% higher than the

SSZ (Figure 6.2 (a) and (b) and Figure 6.4 (a)). The difference was smaller in the top faces of the slabs, the SZ values being approximately 30% higher than the SSZ values. However, the SZ values of the bottom faces of the slabs were approximately 60% higher than the SSZ values. This effect was generally less apparent in the 50 MPa OPC concretes.

Like the 12 months winter results, a change in the SZ and SSZ profiles was observed in the 12 months summer results of the two OPC concretes. The difference between the SZ and SSZ of the concretes in each microclimate was generally insignificant, the coefficient of air permeability at the SZ of the east/west and top/bottom faces being either lower or similar to the SSZ, as shown in Figure 6.3. Further, the lower air permeability values at the surface (5mm) were more prevalent in the 0 and 2 days cured blocks than those cured for 4 and 6 days

For the OPC/GGBS concrete, the air permeability values of the blocks at 3 months were, on average, 25-30% higher at the SZ than the SSZ (Figure 6.10 and Tables B1.5 in Appendix B). Unlike the winter results, the range of measured permeability values was large in each microclimate i.e. the difference in permeability values due to hessian curing duration was distinct (Figures 6.10 and 6.11).

Contrary to the two OPC concretes, the coefficients of air permeability of the OPC/GGBS concrete at 12 months were between 15-50% higher at the SZ than the SSZ of the all the samples. The surface 5-mm permeability values were lower than the 10 mm values in the east and west faces of the 0 and 2 days hessian cured blocks (see Figure 6.11 (a) and (b)). This effect was not as widespread as was in the 30 MPa OPC concrete,

Generally, the air permeability profiles of the slag concrete displayed a distinctive sharp reduction with increasing depth from the surface in the SZ, followed by a more gradual reduction in the SSZ (see Figure 6.11). Like the OPC concretes, the variations in the air permeability profiles at the SSZ were insignificant.

## 6.4.2 30 MPa OPC Concrete

### *Microclimate*

Figures 6.2 and 6.3 show the effect of microclimate on the air permeability profiles of the 30 MPa OPC concrete samples at the ages of 3 and 12 months respectively. The results with statistical analysis are presented in Appendix B, Tables B1.1 and B1.2 (a) & (b), for the 3 and 12 months tests respectively.

The east and bottom faces of the concrete blocks were more permeable than the west and top faces of the same concrete blocks respectively. At 3 months, the east faces of the vertical blocks were approximately 30% more permeable than the west faces at the SZ and SSZ, as can be seen from Figure 6.2 (a) and (b) (values are given in Table B1.1 (a) in Appendix B). The bottom faces were approximately 65% and 40% more permeable than the top faces of the slabs, at the SZ and SSZ respectively (Figure 6.2 (c) and (d)).

At the age of 12 months, the east faces of the vertical blocks were, on average, 30% more permeable than the west faces, at the SZ and SSZ (Figure 6.3 (a) and (b)). The bottom faces were approximately 50% more permeable than the top faces of the slabs in the SZ. In the SSZ, the coefficients of air permeability of the bottom faces were, on average, 20% more permeability than the top faces (Figure 6.3 (c) and (d) and Table B1.4 (b)).

### *Duration of hessian curing*

The relationship between the air permeability and hessian curing duration of the 30 MPa OPC concrete is presented in Figures 6.4 and 6.5, (a) and (b), at the ages of 3 and 12 months respectively.

As can be seen from the 3 months graphs (Figure 6.4 (a) and (b)), the air permeability values decreased with increased hessian curing duration in the 4 microclimates. The improvement in the air permeability values was more prominent in the SZ than the SSZ, and in the east and bottom faces than the west and top faces of the concrete blocks. The improvements in the SZ of the east faces from 0-2, 2-4, and 4-6 days hessian curing were 15, 20 and 30% respectively; and 6, 8 and 25% respectively in the west faces. In the SSZ, there

was, on average, 5% improvement in the air permeability with increased hessian curing duration (0-6 days) of the east and west faces. The improvement due to increased curing duration (0-6 days) was approximately 25 and 10% for the top and bottom faces of the slabs respectively.

Except for the east facing concrete blocks, the variations in the air permeability due to curing duration were significantly smaller after 12 months of field exposure. For the east faces, the air permeability of the 4 and 6 days cured blocks were approximately 40% lower than the 0 and 2 days cured blocks at the SZ and SSZ. The difference in quality between the west facing blocks and slabs were generally small in all samples regardless of curing duration. It is of note that the air permeability of the 0 and 2 days cured samples appear to have improved with age to a greater extent than the blocks that received 4 and 6 days hessian curing (west, top and bottom faces).

#### *Age*

Figures 6.6 and 6.7 illustrate the typical relationship between air permeability and age at the SZ and SSZ respectively.

The coefficients of air permeability at the SZ of the blocks were lower after 12 months of exposure. The reduction in the permeability values with time was more significant in the SZ than the SSZ, and in the east and bottom faces than the top and west faces. Surprisingly, the east and west faces of the blocks exhibited no improvement in the permeability with age at the SSZ.

There was, approximately between 50-80% improvement in the air permeability indices (lower permeability) with age, at the SZ of the east/west and top/bottom faces of the blocks. Although the permeability of the 4-6 days cured blocks were generally lower at 12 months, the improvement in the air permeability with age was more significant in the 0-2 days cured blocks than the 4-6 days cured blocks (see Figure 6.6). The permeability of 0-2 days cured blocks improved by over 75% with age, compared to approximately 50% for the 4-6 days cured blocks. Generally, the coefficients of air permeability of the 12 months old samples were about 2 to 5 times lower than the 3 months old

samples, especially at the surface. Like the winter series, the difference in magnitude between the SZ and the SSZ permeability values (in all microclimates) in the 12 months old samples was also smaller than the 3 months old samples. The difference in magnitude between the SZ and SSZ was reduced by approximately 15% in the east and west faces, and 25% in the top and bottom faces after 12 months of exposure.

#### 6.4.3 50 MPa OPC Concrete

##### *Microclimate*

Figures 6.8 and 6.9 show the effect of microclimate on the air permeability profiles of the 50 MPa OPC concrete samples at the ages of 3 and 12 months respectively. The results with statistical analysis are presented in Appendix B, Tables B1.3 and B1.4 (a) & (b), for the 3 and 12 months tests respectively.

The air permeability indices of the 50 MPa OPC concrete were generally comparable, the variations due to microclimate (or curing) being small (see Figure 6.8). At the age of 3 months, the average air permeability at the SZ (10mm) of the east faces of the blocks was  $1.5 \times 10^{-16}$  compared to  $1 \times 10^{-16}$  for the west faces of the blocks. The air permeability values at the SSZ of the east faces were marginally higher than the west faces (Table B1.3 (a) in Appendix). Similarly, the bottom faces of the slabs were approximately 30% more permeable than the top faces at the SZ, with the variation between the two faces at the SSZ being generally marginal (Figure 5.15 (c) and (d)).

The effect of microclimate remained largely the same after 12 months of exposure. The east faces of the blocks were approximately 10% more permeable than the west faces at the SZ and SSZ. Similarly, the bottom faces were, on average, 30% more permeable than the top faces at the SZ. The variations between the top and bottom faces at the SSZ were marginal.

### *Duration of hessian curing*

The relationship between air permeability and curing duration of the 50 MPa OPC concrete is presented in Figures 6.4 and 6.5, (b) and (c), at the ages of 3 and 12 months respectively.

As can be seen, the effect of hessian curing duration on the 50 MPa concrete at both ages was not significant. The 50 MPa OPC concrete was the least sensitive to curing of the 3 mixes, the differences in the air permeability due to curing being generally marginal in all samples (in the 4 microclimates).

### *Age*

The relationship between air permeability and age of the 50 MPa OPC concrete is shown in Figures B1.1 and B1.2 in Appendix B, for the SZ and SSZ respectively.

The coefficients of air permeability of the 12 months old samples were approximately 2-4 times lower than the 3 months old samples in the 4 microclimates (see Table B1.3 and B1.4 in Appendix B).

## **6.4.4 30 MPa OPC/GGBS Concrete**

### *Microclimate*

Figures 6.10 and 6.11 show the effect of microclimate on the air permeability profiles of the 30 MPa OPC/GGBS concrete samples at the ages of 3 and 12 months respectively. The results with statistical analysis are presented in Appendix B, Tables B1.5 and B1.6 (a) & (b), for the 3 and 12 months tests respectively.

The east faces of the blocks were more permeable than the west faces. At 3 months, the coefficient of air permeability was higher in the east faces by approximately 20 and 25% (on average) at the SZ and SSZ respectively. The bottom faces of the slabs were, on average, 35% more permeable than the top faces at the SZ and SSZ.

At 12 months, the coefficients of air permeability of the east faces were higher than the west faces by approximately 10 at the SZ and SSZ. The bottom faces

of the slabs were approximately 30% more permeable than the top faces at both the SZ. At the SSZ, the air permeability values in the two faces of the slabs were generally similar.

#### *Duration of hessian curing*

The relationship between air permeability and hessian curing duration of the 30 MPa OPC/GGBS concrete at the ages of 3 and 12 is presented in Figures 6.4 and 6.5 (e) and (f), respectively.

The coefficients of air permeability of the OPC/GGBS concrete blocks at the age of 3 months decreased with increased curing duration, in the 4 microclimates. The reduction in the air permeability values with prolonged hessian curing was sharp especially for the east and bottom faces of the blocks (see Figure 6.4 (e) and (f)). The improvement in the SZ permeability values of the east and west faces for the 0-2, 2-4, and 4-6 days cured blocks were 7, 40 and 30%, and 33, 32 and 17% respectively. After 6 days of hessian curing, the air permeability values reduced, on average, by 45% at the SSZ of all the samples.

After 12 months of exposure, the air permeability indices of the 6 days cured blocks were, on average, 70% lower than the non-cured blocks. This is mainly due to the fact that the improvement in the permeability of the non-cured and 2 days cured blocks with age was smaller relative to the 4 and 6 days cured blocks, especially in the east and west faces (Figures 6.4 and 6.5 (e) and (f)). Generally, the improvement due to curing in the air permeability of the blast-furnace slag concrete was more significant compared with the two OPC concretes.

#### *Polythene and curing membrane (C/M) methods*

The air permeability profiles of the air and hessian cured concrete blocks together with the curing membrane and polythene cured blocks are shown in Figures 6.12 and 6.13 for the 3 and 12 months old concretes respectively. The air permeability indices of the polythene and C/M cured samples are given in Tables B1.9 to B1.10 in Appendix B.

The curing membrane (C/M) had no positive effect on the quality of the concrete blocks at the age of 3 months. The permeability of C/M and the non-cured blocks were very similar, their coefficients of air permeability being higher than the 4-6 days hessian cured blocks by approximately 60 and 50% in the east/west and top/bottom faces respectively. Wrapping with polythene sheeting for 6 days produced marginally higher air permeability values than the 4 and 6 days hessian cured blocks. However, the difference between polythene and hessian cured blocks was more significant in the drier microclimates i.e. the east and bottom faces of the blocks, the coefficient of air permeability being approximately 40% higher in the polythene cured blocks compared to the 4 and 6 days hessian cured blocks. The polythene cured blocks were approximately 30% higher than the hessian cured blocks in the west and top faces.

The performance of the wet (hessian) and polythene cured blocks at 3 months was better than the C/M cured concrete blocks. However, the air permeability of the C/M cured blocks improved with age, being similar to or slightly lower than the 2 days hessian cured blocks after 12 months exposure (Figure 6.13). As with the other curing regimes, the improvement in the air permeability was most and least significant in the top and east faces of the blocks respectively.

The permeability of C/M cured blocks improved by more than 30% in the 4 microclimates after 12 months of exposure. These blocks (C/M cured blocks), however, were still approximately 70% more permeable than the 4-6 days hessian cured blocks in the east and west faces. In the top and bottom faces, the C/M cured samples were 10-25% more permeable than the 4-6 days hessian cured blocks. Further, as with the 3 months tests, wrapping with polythene sheeting for 6 days produced marginally higher air permeability values than the 4 days hessian cured blocks. The polythene-cured blocks being 10-30% more permeable than the 4-6 days hessian-cured blocks in the east and west faces. The differences in permeability due to curing regime,

however, were very small in the top and bottom faces, relative to the 3 months results.

#### *Controlled permeability formwork (CPF)*

A comparison between the 3 months air permeability profiles of the CPF-produced concrete and that produced with conventional formwork is given in Figures 6.14 and 6.15. The 3 months permeability indices of the CPF and conventionally produced concrete with statistical analysis are listed in Tables B1.7 and B1.8 in Appendix B.

The CPF-produced concrete was significantly less sensitive to the effect of microclimate than the conventionally produced concrete (see also the 12 months results given in Figures 6.18 and 6.19).

The 3 months results show that regardless of curing method, the coefficients of air permeability of all the CPF-produced concrete blocks were dramatically lower at the surface than the blocks that were cast against conventional formwork. Furthermore, the CPF-produced blocks that received no curing were significantly less permeable at the surface than all cured blocks that were produced with conventional formwork. The results were re-plotted in Figures 6.16 and 6.17 to show the effect of curing at the SZ (10mm) and SSZ (20-50mm) respectively. Generally, the surface air permeability values (Figure 6.16) in all samples were between 2 to 10 times lower in the CPF blocks compared to conventional formwork blocks. However, the difference between CPF and conventional formwork blocks was most striking in the top and bottom faces of the air and 2 days cured blocks; the permeability values being between 15 to 50 times lower in the CPF-produced concrete blocks (see Figures 6.14 and 6.16 (c) and (d)). It is interesting to note that not only did the influence of CPF diminish with distance from the surface, the air permeability indices in the SSZ were higher in the CPF-produced blocks than the blocks that were cast against conventional formwork, as shown in Figures 6.17.

The permeability profiles of the samples at 12 months are given in Figures 6.18 and 6.20. The coefficients of air permeability of the samples (12 months)

are listed in Tables B1.9 and B1.10 in Appendix B. The improvement in the permeability of the CPF-produced concrete blocks after 12 months of exposure was larger in the SZ than the SSZ. The 12 months results were re-plotted in Figures 6.20 and 6.21 to show the effect of curing at the SZ and SSZ respectively. The surface permeability of the CPF-produced concrete was, on average, 20 times lower in the east and west faces compared to the conventionally produced concrete. For the top and bottom faces, the CPF concrete was, on average, more than 5 times lower than the conventional formwork concrete. In the SSZ, however, the CPF permeability values were approximately 5 times lower (Figure 6.21) than the 3 months values for the vertical blocks (east/west faces), and almost similar for the slabs (top/bottom faces).

#### *Age*

The coefficients of air permeability of the hessian-cured concrete were generally lower at 12 months than 3 months, at both the SZ and SSZ of the samples. Contrary to most samples, however, the 0 and 2 days hessian cured vertical blocks exhibited an increase in the air permeability with age (see Figure B1.3 in Appendix B). Unlike the 30 MPa OPC concrete, the improvement in the 12 months old samples was more notable at the SSZ than the SZ. The permeability values of the east and west faces at 12 months were approximately 10-20% lower than the 3 months samples at the SZ, and 30-60% lower at the SSZ. For the top and bottom faces of the slabs, the permeability values were lower than the 3 months old samples by between 40-50% at the SZ and 60-80% at SSZ.

The air permeability of the C/M and polythene cured samples reduced by approximately 15-20% at the SZ of the vertical blocks. The improvement with age was larger for the polythene cured samples than the C/M samples, and at the SZ of the slabs (top/bottom faces) than the SSZ. The 12 months air permeability of the samples at the SZ was approximately 2-4 times lower than

the 3 months samples. At the SSZ, the permeability values of all samples were 2-4 times lower than the 3 months old samples.

The air permeability of the CPF-produced concrete improved substantially with age at both the SZ and SSZ, however, the improvement was most significant at the SZ. Generally, the coefficients of air permeability of the CPF-produced concrete were between 5 to 30 times lower at 12 months than the 3 months old samples, at the SZ and SSZ (see Tables B1.7 to B1.10). Meanwhile, the improvement in the air permeability from 3 to 12 months of the identical concretes that were conventionally produced was between 20-50% at the SZ and SSZ, in the 4 microclimates.

## **6.5 SORPTIVITY**

### **6.5.1 Introduction**

The sorptivity calculations as well as the repeatability and reproducibility of the test results were discussed earlier in Section 5.5.1.

Like the 3 months winter results, the sorptivity of the concrete samples at the age of 3 months were higher at the SZ (10mm) than the SSZ (20-50mm), with the variation in the sorptivity indices being generally marginal at the SSZ. The difference in the sorptivity indices between the SZ and SSZ was most significant in the 30 MPa OPC concrete (15-30%) and least apparent in the 50 MPa OPC concrete (5%). This is inconsistent with the air permeability results (conducted on the same samples) where the difference in the air permeability between the SZ and SSZ was larger for the OPC/GGBS than the 30 MPa OPC concrete.

Similar to the 12 months winter sorptivity results, a change in the SZ/SSZ profile trends was observed in the 12 months summer concrete. The SZ values (5-20mm) of the two OPC concretes were lower than the SSZ (20-40mm) by more than 50% in all cases. This effect was only prevalent at 5mm from the surface of some OPC/GGBS concrete samples, the 10mm values being approximately 10-15% higher than the SSZ values. This is generally in

agreement with the air permeability results, which were distinct and more conspicuous than the sorptivity (compare Figure 6.11 with Figure 6.31).

## 6.5.2 30 MPa OPC Concrete

### *Microclimate*

Figures 6.22 and 6.23 show the effect of microclimate on sorptivity profiles of the 30 MPa OPC concrete samples at the ages of 3 and 12 months respectively. The results with statistical analysis are presented in Appendix B, Tables B1.11 and B1.12 (a) & (b), for the 3 and 12 months tests respectively.

As with the air permeability, the sorptivity of the east and bottom faces of the concrete blocks were higher than the west and top faces of the concrete blocks respectively. The microclimate influence, however, was more distinct in the air permeability results than the sorptivity (compare Figure 6.2 with 6.22). At the age of 3 months, the sorptivity indices of the east faces of the blocks were, on average, 10% higher than the west faces at the SZ and SSZ (sorptivity values are given in Table B1.11 (a) in Appendix B). The sorptivity indices of the bottom faces were approximately 25% and 15% higher than the top faces of the slabs, at the SZ and SSZ respectively (Figure 6.22 (c) and (d)).

The effect of microclimate remained unchanged after 12 months. The sorptivity of the east faces of the blocks was approximately 15% and 5% higher than the west faces at the SZ and SSZ respectively (Figure 6.23 (a) and (b)). The sorptivity indices of the bottom faces were approximately 25% and 15% higher than the top faces of the slabs at the SZ and SSZ respectively.

### *Duration of hessian curing*

The relationship between the sorptivity and hessian curing duration of the 30 MPa OPC concrete is presented in Figures 6.24 and 6.25, (a) and (b), at the ages of 3 and 12 months respectively.

As with the air permeability, (Figure 6.4 (a) and (b)), the sorptivity indices decreased with increased hessian curing duration in all samples. Similarly, the improvement in the sorptivity values due to curing was more noticeable

in the SZ than the SSZ. However, as previously noted, the influence of curing was more manifest in the air permeability results than the sorptivity (compare Figures 6.4 with 6.24 (a) and (b)). The SZ sorptivity indices were 15% to 25% lower after 6 days hessian curing, relative to the non-cured blocks, in the 4 microclimates. The reduction in the sorptivity due to increased hessian curing duration (0-6 days) at the SSZ was between 5 to 15%.

Surprisingly, the differences in the sorptivity values between the 0, 2, 4 and 6 days hessian cured concrete blocks were very small at 12 months (see Figure 6.25 (a) and (b)). The sorptivity indices were generally similar at both the SZ and SSZ regardless of curing duration, in the 4 microclimates.

#### *Age*

Figures 6.26 and 6.27 illustrate the typical relationship between air permeability and age at the SZ and SSZ respectively.

The sorptivity decreased with age at the SZ of the samples, however, it exhibited a slight increase at the SSZ after 12 months of exposure. At the SZ, the sorptivity of the samples were 2-3 times lower at 12 months compared to the 3 months results. Interestingly, the sorptivity of the 0 and 2 days cured blocks appear to have improved with age at a similar or slightly better rate than the 4 and 6 days cured blocks, especially in the east and west faces of the blocks (see Figure 6.26 (a) and (b)). At the SSZ, the sorptivity increased by approximately 10% after 12 months, in the 4 microclimates. Although this is generally in agreement with the air permeability findings, the SSZ air permeability and sorptivity results of the slabs were inconsistent (compare Figure 6.7 with 6.27, (c) and (d)).

### **6.5.3 50 MPa OPC Concrete**

#### *Microclimate*

Figures 6.28 and 6.29 show the effect of microclimate on the sorptivity profiles of the 50 MPa OPC concrete samples at the ages of 3 and 12 months

respectively. The results with statistical analysis are presented in Appendix B, Tables B1.13 and B1.14 (a) & (b), for the 3 and 12 months tests respectively.

Similar to the air permeability results, the variations in the sorptivity indices due to microclimate (or curing) were small (Figure 6.28). The sorptivity of the east faces at 3 months was, on average, 5% higher than the west faces at the SZ and SSZ. The sorptivity of the bottom faces was higher than the top faces by approximately 25 and 10%, at the SZ and SSZ respectively.

The effect of microclimate after 12 months was negligible. As can be seen from Figure 6.29, the sorptivity indices of the blocks were general similar in the 4 microclimates.

#### *Duration of hessian curing*

The relationship between air permeability and curing duration of the 50 MPa OPC concrete is presented in Figures 6.24 and 6.25, (b) and (c), at the ages of 3 and 12 months respectively.

Similar to the air permeability results, the effect of hessian curing duration on the 50 MPa concrete at both ages minimal. As shown in Figures 6.24 and 6.25 (c) and (d), the differences in the sorptivity due to curing at both ages were very small in all samples (in the 4 microclimates). This in agreement with the air permeability results.

#### *Age*

The relationship between air permeability and age of the 50 MPa OPC concrete is shown in Figures B1.1 and B1.2 in Appendix B, for the SZ and SSZ respectively.

The sorptivity of the 12 months old samples were approximately 2-2.5 times lower than the 3 months old samples in the 4 microclimates.

#### 6.5.4 30 MPa OPC/GGBS Concrete

##### *Microclimate*

Figures 6.30 and 6.31 show the effect of microclimate on the sorptivity profiles of the 30 MPa OPC/GGBS concrete samples at the ages of 3 and 12 months respectively. The results with statistical analysis are presented in Appendix B, Tables B1.15 and B1.16 (a) & (b), for the 3 and 12 months tests respectively.

Similar to the air permeability results, the sorptivity of the east and bottom faces of the blocks was higher than the west and bottom faces. At 3 months, the sorptivity of the east faces was, on average, 25% higher than the west faces at the SZ and SSZ. The sorptivity of the bottom faces of the slabs were, on average, 15% higher than the top faces at the SZ and SSZ.

The influence of microclimate remained predominantly unchanged after 12 months of exposure. The sorptivity of the east faces and bottom faces were, on average, 25% and 15% higher than the west and bottom faces respectively, at the SZ and SSZ.

##### *Duration of hessian curing*

The relationship between the sorptivity and hessian curing duration of the 30 MPa OPC/GGBS concrete at the ages of 3 and 12 is presented in Figures 6.24 and 6.25 (e) and (f), respectively.

The sorptivity of the concrete blocks decreased with increased curing duration, in the 4 microclimates. Although less pronounced than the air permeability, the reduction in the sorptivity values with prolonged hessian curing was similarly distinct, especially for the east and bottom faces of the blocks (see Figure 6.24 (e) and (f)). At 3 months of age, the sorptivity of the east and west faces of the blocks decreased gradually with increased hessian curing duration, the difference between the 0-6 days cured blocks being approximately 50 and 45% at the SZ and SSZ respectively. The reduction in the sorptivity of the slabs with prolonged hessian curing duration was not as significant as the vertical blocks. The sorptivity of the 6 days cured, top and

bottom faces of the slabs was, on average, 20 and 25% lower at the SZ and SSZ respectively than the non-cured samples.

After 12 months of exposure, the SZ and SSZ sorptivity indices of the 6 days cured blocks were, on average, 35% lower than the non-cured blocks in the 4 microclimates. As with the air permeability results, the effect of hessian curing duration on sorptivity of the blast-furnace slag concrete was more critical compared with the two OPC concretes.

#### *Polythene and curing membrane (C/M) methods*

The sorptivity profiles of the air and hessian cured concrete blocks together with the curing membrane and polythene cured blocks are shown in Figures 6.32 and 6.33 for the 3 and 12 months old concretes respectively. The air permeability indices of the polythene and C/M cured samples are given in Tables B1.17 to B1.18 in Appendix B.

The 3 months sorptivity results revealed that the application of curing membrane (C/M) was generally slightly more effective than the 2 days hessian curing method in the vertical blocks, and as effective as the 4/6 days hessian curing in the slabs. Interestingly, this result contradicts the air permeability result, where the C/M was shown to have no positive effect on the early age quality of the concretes (compare Figures 6.12 with 6.32). Unlike the air permeability, the range of measured sorptivity values for the samples cured with the various methods were very small. This is more apparent in the sorptivity results of the slabs (Figure 6.32 (c) and (d)) where the difference between the C/M method and other curing methods was insignificant. For the vertical blocks, wrapping with polythene sheeting was slightly more effective than the C/M method and less effective than the 4 days hessian curing method. The difference in the sorptivity between polythene curing and the other curing methods in the slabs (top/bottom faces) was very small.

The effect of the C/M and polythene curing methods on the sorptivity at 12 months was mainly similar to that observed at 3 months. Generally, the sorptivity of the C/M blocks was slightly lower than the 2 days hessian cured

blocks. Similarly, the sorptivity of the 6 days polythene-cured blocks was mostly comparable with the 4/6 days hessian cured blocks. However, as previously stated, the variations in magnitude of the sorptivity indices due to curing regime were generally very small.

#### *Controlled permeability formwork (CPF)*

A comparison between the sorptivity profiles of the CPF-produced concrete and that produced with conventional formwork is given in Figures 6.34 and 6.35. The 3 months sorptivity indices of the CPF and conventionally produced concrete with statistical analysis are listed in Tables B1.17 and B1.18 in Appendix B.

As shown in Figures 6.34 and 6.35, the microclimate influence on the sorptivity of the CPF-produced concrete was notably smaller than the conventionally produced concrete (see also Figures 6.38 and 6.39). This is in agreement with the air permeability results.

As with the air permeability, the 3 months sorptivity of all the CPF-produced concrete blocks were substantially lower at the surface than the blocks that were cast against conventional formwork. Further, the differences in the measured surface sorptivities due to curing regime were significantly smaller for the CPF concretes relative to that cast against conventional formwork. The results were re-plotted in Figures 6.36 and 6.37 to show the effect of curing at the SZ (10mm) and SSZ (20-50mm) respectively. For the east and west faces, the surface sorptivity values of the 0 and 2 days hessian cured CPF blocks were 2-4 times lower than the conventional formwork blocks. However, the sorptivity values of the CPF and conventional formwork blocks were similar for the C/M and polythene cured samples, being between 0-20% lower for the CPF-produced concrete. The difference in quality between the CPF and normal formwork samples was larger in the top and bottom faces of the slabs. The sorptivity of the 0/2 days cured CPF blocks was between 4-10 times lower than the conventionally produced samples. However, the sorptivity of the CPF produced concrete that was cured with C/M and polythene was

generally comparable with the conventionally produced concrete. The influence of CPF decreased with distance from the surface, the sorptivity indices in the SSZ being generally similar to the conventionally produced concretes, as shown in Figures 6.37.

The sorptivity profiles of the samples at 12 months are given in Figures 6.38 and 6.39. The 12 months sorptivity indices of the samples are listed in Tables B1.18 and B1.20 in Appendix B. As with the air permeability, the improvement in the sorptivity of the CPF concrete blocks with age was larger in the SZ than the SSZ. The 12 months results were re-plotted in Figures 6.40 and 6.41 to show the effect of curing at the SZ and SSZ respectively. The surface sorptivity of the CPF-produced concrete was, on average, 2-4 times lower in the east and west faces compared to the conventionally produced concrete. The difference in the sorptivity values was much smaller for the top and bottom faces, the CPF concrete being between 25-50% lower than the conventional formwork concrete. Like the 3 months results, the sorptivity at the SSZ of the CPF and conventional formwork concretes were very similar (Figure 6.41). Although the general trends in the air permeability and sorptivity results were broadly similar, the differences in quality due to microclimate, curing and CPF were more apparent in the air permeability than the sorptivity results.

#### *Age*

The sorptivity of the hessian-cured OPC/GGBS concrete was lower at 12 months than 3 months, at both the SZ and SSZ of the samples. It is noteworthy that the sorptivity of the 0 and 2 days hessian cured vertical blocks decreased with age, whereas the air permeability of the same blocks increased after 12 months of exposure (the two tests were conducted on the same samples; see Figures B1.3 and B1.7 in Appendix B). Unlike the two OPC concretes, the improvement in the sorptivity with age of the 0 and 2 days cured OPC/GGBS samples was notably slower than the samples that received longer duration of curing (4/6 days). Furthermore, both test results showed

distinct variations in quality due to curing of the blast-furnace slag concrete, which was less apparent in the OPC concrete. The sorptivity values of all the samples decreased by, on average, 20-40% after 12 months of field exposure at both, the SZ and SSZ. The reduction in the sorptivity with age, however, was generally greater in the 4/6 days cured samples.

The sorptivity of the C/M and polythene cured samples decreased after 12 months by approximately 15-25% at the SZ of the vertical blocks. The reduction rate was fractionally greater in the polythene-cured samples than the C/M samples. The sorptivity of the bottom faces of the slabs decreased by approximately 30-40% at the SZ, whereas that of the top faces remained similar to the 3 months values. At the SSZ, the C/M and polythene cured samples improved by 25-40%, the improvement rate generally being more significant in the polythene-cured concrete.

The sorptivity of the CPF-produced concrete generally improved with age at both the SZ and SSZ. However, the improvement in the sorptivity with age was not as dramatic as in the air permeability results of the same concretes. The improvement due to age in the sorptivity of the 0/2 days hessian cured CPF concretes was less marked than that of the C/M and polythene cured concretes. For the 0/2 days hessian cured vertical blocks, the sorptivity was 1.5-2 times lower than the 3 months results at the SZ, and less than 10% lower at the SSZ. Surprisingly, the sorptivity of the 0/2 days hessian-cured CPF slabs generally increased with age. This is consistent with the air permeability results. For the C/M and polythene-cured CPF concretes, the sorptivity at the SZ was generally 3.5-4.5 times lower than that obtained at 3 months, and 1.5 times lower at the SSZ of all the samples regardless of curing. Although the effect of CPF and age was more marked in the air permeability than the sorptivity test results, the general trends in the results of both tests were similar.

## 6.6 CARBONATION

### 6.6.1 Introduction

The carbonation test was discussed earlier in Sections 4.6 and 5.6.1.

The effect of microclimate and duration of hessian curing on the carbonation depth of the three concrete mixes is presented graphically in Figures 6.42 and 5.43 at the ages of 6 and 12 months respectively. The results are also presented in Appendix B, Tables B1.21 and B1.22 for the 6 and 12 months tests respectively.

### 6.6.2 30 MPa OPC Concrete

#### *Microclimate*

The carbonation of concrete was higher in the east and bottom microclimates than the west and top microclimates at both ages, 6 and 12 months. The carbonation depth of the east and bottom faces was, on average, 10% and 40% higher than the west and top faces respectively at 6 months. At 12 months, the average carbonation depth of the east faces was 6-mm compared to 5-mm of the west faces (17% higher than the west faces). The average carbonation depth of the bottom faces was 6-mm compared to 4.5mm of the top faces (25% higher than the top faces).

#### *Duration of hessian curing*

As can be seen from the 6 and 12 months graphs, carbonation decreased as curing duration was increased from 0 to 6 days in the 4 microclimates.

Generally, the variation in the carbonation depth due to curing duration between the samples at 12 month was similar to 6 months. There was no significant difference in carbonation depth between the 0-2 days hessian cured blocks at both ages, being, on average, 10% greater for the non-cured blocks. Increased curing to 4 days reduced carbonation by, on average, 25%, while 6 days curing gave a further reduction of approximately 15%.

## *Age*

Figure 6.44 presents the carbonation results after 6 and 12 months of exposure for the 30 MPa OPC concrete. As shown, the carbonation depth increased with age in all the samples. However, the rate of carbonation was higher in the first 6 months of exposure, as the increase in carbonation in the second 6 months of exposure was not as significant. After 12 months of exposure, the carbonation depth increased by, on average, 20% and 15% in the east and west faces of the blocks respectively, relative to the 6 months results. The average increase in carbonation with age in the top and bottom faces was 20 and 10% respectively (see Tables B1.21 and B1.22).

### **6.6.3 50 MPa OPC Concrete**

#### *Microclimate*

Like the 30 MPa OPC concrete, the 50 MPa OPC concrete carbonated to a greater extent in the east and bottom microclimates than the west and top microclimates. In the east microclimate, all blocks carbonated at 6 months of age (average carbonation 2-mm) while in the west microclimate, only the 0-2 days cured blocks carbonated (average depth 1.5-mm). Similarly, the carbonation depth of the bottom faces was almost double that of the top faces for the 0-2 days cured blocks, and was slightly higher for the 4-6 days cured blocks (see Figure 6.42).

After 12 months of exposure, the average carbonation depth of the east and bottom faces of the blocks was approximately 3-mm compared to 1.5-mm for the west and top faces.

#### *Duration of hessian curing*

Carbonation depth decreased with increased curing duration. The early influence of curing duration remained unchanged with age. The reduction in carbonation with curing duration was gradual up to 4 days hessian curing. The carbonation curves generally tapered off after 4 days curing indicating only a small improvement beyond 4 days hessian curing. At 12 months, the

carbonation of the 2 days and 4 days hessian-cured blocks was, on average, 25 and 50% lower than the non-cured blocks. The carbonation depth of the 4 and 6 days-cured blocks were generally comparable at both ages.

#### *Age*

Figure 6.45 presents the carbonation results after 6 and 12 months of exposure for the 50 MPa OPC concrete. As can be seen from the graphs, the carbonation depth was small at 6 months, the average carbonation being less than 2-mm in the 4 microclimates. The progress of carbonation was slower in the second 6 months of exposure, the depth of carbonation after 12 months being, on average, less than 3-mm.

#### **6.6.4 30 MPa OPC/GGBS Concrete**

##### *Microclimate*

As with the two OPC concretes, the carbonation depth of the blast-furnace slag concrete was higher in the east and bottom microclimates than the west and top microclimates respectively. The carbonation depth of the east and bottom faces at 6 months being, on average, 20-30% higher than the west and top faces respectively.

The microclimate effect remained similar after 12 months of exposure, the average carbonation depth being higher in the east and bottom than the west and top microclimates by approximately 20% (average depths of the east, west, top and bottom faces being 10, 8, 6 and 8 mm respectively).

##### *Duration of hessian curing*

As shown in Figures 6.42 and 6.43, the carbonation of the OPC/GGBS decreased with increased curing duration. The reduction in the carbonation depth was sharp from 0-4 days curing, with the improvement beyond 4 days of curing being generally small. The differences in carbonation depth due curing became greater after 12 months of exposure. Furthermore, the carbonation rate was slower for the 4/6 days hessian cured blocks as they showed smaller increase in carbonation depth with age compared to the non-

cured and 2 days hessian cured blocks. At 12 months, the carbonation depth of the 6 days cured blocks was, on average, 45, 40 and 15% lower than the 0, 2 and 4 days hessian cured blocks respectively.

#### *Polythene and curing membrane (C/M) methods*

The 6 days polythene cured blocks showed lower carbonation levels than the curing membrane cured blocks (Figure 6.48). At 12 months, the carbonation depth of the polythene-cured samples was on average, 20% lower than the C/M cured samples. The curing membrane and 6 days polythene cured block initially (at 6 months of age) showed lower levels of carbonation than the 4 days hessian cured blocks. At 12 months, however, their carbonation depth was generally higher than the 4 days hessian cured blocks and lower than the 2 days hessian cured blocks (see Figure 6.48).

#### *Controlled permeability formwork (CPF)*

Figures 6.46 to and 6.47 present the carbonation results at 6 and 12 months respectively of the OPC/GGBS concrete blocks cast with and without controlled permeability formwork system (CPF). The carbonation data is given in Tables B1.21 and B1.22 (b) in Appendix B.

The carbonation of the CPF-produced blocks was significantly lower than the blocks cast with conventional formwork regardless of curing method; the depth of carbonation being, on average, 3 times lower in the CPF-produced concrete (see Tables B1.21 and B1.22, (b)). Further, the differences in carbonation depth due to curing regime were not as significant in the CPF-produced blocks compared to the conventional formwork blocks, especially at 12 months.

Surprisingly, the 0-2 days cured CPF-blocks showed lower depth of carbonation than the 6 days polythene and C/M cured CPF-blocks at 6 months. However, the polythene cured blocks were the least carbonated at 12 months, while the C/M cured blocks showed higher or similar carbonation depths to the 0-2 days hessian cured blocks. There was no real difference in carbonation between the non-cured and the 2 days hessian cured CPF-blocks.

It is worth to mention that the non-cured CPF-produced concrete blocks exhibited lower carbonation depth than all the cured blocks that were cast against conventional formwork

#### *Age*

Figure 6.48 presents the carbonation results after 6 and 12 months of exposure for the OPC/GGBS concrete made with conventional formwork.

The increase in carbonation with age was higher in the east and west microclimates compared to the top and bottom microclimates. Further, the rate of carbonation was lower for the 2, 4 and 6 days hessian cured blocks relative to the non-cured, curing membrane and 6 days polythene cured blocks.

The carbonation depth of the east faces increased from an average depth of 6-mm at 6 months to 10-mm at 12 months, and from 5-mm to 9-mm in the west faces. In the top faces of the slabs, the average carbonation depth increased from 4-mm at 6 months to 6-mm at 12 months, while in the bottom faces it increased from 5 to 8-mm at 12 months.

Figure 6.49 show the 6 and 12 months carbonation results of the CPF-produced OPC/GGBS concrete. The carbonation of the CPF-produced concrete increased with age but at a markedly slower rate than the normally produced concrete. Although the 0/2 days hessian cured blocks showed lower carbonation depth at 6 months, the rate of carbonation in the same samples was higher during the second 6 months of exposure. After 12 months, the carbonation depth of the 0/2 days hessian cured samples increased by more than 3 times compared to 6 months. The carbonation depth of the C/M and polythene cured blocks increased by, on average, 10-20% compared to the 6 months results.

## 6.7 THERMOGRAVIMETRY

### 6.7.1 Introduction

The repeatability and reproducibility of the TG test results were discussed earlier in Section 5.7.1.

The thermogravimetric analysis curves (TG) of the summer series concrete and derivatives (DTG) are given in Appendix B, Figures B1.9 to B1.12. The weight losses due to the decomposition of the various phases of the hydrated matrix at the corresponding temperatures were identified from the peaks of the DTG curves. These were discussed previously in Section 5.7.1, Chapter 5.

The hydrates water and calcium hydroxide (lime) content profiles of the two OPC concrete mixes are given in Figure 6.50. The 30 MPa OPC concrete exhibited an increase in the hydrate water and lime contents with increased depth from the surface, both parameters being greatest at 20mm. However, the increase in both parameters was relatively small, being slightly greater for the 0/2 days cured samples (approximately 2%) than the 4/6 days cured samples. The hydrates water and lime contents of the 50 MPa concrete increased with depth up to 10mm from the surface and generally tended to decrease beyond 10mm as shown in Figure 6.50 (c) and (d). Both parameters, however, were higher at 20mm than 5mm from the surface. As with all samples, the increase in the two parameters was very small.

### 6.7.2 30 MPa OPC Concrete

#### *Duration of hessian curing*

The effect of hessian curing duration on the hydrate water and lime contents is presented graphically in Figure 6.51 (a) and (b) respectively.

The results show no real increase in the hydrate water with increased hessian curing duration at the surface (10mm) and subsurface zone (20mm). The increase in the hydrate water after 6 days of curing was generally insignificant.

The lime content of the samples exhibited a small gradual increase with increased curing duration at the SZ (Figure 6.51 (b)). At the SSZ, however, the lime content remained virtually constant for all samples regardless of curing. Like the hydrate water, the variation in the lime content with increased curing duration from 0-6 days was insignificant.

### **6.7.3 50 MPa OPC Concrete**

#### *Duration of hessian curing*

The effect of hessian curing duration on the hydrate water and lime contents is presented graphically in Figure 6.51 (c) and (d) respectively.

The hydrate water and lime content of the 2 days hessian cured samples showed a slight increase (approximately 1%) relative to the non-cured samples. However, both parameters subsequently decreased with increased curing duration from 2 to 6 days. It is interesting to note that both parameters followed a strikingly similar trend.

## **6.8 MERCURY INTRUSION PROSIMETRY (MIP)**

### **6.8.1 Introduction**

The MIP test methodology, the apparatus and the sample preparation method for the test are described in detail in Section 4.8.

The adopted sampling procedure initially produced variable results with coefficients of variation between duplicate samples of up to 30-40% (in the 12 months winter results which were excluded from the analysis). The reproducibility of the results was subsequently improved by testing small prisms of approximately equal size chiselled from the central section of the discs, and by increasing the equilibrium time at each intrusion step from 15 to 30 seconds to enable better intrusion. This gave results with a coefficient of variation within 15% in the 12 months summer series. Better accuracy can probably be achieved by determining the paste content of the mortar samples and calculating the pore volume as a percent of the paste volume (e.g.

Marchand et al, 1996; Feldman, 1986). This normally requires the removal of mercury from the samples after the test and subsequent determination of the paste content by acid extraction methods. However, this elaborate procedure was not considered practical since porosity (nominal porosity due to the presence of the non-porous sand in the samples) comparisons are valid, as the sand content in the original mixes was the same (fractionally lower for the 50 MPa mix).

The total porosity represents the volume of mercury intruded at 207 MPa. The pore size distribution curves as a function of curing duration and depth from the exposed surface for the 3 concrete mixes are shown in Appendix B, Figure B1.13. The total porosity data for the 3 concretes is given in Table B1.24 in Appendix B.

It has long been established that the permeability of cement composites is a function of pore size distribution rather than the total pore volume or porosity (Nyame and Illston, 1980; Goto and Roy, 1981). More precisely, the permeability of the cement matrix was found to depend on the volume of coarse pores (coarse capillary pores), i.e. pores with diameter larger than  $0.1\mu\text{m}$ , which is also referred to as the relevant or effective porosity (Bagel and Zivica, 1997; Meng, 1994; Young, 1988; Mehta and Manmohan, 1980). Pores larger than  $10\mu\text{m}$  in diameter are considered air or compaction voids in accordance with Powers and IUPAC classification of pores (Young, 1988). Air voids are often isolated and therefore have little effect on the transport properties of the material. Hence, the discussion of results has been based on the porosity that corresponds to the intrusion of pore sizes in the range from  $10\mu\text{m}$  down to  $0.006\mu\text{m}$  diameter (the instrument used in this investigation calculates pore volumes and distributions in the range  $300$  to  $0.006\mu\text{m}$ ; this data is shown in Figure B1.9 and Table B1.23). On this basis, porosity data is listed in Table 6.4 over two pore size ranges to represent large or coarse capillary pores with pore diameter from  $0.1$  to  $10\mu\text{m}$ , and smaller pores (smaller capillary pores and large meso pores) with pore diameter from  $0.1$  to

0.006  $\mu\text{m}$ . For brevity, the volume of large pores (0.1 to 10  $\mu\text{m}$ ) will be referred to as coarse capillary porosity (conventionally, capillary pore sizes range from 0.01 to 10  $\mu\text{m}$ ).

### 6.8.2 30 MPa OPC Concrete

Figures 6.52 and 6.53 present graphically the effect of hessian curing duration at various depths from the surface on the pore size distribution of the 30 MPa OPC mortars. Table 6.4 lists the fraction porosity in two ranges of pore size, at depths of 5, 10 and 20mm from the exposed surface.

#### *Depth*

The porosity profile trends of the 0-2 days cured blocks were contradictory to that of the 4-6 days cured blocks. In the 0-2 days cured blocks, the pore volume increased with depth from the exposed surface while it decreased with depth in the 4-6 days cured blocks.

The volume of coarse capillary pores was higher at 5-mm than 10mm depth from the surface, while the volume of smaller pores (smaller than 0.1  $\mu\text{m}$ ) increased with depth. This effect was reversed in the 4-6 days cured blocks, the volume of coarse capillary pores being lower in the surface than the subsurface while the volume of smaller pores decreased with depth (see Table 6.4).

#### *Duration of hessian curing*

The non-cured and 2 days cured blocks had the largest pore volume at the SZ (10mm) and SSZ (20mm), followed by the 4 and 6 days cured blocks respectively. The pore volume at the surface (10mm) of the 6 days hessian cured samples was 30 and 15% lower than the 0/2 and 4 days hessian cured samples respectively. At 20mm from the surface, the 6 days cured blocks had, on average, 40 and 15% lower pore volume than the 0-2 and 4 days cured blocks respectively.

The volume of coarse capillary and smaller pores decreased with prolonged curing duration. However, contrary to expectation, the reduction in porosity

with prolonged curing was more significant in the volume of small pores than in the coarse capillary pores.

### **6.8.3 50 MPa OPC Concrete**

Figures 6.54 and 6.55 present graphically the effect of hessian curing duration at various depths from the surface on the pore size distribution of the 50 MPa OPC mortars.

#### *Depth*

Generally, the total pore volume was lower at 5mm than at 10mm from the surface with it being lowest at 20mm from the exposed surface.

The volume of large and smaller pores was higher at the 10mm than at 20mm deep with the exception of the 6 days cured blocks where both parameters increased with depth (see also Table 6.4).

#### *Duration of hessian curing*

Contrary to the 30 MPa concrete, the average reduction in pore volume with prolonged curing duration was smaller in the 50 MPa concrete especially at the SSZ. The non-cured blocks had a slightly higher pore volume (10%) than the 2 and 4 days cured blocks at 10 and 20mm from the surface. Similarly, the difference in the porosity between the 2 and 4 days cured samples was small (5-10%) at all depths. However, 6 days curing gave a significant reduction in the pore volume (over 40%) especially at 5 and 10mm from the surface.

Like the 30 MPa concrete, the reduction in the volume of small pores with prolonged curing duration was more significant than the reduction in coarse capillary pores.

### **6.8.4 30 MPa OPC/GGBS Concrete**

Figures 6.56 and 6.57 present graphically the effect of hessian curing duration at various depths from the surface on the pore size distribution of the 30 MPa OPC/GGBS mortars.

### *Depth*

The total pore volume, volume of coarse capillary and smaller pores decreased sharply with depth from the exposed surface (see Table 6.4). The reduction in porosity from 5 to 10 mm from the surface was particularly notable especially in the non-cured and 2 days hessian cured samples.

### *Duration of hessian curing*

The pore volume of the blast-furnace slag concrete reduced significantly with prolonged curing duration. At 5mm from the exposed surface, the pore volume of the non-cured blocks was approximately 1.5, 3 and 3.5 times higher than the pore volume of the 2, 4 and 6 days cured blocks respectively. At 10 and 20mm from the surface, the differences in the pore volume between the non-cured blocks and the 2, 4, and 6 days cured blocks was on average, 20, 30 and 40% respectively.

The volume of coarse capillary pores and smaller pores reduced sharply with increased curing duration. The reduction in the volume of coarse capillary pores with improved curing was more noticeable at the surface (5mm) than the subsurface, being more than 4 times lower after 6 days curing relative to the non-cured blocks. Like the other two mixes, the reduction in the volume of smaller pores was more significant than the reduction in coarse capillary pores.

**Table 6.1** Weather data during curing period (curing environment)

Concrete reference	Mean weekly temperature.(°C)	Mean weekly relative humidity (%)	Wind direction
A	15	68	south west
	16.8	70	south west
B	17.4	68	north east
	19.6	69	north east
C	16.9	70	west
	19.5	68	west
	14.0	67	south west
	14.6	68	west
	14.4	72	east

Concrete: A = 30 MPa OPC, B = 50 MPa OPC, C = 30 MPa OPC/GGBS

**Table 6.2** Weather data during the first three months of exposure

Month (1996)	Average temperature (°C)	Average monthly relative humidity (%)	Wind direction
July	17.6	68.9	west
August	16.8	70.2	north west
September	13.5	73.9	east
October	11.7	74.3	east
November	5.7	76.4	east
December	2.7	78.1	east

**Table 6.3** Compressive strength results

Concrete reference	Design strength (MPa)	Actual strength* (MPa)
A	30	29-33
B	50	47-52
C	30	29-31

Concrete: A = 30 MPa OPC, B = 50 MPa OPC, C = 30 MPa OPC/GGBS,

\* Average of six tests

**Table 6.4** Porosity and fraction of pore volume in selected sizes of OPC and OPC/GGBS concrete at various depths from the exposed surface (east faces)

Concrete mix		30 MPa OPC concrete			50 MPa OPC concrete			30 MPa OPC/GGBS concrete		
Curing regime	Depth (mm)	5	10	20	5	10	20	5	10	20
	Pore diameter (µm)	fraction of volume in pores (cc/g) x 10 <sup>-2</sup>			fraction of volume in pores (cc/g) x 10 <sup>-2</sup>			fraction of volume in pores (cc/g) x 10 <sup>-2</sup>		
No cure	10 - 0.1	3.01	2.74	3.49	2.77	2.11	2.68	16.63	4.28	3.55
	0.1 - 0.006	6.95	7.92	9.15	3.98	5.23	3.87	10.45	8.93	9.63
	Total porosity	9.96	10.66	12.64	6.75	7.34	6.55	27.08	13.21	13.18
+2 days H	10 - 0.1	5.41	2.76	2.86	2.87	2.08	1.80	7.21	4.04	3.67
	0.1 - 0.006	5.82	8.74	8.74	4.42	4.05	4.38	9.41	7.66	6.46
	Total porosity	11.23	11.50	11.60	7.29	6.13	6.18	16.62	11.70	10.13
+4 days H	10 - 0.1	2.42	3.92	3.05	2.29	3.61	1.94	4.12	4.94	3.18
	0.1 - 0.006	7.07	5.37	5.65	4.75	3.81	3.95	5.13	5.06	5.54
	Total porosity	9.49	9.29	8.70	7.04	7.42	5.89	9.25	10.00	8.72
+6 days H	10 - 0.1	2.75	3.09	2.86	0.62	2.20	2.36	3.53	4.04	3.66
	0.1 - 0.006	5.75	4.78	4.43	2.04	2.62	3.65	4.52	3.66	4.02
	Total porosity	8.50	7.87	7.29	2.66	4.82	6.01	8.05	7.70	7.68

Key: +2 days H = 2 days hessian cured plus one days in the mould

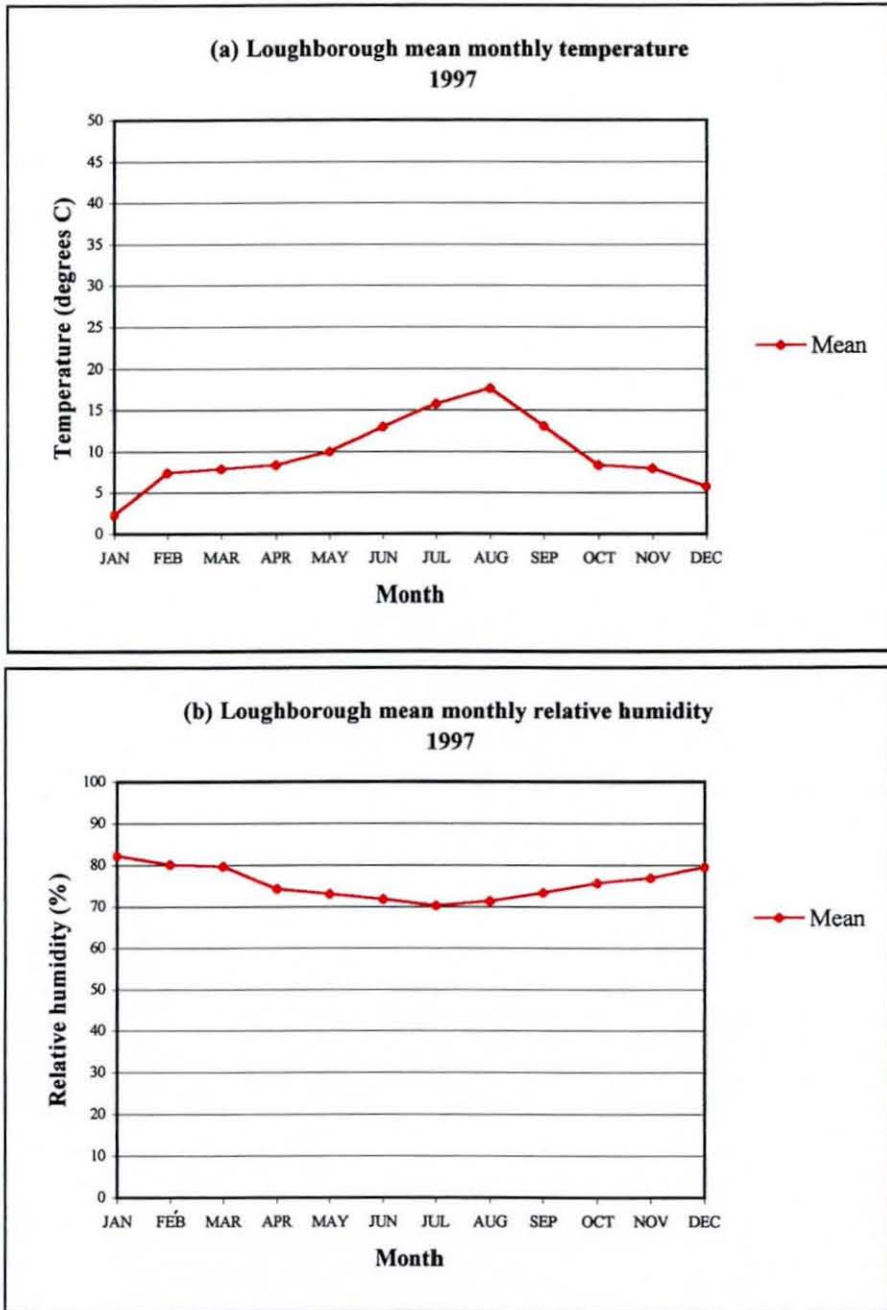
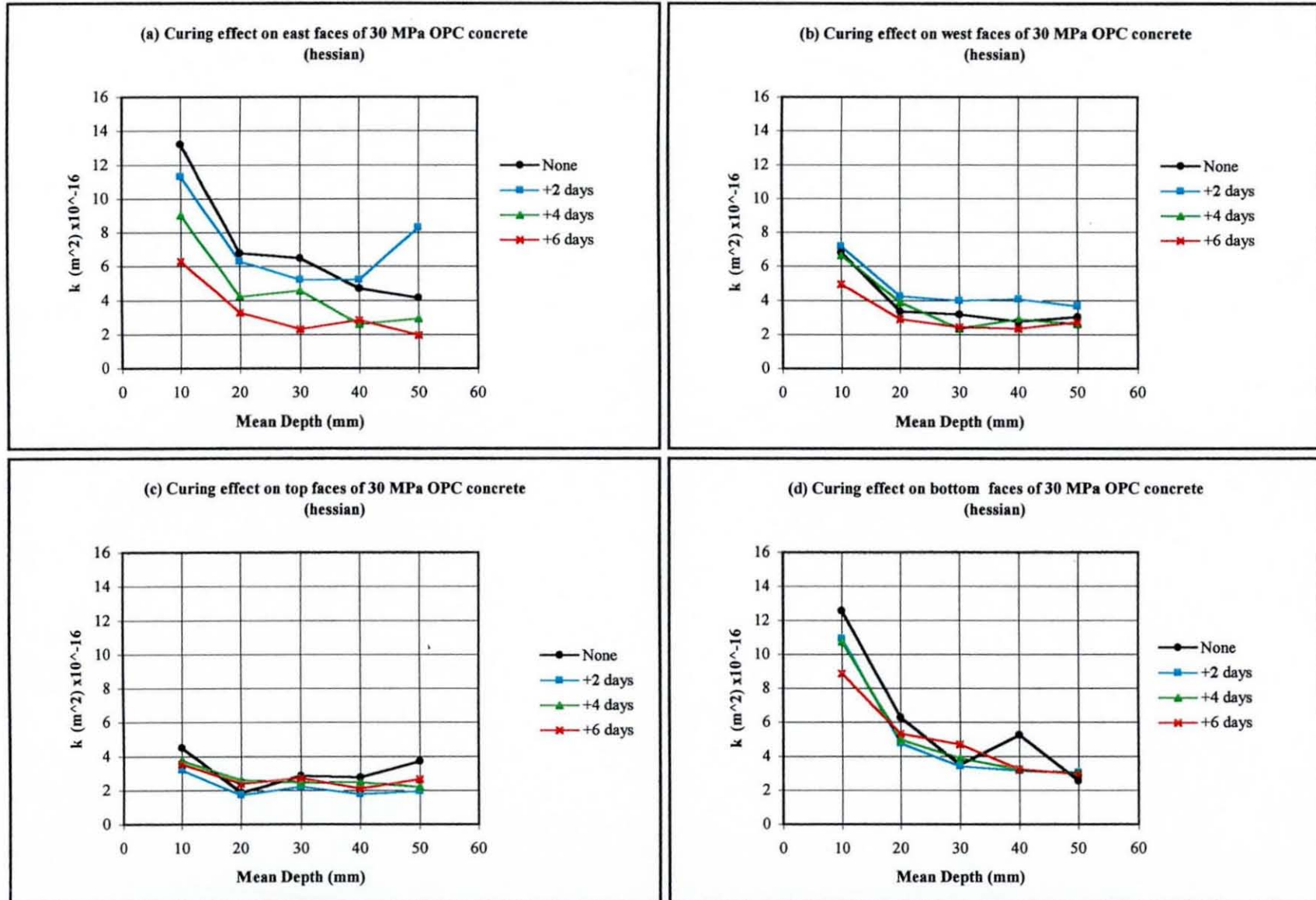


Fig. 6.1 Mean monthly temperature and relative humidity - Loughborough 1997



**Fig. 6.2** Effect of curing regime on the air permeability profiles for the 30 MPa OPC concrete - 3 months summer series

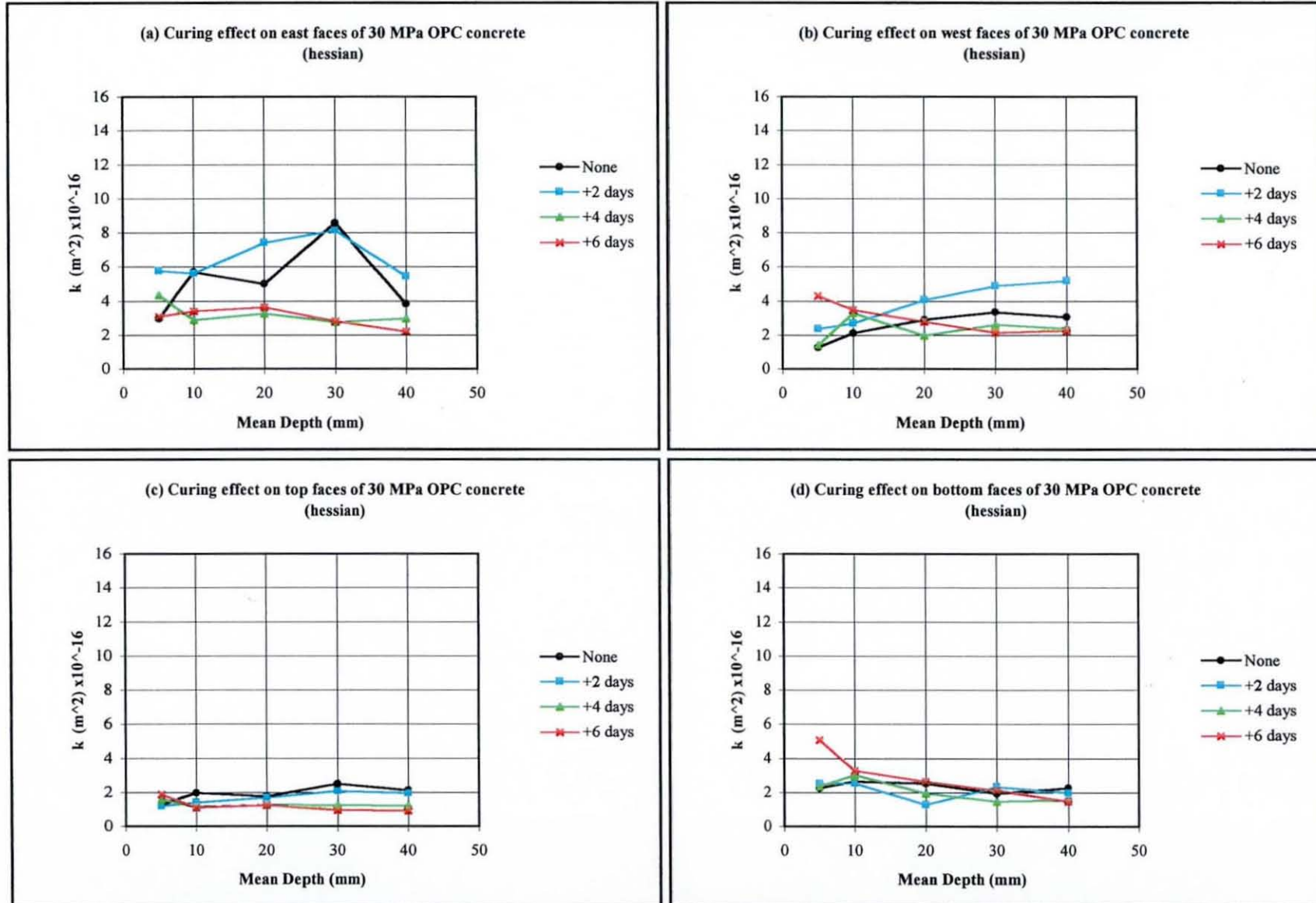


Fig. 6.3 Effect of curing regime on the air permeability profiles for the 30 MPa OPC concrete - 12 months summer series

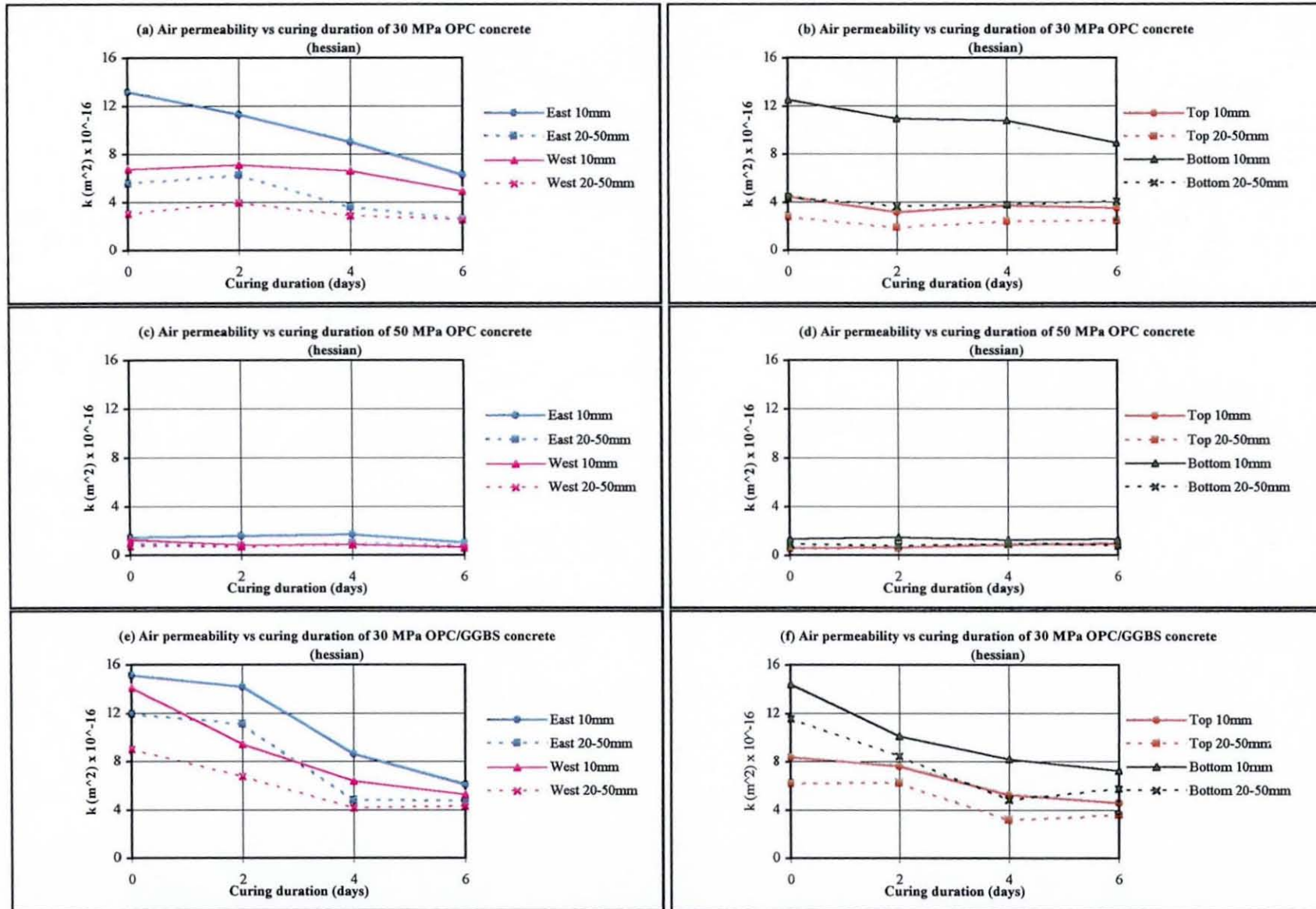


Fig. 6.4 Effect of curing duration on the air permeability for OPC and OPC/GGBS concrete - 3 months summer series

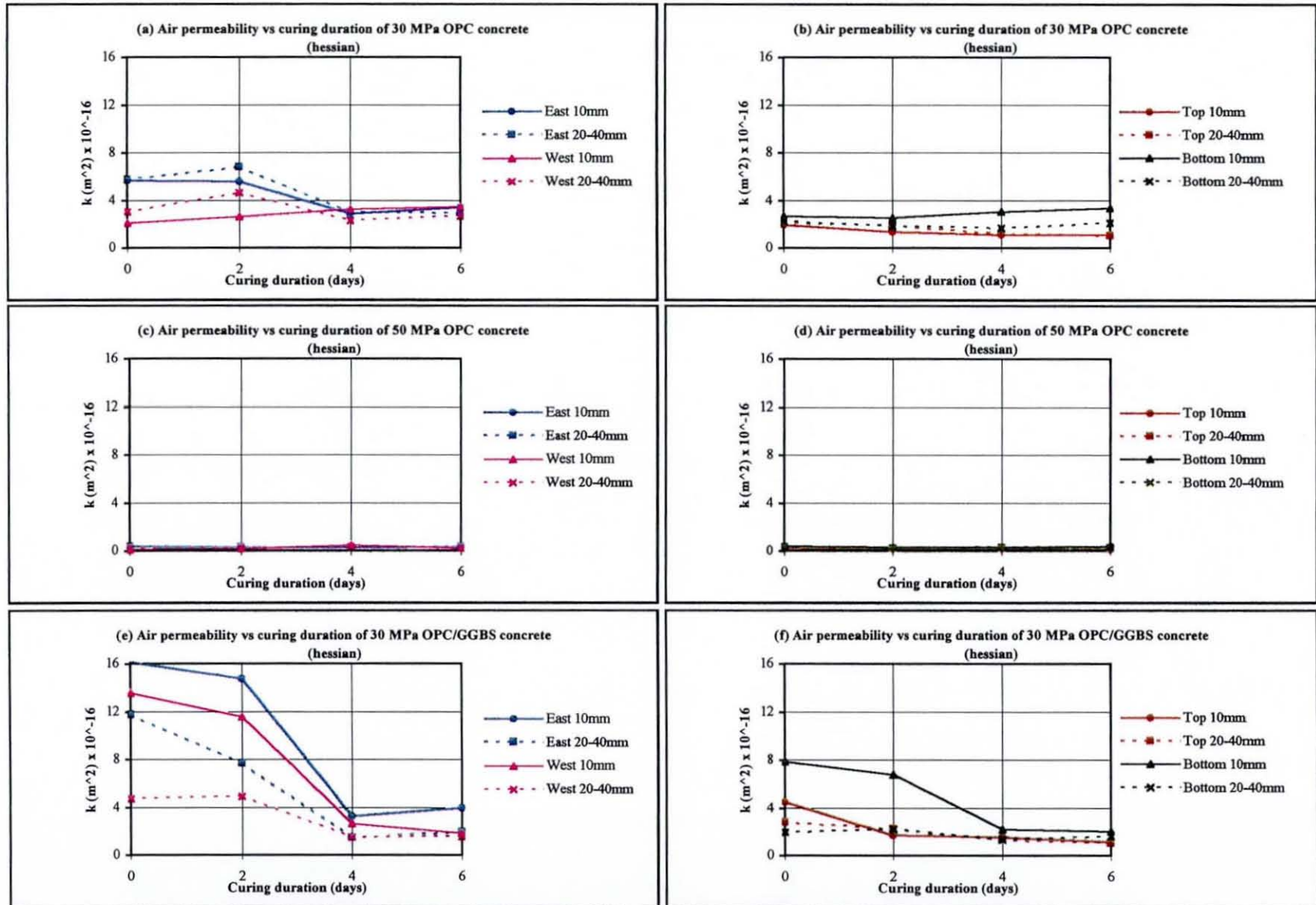


Fig. 6.5 Effect of curing duration on the air permeability for OPC and OPC/GGBS concrete - 12 months summer series

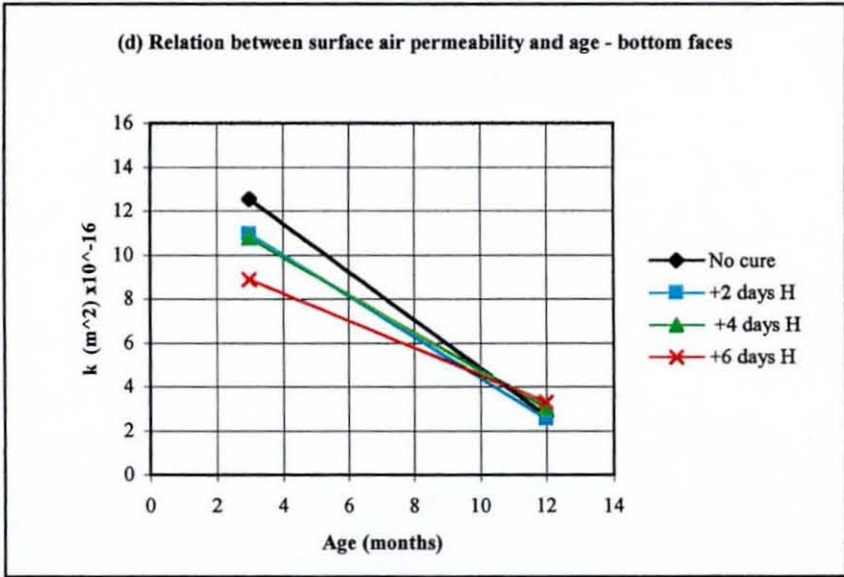
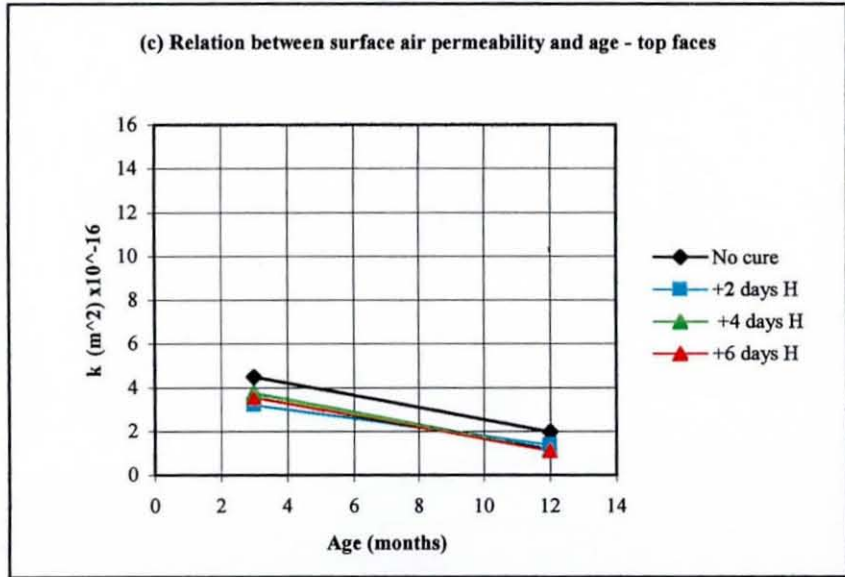
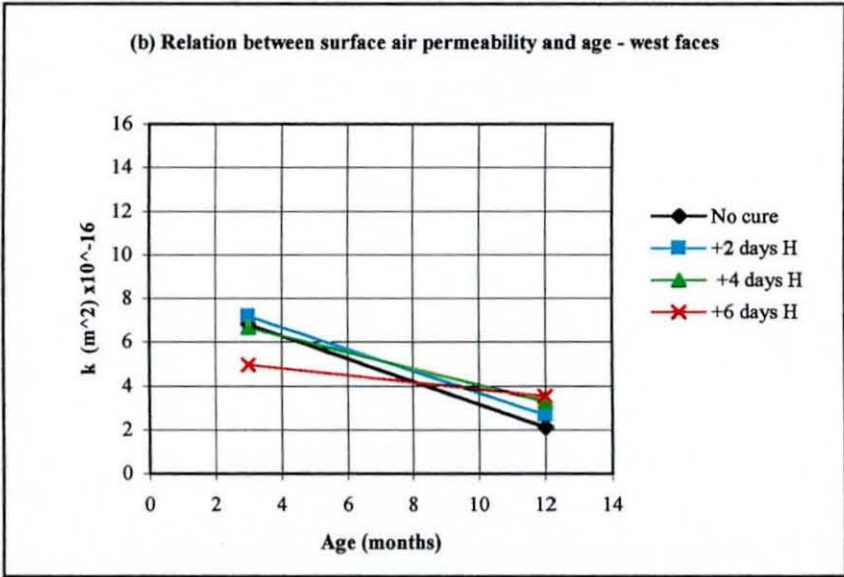
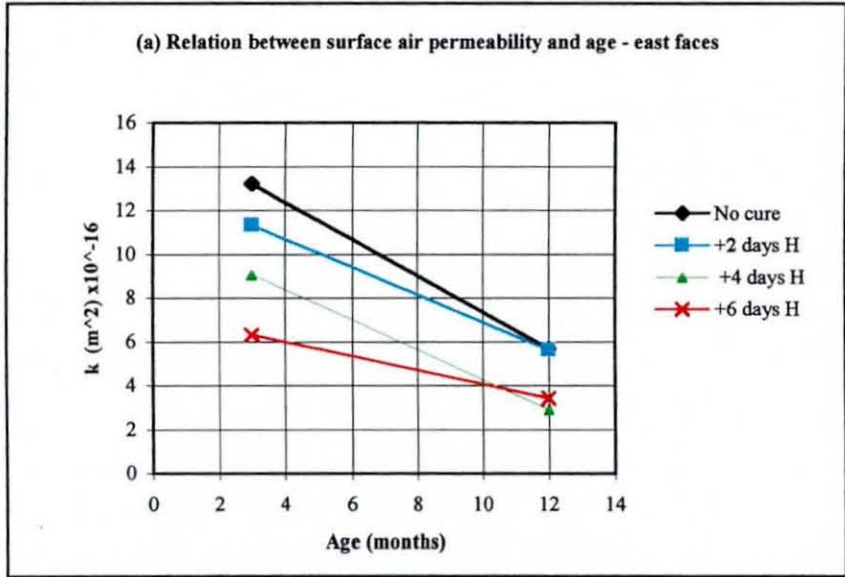


Fig. 6.6 Relationship between surface air permeability and age of the 30 MPa OPC concrete - UK summer

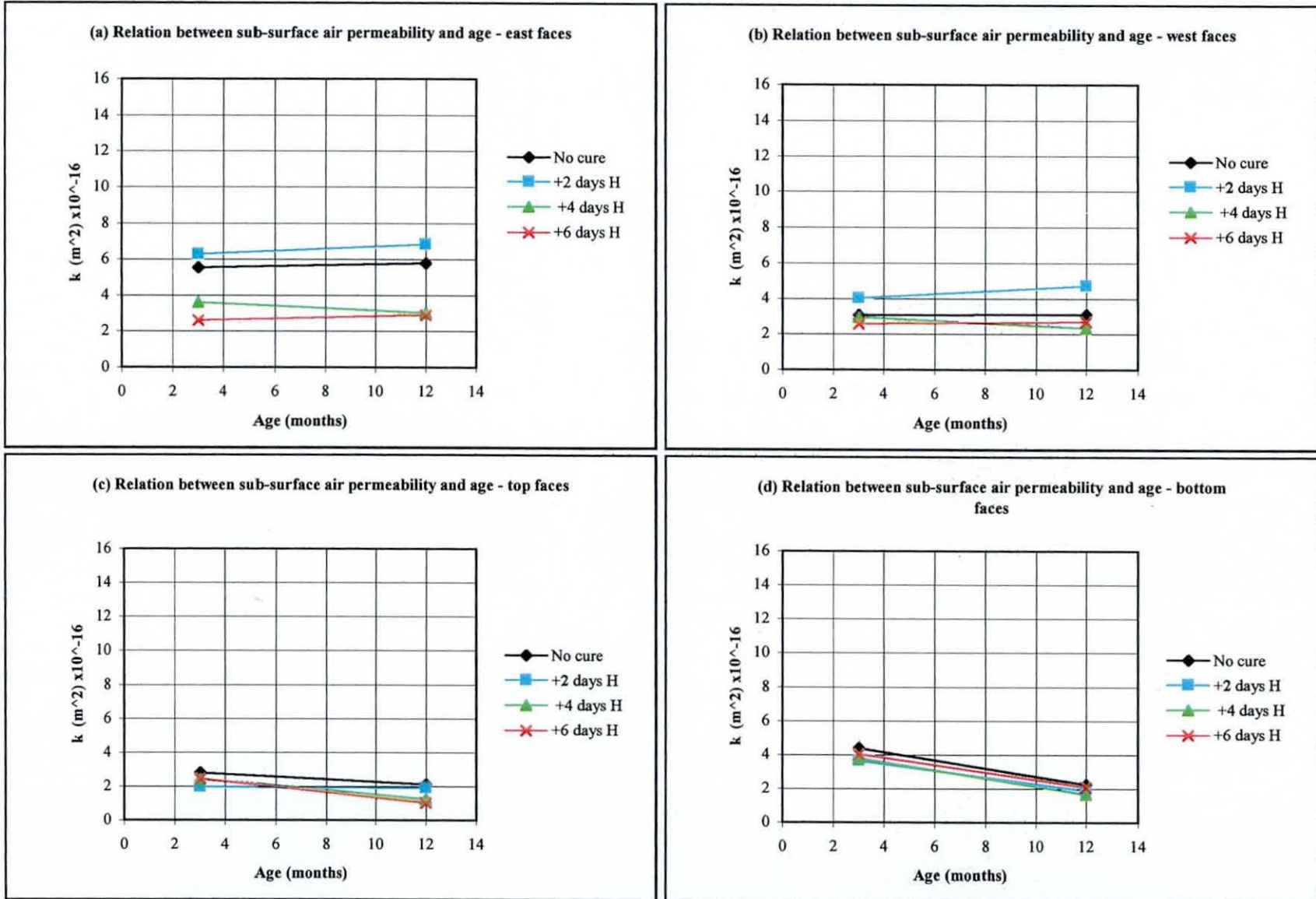


Fig. 6.7 Relationship between sub-surface air permeability and age of the 30 MPa OPC concrete - UK summer

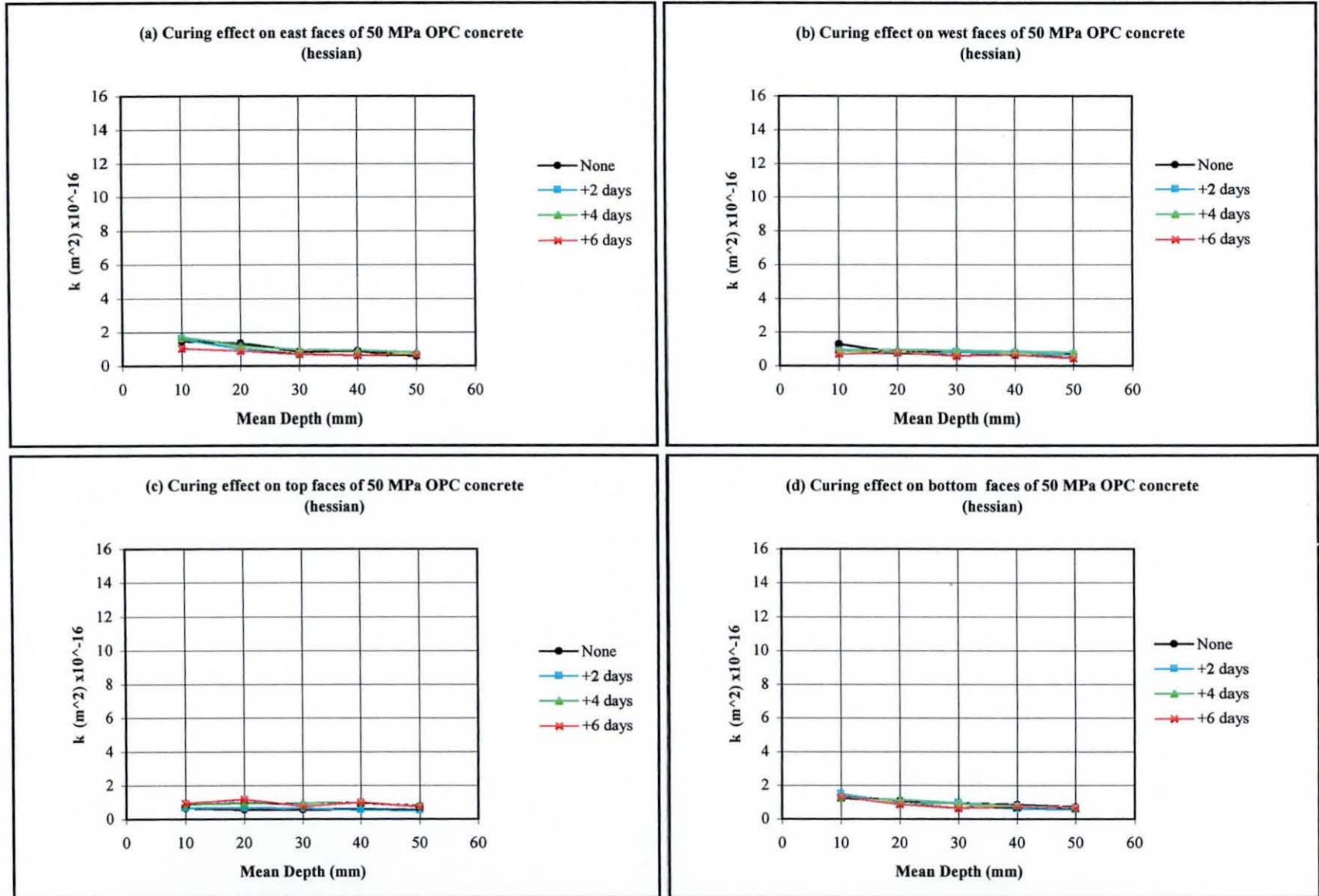


Fig. 6.8 Effect of curing regime on the air permeability profiles for the 50 MPa OPC concrete - 3 months summer series

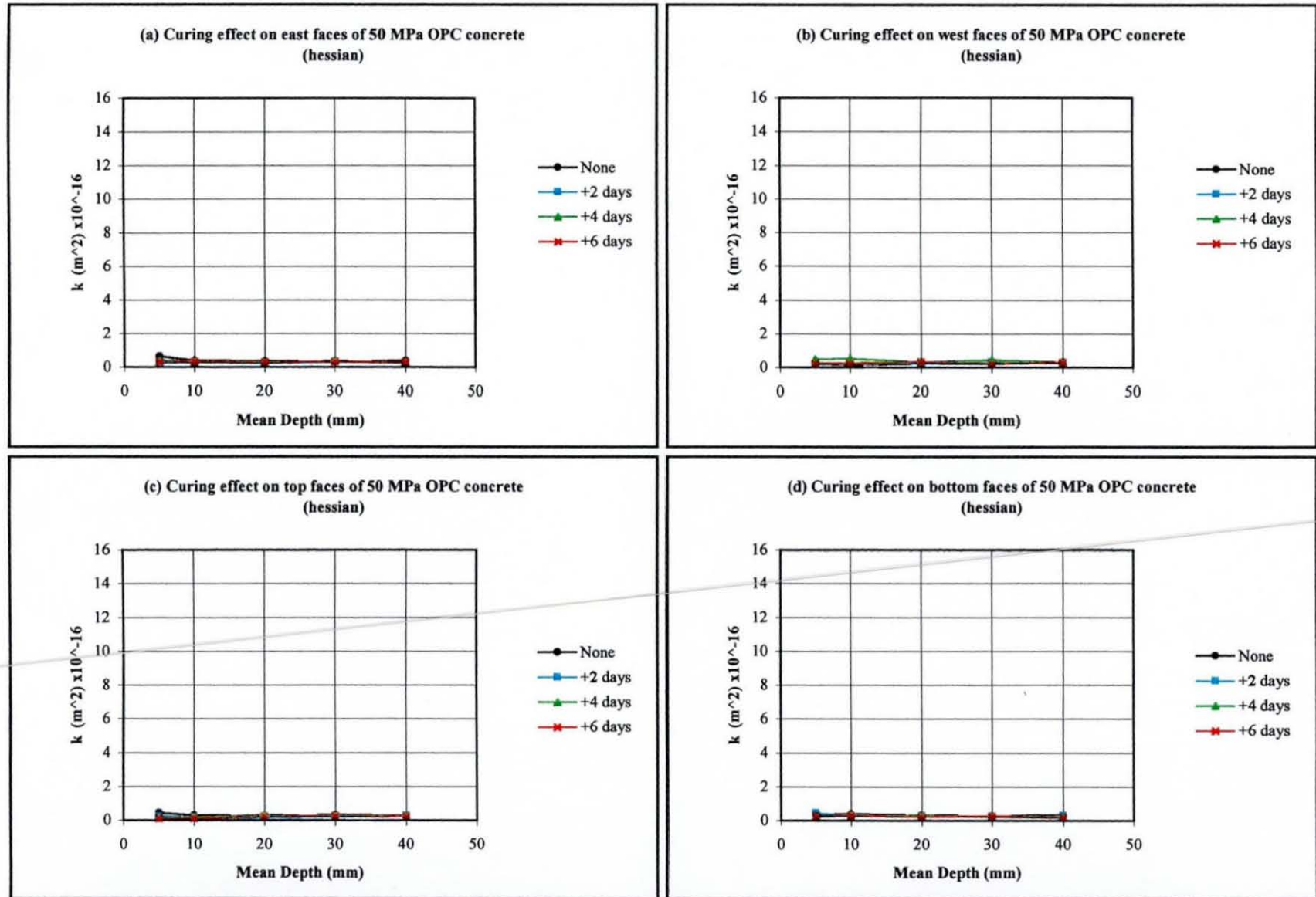


Fig. 6.9 Effect of curing regime on the air permeability profiles for the 50 MPa OPC concrete - 12 months summer series

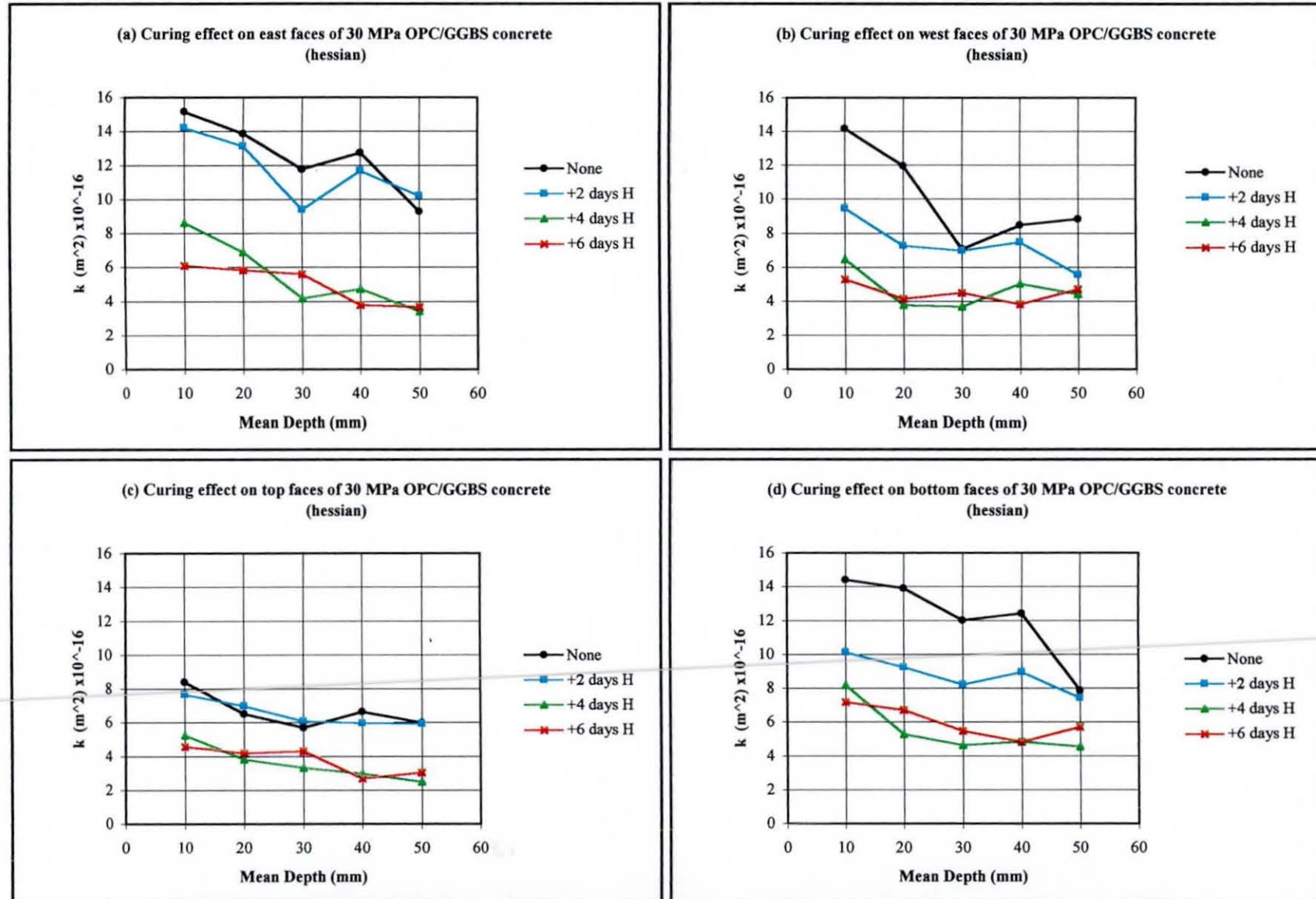


Fig. 6.10 Effect of curing regime on the air permeability profiles for the 30 MPa OPC/GGBS concrete - 3 months summer series

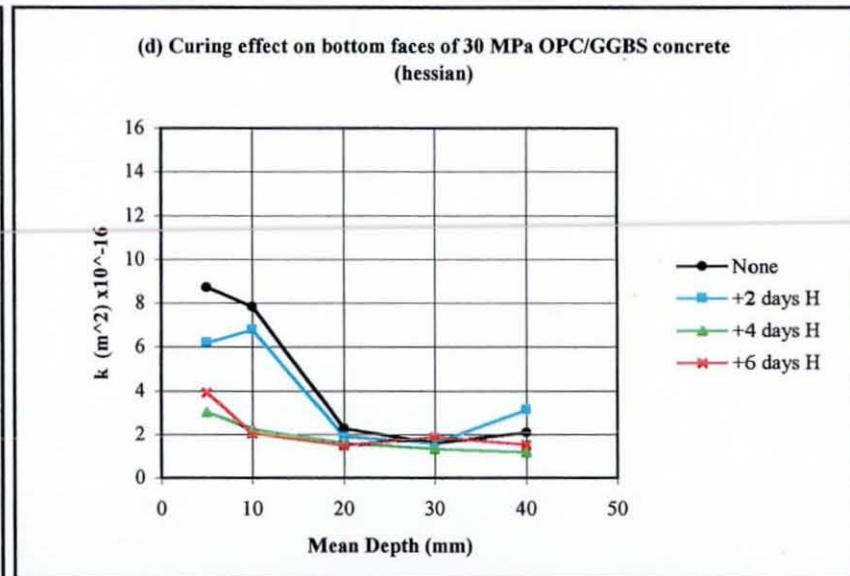
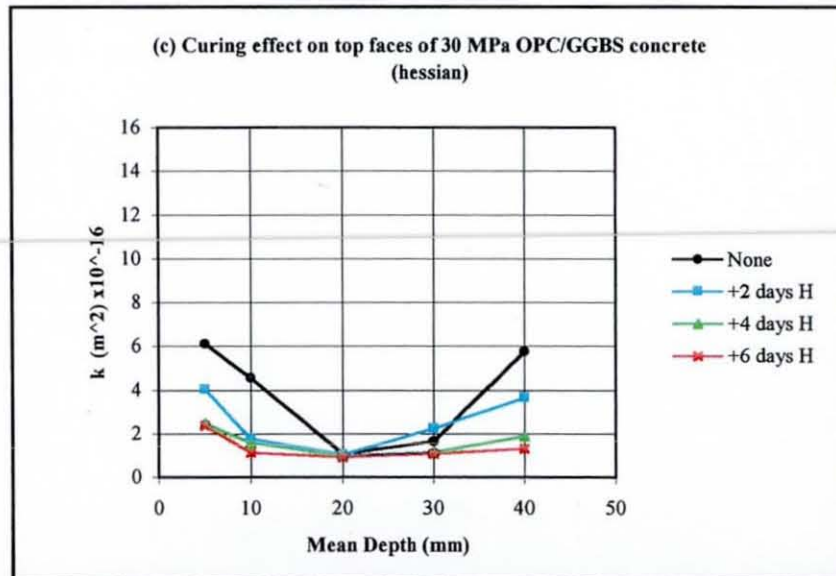
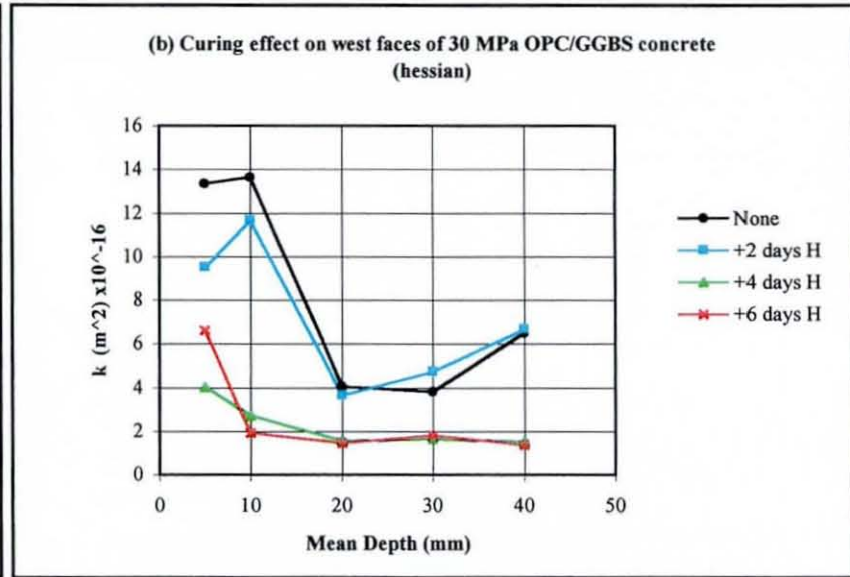
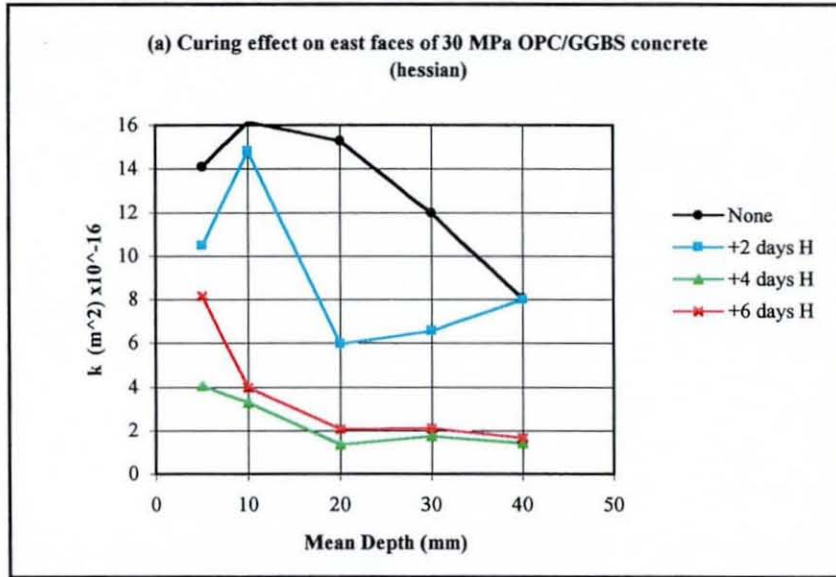
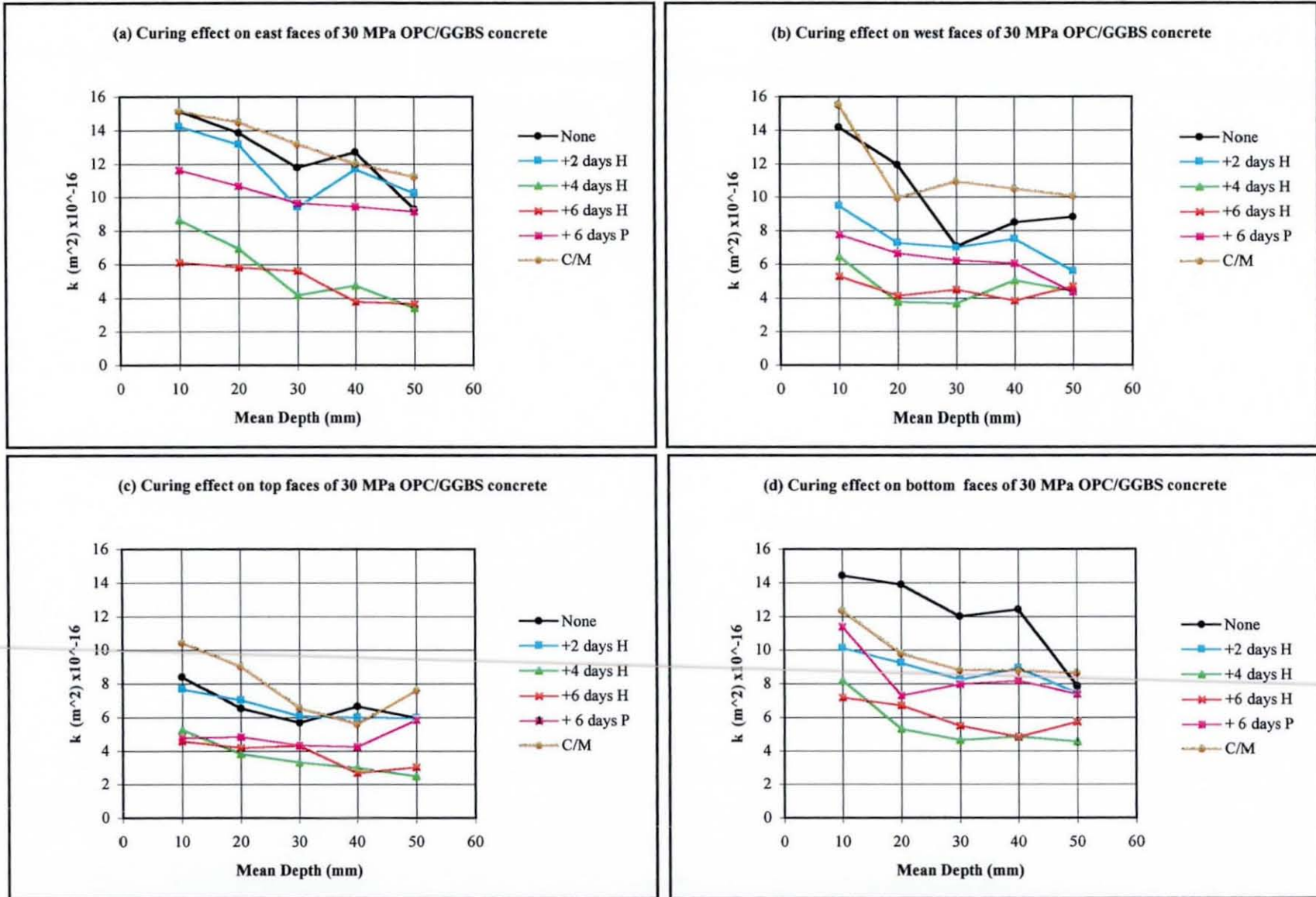
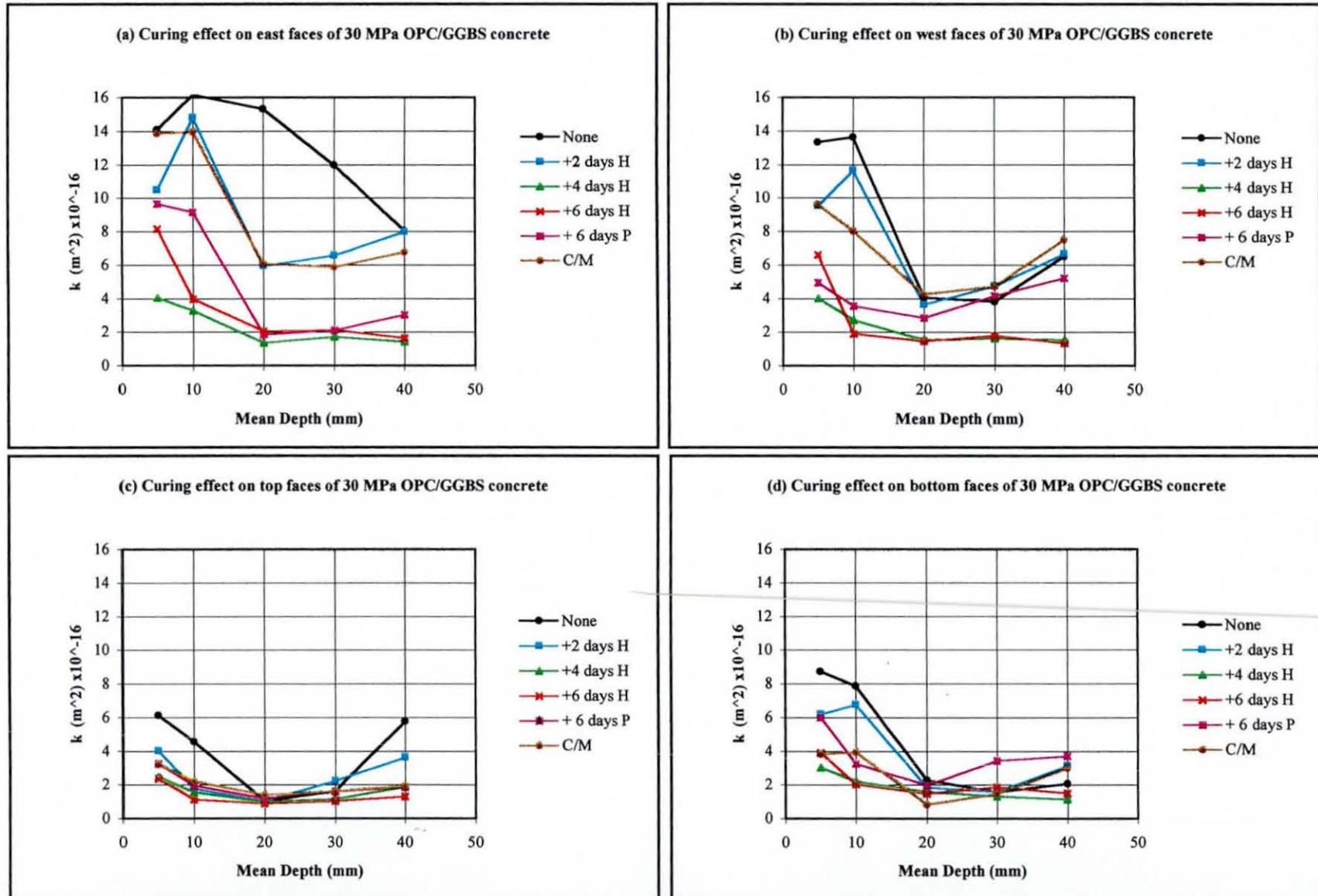


Fig. 6.11 Effect of curing regime on the air permeability profiles for the 30 MPa OPC/GGBS concrete - 12 months summer series



**Fig. 6.12** Effect of curing regime on the air permeability profiles for the 30 MPa OPC/GGBS concrete - 3 months summer series



**Fig. 6.13** Effect of curing regime on the air permeability for the 30 MPa OPC/GGBS concrete - 12 months summer series

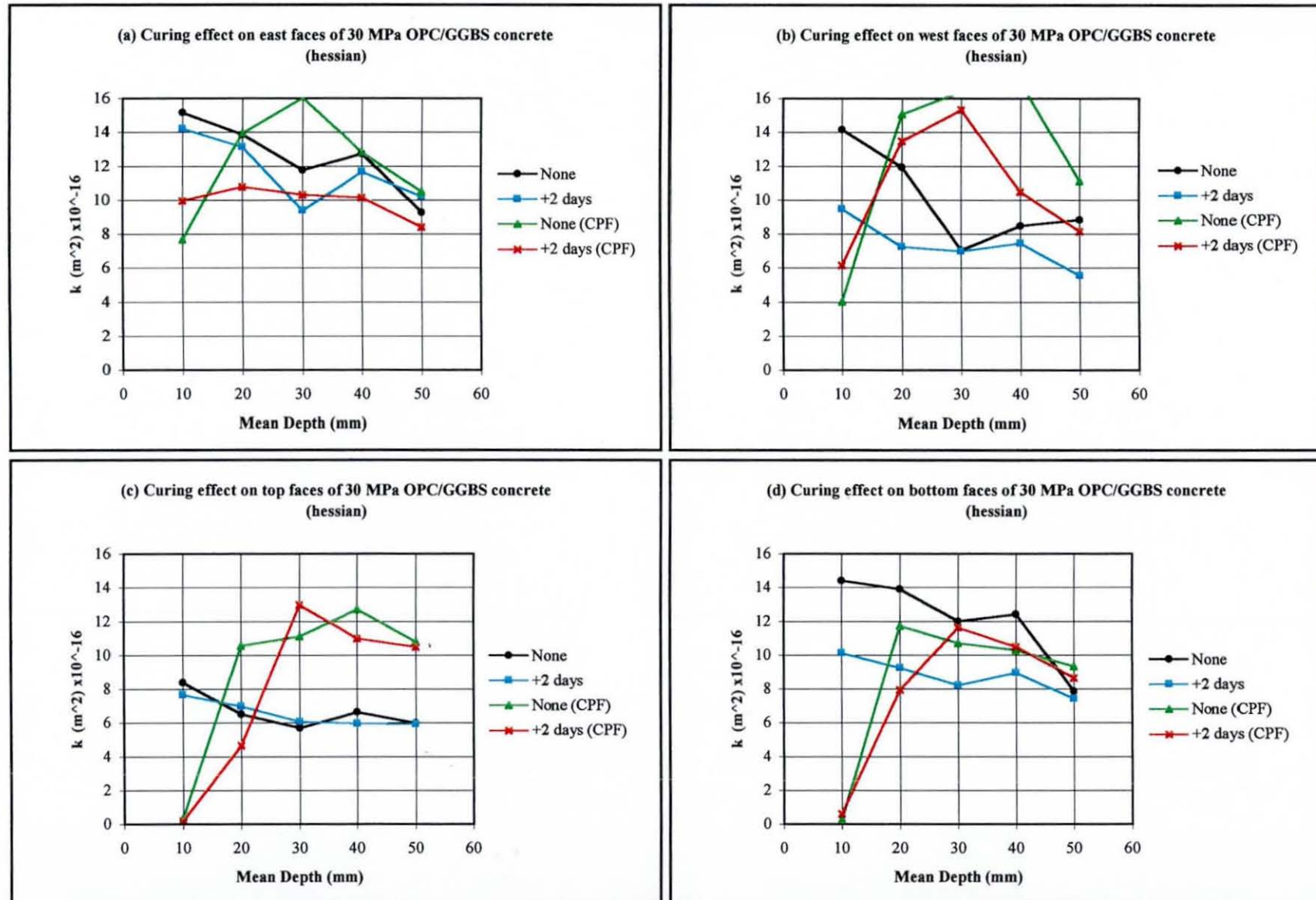


**Fig. 6.14** Effect of curing and CPF on the air permeability profiles for the 30 MPa OPC/GGBS concrete - 3 months summer series

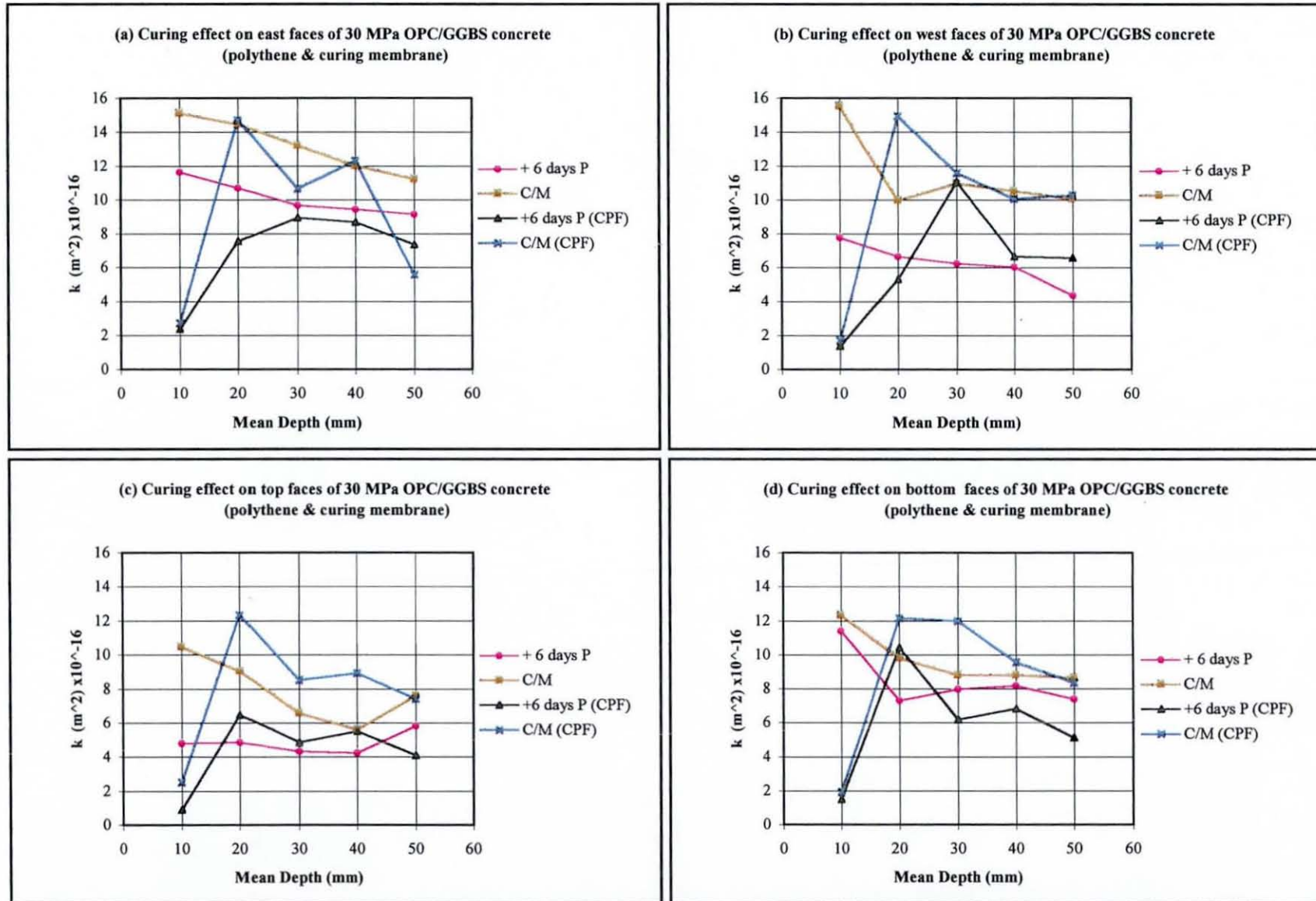


**Fig. 6.15** Effect of curing and CPF on the air permeability profiles for the 30 MPa OPC/GGBS concrete - 3 months summer series

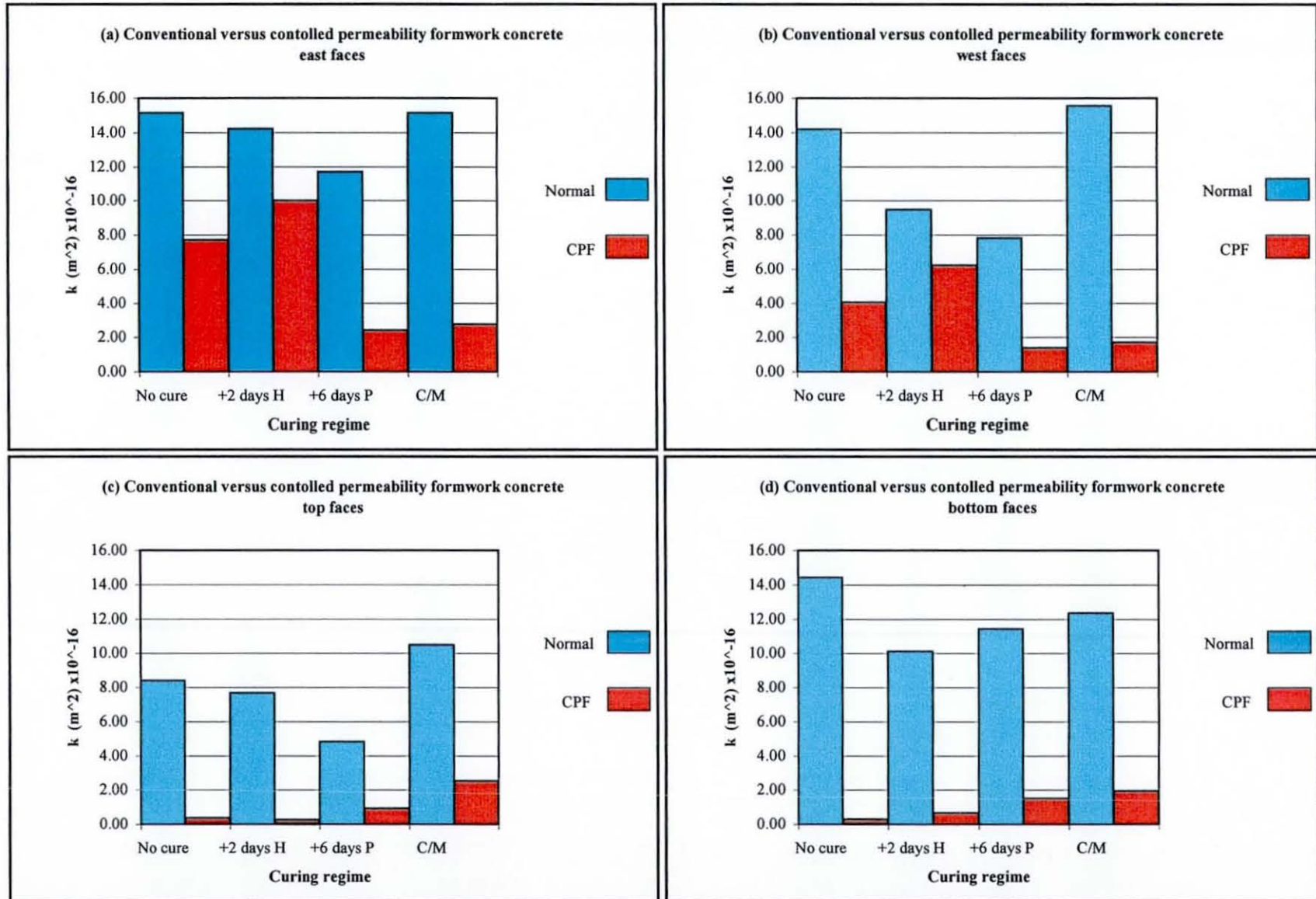


**Fig. 6.16** Effect of curing and CPF on the air permeability of 30 MPa OPC/GGBS concrete at surface (10mm from surface) - 3 months summer series

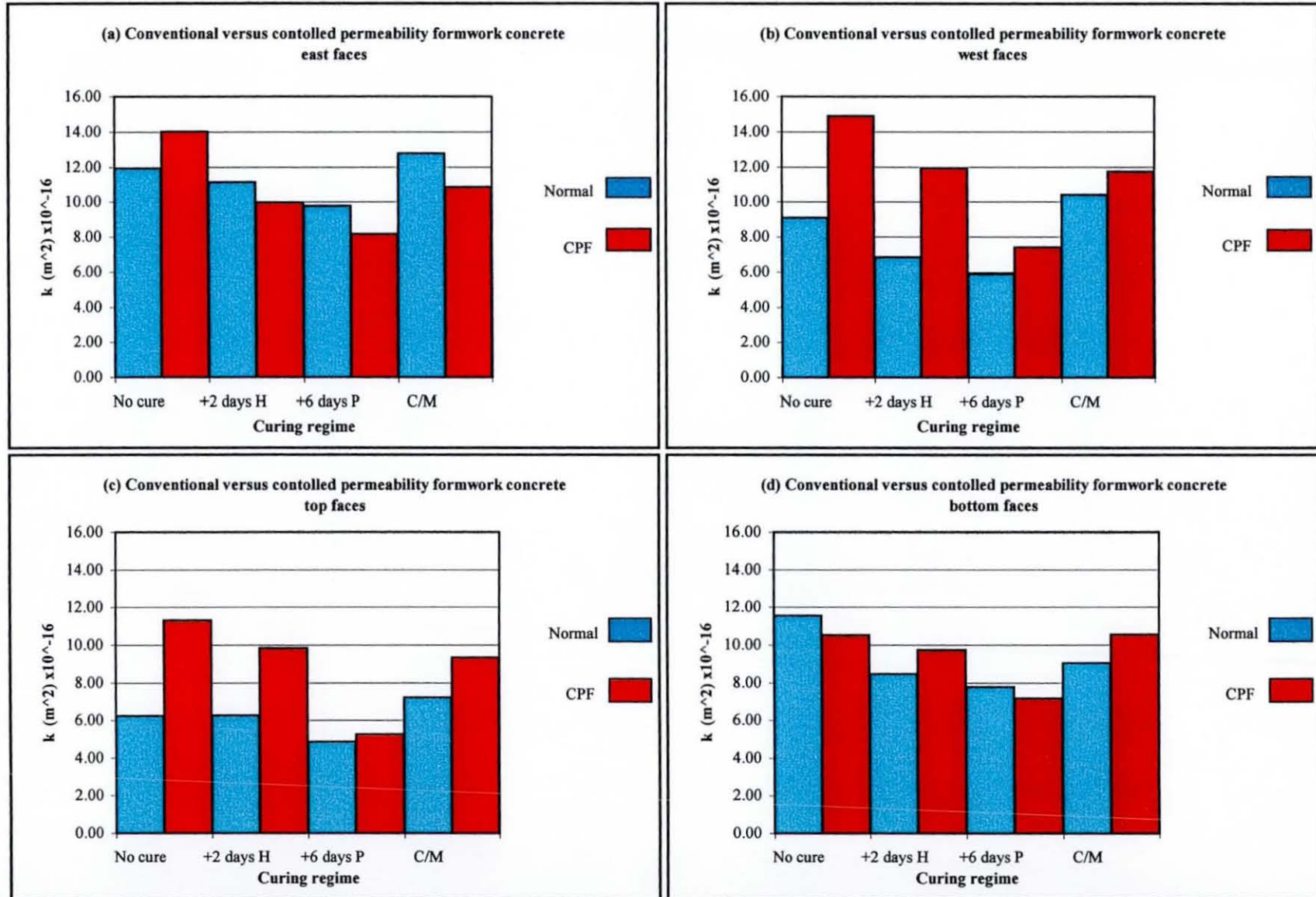
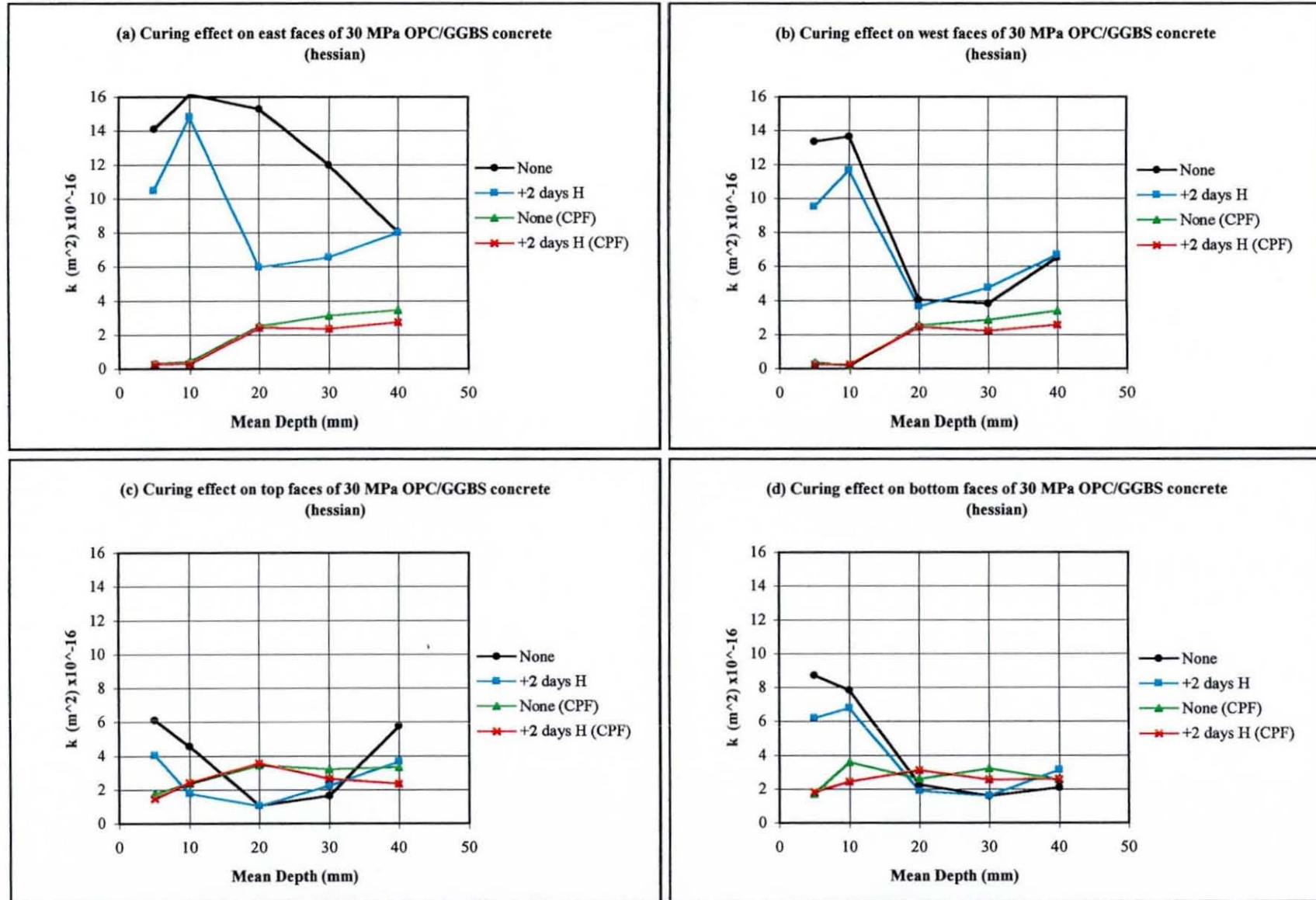


Fig. 6.17 Effect of curing and CPF on the air permeability of 30 MPa OPC/GGRS concrete at subsurface (20-50mm from surface) - 2 months exposure



**Fig. 6.18** Effect of curing and CPF on the air permeability profiles for the 30 MPa OPC/GGBS concrete - 12 months summer series

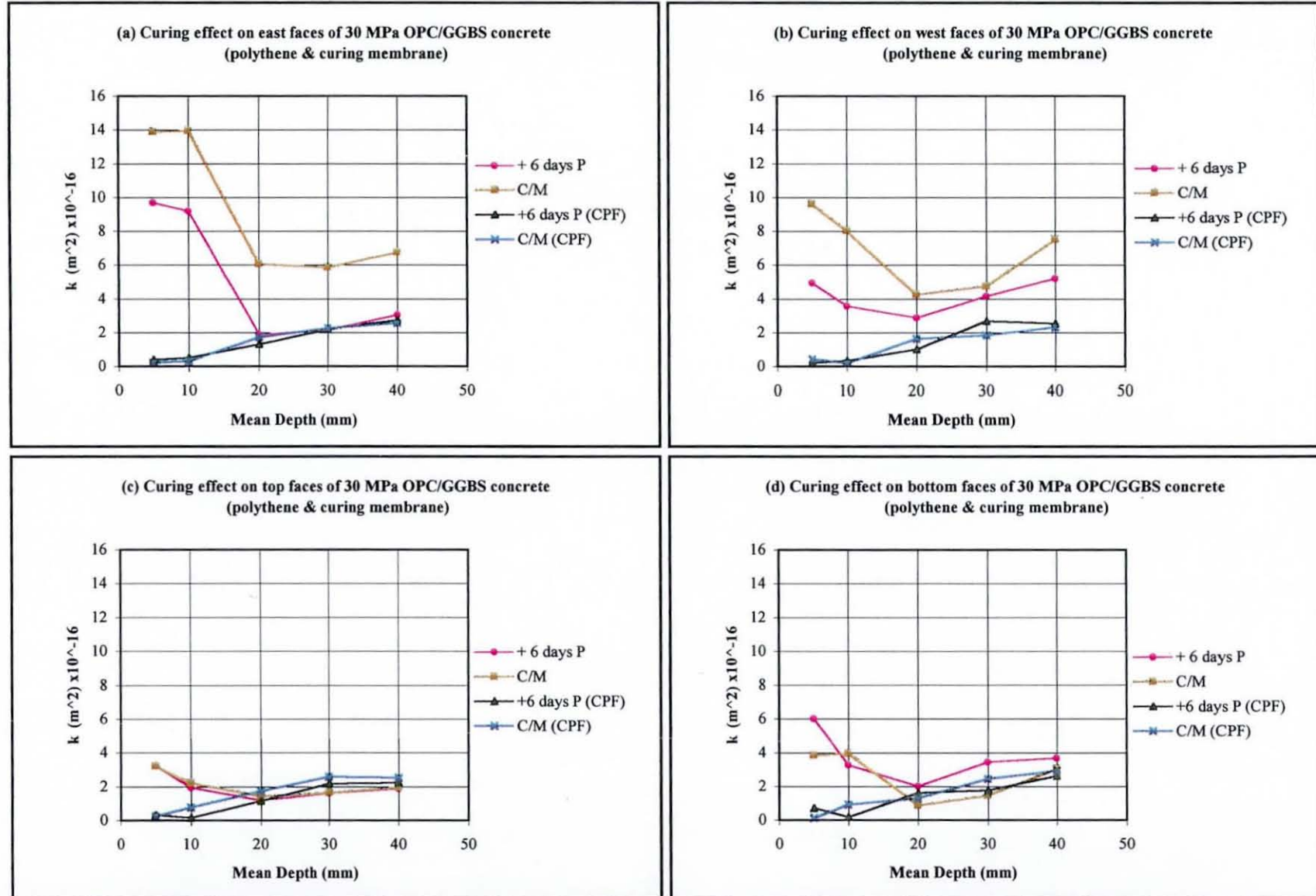


Fig. 6.19 Effect of curing and CPF on the air permeability profiles for the 30 MPa OPC/GGBS concrete - 12 months summer series

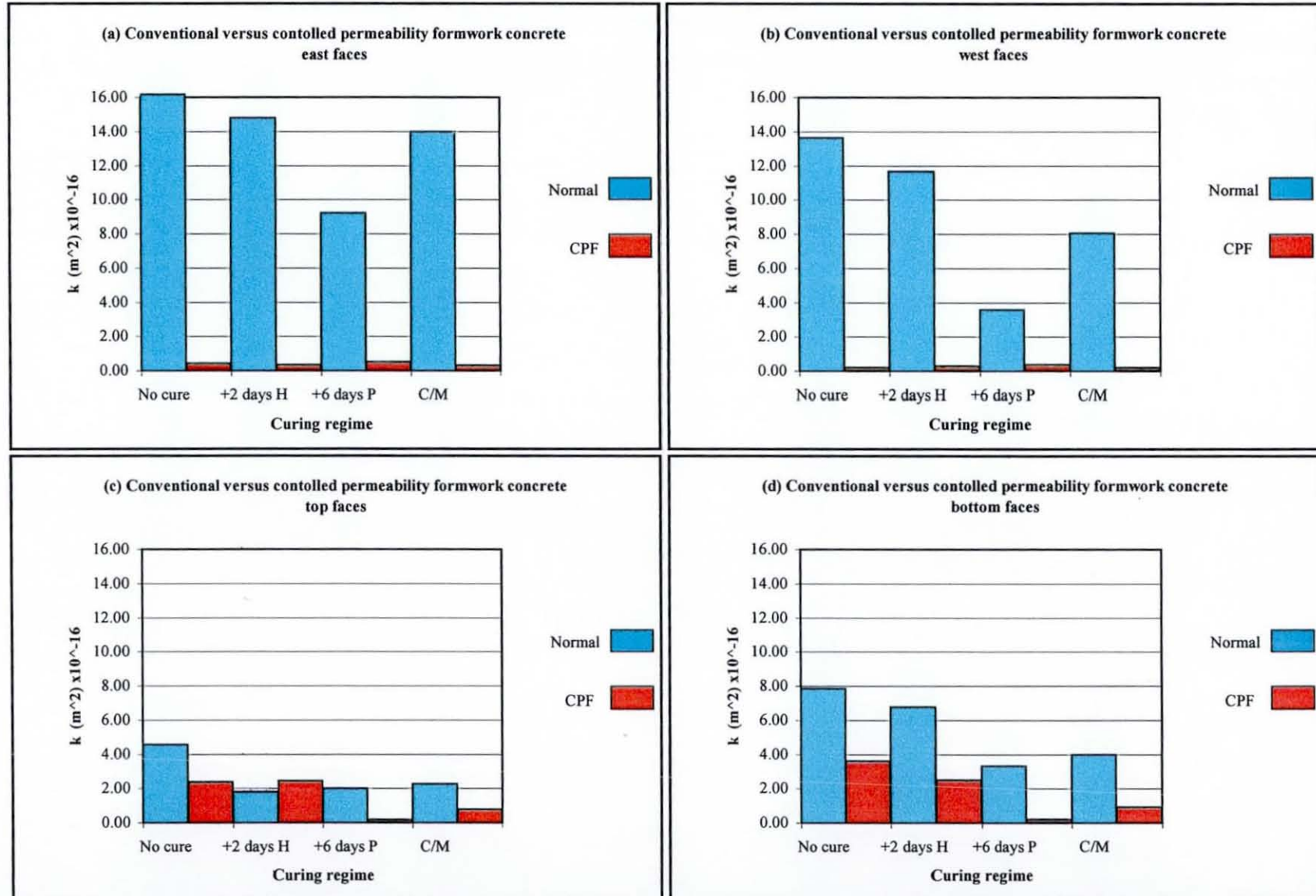


Fig. 6.20 Effect of curing and CPF on the air permeability profiles of 30 MPa OPC/GGBS concrete at surface (10mm from surface) - 12 months summer series

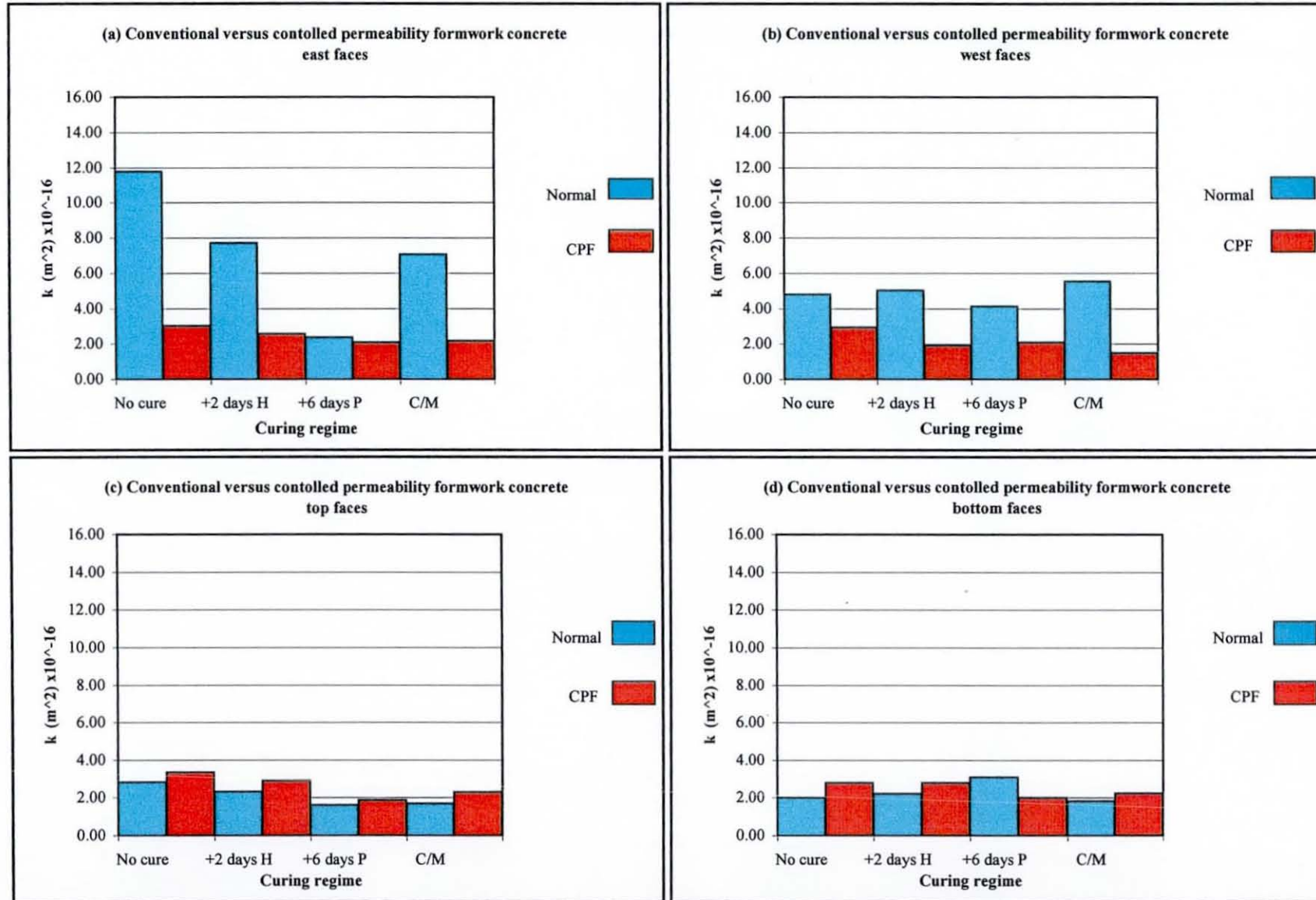


Fig. 6.21 Effect of curing and CPF on the air permeability profiles of 30 MPa OPC/GGBS concrete at subsurface (20-50mm from surface) - 12 months summer series

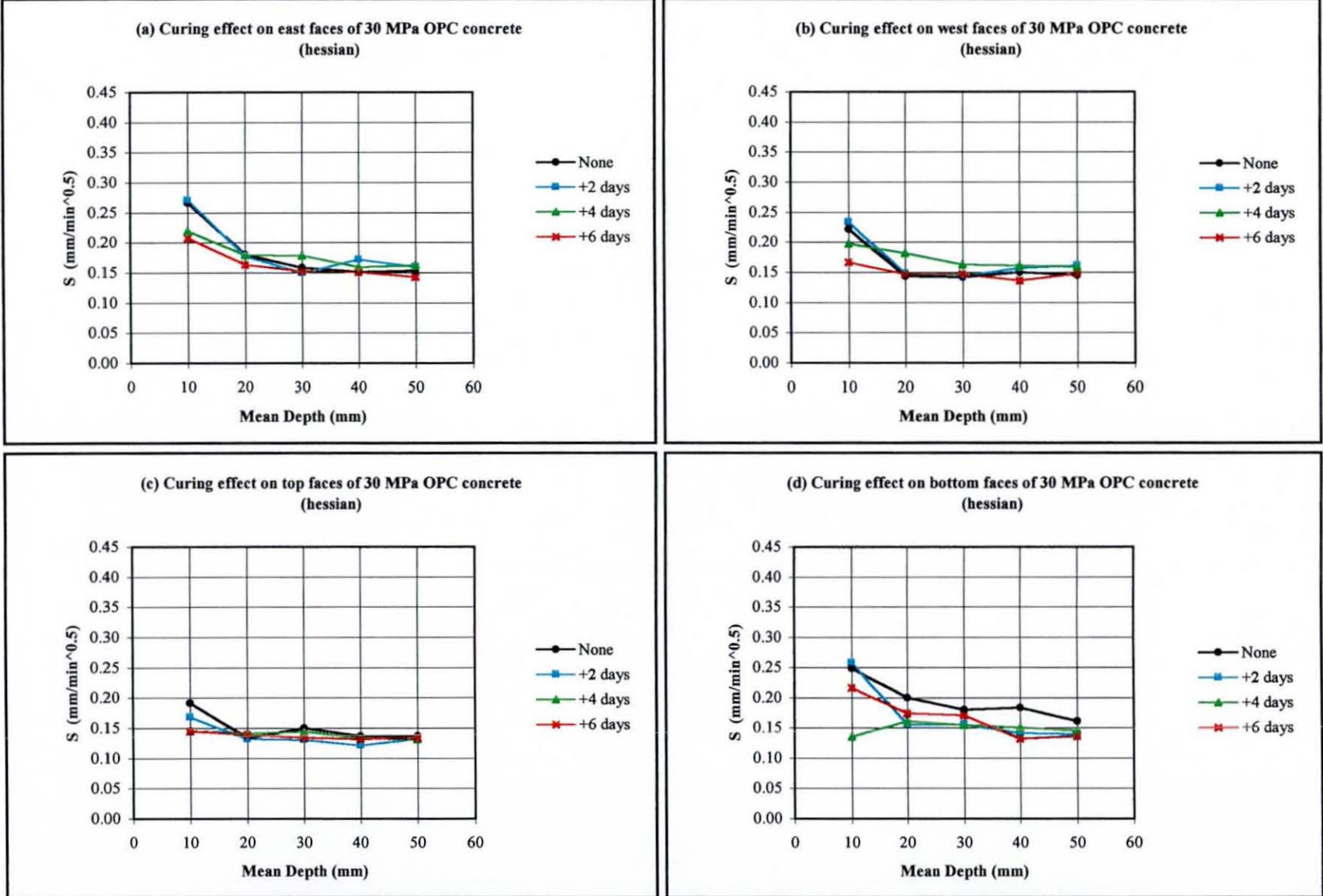


Fig. 6.22 Effect of curing regime on the sorptivity of 30 MPa OPC concrete - 3 months summer series

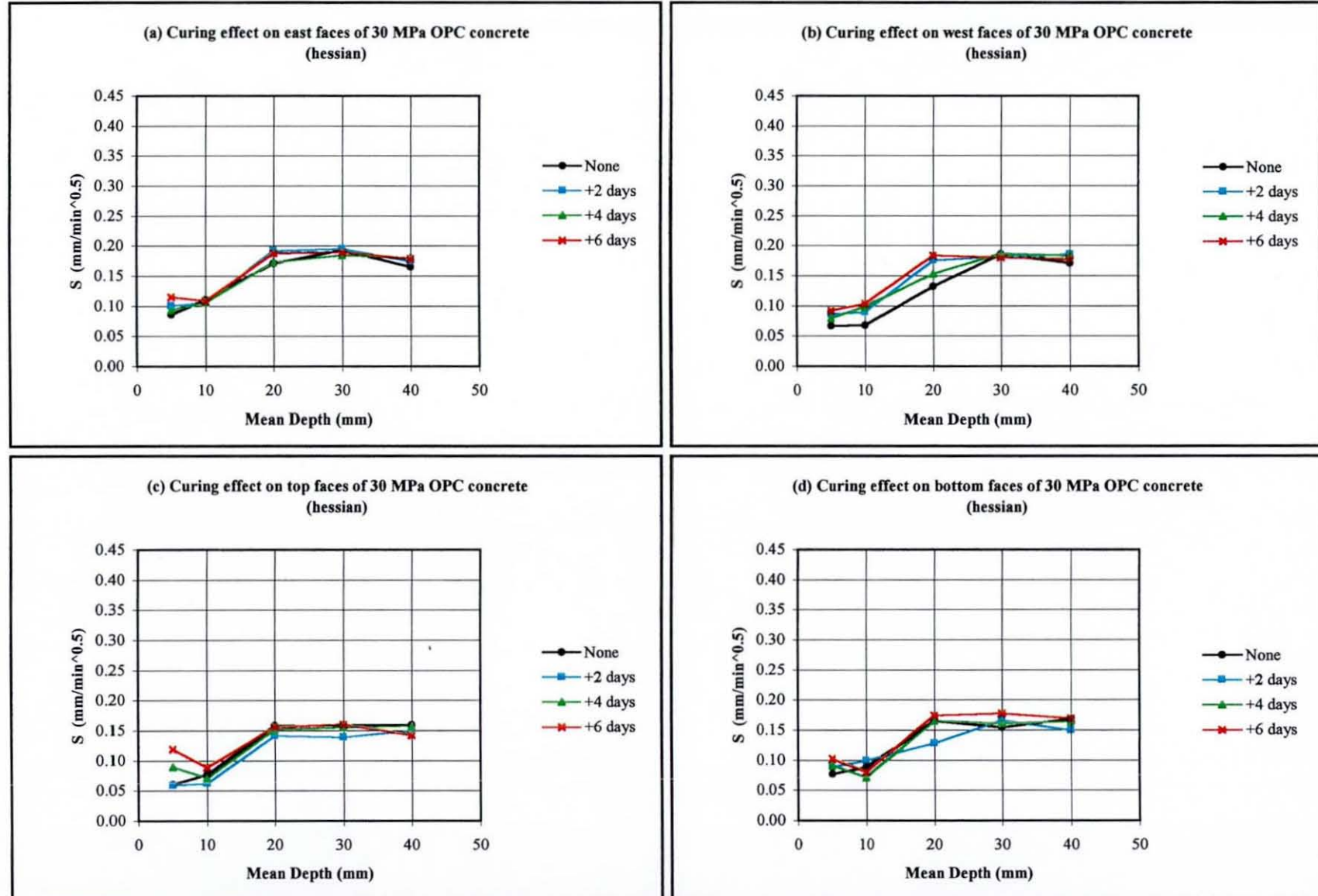


Fig. 6.23 Effect of curing regime on the sorptivity of 30 MPa OPC concrete - 12 months summer series

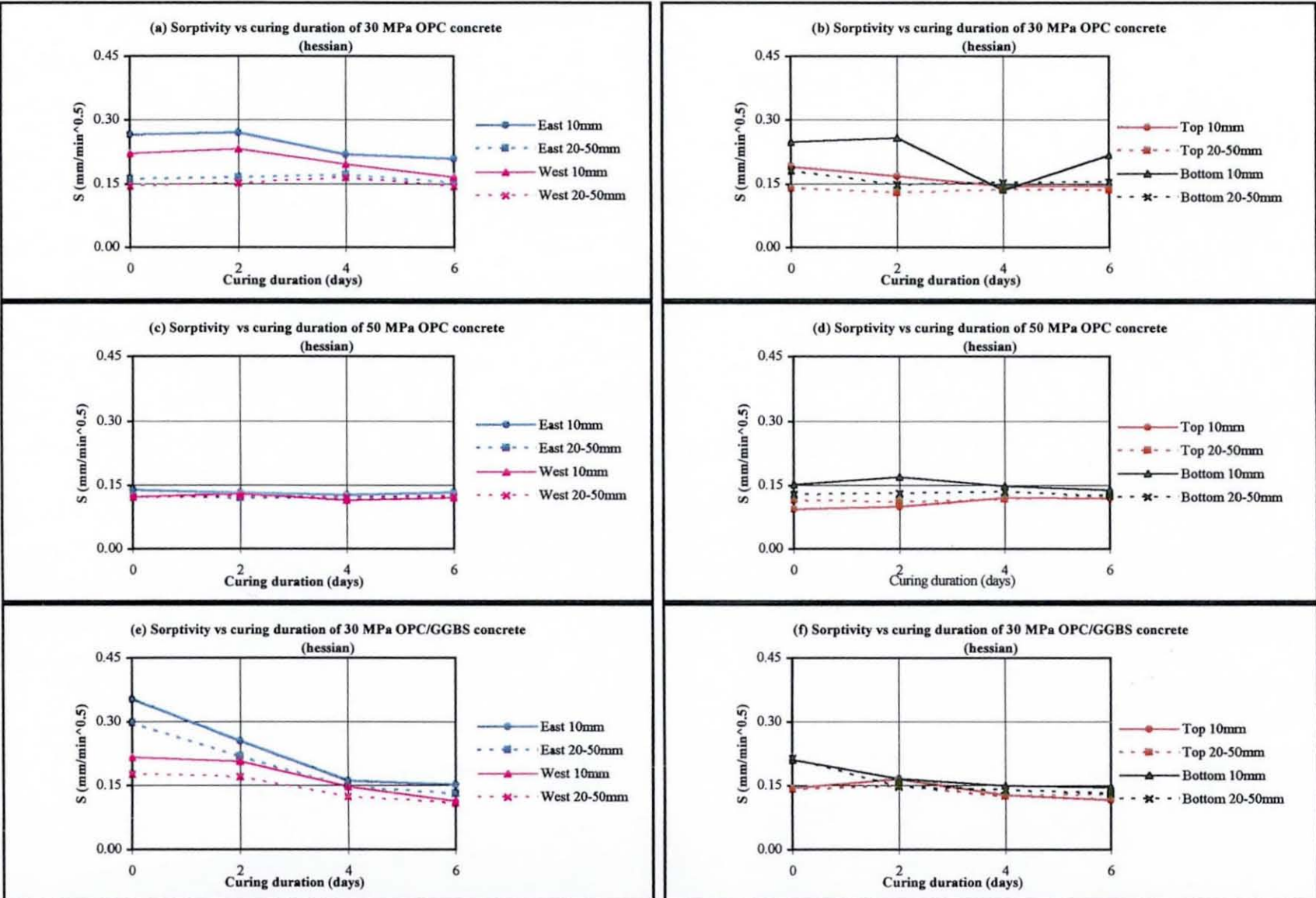


Fig. 6.24 Effect of curing duration on the sorptivity of OPC and OPC/GGBS concrete - 3 months summer series

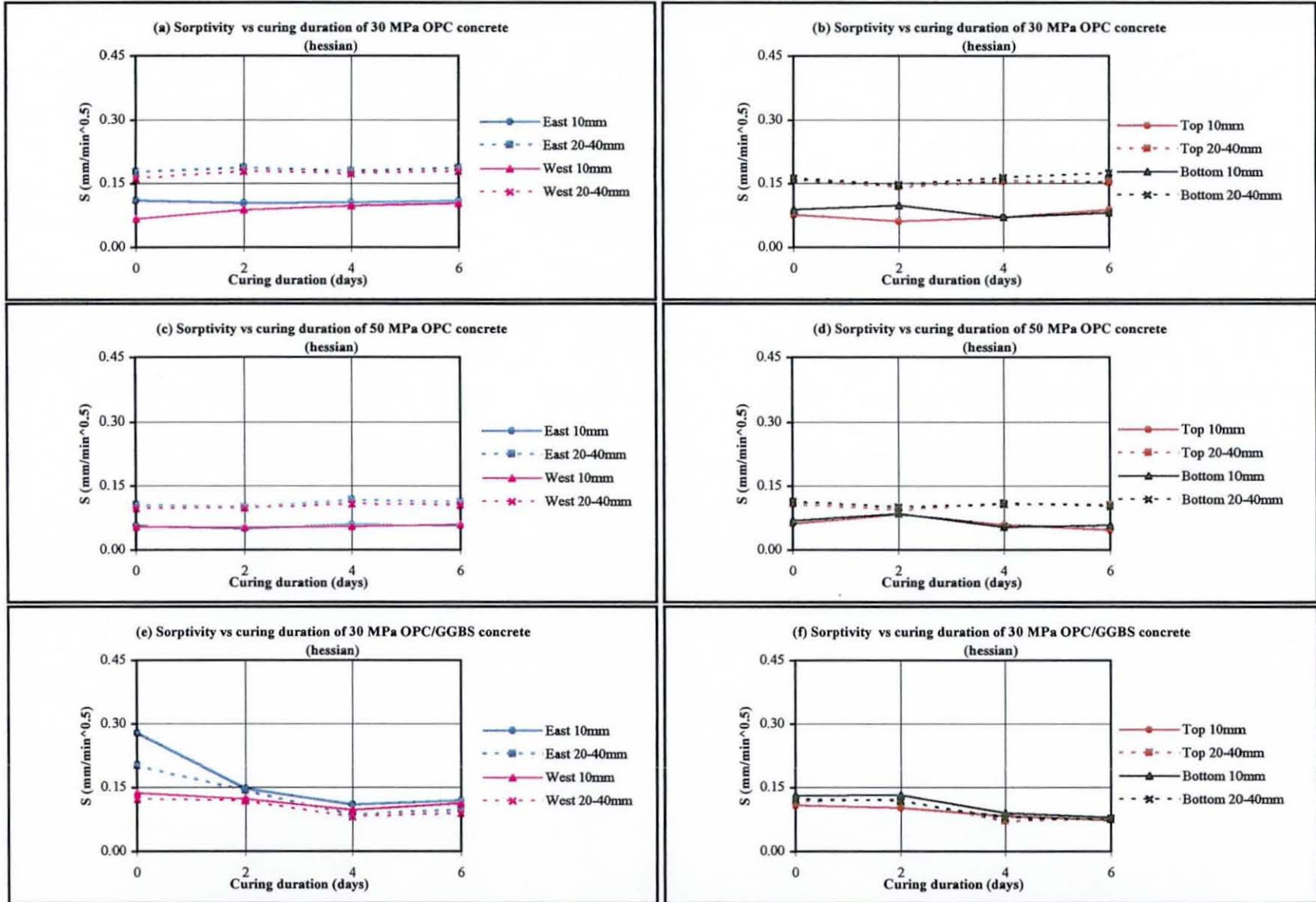


Fig. 6.25 Effect of curing duration on the sorptivity of 30 MPa OPC and OPC/GGBS concrete - 12 months summer series

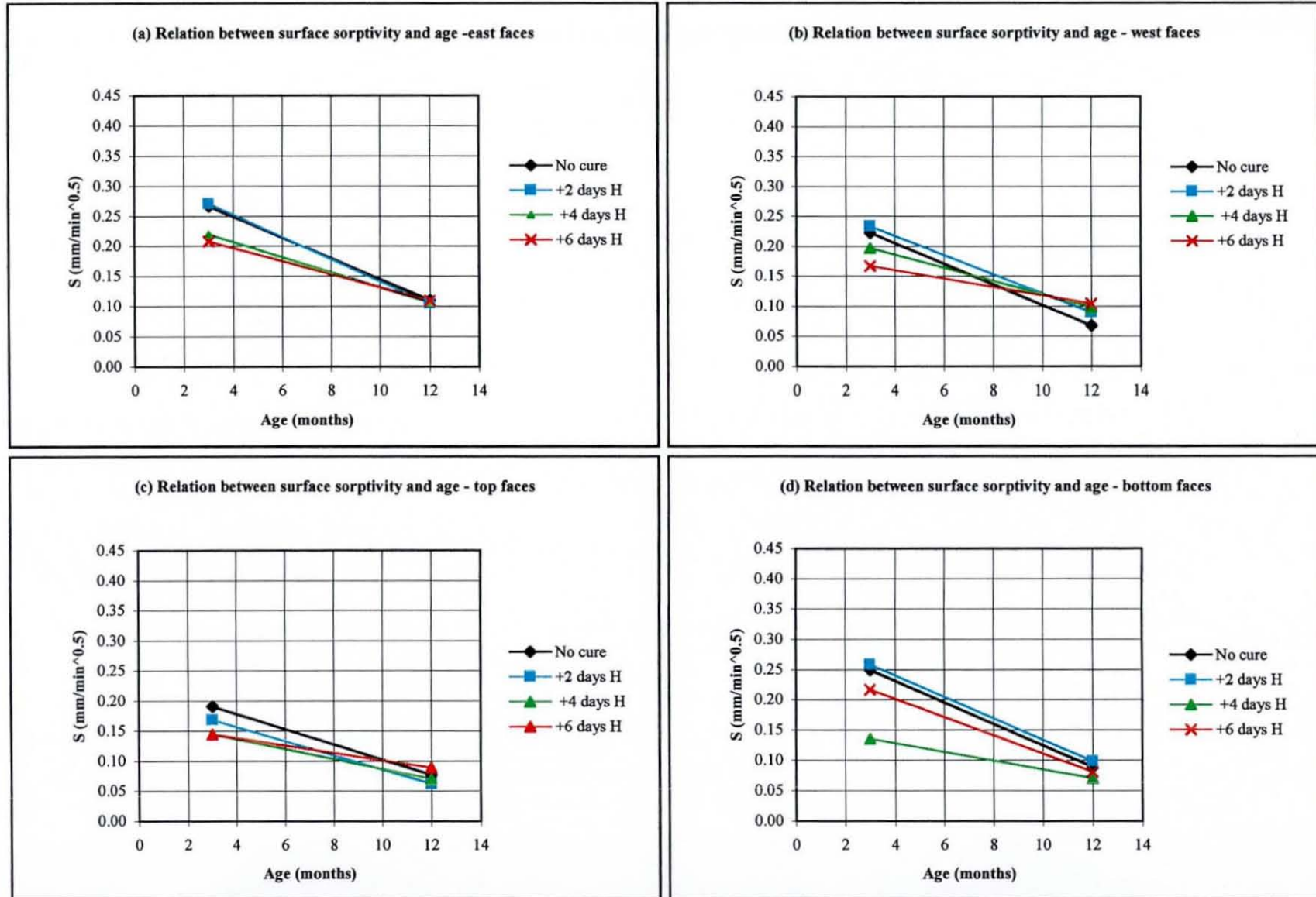


Fig. 6.26 Relationship between surface sorptivity and age of the 30 MPa OPC concrete - IJK summer

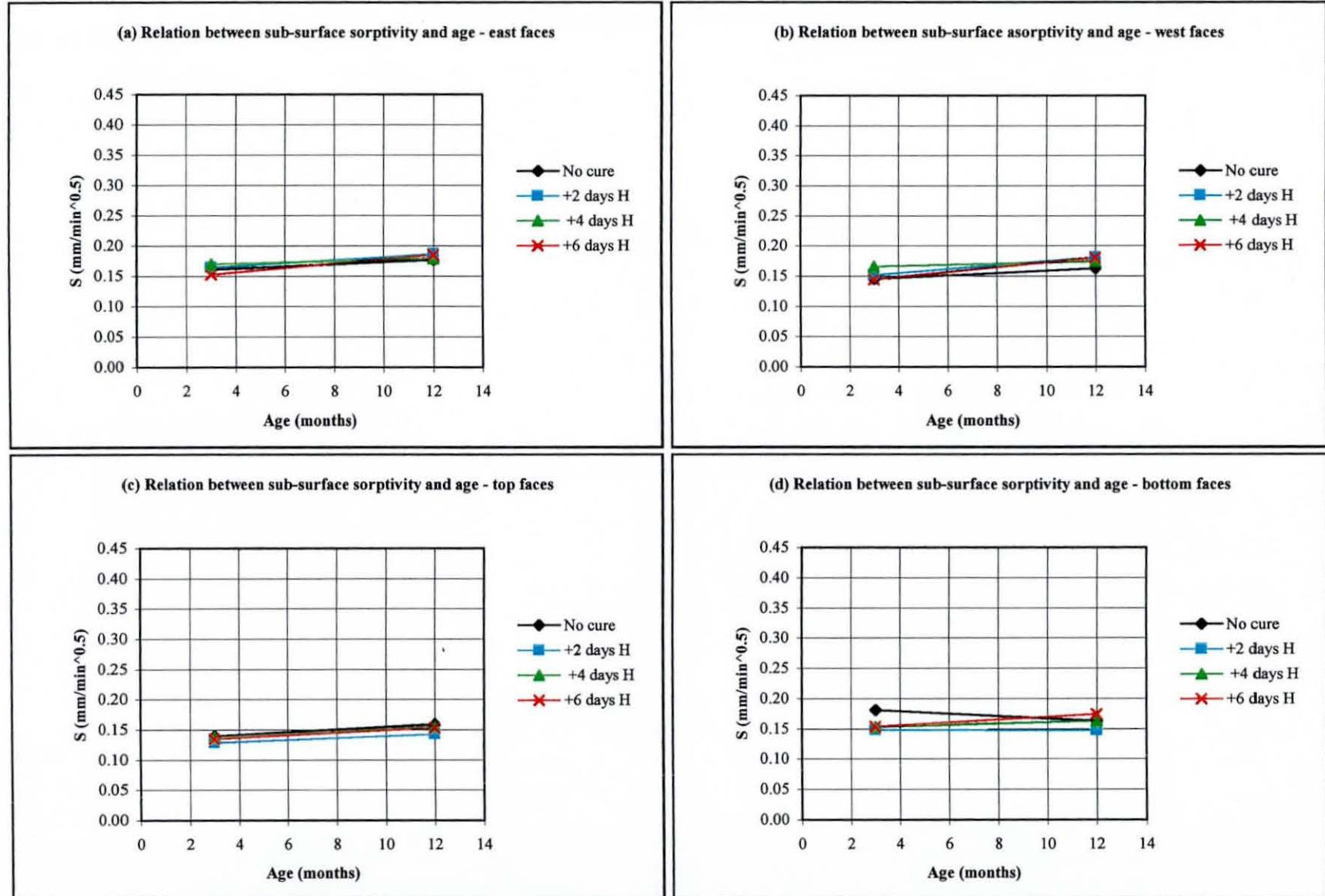


Fig. 6.27 Relationship between sub-surface sorptivity and age of the 30 MPa OPC concrete - UK summer

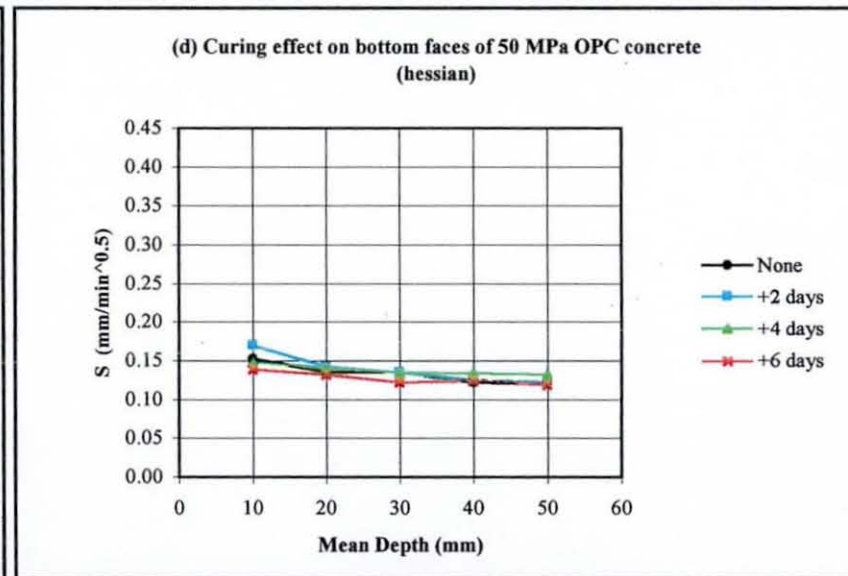
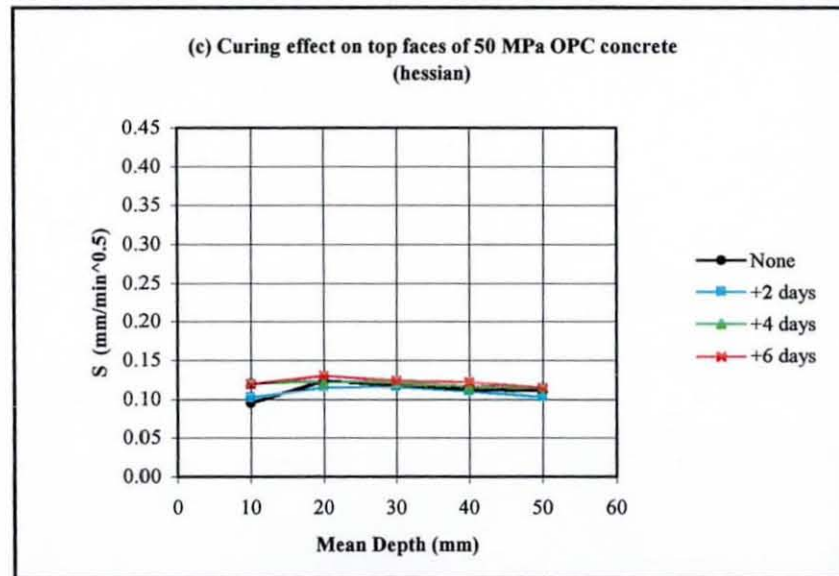
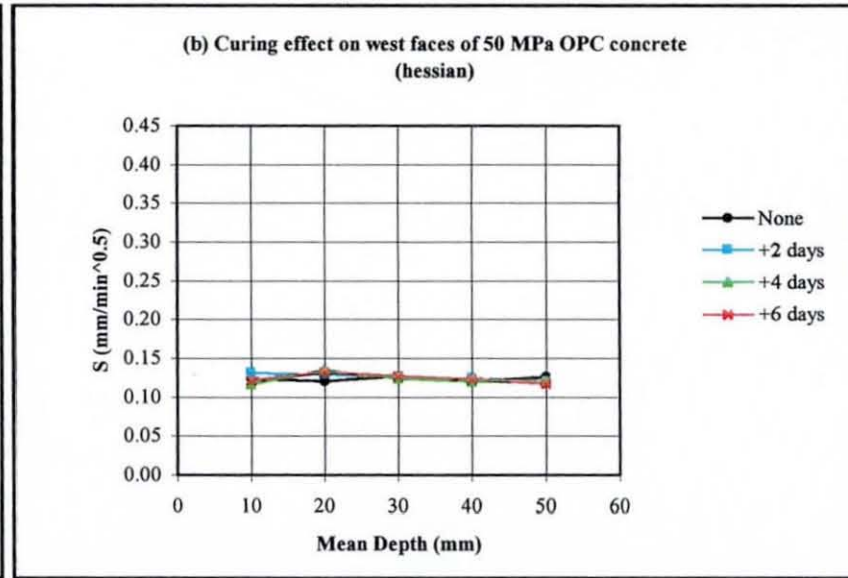
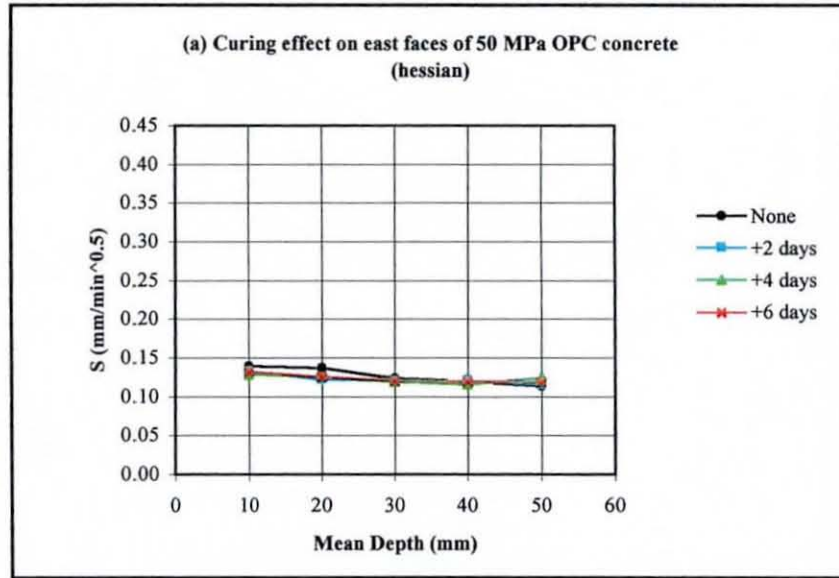


Fig. 6.28 Effect of curing regime on the sorptivity of 50 MPa OPC concrete - 3 months summer series

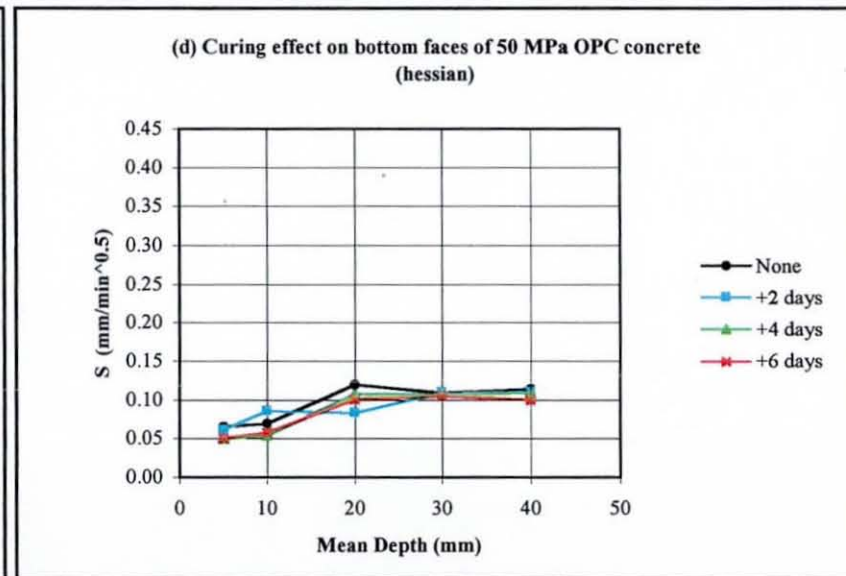
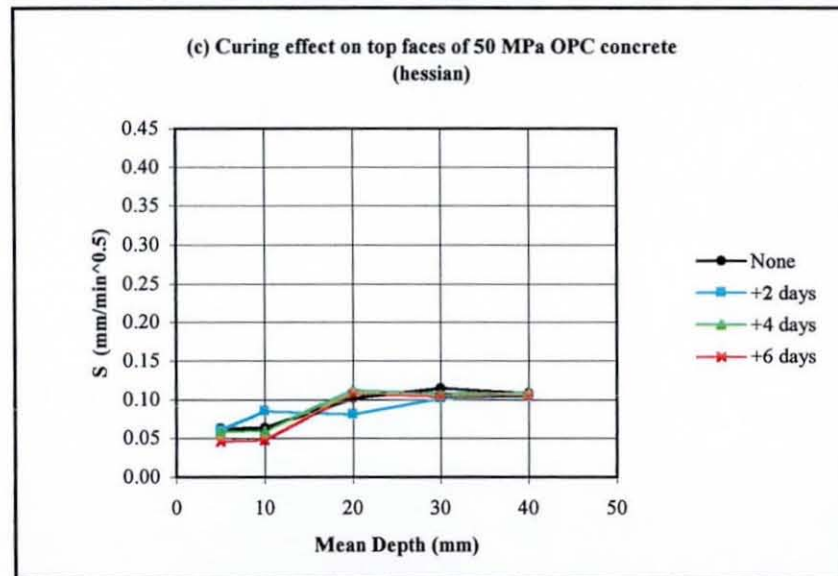
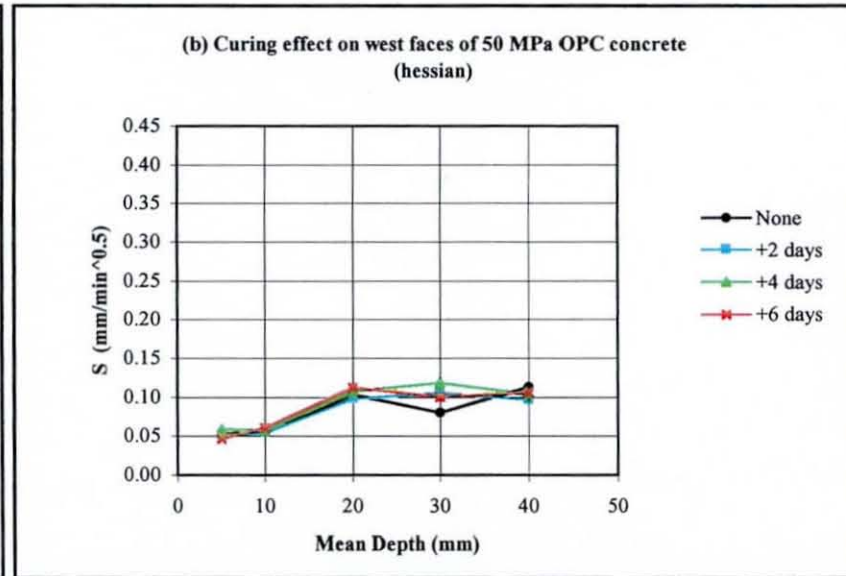
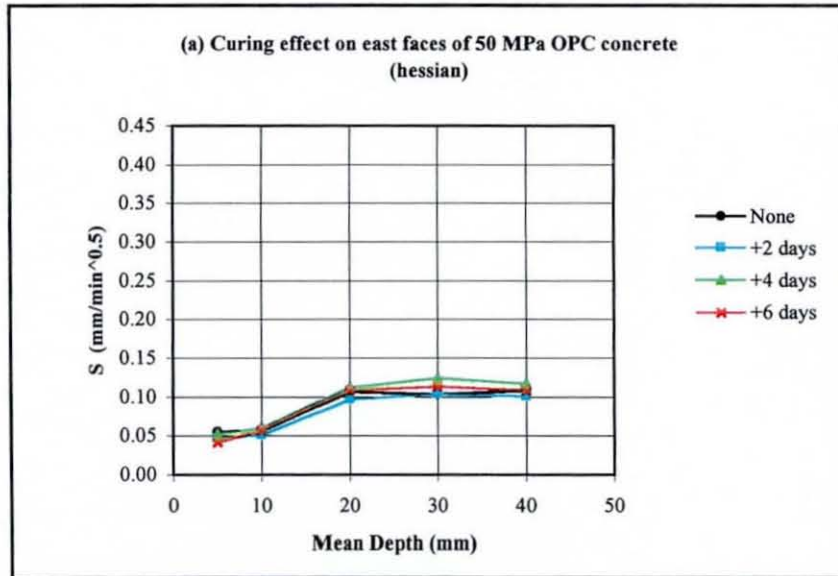


Fig. 6.29 Effect of curing regime on the sorptivity of 50 MPa OPC concrete - 12 months summer series

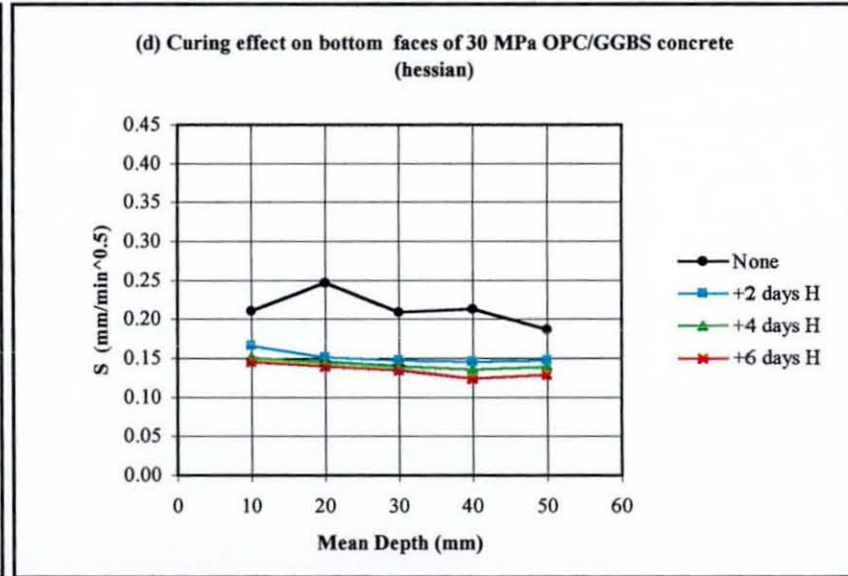
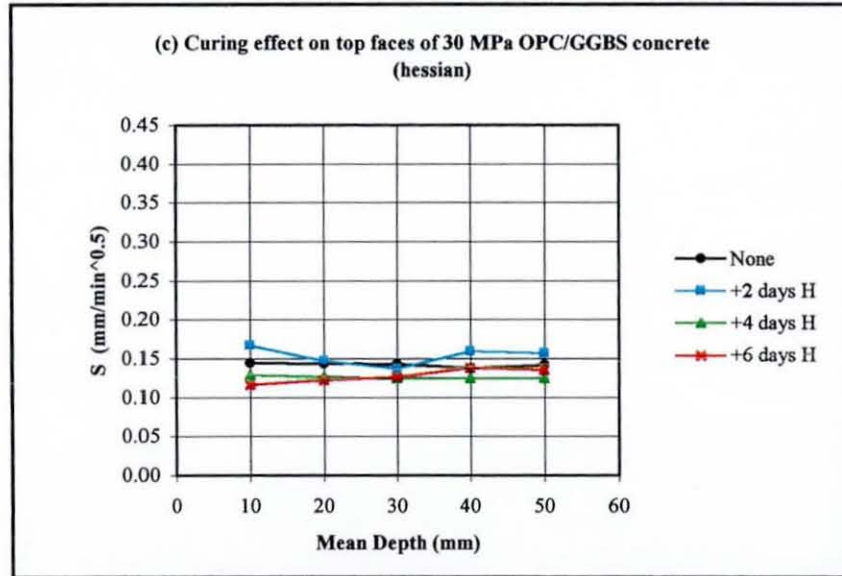
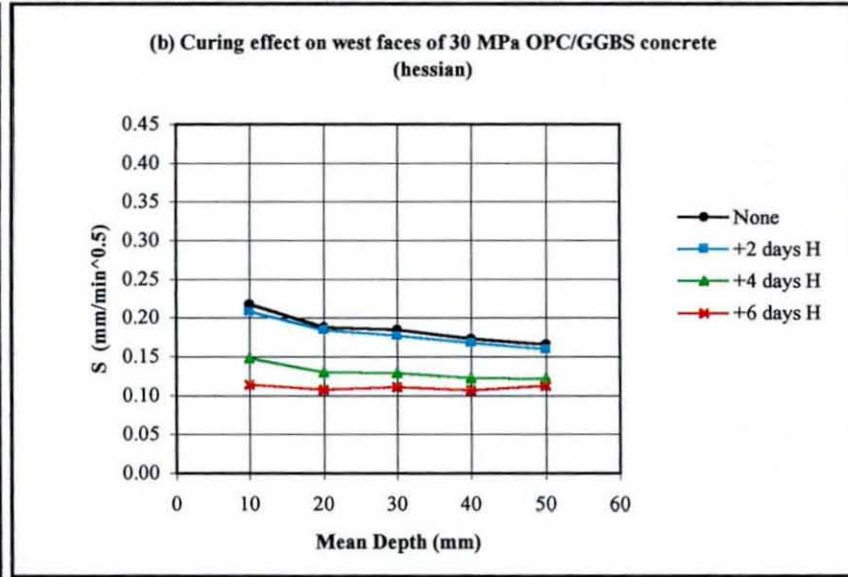
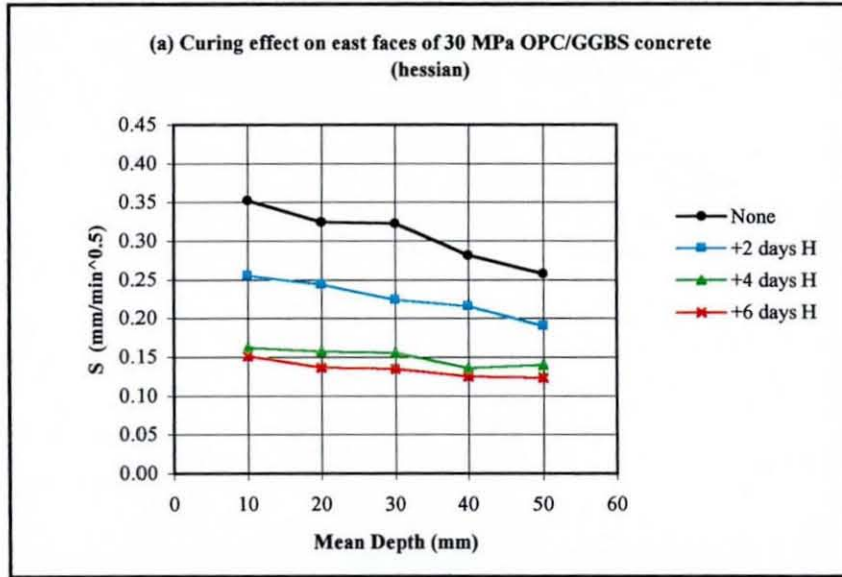


Fig. 6.30 Effect of curing regime on the sorptivity of 30 MPa OPC/GGBS concrete - 3 months summer series

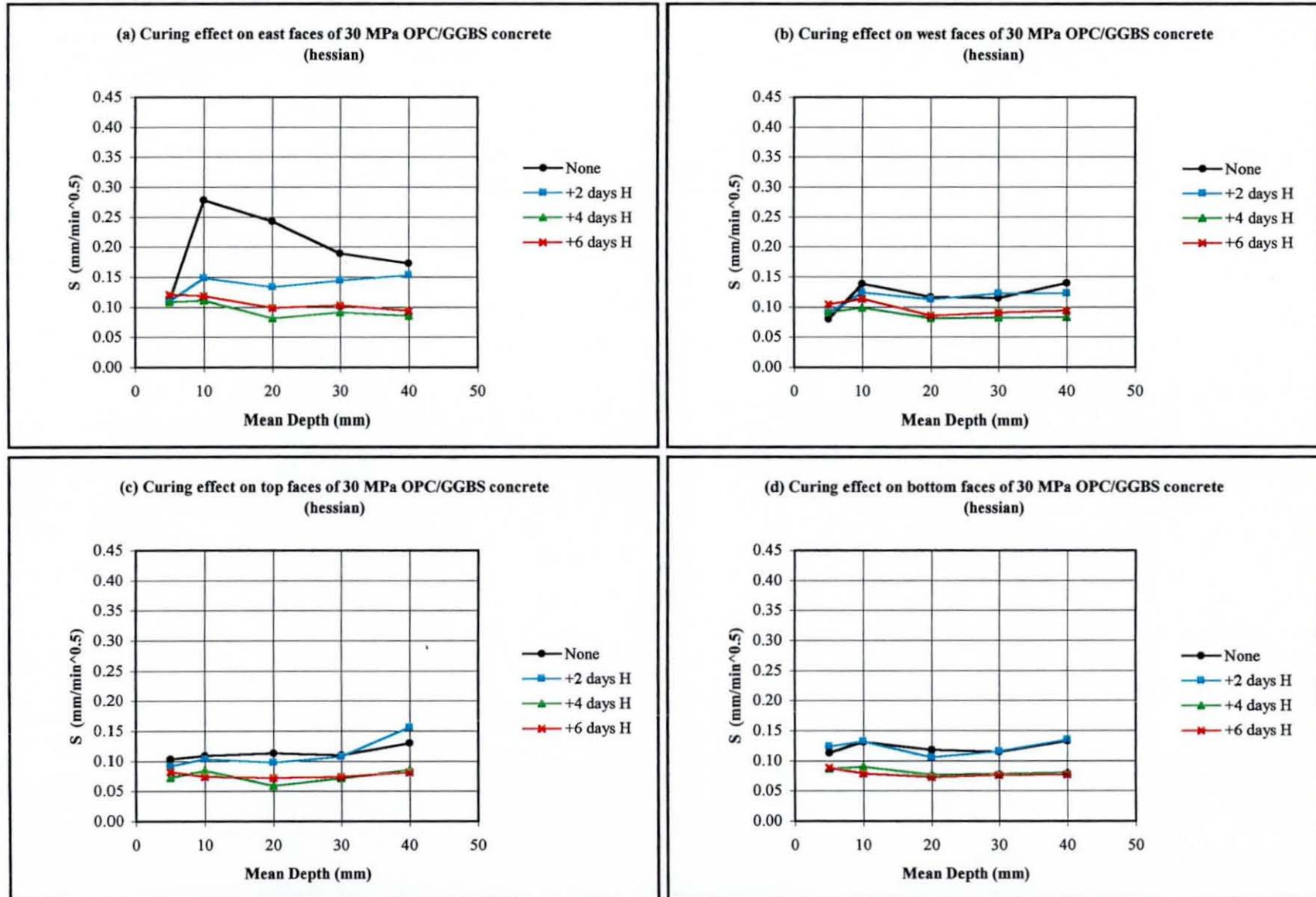


Fig. 6.31 Effect of curing regime on the sorptivity of 30 MPa OPC/GGBS concrete - 12 months summer series

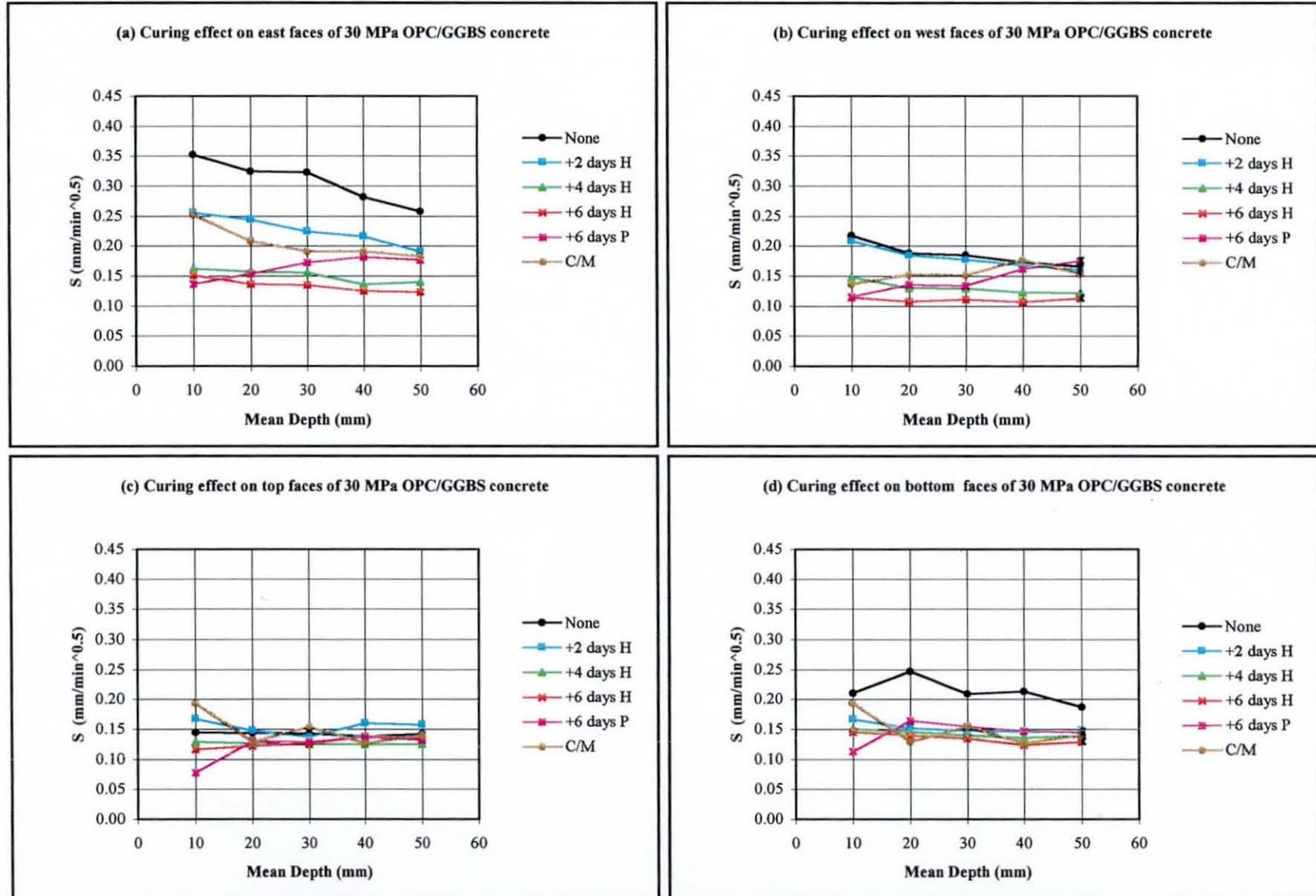


Fig. 6.32 Effect of curing regime on the sorptivity of OPC/GGBS concrete - 3 months summer series

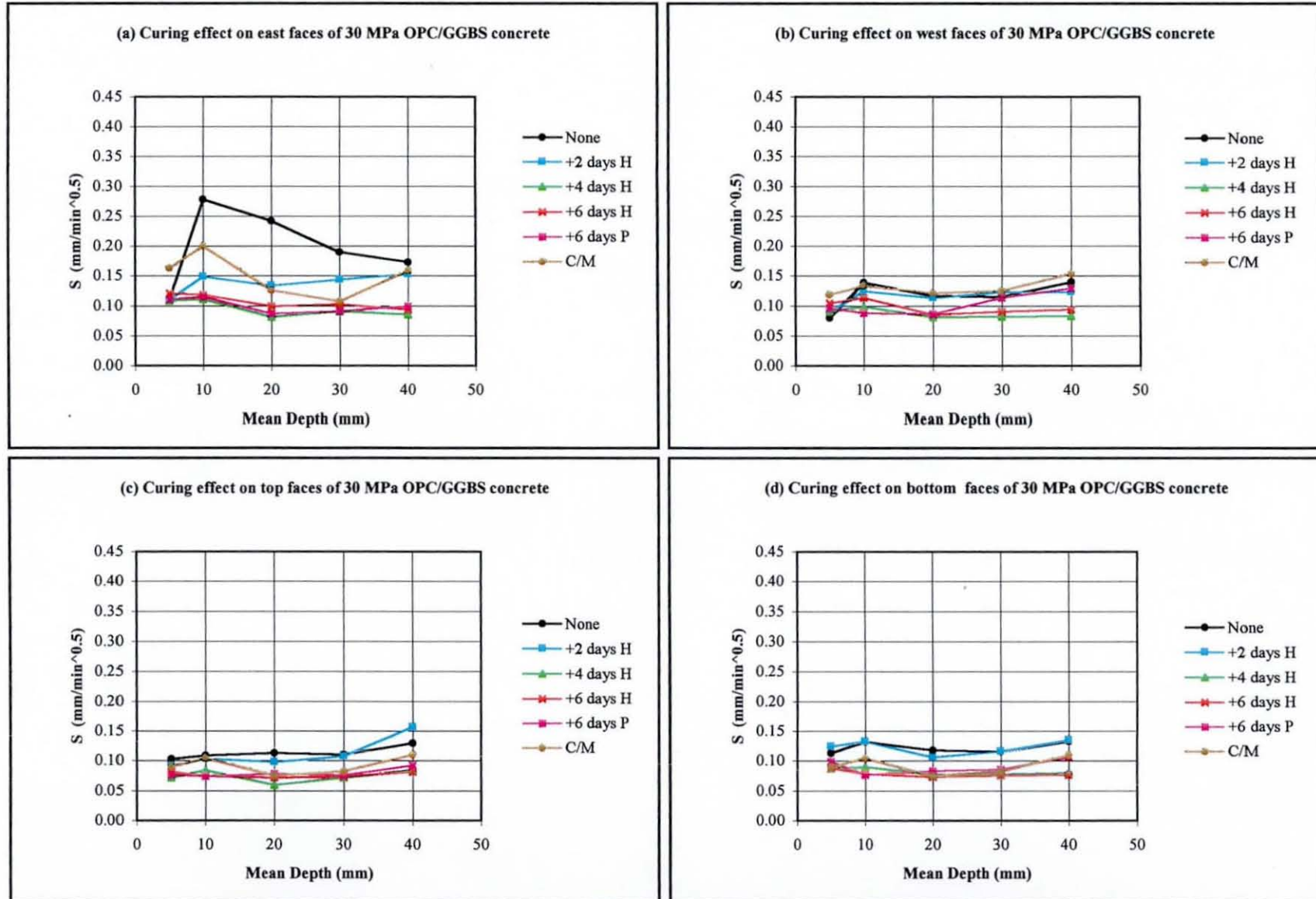


Fig. 6.33 Effect of curing regime on the sorptivity of OPC/GGBS concrete - 12 months summer series

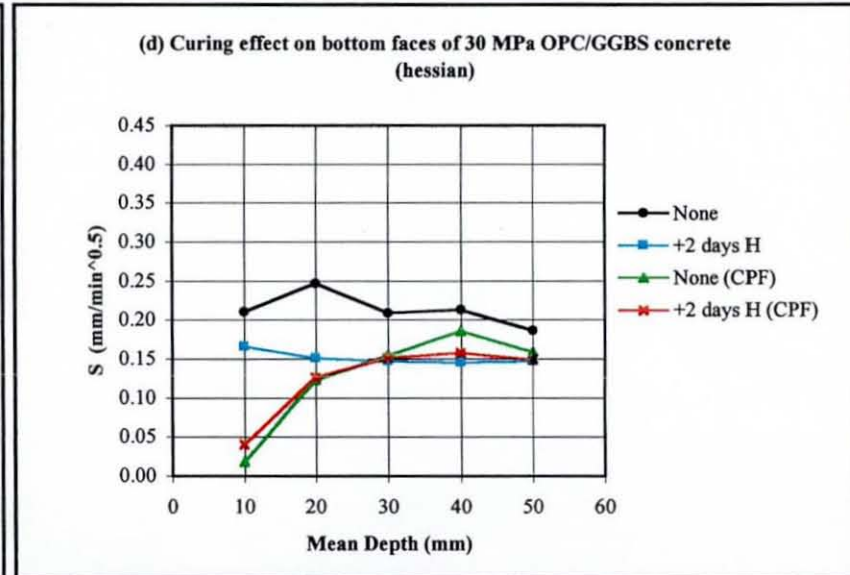
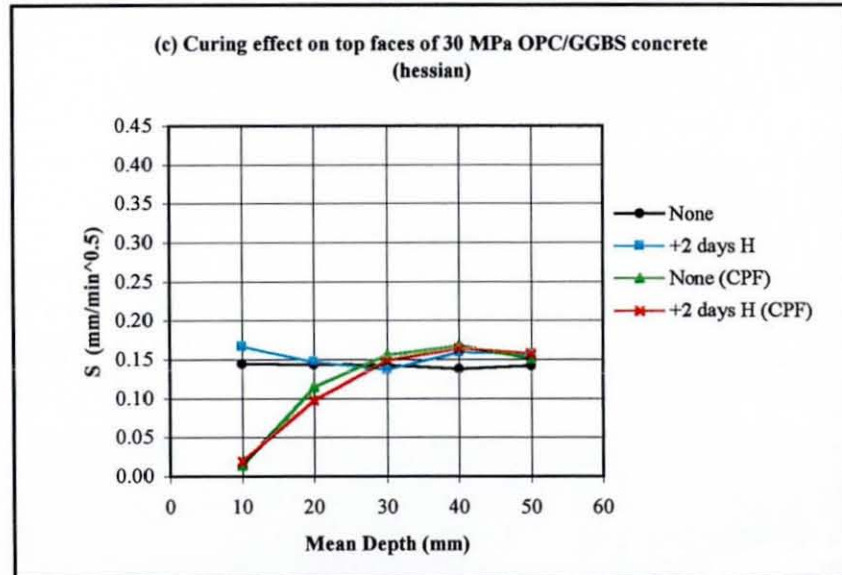
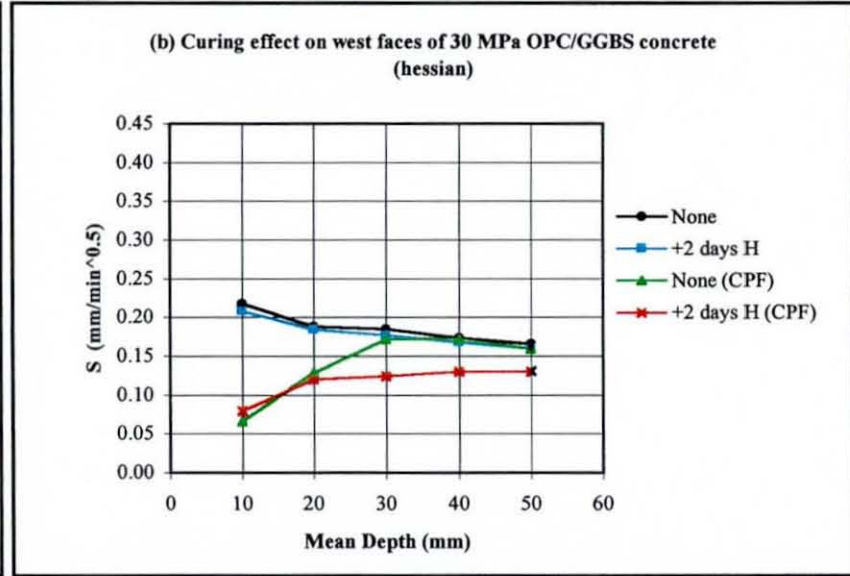
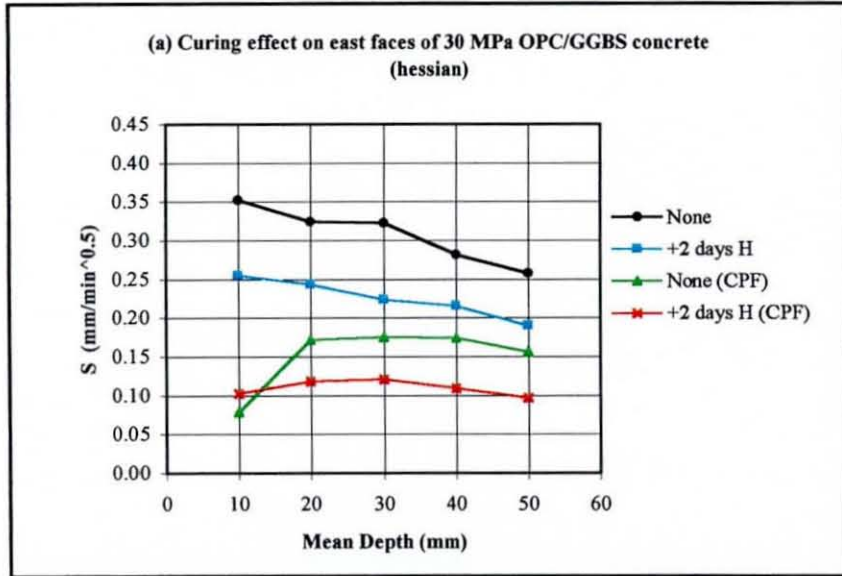


Fig. 6.34 Effect of curing and CPF on the sorptivity of 30 MPa OPC/GGBS concrete - 3 months summer series

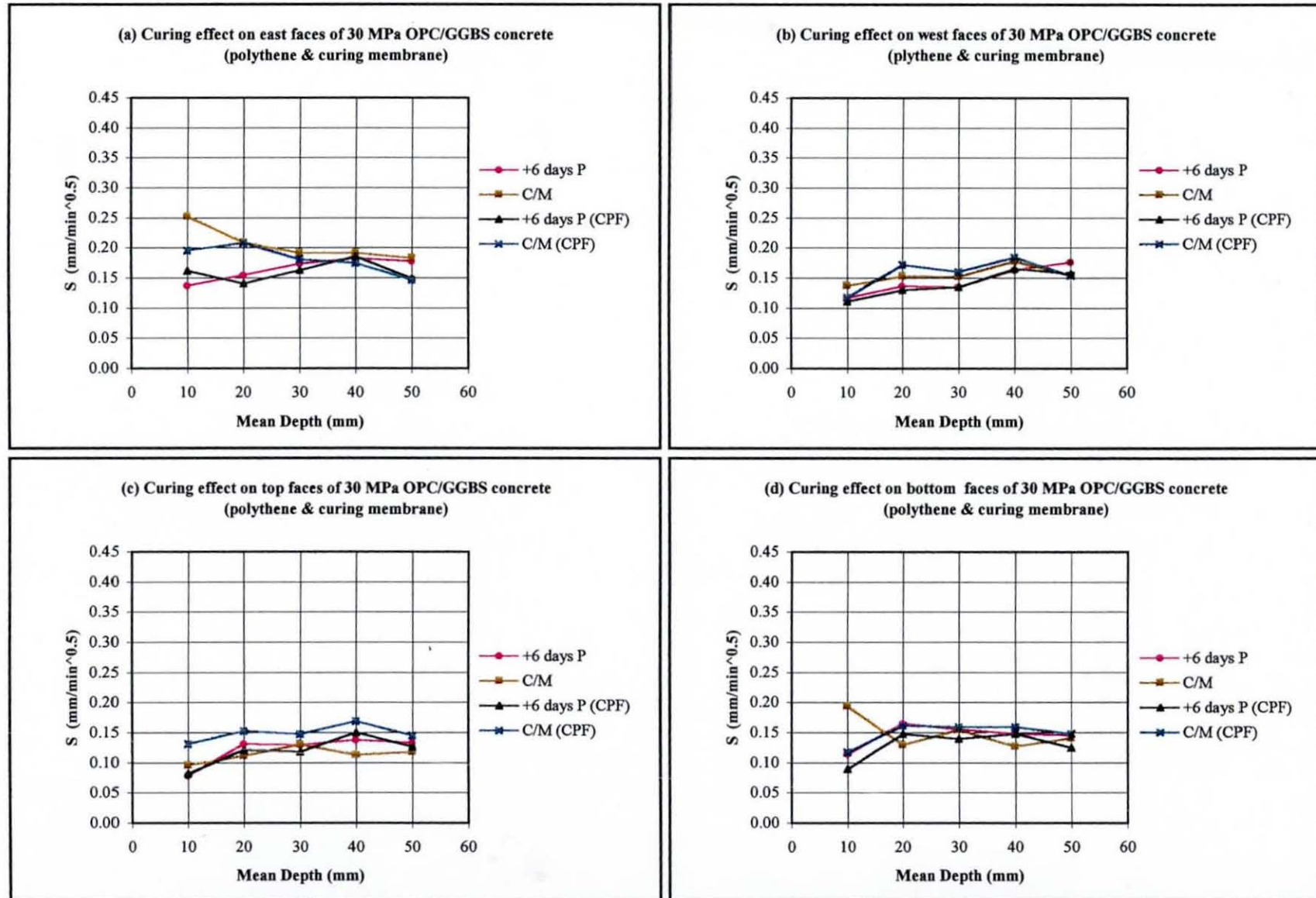


Fig. 6.35 Effect of curing and CPF on the sorptivity of 30 MPa OPC/GGBS concrete - 3 months summer series

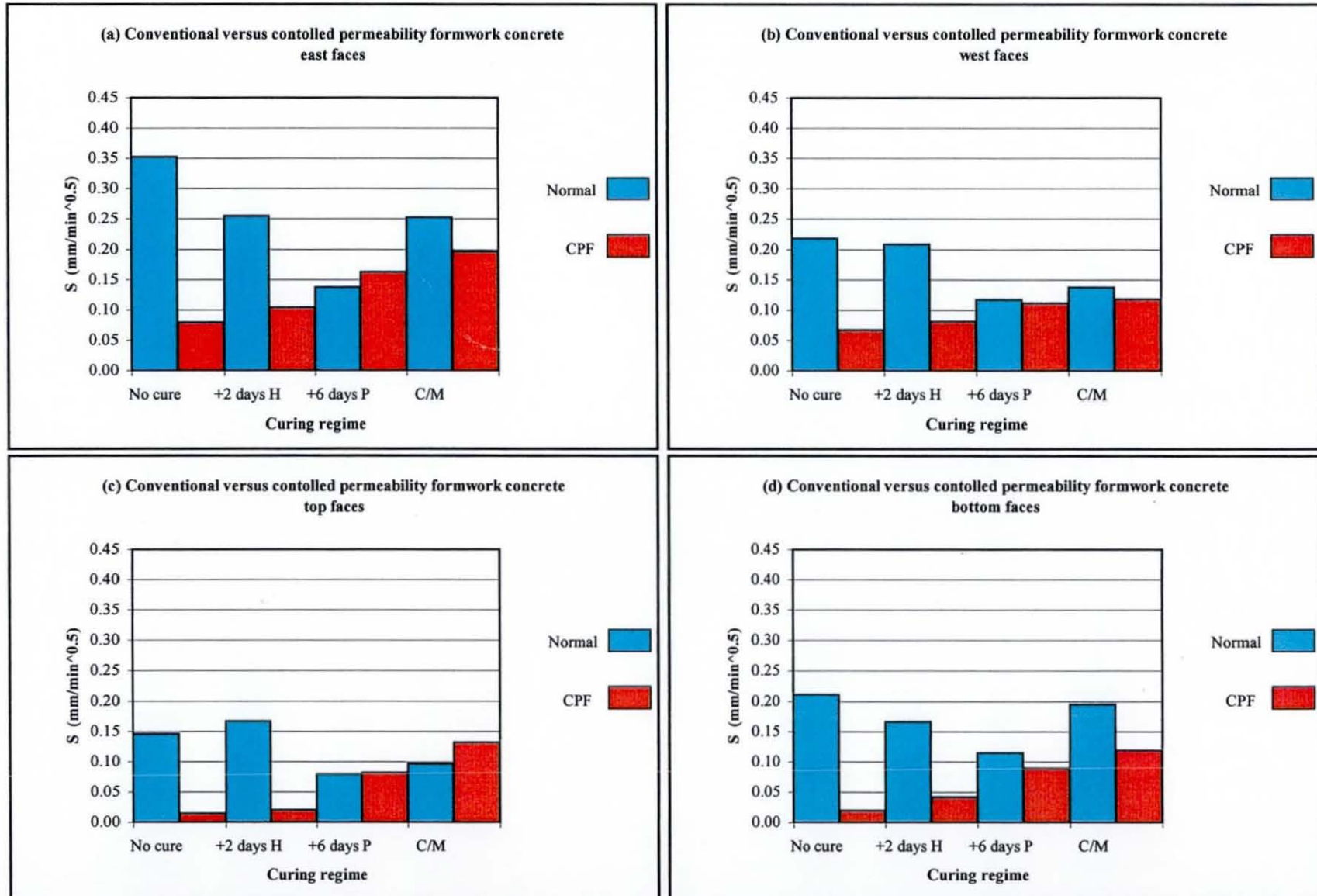


Fig. 6.36 Effect of curing and CPF on the sorptivity of 30 MPa OPC/GGBS concrete at surface (10 mm from surface) - 3 months summer series

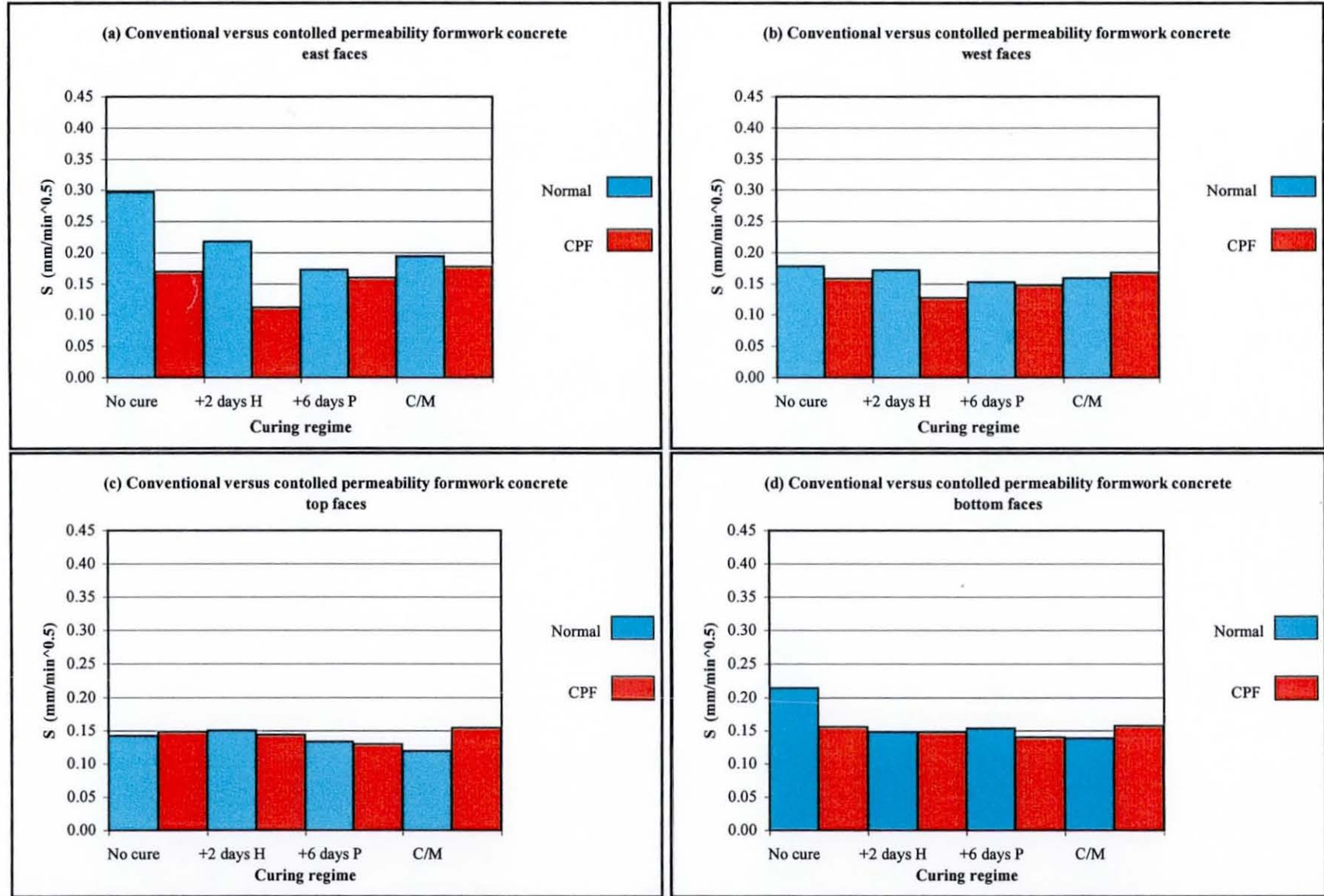


Fig. 6.37 Effect of curing and CPF on the sorptivity of 30 MPa OPC/GGBS concrete at subsurface (20-50mm from surface) - 3 months summer series

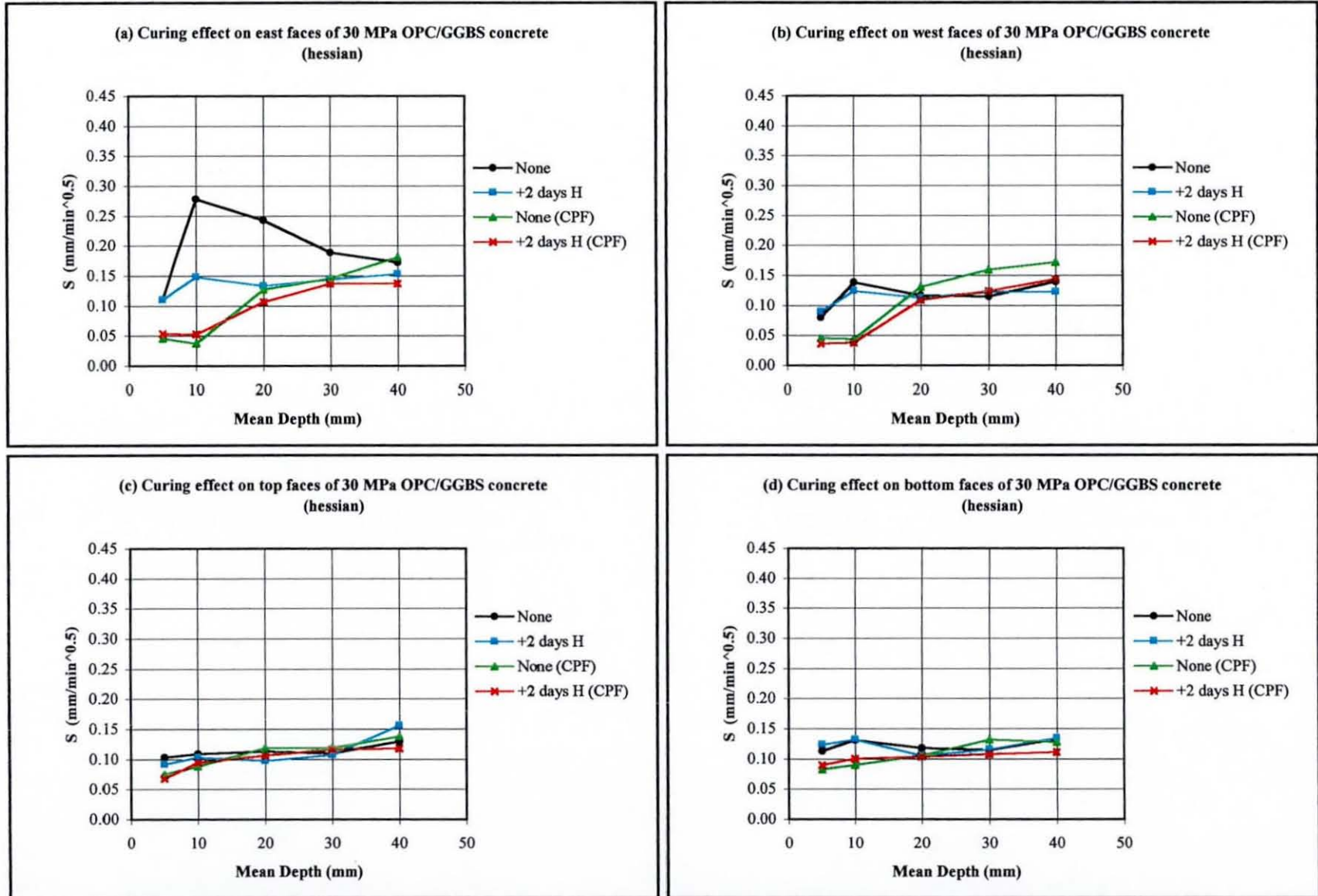


Fig. 6.38 Effect of curing and CPF on the sorptivity of 30 MPa OPC/GGBS concrete - 12 months summer series

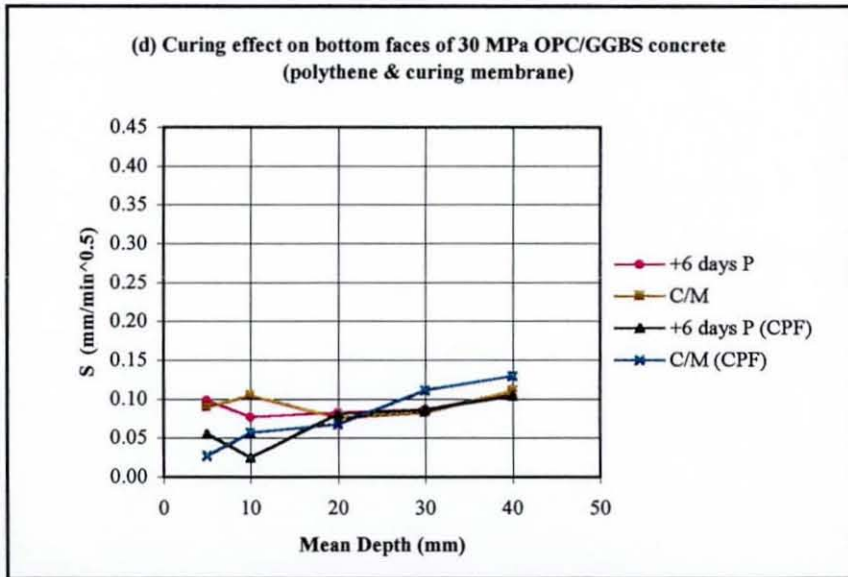
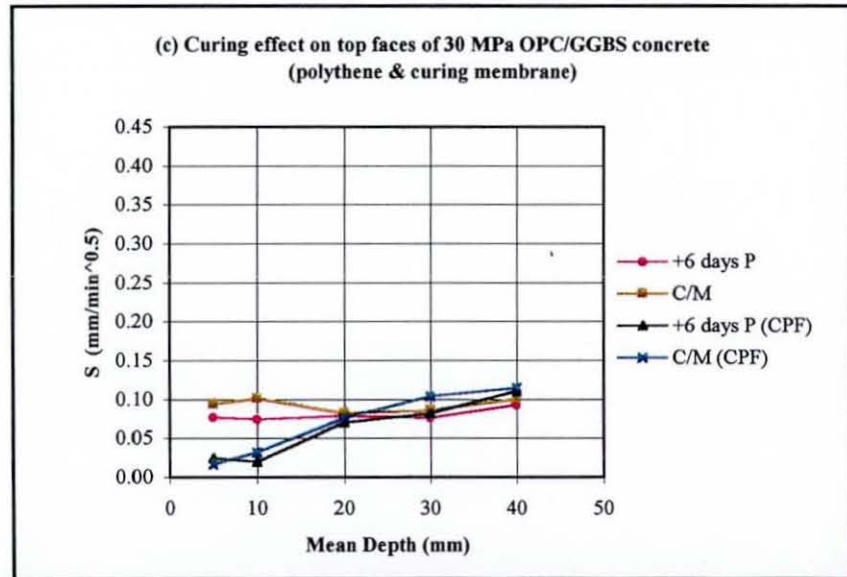
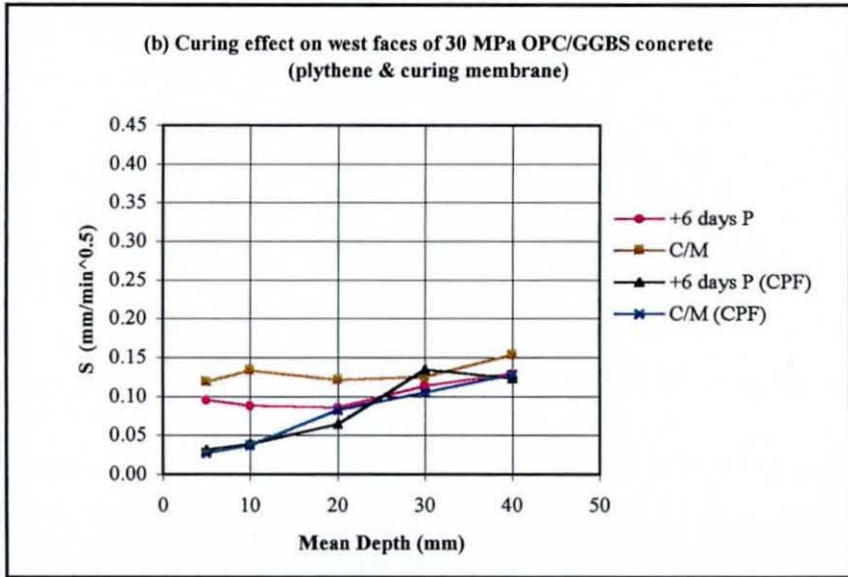
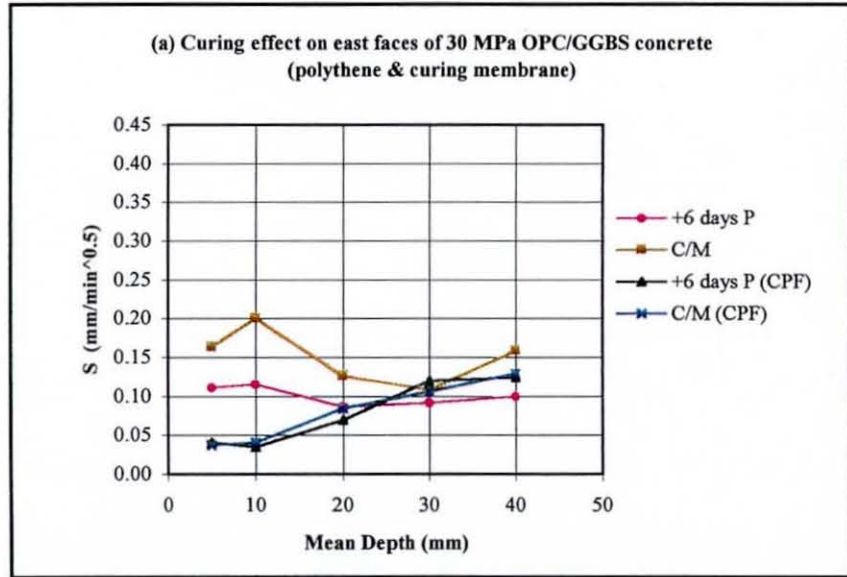


Fig. 6.39 Effect of curing and CPF on the sorptivity of 30 MPa OPC/GGBS concrete - 12 months summer series

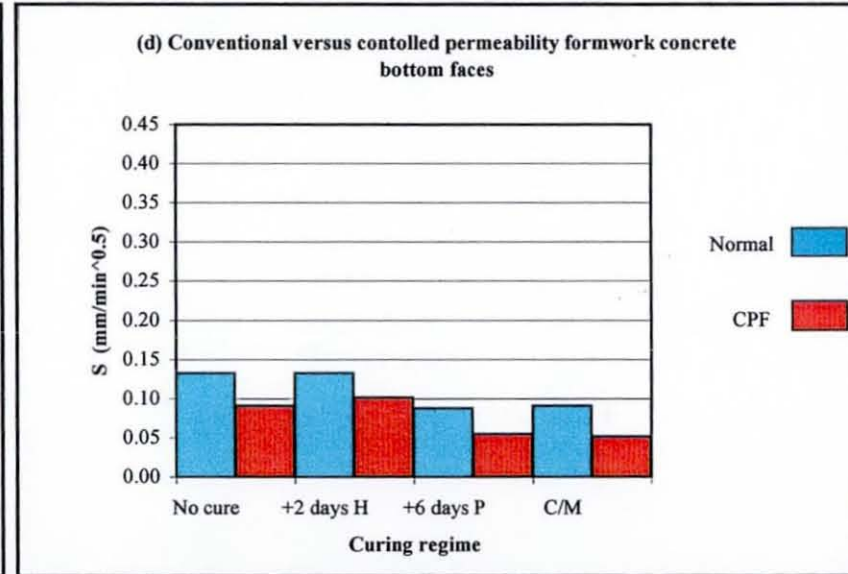
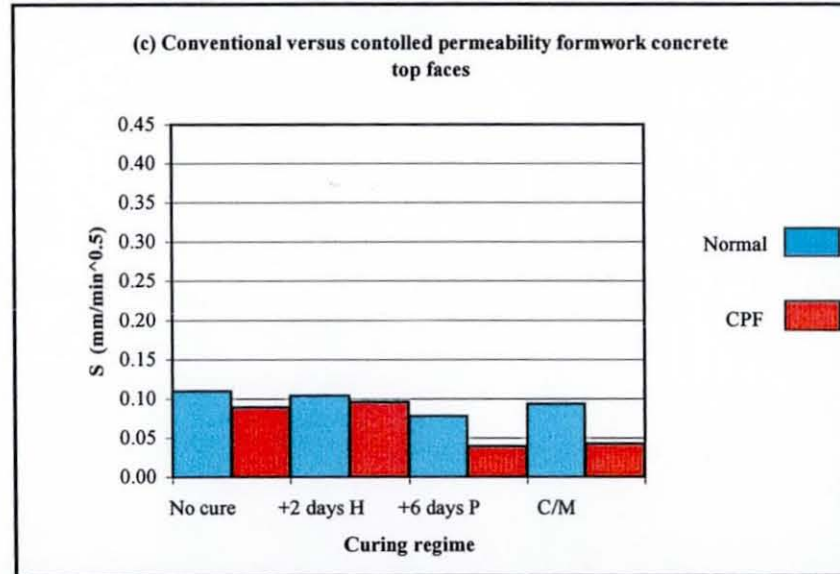
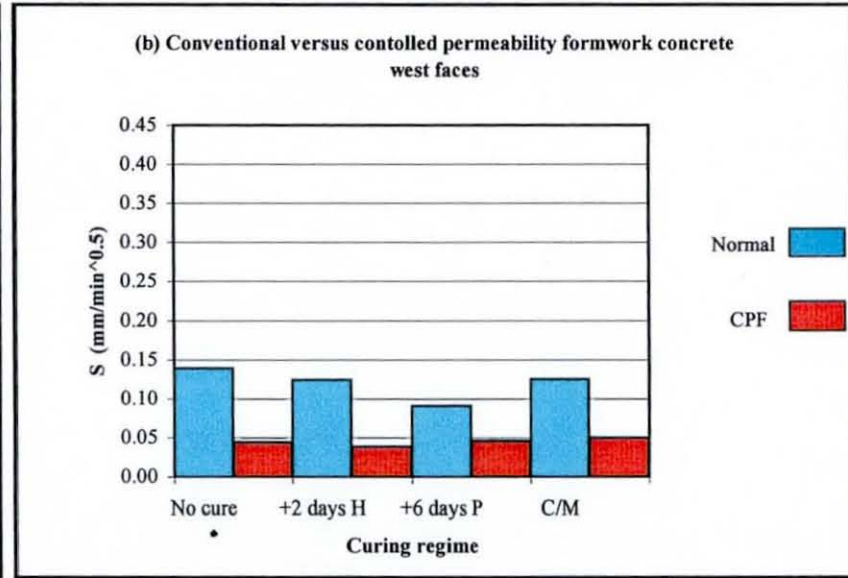
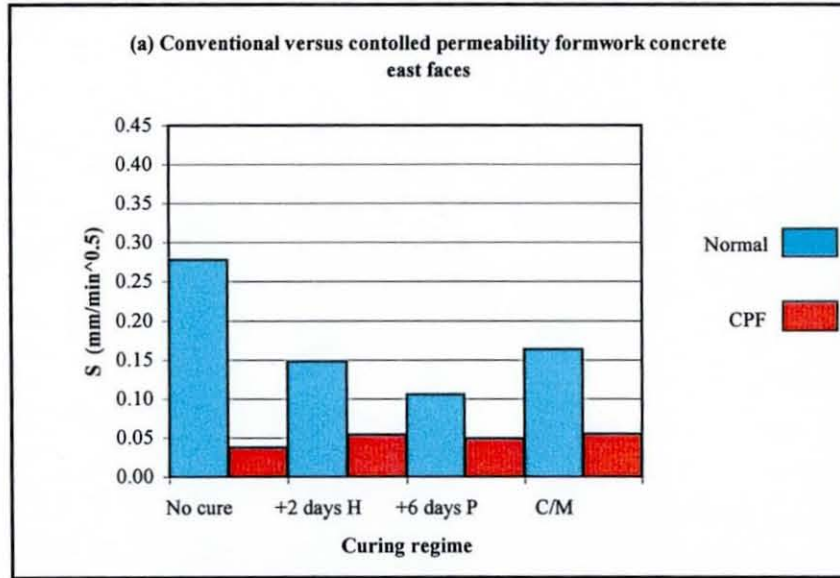


Fig. 6.40 Effect of curing and CPF on the sorptivity of 30 MPa OPC/GGBS concrete at surface (10mm from surface) - 12 months summer series

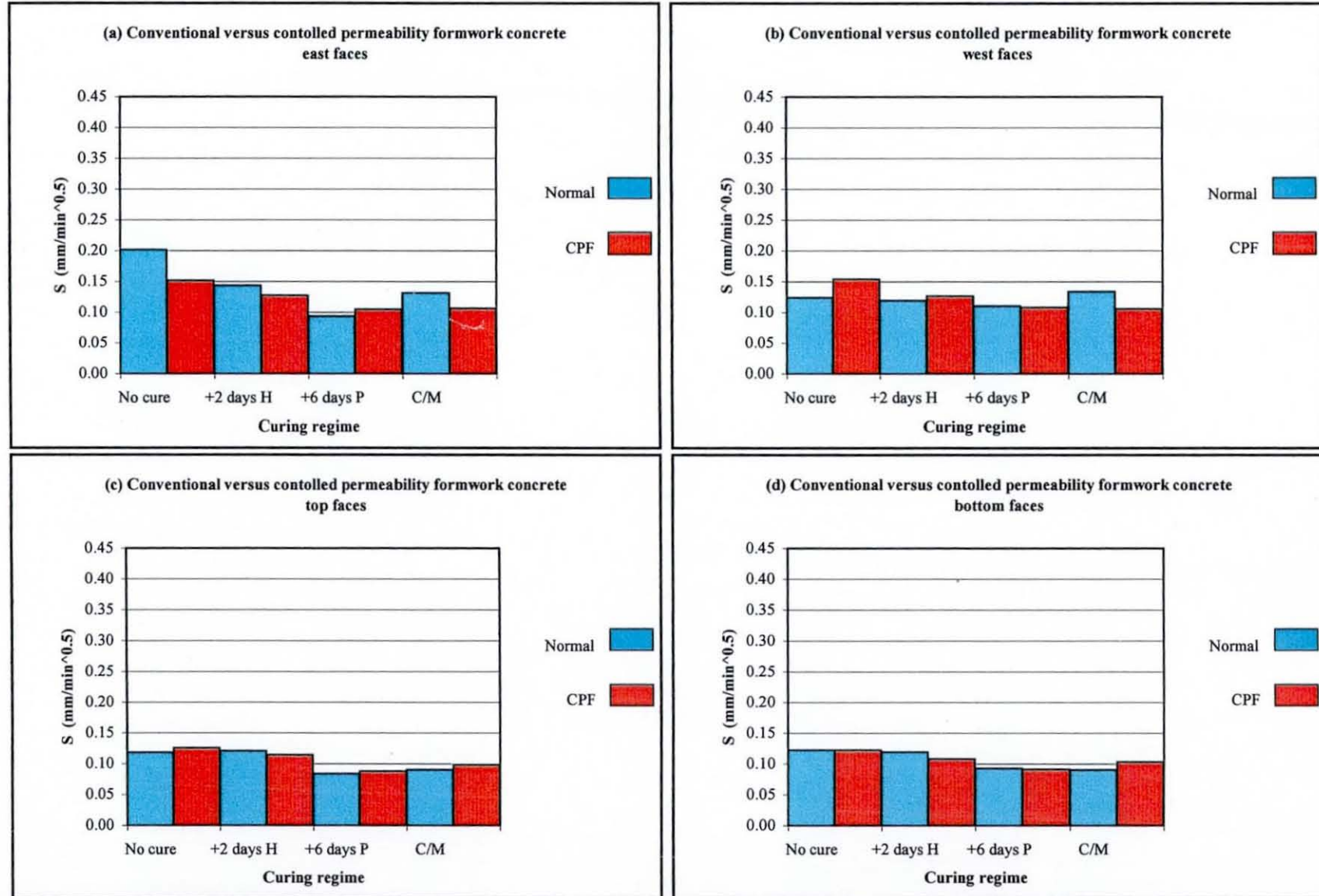


Fig. 6.41 Effect of curing and CPF on the sorptivity of 30 MPa OPC/GGBS concrete at subsurface (20-50mm from surface) - 12 months summer series

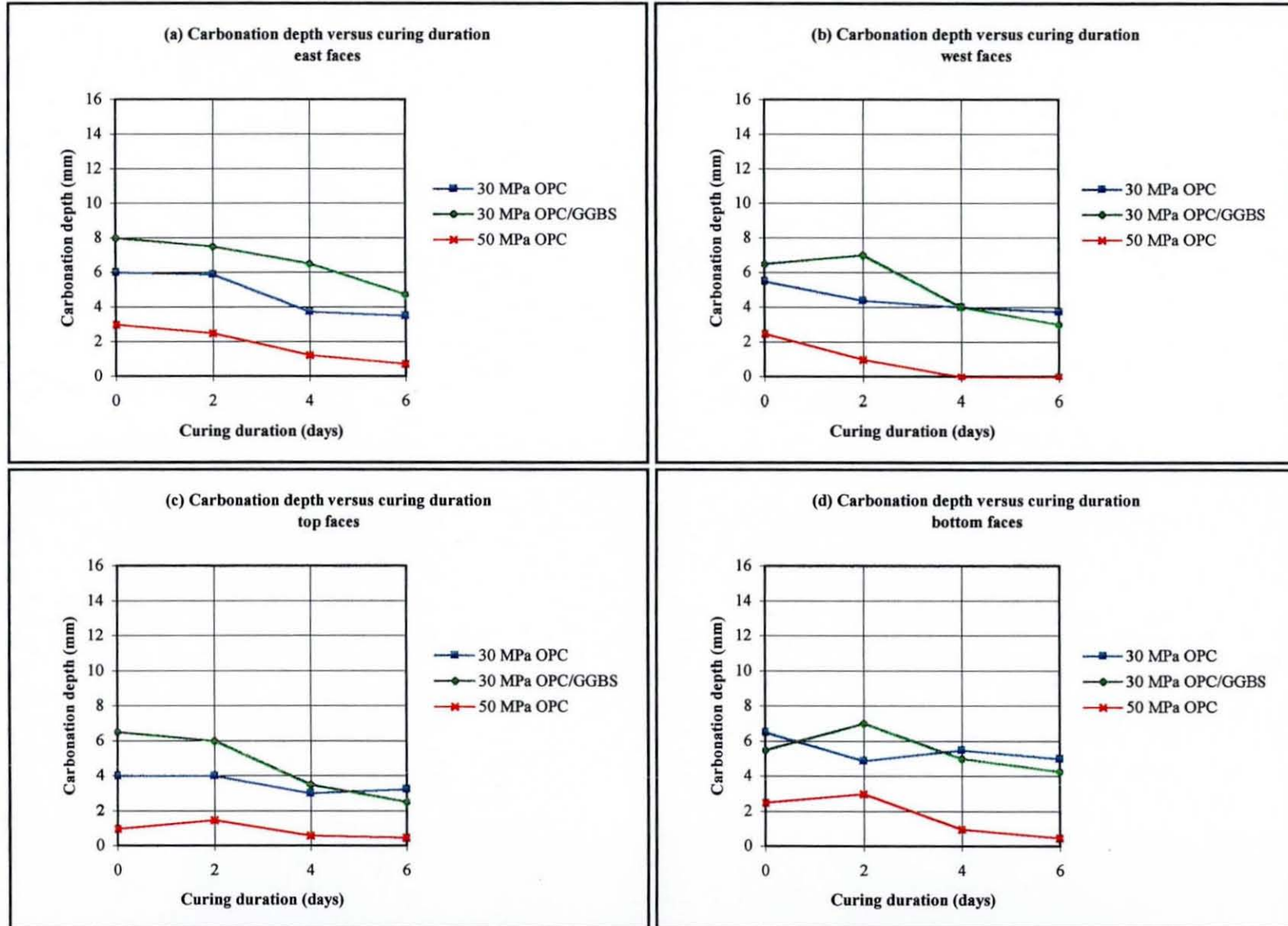


Fig. 6.42 Effect of microclimate, curing and concrete type on carbonation depth - 6 months summer series

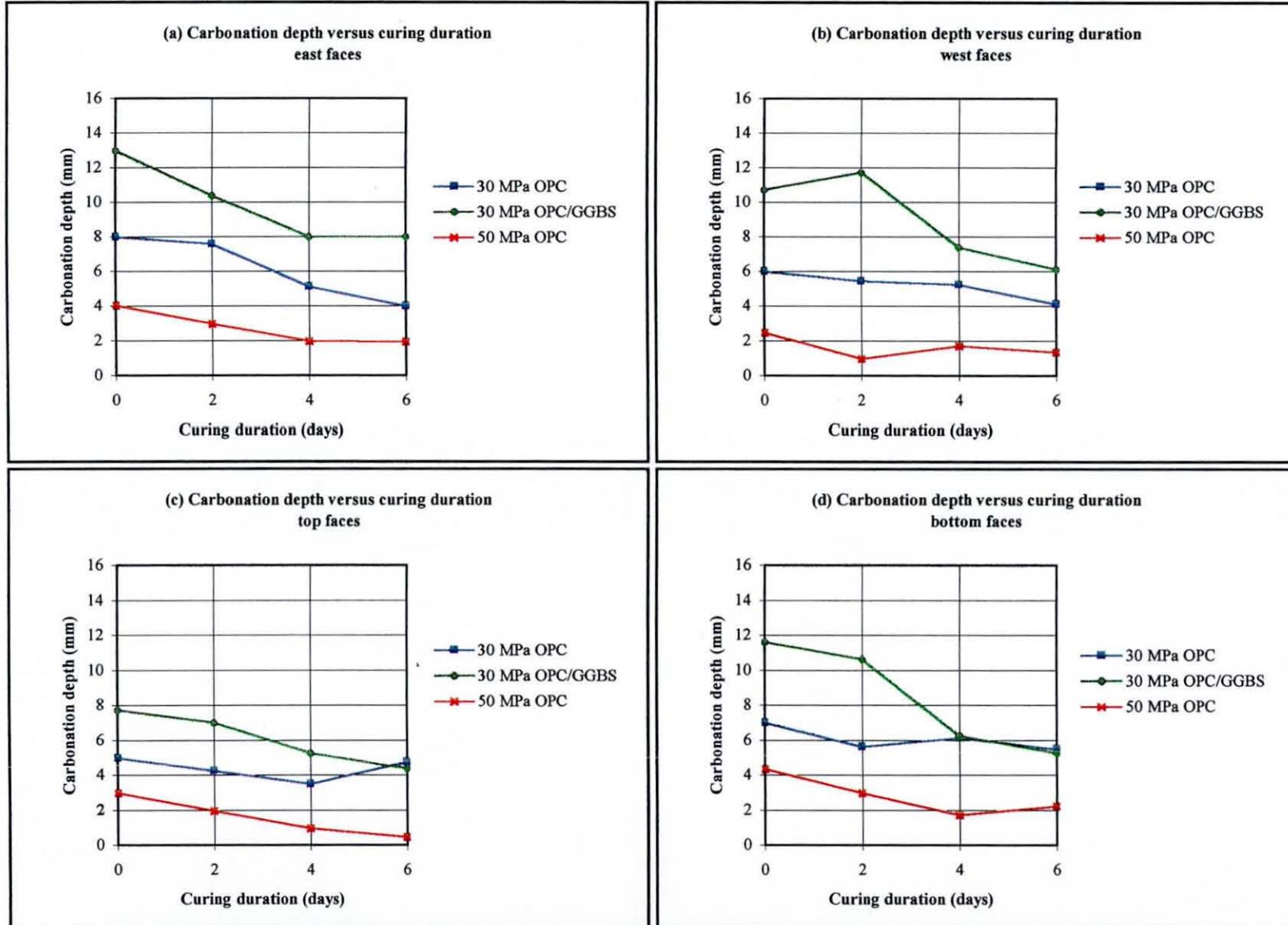


Fig. 6.43 Effect of microclimate, curing and concrete type on carbonation depth - 12 months summer series

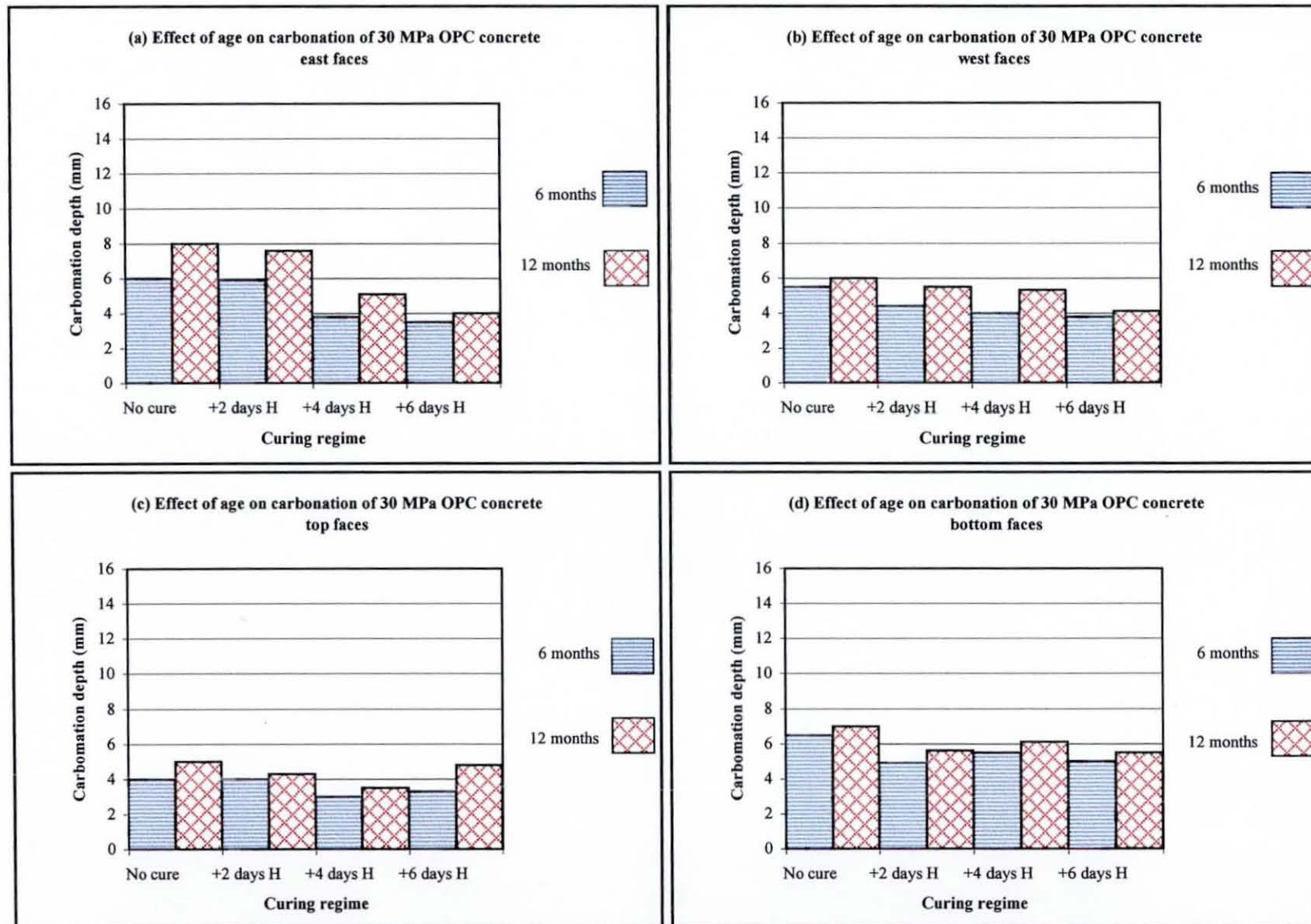


Fig. 6.44 Effect of age on carbonation depth of the 30 MPa OPC concrete - summer series

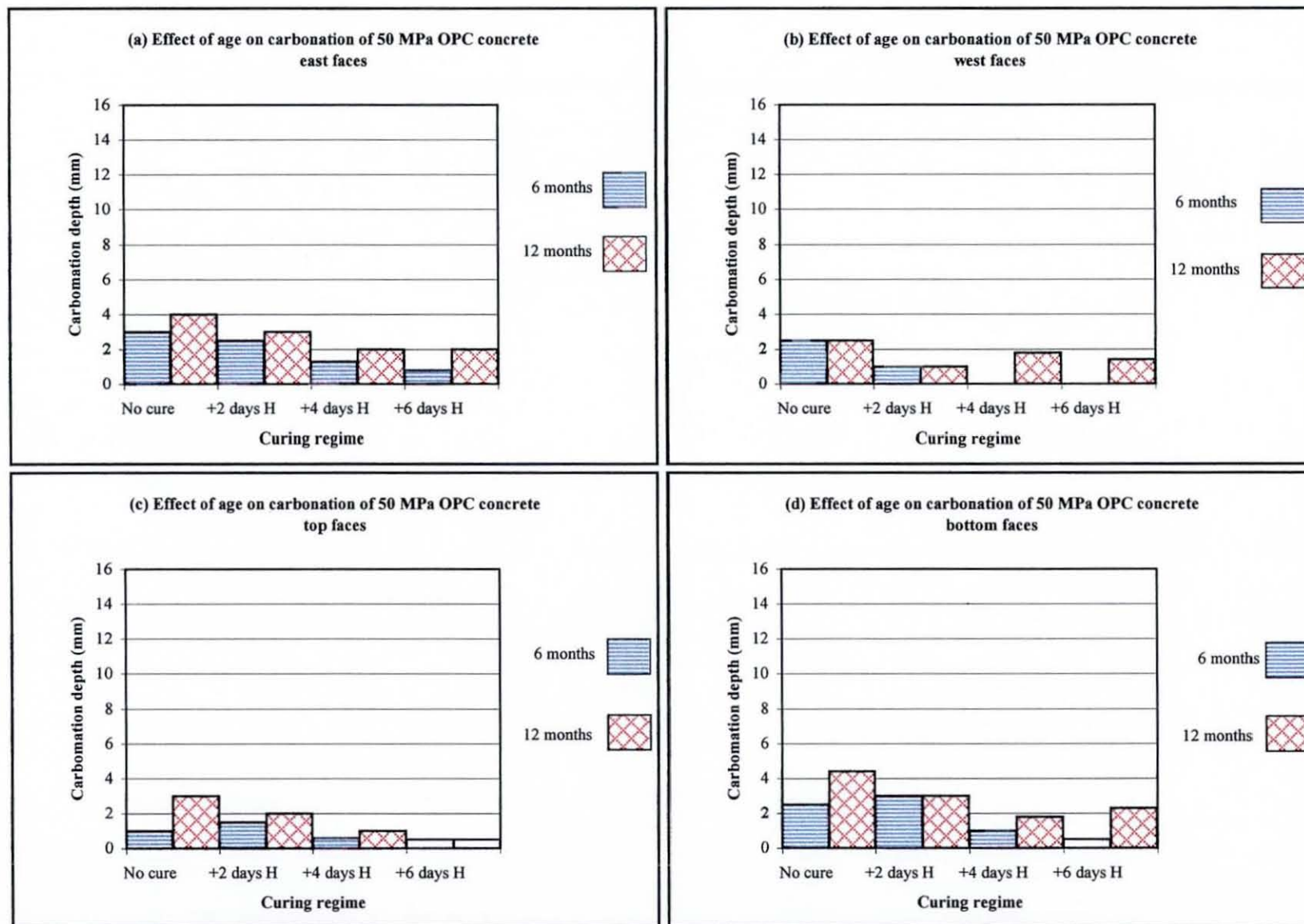


Fig. 6.45 Effect of age on carbonation depth of the 50 MPa OPC concrete - summer series

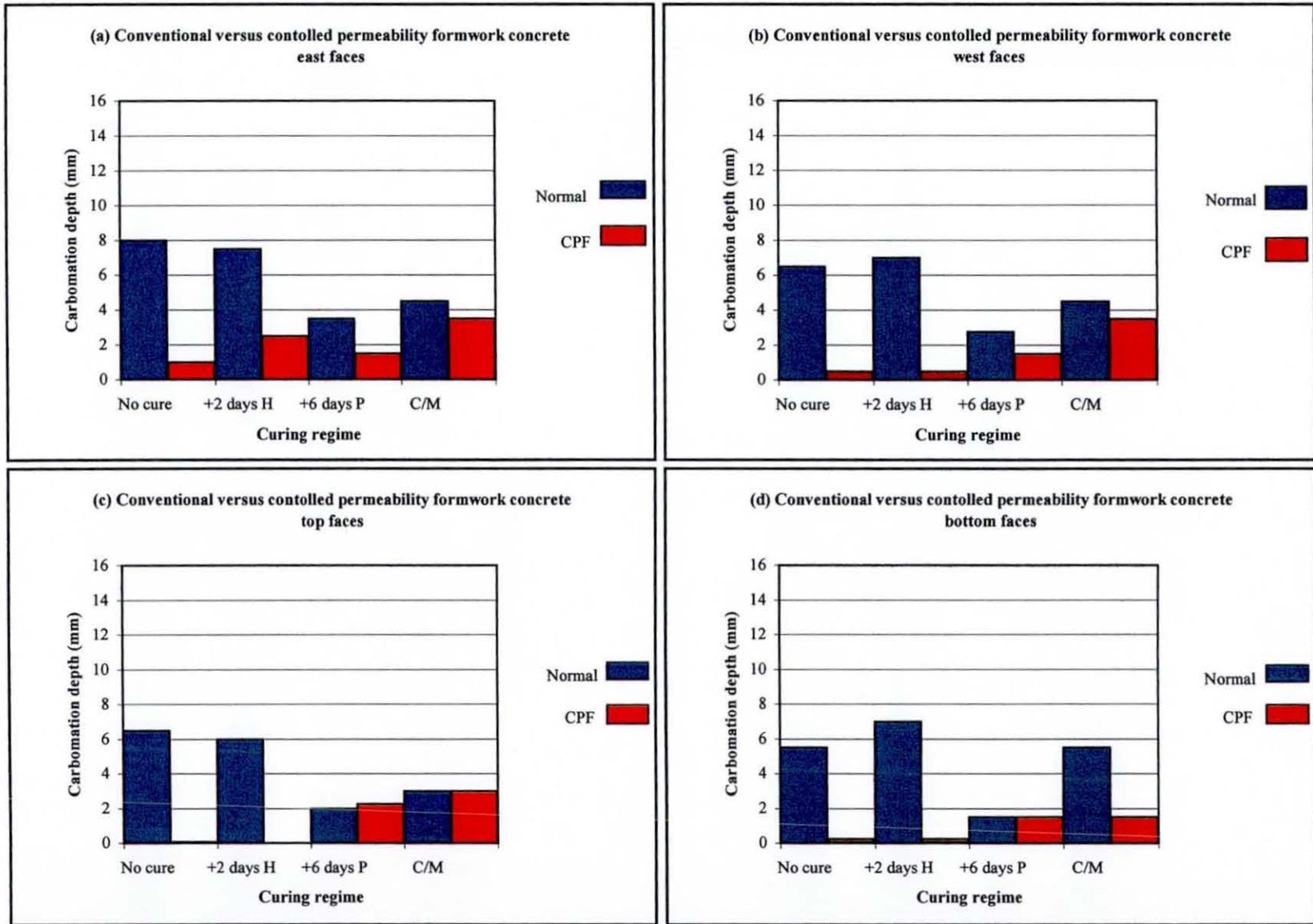


Fig. 6.46 Effect of curing regime and CPF on carbonation of the 30 MPa OPC/GGBS concrete - 6 months summer series

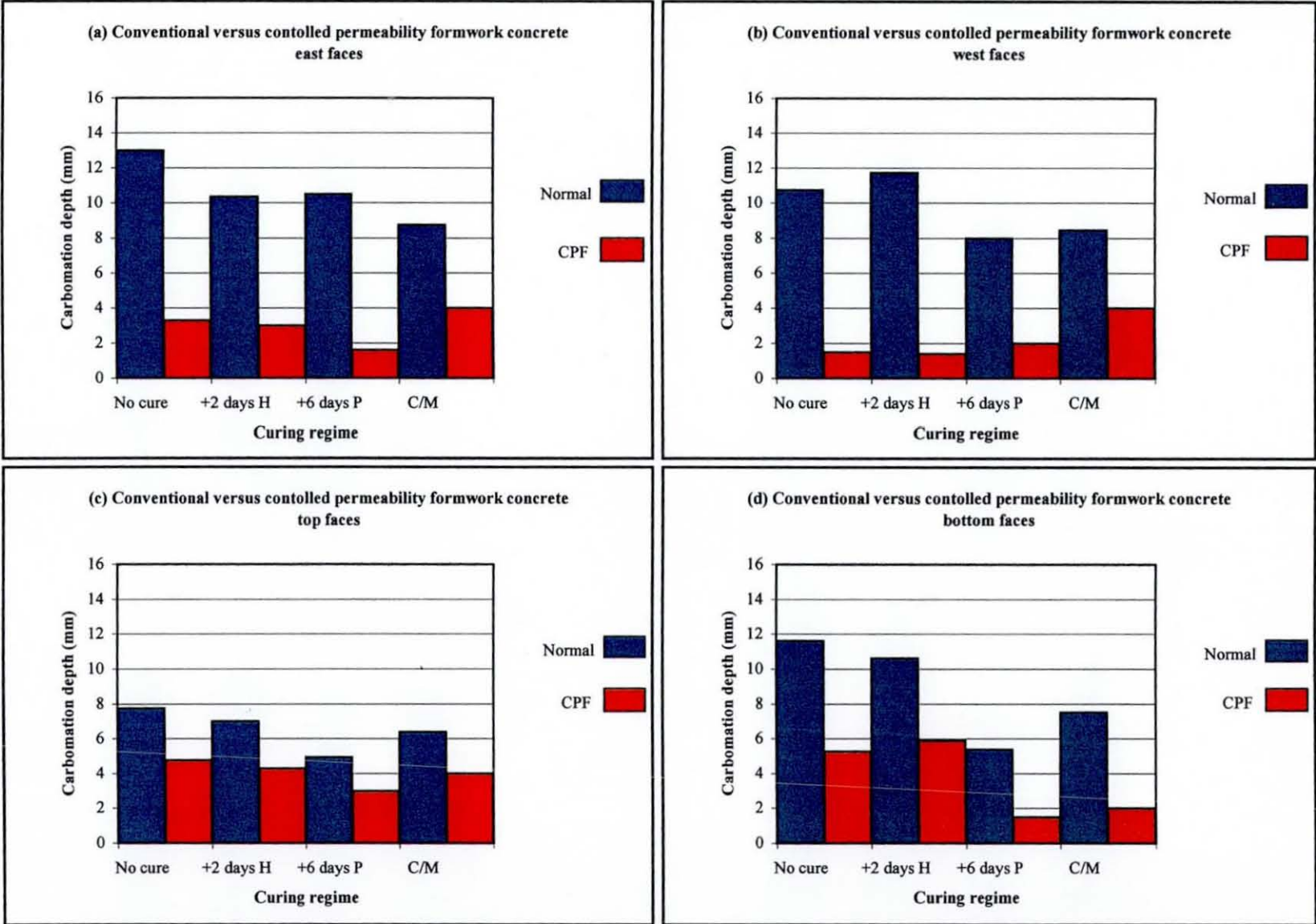


Fig. 6.47 Effect of curing regime and CPF on carbonation of the 30 MPa OPC/GGBS concrete - 12 months summer series

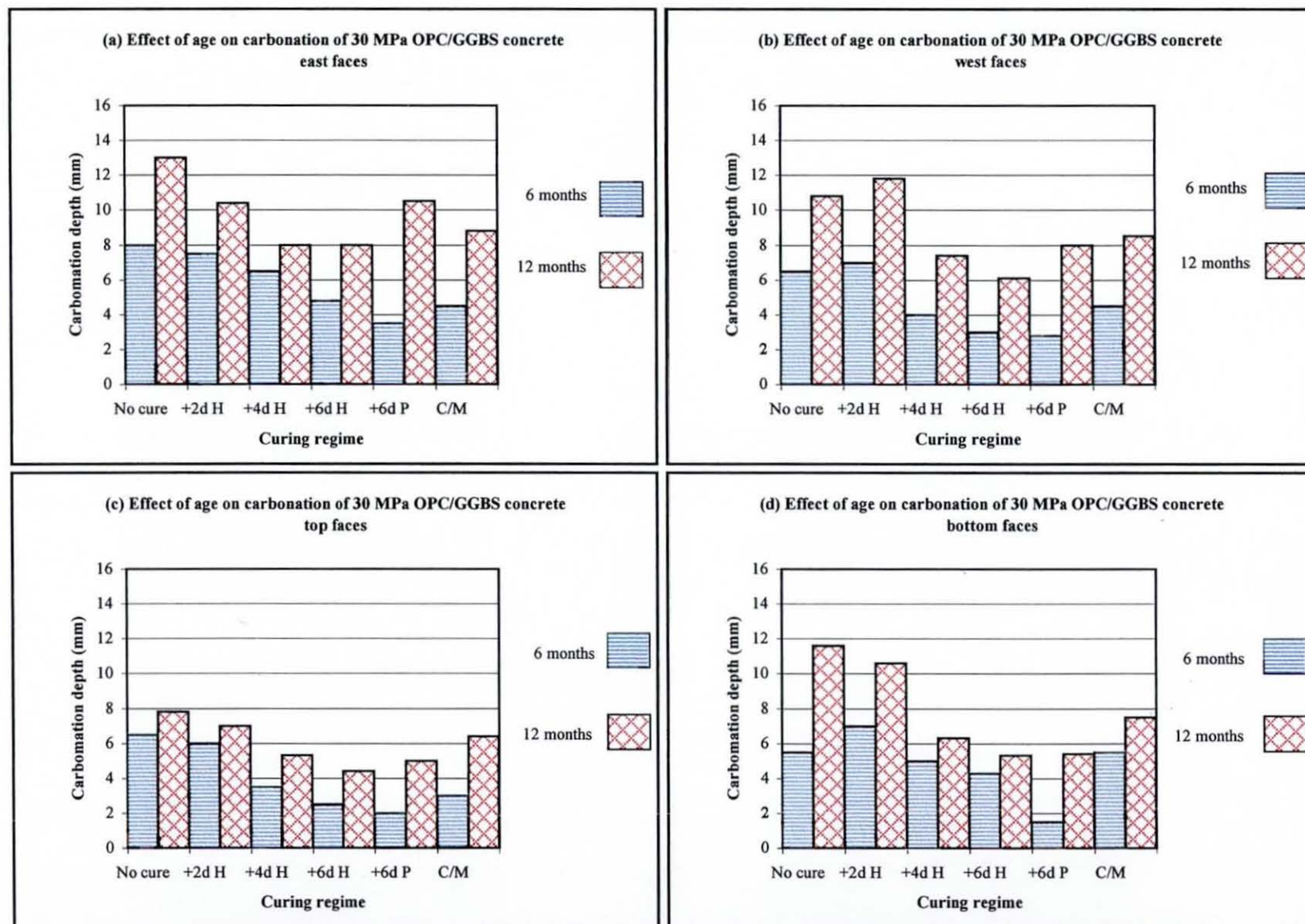


Fig. 6.48 Effect of age on carbonation depth of the 30 MPa OPC/GGBS concrete - summer series

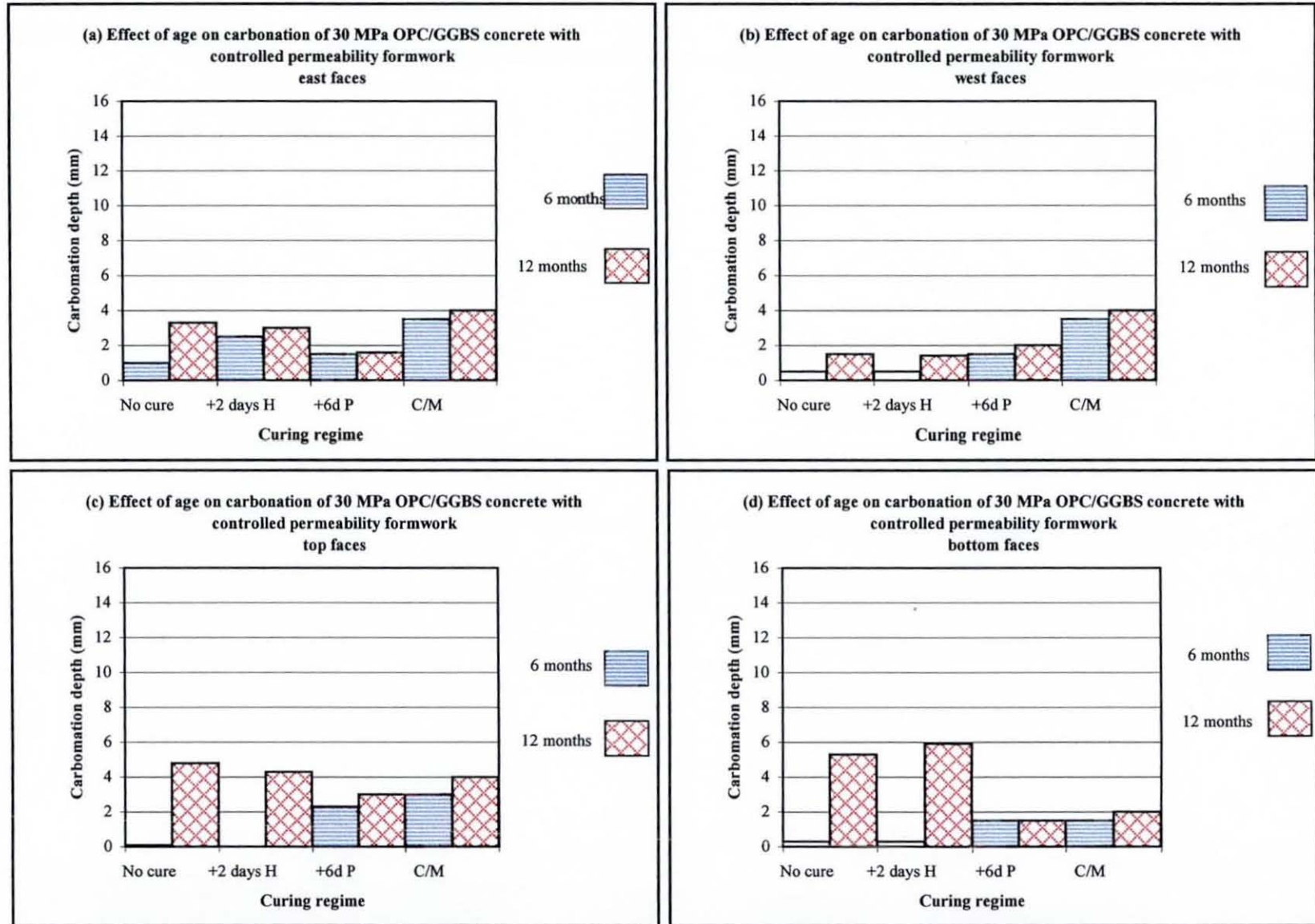


Fig. 6.49 Effect of age on carbonation depth of the CPF-produced, 30 MPa OPC/GGBS concrete - summer series

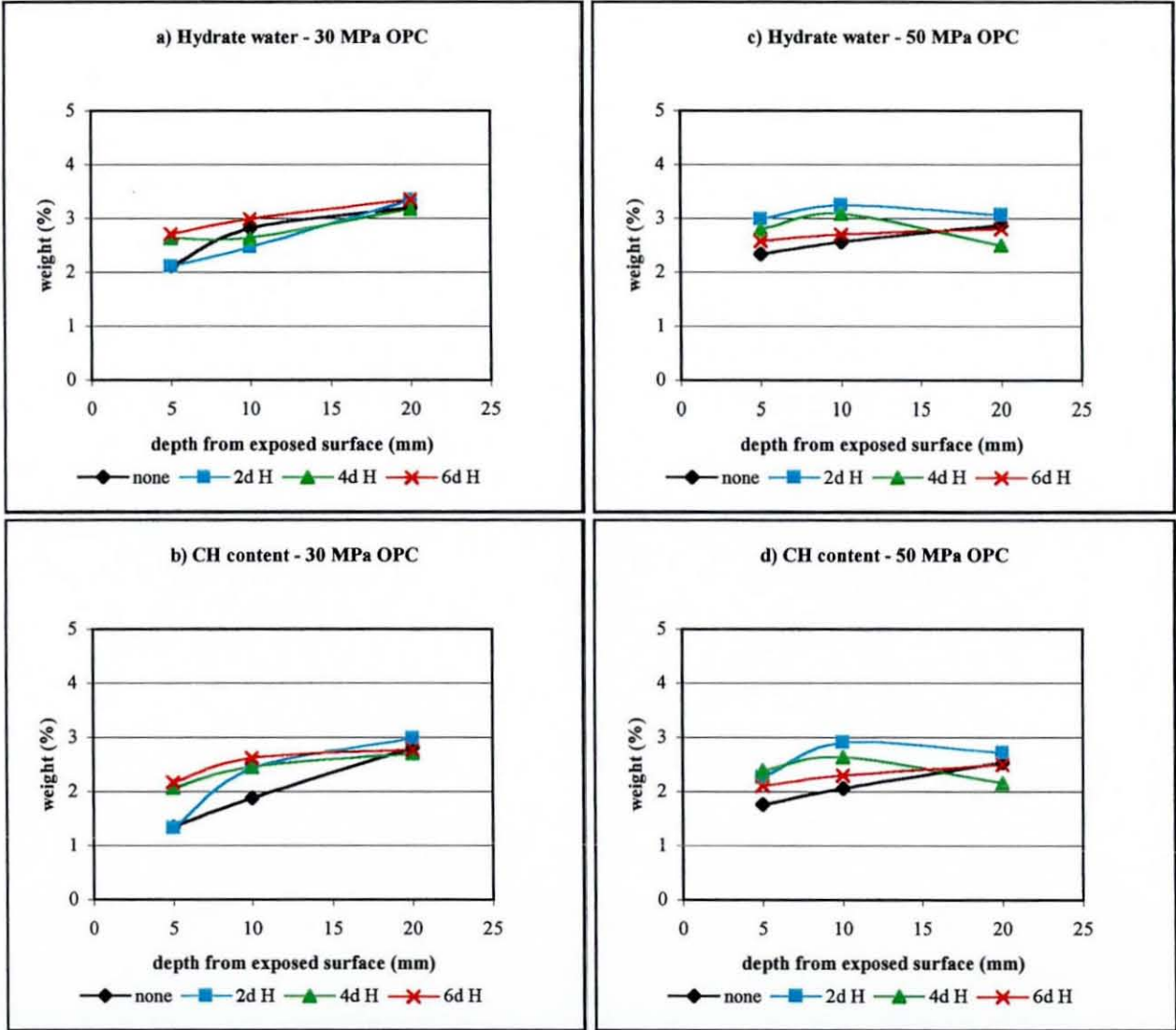


Fig. 6.50 Hydrate water and lime content profiles of the OPC concretes - 12 months summer (from Table R1.23)

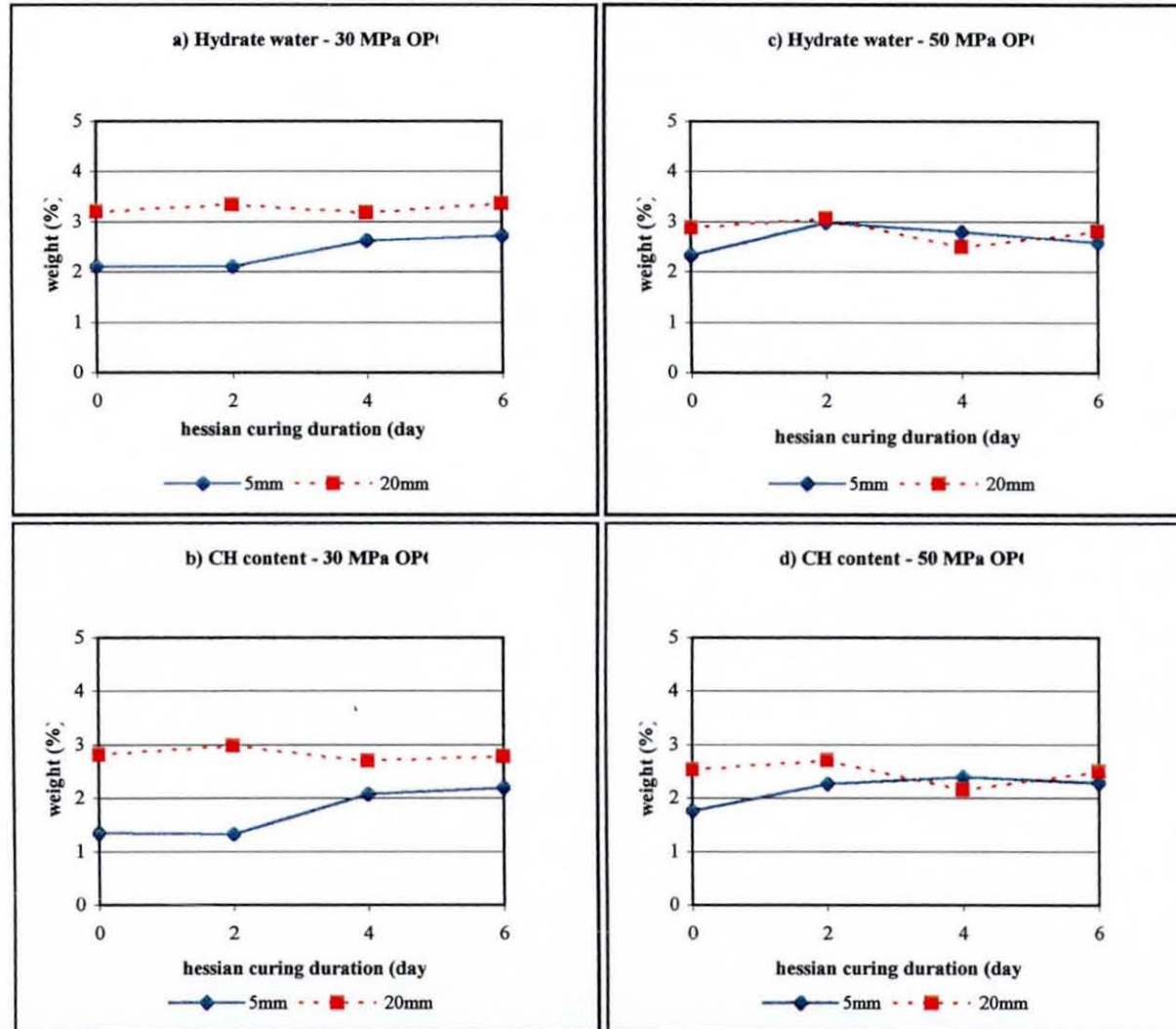


Fig. 6.51 Hydrate water and lime content at the surface (5mm) and subsurface (20mm) layers of concrete - 12 months summer (from Table B1.23)

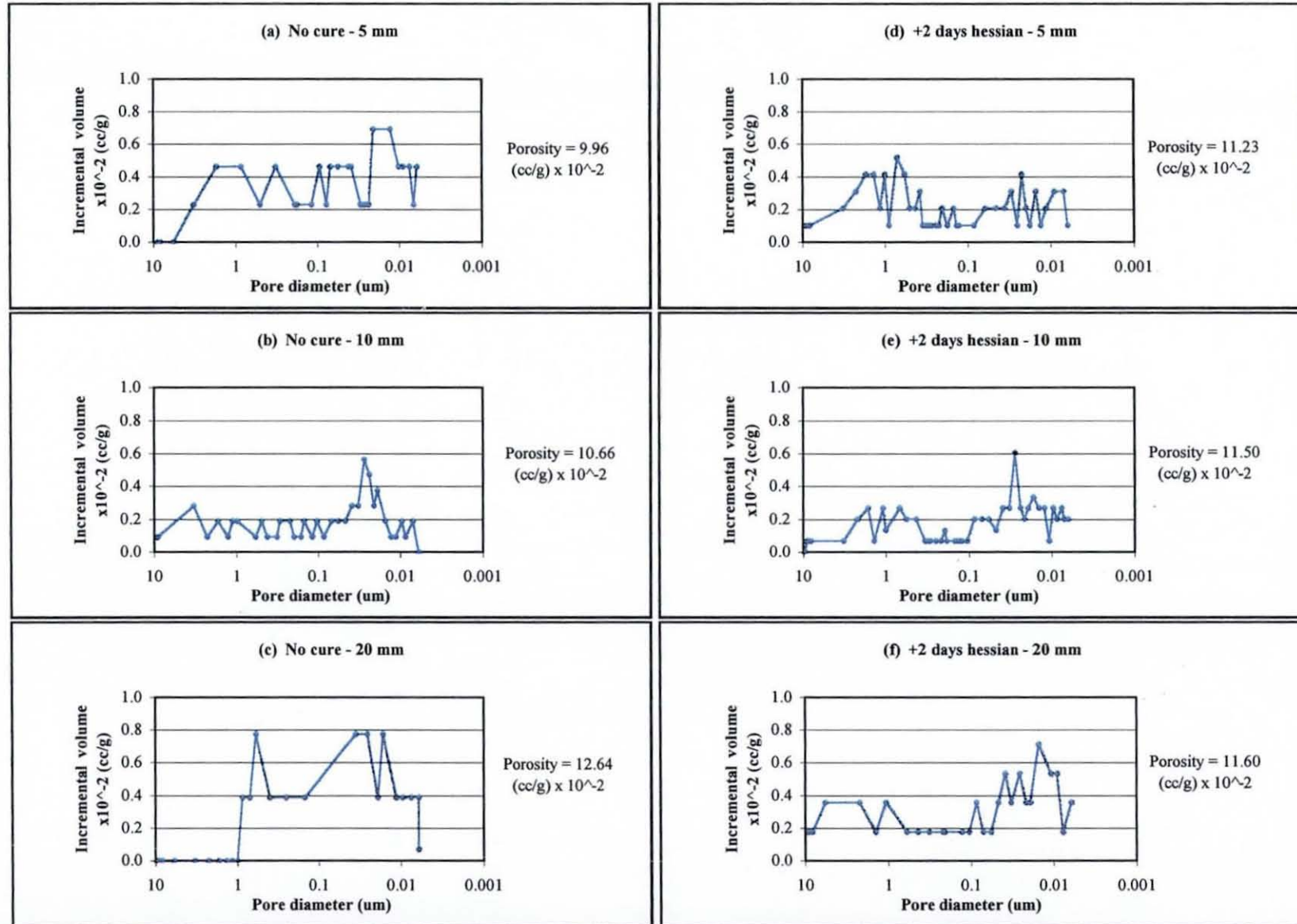


Fig. 6.52 Influence of curing on pore size distribution of 30 MPa OPC concrete at various depths from exposed surface - 17 months summer series

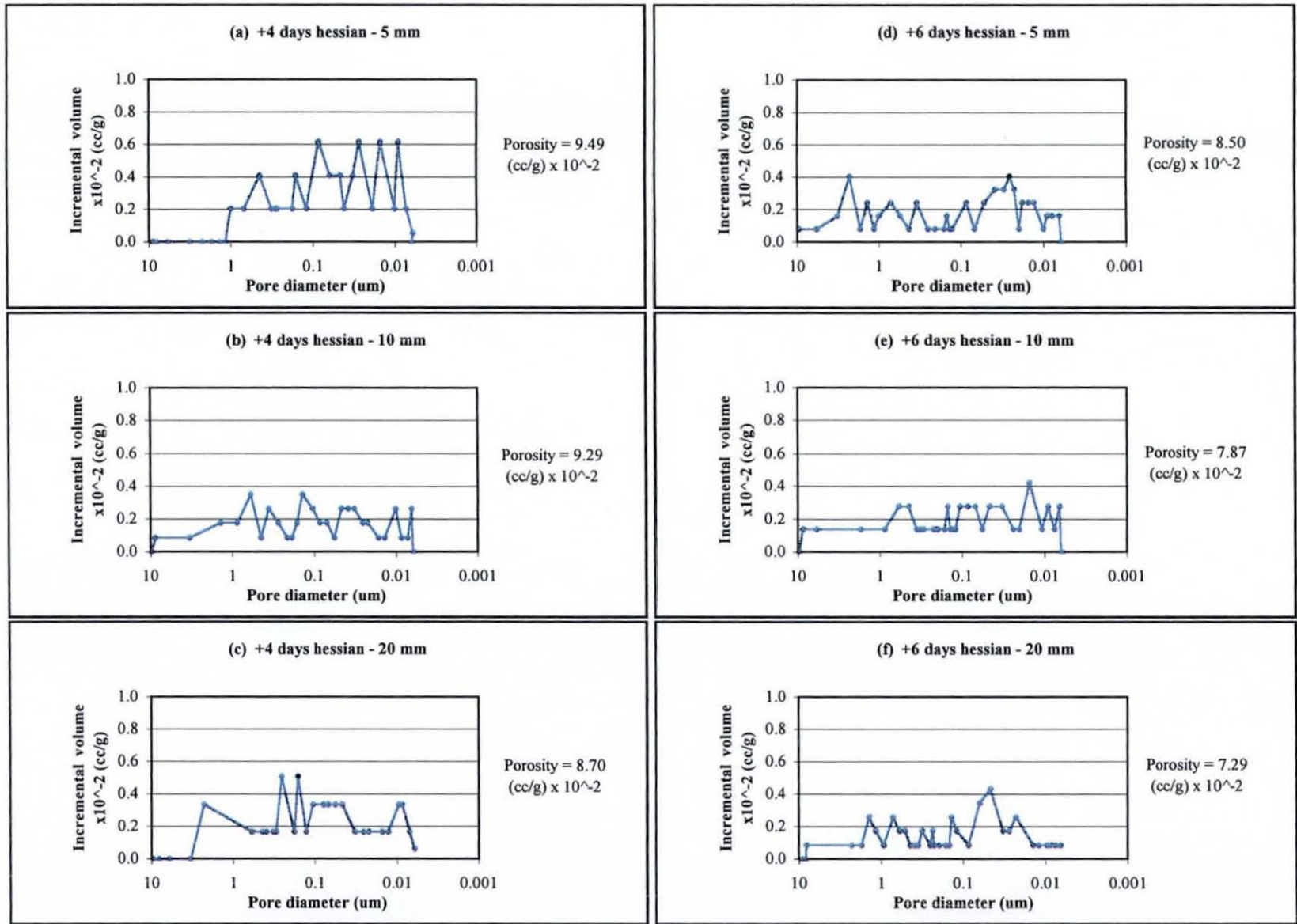


Fig. 6.53 Influence of curing on pore size distribution of 30 MPa OPC concrete at various depths from exposed surface - 12 months summer series

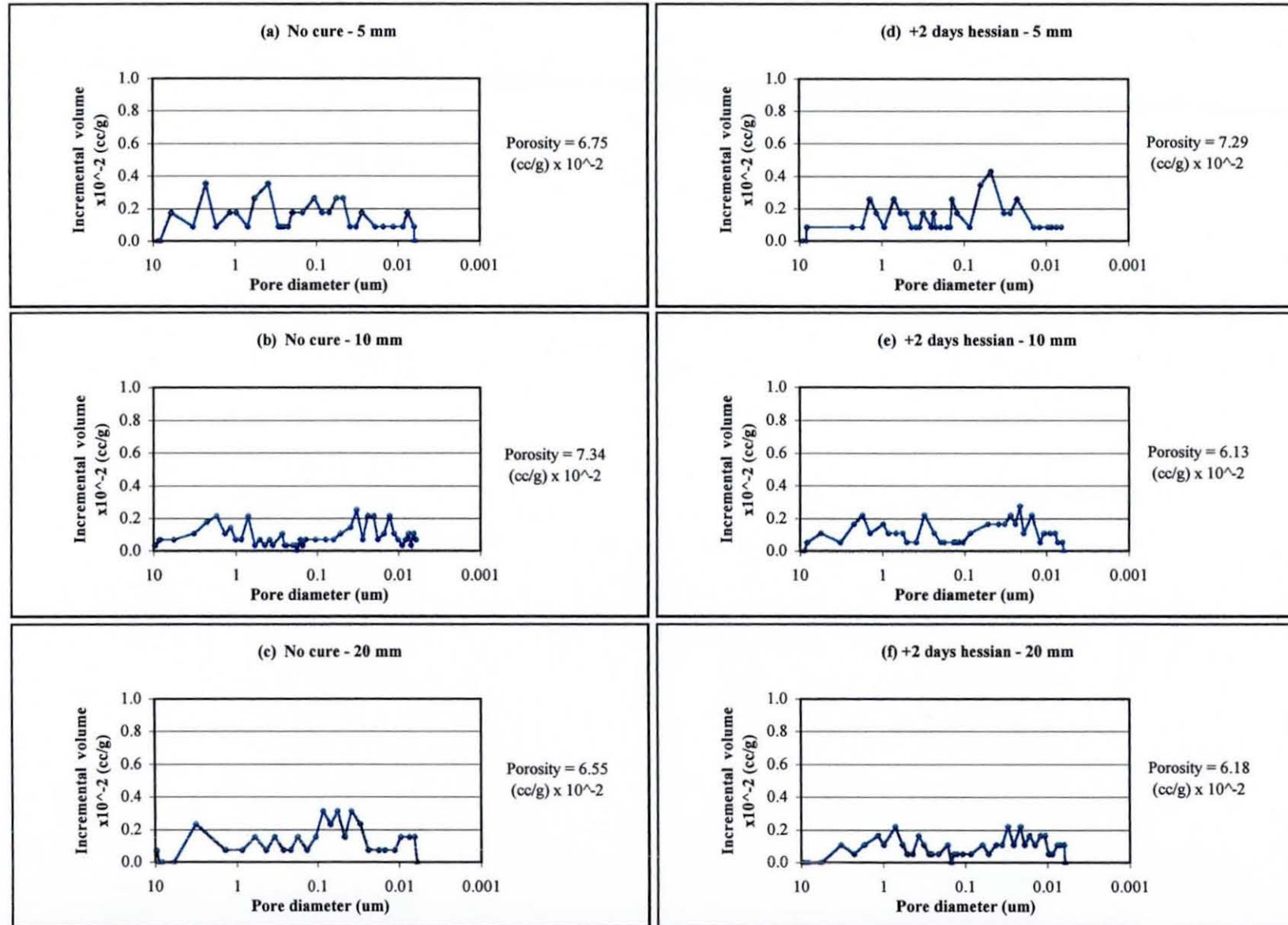


Fig. 6.54 Influence of curing on pore size distribution of 50 MPa OPC concrete at various depths from exposed surface - 12 months summer season

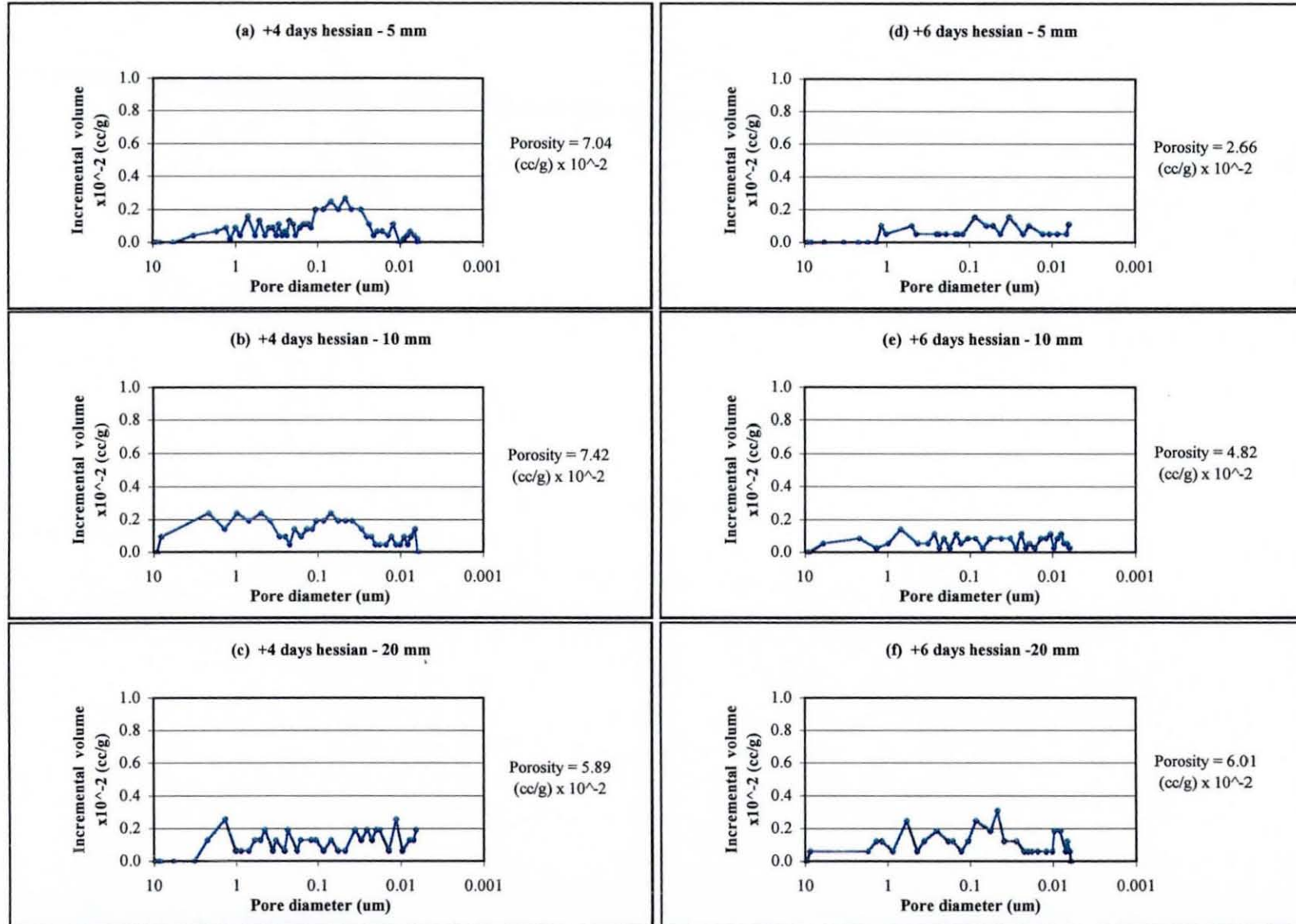


Fig. 6.55 Influence of curing on pore size distribution of 50 MPa OPC concrete at various depths from exposed surface - 12 months summer series

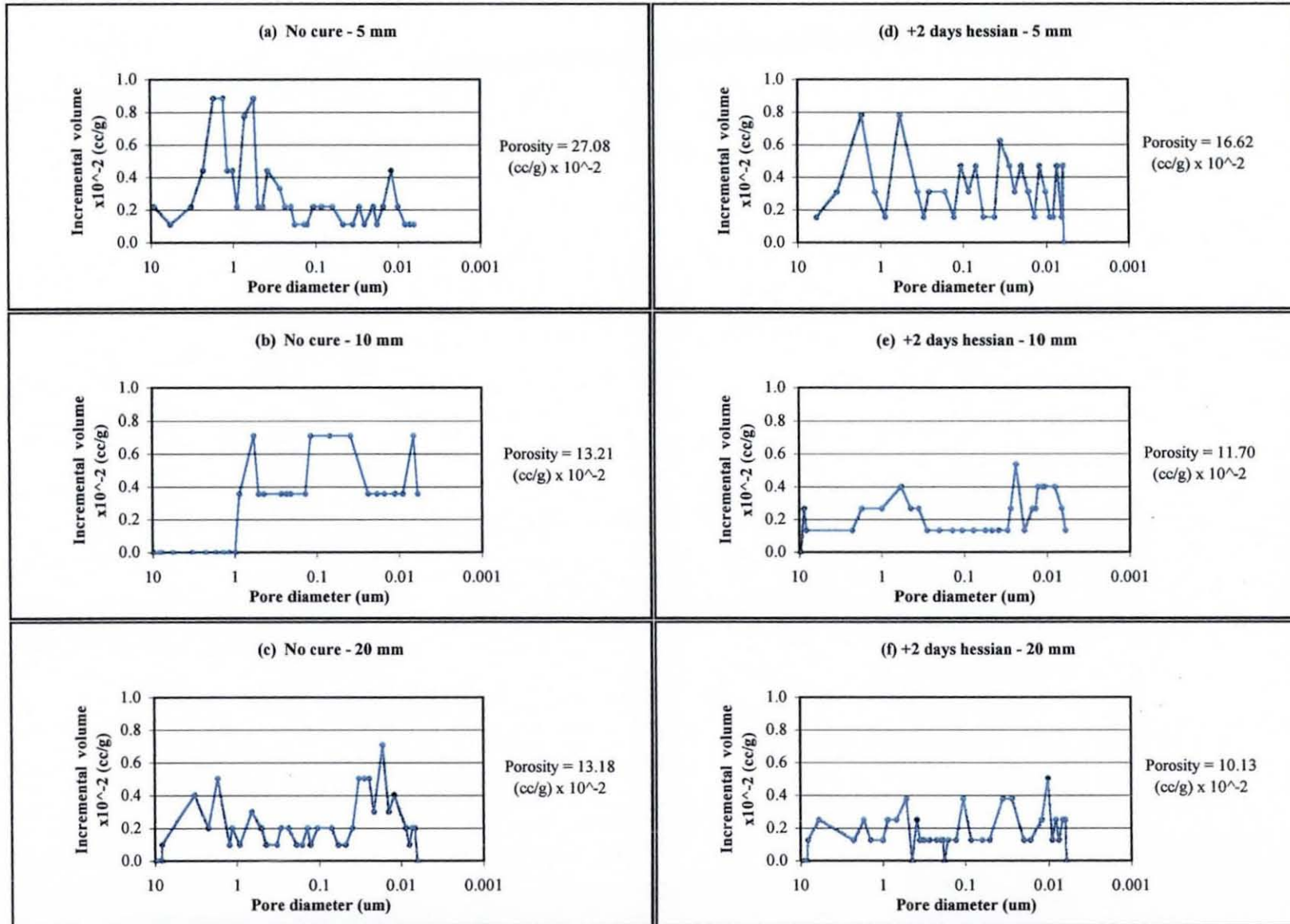


Fig. 6.56 Influence of curing on pore size distribution of 30 MPa OPC/GGBS concrete at various depths from exposed surface - 12 months summer series

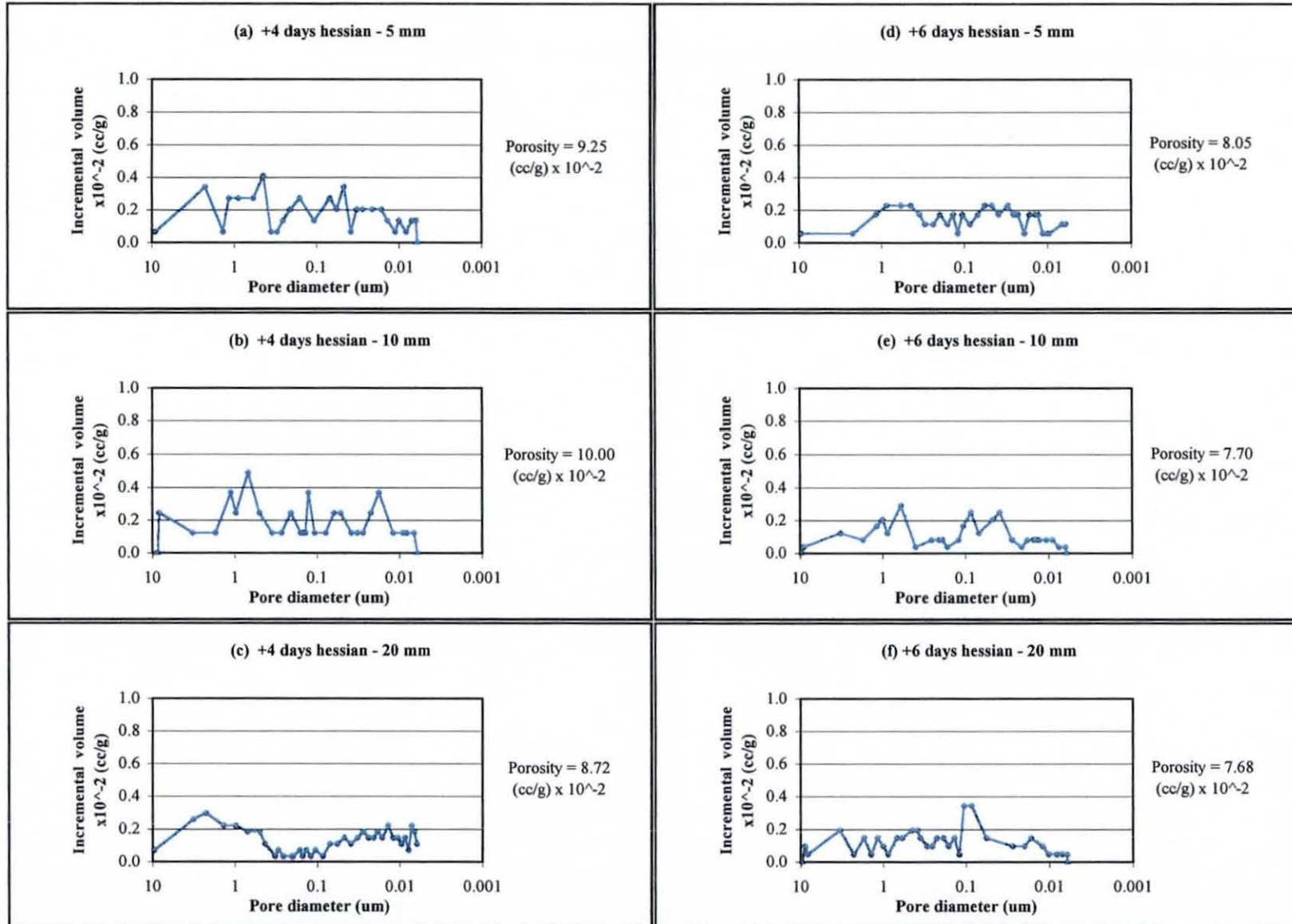


Fig. 6.57 Influence of curing on pore size distribution of 30 MPa OPC/GGBS concrete at various depths from exposed surface - 12 months summer series

## Chapter 7 Muscat Summer Climate

---

### 7.1 INTRODUCTION

The sorptivity test was performed on the two concrete mixes that constitute the Muscat series, the 30 MPa OPC and OPC/GGBS concretes, after 3 and 12 months of local site exposure. This chapter presents the results of the sorptivity tests of the two concretes as influenced by microclimate, curing methods and duration and exposure time. Along with the two Loughborough series, the results and trends of the Muscat series are discussed in detail in Chapter 8.

As previously reported, the Muscat series was air freighted from Loughborough immediately after the curing period (one week) to a suitable exposure site at Sultan Qaboos University (SQU) in Muscat. Due to resources and time constraints, a limited number of the concrete blocks (no slabs) could be transported to Muscat. Hence, two mixes instead of three were evaluated, with the microclimate effect assessed on either side of the vertical blocks (east/west). The same testing, sample preparation and conditioning procedures (Chapter 4) that were adopted at Loughborough were followed for the Muscat tests.

### 7.2 WEATHER DATA

Figures 7.1 and 7.2 and Tables 7.1 and 7.2 give the mean and extreme monthly temperatures and relative humidity, and the prevailing wind direction during 1996 and 1997 respectively.

The average temperature and relative humidity during the curing week of the concretes at Loughborough was 16.8 °C and 67% respectively. The mean temperature during the first 3 months of exposure, August, September and October in Muscat was 35, 34 and 33 °C respectively. The temperature extremes (max-min) during these months were 42-25, 40-22 and 37.5-16.6 °C (see Table 7.1 and Figure 7.1). The mean relative humidity during the 3 months was 87, 86 and 74%, whereas the extreme max and minimum were 95-24, 94-25 and 89-4%. The prevailing wind direction during the initial curing period at Loughborough was northerly and north easterly during the first 3 months of exposure in Muscat. The weather data during for the full exposure year (August 1996-1997) is shown in Tables 7.1 and 7.2.

### 7.3 COMPRESSIVE STRENGTH

The compressive strength test results of the Muscat series are given in Table 7.3 below. The coefficients of variation between nominally identical samples for the two mixes were within 10%.

**Table 7.3** Compressive strength results

Concrete mix	Design strength (MPa)	Actual strength (MPa)
OPC	30	29-34
OPC/GGBS	30	28-32

### 7.4 SORPTIVITY

#### 7.4.1 Introduction

The water sorptivity was calculated as described before in Chapter 5, Section 5.4.1. As with the two Loughborough series, the sorptivity plot conformed well to equation (4.11), the best-fit lines being linear with correlation coefficients  $r \approx 0.99$  in all cases. Representative sorptivity plots from a

selection of samples and their duplicates (reproducibility samples), showing the sorptivity and intercept indices, are given in Appendix C, Figures C1.1 to C1.8.

At the age of 3 months, the sorptivity indices of the east and west faces of the OPC and OPC/GGBS concretes were consistently higher at the surface than subsurface. It is interesting to note, however, that the curing affected zone (CAZ) for the Muscat concretes was notably larger than that of the two Loughborough concrete series. Generally, the sorptivity decreased sharply with depth from the exposed surface to a depth of 30-40mm below, at which the sorptivity profiles tended to level off (see Figures 7.3, 7.4 and 7.7). The curing affected zone was slightly larger in the blast-furnace slag concrete (40mm) than the OPC concrete, especially after 12 months of exposure (Figure 7.7). Further, the reduction in the sorptivity from the surface (10mm) down to 40mm was approximately 25% for the OPC concretes and almost 50% for the OPC/GGBS concrete. The variations in the sorptivity beyond 40mm deep were generally marginal.

Whereas the sorptivity of the Loughborough OPC concretes became lower at the SZ than the SSZ after 12 months of exposure, the sorptivity of the Muscat concretes remained invariably higher at the surface. However, unlike the OPC concrete (Figure 7.3), the difference between the surface (10mm) and subsurface sorptivity values increased markedly with age in the blast-furnace slag concrete (Figure 7.7).

#### **7.4.2 30 MPa OPC Concrete**

##### *Microclimate*

Figures 7.3 show the effect of microclimate on the sorptivity profiles of the hessian cured 30 MPa OPC concrete samples at the ages of 3 and 12 months. The effect of microclimate on the curing membrane and polythene cured OPC samples at the ages of 3 and 12 months is shown in Figure 7.4. The sorptivity indices with statistical analysis are listed in Tables C1.1 to C1.4 in Appendix C for the 3 and 12 months tests respectively.

The differences in the sorptivity indices due to microclimate were insignificant at both ages. At 3 months, the average surface (10mm) sorptivity value of the east faces was 0.313 compared to 0.316 ( $\text{mm}/\text{min}^{0.5}$ ) for the west faces. Similarly at the SSZ (20-50mm), the average sorptivity value of the east and west faces was 0.241 and 0.239 respectively.

At 12 months of age, the average surface sorptivity value of the east faces was 0.287 compared to 0.291 ( $\text{mm}/\text{min}^{0.5}$ ) for the west faces. At the SSZ, the sorptivity values of the east and west faces were 0.251 and 0.249 ( $\text{mm}/\text{min}^{0.5}$ ) respectively.

#### *Duration of hessian curing*

The relationship between the sorptivity and hessian curing duration of the 30 MPa OPC concrete at the ages of 3 and 12 is presented in Figure 7.5 (a) and (b) respectively.

As can be seen from the graphs, the effect of hessian curing duration on the sorptivity of OPC concrete was small. As previously observed, the range of measured sorptivity indices due to curing was narrow with the differences between the non-cured and 6 days cured samples being generally very small. This is apparent at both, the SZ and SSZ and at both ages (Figure 7.5 (a) and (b)). Nevertheless, the sorptivity decreased with increased hessian curing duration in all samples with the difference between the 0 and 6 days cured samples being approximately 10%. The magnitude of improvement in the sorptivity at the SZ and SSZ was similar.

#### *Curing membrane (C/M) and polythene curing methods*

The effect of hessian curing duration, curing membrane and polythene curing on the sorptivity of the concrete samples at 3 and 12 months of age is shown in Figure 7.6.

As shown, the difference between the 6 curing regimes after 3 and 12 months of exposure was small. At 3 months, the surface (10mm) sorptivity of the polythene-cured concrete was relatively higher than all samples in the east

and west microclimates. The surface sorptivity of the C/M cured concrete was generally similar to the hessian cured blocks. There was no real difference in the sorptivity between the various samples at the SSZ (see Figure 7.6 (c) and (d)).

After 12 months of exposure, the C/M and polythene cured concrete exhibited similar sorptivity values at the surface, being higher than all hessian cured samples by approximately 10%. The differences in the sorptivity of the samples at the SSZ were very small in both microclimates (Figure 7.6 (c) and (d)).

#### *Age*

The sorptivity of the OPC concrete decreased with age at the SZ and increased fractionally at the SSZ, as shown in Figure 7.6. The improvement in the SZ values with ages was generally small, being on average, 10% lower than the 3 months values. This is in line with the Loughborough results for the OPC concrete, although the reduction in the surface sorptivity of the samples with age was considerably larger. At the SSZ, the difference between the 3 and 12 months sorptivity values was less than 5% (see Figure 7.6 (c) and (d)).

### **7.4.3 30 MPa OPC/GGBS Concrete**

#### *Microclimate*

Figures 7.7 show the effect of microclimate on the sorptivity profiles of the 30 MPa OPC/GGBS concrete samples at the ages of 3 and 12 months. The effect of microclimate on the curing membrane and polythene cured OPC/GGBS samples at the ages of 3 and 12 months is shown in Figure 7.4. The sorptivity indices with statistical analysis are listed in Tables C1.5 and C1.6 in Appendix C for the 3 and 12 months tests respectively.

As with the OPC concrete, the variation in the sorptivity of the blast-furnace slag concrete due to microclimate were very small at both ages. The difference in the sorptivity values of the east and west faces of the concrete blocks was generally less than 5% for all samples (see Tables C1.3 to C1.6 for values).

### *Duration of hessian curing*

The relationship between the sorptivity and hessian curing duration of the 30 MPa OPC/GGBS concrete at the ages of 3 and 12 is presented in Figure 7.5 (c) and (d) respectively.

The sorptivity of the samples at 3 months of age decreased gradually as hessian curing was increased. It is interesting that the variation in the sorptivity due to curing was relatively more pronounced in the OPC/GGBS concrete than the OPC concrete, which is also true for the two Loughborough series. The east faces of the concrete blocks improved steadily with increased curing duration from 0-6 days, the SZ sorptivity being on average, 15% lower after 6 days of curing relative to the non-cured samples. The improvement in the sorptivity indices was larger in the west faces of the blocks, being approximately 30% lower at the SZ than the non-cured concrete blocks after 6 days curing. At the SSZ, the sorptivity of the 6 days cured blocks was approximately 25% lower than the non-cured blocks in the east and west faces.

After 12 months of exposure, no real advantage due to curing was evident in the east faces of the concrete blocks, the sorptivity of all east-facing blocks being similar regardless of curing duration. For the west facing samples, the 4/6 days hessian cured blocks showed lower sorptivity than the 0/2 days cured blocks; the sorptivity of the 6 days cured samples being the lowest of all samples. At the SSZ, the sorptivity decreased slightly with increased curing duration (Figure 7.5 (d)).

### *Curing membrane and polythene curing methods*

The effect of hessian curing duration, curing membrane and polythene curing on the sorptivity of the concrete samples at 3 and 12 months of age is shown in Figure 7.8.

After 3 months of exposure, the sorptivity of the C/M cured blocks was approximately 10% higher than the blocks that received 6 days polythene curing, however, both methods exhibited higher sorptivity values (10-20%)

than the hessian-cured concretes. After 12 months of exposure, the sorptivity of the C/M and polythene cured samples was lower than the 2/4 days cured samples and generally similar to the 6 days hessian cured samples. The difference between C/M and polythene curing was generally small (the sorptivity values are listed in Tables C1.3 to C1.6).

#### *Age*

Unlike the OPC concrete, the sorptivity of the blast-furnace slag concrete increased with age in almost all samples, as shown in Figure 7.8. The increase in the sorptivity of the samples ranged from 10-30% and was more significant at the surface than the layers below. It is worth to note, however, that despite the increased sorptivity of the OPC/GGBS concrete after 12 months, the sorptivity values at the SSZ were lower than that of the OPC concrete (compare Figures 7.6 with 7.8, (c) and (d)).

Table 7.1 Weather data - Muscat 1996 (Figure 7.1)

Month	Air temperature (c)					Relative humidity (%)					Prevailing wind direction	
	mean			extreme		mean			extreme		(degrees)	direction
	mean	max	min	max	min	mean	max	min	max	min		
JAN	20.4	24.2	16.6	28.5	12.8	64	81	47	96	28	210	SW
FEB	21.7	25.6	17.8	29.1	14.1	69	84	54	99	34	60	NE
MAR	24.4	28.7	20.8	36.5	15.4	69	86	49	97	24	60	NE
APR	28.8	33.9	23.8	41.5	19.2	50	71	33	94	11	270	S
MAY	34.1	39.6	29	45.2	22.4	41	64	21	89	8	210	SW
JUN	34.4	39.5	30.2	47.8	27.1	54	74	34	91	8	60	NE
JUL	34.6	39.9	30.4	44.1	27.3	54	80	32	100	11	60	NE
AUG	31.2	34.8	28.5	42.1	25.3	74	87	59	95	24	60	NE
SEP	29.7	34.1	26	39.8	22.2	70	86	52	94	25	60	NE
OCT	27.5	33.1	22.1	37.5	16.6	52	74	30	89	4	60	NE
NOV	23.6	28.3	18.3	32.3	12.8	57	72	41	89	24	60	NE
DEC	20.6	25.2	15.6	28.4	10.9	61	75	46	90	22	210	SW

Table 7.2 Weather data - Muscat 1997 (Figure 7.2)

Month	Air temperature (c)					Relative humidity (%)					Prevailing wind direction	
	mean			extreme		mean			extreme		(degrees)	direction
	mean	max	min	max	min	mean	max	min	max	min		
JAN	20.1	24.5	15.4	28	12.6	60	75	42	95	9	210	SW
FEB	21.9	26.2	17.8	31.8	14.9	65	81	46	98	24	330	SE
MAR	23	27.3	19.1	33.9	15.4	66	84	45	97	8	60	NE
APR	26.5	31.1	22.1	38	17.7	61	81	41	97	16	60	NE
MAY	32.2	37.8	26.2	44.4	21	42	67	22	94	7	210	SW
JUN	33.2	38.1	28.9	46.6	26.1	60	81	39	97	9	60	NE
JUL	33.5	37.7	30.1	46.7	28	61	78	43	91	12	60	NE
AUG	31.5	35.8	28.4	39	27.1	73	89	53	95	16	60	NE
SEP	31.1	36.3	26.7	42.2	23.8	68	88	45	96	14	60	NE
OCT	29.6	34.2	25.4	38.6	22.6	60	77	42	95	16	60	NE
NOV	24.9	28.6	20.9	31.3	17.8	66	81	51	89	40	60	NE
DEC	22.3	26.6	18.2	29.4	15.2	63	77	46	90	31	210	SW

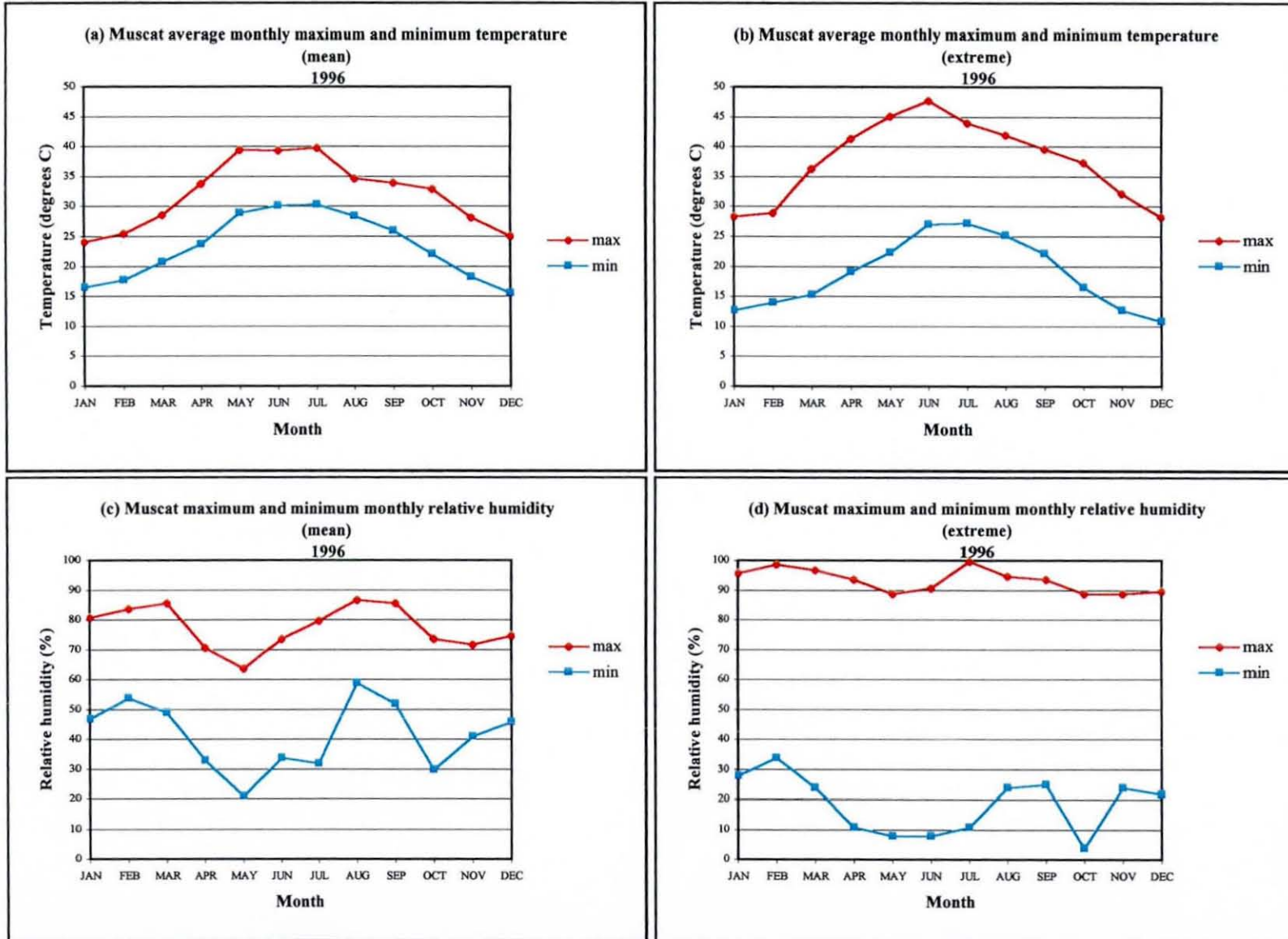


Fig. 7.1 Average monthly maximum and minimum temperature and relative humidity - Muscat 1996 (Table 7.1)

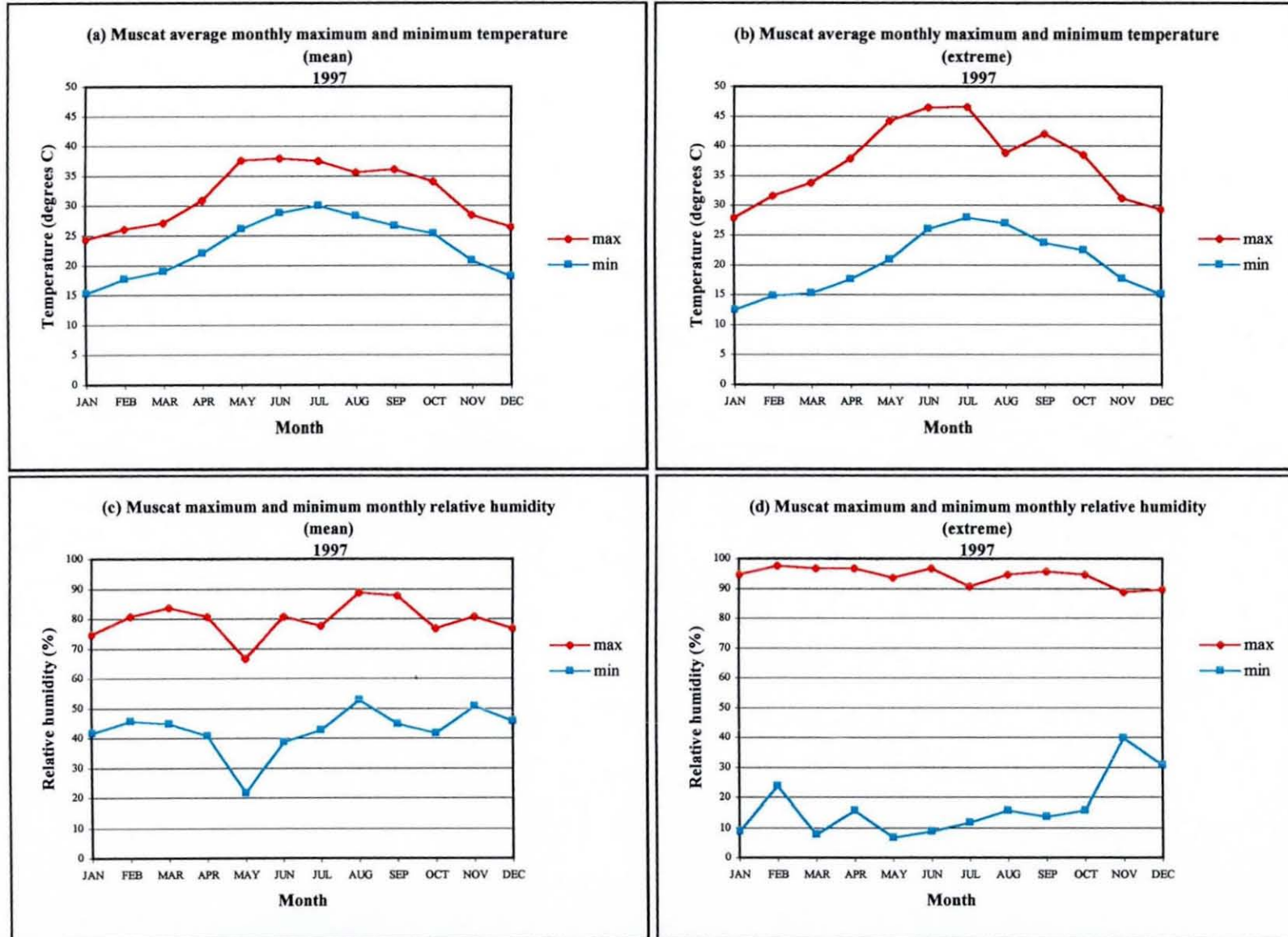


Fig. 7.2 Average monthly maximum and minimum temperature and relative humidity - Muscat 1997 (Table 7.2)

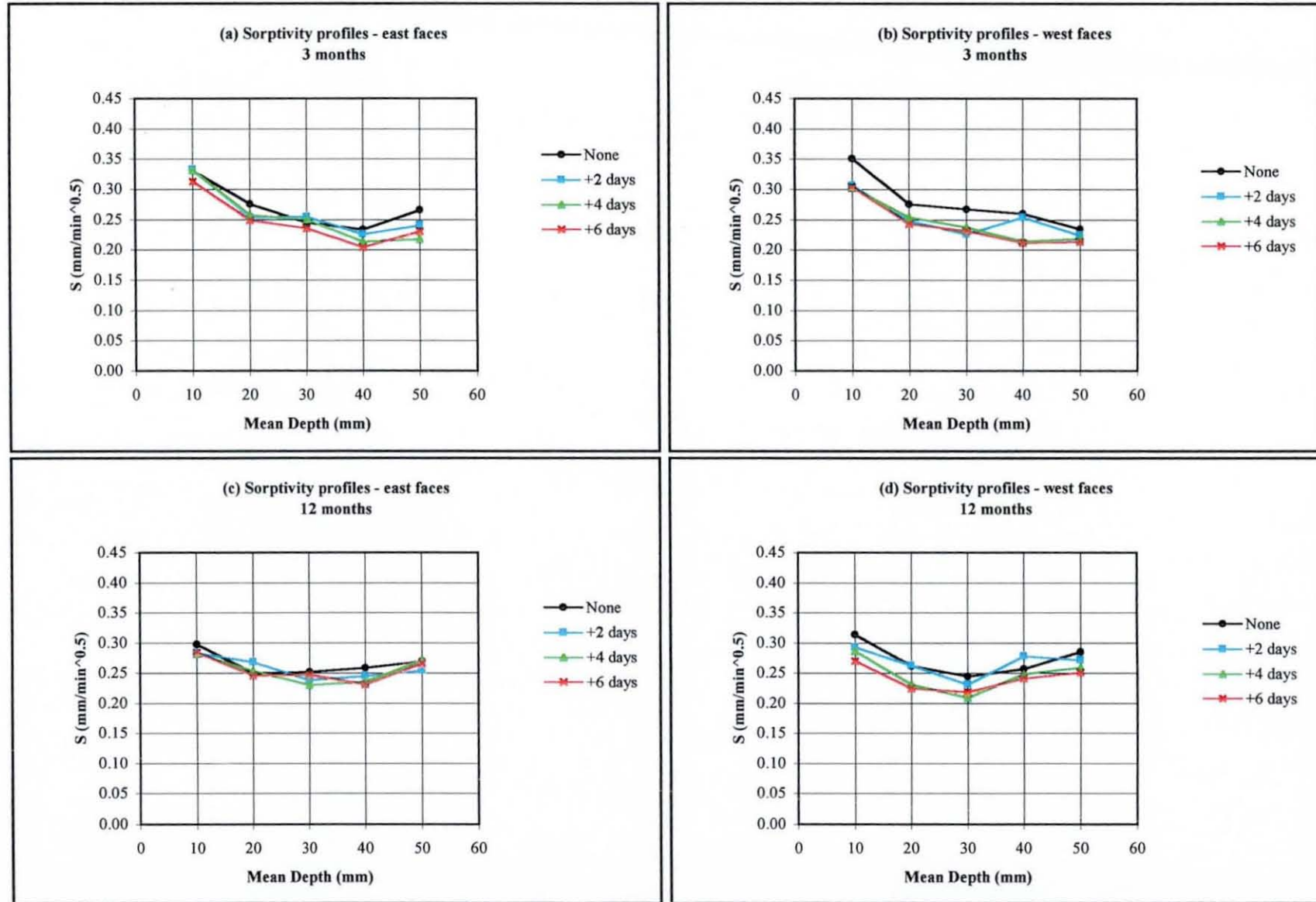


Fig. 7.3. Effect of hessian curing duration on the sorptivity profiles of 30 MPa OPC concrete after 3 and 12 months of field exposure -Muscat summer series

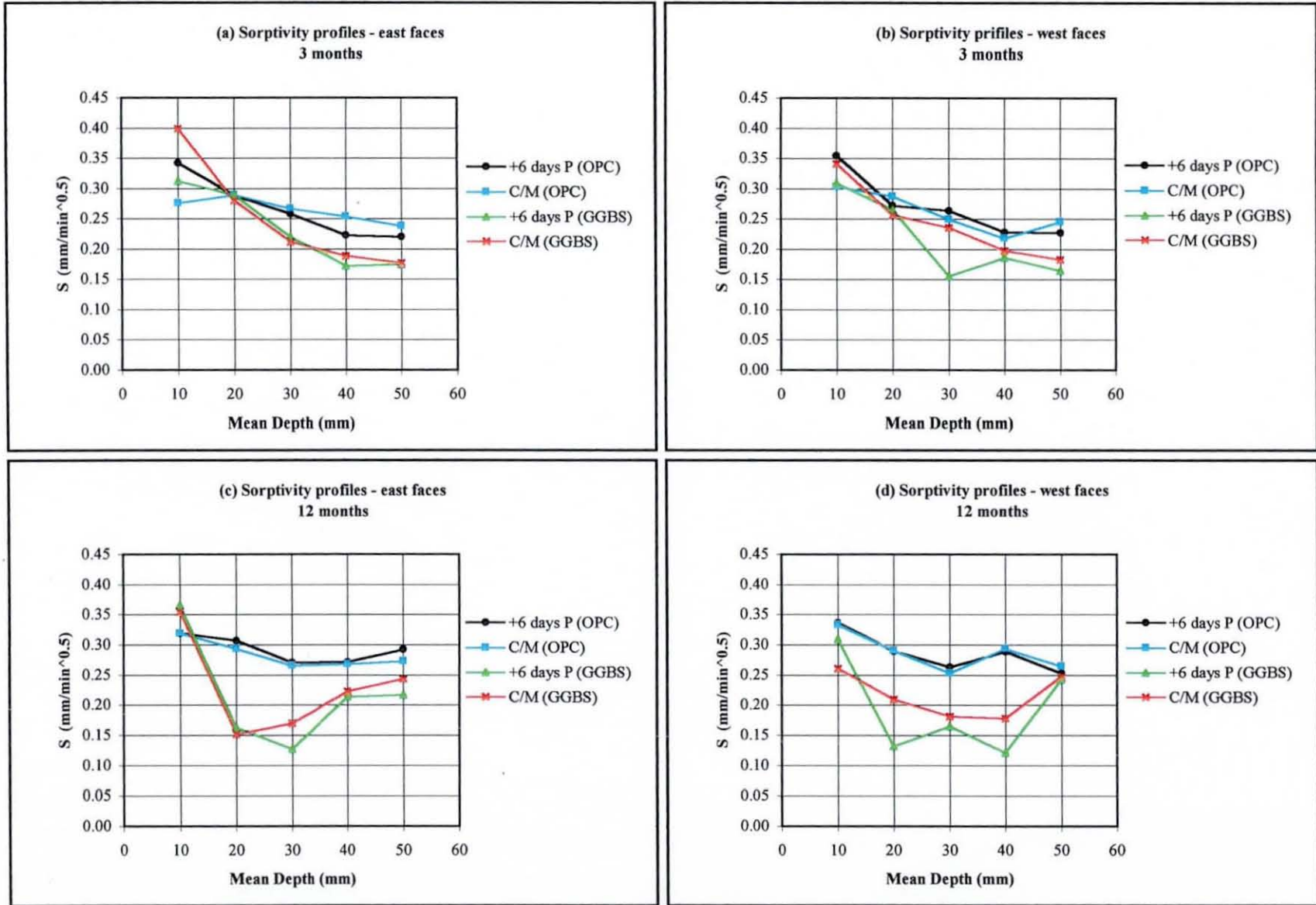


Fig. 7.4 Effect of curing regime on the sorptivity of 30 MPa OPC and OPC/GGBS concrete - 3 and 12 months Muscat summer series

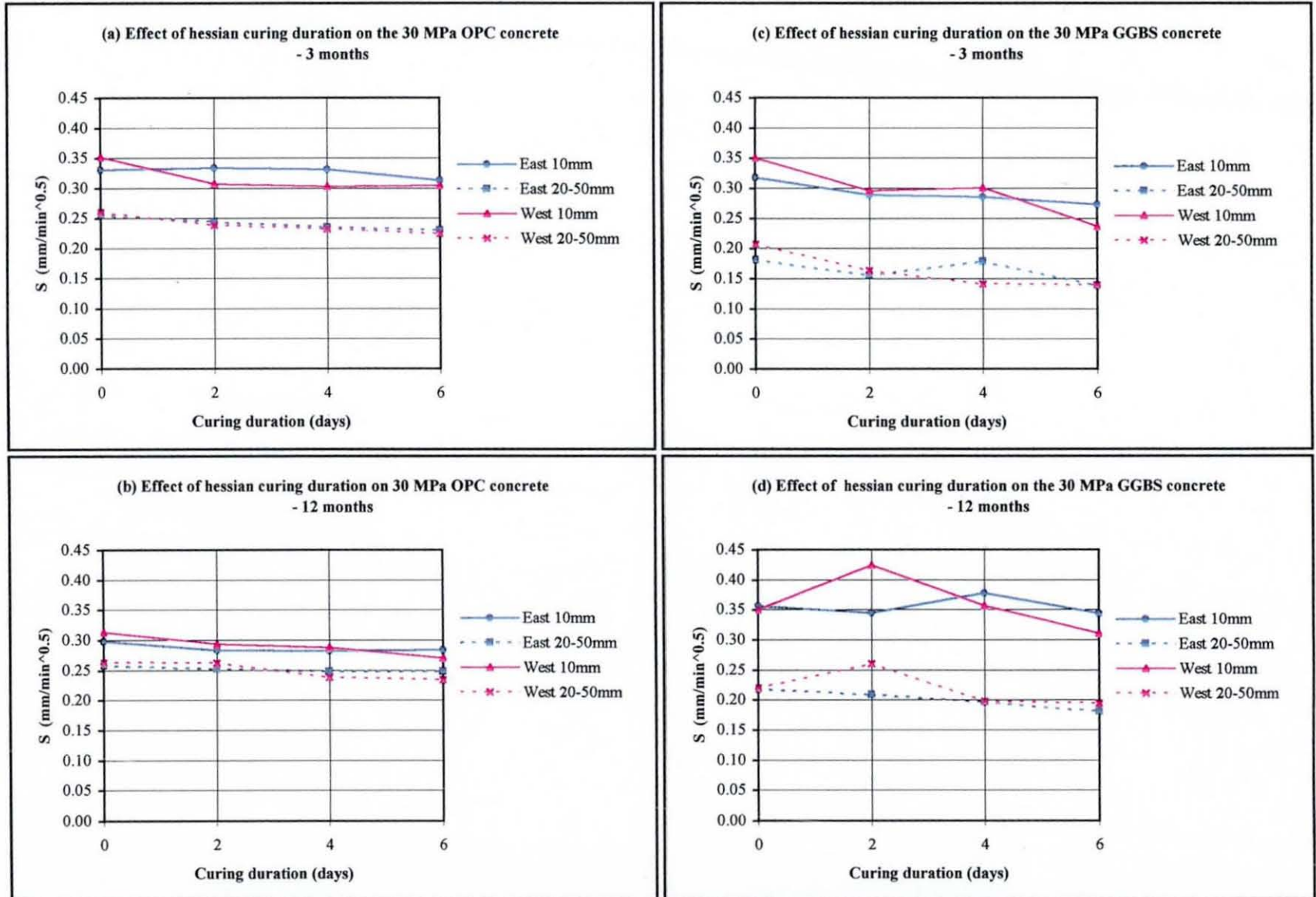
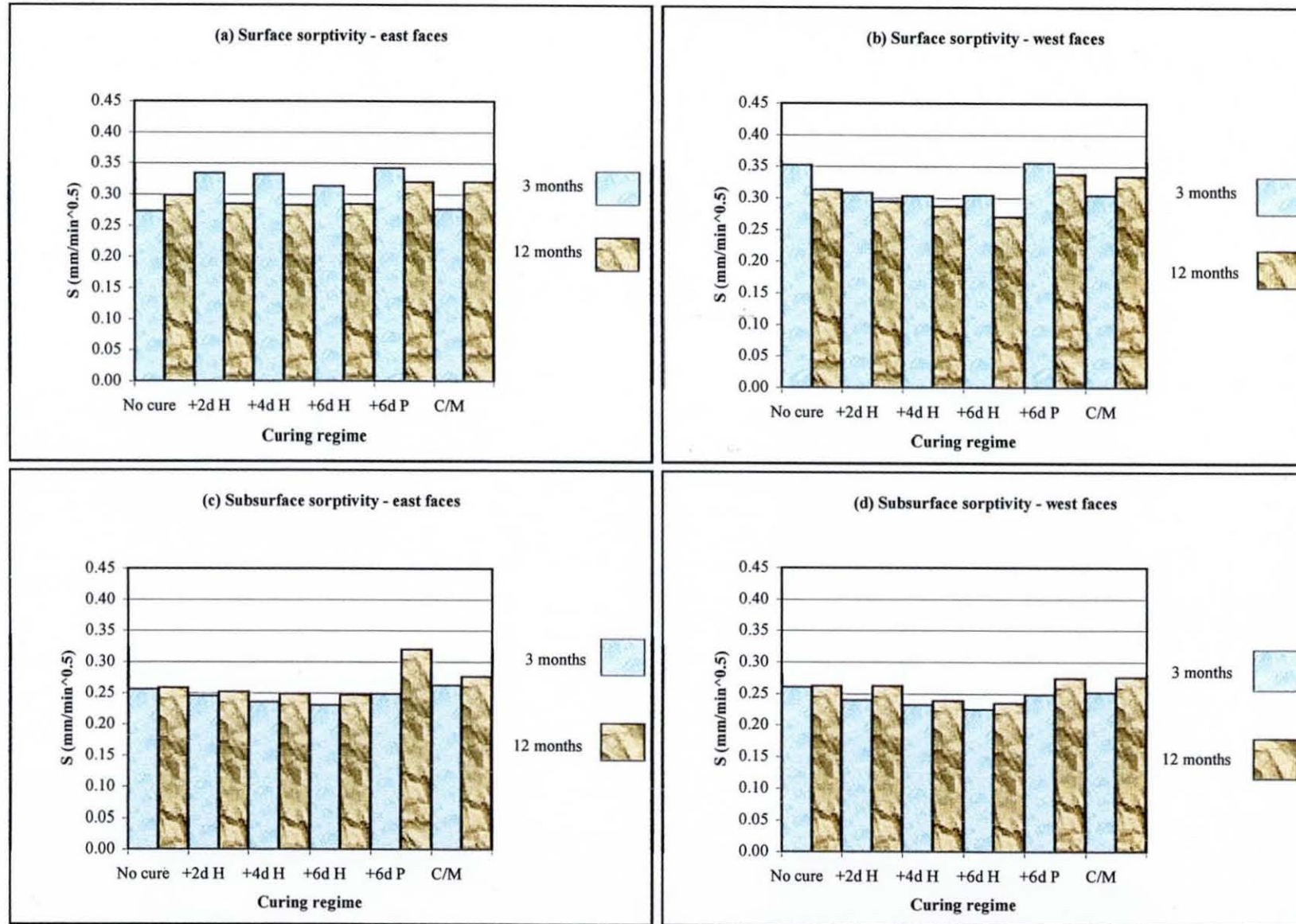
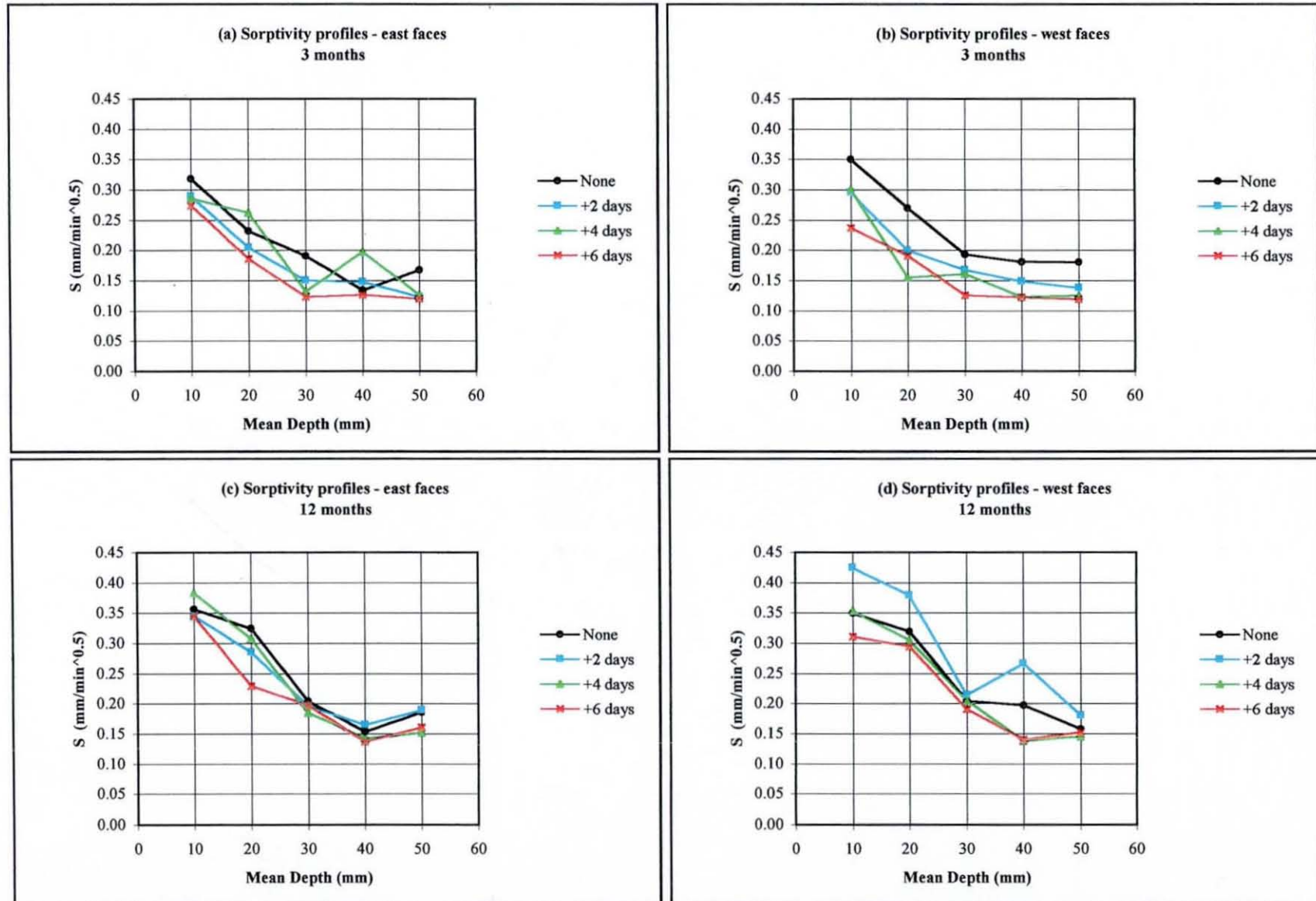


Fig. 7.5. Effect of hessian curing duration on the sorptivity of 30 MPa OPC and OPC/GGBS concrete - 3 and 12 months Muscat summer series



**Fig. 7.6** Effect of curing regime on the surface and subsurface sorptivity of the 30 MPa OPC concrete - 3 and 12 months Muscat summer series



**Fig. 7.7** Effect of hessian curing duration on the sorptivity profiles of 30 MPa OPC/GGBS concrete after 3 and 12 months of field exposure - Muscat summer series

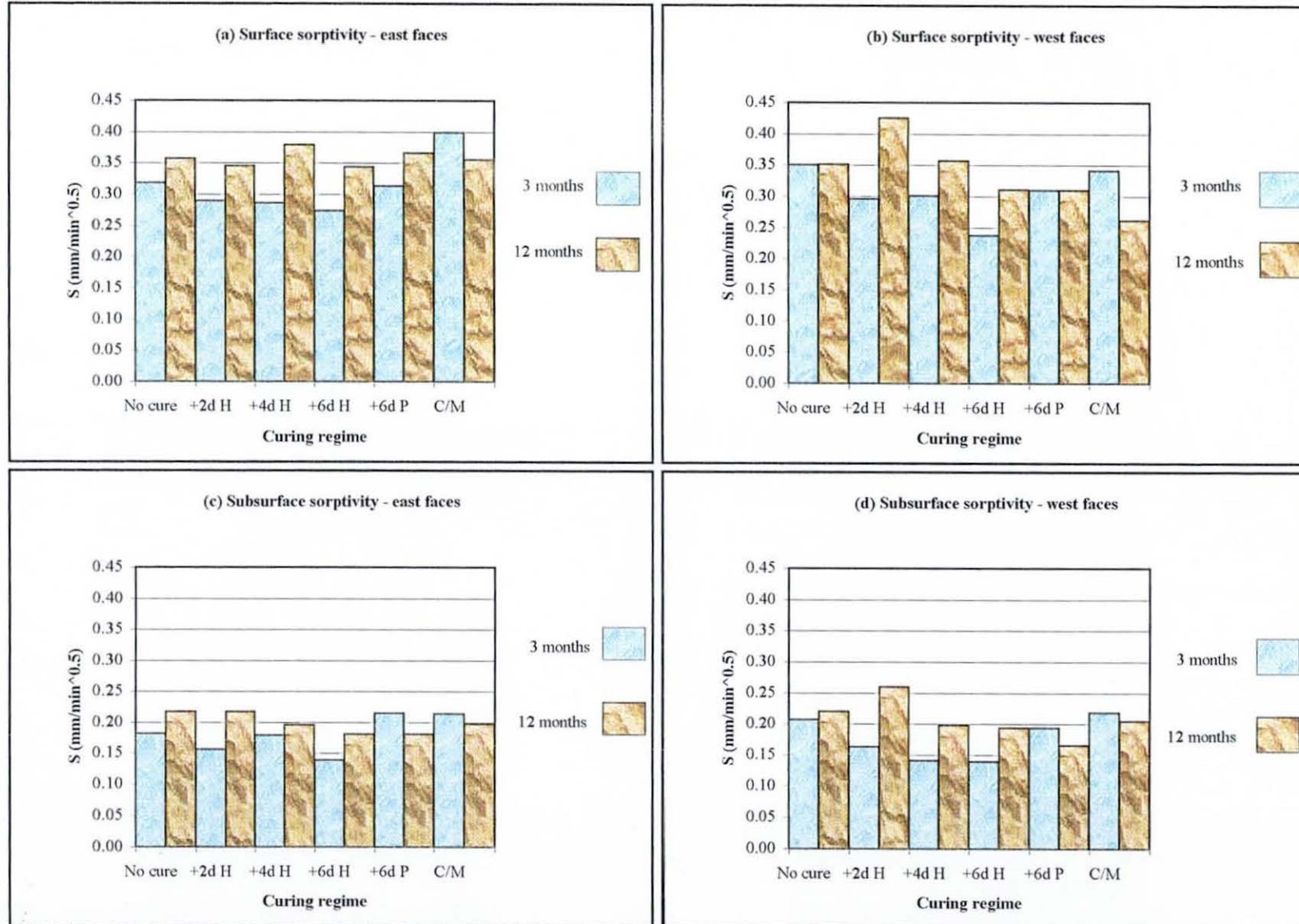


Fig. 7.8. Effect of curing regime on the surface and subsurface sorptivity of the 30 MPa OPC/GGBS concrete - 3 and 12 months Muscat summer series

## Chapter 8 Trends and Discussion

---

### 8.1 INTRODUCTION

The air permeability and sorptivity tests were performed on over 1200 and 1500 concrete specimens respectively during the course of the experimental investigations. The carbonation test was performed on all the concrete blocks investigated (surface samples) whereas the TGA and MIP were conducted on a selection of samples at the age of 12 months. Systematic variations of the measured tests parameters i.e. coefficient of air permeability, sorptivity, carbonation depth, porosity and hydration within the cover concrete (the first 50-mm from the exposed concrete surface) have been detected. The effect of macro and microclimate, hessian-curing duration, curing regime, controlled permeability formwork, exposure duration and concrete type are discussed. Comparisons are then made between the results of physical property tests and microstructural tests to assess correlation.

### 8.2 DEPTH AND CURING AFFECTED ZONE (CAZ)

#### 8.2.1 Permeability and Sorptivity

The air permeability and sorptivity were higher at the surface zone than the subsurface zone in the 3 concrete mixes of the winter and summer series at the age of 3 months. Generally, the curing profile graphs showed a sharp reduction in the two parameters (coefficients of air permeability ( $k$ ) and sorptivity ( $S$ )) with increasing depth at the SZ, followed by a more gradual reduction at depths beyond 20mm, within the SSZ. Thus, curing largely affected the penetrability properties to a depth of approximately 20mm from

the outer surface. However, the curing affected zone varied according to curing and microclimate conditions as well as concrete strength and type. The curing affected zone was generally larger i.e. up to 30-40mm for the OPC/GGBS concretes and for the OPC concretes that were subjected to the dry microclimates (east faces and bottom faces of the blocks). The extent of the curing affected zone of the 50 MPa OPC concretes was generally small (average 10mm). The variation in the air permeability with depth between the different samples was larger and more marked than the sorptivity, with the profile trends of the former being the most distinct (e.g. compare Figure 6.2 with 6.22).

The variation in the air permeability and sorptivity with depth from the exposed surfaces comes as a result of quality gradients within the concrete (perpendicular to and in the direction of casting), which is usually attributable to two main factors. The first is the inherent heterogeneity of concrete arising from the migration and settlement of water and aggregates respectively, during compaction and placing (Kreijger, 1984; Dhir et al, 1986). The second factor is drying caused by: (1) the evaporation of water from the surface due to relative humidity, temperature and wind conditions of the surrounding environment or microclimate; and (2) self desiccation of concrete which is caused by the consumption of water during hydration (Killoh et al 1989; Dinku and Reinhardt, 1997). These factors lead to variation in cement-aggregate and moisture content, leading to differences in cement hydration and porosity with depth from an exposed concrete surface. Surface drying has been found by many researchers (e.g. Patel et al, 1985; Mangat and El-Khatib, 1992) to increase both the pore size and continuity owing to the driving off of water from the pores and cessation of hydration in the absence of water. In addition, early surface drying may cause crazing or cracking of the surface since the concrete has not attained sufficient strength to resist the tensile forces that developed as a result of the rapid moisture loss (Waters, 1955; Al-Ani and Al-Zaiwary, 1988). Previous studies indicated that for a good quality concrete, there is a 21% increase in porosity laterally from the core to the

surface (Kreijger, 1984). These findings were manifested in the observed higher air permeability and sorptivity values in the outermost layers of concrete at early age.

The sharp reduction in the permeability and sorptivity values with increasing depth in the SZ (0-20 mm from the surface), which was more apparent in the blast-furnace slag concrete, is an indication of the continuity of the pores in this region of concrete, as interpreted by the percolation theory (Parrott, 1992; Garboczi, 1995). This sharp reduction was followed by a transition phase at 20mm which marked the shift from the continuous to discontinuous pores in the SSZ. The pore size and continuity in the SSZ of concrete are reduced due to continued hydration (the pore filling process due to hydration) where adequate pore water is still available (Patel et al, 1988). This is generally supported by the porosity and hydration results (see Tables 6.4, A1.15 and A1.16). As shown, the porosity decreased sharply with depth for the OPC/GGBS concrete, especially for the non-cured samples. Similarly, the evaporable water was higher for the OPC/GGBS concrete, which indicates higher capillary porosity than the OPC concrete. Also, the calcium hydroxide content was lower at the surface and, together with the combined water for most samples, tended to generally increase with depth from the exposed surface, indicating continued hydration reaction and pore segmentation in the inner layers of concrete. Air and water flow is slower and more restricted in these discontinuous pores, hence the lower air permeability and sorptivity values in the SSZ.

The difference between the SZ and SSZ permeability and sorptivity values generally reduced with age, especially in OPC concrete. The reduction was most significant in the blocks that were hessian cured for 4 and 6 days, and in the west and top faces of the blocks. Additional initial curing in the 4 and 6 days cured blocks as well as the longer curing due to rain on the west and top faces of the blocks during exposure (Ho et al, 1989), resulted in better hydration in the surfaces of these samples and, therefore, reduced pore size and volume. Conversely, the east and bottom sides of the blocks were

sheltered from the beneficial effect of rain during the entire exposure period, which led to their consistently higher permeability and sorptivity at the SZ compared to the west and top faces of the blocks. This corroborates findings (Osborne, 1994 and Parrott,1992) that the exposed surfaces may benefit from rain to a greater extent than the possible drying effect due to solar radiation and wind, depending on the conditions obtaining.

Contrary to the 3 months results, the air permeability and sorptivity of the two OPC concretes were generally lower at the surface (5 and 10mm values) than the subsurface (20-50mm) at 12 months. This effect was not prevalent in OPC/GGBS concrete where the surface values (most apparent in air permeability results) continued to be higher than the subsurface (see Figures 6.13 and 6.33). This is consistent with the porosity results (Table 6.4). The variation with depth in the porosity and pore size distribution of the two OPC concretes was distinctly different than the OPC/GGBS concrete. Generally, the total pore volume and the volume of small pore ( $< 0.1 \mu\text{m}$ ) were lower at the surface than the inner sections of the samples. This effect was also reported by many researchers who observed lower permeability and porosity at the surface than the subsurface of OPC concrete and vice versa in slag concrete (e.g. Bier et al, 1989; Thomas et al, 1990; Parrott, 1992). The thermal analysis results confirmed that the lower porosity at the surface was not due continued hydration, since the hydrate and calcium hydroxide waters tended to increase with depth from the exposed surface (Tables A1.15 and B1.23). The lower surface porosity of the OPC concrete may be explained in light of the reported carbonation effect on concrete pore structure (Section 8.2.2).

### **8.2.2 Carbonation**

Carbonation of concrete is reported to reduce the surface area, capillary pore volume and continuity of the cement matrix of OPC concrete, and increase capillary porosity in slag concrete (Beir et al, 1989; Thomas et al, 1990; Parrott, 1992, Balen and Gemert, 1994). This was attributed to the deposition of calcium carbonate ( $\text{CaCO}_3$ ) which is formed by the decomposition of  $\text{Ca(OH)}_2$

during reaction with  $\text{CO}_2$  in the pores of the cement matrix in OPC concrete thereby reducing the volume and continuity of its pores.

For concretes with high slag content, the low  $\text{Ca}(\text{OH})_2$  can easily be expended upon carbonation which results in the carbonation and decomposition of the C-S-H into  $\text{CaCO}_3$  and a highly porous silica gel (pores in the range 0.1-10  $\mu\text{m}$ ). Parrott (1996) reported that carbonation of calcium silicate hydrate leads to an increase of gas permeability and carbonation of calcium hydroxide leads to a decrease of gas permeability. The higher surface permeability and sorptivity values of the blast-furnace slag concrete were generally more apparent in the 12 months old samples that had carbonated most (e.g. compare Figures 5.11 & 6.11 with 5.25 & 6.43 respectively), which supports the reported negative effect of carbonation on its pore structure. As a result, and contrary to OPC concrete, the difference between the SZ and SSZ permeability and sorptivity values of the 12 months old OPC/GGBS concrete was higher than the 3 months old concrete, despite the small reduction at 5mm from the surface which was observed in some samples.

It is interesting that although there is agreement in the literature on the effect of carbonation in reducing the local porosity at the concrete surface, the reports are conflicting on the pore sizes most affected. Some workers (e.g. Litvan and Meyer, 1986; Thomas et al, 1990) observed a reduction in the volume of small pores ( $\leq 0.009 \mu\text{m}$ ) upon carbonation, while others (e.g. Patel et al, 1985) reported a reduction in the volume of larger pores. Interestingly, both these effects were observed in different samples in this work although the reduction in the volume of large pores was more noticeable.

However, it is of note that some OPC concrete samples showed lower surface (5-10mm) air permeability and sorptivity values than the SSZ despite the fact that these exhibited no or very little carbonation (e.g. compare the sorptivity of the 0 and 2 days cured samples in Figure 5.21 (c) with its carbonation in Figure 5.25 (c)). Similarly, some OPC/GGBS concrete samples showed lower surface penetrability than other samples with similar carbonation levels.

Apart from possible inconsistencies that are often encountered in field investigated concrete, no definite explanation could be proposed, especially in the absence of porosity and hydration measurements for these samples.

### 8.2.3 Porosity and Hydration

The pore volume and coarse capillary porosity of the 50 MPa OPC concrete was notably lower than the 30 MPa OPC and OPC/GGBS concrete at all depths (see Sections 8.8.1 and 8.8.2). This is in agreement with the permeability and sorptivity results, which were significantly lower in the 50 MPa OPC concrete than the 30 MPa OPC and OPC/GGBS concrete. The strength-porosity relationship has been studied extensively and is well understood. It has long been ascertained that the strength and permeability of a cement matrix are both determined by its porosity and pore size distribution, which for the same degree of hydration are determined by the W/C ratio (e.g. Nyame and Illston, 1981; Odler and Koster, 1986; Rahman, 1984; Taylor, 1990). Decreasing the W/C ratio was found to decrease the porosity and volume of coarse pores and subsequently decreases permeability and increases strength (e.g. Yudenfreund et al, 1972; Mehta and Manmohan, 1980; Midgley and Illston, 1983; Odler and Koster, 1986; Dinku and Reinhardt, 1997). Therefore, the reduction in the pore volume and coarse capillary porosity of the 50 MPa OPC concrete relative to the two 30 MPa concretes is solely attributable to its increased cement content and the associated reduction in the W/C ratio, since the hydration conditions (compaction, curing, exposure and age) of the three concretes were the same. Apart from the increased volumes of hydration products which created denser pore structure in the 50 MPa concrete, the reduced water content increased the concentration of solids in the matrix by closer particle packing, which means that there was initially insufficient water to form what later becomes water/air voids.

The change in porosity with depth in the OPC/GGBS concrete was much more dramatic than OPC concrete. This was detected by the air permeability

(Figure 5.11 and Figures 6.10 to 6.13) but was significantly less marked in the sorptivity results (Figures 5.23 and Figures 6.31 to 6.33). Furthermore, unlike the OPC concretes the total pore volume and coarse capillary porosity was consistently higher at the surface than the inner sections of the samples (see Table 6.4). This coincides with the 12 months air permeability and sorptivity of the slag concrete where these were higher at the surface than the subsurface.

The higher porosity of the slag concrete, especially at the surface, can be attributed to a number of reasons, some of which were discussed earlier. Blast-furnace slag concrete's slower initial reaction and pore structure development facilitates evaporation of water from the outermost layers at early age (on drying) and hinders hydration, leading to higher porosity and permeability at the surface. Parrott (1991a) observed greater weight losses for the OPC/GGBS concrete than plain OPC concrete at all ages considered. Furthermore, in the context of carbonation, blast-furnace slag concrete and in particular those with high OPC replacement levels also undergo change to its pore structure upon carbonation. The consumption of the low  $\text{Ca(OH)}_2$  of slag concrete upon carbonation leads, on continued  $\text{CO}_2$  diffusion, to the carbonation of the C-S-H which results in its decomposition into  $\text{CaCO}_3$  and a highly porous silica gel (pores in the range 0.1-10  $\mu\text{m}$ ). This further increases the pore volume and the volume of coarse capillary pores at the surface, which subsequently leads to higher permeability as confirmed by the earlier findings.

The progress of hydration with depth was estimated by the bound water and calcium hydroxide water contents of a selection of concrete samples (east facing blocks). The profile curves of both parameters were remarkably similar in shape and absolute values (Figures 5.30 and 6.50). The hydrate water and lime water contents of the two OPC concretes generally increased with depth from the exposed surface up to 10mm, beyond which the profile curves exhibited a downward curvature with the 20mm values being generally lower than the values at 10mm from the surface. Surprisingly, this trend was

reversed for the OPC/GGBS concrete where the two parameters generally decreased with increasing depth from the exposed surface with the 5mm surface values showing the highest hydrate and calcium hydroxide water contents (Figures 5.30 (e) and (f)).

The TGA results of the two OPC concretes of the winter and summer series indicate that the inner layers (10-20mm values) of concrete hydrated to a greater extent than the surface layer (5mm) and vice versa for the OPC/GGBS concrete. However, the variation in the extent of hydration between the three depths was small in all cases and does not appear to reflect quantitatively the observed air permeability, sorptivity and porosity gradients with depth from the surface. The hydration results of the OPC concretes are in agreement with what might be expected and verify, as stated earlier, that the lower surface permeability, sorptivity and porosity at 12 months were not due to an improvement in the sample's hydration. Similar findings were reported by Patel and his co-workers (1985) where the surface porosity (up to 6mm from the surface) and diffusion rates were lower than the inner layers of the samples although their degree of hydration was lower than the internal sections of concrete. The authors ascribed this to the consolidating effect of carbonation as previously discussed.

Contrary to expectation, the hydration profile results of the OPC/GGBS indicate that the surface layer hydrated to a greater extent than the inner layers of the samples. This is inconsistent with the air permeability, sorptivity and porosity results, however due to the limited number of results obtained, no definite explanation could be offered.

## **8.3 MACROCLIMATE**

### **8.3.1 Loughborough Winter versus Loughborough Summer**

All hessian cured blocks in the winter and summer series were sprayed with water once every 24 hours during the curing period to represent site curing. The ambient conditions in the two seasons, however, were entirely different.

Despite the slightly favourable relative humidity conditions during daytime in the winter compared to summer, the ambient conditions, in general, were very cold and dry in the winter. Unlike the summer, the hessian were often found dry and occasionally frozen hours after being sprayed with water in the winter. Additional rainfall in the summer has also contributed to the overall curing of the summer blocks, especially when it occurred during the curing period of the blocks. These conditions resulted in improved concrete quality with prolonged hessian curing duration in the summer and vice versa in the winter. As a result, the air permeability and sorptivity values of the summer series concrete were generally lower for the OPC/GGBS and 50 MPa OPC concrete than the winter series (see Table 8.1). The air permeability and sorptivity values of the 30 MPa OPC concrete in the summer series were generally comparable with the winter series concrete (compare Figures 5.3 with 6.3 and 5.15 with 6.23).

The 3 concrete mixes that were cast in the summer season exhibited higher carbonation rates after 6 months of exposure than the same mixes that were cast during winter. This trend, however, was changed after 12 months of exposure. At 6 months of age, the 30 MPa OPC and OPC/GGBS concrete blocks that were cast in the summer carbonated respectively by, on average, 40% and almost 100% more than the equivalent winter-cast blocks (Tables A1.13 and B1.21). The winter-cast 50 MPa OPC concrete blocks showed no sign of carbonation after 6 months of exposure, while the summer-cast blocks carbonated to a depth of approximately 2mm in the dry east and bottom faces and 1mm in the west and top faces.

The higher initial carbonation rates of the summer series were most probably due to the relatively higher ambient temperature and lower relative humidity during the early stages of exposure in the summer, compared to winter. The average temperatures during the initial curing and exposure periods of the summer series were almost 10 °C higher than the winter series (average summer temperature was 15 °C). The relative humidity was, on average, 20%

lower in the summer especially during the longer daytimes. However, the additional rainfall in the summer was expected to slow down the diffusion of carbon dioxide into concrete, especially since this aided the overall curing of the blocks and led to an improvement in their permeability compared to the winter blocks. Nevertheless, an increase in the ambient temperature increases the rate of carbonation even in situation where higher relative humidity or rain prevail (Richardson, 1998). It has been suggested that elevated temperatures enhance CO<sub>2</sub> diffusion, and may increase the pore space within concrete through drying, thereby facilitating diffusion (Roy et al, 1996; Kropp, 1995).

After 12 months of exposure, the carbonation depth trends were different to those observed at 6 months. The carbonation depth of the winter and summer-cast, 30 MPa OPC concrete were similar (average 4-7mm); while the carbonation depth of the summer-cast 50 MPa OPC concrete was, on average, 30% higher than that cast in the winter (winter values from 0-2.5mm). The carbonation depth of the winter-cast, 30 MPa OPC/GGBS concrete blocks were, on average, 20% higher than the summer-cast blocks (winter values range from 7-13mm, depending on microclimate and curing), despite it being initially lower in the winter blocks at 6 months (see Tables A1.14 and B1.22). A possible explanation is that the higher summer temperatures (average 10 °C higher than winter during initial exposure) initially triggered higher diffusion of CO<sub>2</sub> into the summer-cast concrete, however, this was being gradually buffered by the continuous development of the pore system that was afforded by the better overall curing conditions. This resulted in lower carbonation rates in the summer series' OPC and OPC/GGBS concretes over the second 6 months of exposure. The more permeable winter blocks, on the other hand, continued to carbonate steadily with time, consequently attaining higher carbonation depths than the summer blocks after 12 months of exposure.

The 12 months carbonation results of the winter and summer series are generally in agreement with their air permeability and sorptivity results. Like carbonation, the winter and summer air permeability and sorptivity values of

the 30 MPa OPC concrete were generally comparable at 12 months. Furthermore, the higher carbonation depths of the winter-cast, 30 MPa OPC/GGBS coincide with its higher air permeability and sorptivity results. This was confirmed by reports that higher air permeability and capillary absorption of concrete favours higher rates of carbonation (Osborne, 1989; Parrott, 1992; Kropp, 1995).

The hydration results are consistent with the permeation and carbonation results of the two Loughborough series. Although the differences were small, the results generally indicated that the extent of hydration of the summer concretes was relatively greater than the winter series samples (see Tables A1.15 and B1.23)

### **8.3.2 Loughborough versus Muscat**

The sorptivity of the concrete that was exposed to the hot climate of Muscat was higher than the equivalent concrete exposed to the Loughborough climate at both ages (see Table 8.1). The sorptivity of the Muscat OPC concrete was approximately 2.5 to 3 times higher at the surface (10mm) than the Loughborough-exposed OPC concrete (compare Figure 7.3 with 6.22 and 6.23 (a) and (b)). In the SSZ, the sorptivity of the Muscat samples was on average 30% higher than the Loughborough samples. For the OPC/GGBS concrete, the sorptivity of the Muscat samples (Figures 7.4 and 7.7) was more than 3 times higher at the surface than the equivalent Loughborough samples (Figure 6.33) and 15-50% higher at the SSZ (20-50mm). The curing affected zone for the Muscat concrete extended to approximately 40mm below the surface for the OPC concrete and as much as 50mm for the OPC/GGBS concrete (see Figure 7.7). This is compared to approximately 20mm below the surface for the plain Portland cement and blast-furnace slag cement concretes of the Loughborough series.

The difference in the climatic condition during the exposure year of the Muscat and Loughborough exposed samples is remarkable. Comparing the average temperatures during the exposure year, the air temperature in

Muscat was over 20 °C higher. The combined effect of high air temperature and solar radiation elevates the temperature of the concrete to as high as 70 to 80 °C at the surface during a typical summer's day. Whereas the daily and monthly fluctuations in temperature were generally small at Loughborough, the difference between the extreme maximum and minimum temperature in Muscat was as high as 17-20 °C during the summer period. Similarly, variation between maximum and minimum daily relative humidity of up to 85-90% are typically encountered throughout the year in Muscat (see Tables 7.1 and 7.2 for extreme monthly values). Such rapid and continuous temperature and relative humidity cycles cause constant cycles of expansion/contraction and hydration/dehydration which can give rise to significant micro cracking and enhanced permeability of concrete (Al-Amoudi et al, 1993). Furthermore, the high temperature combined with drying winds causes excessive evaporation of moisture from the concrete especially at the surface. This excessive evaporation severely hinders the hydration reaction and the development of the microstructure (densification of the cement matrix) and creates pathways through the emptied pores (dried pores) for the ingress of substances from the environment. These effects are evident not only from the higher sorptivity of the Muscat concretes relative to the concrete stored at Loughborough, but also from the higher sorptivity of the OPC/GGBS concrete at 12 months (Muscat) compared to that measured at 3 months. This is an indication of continued moisture loss with time, which not only impaired the pore blocking process by continued hydration but also coarsened the pores through drying. However, it is worth noting that exposure to elevated temperature such as those experienced in hot weather countries also has a fundamental effect on concrete microstructure, which is often overlooked. Experimental evidence suggests that the rate of diffusion of the hydration products of concretes subjected to high temperature exposure such as that encountered in Oman does not permit even dispersion of the hydrates, which results in the development of a different microstructure than that developed under temperate conditions. This microstructure is

characterised by a relatively dense structure immediately around the cement grains and an open, porous structure between the grains (Verbeck and Helmuth, 1968; Detwiler et al, 1994).

The results of the Muscat series concrete are interesting, especially in view of the fact that these samples were cast and cured in temperate weather conditions at Loughborough. Apart from some emphasis on materials quality and mix design, most of the deterioration problems are often associated with the effects of hot weather on the properties of fresh concrete and its curing efficiency thereafter (e.g. Rasheeduzzafar and Al-Kurdi, 1993). These effects include increased water demand and slump loss, premature setting resulting in difficulty in placement and compaction, and enhanced tendency for plastic shrinkage and thermal cracking. Additionally, high rates of evaporation of mix and curing water can seriously impair hydration, thus seriously affecting concrete's strength and durability. However, the results of this work clearly demonstrate that the effect of exposure conditions, per se, on the hardened concrete are of equal significant importance. The extension of the CAZ to 40-50mm from the surface and the tripling of the surface sorptivity after 12 months of exposure of the Muscat series has considerable implication on the life span of the concrete relative to the nominally identical concrete which was exposed to the temperate Loughborough climate. The results illustrate that regardless of the precautions taken against hot weather during the preparation, mixing, placing and curing of the concrete, attendant measures have to be taken to ensure that concrete can withstand the climatic onslaught during its service years. This can only be ensured through the correct selection of material to suit the service environment and optimum mix design.

## **8.4 MICROCLIMATE**

### **8.4.1 Permeability and Sorptivity**

The air permeability and sorptivity of the east faces of the vertical blocks and the bottom faces of the horizontal blocks (slabs) were consistently higher than the west and top faces respectively, for the three concrete mixes of the winter

and summer series. Significant variation in the air permeability and sorptivity of as much as 50% were measured between the two faces of the concrete blocks and more than 100% between the vertical blocks and slabs (e.g. between the top faces of the slabs and the east faces of the blocks). The influence of microclimate can be readily seen from Figure 8.1, which shows the surface and subsurface air permeability and sorptivity results of the winter and summer series for the 3 concrete mixes.

However, the variations in the air permeability due to microclimate were more conspicuous and marked than the sorptivity. Considering the Loughborough summer series, for examples, the lowest average SZ air permeability and sorptivity values obtained from the same samples were  $1.43 \times 10^{-16} \text{ m}^2$  and  $0.076 \text{ mm}/\text{min}^{0.5}$  (top faces of the slabs) and the highest were  $4.42 \times 10^{-16} \text{ m}^2$  and  $0.108 \text{ mm}/\text{min}^{0.5}$  (east faces of the blocks). The difference between the lowest and highest values, therefore, is 3 fold in the air permeability results compared to only 30% in the sorptivity results. This is typical of all the results as illustrated in Table 8.1, which shows average air permeability and sorptivity values for the Loughborough and Muscat series at the age of 12 months.

The microclimate on the west and topsides of the blocks were similar. Both sides were open to weather elements such as solar radiation, rain and wind, although the vertical west faces were more open to direct wind because of its orientation. The microclimates on the east and bottom sides of the blocks were similar in that both sides were sheltered from direct solar radiation and rain. However, unlike the eastside, the bottom faces of the slabs were not susceptible to direct wind. In situ measurement showed that the differences in the ambient relative humidity in the 4 microclimates were generally not significant. The prevailing wind directions during the early stages of curing were mainly easterly during winter and south westerly during summer, as presented in the results (Tables 5.1-5.2 and 6.1-6.2). There was more rainfall during the curing and exposure periods of the summer series than the winter series. The dry wind during the curing period of the winter blocks may have

had an early drying influence on the concrete. On the other hand, the westerly wind accompanied with rain during the curing period of the summer blocks could have resulted in an early beneficial effect on these concretes.

Considering the whole exposure period, however, the results suggest that the exposure of the west and top faces to rain and directional rain was more beneficial than the possible drying effect due to solar radiation and wind. This was also found by other researchers (e.g. Ho et al, 1989 and Parrott, 1992). Apart from being less open to direct wind than the west faces of the vertical blocks, the top (horizontal) faces of the slabs benefited most from rain because of its orientation and were the least permeable of all the surfaces as a result. The improvement in the permeability and sorptivity of the bottom faces with age was probably due to the fact that these faces were protected from the effect of direct wind combined with more favourable humidity conditions (partly sheltered) compared to the wholly open west faces.

The effect of microclimate on the sorptivity of the Muscat concrete was generally insignificant (see Table 8.1). Although the wind direction throughout the exposure period was predominantly north easterly (9 months NE and 3 months SW), the sorptivity indices of the east and west faces of the blocks were generally very similar. This implies that under these exposure conditions, temperature and solar radiation played a more influential role on concrete quality than wind. The relative humidity on either side of the concrete blocks were similar (both sides were open to the atmosphere).

#### **8.4.2 Carbonation**

The progress of carbonation in the 4 microclimates was not clearly defined at 6 months, but it became more distinct with age as revealed by the 12 months results. The differences in carbonation of the blocks due to microclimate were similar in the winter and summer seasons. The carbonation of the east and bottom faces of the blocks was consistently greater than the west and top faces respectively (Figures 5.25 and 6.43). This is in agreement with the air permeability and sorptivity results discussed above. The microclimate

influence on carbonation is evident from the relationship between air permeability and sorptivity of the samples with their carbonation depth given in Figure 8.2.

Considering the winter and summer results for all samples (average values of all blocks in each microclimate), the carbonation depths of the east faces of the blocks were approximately 25% greater than the west faces of the same blocks (see Tables A1.14 and B1.22). Similarly, the carbonation depths of the top faces of the slabs were approximately 50% greater than the bottom faces of the same slabs. Although the above figures provide a sound estimation of the influence of microclimate (since all blocks were cured in exactly the same manner on either side of the blocks), comparing the carbonation results of the non-cured blocks alone (air cured) in the 4 microclimates affords a more accurate quantification of the microclimate influence. This showed that the carbonation depths of the east faces of the non-cured blocks were between 10-50% greater than the west faces, and between 20-100% greater in the bottom faces than the top faces of the same blocks.

The drier microclimates of the partly sheltered east and bottom faces are conducive to higher rates of carbonation than the fully exposed west and top faces of the blocks. Numerous researchers found that the progress of carbonation is predominantly influenced by the microclimate and exposure conditions around the structure (e.g. Osborne, 1994; Parrott, 1987). The observed different rates of carbonation in each microclimate were most probably due to the different moisture content of the permeable pores of the blocks, which determines its permeability to carbon dioxide. Exposure to rain initially increases the pore water content, which hinders CO<sub>2</sub> diffusion and, at the same time, leads to better hydration. This is corroborated by findings of many workers that concrete elements subjected to sheltered outdoor exposure exhibited higher rates of carbonation than exposed concrete (Hudec et al, 1986; Peteresson, 1996; Dunster et al, 1996). The diffusion of carbon dioxide is reported to be around six orders of magnitude slower in water than air (Richardson, 1998).

The carbonation rates of the blocks in the drier east and bottom microclimates were strikingly similar, which confirms the dominant role of exposure in governing the rates of carbonation. Meanwhile, the rates of carbonation of the west and top faces were notably different. The top faces of the slabs benefit more from rain due to its horizontal orientation, and additionally, they were not as prone to drying wind as the vertical west faces. Further, the weather conditions prevailing during the early stages of curing and exposure of the winter and summer blocks may have had an early influence on carbonation, however, this does not appear to have been significant, as no critical differences due to microclimate were detected from the 6 months results. This is a further indication that the long-term exposure conditions of structures play a determining role on carbonation. Additional to exposure to wetting, the microclimate's relative humidity and temperature can influence the rate of carbonation (Parrott, 1987). However, the differences in temperature and relative humidity on either side of the blocks were not generally significant, as all blocks were open to the atmosphere (the east and bottom faces were partly sheltered). Considering the whole exposure period, the exposure of the west and top faces to wetting due to rain and directional rain had a greater influence than the possible drying effect due to solar radiation and wind.

## **8.5 DURATION OF HESSIAN CURING**

### **8.5.1 Permeability and Sorptivity**

Contrary to expectation, the air permeability and sorptivity of the winter series' concretes were generally higher with increased curing duration. The permeability and sorptivity values exhibited no real improvement with increased hessian curing duration, with the non-cured blocks having lower or similar values to the 6 days hessian cured blocks (Figure 5.4 and 5.16). The same trend was observed at 12 months (Figure 5.5 and 5.17). This effect is illustrated in Figure 8.3, which presents the air permeability results plotted against the sorptivity results of the same samples as influenced by curing for the 3 concrete mixes. The agreement between the air permeability and

sorptivity (and carbonation) results and the consistency of the test results at the two ages eliminated any possible uncertainties in the results due to experimental error.

This phenomenon could be explained by the argument raised by Cather (1994) that hessian can act as a wick to remove water from the concrete surface if it is allowed to dry during curing. The hessian, which was deliberately sprayed with water only once in 24 hours to represent poor site curing, was often found dry even after only 4 to 6 hours from being sprayed with water. The wick effect concept is supported by the observation that the concrete in the two driest microclimates, the east and bottom sides of the blocks, suffered most from the longer hessian curing periods. Furthermore, this effect was more striking in the OPC/GGBS concrete than OPC concrete, especially at 12 months (Figures 5.5 and 5.17 (e) and (f)). The significance of these observations are two-fold: firstly, they confirm the reported sensitivity of OPC/GGBS concrete to inadequate curing due to its slower initial rate of reaction compared to OPC concrete (e.g. Osborne, 1986 and Gowripalan et al, 1990); and secondly, they substantiate the suggested detrimental effect of dry hessian on the quality of concrete.

Hessian is rarely kept moist during the required curing period and is often found dry in practice, especially in hot climate countries like Oman. This is not at all surprising since, in a temperate climate country like the UK, hessian was getting dry within hours of wetting. It is rather surprising that this potentially important characteristic of hessian curing remained unnoticed or, at least, unreported despite the numerous studies on curing that have been carried out over the past years in both temperate and hot climates. It is also relevant to mention at this juncture that the effect of practical site curing on the development of durability related properties is not well documented.

While the winter series revealed the unexpected relationship between air permeability and sorptivity with hessian curing, the relationship for the summer series concretes was conventional; the air permeability and sorptivity

decreased with increased hessian curing duration at both the SZ and SSZ, as illustrated in Figure 8.4. The improvement in the air permeability and sorptivity with increased curing was most dramatic in the OPC/GGBS concrete and in the east and bottom faces of the blocks respectively. The reduction in the penetrability properties of the summer concretes was due to the long established beneficial effect of increased curing duration in promoting cement hydration and, therefore, improving the pore structure and reducing the permeability. As stated earlier, the hessian was kept wet for longer duration in the summer due to rain, compared to the winter.

It is of importance to note that the changes in the water sorptivity due to variation in curing were very small. The differences in the air permeability results were much clearer and the trends were more distinct. This suggests that sorptivity test is not very sensitive to the effects of site curing. However, it was interesting to observe that the variation in the sorptivity results due to curing, microclimate and depth from the exposed surface were more marked and conspicuous for the blast-furnace slag concrete, while the responses to the same variables were smaller for the 30 MPa OPC concrete and very small for the 50 MPa OPC concrete (see Figures 6.23, 6.29 and 6.31). The higher permeation, carbonation and porosity of the OPC/GGBS concrete suggests that the capillary absorption test may be more relevant over a certain threshold of pore size ranges corresponding to larger capillary pores. Comparison of the porosity data of the two OPC concretes and the OPC/GGBS concrete (Table 6.4) reveal that the later concrete possesses greater volume of pores with a diameter larger than  $0.1\mu\text{m}$ . In view of the more distinct sorptivity plots for the GGBS concrete (compare figures 6.23(a), 6.29(a) and 6.31(a)) therefore, the implication is that the capillary absorption test is more able to reflect the microstructure and porosity of concretes that are predominantly characterised by coarser pores with diameter greater than  $0.1\mu\text{m}$ . Significant differences, on the other hand, were detected in the air permeability of the three concretes due to curing and microclimate with depth

from the exposed surface, indicating its reliability in assessing changes in concrete over a wide quality (porosity) range.

### 8.5.2 Carbonation

The winter series exhibited higher carbonation depth with increased hessian curing at 12 months. This is apparent, despite some scatter in the results, from Figures 8.5 and 8.6, which shows the relationships between air permeability and sorptivity with carbonation depth as influenced by curing duration. Furthermore, the carbonation was highest in the concrete blocks that received longer hessian curing during the second 6 months of exposure, as some of these blocks exhibited lower carbonation depths initially at 6 months of age. This is in agreement with the winter air permeability and sorptivity results.

Carbonation of concrete is determined by the rate of CO<sub>2</sub> diffusion which depends on concrete's porosity (e.g. Parrott, 1987). Further, concrete porosity and pore structure development is mainly dependent on its degree of hydration (and of course, the W/C ratio), which in turn is determined by the length and effectiveness of curing. It was suggested above that the untimely drying of hessian during curing had a detrimental effect on the quality of concrete. The wick effect of dry hessian caused premature drying and desiccation of the surface layers of concrete, which impeded hydration and microstructure development, resulting in a coarser and more continuous pore system in these layers. This was manifested in the higher air permeability, sorptivity and carbonation in the surface zone of concrete, with increased hessian curing duration. Higher concrete permeability was found to correlate with higher rates of carbonation providing that the concrete is not completely dry, i.e. sufficient moisture is present to enable carbonation reaction (gaseous CO<sub>2</sub> is not reactive) to take place (e.g. Kropp, 1995; Osborne, 1989). As a result, concrete's permeability properties are often being used to indicate its resistance to carbonation (Richardson, 1998).

The OPC/GGBS concrete was most affected by inadequate curing. The depths of carbonation were highest in the slag concrete after 12 months of exposure,

with the carbonation being greater in the 4-6 days hessian cured blocks (Figures 8.5 and 8.6). The carbonation results reaffirms previous statements on the negative effect of dry hessian and confirms slag concrete's reported sensitivity to poor curing (Uomoto and Kobayashi, 1989; Osborne, 1986).

Contrary to the winter results, carbonation decreased with increased curing in the summer series concrete. The 6 and 12 months results showed lower carbonation depths for the concrete blocks that received longer curing duration. The beneficial effect of curing on the carbonation is illustrated in Figures 8.7 and 8.8, which presents the relationships between the air permeability and sorptivity with carbonation depth of the 3 concrete mixes. Curing with hessian for 2 days produced, on average, 10% lower carbonation depths than taking no measure (air curing). The most significant improvements in carbonation were achieved after 4 days of hessian curing; the average reduction in carbonation depths from 0-4 days being approximately 25-30%. Increasing the curing duration from 4 to 6 days resulted in a further average reduction of 15% in carbonation depths.

As previously discussed, the reduction in the penetrability of the summer concrete came as a result of the wetter summer conditions which aided the overall curing of the summer concrete. The observed reduction in carbonation rates due to increased curing time in the summer series is well understood. The influence of curing on hydration and porosity was discussed earlier. Numerous researchers found the rate of carbonation to increase with poor curing or a reduction in the length of curing time (e.g. Osborne, 1986; Parrott, 1987; Peterson, 1996; Bamforth, 1997).

### 8.5.3 Porosity and Hydration

The general trend of the hydration results of the winter series is consistent with the penetrability and carbonation results. With the progress of hydration, the volume of hydration products i.e. calcium silicate hydrates (C-S-H) & calcium hydroxide (CH), calcium aluminate hydrates (C-A-H) and tetracalcium aluminoferrite hydrates (C-F-H) increases and therefore the

amount of chemically combined water and calcium hydroxide content increases. However, Figure 5.31 shows that there was no real increase in the hydrates and calcium hydroxide water contents of the 30 MPa OPC concrete with prolonged hessian curing. Furthermore, although the hydrate water content was slightly higher for the OPC/GGBS concrete than the plain OPC concrete, the adverse drying effect of hessian was more conspicuous in the OPC/GGBS results as the hydrates water content appeared to decrease (indicating poorer quality) with increased hessian curing at the surface and subsurface layers. The limited data of the 50 MPa OPC concrete does not enable comparison with the penetrability and carbonation results (see Table A1.15). Further, it was surprising to see that the differences in the calcium hydroxide content between the 3 mixes were small despite the noted differences in their cement contents.

The effect of hessian curing duration on the total pore volume and coarse capillary porosity of the two OPC concretes of the summer series was much less dramatic than the OPC/GGBS concrete. Surprisingly, the difference in pore volume between the non-cured and 2 days cured blocks of the 30 and 50 MPa OPC concrete was not significant. However, notable reduction in the total pore volume and the volume of coarse capillary pores of both concretes was achieved after 4 and 6 days curing. Contrary to expectation, the reduction in the volume of smaller pores of the two OPC concretes with improved curing was more significant than the volume of capillary pores.

The non-cured OPC/GGBS concrete blocks had the highest pore volume (see Table 6.4 and Figure B1.13). Significant improvement in the pore volume was achieved with continued curing (summer series concrete) with the 6 days cured blocks having a substantially lower total pore volume than the other blocks. Surprisingly the improvement in the coarse capillary pore volume was only significant at the surface, as it remained virtually constant in the inner layers of the concrete regardless of curing time.

The reduction of porosity with prolonged curing of the summer series' concrete indicates the effectiveness of curing in promoting cement hydration.

Continued hydration sustained the production of hydrates, which were concurrently deposited in the pore space thereby reducing the pore volume and its continuity. The TG results suggest that the hydration at the surface of the samples progressed steadily with prolonged curing of the summer concrete. The chemically bound water in the cement hydrates and calcium hydroxide increased as the production of hydrates increased due to increased curing duration from 0 to 6 days for both concretes. There was no improvement in both parameters at the subsurface, as shown in Figure 6.51. However, the magnitude of improvement due to curing at the surface layer was small and it does not appear to reflect the change in quality as detected by the air permeability and sorptivity tests. Similar remarks were made by other researchers who observed no significant variations due to curing in the calcium hydroxide and combined water contents as determined by TG (Odler and Chen, 1995). Further, it was also surprising that the differences between the hydrates water and calcium hydroxide water contents were very small. This is because in a fully hydrated concrete samples, the C-S-H are expected to constitute 70% of the total weight of the solid material compared to approximately 20% CH (Barker and Barnes, 1984). Furthermore, the hydrate water and lime water contents of the 50 MPa OPC concrete was expected to be notably higher than the 30 MPa OPC concrete due to its higher cement content.

## **8.6 CURING METHOD**

### **8.6.1 Permeability and Sorptivity**

The results of the summer series, where a wider range of curing regimes were tested, showed that the wet hessian curing method was more effective in improving the surface penetrability properties than the water retention methods, i.e. covering with polythene sheets and curing membrane. The differences between the various curing methods reduced with age. The application of curing membrane produced similar quality concrete to the 2 days hessian cured concrete at 12 months, however, the C/M appeared to be

more effective on the horizontal surfaces (slabs) than the vertical blocks (see Figures 6.13 and 6.33). Covering the blocks with polythene sheets for 6 days generally produced similar quality to the 4 days hessian cured concrete. These findings are in agreement with numerous reports about the effectiveness and advantages of the wet curing methods over the moisture retention methods in improving concrete quality (e.g. CIRIA, 1984; Petersson 1996). Wet methods have an additional cooling effect on the concrete surface and may provide additional water that can be imbibed by the surface layers, thereby promoting hydration. Many researchers found that hydration of concrete was severely hindered if the curing relative humidity falls below a critical level that corresponds to an internal relative humidity within the concrete of about 80% (e.g. Killoh et al, 1989; Patel et al, 1988, 1985; Parrott et al, 1986; Ho et al, 1989).

### **8.6.2 Carbonation**

The 6 days polythene-curing regime produced a slightly higher carbonation depth than 4 days hessian curing, and approximately 10% lower carbonation depths than the curing membrane regime.

## **8.7 CONTROLLED PERMEABILITY FORMWORK**

### **8.7.1 Permeability and Sorptivity**

The application of CPF was effective in reducing the air permeability and sorptivity of the cover concrete. The results showed dramatic reduction in the air permeability values at the surface of the CPF-produced concrete compared to that cast against conventional formwork. For the east and west faces of the blocks, the CPF-produced concrete was on average 20 times less permeable than the conventional formwork samples after 12 months of field exposure.

The difference between the CPF and conventional formwork samples was smaller for the slabs, the CPF concrete being approximately 5 times less permeable. The differences between the CPF and normal formwork concretes as detected by the sorptivity test were significantly less marked than the air permeability. For the east and west faces of the blocks, the sorptivity of the

CPF concretes was 2-4 times lower than the companion conventional formwork samples. Similarly, the capillary absorption of the CPF slabs was only 25-50% lower than the conventionally produced samples. This verifies the results of tests (performed mainly on laboratory size specimens) reporting the benefit of CPF in significantly improving the surface permeability and strength, reducing the surface W/C ratio and enhancing the resistance of concrete to carbonation and chlorides (Price, 1993; Wilson, 1994; Long et al, 1996; Serafini et al, 1997).

It is remarkable that the surface air permeability and sorptivity of the CPF-produced OPC/GGBS concrete became comparable with that of the 50 MPa OPC concrete that was conventionally produced (Compare Figures 6.9 and 6.29 with Figures 6.20, 6.40 and 6.41). This demonstrates that CPF can be effective in mitigating blended cement concrete's sensitivity to curing. Furthermore, CPF-produced concrete was significantly less sensitive to the effects of curing and microclimate than nominally identical concrete cast against normal formwork. In addition, the surface appearance of the CPF-produced concrete was improved considerably, resulting in an almost blowhole-free surface.

These results confirm the suggested beneficial effect of CPF systems in improving the surface permeation properties and appearance. The magnitude of improvement in the surface penetrability properties has encouraging implications for concrete's service performance and longevity. The benefits of the CPF systems comes from its ability to effectively drain excess water and entrapped air from the fresh concrete during compaction through its filter fabric combined with retention of cement, which modifies the W/C ratio close to the interface with the formwork. As a result, the W/C ratio and capillary porosity is significantly reduced in the near surface region of concrete resulting in a denser less permeable matrix (Richardson, 1993 and Long et al, 1996). The 3 months air permeability results (see Figure 6.14) initially raised concern on the depth of influence of CPF, as the inner layers (from 20-50 mm) of CPF-produced concrete were constantly more permeable relative to

conventional formwork concrete. However, the results after 12 months showed that CPF concrete had improved concrete permeability from the surface down to around 10-20mm deep.

### 8.7.2 Carbonation

The carbonation of the OPC/GGBS concrete blocks that was cast against controlled permeability formwork liners was notably lower than similar blocks cast against conventional formwork, regardless of curing method. The depth of carbonation of the CPF-produced concrete being, on average, 3 times lower. Moreover, the non-cured CPF-produced concrete blocks exhibited lower carbonation than any cured concrete blocks that were cast against conventional formwork. Hence, the benefit of CPF by itself was more significant in this case than any benefit that originated from curing. As with the air permeability and sorptivity results, the variation in the carbonation depths of the CPF-produced samples were less pronounced than the companion conventionally produced concrete, indicating lower sensitivity to the differing curing regimes. By comparing the carbonation results of the CPF-produced OPC/GGBS concrete with that of the 50 MPa OPC concrete (Figure 6.43 with 6.47), it is apparent that the benefit, in terms of penetrability and carbonation, of using CPF systems almost equates to that of adopting a higher strength concrete.

The effect of CPF on carbonation control is quite significant when viewed in terms of the assumed proportional progress of carbonation with the square root of time. This shows that, under the same exposure conditions, the CPF-produced concrete have approximately 9 times the life expectancy of the conventionally produced concrete when considering carbonation induced corrosion.

## 8.8 CONCRETE TYPE

### 8.8.1 OPC Concretes: 30 MPa versus 50 MPa

The permeation properties (permeability and sorptivity), carbonation depth and porosity of the 50 MPa OPC concrete were significantly lower than the lower strength class, 30 MPa OPC concrete. This can readily be acknowledged from the results presented in Figures 8.1 to 8.8 and Tables 8.1 and 6.4. Furthermore, the 50 MPa concrete was far less sensitive to microclimate and inadequate curing effects than the 30 MPa concrete. In addition, the difference in magnitude between the SZ and SSZ permeability and sorptivity values was much lower than the 30 MPa concrete. This implies that the quality of surface concrete of the 50 MPa is superior to the lower strength class, 30 MPa OPC concrete. Generally, the air permeability and sorptivity of the 50 MPa were respectively between 3-12 and 1.5-2 times lower than the equally cured 30 MPa OPC concrete. Similarly, the carbonation depth was on average 2-3 times lower than the 30 MPa OPC samples and the porosity was 40-50% lower.

The notable improvement in the performance of the 50 MPa concrete is mainly attributable to its increased cement content and lower W/C ratio, which has two main effects on the matrix. The first is the increased volume of hydration products produced (under the same conditions), which leads to better densification of the pore structure (more hydrates to fill the pores) and subsequent reduction in the pore volume and its continuity. The second effect is the closer particle packing in the matrix and the reduction in the water occupied space, which results in a reduction in the volume of larger pores. This is supported by the significantly reduced total pore volume and capillary porosity especially in the samples that received longer curing time.

It has long been ascertained that concrete's protection against carbonation induced corrosion is chiefly afforded by the high alkalinity of its pore water, which is mainly attributable to the presence of calcium hydroxide. The calcium hydroxide ( $\text{Ca}(\text{OH})_2$ ) originates from the reaction of the two major compounds of Portland cement, Alite ( $\text{C}_3\text{S}$ ) and Belite ( $\text{C}_2\text{S}$ ) (see Section 2.1.2).

Numerous researchers reported that the rate of carbonation is increased with decreased cement or  $\text{Ca(OH)}_2$  content (e.g. Bier et al, 1989; Parrott, 1987; Soroka, 1993; Neville, 1995). However, the higher resistance of the 50 MPa concretes to carbonation is not only brought about by its higher calcium hydroxide content, but probably more significantly, also by the lower W/C ratio usually associated with increased cement content. A reduction in W/C ratio greatly reduces the measured depth of carbonation (e.g. Skjolsvold, 1986; Parrott, 1987). This is because lower W/C ratio, with provision of effective curing, is known to result in lower concrete porosity and permeability or diffusivity (e.g. RILEM, 1995). As a result of the close relation of cement content, W/C ratio and curing to concrete's strength, good correlations were obtained directly between compressive strength and depth of carbonation (e.g. Osborne, 1986; Parrott, 1987). Although the strength/carbonation relationship is not unique (carbonation also depends on other factors such as CaO content and  $\text{CO}_2$  concentrations), it is generally presumed that carbonation rate is inversely proportional to strength (e.g. Hilsdorf, 1995; Richardson, 1998).

### **8.8.2 30 MPa Concretes: OPC versus OPC/GGBS**

The plain OPC concrete was consistently less permeable to air and water than the OPC/GGBS concrete. After 12 months of exposure, the air permeability values of the slag concrete were approximately 2 times higher than the plain Portland cement concrete in the winter and summer series especially at the surface (see Table 8.1). The sorptivity of the OPC/GGBS concrete was 10-25% higher than the equivalent OPC samples particularly at the surface (Table 8.1). Further, the ground granulated blast-furnace slag concrete was significantly more susceptible to carbonation than plain Portland cement concretes, the carbonation depth being on average two times higher (average 11mm) than the plain OPC concrete samples (average 6mm).

It has been reported that slag concrete and in particular that with high OPC replacement levels is more vulnerable to carbonation than equivalent plain

OPC concretes (e.g. Bier et al 1989; Osborne, 1986 and 1994; Parrott, 1996). However, views as to the basic reasons behind this tendency when given have been vague and conflicting. On the one hand, this has been attributed to slag concrete's lower  $\text{Ca(OH)}_2$  content, as depths of carbonation were found to be greater with reduced amount of  $\text{Ca(OH)}_2$  in concrete (Parrott, 1996; Neville, 1995; Soroka, 1993). Others, on the other hand, ascribe slag's higher carbonation to its greater sensitivity to inadequate curing, which results in a coarser pore system that facilitates carbonation (Sims, 1994; Osborne 1986). The first argument has not been explained against the logical inference that carbonation of concrete with low  $\text{Ca(OH)}_2$  is anticipated to be severely retarded upon its exhaustion, especially since the amount of other present alkalis ( $\text{K}_2\text{(OH)}_2$  and  $\text{Na}_2\text{(OH)}_2$ ) that can react with  $\text{CO}_2$  are small. This is particularly relevant in view of the repeated reports that it is the dissolution of OH ions from the  $\text{Ca(OH)}_2$  which accentuates carbonation (i.e. the reduction of alkalinity) and not the formation of  $\text{CaCO}_3$  by it self (Litvan and Meyer, 1986; Sims, 1994; Taylor, 1990). The second argument may explain the higher initial rates of carbonation of slag concretes, but does not offer a viable justification to the reported, ultimately higher carbonation depths of slag concretes compared to OPC concretes, especially since the former has a significantly lower  $\text{Ca(OH)}_2$  content to undergo conversion (further reduction in alkalinity). It has been suggested that when all  $\text{Ca(OH)}_2$  have been consumed,  $\text{CO}_2$  can react with all other cement hydrates, such as C-S-H and the various calcium aluminate and ferro-aluminate phases (Parrott, 1987; Neville, 1995; Kropp, 1995). Consequently, the C-S-H decomposes into  $\text{CaCO}_3$  and a highly porous silica gel with pores larger than 100 nm (capillary pores sizes range from 10-10,000 nm), which facilitates further carbonation.

It is proposed that a more reasonable explanation of the higher carbonation rates of the OPC/GGBS concrete can be given in the light of its significantly higher air permeability and sorptivity results, compared to OPC concretes. This becomes more apparent when comparing the carbonation results of the slag concretes made with and without the CPF liners, as the carbonation

depth was more than 3 times lower for CPF-produced samples. Indeed as mentioned before, the carbonation depth of the CPF-produced OPC/GGBS concretes was notably lower than the equivalent strength plain OPC concrete and similar to the 50 MPa OPC concrete which were produced with conventional formwork. It has been pointed out earlier that slag concrete requirement for curing exceeds that of its equivalent strength OPC concrete, if similar permeation resistance is to be achieved. Moreover, the initially reduced  $\text{Ca(OH)}_2$  (alkalinity) of the slag concrete due to OPC replacement would have undoubtedly influenced the short term carbonation readings of this investigation. Calcium hydroxide is solely produced by OPC upon hydration, as GGBS cements on hydration do not produce significant amounts of  $\text{Ca(OH)}_2$ . In the OPC/GGBS concrete of this investigation, 70% of the OPC was replaced with GGBS cement, and as such the  $\text{Ca(OH)}_2$  content would have been significantly lower compared to its equivalent plain OPC concrete. However, the lower content of  $\text{Ca(OH)}_2$  is not only due to OPC replacement, but also to the consumption of  $\text{Ca(OH)}_2$  by the slag cement during its reaction (Kokubu et al 1989; Litvan and Meyer, 1986). Neville (1995) stated that reduced amounts of  $\text{Ca(OH)}_2$  in concrete means that lower levels of  $\text{CO}_2$  can readily deplete all  $\text{Ca(OH)}_2$  during their reaction to form  $\text{CaCO}_3$ . Nevertheless, it is thought that better distinction between the influence of the initial  $\text{Ca(OH)}_2$  content and permeability on the carbonation of blast-furnace slag concrete can only be afforded through long term physical and microstructural data of comparable OPC and GGBS concretes.

Generally, the pore volume of the OPC concrete was significantly lower than the OPC/GGBS concrete. The difference in porosity between the two mixes was particularly striking at the surface layer (5mm) and with poor curing. The total pore volume of the non-cured blocks being on average, more than 60 % higher in the slag concrete than the OPC concrete. This confirms that lack of curing has a more damaging effect on slag concrete than the equivalent OPC concrete. The difference in porosity between the two concretes reduced with increasing depth from the surface and with increased curing duration.

However, after 6 days curing the volume of coarse capillary pores was approximately 30% higher in the slag concrete than the OPC concrete (Table 6.4).

The reasons behind slag concrete's higher porosity compared to OPC concrete were discussed earlier. The results illustrated that poor or lack of curing results in increased total pore volume and the volume of coarse pores owing to the cessation of hydration especially in slag concrete. Slag concrete's extra vulnerability to the effects of inadequate curing and premature drying that stems for its slower initial rate of hydration and pore structure development was evident. This was demonstrated by the fact that after 6 days curing, the pore volume of slag concrete was, on average, 30% higher than identically cured OPC concrete. This clearly confirms that slag concrete requirement for curing exceeds that of equivalent OPC concrete if it is to achieve similar performance levels.

It is appropriate to point out at this point that the accuracy of porosity results can be compromised owing to the limitations of the mercury intrusion technique exceptionally when applied to blended cement samples such as slag. Feldman (1986) reported that high pressure mercury intrusion can cause damage to the pores of samples particularly those made of blended cements. However, the porosity results of the OPC/GGBS samples can be viewed with confidence since they are in good agreement with the results obtained from the permeation and carbonation tests.

## **8.9 AGE: 3 MONTH VERSUS 12 MONTHS**

### **8.9.1 Permeability and Sorptivity**

The air permeability and sorptivity of the 3 concrete mixes of the Loughborough series generally improved with age. The variations in the air permeability indices due to age were noticeably more marked than the sorptivity. It is interesting to note that the improvement with age in the air permeability and sorptivity was greater in the summer series than the winter

series concrete. This is consistent with the general trend of the results of the two series where the performance of the Loughborough summer series was largely better than the winter series. Further, the improvement in the permeability and sorptivity indices with age was greater in the two OPC concretes than the OPC/GGBS concrete although the performance of some OPC/GGBS samples was slightly better at the SSZ.

For the winter series concrete, the air permeability of the two OPC concretes was generally 2 times lower at 12 months compared to 3 months. This is compared to approximately 10-20% improvement in the air permeability indices of the 30 MPa OPC/GGBS concrete after 12 months of exposure. The sorptivity test results indicated between 25-50% and 25% improvement in the sorptivity indices of the two OPC concretes and OPC/GGBS concrete respectively after 12 months of field exposure. For the Loughborough summer series, the air permeability of the two OPC and OPC/GGBS concrete after 12 months of exposure was 2-5 times and 10-20% lower respectively than at 3 months of age. This is compared to 2-3 times reduction in the sorptivity indices of the two OPC concretes and 20-30% reduction for the OPC/GGBS concrete after 12 months of exposure.

The sorptivity of the OPC concrete of the Muscat series showed a slight improvement of approximately 10% with age. However, the capillary absorption of the OPC/GGBS concrete increased after 12 months of exposure by approximately 10-30% relative to the 3 months results particularly at the surface.

The improved permeability of OPC concrete with age and the adverse effect in the OPC/GGBS concrete (especially at the SZ) can be explained by the differences in the development of their pore structure. At early age, the pore structure of concrete is characterised by a continuous pore system termed "capillary porosity". If water is available, hydration will continue and capillary porosity will reduce due to the formation of additional hydration products, which continuously fill the pores. Thus, the reduction in capillary

porosity is essentially a function of the extent of hydration. This seems to have taken place in OPC concrete resulting in a significant reduction in its permeability (which is a function of porosity) with age. However, due to its slower initial rate of hydration, the formation of hydrates at early age of slag concrete is reduced, resulting in a coarser and more continuous capillary porosity, which under the same drying conditions leads to increased loss of moisture (evaporation) that would otherwise be available for hydration to continue (Parrott, 1995; ACI, 1995). This is particularly apparent from the sorptivity results of the Muscat series where the hot weather effect had a more adverse effect on the OPC/GGBS concrete than the plain OPC concrete. In addition to its serious effect on hydration, water evaporation from the surface invariably leads to surface cracking, which further influences the permeability. This, in turn, reaffirms the earlier statement, made in view of the results, about slag's requirements for more stringent curing measures relative to OPC concrete. The improvement in the air permeability and sorptivity of the Loughborough summer series with age comes as a result of the improved early curing conditions in the summer as discussed earlier.

### **8.9.2 Carbonation**

The carbonation depth increased with exposure time of the Loughborough winter and summer series. However, the carbonation rate varied substantially in the various samples, depending on the curing regime, concrete strength, cement type, micro and macroclimates involved, as shown in the preceding sections. Generally, the increase in carbonation depth with age was greater in the winter than the summer, in the drier east and bottom microclimates, in OPC/GGBS concrete than equivalent OPC concrete, in lower concrete grade and with poor curing. These results are in agreement with numerous reports on the factors influencing the rate of carbonation of concrete which were mainly related to two factors, namely: (1) concrete materials i.e. mix proportions, cement type and curing; and (2) exposure conditions i.e. temperature, relative humidity, rain, wind and CO<sub>2</sub> concentration.

The rate of carbonation of concrete is generally assumed to follow a square root of time relationship (e.g. Richardson, 1998; Bamforth, 1997; Balen and Gemert, 1994). However, the substantial variation in carbonation rates depending on the numerous variables above, together with the limited short term, 6 and 12 months data available rendered the modelling of carbonation impossible. Nevertheless, these variations clearly highlighted the limitation of the assumed theoretical relationship between carbonation and the square root of time particularly in modelling field concrete. However, if a square root relationship is to be considered as a starting point, then a rate of carbonation model similar to that proposed by Richardson may be applicable to predict carbonation of concrete in the field (Richardson, 1998). Based on the results from this work, the model will need to account for several important factors such as exposure conditions (e.g. dry or wet), permeability or diffusivity, cement type and W/C ratio. Such a model can be expressed as:  $d = (f_1 \text{ to } f_n) t^e$ , where  $d$  is depth of carbonation after  $t$  years of natural exposure,  $f_1$  to  $f_n$  are factors including those listed above, and  $e$  is a power exponent related to exposure. Validation with substantial carbonation data from field concrete is essential if successful prediction of future behaviour is to be achieved.

## **8.10 CORRELATIONS BETWEEN PROPERTIES**

### **8.10.1 Permeability and Sorptivity**

The relationship between the coefficient of air permeability and sorptivity of the winter and summer series at the surface and subsurface is presented in Figure 8.9. As can be seen, the correlation between the two test results was poor with the average coefficient of correlation being 68% significant. This finding is similar to that of Parrott (1996) who found that there was no close correlation between the 4 hour water absorption ( $\text{kg}/\text{m}^2$ ) and coefficient of air permeability ( $\text{m}^2$ ).

### 8.10.2 Carbonation

Figure 8.10 presents the relationship between depth of carbonation with surface air permeability and sorptivity, after one year of field exposure for the winter and summer series. The best correlation was obtained between carbonation depth and air permeability with an average correlation coefficient of approximately 0.90 for the winter and summer results. Plotting the winter and summer air permeability results together against carbonation depth gave weaker correlation ( $r = 0.85$  compared to 0.92). This is an indication of the influential effect of exposure and curing environment on the development of carbonation. The correlation between the carbonation depth and sorptivity was a lot weaker than with air permeability, with an average correlation coefficient of 0.75 for the winter and summer results. Dhir et al (1994) noted that correlation between surface absorption and chemically related durability characteristics, e.g. carbonation and chloride diffusion, is less strong than the correlations with physical durability aspects (e.g. freeze/thaw and abrasion resistance). The poor correlation demonstrates that the capillary suction transport process is not indicative of  $\text{CO}_2$  diffusion characteristics. However, the linearity in the sorptivity-carbonation relationship is evident despite the scatter of results. It is worth noting that the results of the air permeability, sorptivity and carbonation tests were obtained from the same surface discs.

The relationships between the carbonation depth with coarse capillary porosity, volume of small pores and total porosity of the summer series concretes are presented graphically in Figure 8.11. The correlation coefficients for the three relationships respectively were 0.89, 0.79 and 0.86. The influence of curing and concrete type on the carbonation and porosity of the samples is apparent from the graphs.

As with the air permeability, the best correlation was obtained between carbonation depth and coarse capillary porosity ( $r = 0.89$ ). The diffusion of  $\text{CO}_2$  into concrete was shown to be influenced by the volume of coarse capillary pores and increased linearly with increased volume of these pores, as shown Figure 8.11 (a, b). The carbonation depth exhibited lesser

dependence on the volume of smaller pores ( $r = 0.79$ ). This finding contradicts the theoretical postulation that the entire pore volume above  $0.001 \mu\text{m}$  in radius is relevant for gas diffusion and that the diffusion coefficient is independent of pore size or surface (Meng, 1994).

Capillary porosity was taken as the total intruded volume corresponding to the pore diameter size range from  $10 \mu\text{m} - 0.006 \mu\text{m}$  ( $6 - 10,000 \text{ nm}$ ) i.e. from the larger gel pores (meso pores) to the largest capillary pores according to Powers pore size classification (Young, 1988). Numerous workers found correlations between carbonation depth and porosity (e.g. RILEM, 1995). Although the surface porosity results are relatively limited to permit accurate assessment of the relationship with carbonation, the available results readily indicate that carbonation diffusion is eased with increased capillary porosity.

### 8.10.3 Porosity

The relationship between the coefficient of air permeability and coarse capillary porosity, volume of smaller pores and total porosity was investigated separately and is presented graphically in Figure 8.12. The graphs also illustrate the influence of curing and concrete type on the air permeability and porosity. The best correlation was obtained between the surface air permeability and surface coarse capillary porosity with a correlation coefficient of 0.89 (Figure 8.12 (a, b)). The first two relationships were plotted by considering the surface values (5mm) of the investigated variables. The air permeability-total porosity relationships were evaluated using the surface and subsurface permeability and porosity data, i.e. taking into consideration the effect of depth (5 to 20 mm from the surface).

The better correlation between air permeability and coarse capillary porosity emphasises the importance of large capillary pores ( $> 0.1 \mu\text{m}$ ) in the transport process of fluids into concrete. The relationship clearly illustrates that higher volume of coarse capillary pores results in increased permeability to air. However, the relationship between the air permeability and porosity in general was reasonably good, as verified by its plot against the volume of

small pores and total porosity, the coefficients of correlation respectively being 0.83 and 0.76. As shown in Figure 8.12, the air permeability increased approximately linearly with an increase in the volume fraction of pores in all pore size ranges and varied with depth accordingly.

Contrary to expectation, the regression analysis of sorptivity and porosity exhibited poor correlation with all three porosity parameters; the correlation coefficients with capillary porosity, volume of small pores and total porosity being 0.61, 0.58 and 0.59 respectively, as shown in Figure 8.13. It was anticipated that a better relationship should exist particularly between sorptivity i.e. water absorption due to capillary suction and capillary porosity, since theoretically, water suction by capillarity takes place in the same pore size range considered. Further, capillary suction relies principally on the same porosity fraction as permeability and the same pore size is expected to influence both parameters (Meng, 1994). This is further complicated by the fact that water sorptivity obeyed almost perfectly the  $\sqrt{t}$  relationship ( $r > 0.99$ ). The poor correlation, therefore, cannot be attributed to the possible complication that may arise from the interaction between water and concrete during water transport through it. Such interaction include, for example, the restriction of flow due to hydration, solubility of gases and solids in the pore ways during water migration or changes in water viscosity and surface tension as a result of the changing pore geometry which affects flow. A good implication from these variations is that different pore size ranges in the same concrete are involved in different transport processes depending on the physical and chemical characteristics of the transport process and the medium transported.

**Table 8.1** Summary of air permeability and sorptivity results of the 3 concrete mixes at the age of 12 months at the surface and subsurface as influenced by the macro and microclimate (average values)

Macroclimate	Microclimate	30 MPa OPC concrete				50 MPa OPC concrete				30 MPa OPC/GGBS concrete			
		Air Perm. ( $10^{-16}$ ) m <sup>2</sup>		Sorptivity (mm/min <sup>0.5</sup> )		Air Perm. ( $10^{-16}$ ) m <sup>2</sup>		Sorptivity (mm/min <sup>0.5</sup> )		Air Perm. ( $10^{-16}$ ) m <sup>2</sup>		Sorptivity (mm/min <sup>0.5</sup> )	
		SZ	SSZ	SZ	SSZ	SZ	SSZ	SZ	SSZ	SZ	SSZ	SZ	SSZ
Loughborough Winter	E	5.33	3.66	0.165	0.193	0.49	0.47	0.073	0.113	12.8	6.87	0.176	0.126
	W	2.92	2.61	0.121	0.175	0.36	0.38	0.053	0.104	8.77	6.93	0.127	0.118
	T	1.15	1.27	0.082	0.142	0.23	0.36	0.061	0.099	5.53	2.56	0.103	0.084
	B	1.92	1.62	0.098	0.162	0.67	0.51	0.071	0.114	6.66	3.59	0.116	0.098
Loughborough Summer	E	4.42	4.65	0.108	0.182	0.36	0.36	0.056	0.109	9.58	5.75	0.164	0.133
	W	2.92	3.22	0.091	0.175	0.32	0.33	0.057	0.104	7.5	3.28	0.119	0.104
	T	1.43	1.6	0.076	0.153	0.23	0.29	0.065	0.105	2.29	1.92	0.093	0.093
	B	2.91	1.99	0.086	0.163	0.35	0.3	0.067	0.107	4.75	1.82	0.109	0.099
Muscat Summer	E			0.287	0.251							0.356	0.202
	W			0.291	0.249							0.361	0.218

**Key:** SZ= 10mm values; SSZ= 20-40mm values; E, W, T and B = east, west, top and bottom faces of the blocks respectively

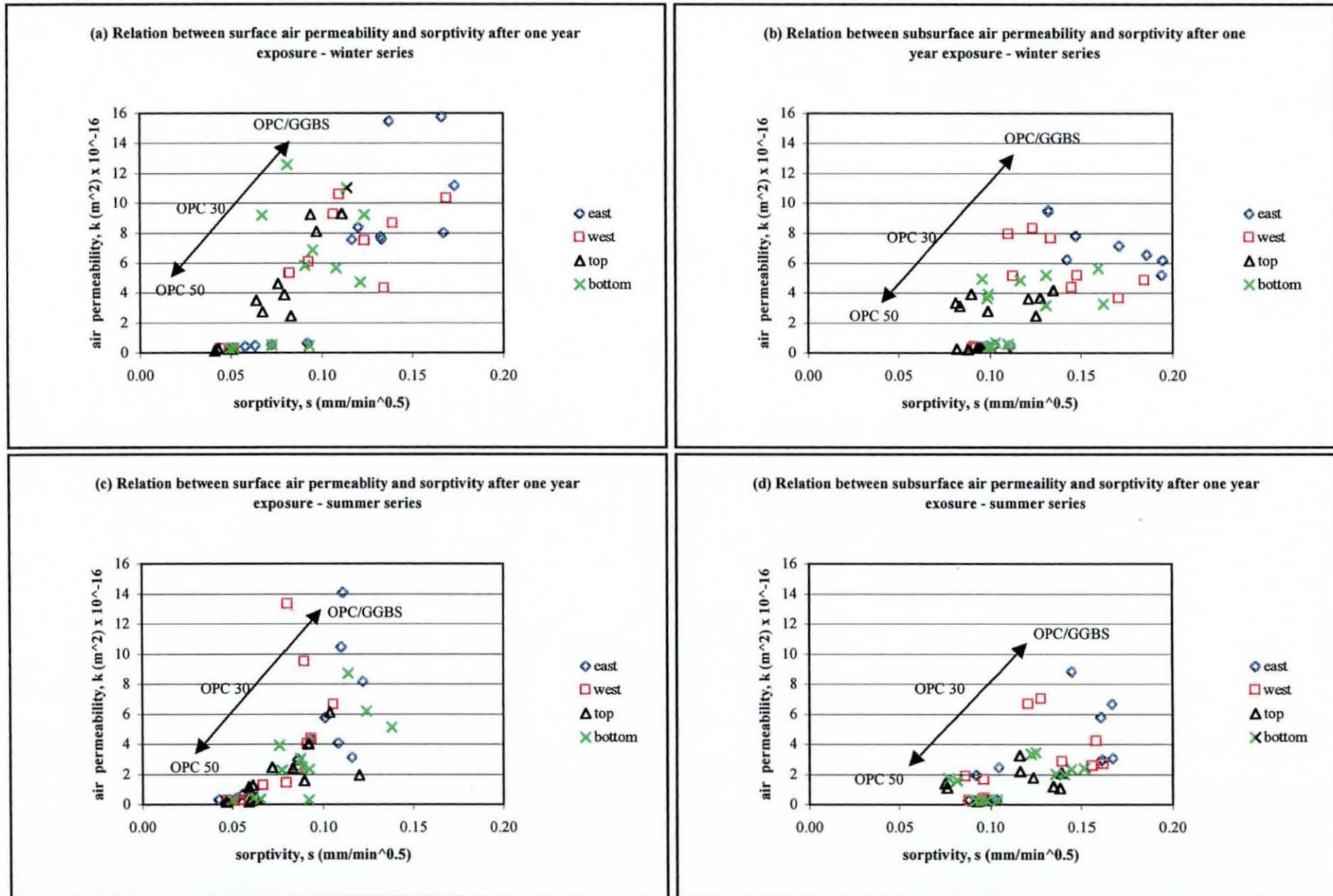


Fig. 8.1 Relationship between air permeability and sorptivity after one year of exposure of winter and summer series - effect of micro and macro climate

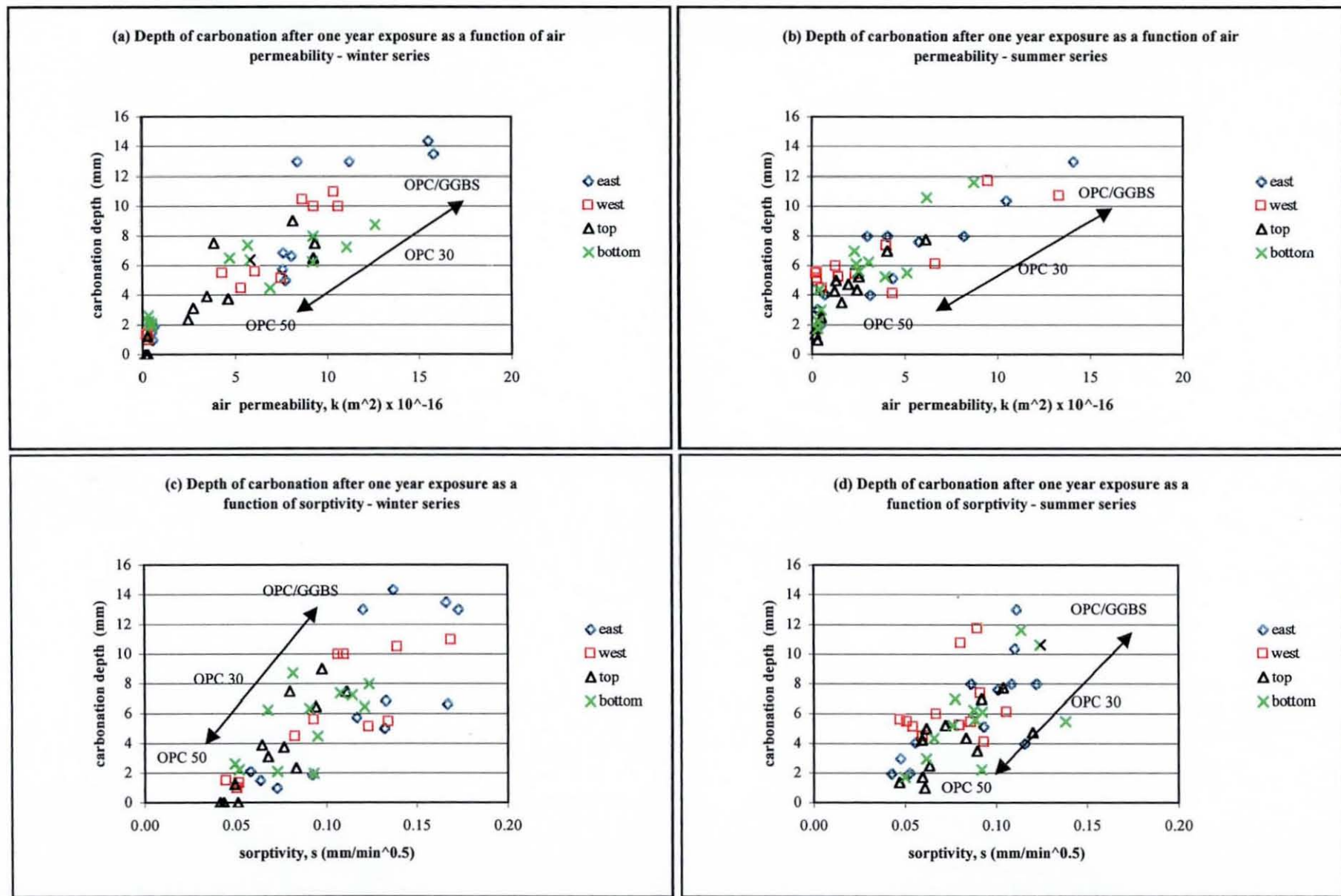


Fig. 8.2 Relationship between air permeability and sorptivity with carbonation after one year of exposure of winter and summer series- effect of micro and macro climate

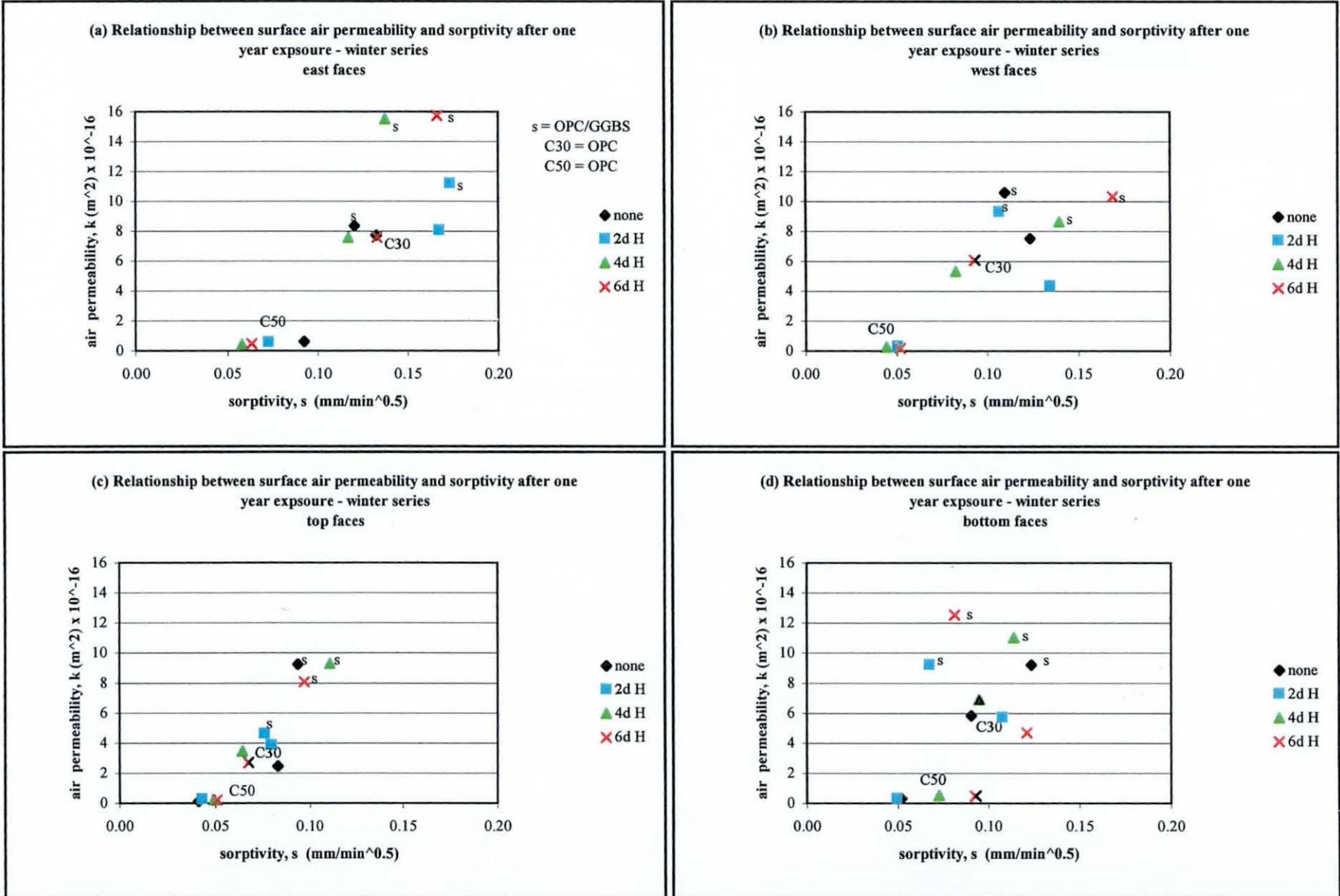


Fig. 8.3 Relationship between air permeability and sorptivity of the winter series after one year of exposure - effect of microclimate, curing and concrete type

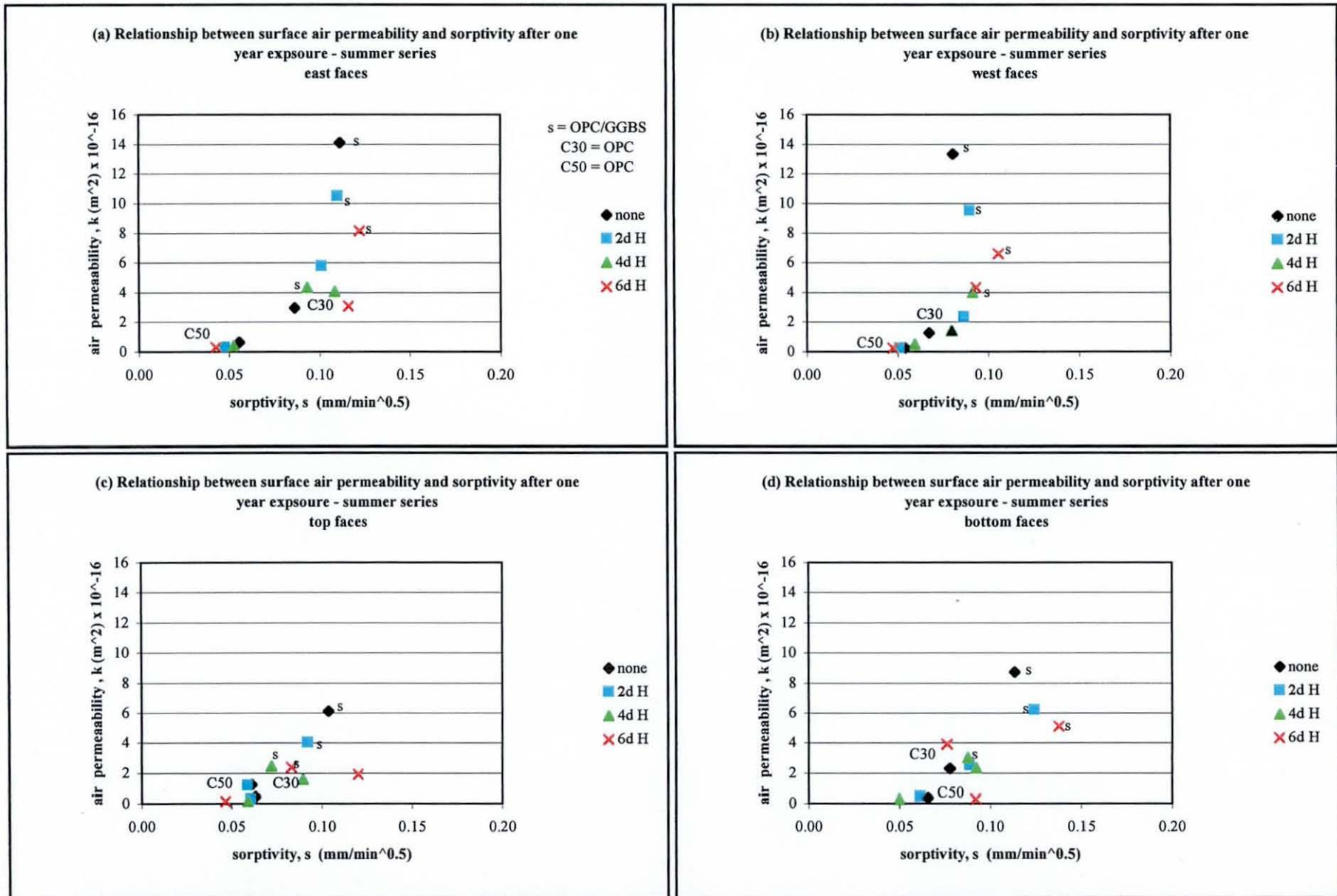


Fig. 8.4 Relationship between air permeability and sorptivity of the summer series after one year exposure - effect of microclimate, curing and concrete type

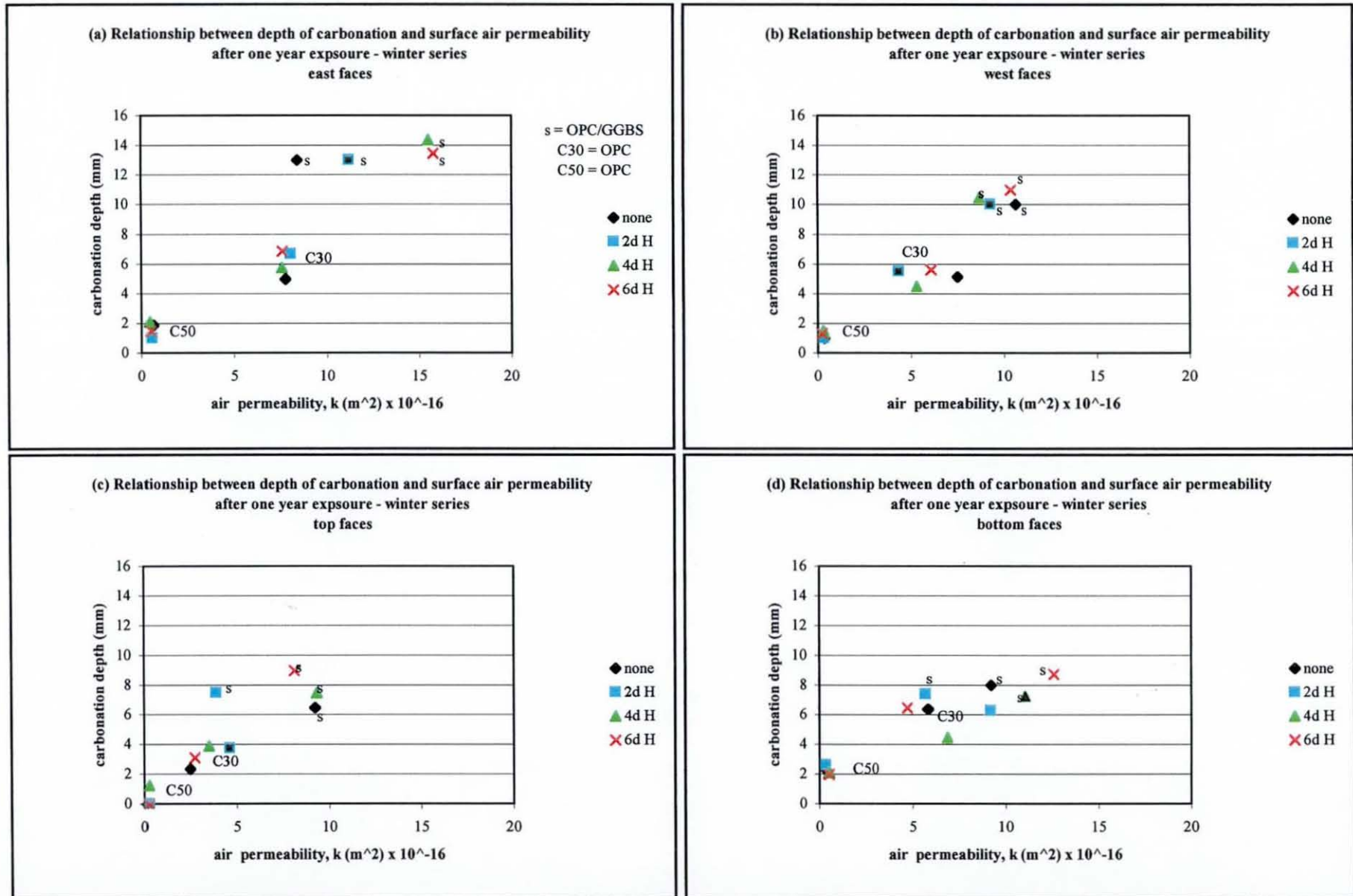


Fig. 8.5 Relationship between air permeability and depth of carbonation of the winter series after one year of exposure - effect of microclimate, curing and concrete type

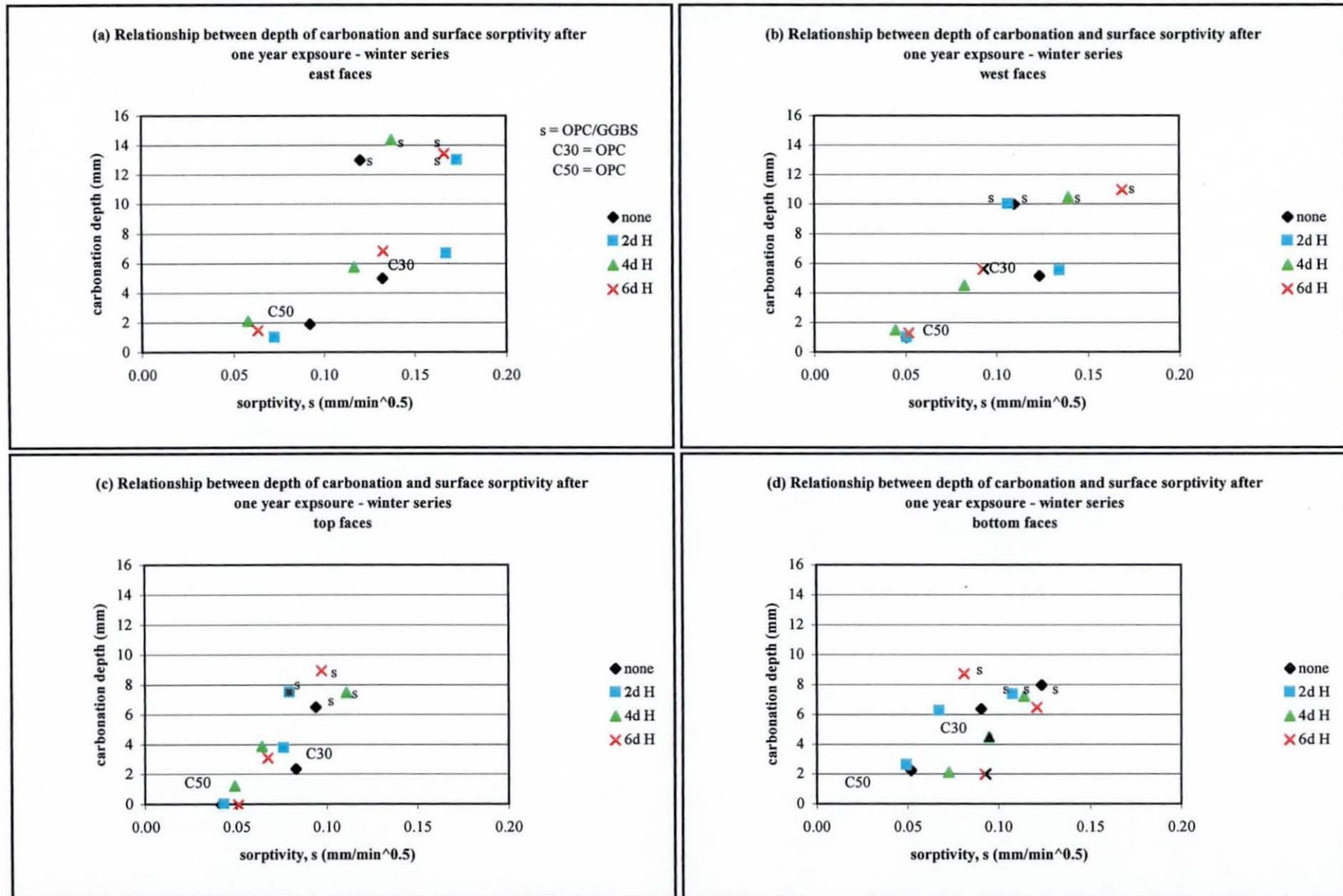


Fig. 8.6 Relationship between surface sorptivity and depth of carbonation of the winter series after one year of exposure - effect of microclimate, curing and concrete type

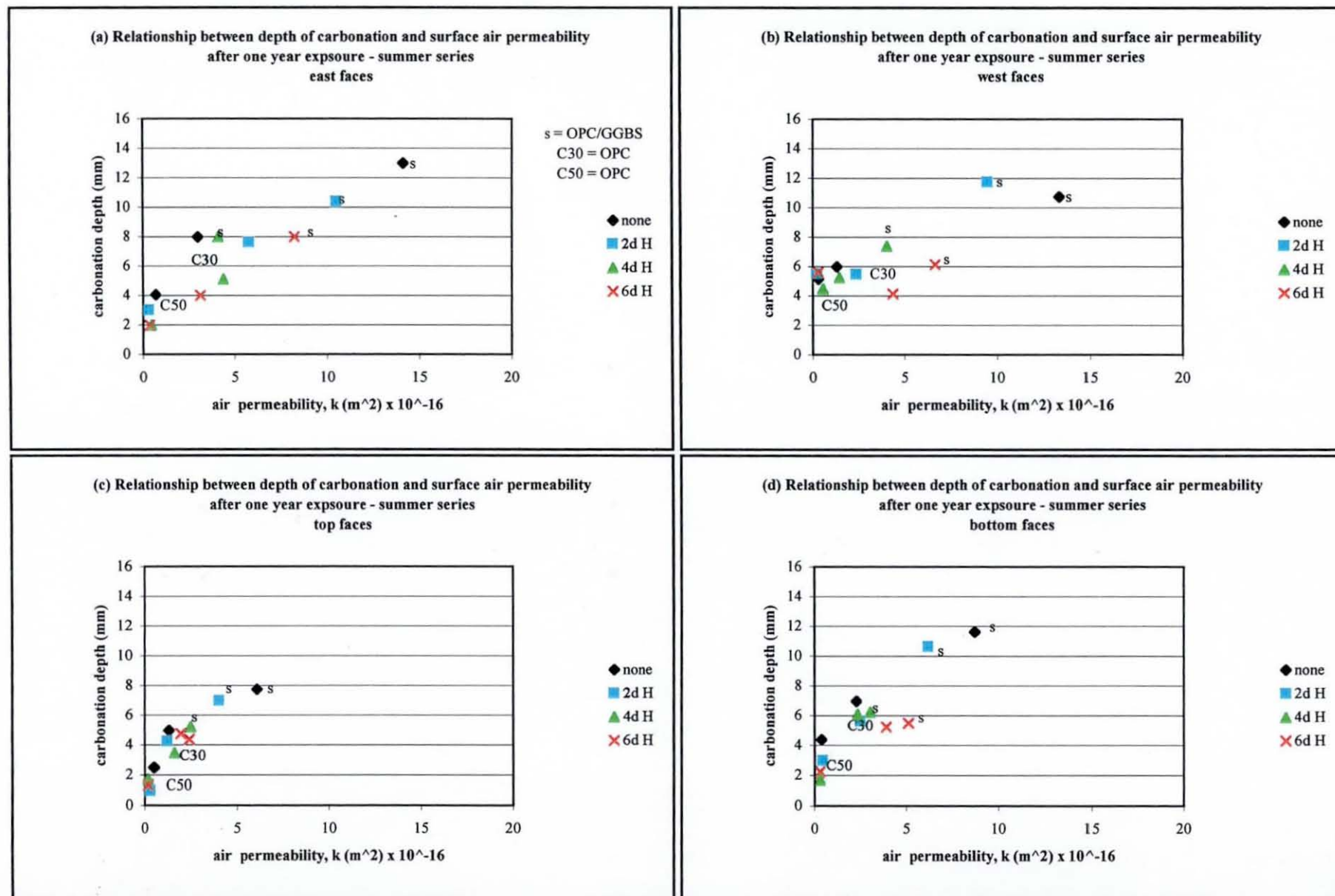


Fig. 8.7 Relationship between air permeability and depth of carbonation of the summer series after one year of exposure - effect of microclimate, curing and concrete type

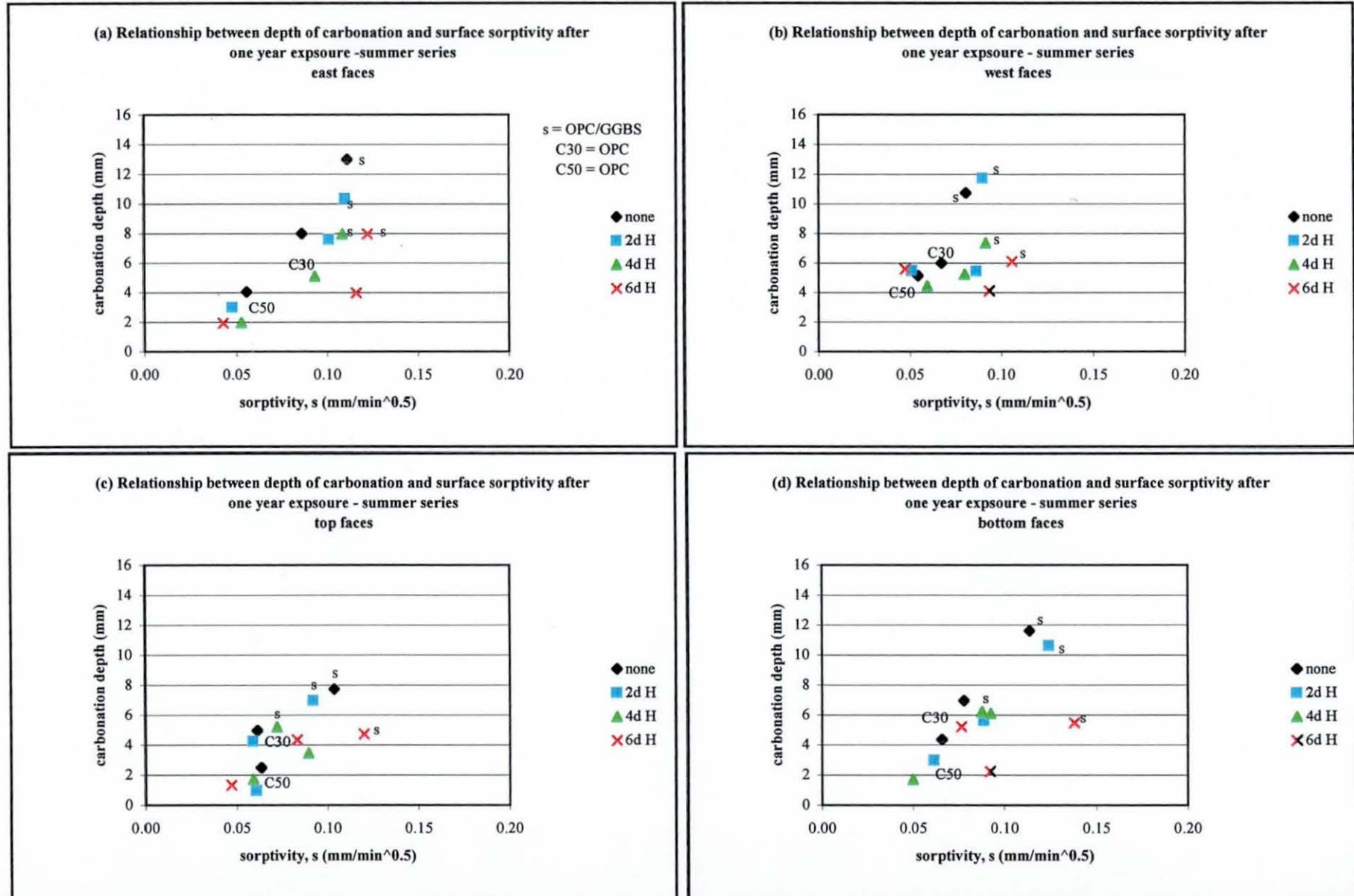


Fig. 8.8 Relationship between depth of carbonation and surface sorptivity of the summer series after one year of exposure - effect of microclimate, curing and concrete type

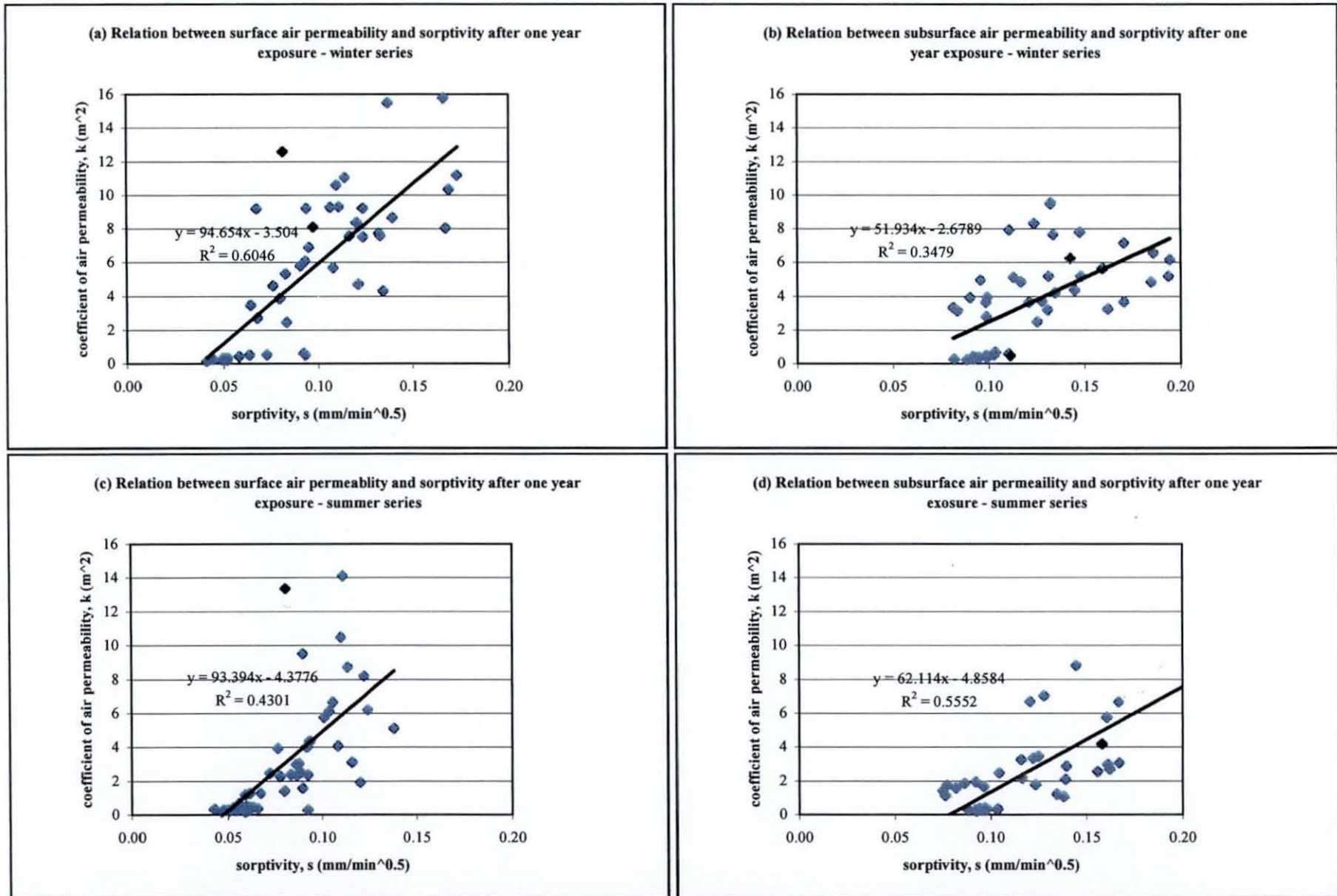


Fig. 8.9 Relationship between air permeability and sorptivity in the surface and subsurface zones after one year field exposure

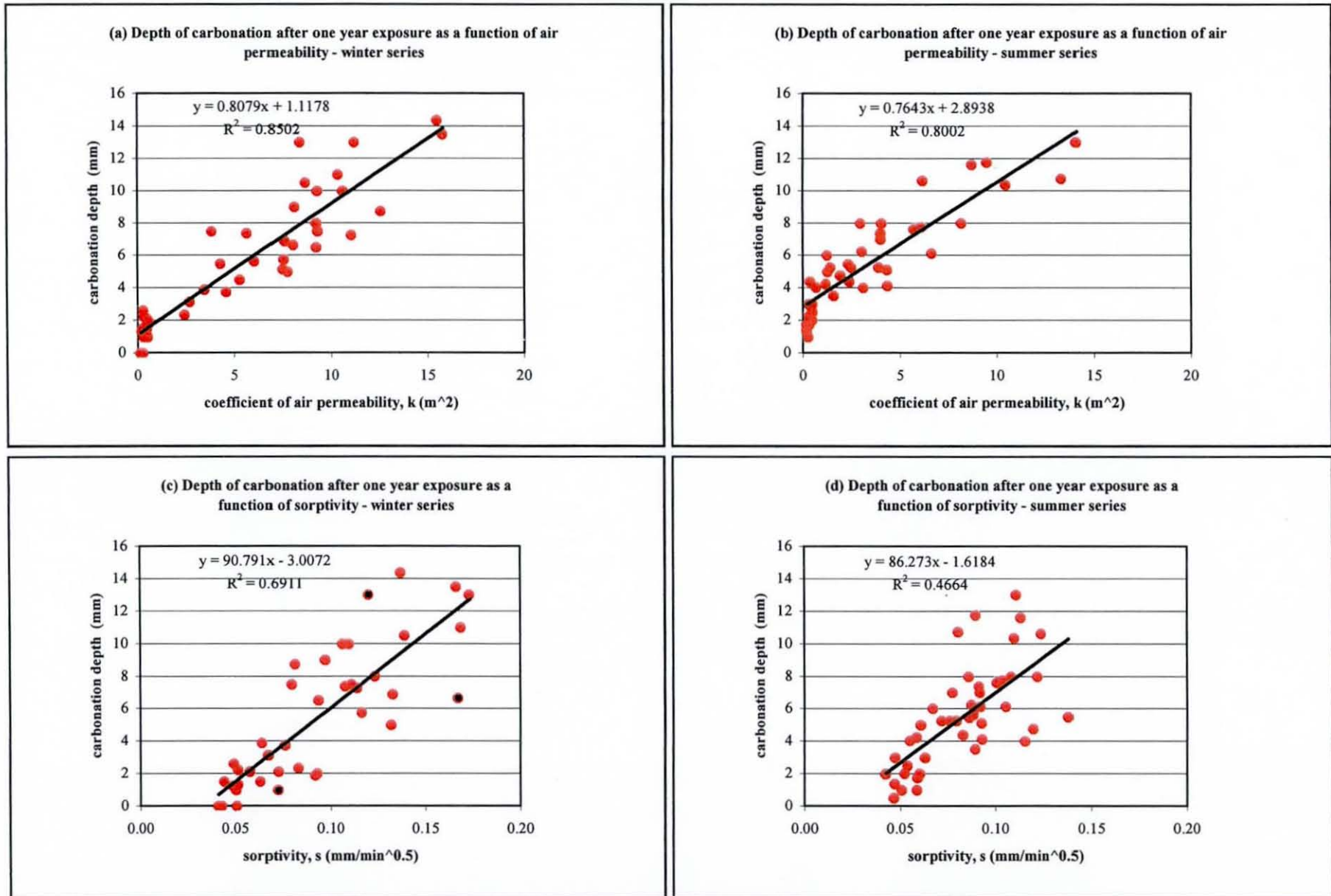


Fig 8.10 Relation between depth of carbonation, air permeability and sorptivity after one year field exposure

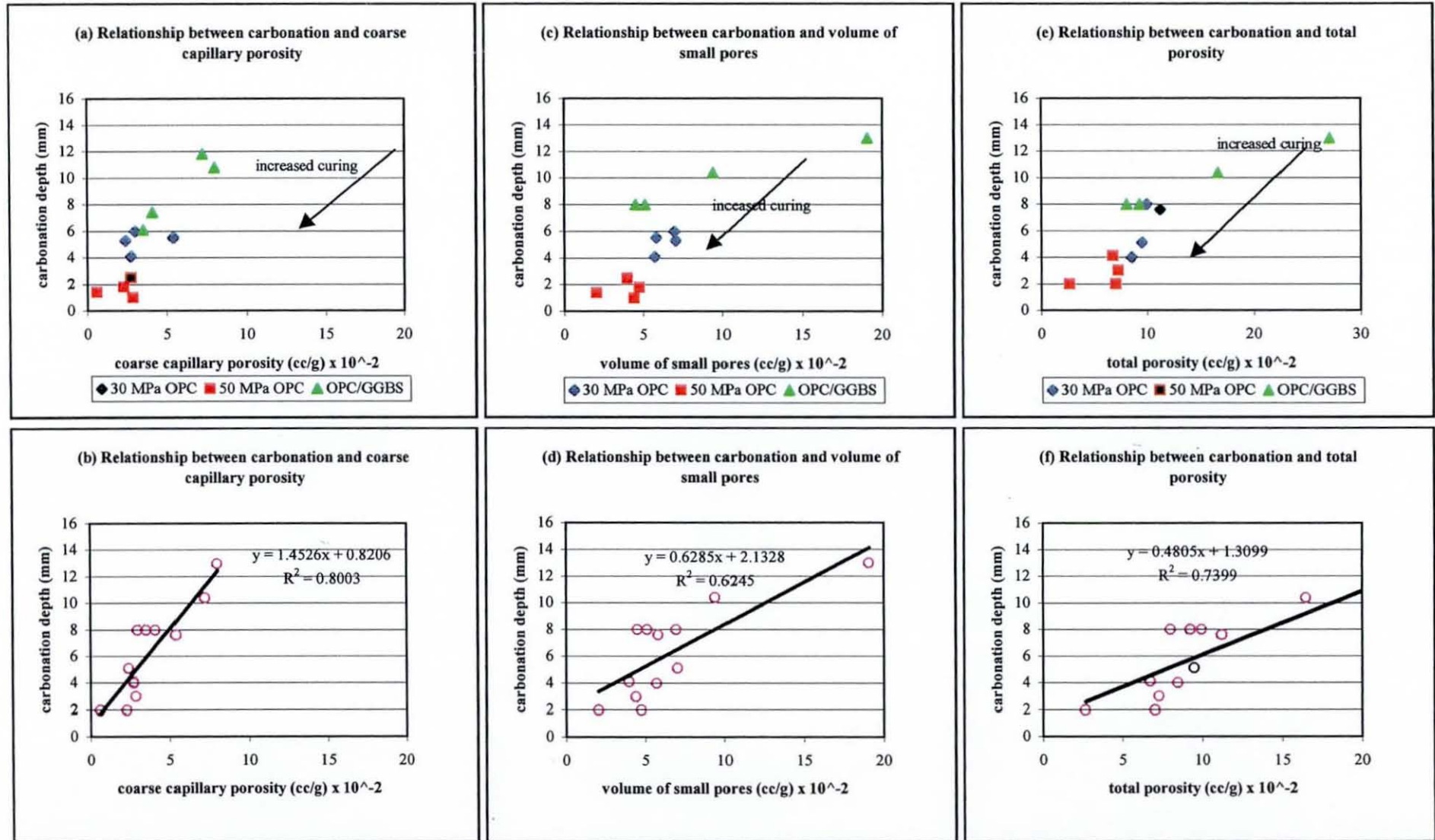


Fig. 8.11 Relation between carbonation and coarse capillary porosity, volume of small pores and total porosity after one year of field exposure - (east faces) summer serie

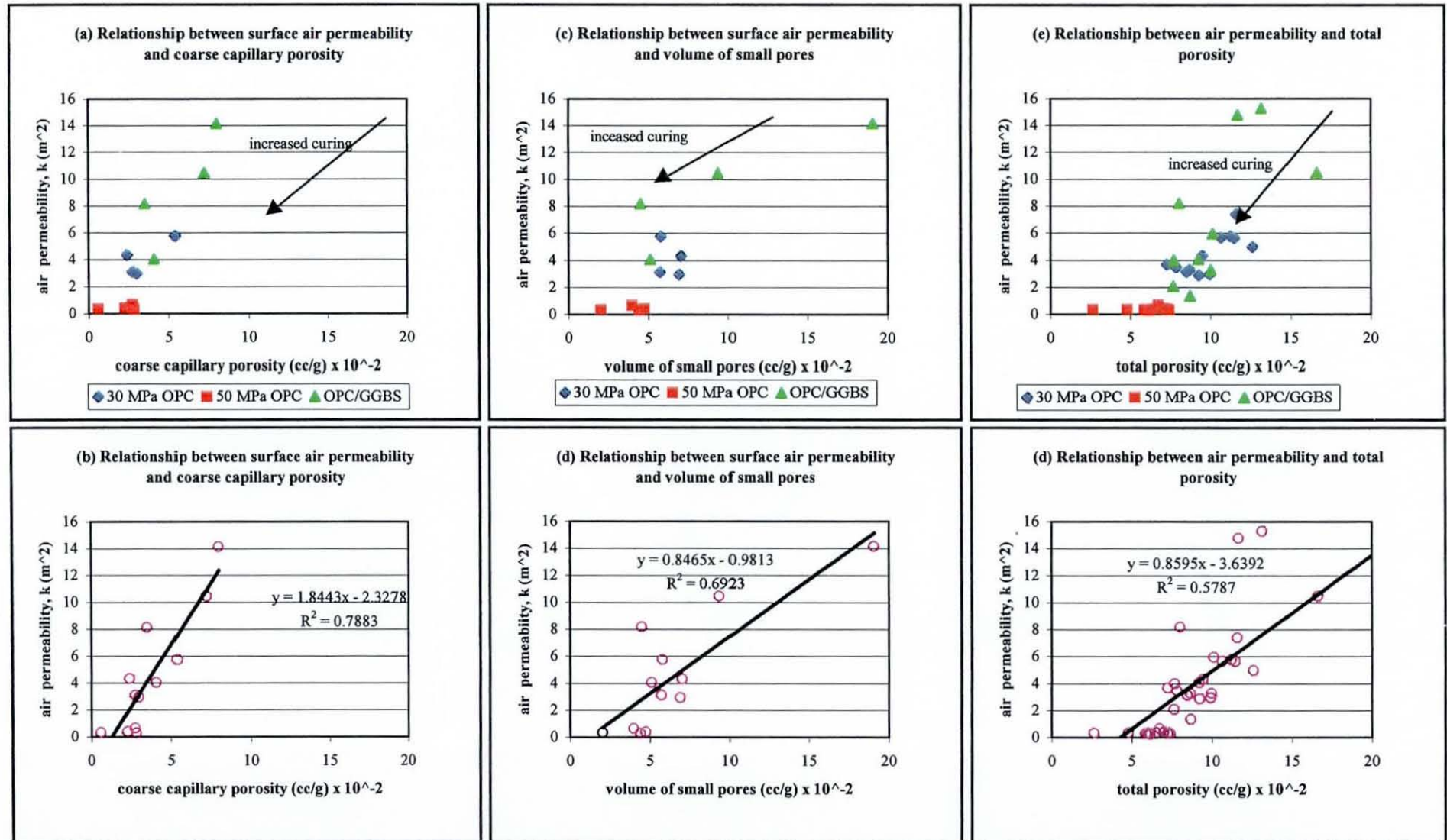


Fig. 8.12 Relation between air permeability and coarse capillary porosity, volume of small pores and total porosity after one year of field exposure - (east faces) summer series

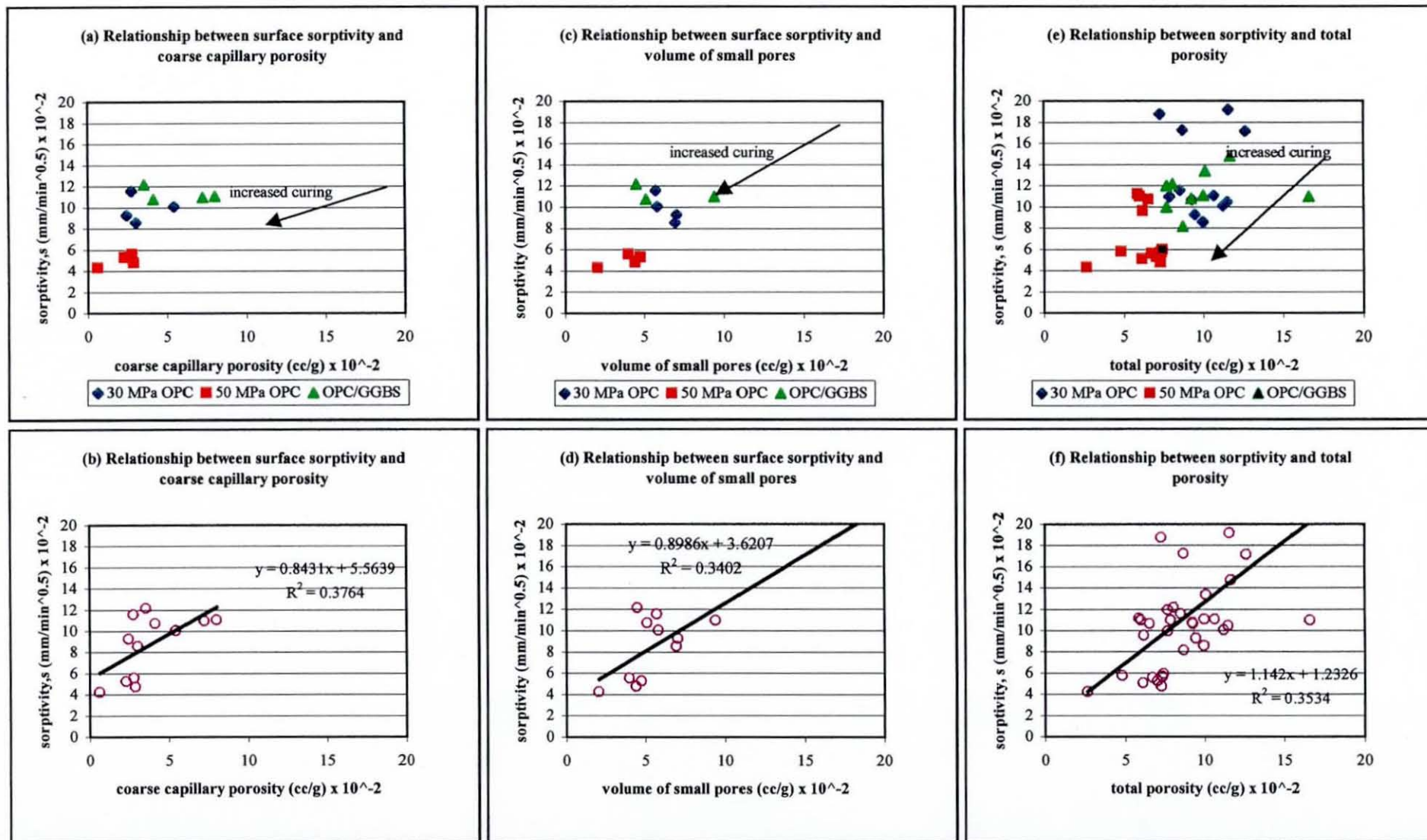


Fig. 8.13 Relation between sorptivity and coarse capillary porosity, volume of small pores and total porosity for concrete of 5-11 mm size (continued)

## Chapter 9 Conclusions and Recommendations

---

### 9.1 CONCLUSIONS

#### 9.1.1 The Curing Affected Zone

The test results revealed that the extent of the curing affected zone depends on concrete's curing and exposure environments, concrete strength and mix composition. Generally, curing affected the penetrability properties of concrete to a depth of approximately 20mm below the exposed surface for the two Loughborough concrete series. However, where the exposure conditions were particularly dry, the curing affected zone extended to depths of 30-40 mm from the exposed surface. This was especially applicable to the 30 MPa ground granulated blast-furnace slag concrete which displayed distinct penetrability properties characterised by a coarser and more continuous pore system relative to the equivalent strength, plain OPC concrete. The curing affected zone was smallest for the higher strength class, 50 MPa plain OPC concrete.

For the concretes exposed to the hot and dry climate of Muscat, curing affected the penetrability of the OPC concrete to a depth of approximately 40mm below the exposed surface. The curing affected zone of the OPC/GGBS concrete extended to a depth of nearly 50mm below the outer surface.

Large quality gradients were detected (in terms of the penetrability properties and porosity) within the 50mm surface region of concrete. The extent of these quality differences within the same concrete element suggests that measurements of properties from bulk concrete will give misleading results and will not reflect the true performance potential of concrete. Averaging of

properties or detailing the precise location of measurement within the material is imperative if an accurate assessment of concrete's state of service is to be made.

### **9.1.2 Climatic Effects**

The microclimate to which the concrete is exposed has a significant effect on its quality and microstructure development. Experimental evidence showed that variation in the penetrability properties within the surface region of concrete could vary by as much as 50% between the two faces of a concrete element exposed to two different microclimates. Concrete elements representing slab members, i.e. stored in-situ in a horizontal orientation exhibited a notably superior performance than identically cast and cured concrete elements, which were orientated in-situ to represent vertical members. Further, a predominantly dry microclimate where occasional wetting prevailed proved to be the most hostile, in relative terms, to concrete's quality and performance. This was displayed in the higher penetrability properties (permeability and sorptivity) and carbonation for the concrete in that microclimate. The quality variations due to microclimate effect demonstrate that curing requirements of concrete structures differ depending on their exact location and orientation within the same structure. The selection of different construction materials for different members of the same structures to suit their location and microclimate exposure is required to achieve uniform performance, integrity and durability of the whole structure.

Seasonal variation within the same country has an early influence on concrete's service life and performance depending on the particular seasonal conditions in which it was cast and cured. The overall performance of concretes cast and cured during a moderate, rainy UK summer season was better than identical concrete cast and cured during a particularly cold and dry UK winter season.

The surface sorptivity of concrete which was cast and cured during temperate weather conditions in the UK, but exposed to the hot and dry climatic

conditions of Oman, was 2-3 times higher after one year of exposure than nominally identical concrete exposed to UK climate. This, together with the large extension of the curing affected zone of the concretes exposed in Oman, relative to that stored in the UK, have considerable implication for the durability and life span of concrete in hot climate. Furthermore, whereas the penetrability properties of the UK concretes generally improved with age, the penetrability of the OPC/GGBS concretes exposed in Oman increased particularly at the surface as a result of the severe drying conditions.

### 9.1.3 Curing Method

The performance of the wet curing method (hessian) in improving the penetrability characteristics of the surface region of concrete was better than the water retention methods (polythene and curing membrane). The porosity, air permeability, sorptivity and carbonation were reduced with increased hessian curing duration. However, allowing wet hessian to dry prematurely during the course of curing proved to be more damaging to concrete's quality than taking no curing measure at all. The untimely drying of wet hessian produced concrete of higher permeability, sorptivity and carbonation than non-cured concrete. The OPC/GGBS concrete mixes were particularly susceptible to the adverse effect of dry hessian.

Curing with hessian for 6 days, when sufficiently moist, produced concrete with the lowest air permeability, sorptivity and carbonation whereas wrapping with polythene sheeting for 6 days produced similar quality to the 4 days hessian cured concrete. The application of curing membrane produced similar quality concrete to the 2 days hessian cured concrete however the C/M appeared to be more effective on the horizontal surfaces (slabs) than the vertical blocks.

The application of controlled permeability formwork system (CPF) was very effective in substantially improving the penetrability properties and carbonation resistance of concrete. Furthermore, the sensitivity of the CPF-produced concrete to the effects of curing and microclimate was significantly

lower than companion concretes, which were produced with conventional formwork. In addition, CPF application enhanced the surface appearance of concrete considerably, ensuing in an almost blowhole-free surface. Whereas the conventionally produced 30 MPa OPC/GGBS concrete mix displayed the poorest performance in terms of surface penetrability properties and carbonation resistance relative to the plain OPC concrete mixes, the penetrability properties and carbonation of the same mix cast against CPF became comparable with those of the higher strength class, 50 MPa OPC concrete. In terms of cost effectiveness, therefore, the utilisation of CPF was as effective as almost doubling the design strength of the concrete mix. However, a further benefit is that the employment of CPF can be effective in mitigating the effects that arise from the sensitivity of blended cement concretes to curing.

#### **9.1.4 Microstructural Effects**

Measurement of the penetrability properties of the surface region from thin concrete sections enabled the detection of small differences in concrete quality within this region due to curing and exposure conditions. However, the air permeability test proved to be more sensitive and reliable in detecting these small variations in concrete quality than the sorptivity test. Nevertheless, it is interesting that the sensitivity of the sorptivity test to variations in curing, macro/microclimate and concrete type was improved for young concretes and concretes of relatively poorer quality, i.e. concretes characterised by coarser pore systems. This was manifested in a relatively more marked and conspicuous sorptivity indices (in response to the above variables) for the OPC/GGBS concretes generally and the 3 months old 30 MPa OPC concretes which were subjected to the dry microclimate. This was also apparent from the results of the concretes that were exposed to the Muscat climate. This implied that the capillary suction test is able to assess the microstructure and porosity of concretes over a narrower quality range than the air permeability test. The indication from the limited porosity data is that capillary suction is

principally able to reflect changes in the pore system of concrete over a certain pore size range with a minimum threshold diameter near to 0.1 $\mu$ m.

The carbonation results reflected the effects of curing and exposure conditions on the quality of concrete as were detected by the air permeability and sorptivity results. The results showed that concrete type (concrete grade and composition), temperature and curing have an early influence on carbonation in the same order of importance, however, long term exposure and microclimate conditions play a determining role in the progress of carbonation. The carbonation of OPC concretes caused a reduction in the local surface porosity whereas that of the OPC/GGBS caused it to increase, as was reflected by the air permeability, sorptivity and porosity results. In terms of durability, however, the improvement in the surface porosity of OPC concretes is counteracted by the loss of the calcium hydroxide in that region.

The surface porosity of the OPC concretes improved markedly with increased curing duration, however, the improvement rate in the surface porosity of the OPC/GGBS concrete was more significant. The results showed that taking no curing measure resulted in higher intruded pore volume and coarser pore structure, exceptionally for the OPC/GGBS concrete. Although the porosity measurements were comparatively limited, the results obtained reflected the penetrability properties of the surface region of concrete as characterised by the air permeability and sorptivity and provided an insight into the effects of carbonation on concrete's surface. The hydration results, on the other hand, were difficult to explicate and did not accurately mirror the observed changes as detected by the other tests.

#### **9.1.5 Concrete Type**

The surface air permeability, sorptivity, carbonation rate and porosity of the 50 MPa OPC concrete were notably lower than the 30 MPa OPC concrete. The smaller difference in the measured penetrability properties between the outermost surface layer and subsurface layers is a further measure of the superior surface quality of the 50 MPa concrete to the 30 MPa OPC concrete.

In addition, the sensitivity of the higher strength class concrete to the effects of poor curing and microclimate was significantly lower than the lower strength class, 30 MPa OPC concrete.

The 30 MPa OPC/GGBS concrete exhibited the poorest performance of the three concrete mixes in both, the temperate and hot climate exposures. The air permeability, sorptivity, carbonation, capillary and total porosity of the 30 MPa OPC/GGBS concrete was higher than the equivalent strength class, plain OPC concrete. Further, the OPC/GGBS concrete was significantly more sensitive to the effects of inadequate curing and dry exposure conditions than the OPC concrete.

Generally, the effect of concrete strength and mix composition on the penetrability properties of the cover region of concrete was greater than that of curing and exposure conditions.

## **9.2 RECOMMENDATIONS**

### **9.2.1 Depth of Cover**

Cover to reinforcement should be specified in view of the extent of the curing affected zone within the concrete, which has been found to vary in accordance with concrete grade, concrete composition, and macro and microclimate conditions of exposure. Therefore, the cover requirements for the various members within the same structure will vary according to these variables. Whereas most current codes of practice recognise the effects of exposure environment and concrete type when specifying the cover to reinforcement, little attention has been given to the variation in the macro and microclimate effects. It is recommended that cover specifications should be considered in light of the likely penetrability characteristics of the surface region of the proposed construction mix while taking into account the macro and microclimate conditions that the various structural elements of the concrete will be subjected to in service.

### 9.2.2 Curing Method

The advantages of the wet curing or water adding methods over the water retaining methods are well recognised. However, due care should be taken when wet hessian or burlap is adopted, especially where concrete is subjected to drying conditions of exposure during its service. As demonstrated, allowing hessian to dry prematurely during curing has adverse effects on the penetrability properties of the cover region of concrete, which can seriously influence its performance and durability. This is particularly applicable to hot climate concreting where curing is often interrupted or intermittent and dry hessian during the course of curing is a commonly encountered phenomenon. The use of a combination of curing materials such as hessian and polythene wrapping instead of hessian alone should be the rule rather than the exception, as is the case now.

The application of curing membranes in temperate weather exposure like the UK is recommended as an alternative to the more conventional curing methods where these are difficult or uneconomical to perform. Their application to horizontal surfaces such as slabs or large beams is preferred, as this is more effective than on wall members or columns. However, in hot countries like Oman where the W/C ratio of the mixes is typically low (lower than 0.42), water addition methods of curing are preferred and the use of curing membrane is not strongly recommended.

The utilisation of controlled permeability formwork liner systems is recommended, as it offers a viable and effective option that can work alongside curing to improve the surface permeability and appearance significantly, thereby enhancing concrete's performance and durability. The employment of CPF in concrete construction is particularly recommended for Oman, where the unforgiving hot and dry weather conditions and the scarcity and cost of water warrants the exploitation of alternative curing methods and materials that aid curing in such conditions.

Ordinary Portland cement concrete mixes incorporating high level of blast-furnace slag cement require longer and more stringent curing measures to achieve similar level of performance to the equivalent strength plain OPC concretes.

### **9.2.3 Test Method**

The air permeability test is a sensitive and reliable measure of concrete performance and it correlates well with durability characteristics. It is recommended that concrete should be specified, amongst other things, to have low air permeability and adequate cover to reinforcement to minimise risk of corrosion. It is further recommended that the test be routinely used to monitor and verify durability compliance.

### **9.2.4 Concrete Type**

The use of higher strength grade OPC concrete (e.g. > 40 MPa) is recommended in situations where low permeability concrete is required, provided that proper curing procedures are strictly followed and adhered to. This is especially pertinent in severe exposure conditions like those experienced in Oman where the foremost problem is concrete's penetrability to chloride, sulphates and other aggressive media which ultimately lead to corrosion of reinforcement and sulphate attack. Additional to its lower permeability, other advantages of higher strength OPC concretes include lower risk of drying shrinkage due to its lower W/C ratio and better resistance to cyclic wetting/drying and daily temperature gradients.

Ordinary Portland cement concrete mixes containing high replacement levels of ground granulated blast-furnace slag of up to 70% exhibited extra sensitivity to inadequate curing and poor overall performance and, therefore, is not recommended for hot weather construction or where low permeability concrete is crucial. Whereas the industrialised nations can afford to, and indeed should, experiment with cement replacements, as these are mostly disposable by-products of industry, the situation for the emerging countries

like Oman is entirely different. The high cost of importing these materials as well as the severe weather conditions and the associated difficulties in achieving effective curing renders their use currently uncertain and uneconomical.

### **9.3 FURTHER RESEARCH**

The research work carried out in this thesis has identified a need for further research in several areas. It is therefore recommended that future investigation should be directed into the following areas:

1. Investigation of the penetrability properties should be carried out on extended areas of the surface region of up to 70-100mm from the surface using thin sections of 10mm thick or less with smaller aggregate size with an aim to detect variations due to exposure and curing with better degree of accuracy and resolution.
2. The determination of internal relative humidity within the surface concrete provides important information on concrete internal structure, curing and exposure conditions. There is therefore a need for the development of practical methods for the monitoring and determination of the internal relative humidity of the surface region of in-situ concrete.
3. In view of the water scarcity and high cost in hot weather countries like Oman, the applicability and efficiency of alternative curing methods to water addition need to be investigated with respect to improving concrete's surface properties and performance.
4. There is an indication that the pore structure and penetrability of slag concrete is adversely affected by carbonation and drying, especially in hot weather conditions. The potential benefits of the use of cement replacements in hot weather, especially for chloride durability, justify further examination. Long term investigation, with the aid of porosity measurements, of the surface penetrability properties and carbonation of

slag concretes incorporating different levels of binder replacement is needed.

5. The suitability of the sorptivity test as an indicator of curing efficiency and concrete performance has been studied extensively in this work, however, the rapidity and simplicity of the test warrants further investigation into its sensitivity and response to the various exposure variables. Work with the aid of porosity and hydration measurements should aim to establish its degree of sensitivity over a wide range of materials with a wide range of pore structure characteristics.
6. There is a strong need for the development of a non-destructive and practical test method for the in-situ measurement of concrete's penetrability characteristics.

## REFERENCES

- ACI COMMITTEE 224 REPORT, 1984:  
"Causes, evaluation and repair of cracks in concrete structures", ACI Journal, May-June, pp.211-229.
- ACI COMMITTEE 308 REPORT, 1990:  
"Standard practice for curing concrete", ACI 308-81, ACI Manual of Concrete Practice, Part 2, Construction Practices and Inspection Pavements.
- ACI COMMITTEE 306 REPORT, 1990:  
"Cold weather concreting", ACI 306R-88, ACI Manual of Concreting Practice, Part 2, Construction Practices and Inspection Pavements.
- ACI COMMITTEE 305 REPORT, 1991:  
"Hot weather concreting", ACI 305-91, ACI Materials Journal, Vol.88, No.4, August.
- ACI COMMITTEE 233 REPORT, 1995:  
"Ground granulated blast-furnace slag as a cementitious constituent in concrete", ACI 233R-95, Detroit.
- AL-ABIDEEN, H.M.Z., 1996:  
"Environment differences in Gulf countries – effects on concrete practice", Conference on Deterioration of Reinforced Concrete in the Gulf and Methods of Repair, 15-17 December, Muscat, Sultanate of Oman, pp.31-60.
- AL-ABIDEEN, H.M.Z., 1998:  
"Concrete practices in the Arabian Peninsula and the Gulf", Materials and Structures, Vol.31, May, pp.275-280.
- AL-AMOUDI, O.S.B., RASHEEDUZZAFAR, MASLEHUDDIN, M. , ALMUSALLAM, A.A., 1993:  
"Improving concrete durability in the Arabian Gulf", Proceedings, 4<sup>th</sup> International Conference on Deterioration and Repair of Reinforced Concrete in the Arabian Gulf, Bahrain, No.2, pp.927-942.
- AL-ANI, S.H., AL-ZAIWARY, M.A.K., 1988:  
"The Effect of Curing Period and Curing Delay on Concrete in Hot Weather", Materials and Structures, 21, pp.205-212.
- ALEXANDER, M.G., MINDESS, S., DIAMOND, S., QU, L., 1995:  
"Properties of paste-rock interfaces and their influence on composite behaviour", Materials and Structures, 28, pp.497-506.
- AL-GAHTANI, H.J., ABBASI, A.G.F., AL-AMOUDI, O.S.B, 1998:  
"Concrete mixture design for hot weather: experimental and statistical analysis", Magazine of Concrete Research, 50, No.2, June, pp.95-105.
- ALI, M.A., MARSH, B.K., 1994:  
"Assessment of the effectiveness of curing on the durability of reinforced concrete", Proceedings, PK Mehta Symposium on Durability of Concrete, ACI CANMET, Nice, pp.1161-1176.
- AMERICAN SOCIETY FOR TESTING AND MATERIALS, 1991:  
"Standard test method for water retention by concrete curing materials", C171-91, Washington DC, December.
- AMERICAN SOCIETY FOR TESTING AND MATERIALS, 1991:  
"Standard test method for water retention by concrete curing materials", C1151-91, Washington DC, December.

- AMERICAN SOCIETY FOR TESTING AND MATERIALS, 1993:  
 "Standard test method for water retention by concrete curing materials", C156-93,  
 Washington DC, August.
- ARAFAH, A., AL-ZAID, R., AL-HADDAD, M., 1996:  
 "Influence of non-standard curing on the strength of concrete in arid areas", Cement and  
 Concrete Research, Vol.26, No.9, pp.1341-1350.
- ASTM SPECIAL TECHNICAL PUBLICATION 169B, 1978:  
 "Significance of tests and properties of concrete and concrete-making materials",  
 American Society for Testing and Materials, STP 169B.
- AUSTRALIAN PRE-MIXED CONCRETE ASSOCIATION, 1995:  
 "Hot weather concreting", Technical Bulletin 95/2, North Sydney, pp.4.
- BAGEL, L., ZIVICA, V., 1997:  
 "Relationship between pore structure and permeability of hardened cement mortars: on  
 the choice of effective pore structure parameter", Cement and Concrete Research, Vol.27,  
 No.8, pp.1225-1235.
- BAILEY, J.E., STEWART, H.R., 1984:  
 "Relationship between microstructural development and physio-chemical nature of OPC  
 pastes", The Chemistry and Chemically Related Properties of Cement, Proceedings,  
 British Ceramic, No.35, Stoke on Trent, British Ceramic Society, September, pp.193-206.
- BALEN, K.V., GERMERT, D.V., 1994:  
 "Modelling lime mortar carbonation", Materials and Structures, 27, pp.393-398.
- BALLIM, Y., 1993:  
 "Curing and the durability of OPC, fly ash and blast-furnace slag concretes", Materials  
 and Structures, 26, pp.238-244.
- BAMFORTH, P.B., 1986:  
 "Alternative cements for hot climates", Concrete, February, pp.18-20.
- BAMFORTH, P.B., 1987:  
 "The relationship between permeability coefficients for concrete obtained using liquid  
 and gas", Magazine of Concrete Research, Vol.39, No.138, March, pp.3-11.
- BAMFORTH, P., POCOCK, D., 1990:  
 "Minimising the risk of chloride induced corrosion by selection of concreting materials",  
 Proceedings, 3rd Symposium on the Corrosion of Reinforcement on Concrete  
 Construction, Royal Society of Chemical Industry, London, pp.119-131.
- BAMFORTH, P.B., 1995:  
 "Improving the durability of concrete by the use of mineral additions", Proceedings,  
 Conference on Concrete Durability in the Arabian Gulf, (Ed. MacMillan), Bahrain Society  
 of Engineers, pp.67-92.
- BAMFORTH, P.B., SUMMERS, G.R., 1997:  
 "Carbonation data from 6 years exposure of blended cement concretes in Bahrain",  
 Proceedings, 5<sup>th</sup> International Conference on the Deterioration and Repair of Reinforced  
 Concrete in the Arabian Gulf, 27-29 October, Bahrain, pp.389-401.
- BAMFORTH, P.B., 1997a:  
 "Improving the durability of concrete by the use of mineral additions", Proceedings, 5<sup>th</sup>  
 International Conference on the Deterioration and Repair of Reinforced Concrete in the  
 Arabian Gulf, 27-29 October, Bahrain, pp.749-765.
- BARKER, A.P., BARNES, P., 1984:  
 "Characterisation of calcium hydroxide in set cements using some established and novel  
 techniques", The Chemistry and Chemically Related Properties of Cement, Proceedings,  
 British Ceramic, No.35, Stoke on Trent, British Ceramic Society, September, pp.25-40.

- BARNES, B.D., ORNDORFF, R.L., ROTEN, J.E., 1977:  
 "Low initial curing temperature improves the strength of concrete test cylinders", *Journal of American Concrete Institute*, 74, No.12, pp.612-615.
- BASHEER, P.A.M., 1993:  
 "A brief review of methods for measuring the permeation properties of concrete in-situ", *Proceedings, Institute of Civil Engineers (Structures and Buildings)*, 99, February, pp.74-83.
- BASMA, A.A., ABDEL-JAWAD, Y., 1995:  
 "Probability model for the drying shrinkage of concrete", *ACI Materials Journal*, Vol.88, No.4, June.
- BENTUR, A., KUNG, J.H., BERGER, R.L., YOUNG, J.F., MILESTONE, N.B., MINDESS, S., LAWRENCE, F.V., 1980:  
 "Influence of microstructure on the creep and drying shrinkage of calcium silicate pastes", *7<sup>th</sup> International Symposium on the Chemistry of Cement, Paris, Vol.3*, pp.VI26-VI31.
- BENTUR, A., GOLDMAN, A., 1989:  
 "Concrete effects, strength and physical properties of high strength silica fume concretes", *Journal of Materials in Civil Engineering*, Vol.1, No.1, February, pp.46-58.
- BERHANE, Z., 1984:  
 "Evaporation of water from fresh mortars and concrete at different environmental conditions", *ACI Journal*, November/December, pp.560-565.
- BERNAL, J.D., 1952:  
 "The structure of cement hydration compounds", *Proceedings, 3<sup>rd</sup> International Symposium on the Chemistry of Cement, London*, pp.216-236.
- BIER, T.A., LUDIRDJA, D., YOUNG, F., BERGER, R.L., 1989:  
 "The effect of pore structure and cracking on the permeability of concrete", *Proceedings, Materials Research Society Symposium, Edited by Roberts, L.R., and Skalny, J.P.*, 28-30 November, Boston, Massachusetts, USA, Vol.137, pp.235-241.
- BIJEN, J.M.J.M., 1985:  
 "On the durability of Portland blast furnace slag cement concrete in hot marine environment", *Proceedings, 1<sup>st</sup> International Conference on Deterioration and Repair of Reinforced Concrete in the Arabian Gulf, 26-29 October, Bahrain*, pp.215-232.
- BOGUE, R.H., 1955:  
 "The chemistry of Portland cement", 2<sup>nd</sup> Edition, Reinhold Publishing Corporation, New York.
- BRITISH STANDARD INSTITUTION, 1975:  
 "Sampling and testing of mineral aggregate, sand and filler", BS812: Part 1 & 2, London.
- BRITISH STANDARDS INSTITUTION, 1982:  
 "Specification for Accelerating Admixtures, Retarding Admixtures and Water Reducing Admixtures", BS5075, Part 1, London.
- BRITISH STANDARD INSTITUTION, 1985:  
 "Structural Use of Concrete", BS8110, Part 1, Code of Practice for Design and Construction, BSI, London.
- BRITISH STANDARD INSTITUTION, 1991:  
 "Specification for Portland Cements", BS12, London.
- BROOKES, J.J., 1989:  
 "Influence of mix proportions, plasticisers and superplasticisers on creep and drying shrinkage of concrete", *Magazine of Concrete Research*, 41, No.148, pp.145-154.
- BROWN, M.E., 1988:  
 "Introduction to thermal analysis", Chapman and Hall (Ed.), London.

- CABRERA, J.C., LYNSDALE, C.J., 1988:  
 "A new gas permeameter for measuring the permeability of mortar and concrete",  
 Magazine of Concrete Research, Vol.40, No.144, September, pp.177-182.
- CABRERA, J.G., GOWRIPALALN, N., WAINWRIGHT, P.J., 1989:  
 "An assessment of concrete curing efficiency using gas permeability", Magazine of  
 Concrete Research, Vol.41, No.149, December, pp.193-198.
- CADY, P.D., 1978:  
 "Corrosion of reinforcing steel", in Significance of Tests and Properties of Concrete and  
 Concrete-Making Materials, American Society for Testing and Materials, ASTM STP  
 169B, pp.275-279.
- CAMBUREAU RECOMMENDATIONS, 1989:  
 "The determination of the permeability of concrete to oxygen by the Cambureau method  
 - a recommendation", Materials and Structures, 22, pp.225-230.
- CARRIER, R.E., 1983:  
 "Concrete curing tests", Concrete International, April, pp.23-26.
- CATHER, J.W., FIGG, J.W., MARSDEN, A.F., O'BRIEN, T.P., 1984:  
 "Improvements to the figg method for determining the air permeability of concrete",  
 Magazine of Concrete Research, Vol.36, No.129, December, pp.241-245.
- CATHER, B., 1994:  
 "Curing: the true story?", Magazine of Concrete Research, 46, No.168, September, pp.157-  
 161.
- CHERN, J.C., CHAN, Y.W., 1989:  
 "Effect of temperature and humidity conditions on the strength of blast furnace slag  
 cement concrete", Proceedings, 3<sup>rd</sup> International Conference on Fly Ash, Silica Fume, Slag  
 and Natural Pozzolans in Concrete, Trondheim, Norway, June.
- CIRIA Special Publication 31, 1984:  
 "The CIRIA Guide to Concrete Construction in the Gulf Region", CIRIA, pp.13-87.
- CLARKE, L.A., SHAMMAS-TOMA, M.G.K., SEYMOUR, D.E., PALLETT, P.F., MARSH, B.K.,  
 1997:  
 "How can we get the cover we need?", The Structural Engineer, Vol.75, No.17,  
 September, pp.289-296.
- CONCRETE SOCIETY, 1988:  
 "Permeability testing of site concrete: a review of methods and experience", Report of a  
 Concrete Society Working Party, London, August, Concrete Society Technical Report 31.
- CONCRETE SOCIETY, 1996:  
 "Developments in durability design and performance-based specification of concrete",  
 Concrete Society Special Publication CS109, pp.69.
- DANIELSSON, V., 1974:  
 "An apparatus for easy determination of the amount of bound water in cement pastes  
 yielding highly reproducible results", Materiaux et Constructions, Vol.7, No.40, pp.231-  
 246.
- DAY, P.D., 1978:  
 "Corrosion of reinforcing steel", in Significance of Tests and Properties of Concrete and  
 Concrete-Making Materials, ASTM, STP 169B, pp.275-299.
- DAY, R.L., ILLSTON, J.M., 1983:  
 "The effect of rate of drying on the drying/wetting behaviour of cement paste", Cement  
 and Concrete Research, Vol.13, pp.7-17.

- DETWILER, R.J., KJELLEN, K.O., GJORV, O.E., 1991:  
 "Resistance to chloride intrusion of concrete cured at different temperatures", *ACI Materials Journal*, January-February, pp.19-24.
- DETWILER, R.J., FAPOHUNDA, C.A., NATALE, J., 1994:  
 "Use of supplementary cementing materials to increase the resistance to chloride ion penetration of concretes cured at elevated temperatures", *ACI Materials Journal*, January-February, pp.63-66.
- DHIR, R.K., HEWLETT, P.C., CHAN, Y.N., 1986:  
 "Near-surface characteristics and durability of concrete: an initial appraisal", *Magazine of Concrete Research*, Vol.38, No.134, March, pp.54-56.
- DHIR, R.K., HEWLETT, P.C., CHAN, Y.N., 1989:  
 "Near surface characteristics of concrete: intrinsic permeability", *Magazine of Concrete Research*, 41, No.147, June, pp.87-97.
- DHIR, R.K., HEWLETT, P.C., CHAN, Y.N., 1989a:  
 "Near-surface characteristics of concrete: prediction of carbonation resistance", *Magazine of Concrete Research*, 1989, 41, No.148, September, pp.137-143.
- DHIR, R.K., LEVITT, M., WANG, J., 1989b:  
 "Membrane curing of concrete: water vapour permeability of curing membranes", *Magazine of Concrete Research*, 41, No.149, December, pp.221-228.
- DHIR, R.K., JONES, M.R., AHMED, H.E.H., SEREVIRATNE, A.M.G., 1990:  
 "Rapid estimation of chloride diffusion coefficient in concrete", *Magazine of Concrete Research*, 42, No.152, September, pp.177-185.
- DHIR, R.K., JONES, M.R., AHMED, H.E.H., 1991a:  
 "Determination of total soluble chlorides in concrete", *Cement and Concrete Research*, Vol.20, pp.579-590.
- DHIR, R.K., JONES, M.R., AHMED, H.E.H., 1991b:  
 "Concrete durability: estimation of chloride concentration during design life", *Magazine of Concrete Research*, 43, No.154, March, pp.37-44.
- DHIR, R.K., HEWLETT, P.C., CHAN, Y.N., 1991:  
 "Near-surface characteristics of concrete: abrasion resistance", *Materials and Structures*, 24, pp.124-128.
- DHIR, R.K., JONES, M.R., ELGHALY, A.E., 1993:  
 "PFA concrete – exposure temperature effects on chloride diffusion", *Cement and Concrete Research*, Vol.23, No.5, pp.1105-1114.
- DHIR, R.K., BYARS, E.A., 1993a:  
 "PFA concrete – permeation properties of cover to steel reinforcement", *Cement and concrete Research*, Vol.23, No.3, pp.554-566.
- DHIR, R.K., BYARS, E.A., 1993b:  
 "Pulverised fuel-ash concrete – intrinsic permeability", *ACI Materials Journal*, Vol.90, No.6, pp.571-580.
- DHIR, R.K., BYARS, E.A., 1993c:  
 "PFA concrete: chloride diffusion rates", *Magazine of Concrete Research*, 45, No.162, March, pp.1-9.
- DHIR, R.K., SHAABAN, I.G., CLAISSE, P.A., BYARS, E.A., 1993d:  
 "Preconditioning insitu concrete for permeation testing 1. Initial surface-absorption", *Magazine of Concrete Research*, Vol.45, No.163, pp.113-118.
- DHIR, R.K., JONES, M.R., MCCARTHY, M.J., 1993e:  
 "PFA concrete – chloride ingress and corrosion in carbonated cover", *Proceedings, Institution of Civil Engineers – Structures and Buildings*, Vol.99, No.2, pp.167-172.

- DHIR, R.K., JONES, M.R., BYARS, E.A., SHABAAN, I.G., 1994:  
 "Predicting concrete durability from its absorption", CANMET/ACI 3<sup>rd</sup> International Conference on Concrete Durability, Edited by V.M. Malholra, Nice, France, May, ACI SP145, pp.1177-1182.
- DHIR, R.K., HEWLETT, P.C., LOTA, J.S., DYER, T.D., 1994a:  
 "An investigation into the feasibility of formulating 'self-cure' concrete", Materials and Structures, 27, pp.606-615.
- DHIR, R.K., HEWLETT, P.C., BYARS, E.A., BAI, J.P., 1994b:  
 "Estimating the durability of concrete in structures", Concrete, November, pp.25-30.
- DHIR, R.K., JONES, M.R., MCCARTHY, M.J., 1994c:  
 "PFA concrete: chloride-induced reinforcement corrosion", Magazine of Concrete Research, Vol.46, No.169, pp.269-277.
- DHIR, R.K., HEWLETT, P.C., BYARS, E.A., SHAABAN, I.G., 1995:  
 "A new technique for measuring the air permeability of near-surface concrete", Magazine of Concrete Research, 47, No.171, June, pp.167-176.
- DHIR, R.K., HEWLETT, P.C., DYER, T.D., 1995a:  
 "Durability of self-cure concrete", Cement and Concrete Research, Vol.25, No.6, pp.1153-1158.
- DHIR, R.K., JONES, M.R., MCCARTHY, M.J., 1996:  
 "Binder content influences on chloride ingress in concrete", Cement and Concrete Research, Vol.26, No.12, pp.1761-1766.
- DHIR, R.K., HEWLETT, P.C., DYER, T.D., 1996a:  
 "Influence of microstructure on the physical properties of self-curing concrete", ACI Materials Journal, Vol.93, No.5, pp.465-471.
- DHIR, R.K., ELMOHR, M.A.K., DYER, T.D., 1996b:  
 "Chloride binding in GGBS concrete", Cement and Concrete Research, Vol.26, No.12, pp.1767-1773.
- DHIR, R.K., ELMOHR, M.A.K., DYER, T.D., 1997:  
 "Developing chloride resisting concrete using PFA", Cement and Concrete Research, Vol.27, No.11, pp.1633-1639.
- DHIR, R.K., HEWLETT, P.C., BYARS, E.A., SHAABAN, I.G., 1997a:  
 "A new technique for measuring the air permeability of near-surface concrete" A Reply, Magazine of Concrete Research, Vol.49, No.181, pp.367-368.
- DHIR, R.K., HEWLETT, P.C., DYER, T.D., 1998:  
 "Mechanisms of water retention in cement pastes containing a self-curing agent", Magazine of Concrete Research, Vol.50, No.1, pp.85-90.
- DHIR, R.K., JONES, M.R., NG, S.L.D., 1998a:  
 "Prediction of total chloride content profile and concentration time-dependent diffusion coefficients for concrete", Magazine of Concrete Research, Vol.50, No.1, pp.37-48.
- DINKU, A., REINHARDT, H.W., 1997:  
 "Gas permeability coefficient and cover concrete as a performance control", Materials and Structures, Vol.30, August-September, pp.387-393.
- DUNSTER, A.M., BIGLAND, D.J., HOLLINSHEAD, K., CARMOND, N.J., 1996:  
 "Studies of carbonation and reinforcement corrosion in high alumina cement concrete", Proceedings, 4<sup>th</sup> Symposium on the Corrosion of Reinforcement in Concrete Construction, Royal Society of Chemistry, July, pp.191-199.
- EGAN, P.J., 1995:  
 "How admixtures can help young concrete", Concrete, May/June, pp.18-20.
- EUROPEAN STANDARD ENV 206, 1992:  
 "Concrete: performance, production, placing and compliance criteria".

- EUROPEAN STANDARD FIRST DRAFT prEN 104-837, 1995:  
 "Products and systems for the protection and repair of concrete structures – Tests methods – Determination of capillary absorption", CEN/TC 104/SC8, pp.13.
- EWERSTON, C., PETERSSON, P.E., 1993:  
 "The influence of curing conditions on the permeability and durability of concrete – results from a field exposure test", Cement and Concrete Research, Vol.23, pp.683-692.
- FELDMAN, R.F., 1986:  
 "The effect of sand/cement ratio and silica fume on the microstructure of mortars", Cement and Concrete Research, Vol.16, pp.31-39.
- FEDERATION INTERNATIONALE DE LA PRECONTRAINTE, 1986:  
 FIP Guide to good practice: "Concrete construction in hot weather", Published by Thomas Telford Ltd., London, pp.16.
- FOOKES, P.G., 1993:  
 "Concrete in the Middle East – past, present and future: a brief review", Concrete, July-August, pp.14-20.
- FOOKES, P., 1995:  
 "Concrete in hot dry salty environment", Concrete, January/February, pp.34-39.
- GARBOCCZI, E.J., 1995:  
 "Microstructure and transport properties of concrete", in Performance Criteria for Concrete Durability, RILEM Report 12, J. Kropp and H.K. Hilsdart (Ed.), pp.198-211.
- GAYNOR, R.D., MERNNGER, R.C., KHAN, T.S., 1983:  
 "Effect of temperature and delivery time on concrete proportions", in Temperature Effects on Concrete, ASTM, Sp. Tech. Publication No.858, pp.68-87.
- GEBLER, S., 1983:  
 "Predict evaporation rate and reduce plastic shrinkage cracks", Concrete International, April 1983, pp.19-22.
- GEIKER, M., EDVARSEN, C., 1997:  
 "Effects of cracks in reinforced concrete", Proceedings, 5<sup>th</sup> International Conference on the Deterioration and Repair of Reinforced Concrete in the Arabian Gulf, 27-29 October, Vol.1, pp.305-319.
- GEISELER, J., KOLLO, H., LANG, E., 1995:  
 "Influence of blast furnace cements on durability of concrete structures", ACI Materials Journal, Vol.88, No.4, June.
- GOTO, S., ROY, D.M., 1981:  
 "The effect of w/c ratio and curing temperature on the permeability of hardened cement paste", Cement and Concrete Research, 11, No.4, pp.575-579.
- GOWRIPALAN, N., CABRERA, J.G., CUSENS, A.R., WAINWRIGHT, P.J., 1990:  
 "Effect of curing on durability", Concrete International, Vol.12, No.2, February, pp.47-54.
- GUMMERSON, R.J., HALL, C., HOFF, W.D., 1980:  
 "Water movement in porous building materials – II. Hydraulic suction and sorptivity of brick and other masonry materials", Building and Environment, Vol.15, pp.101-108.
- GUMMERSON, R.J., HALL, C., HOFF, W.D., 1981:  
 "Water movement in porous building materials – III. Asorptivity test procedure for chemical injection damp proofing", Building and Environment, Vol.16, No.3, pp.193-199.
- HALAMICKOVA, P., DETWILER, R.J., BENTZ, D.P., GARBOCZI, J., 1995:  
 "Water permeability and chloride ion diffusion in Portland cement mortars: relationship to sand content and critical pore diameter", Cement and Concrete Research, Vol.25(4), pp.790-802.
- HALL, C., 1977:  
 "Water movement in porous building materials – I. Unsaturated flow theory and its applications", Building and Environment, Vol.12, pp.117-125.

- HALL, C., 1981:  
 "Water movement in porous building materials – IV. The initial surface absorption and sorptivity", *Building and Environment*, Vol.16, No.3, pp.201-207.
- HALL, C., TSE, T.K., 1986:  
 "Water movement in porous building materials – VII. The sorptivity of mortars", *Building and Environment*, Vol.21, No.2, pp.113-118.
- HALL, C., 1987:  
 "Water movement in porous building materials – IX. The water absorption and sorptivity of concrete", *Building and Environment*, Vol.22, No.1, pp.77-82.
- HALL, C., 1989:  
 "Water sorptivity of concrete: a review", *Magazine of Concrete Research*, Vol.41, No.147, June, p.51-61.
- HAQUE, M.M., 1990:  
 "Some concretes need 7 day initial curing", *Concrete International*, Vol.12, No.2, pp.42-46.
- HARRISON, T.A., 1996:  
 "The specification of durability by performance-when?", in *Radical Concrete Technology*, Edited by R.K. Dhir and P.C. Hewlett, Published by E&FN Spon, pp.413-425.
- HIGHWAY RESEARCH BOARD, 1952:  
 "Curing concrete pavements", *Current Road Problems*, No.1-R, Revised Edition, Washington.
- HILLERBORG, A., 1985:  
 "A modified absorption theory", Vol.15, *Cement and Concrete Research*, pp.809-816.
- HO, D.W.S., HINCZAK, I., CONROY, J.J., LEWIS, R.K., 1986:  
 "Influence of slag cement on the water sorptivity of concrete", *Proceedings, 2<sup>nd</sup> International Conference on the Use of Fly Ash, Blast-Furnace Slag and Silica Fume in Concrete*, Madrid, Vol.2, pp.1463-1470.
- HO, D.W.S., LEWIS, R.K., 1987:  
 "Carbonation of concrete and its prediction", *Cement and Concrete Research*, Vol.17, pp.489-504.
- HO, D.W.S., LEWIS, R.K., 1988:  
 "The specification of concrete for reinforcement protection – performance criteria and compliance by strength", *Cement and Concrete Research*, Vol.18, pp.584-594.
- HO, D.W.S., CUI, Y.Q., RITCHIE, D.J., 1989:  
 "The influence of humidity and curing time on the quality of concrete", *Cement and Concrete Research*, Vol.19, pp.457-464.
- HOLLINSHEAD, K., OSBORNE, G.J., BIGLAND, D.J., 1997:  
 "Durability assessment of concrete", *New Zealand Concrete Construction*, Vol.41, Part 3, pp.26-29.
- HUDEC, P.P., MACINNIS, C., MONKWA, M., 1986:  
 "Microclimate of concrete barrier walls: temperature, moisture and salt content", *Cement and Concrete Research*, Vol.16, pp.615-623.
- HUGHES, D.C., 1985:  
 "Sulphate resistance of OPC, UPC/fly ash and SRPC pastes: pore structure and permeability", *Cement and Concrete Research*, Vol.15, pp.1003-1012.
- HUTCHENSON, 1996:  
*The Hutchenson Encyclopaedia*, Helicon Publishing.
- JACOBES, F.J., MEYER, G., 1992:  
 "Porosity and permeability of autoclaved aerated concrete", *Advances in Autoclaved Aerated Concrete*, Edited by Wittmann, Belkema, Rotterdam, pp.71-75.

- JACOBS, F., 1998:  
 "Permeability to gas of partially saturated concrete", Magazine of Concrete Research, 50, No.2, June, pp.115-121.
- JOLICOEUR, C., SIMARD, M., 1998:  
 "Chemical admixture-cement interactions: phenomenology and physio-chemical concepts", Cement and Concrete Composites, 20, pp.87-101.
- JONES, M.R., DHIR, R.K., GILL, J.P., 1995:  
 "Concrete surface-treatment – effect of exposure temperature on chloride diffusion resistance", Cement and Concrete Research, Vol.25, No.1, pp.197-208.
- JONES, M.R., DHIR, R.K., MAGEE, B.J., 1997:  
 "Concrete containing ternary blended binders: resistance to chloride ingress and carbonation", Cement and Concrete Research, Vol.27, No.6, pp.825-831.
- KAY, T., SLATER, D., 1995:  
 "Specifying concrete for adverse weather", Concrete, May/June, pp.21-23.
- KELHAM, S., 1988:  
 "A water absorption test for concrete", Magazine of Concrete Research, Vol.40, No.143, June.
- KERN, R., CERVINKA, S., WEBER, R., 1995:  
 "Efficiency of curing methods", Darmstadt Concrete, Vol.10, pp.117-122.
- KHATRI, R.P., SIRIVIVATNANON, V., 1997:  
 "Role of permeability in sulphate attack", Cement and Concrete Research, Vol.27, No.8, pp.1179-1189.
- KILLOH, D.C., PARROTT, L.J., PATEL, R.G., 1989:  
 "Influence of curing at different relative humidities on the hydration and porosity of a Portland/fly ash cement paste", Proceedings, 3<sup>rd</sup> International Conference on Fly Ash, Silica Fume, Slag and Natural Pozzolans in Concrete, Trondheim, Norway, June, ACI SP-114, Vol.1, pp.157-174.
- KJELLEN, K.O., DETWILER, R.J., GJORV, E., 1990:  
 "Backscattered electron imaging of cement pastes hydrated at different temperatures", Cement & Concrete Research, Vol.20, pp.308-311.
- KJELLEN, K.O., DETWILER, R.J., GJORV, E., 1990a:  
 "Pore structure of plain cement pastes hydrated at different temperature", Vol.20, pp.927-933.
- KLIEGER, P., 1958:  
 "Effect of mixing and curing temperature on concrete strength", Journal, American Concrete Institute, 54, June, pp.1063-1081.
- KOKUBA, K., TAKAHASHI, S., ANZAL, H., 1989:  
 "Effect of curing temperature on the hydration and adiabatic temperature characteristics of Portland cement – blast furnace slag concrete", Proceedings, CANMET/ACI 3<sup>rd</sup> International Conference on Fly Ash, Silica Fume, Slag and Natural Pozzolans in Concrete, Edited by V.M. Malhotra, Trondheim, Norway, June, ACI SP 114-66, pp.1361-1376.
- KOLLEK, J.J., 1989:  
 "The determination of the permeability of concrete to oxygen by the Cembureau method – a recommendation", Materials and Structures, No.22, pp.225-230.
- KOVLER, K., 1995:  
 "Shock of evaporative cooling of concrete in hot dry climates", Concrete International, October, pp.65-69.
- KREIJGER, P.C., 1984:  
 "The skin of concrete, composition and properties", Materials and Structures Research and Testing, Vol.17, No.100, July/August, pp.275-283.

- KROPP, J., 1995:  
 "Relations between transport characteristics and durability", in RILEM Report 12: Performance Criteria for Concrete Durability, RILEM Technical Committee TC116-PCD, Performance of Concrete as a Criterion of its Durability, Edited by J. Kropp and H.K. Hilsdorf, E&FN Spon, pp.98-111.
- LANGLOIS, M., BEAUPRE, D., PIGEON, M., FOY, C., 1989:  
 "The influence of curing on the salt scaling resistance of concrete with and without silica fume", Proceedings, 3<sup>rd</sup> International Conference on Fly Ash, Silica Fume, Slag and Natural Pozzolans in Concrete, Trondheim, Norway, June.
- LAWRENCE, C.D., 1984:  
 "Transport of oxygen through concrete", British Ceramic Proceedings, 35, The Chemistry and Properties of Cement, April, pp.277-293.
- LEA, F.M., 1970:  
 "The chemistry of cement and concrete", 3<sup>rd</sup> Edition, Edward Arnold, London.
- LITVAN, G.G., MEYER, 1986:  
 "Carbonation of granulated blast furnace slag cement concrete during twenty years of field exposure", Proceedings, 2<sup>nd</sup> International Conference on Fly Ash, Silica Fume, Slag and Natural Pozzolans in Concrete, Madrid, American Concrete Institute, Special Publication No. SP91-71, Vol.2, pp.145-162.
- LONG, A.E., SHAAT, A.A., BASHEER, P.A.M., 1995:  
 "The influence of controlled permeability formwork on the durability and transport-properties of near-surface concrete", Proceedings, 2<sup>nd</sup> CANMET/ACI International Symposium on Advances in Concrete Technology, Las Vegas, NV, 11-14 June, pp. 41-54.
- LONG, A.E., BASHEER, P.A.M., BRADY, P., MCCAULEY, A., 1996:  
 "A comparative study of three types of controlled permeability formwork liners", Radical Concrete Technology, Edited by R.K. Dhir and P.C. Hewlett, E&FN Spon, London, pp.273-290.
- LOO, Y.H., CHIN, M.S., TAM, C.T., ONG, K.C.G., 1994:  
 "A carbonation prediction model for accelerated carbonation testing of concrete", Magazine of Concrete Research, 46, No.168, September, pp.191-200.
- LOVELOCK, P.E.R., 1970:  
 "Laboratory measurement of soil and rock permeability", Institute of Geological Science, London.
- LYDON, F.D., MAHAWISH, A.H., 1991:  
 "Tests of the permeability of concrete to Nitrogen gas", Construction and Building Materials, Vol.5, No.1, March, pp.8-17.
- McCARTER, W.J., EZIRIM, H., EMERSON, M., 1992:  
 "Absorption of water and chloride into concrete", Magazine of Concrete Research, 44, No.158, March, pp.31-37.
- McCARTHY, M.J., DHIR, R.K., JONES, M.R., 1998:  
 "Benchmarking PFA grouts for magnesium sulfate bearing exposures", Materials and Structures, Vol.31, No.209, pp.335-342.
- MACKENZIE, R.C., 1972:  
 "Differential thermal analysis", Vol.2, Academic Press, London and New York.
- MALVIN, S., ODD, E.G., 1992:  
 "High curing temperatures in light weight high strength concrete", Concrete International, December, pp.40-42.
- MANGAT, P.S., EL-KHATIB, J.M., 1992:  
 "Influence of initial curing on pore structure and porosity of blended cement concretes", Proceedings, 4<sup>th</sup> International Conference on fly ash, silica fume, slag and natural Pozzolans in concrete, SP-132, Malholva, V.M. (Ed.), Istanbul, Turkey, pp.813-833.

- MARCHAND, J., HORNAIN, H., DIAMOND, S., PIGEON, M., GUIRAND, H., 1996:  
 "The microstructure of dry concrete products", *Cement and Concrete Research*, Vol.26, No.3, pp.427-438.
- MARCHESE, B., D'AMORE, F., 1990:  
 Discussion on paper published in *Magazine of Concrete Research*, Vol.41, No.147, June, by C. Hall, *Water Sorptivity of Mortars and Concretes: A Review*, *Magazine of Concrete Research*, Vol.42, No.151, June.
- MARSH, B.K., ALI, M.A., 1994:  
 "Assessment of the effectiveness of curing on the durability of reinforced concrete", *CANMET/ACI 3<sup>rd</sup> International Conference on the Durability of Concrete*, Edited by V.M. Malholra, Nice, France, ACI SP145, pp.1161-1176.
- MARSH, B.K., DAY, R.L., BONNER, D.G., 1985:  
 "Pore structure characteristics affecting the permeability of cement paste containing fly ash", *Cement and Concrete Research*, Vol.15, pp.1027-1038.
- MARTIN, M., 1992:  
 "Compressive strength and the rising temperature of field concrete", *Concrete Institute*, December, pp.29-33.
- MEHTA, P.K., MANMOHAN, D., 1980:  
 "Pore size distribution and permeability of hardened cement pastes", *Proceedings, 7<sup>th</sup> International Symposium on the Chemistry of Cement*, Paris, Vol.3, pp.VII-1-VII-5.
- MENG, B., 1994:  
 "Calculation of moisture transport coefficients on the basis of relevant pore structure parameters", *Materials and Structures*, 27, pp.125-134.
- MIDGLEY, H.G., 1979:  
 "The determination of calcium hydroxide in set Portland cement", *Cement and Concrete Research*, Vol.9, pp.77-82.
- MIDGLEY, H.G., ILLSTON, J.M., 1983:  
 "Some comments on the microstructure of hardened cement pastes", *Cement and Concrete Research*, Vol.13, pp.197-206.
- MOURET, M., BASCOUL, A., ESCADEILLAS, G., 1997:  
 "Drops in concrete strength in summer related to the aggregate temperature", *Cement and Concrete Research*, Vol.27, No.3, pp.345-357.
- MURPHY, C.B., 1958:  
 "Differential thermal analysis: review of fundamental developments in analysis", *Analytical Chemistry*, Vol.30, No.4, April, pp.867-872.
- MURPHY, C.B., 1960:  
 "Differential thermal analysis: review of fundamental developments in analysis", *Analytical Chemistry*, Vol.32, No.5, April, pp.169R-171R.
- MURPHY, C.B., 1962:  
 "Differential thermal analysis: review of fundamental developments in analysis", *Analytical Chemistry*, Vol.34, No.5, April, pp.229R-301R.
- NAGATAKI, S., OHGA, H., KIM, E.K., 1986:  
 "Effect of curing conditions on the carbonation of concrete with fly ash and the corrosion of reinforcement in long-term tests", *Proceedings, CANMET/ACI 2<sup>nd</sup> International Conference on Fly Ash, Silica Fume, Slag and Natural Pozzolans in Concrete*, Madrid, ACI SP 91-24, Vol.1, pp.521-540.
- NAGATAKI, S., UJIKE, I., 1986a:  
 "Air permeability of concretes mixed with fly ash and condensed silica fume", *Proceedings, CANMET/ACI 2<sup>nd</sup> International Conference on the Use of Fly Ash, Blast-Furnace Slag and Silica Fume in Concrete*, Madrid, Vol.2, pp.1049-1068.

- NEVILLE, A.M., 1995:  
 "Properties of concrete", 4<sup>th</sup> Edition, Longman Group Ltd., London.
- NILSSON, L.O., 1996:  
 "Interaction between microclimate and concrete – a pre-requisite for deterioration",  
 Construction and Building Materials, Vol.10, No.5, pp.301-308.
- NIREKI, T., 1996:  
 "Service life design", Construction and Building Materials, Vol.10, No.5, pp.403-406.
- NMAI, C.K., 1998:  
 "Cold weather concreting admixtures", Cement and Concrete Composites, 20, pp.121-128.
- NYAME, B.K., ILLSTON, J.M., 1980:  
 "Capillary pore structure and permeability of hardened cement paste", Proceedings, 7<sup>th</sup>  
 International Symposium on the Chemistry of Cement, Paris, Vol.3, pp.VI-181-VI-186.
- NYAME, B.K., ILLSTON, J.M., 1981:  
 "Relationship between permeability and pore structure of hardened cement paste",  
 Magazine of concrete Research, Vol.33, No.116, September, pp.139-146.
- ODLER, I., GLEN, Y., 1995:  
 "Investigations on the ageing of hydrated tricalcium silicate and Portland cement  
 pastes", Cement and Concrete Research, Vol.25, No.5, pp.919-923.
- ODLER, I., KOSTER, H., 1986:  
 "Investigation on the structure of fully hydrated Portland cement and tricalcium silicate  
 pastes", Cement and Concrete Research, Vol.16, pp.893-901.
- OSBORNE, G.J., 1986:  
 "Carbonation of blast furnace slag cement concretes", Durability of Building Materials, 4,  
 pp.81-96.
- OSBORNE, G.J., 1989:  
 "Carbonation and permeability of blast furnace slag cement concretes from field  
 structures", Proceedings, CANMET/ACI 3<sup>rd</sup> International Conference on Fly Ash, Silica  
 Fume, Slag and Natural Pozzolans in Concrete, ACI SP114-59, Trondheim, Norway, June,  
 Vol.2, pp.1209-1237.
- OSBORNE, G.J., 1994:  
 "Effect of microclimate on carbonation of slag cement concrete structures", Proceedings,  
 PH Mehta Symposium on Durability of Concrete, Ed. K.H. Khayat, ACI CANMET, Nice,  
 pp.119-145.
- OSLEN, N.H., SUMMERS, G.R., 1996:  
 "New concepts in the durability and repair of reinforced concrete", Conference on  
 Deterioration of Reinforced Concrete in the Gulf and Methods of Repair, 15-17 December,  
 Muscat, Sultanate of Oman.
- OSLEN, N.H., SUMMERS, G.R., 1997:  
 "Performance of 750 reinforced concrete specimens after 10 years exposure in Bahrain",  
 CANMET/ACI Fourth International Conference on the Durability of Concrete, Edited by  
 Bryant and Catherine Mather, Sidney, Australia.
- OWENS, P.L., 1985:  
 "Effect of temperature rise and fall on the strength and permeability of concrete made  
 with and without fly ash", Temperature Effects on Concrete, ASTM STP858, T.R. Naik  
 (Ed.), American Society for Testing and Materials, Philadelphia, 1985, pp.134-149.
- PAGE, C.L., SHUT, N.R., EL-TERRAS, A., 1981:  
 "Diffusion of chloride ions in hardened cement pastes", Cement and Concrete Research,  
 Vol.11, pp.395-406.

- PARROTT, L.J., KILLOH, D.C., 1984:  
 "Prediction of cement hydration", The Chemistry and Chemically-Related Properties of Cement, British Ceramic Proceedings, No.35, Stoke on Trent, British Ceramic Society, September, pp.41-53.
- PARROTT, L.J., KILLOH, D.C., PATEL, R.G., 1986:  
 "Cement hydration under partially saturated curing conditions", Proceedings, 8<sup>th</sup> Congress on the Chemistry of Cement, Rio de Janeiro, FINEP, Vol.3, pp.46-50.
- PARROTT, L.J., 1987:  
 "A review of carbonation in reinforced concrete", Cement and Concrete Association, Slough, July, pp.42.
- PARROTT, L.J., 1988:  
 "Moisture profiles in drying concrete", Advances in Cement Research, Vol.1, No.3, pp.164-170.
- PARROTT, L.J., GEIKER, M., GUTTERIDGE, W.A., KILLOH, D., 1990:  
 "Monitoring Portland cement hydration: comparison of methods", Cement and Concrete Research, Vol.20, pp.919-926.
- PARROTT, L.J., 1991:  
 "Some factors influencing air permeation in cover concrete", Materials and Structures, 24, pp.403-408.
- PARROTT, L.J., 1991a:  
 "Rate of weight loss during initial exposure as an indicator of cover concrete performance", British Cement Association, Slough.
- PARROTT, L.J., 1991b:  
 "Factors influencing relative humidity in concrete", Magazine of Concrete Research, 43, No.154, March, pp.45-52.
- PARROTT, L.J., 1992:  
 "Water absorption in cover concrete", Materials and Structures, 25, pp.284-292.
- PARROTT, L.J., 1992a:  
 "Variation of water absorption rate and porosity with depth from an exposed concrete surface: effects of exposure conditions and cement type", Cement and Concrete Research, Vol.22, pp.1077-1088.
- PARROTT, L.J., 1994:  
 "Moisture conditioning and transport properties of concrete test specimens", Materials and Structures, 27, pp.460-468.
- PARROTT, L.J., 1995:  
 "Influence of cement type and curing on the drying and air permeability of cover concrete", Magazine of Concrete Research, 47, No.171, June, pp.103-111.
- PARROTT, L.J., 1996:  
 "Water absorption, chloride ingress and reinforcement corrosion in cover concrete: some effects of cement and curing", Proceedings, 4<sup>th</sup> Symposium on the Corrosion of Reinforcement in Concrete Construction, Royal Society of Chemistry, July, pp.146-155.
- PATEL, R.G., PARROTT, L.J., MARTIN, J.A., KILLOH, D.G., 1985:  
 "Gradients of microstructure and diffusion properties in cement paste caused by drying", Cement and Concrete Research, Vol.15, pp.343-356.
- PATEL, R.G., KILLOH, D.L., PARROTT, L.J., GUTTERIDGE, W.A., 1988:  
 "Influence of curing at different relative humidities upon compound reactions and porosity in Portland cement paste", Materials and Structures, Vol.21 (123), May-June, p.192-197.
- PAULINI, P., 1994:  
 "A through solution model for volume changes of cement hydration, Cement & Concrete Research, Vol.24, No.3, pp.488-496.

- PERSSON, B., 1997:  
 "Moisture in concrete subjected to different kinds of curing", *Materials and Structures*, Vol.30, November, pp.533-544.
- PETERSSON, P., 1996:  
 "Curing of concrete – effect on strength and durability", in *Radical Concrete Technology*, Edited by R.K. Dhir and P.C. Hewlett. Published in 1996 by E&FN Spon, pp.381-390.
- POWERS, T.C., 1947:  
 "A discussion of cement hydration in relation to the curing of concrete", Publication No.RX25, Portland Cement Association, Skokie, 12pp.
- PRICE, W.F., 1993:  
 "The improvement of concrete durability using controlled permeability formwork", *Proceedings, 5<sup>th</sup> International Conference on Structural Faults and Repairs*, Vol.2, pp.233-238.
- PRICE, W.H., 1951:  
 "Factors influencing concrete strength", *Journal of American Concrete Institute*, 47, February, pp.417-432.
- PRIEST, A., 1995:  
 "Concrete durability design and performance testing", *Concrete*, January/February, pp.32-33.
- RAHMAN, A.A., 1984:  
 "Characterisation of the porosity of hydrated cement pastes", in the *Chemistry and Chemically Related Properties of Concrete*, British Ceramic Proceedings, No.35, Stoke-on-Trent, pp.249-263.
- RAMEZANIANPOUR, A.A., 1993:  
 "Recommendations for concrete durability in the southern coasts and islands of Iran", *Building Housing and Research Centre*, 1993, pp.49.
- RAMEZANIANPOUR, A.A., MALHOTRA, V.M., 1995:  
 "Effect of curing on the compressive strength, resistance to chloride-ion penetration and porosity of concretes incorporating slag, fly ash or silica fume", *Cement and Concrete Composites*, 17, pp.125-133.
- RASHEEDUZZAFAR, DAKHIL, F.H., GHATANI, A.S., 1984:  
 "The deterioration of concrete structures in the environments of the Middle East", *Journal, American Concrete Institute*, 1, January-February, pp.13-20.
- RASHEEDUZZAFAR, DAKHIL, F.H., GHATANI, A.S., 1985:  
 "Corrosion of reinforcement in concrete structures in the Middle East", *Concrete International*, 7(9), September, pp.48-55.
- RASHEEDUZZAFAR, AL-KURDI, S.M.A., 1992:  
 "Effect of hot weather conditions on the microcracking and corrosion cracking potential of reinforced concrete", SP-139, MacInnis (Ed.), *Durable Concrete in Hot Climates*, International Symposium on "How to produce concrete in hot climates", ACI Fall Convention in San Juan, Puerto Rico, October, pp.1-19.
- RASHEEDUZZAFAR, ALI, M.G., 1992a:  
 "Effect of temperature on cathodic protection criterion for reinforced concrete structures", SP139-2, MacInnis (Ed.), *Durable Concrete in Hot Climates*, International Symposium on "How to Produce Concrete in Hot Climates", ACI Fall Convention in San Juan, Puerto Rico, October, pp.21-40.
- RAVINA, D., SHALON, R., 1968:  
 "Plastic shrinkage cracking", *ACI Journal*, Vol.65, pp.282-292.

- RAVINA, D., SOROKA, I., 1992:  
 "Research on concrete in hot environments at the National Building Research Institute, Haifa, Israel", International Symposium on "How to Produce Durable Concrete in Hot Climates", ACI Fall Convention in San Juan, Puerto Rico, October, SP-139, MacInnis (Ed.), pp.107-129.
- REINHARDT, H.W., AUFRECHT, M., 1995:  
 "Simultaneous transport of an organic liquid and gas in concrete", Materials and Structures, 28, pp.43-51.
- RICHARDSON, M.G., 1993:  
 "Controlled permeability formwork: a review and pilot study of early age and medium term characteristics of inclined concrete surfaces", Department of Civil Engineering, University College Dublin, pp.51.
- RICHARDSON, M.G., 1998:  
 "Permeability and carbonation - making durable concrete", The Institute of Concrete Technology Yearbook, pp.33-45.
- RILEM TECHNICAL COMMITTEE 14-CPC, 1974:  
 "Absorption of water by capillarity", Tentative Recommendations No.11.2, Materials and Structures, Vol.7, No.40, pp.295-297.
- RILEM TECHNICAL COMMITTEE 94-CHC, 1993:  
 "Concrete in hot weather environments", Draft, Part 1: Influence of the Environment of Reinforced Concrete Durability, Part II: Design Approach for Durability.
- RILEM CONCRETE PERMANENT COMMITTEE CPC-18, 1984:  
 "Measurement of hardened concrete carbonation depth", Materials and Structures, Vol.17, No.102, pp.435-440.
- RILEM REPORT 12, 1995:  
 "Performance criteria for concrete durability", RILEM Technical Committee TC116-PCD, Performance of Concrete as a Criterion of its Durability, Edited by J. Kropp and H.K. Hilsdorf, Published by E&FN Spon, London.
- RITTER, H.L., DRAKE, L.C., 1945:  
 "Pore size distribution in porous materials", Industrial and Engineering Chemistry, Vol.17, No.12, pp.782-786.
- ROY, D.M., 1989:  
 "Hydration, microstructure and chloride diffusion of slag-cement pastes and mortars", Proceedings, CANMET/ACI 3<sup>rd</sup> International Conference on the Use of Fly Ash, Silica Fume, Slag and Natural Pozzolans in Concrete, Trondheim, Norway, Vol.2, pp.1265-1281.
- ROY, S.K., BENG, P.K., NORTHWOOD, D.O., 1996:  
 "The carbonation of concrete structures in the topical environment of Singapore and a comparison with published data for temperate climates", Magazine of Concrete Research, 48, No.177, December, pp.293-300.
- RUTLE, J., 1977:  
 "Additives and curing of concrete", Nordisk Betong, Vol.3, pp.21-26.
- SARICIMEN, H., MASLEHUDDIN, M., AL-TAYYIB, A.J., AL-MANA, A., 1995:  
 "Permeability and durability of plain and blended cement concretes cured in field and laboratory conditions", ACI Materials Journal, Vol.92, No.2, March-April, pp.111-115.
- SCANLON, J.M., 1992:  
 "Concrete problems associated with hot climate", ACI Fall Convention in San Juan, Puerto Rico, October, pp.1-19.
- SCANLON, J.M., 1997:  
 "Controlling concrete during hot and cold weather", Concrete International, June, pp.52-58.

- SCRIVENER, K.L., PRATT, P.L., 1984:  
 "Microstructural studies of the hydration of C<sub>3</sub>A and C<sub>4</sub>AF independently and in cement paste", BCP, pp.207-219.
- SCRIVENER, K.L., NEMATI, K.M., 1996:  
 "The percolation of pore space in the cement paste/aggregate interfacial zone of concrete", Cement and Concrete Research, Vol.26, No.1, pp.35-40.
- SENBETTA, E. AND SCHOLER, C.F., 1984:  
 "A new approach for testing concrete curing efficiency", ACI Journal, Jan-Feb., pp.82-86.
- SENEBETTA, E., 1994:  
 "Curing and curing materials", American Society for Testing and Materials, ASTM STP 169C, Significance of Tests and Properties of Concrete and Concrete Making Materials, pp.478-483.
- SERAFINI, F.L., SMOLDERS, K., TONUS, S., WILSON, D., 1997:  
 "Controlled permeability formwork liners (CPF): some important benefits", Proceedings, 5<sup>th</sup> International Conference on Deterioration and Repair of Reinforced Concrete in the Arabian Gulf, 27-29 October, pp.201-216.
- SHA'AT, A., 1997:  
 "The effect of environmental conditions on the chloride ingress on a concrete made with controlled permeability formwork", Proceedings, 5<sup>th</sup> International Conference on the Deterioration and Repair of Reinforced Concrete in the Arabian Gulf, 27-29 October, Bahrain, Vol.1, pp.275-290.
- SHALON, R., RAVINA, D., 1960:  
 "Studies in concreting in hot countries", Proceedings, RILEM Symposium on Concrete and Reinforced Concrete in Hot Countries, Vol.1, Building Research Station, Technion, Haifa.
- SHARP, B., 1997:  
 "Criteria for curing – a 'black hole' ", Concrete, June, pp.34-38.
- SHINGUN, L., ROY, M., 1986:  
 "Investigation of relations between porosity, pore structure, and Cl-diffusion of fly ash and blended cement pastes", Cement and Concrete Research, Vol.16, pp.749-759.
- SIMS, I., 1994:  
 "The assessment of concrete for carbonation", Concrete, 28, No.6, November/December, pp.33-38.
- SKJOLSVOLD, O., 1986:  
 "Carbonation depths of concrete with and without condensed silica fume", ACI SP-91, Madrid Proceedings, Vol.2, pp.1031-1048.
- SOONGSWANG, P., TIA, M., BLOOMQUIST, D., 1991:  
 "Factors affecting the strength and permeability of concrete made with porous limestone", ACI Materials Journal, Vol.88, No.4.
- SOROKA, I., 1993:  
 "Concrete in hot environments", First Edition, Published by E&FN Spon, UK.
- SOROKA, I., RAVINA, D., 1998:  
 "Hot weather concreting with admixtures", Cement and Concrete Composites, 20, pp.129-136.
- SPEARS, R.E., 1983:  
 "The 80 percent solution to inadequate curing problems", Concrete International, pp.15-18.
- TAYLOR, H.F.W., 1964:  
 "The chemistry of cements", Academic Press, Vol.1 and 2, London.

- TAYLOR, H.F.W., 1984:  
 "Studies on the chemistry and microstructure of cement pastes", The Chemistry and Chemically Related Properties of Cement, British Ceramic Proceedings, No.35, Stoke on Trent, British Ceramic Society, September, pp.65-82.
- TAYLOR, H.F.W., 1990:  
 "Cement chemistry", Academic Press.
- TEYCHENNE, D.C., FRANKLIN, F.E., ERNTROY, H.C., 1975:  
 "Design of normal concrete mixes", Department of the Environment, Building Research Establishment, Transport and Road Research Laboratory, HMSO, London.
- THOMAS, M.D.A., OSBORNE, G.J., MATHEWS, J.D., CRIPWELL, J.B., 1990:  
 "A comparison of the properties of OPC, PFA and ggbs concrete in reinforced concrete tank walls of slender section", Magazine of Concrete Research, 42, No.152, September, pp.127-134.
- TSUKINAGA, Y., SHOYA, M., SUGAWARA, R., NONOME, H., 1995:  
 "Improvement in concrete performance and durability using permeable sheet", Proceedings, 2<sup>nd</sup> CANMET/ACI International Symposium on Advances in Concrete Technology, Las Vegas, NV, 11-14 June.
- TURTON, C.D., 1995:  
 "How hot and cold weather affect plastic concrete", Concrete, May/June, pp.24-25.
- UOMOTO, T., KOBAYASHI, K., 1989:  
 "Effect of curing temperature and humidity on strength of concrete containing blast furnace slag admixture", Proceedings, CANMET/ACI 3<sup>rd</sup> International Conference on Fly Ash, Silica Fume, Slag and Natural Pozzolans in Concrete, edited by V.M. Malhotra, Trondheim, Norway, June, ACI SP 114, pp.1345-1359.
- VERBECK, G.J., HELMUTH, R.A., 1968:  
 "Structures and physical properties of cement paste, Proceedings, 5<sup>th</sup> International Symposium on the Chemistry of Cement, Tokyo, Vol.3, pp.1-32.
- WALKER, W., 1996:  
 "Reinforced concrete in the environmental conditions of the Arabian Peninsula – including basic needs and consideration for satisfactory performance and philosophy and use of whole life costing", Conference on Deterioration of Reinforced Concrete in the Gulf and Methods of Repair, 15-17 December, Muscat, Sultanate of Oman, pp.1-17.
- WANG, J., DHIR, R.K., LEVITT, M., 1994:  
 "Membrane curing of concrete – moisture loss", Cement and Concrete Research, Vol.24, No.8, pp.1463-1474.
- WASHBURN, E.W., 1921:  
 "Notes on a method of determining the distribution of pore sizes in a porous materials", Proceedings, National Academy of Science, Vol.7, pp.115-116.
- WATERS, T., 1955:  
 "The effect of allowing concrete to dry before it has fully cured", Magazine of Concrete Research Vol.7, No.20.
- WHITE, R.N., 1997:  
 "Durable concrete facilities to resist severe environments: materials design, structural design, working with owners and a look at the future", Proceedings, 5<sup>th</sup> International Conference, Deterioration and Repair of Reinforced Concrete in the Arabian Gulf, 27-29 October, Bahrain, Vol.2, pp.829-847.
- WHITTMANN, F.H., 1976:  
 "On the action of capillary pressure in fresh concrete", Cement and Concrete Research, 6(1), pp.49-56.

- WILSON, D.J., 1994:  
 "A review of the use of controlled permeability formwork (CPF) systems", Proceedings, Conference Corrosion and Corrosion Protection of Steel in Concrete, Sheffield, pp.1132-1141.
- WILSON, M.A., TAYLOR, S.C., HOFF, W.D., 1998:  
 "The initial surface absorption test (ISAT): an analytical approach", Magazine of Concrete Research, 50, No.2, pp.179-185.
- WINSLOW, D.N., DIAMOND, S., 1970:  
 "A mercury porosimetry study of the evolution of porosity in Portland cement", Journal of Materials, Vol.5, No.3, September, pp.564-585.
- WINSLOW, D., LIU, D., 1990:  
 "The pore structure of paste in concrete", Cement and Concrete Research, Vol.20, pp.227-235.
- WOOD, J.G.M., 1994:  
 "Quantifying and modelling concrete durability performance", Paper to Meeting at Building Research Establishment, November 10<sup>th</sup>.
- WOOD, J.G.M. 1995:  
 "Structures in distress", Queen Mary and Westfield College Symposium, 31<sup>st</sup> January.
- XUEQAN, W., JIANBGO, D., MINGSHU, T., 1997:  
 "Microwave curing technique in concrete manufacture", Cement and Concrete Research, Vol.17, No.2, pp.205-210.
- YONG, J.F., 1988:  
 "A review of the pore structure of cement paste and concrete and its influence on permeability", American Concrete Institute, ACI SP-108, Permeability of Concrete, pp.1-18.
- YOUNG, J., 1967:  
 "Humidity control in the laboratory using salt solutions – a review", Journal of Applied Chemistry, Vol.17, pp.241-245.
- YUDENFREUND, M., ODLER, I., BRAUNAUER, S., 1972:  
 "Hardened portland cement pastes of low porosity: I – Materials and experimental methods", Cement and Concrete Research, Vol.2, pp.313-330.

# Appendix A

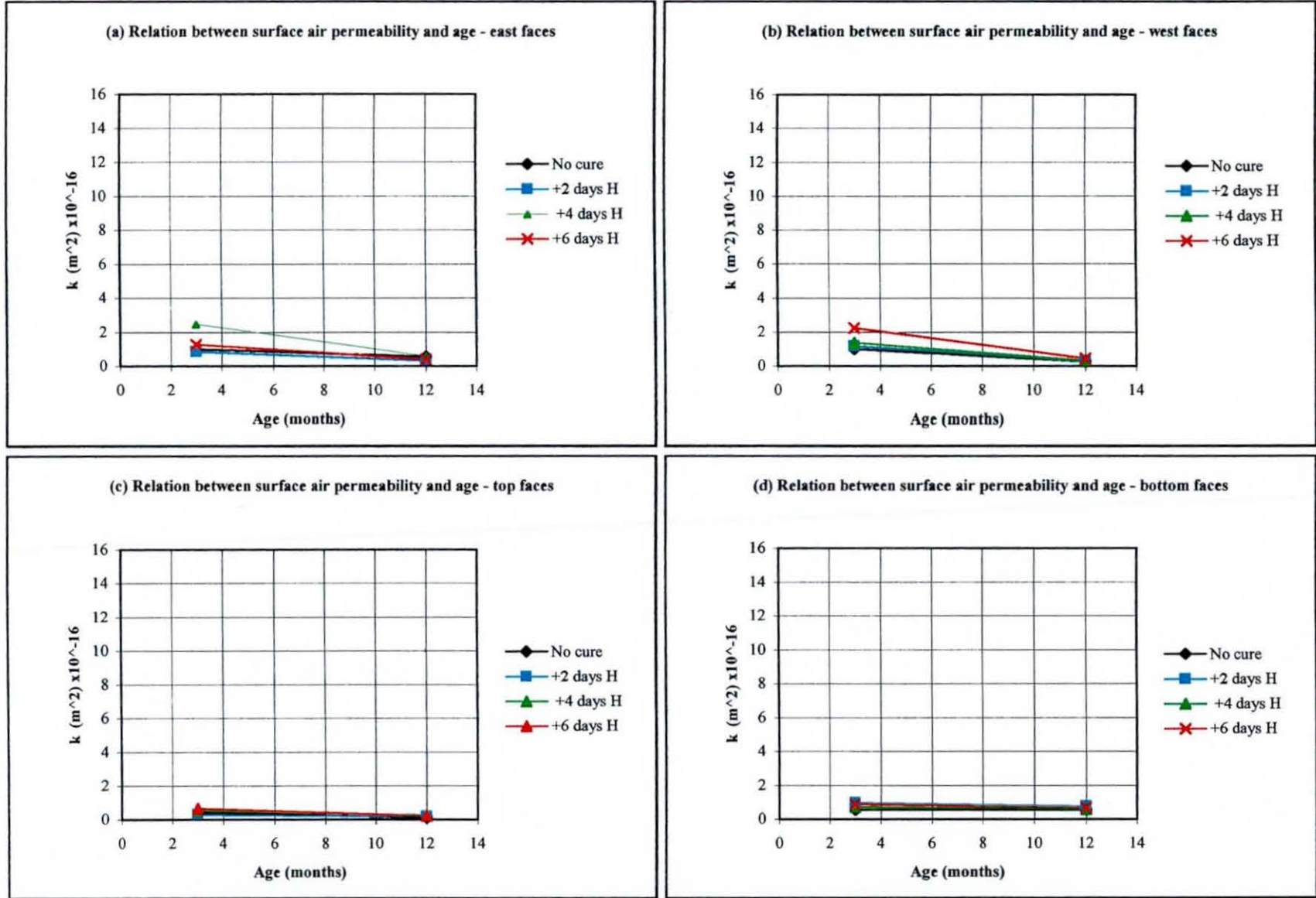


Fig. A1.1. Relationship between surface air permeability and age of the 50 MPa OPC concrete - UK winter

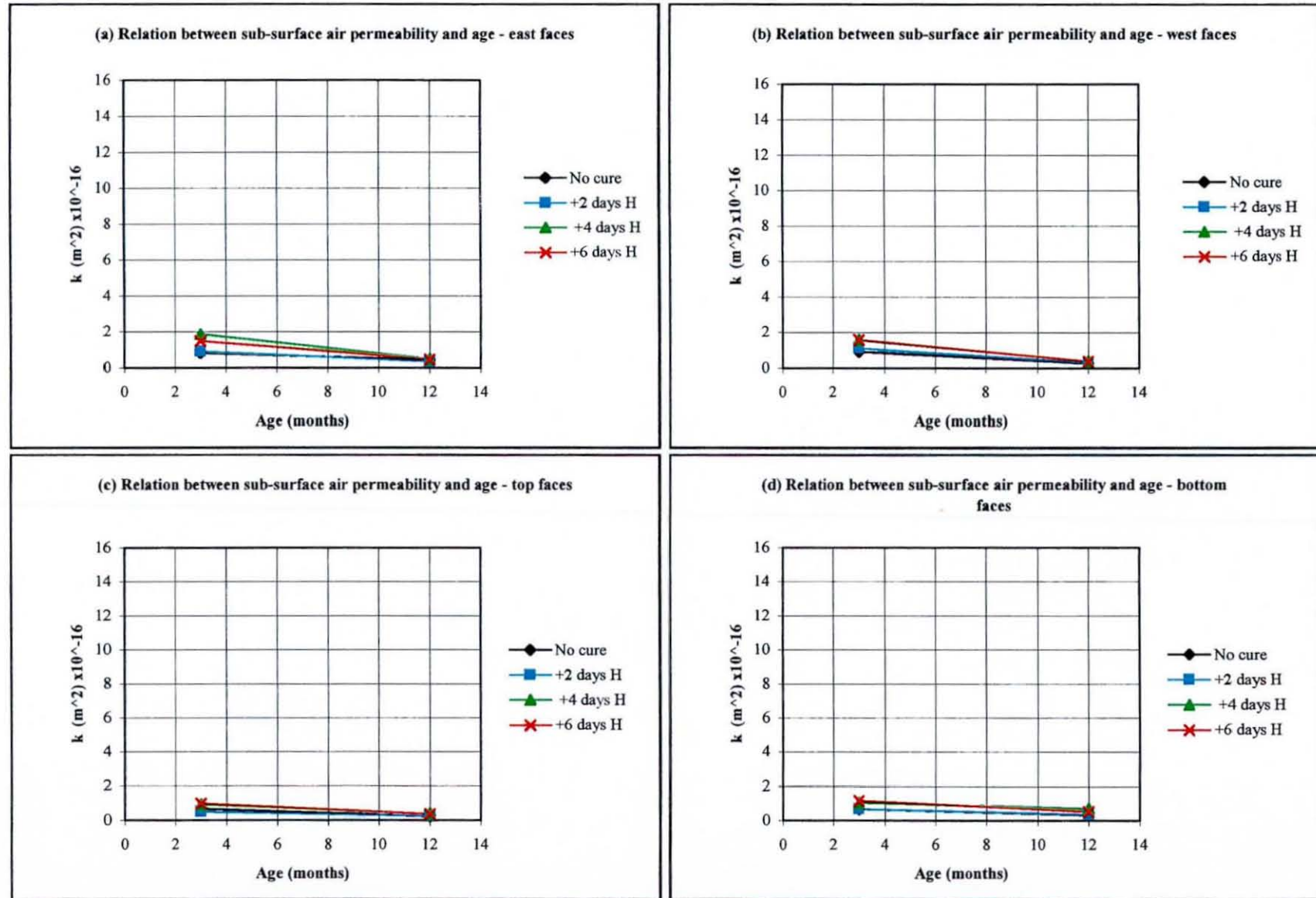


Fig. A1.2 Relationship between sub-surface air permeability and age of the 50 MPa OPC concrete - UK winter

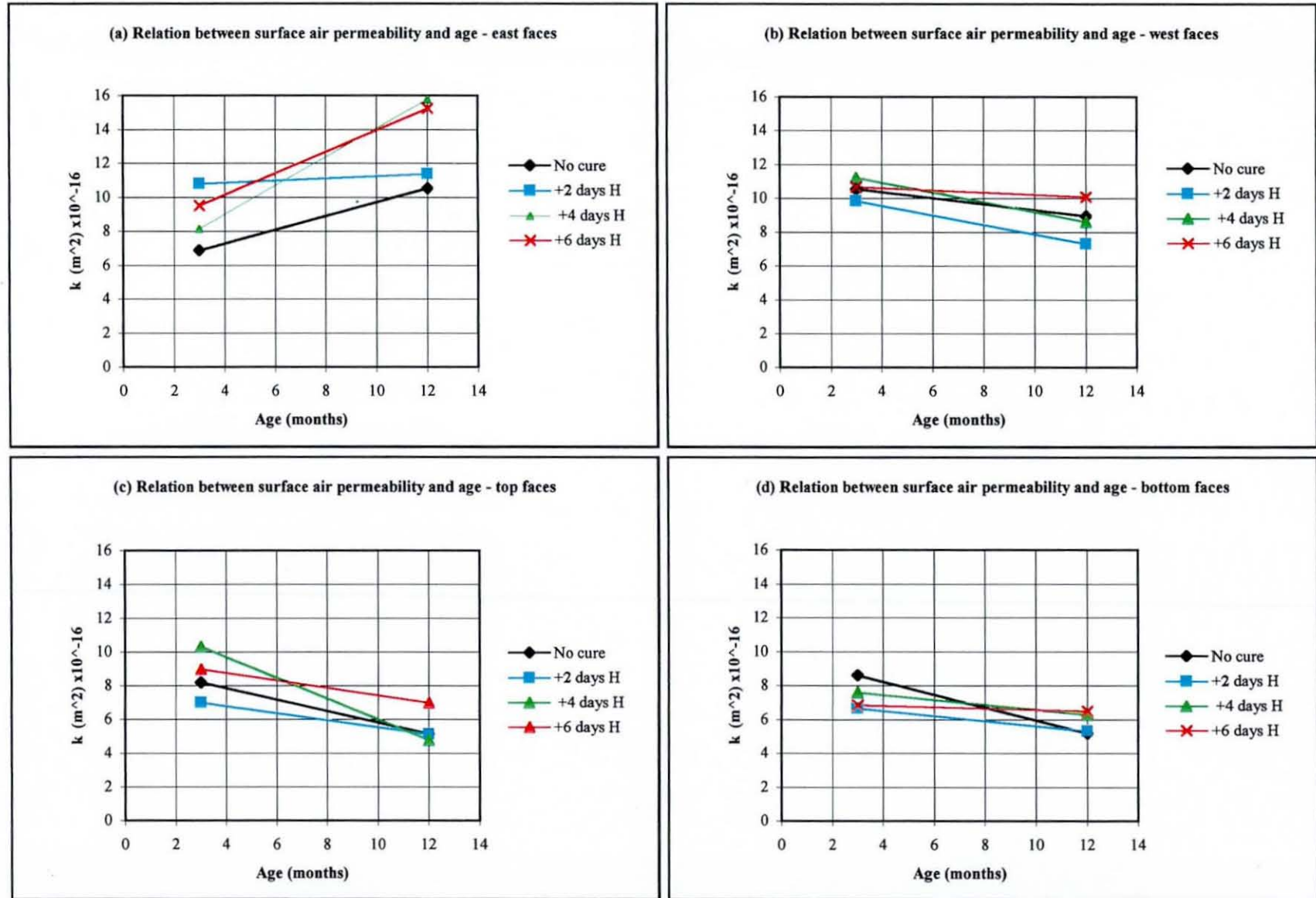


Fig. A1.3. Relationship between surface air permeability and age of the 30 MPa OPC/GGBS concrete - UK winter

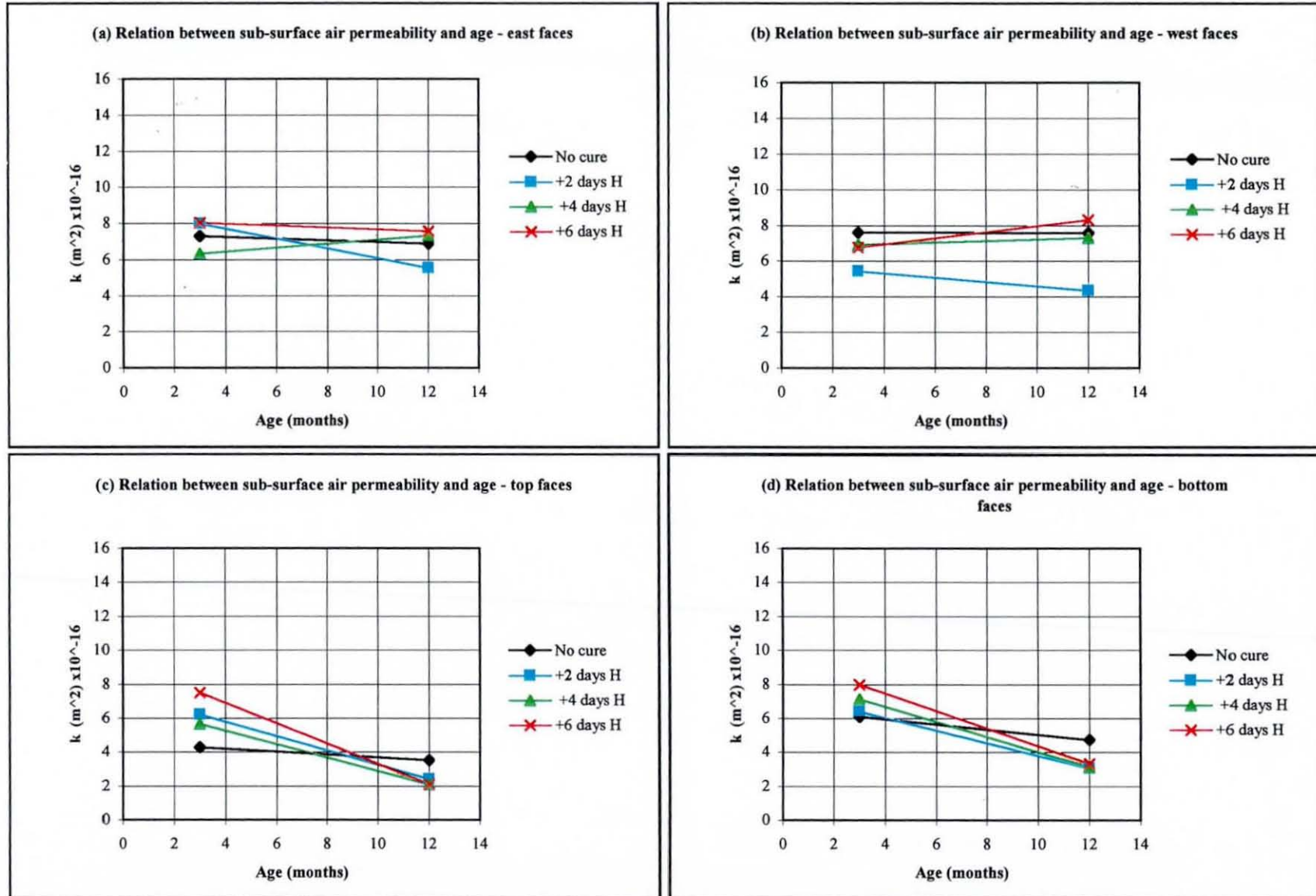


Fig. A1.4 Relationship between sub-surface air permeability and age of the 30 MPa OPC/GGBS concrete - UK winter

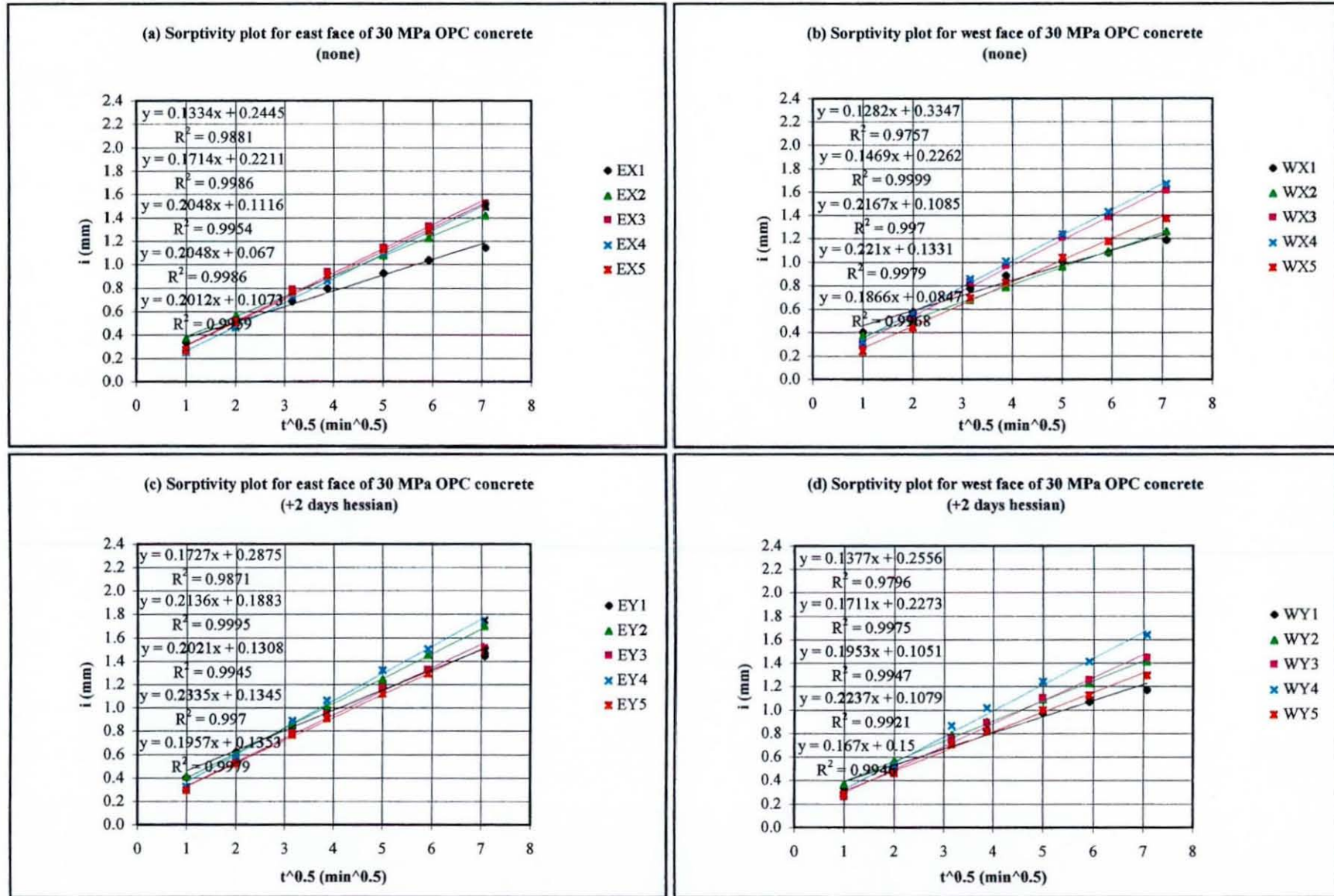


Fig. A1.5 Sorptivity plot for the 30 MPa OPC concrete - 12 months winter series

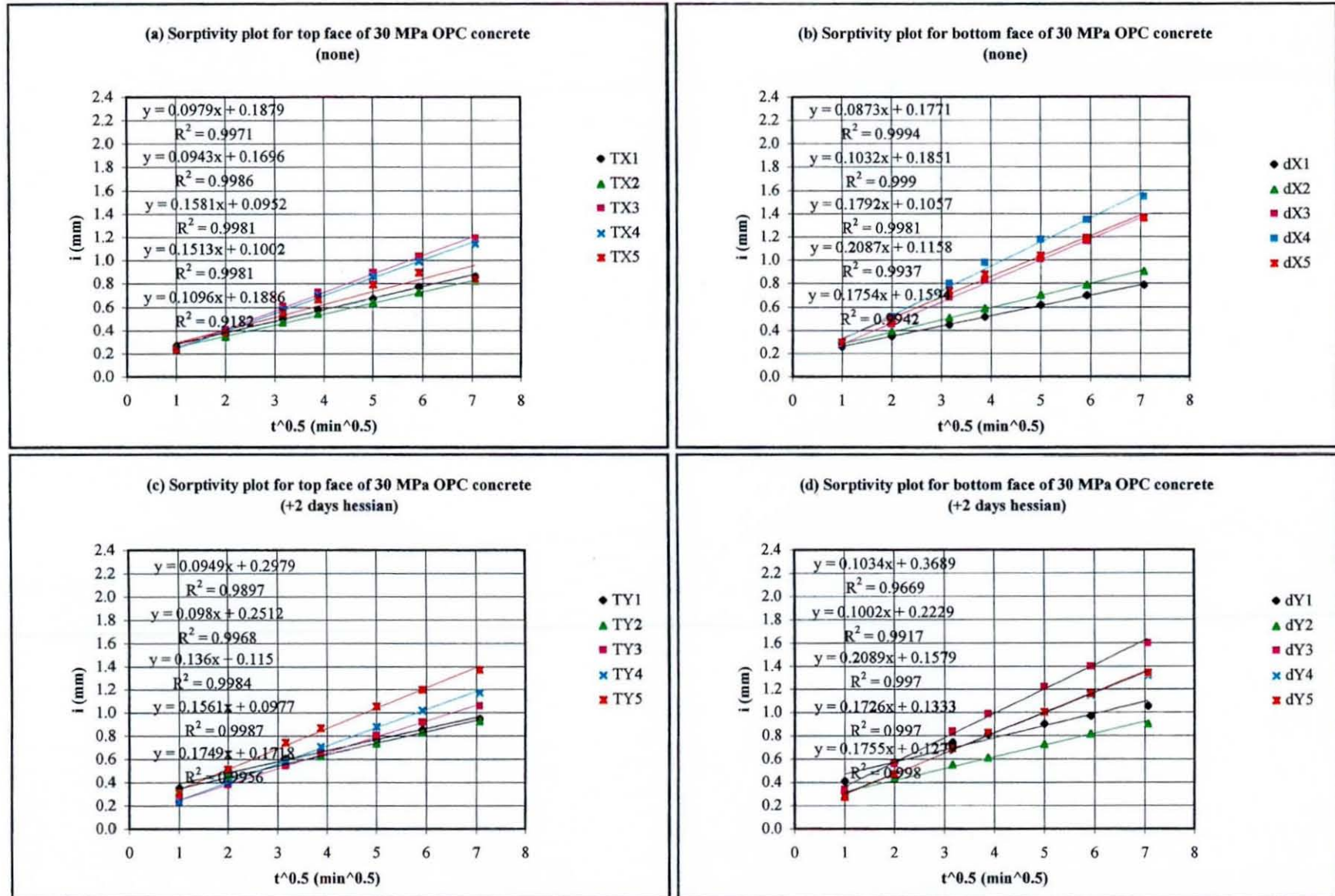


Fig. A1.6 Sorptivity plot for the 30 MPa OPC concrete - 12 months winter series

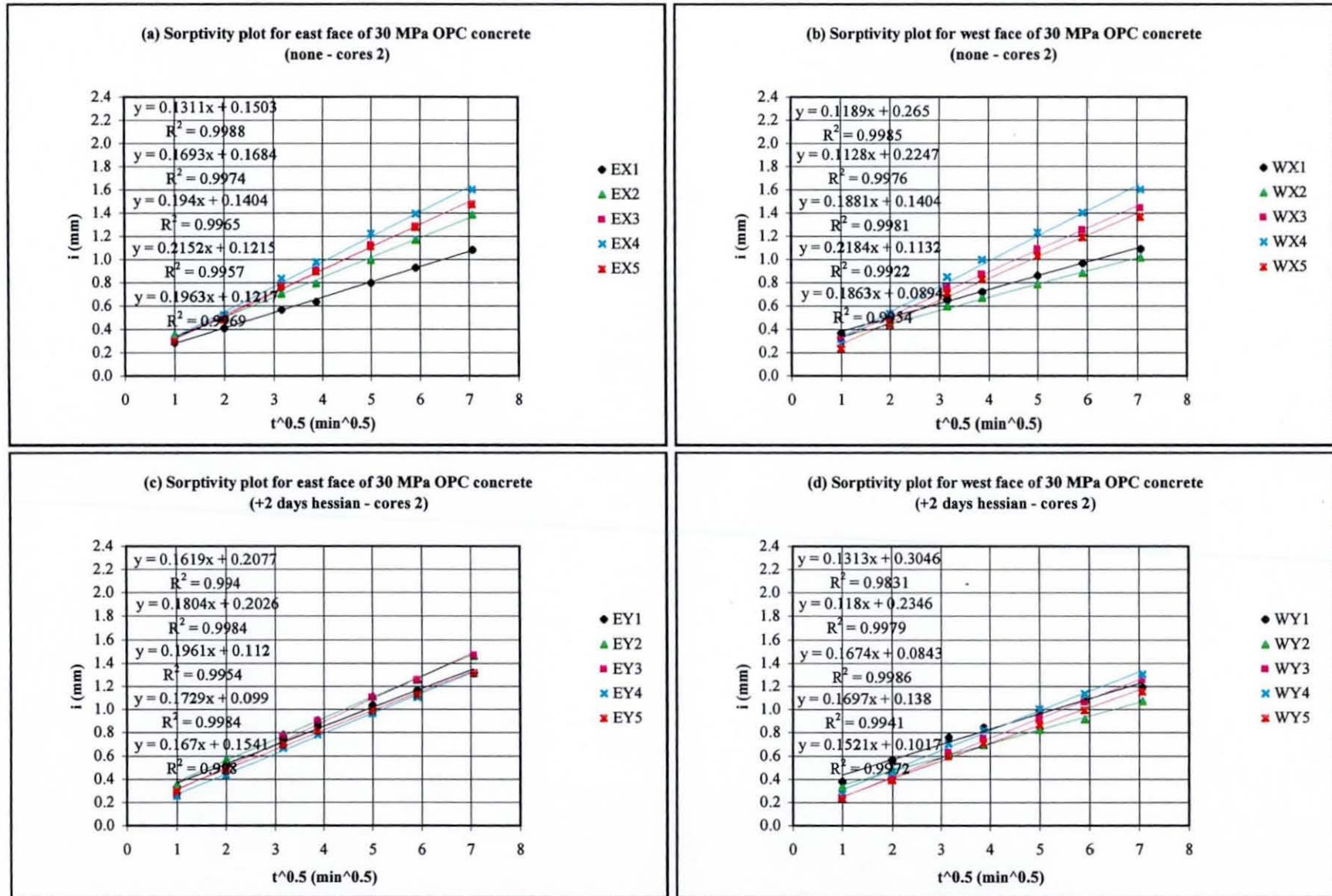


Fig. A1.7 Sorptivity plot for the 30 MPa OPC concrete - 12 months winter series

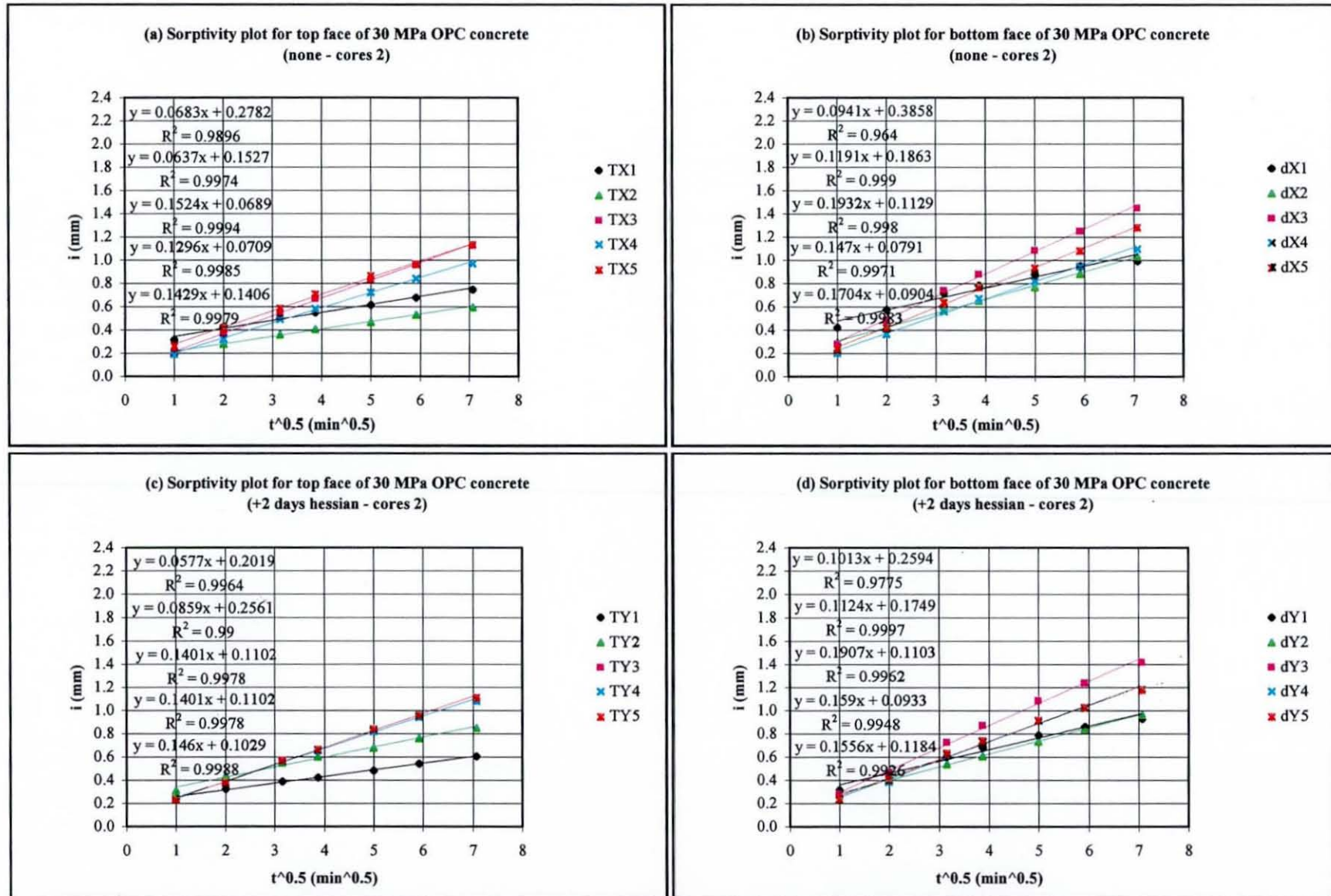


Fig. A1.8 Sorptivity plot for the 30 MPa OPC concrete - 12 months winter series

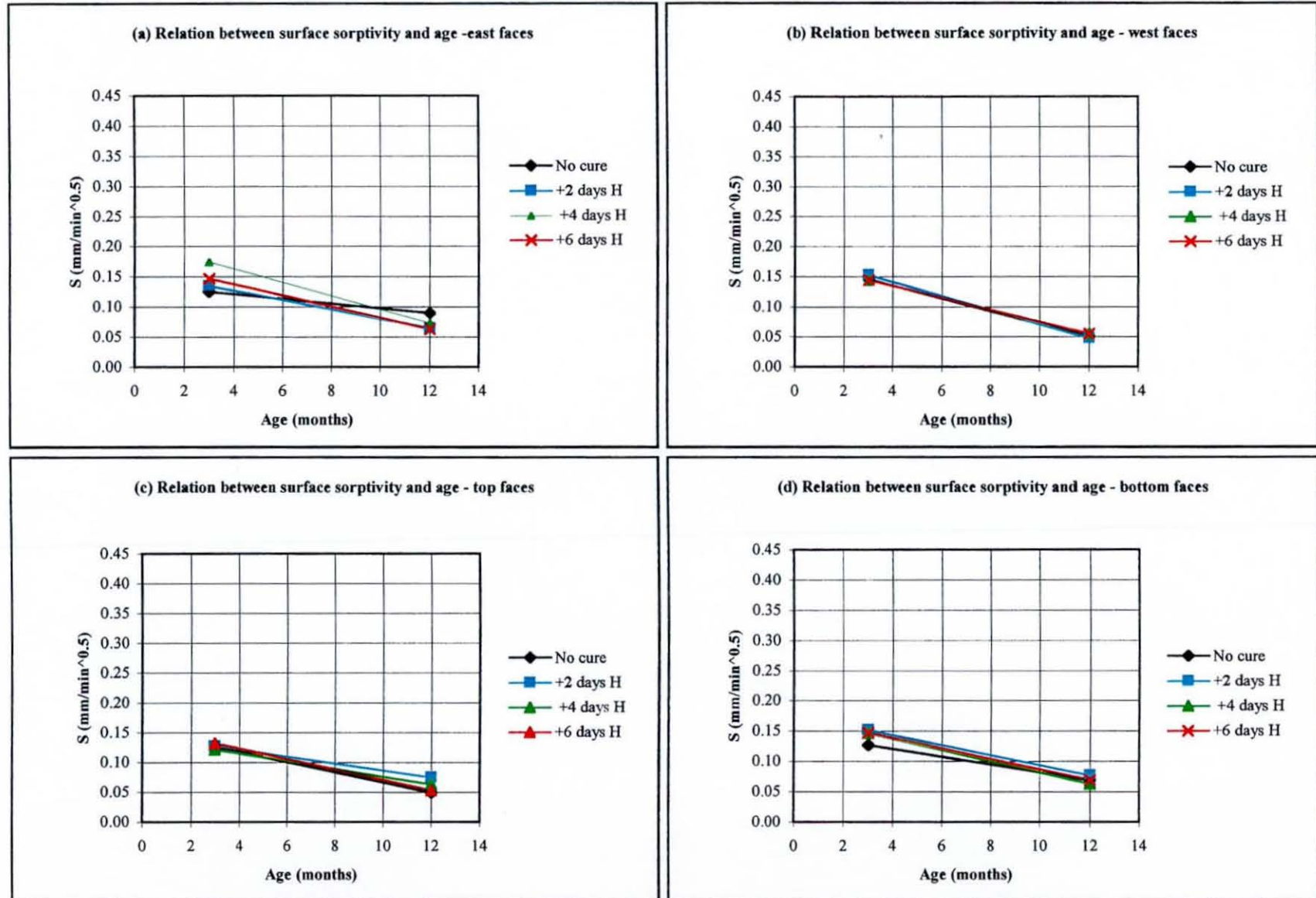


Fig. A1.9 Relationship between surface sorptivity and age of the 50 MPa OPC concrete - UK winter

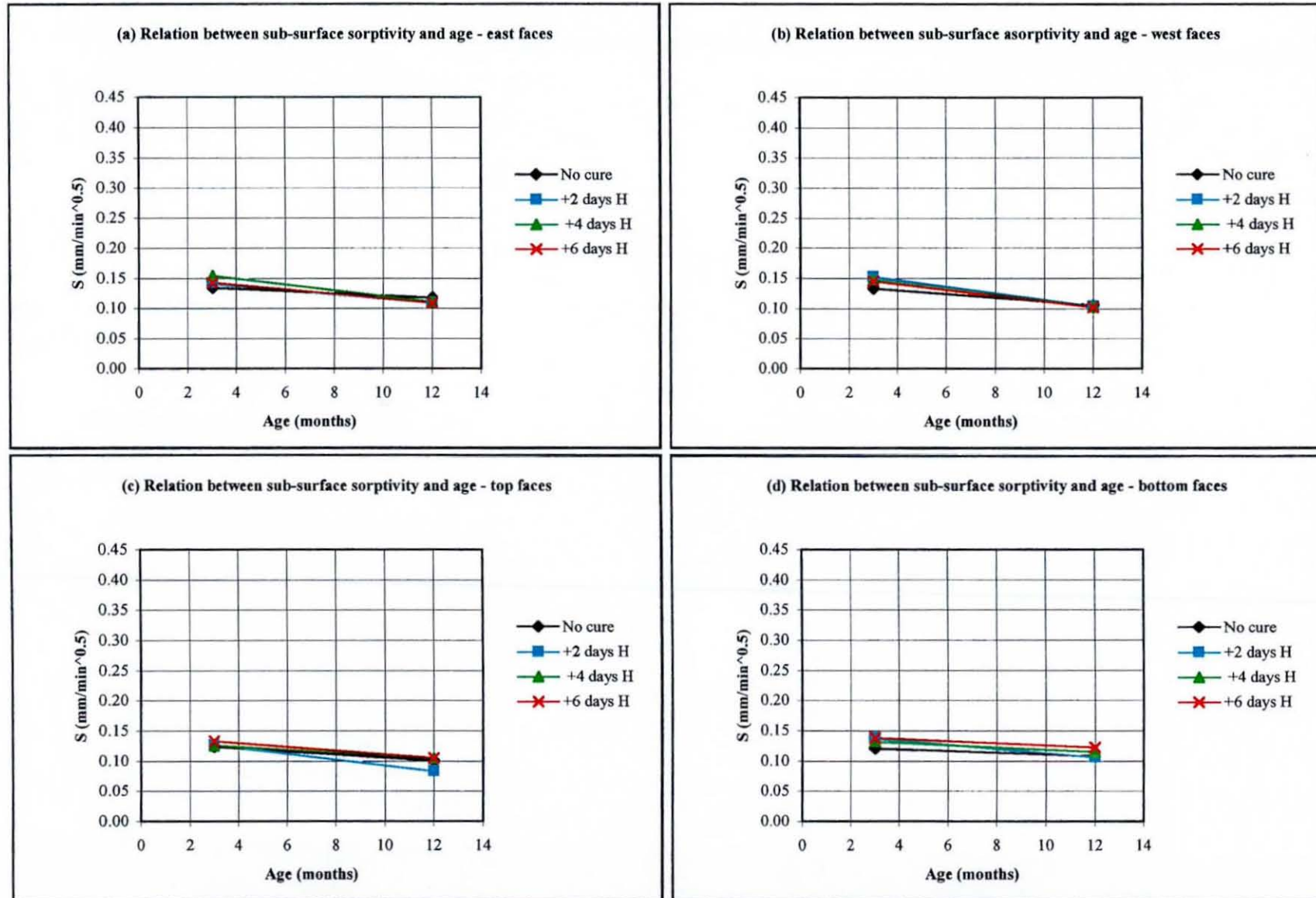


Fig. A1.10 Relationship between sub-surface sorptivity and age of the 50 MPa OPC concrete - UK winter

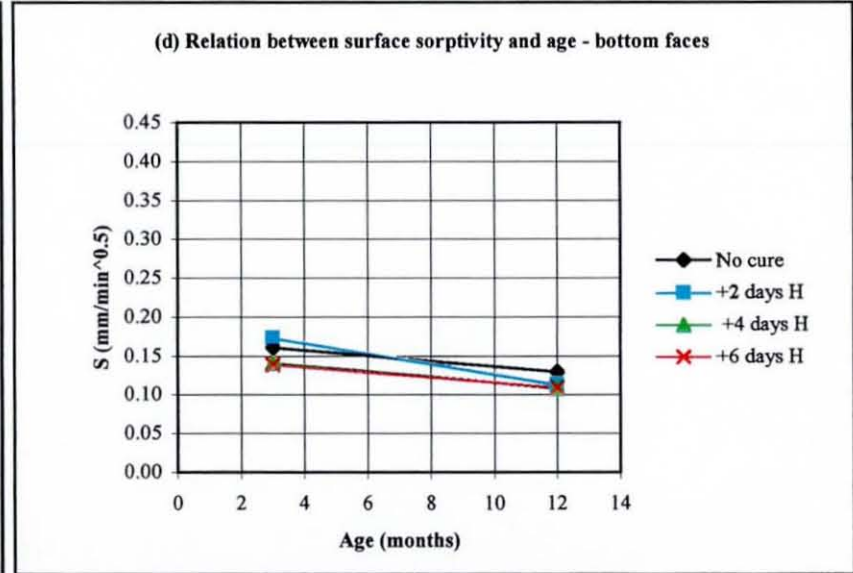
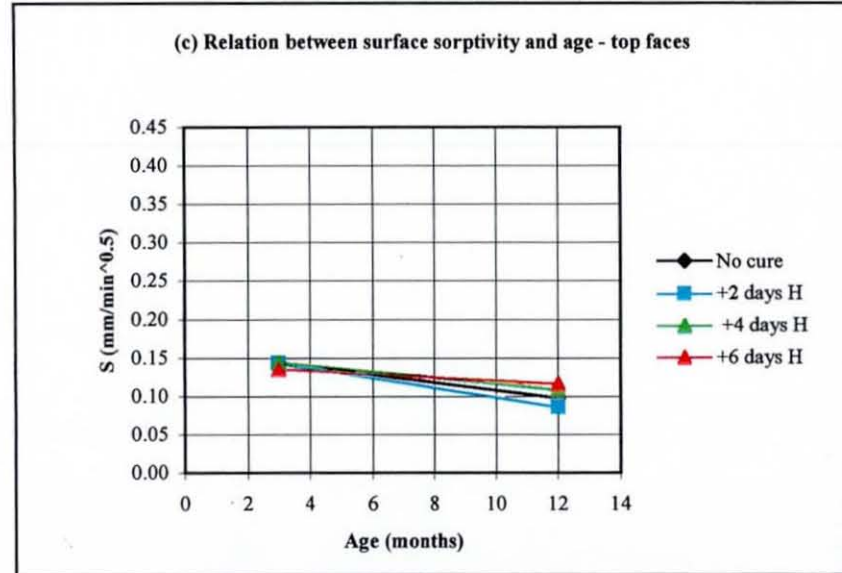
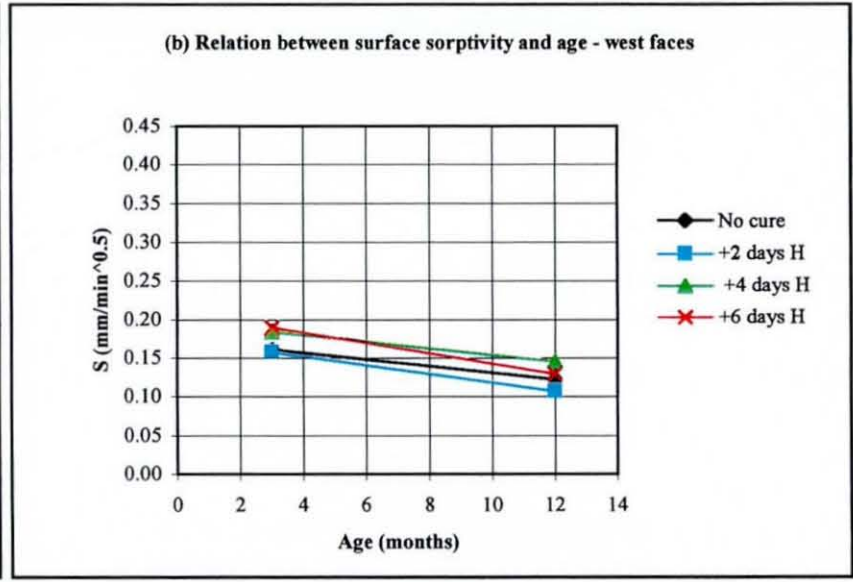
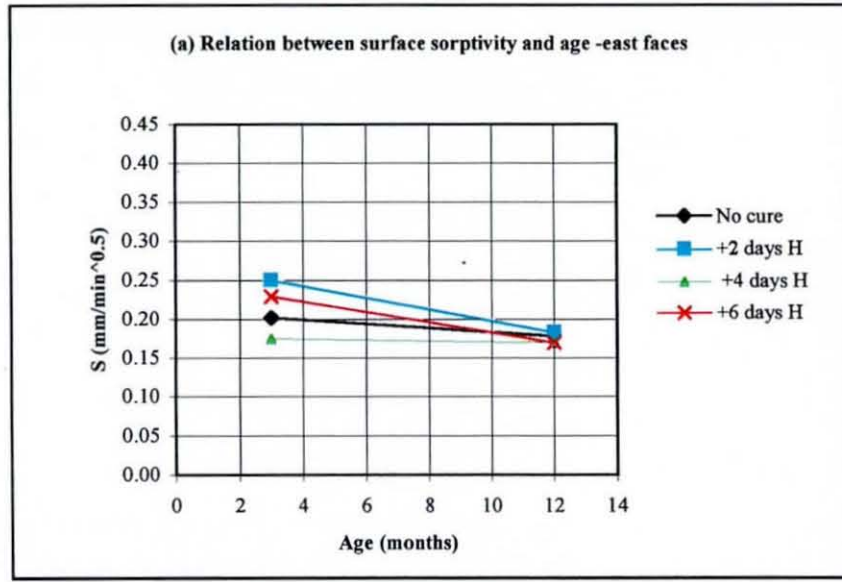


Fig. A1.11 Relationship between surface sorptivity and age of the 30 MPa OPC/GGBS concrete - UK winter

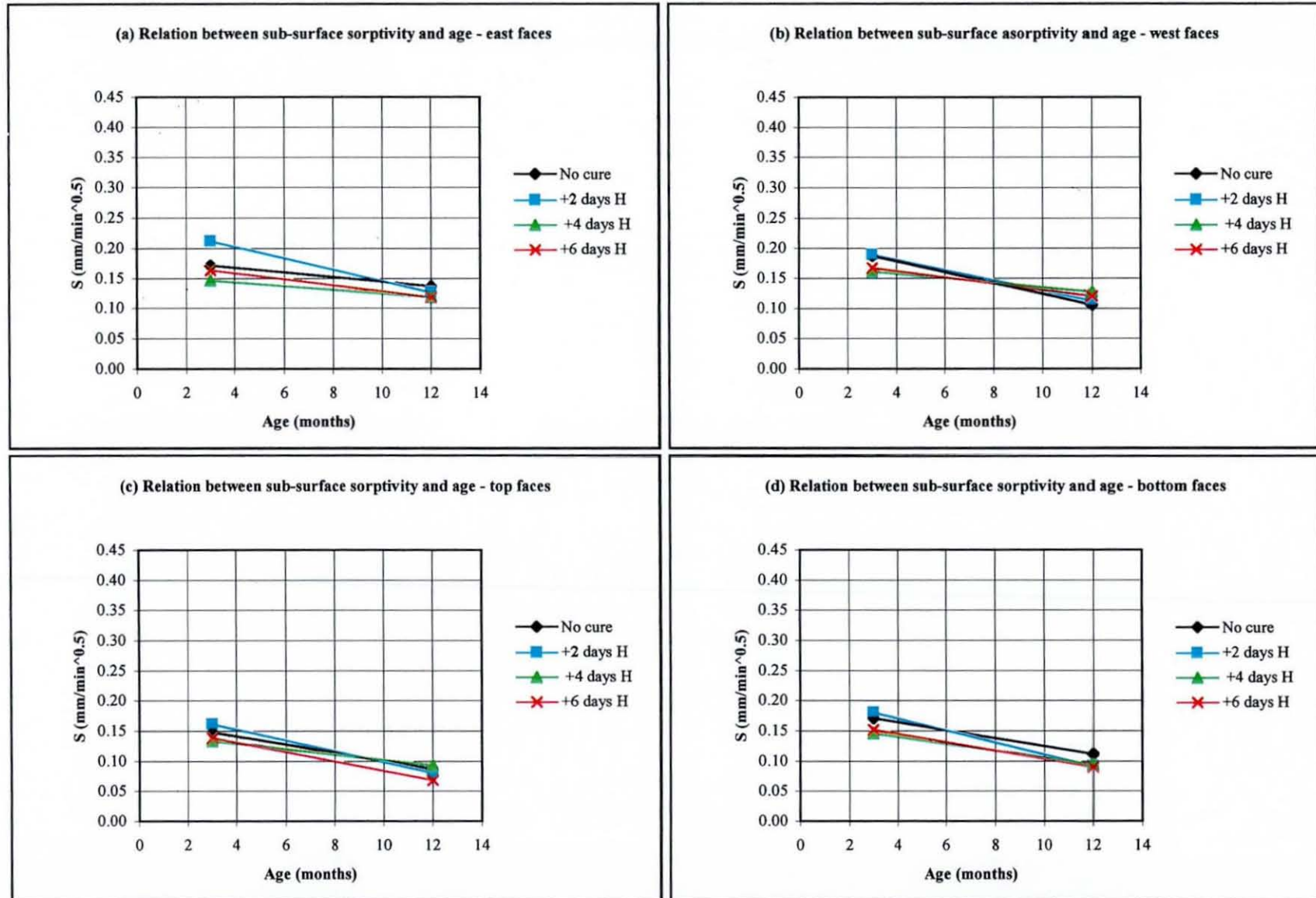


Fig. A1.12 Relationship between sub-surface sorptivity and age of the 30 MPa OPC/GGBS concrete - UK winter

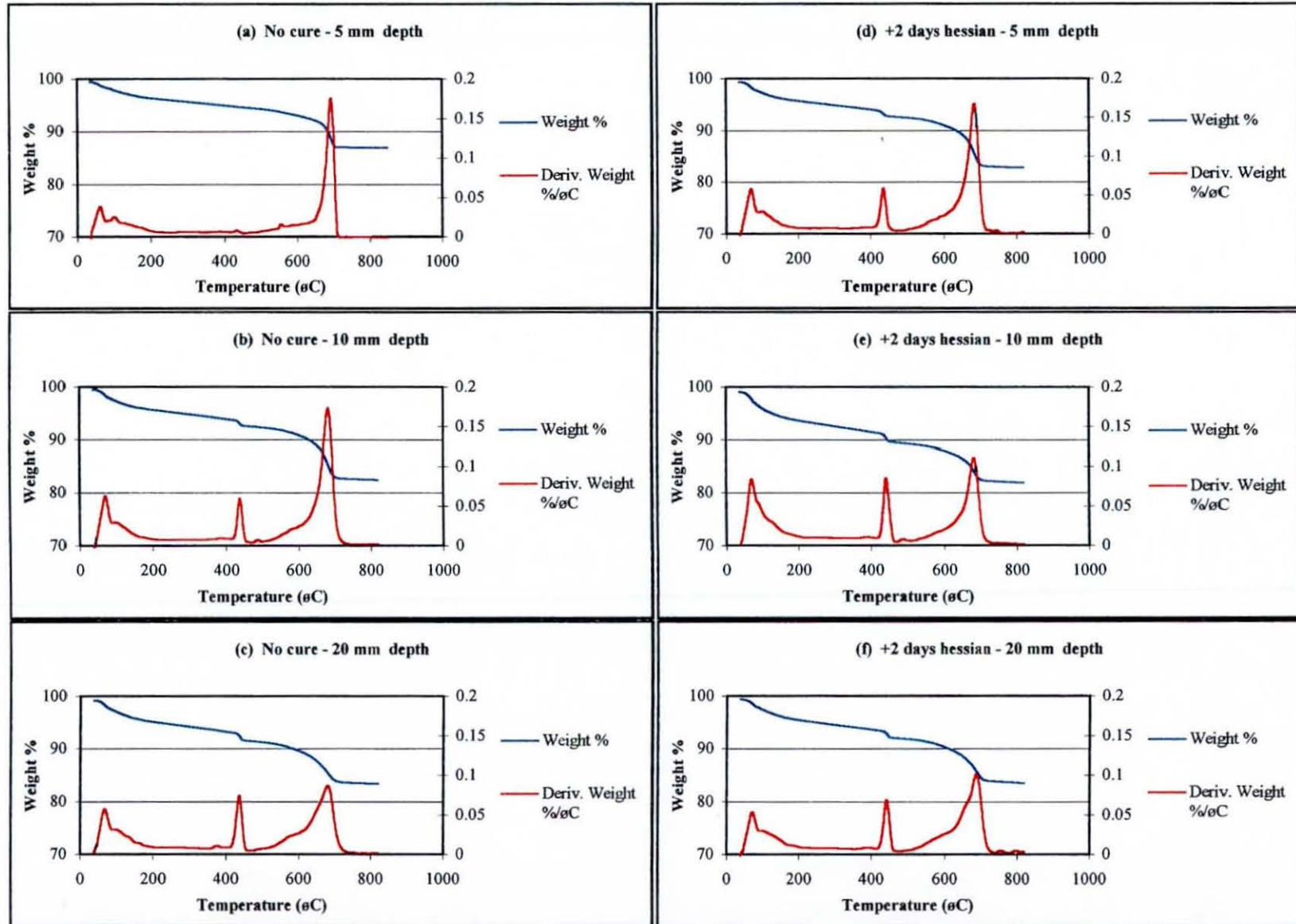
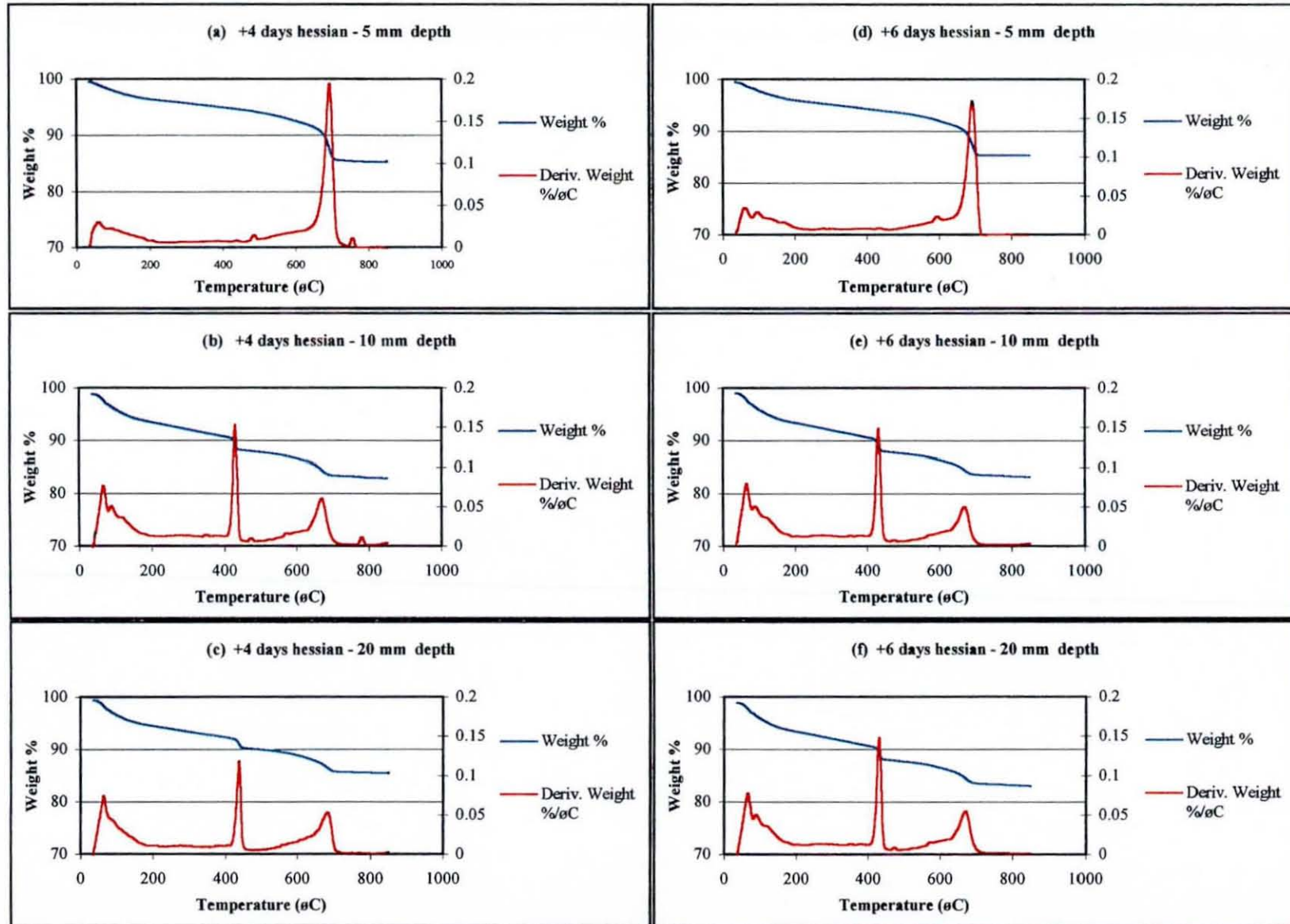


Fig. A1.13 TG and DTG curves of 30 MPa OPC mortar samples at various depths from exposed surface - 12 months winter series



**Fig. A1.14** TG and DTG curves of 30 MPa OPC mortar samples at various depths from exposed surface - 12 months winter series

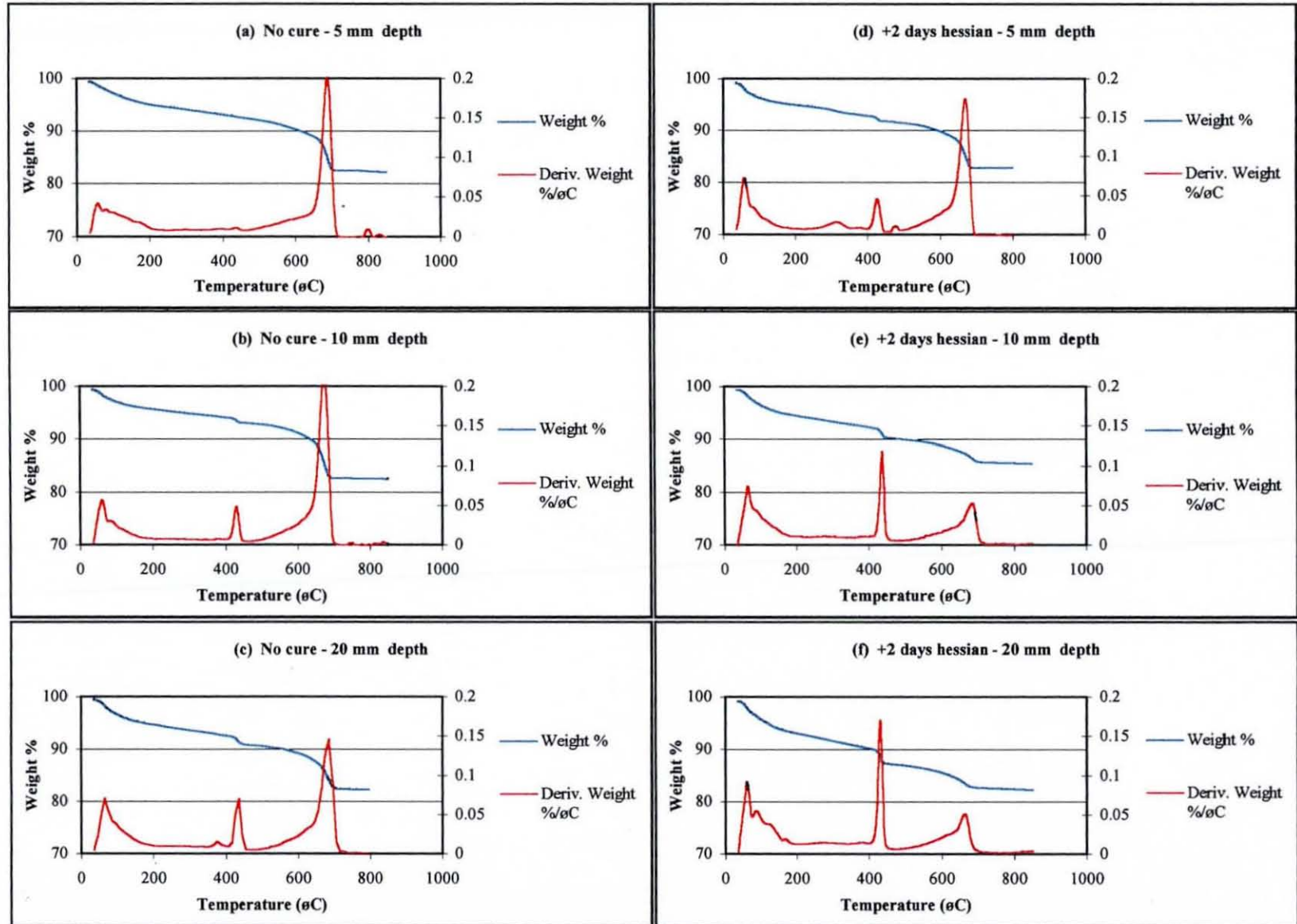


Fig. A1.15 TG and DTG curves of 50 MPa OPC mortar samples at various depths from exposed surface - 12 months winter series

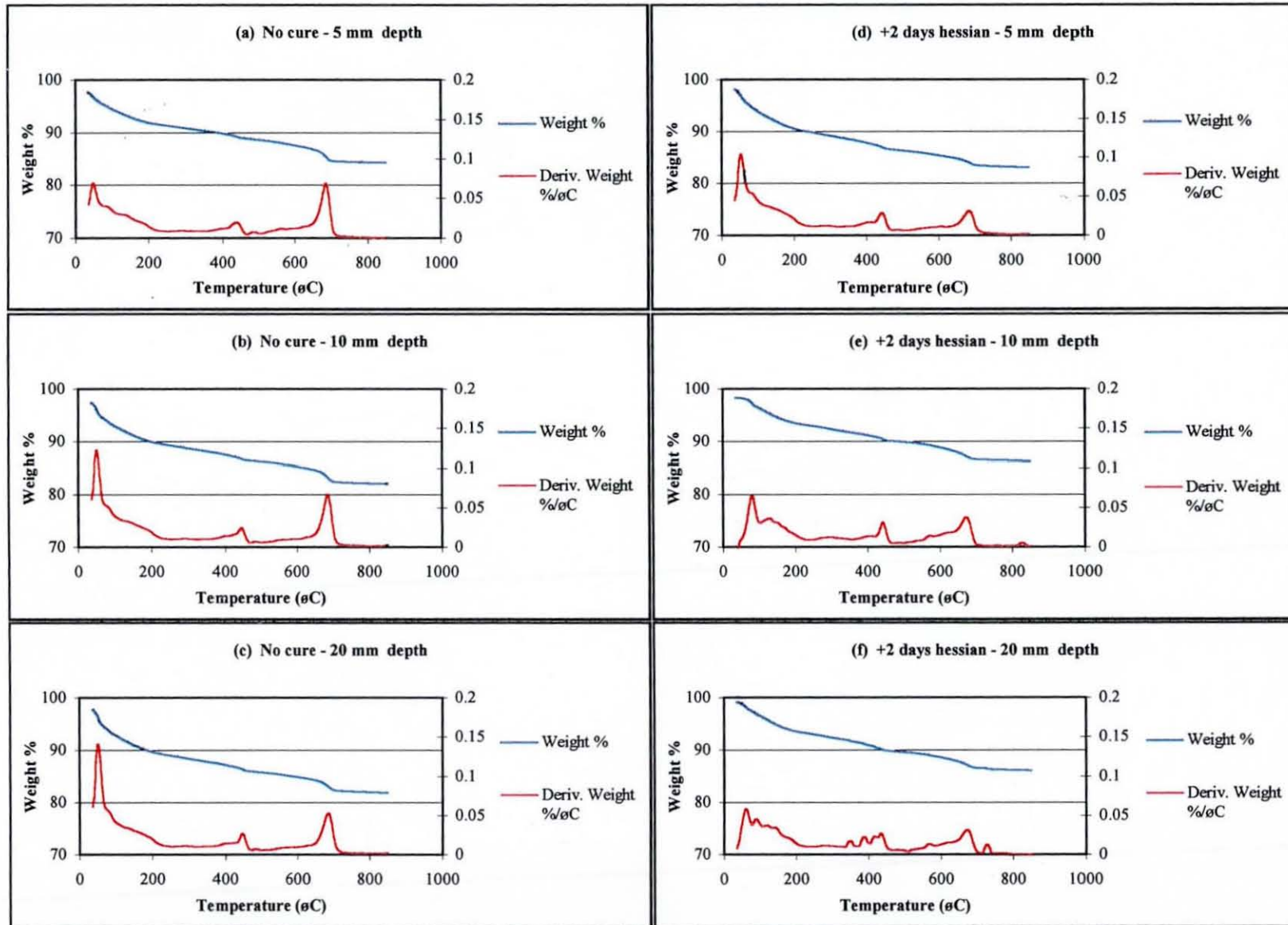


Fig. A1.16 TG and DTG curves of 30 MPa OPC/GGBS mortar samples at various depths from exposed surface - 12 months winter series

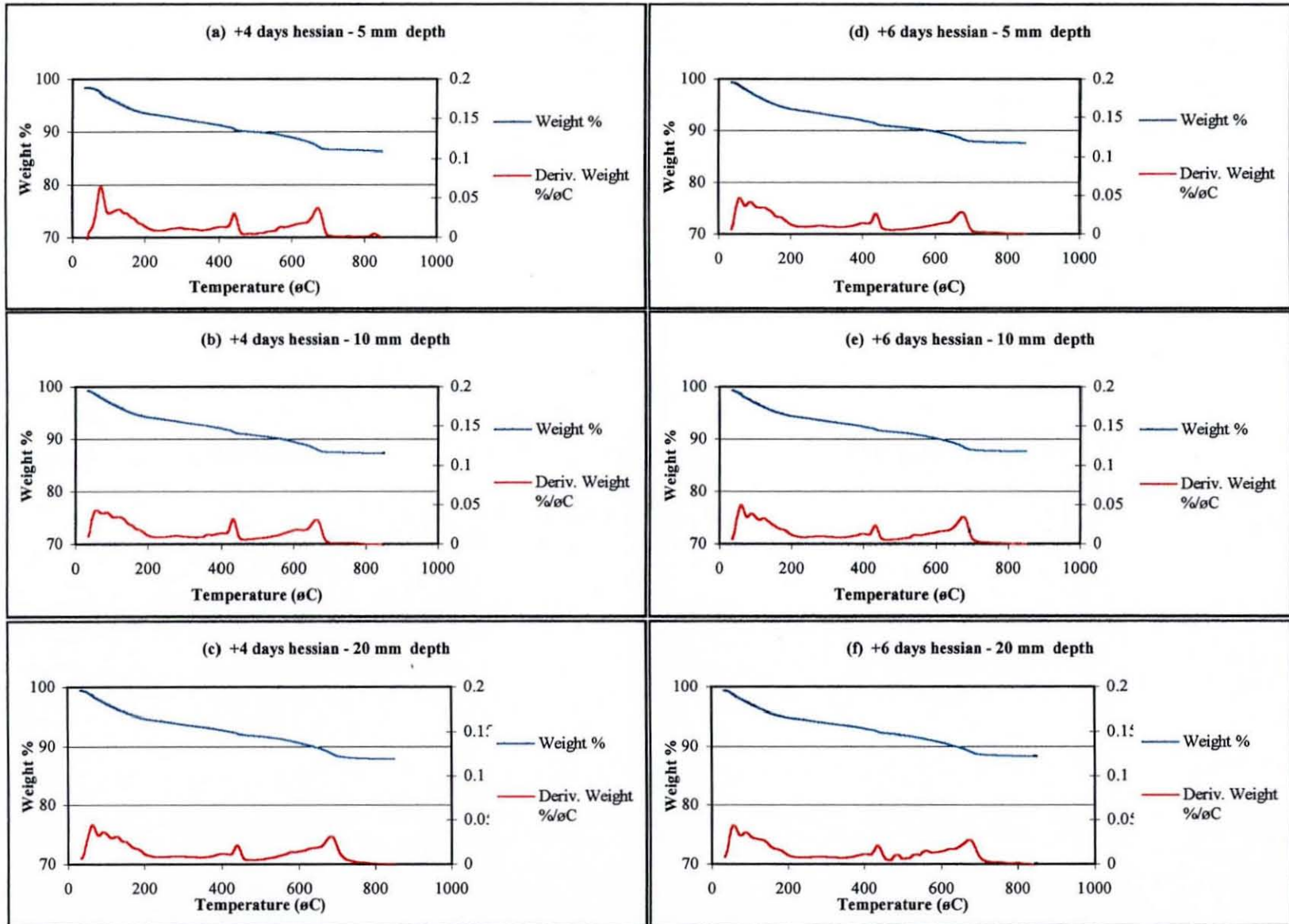


Fig. A1.17 TG and DTG curves of 30 MPa OPC/GGBS mortar samples at various depths from exposed surface - 12 months winter series

**Table A1.1(a).** Coefficient of air permeability  $k$  ( $m^2 \times 10^{-16}$ ) for the 30 MPa OPC concrete (east/west) - 3 months winter series

Orientation	Curnig regime		Average depth from outer surface (mm)					Surface (10mm)	Sub-surface (20-50mm)
			10	20	30	40	50		
East	No Cure	Cores 1	5.83	6.05	6.62	5.06	6.83	5.83	6.14
		Cores 2	9.68	4.98	5.62	6.59	7.69	9.68	6.22
		Average	<b>7.75</b>	<b>5.52</b>	<b>6.12</b>	<b>5.82</b>	<b>7.26</b>	<b>7.75</b>	<b>6.18</b>
		C of V (%)	24.8	9.6	8.2	13.1	5.9	24.8	0.6
	+2 days H	Cores 1	9.76	7.30	4.80	4.96	4.55	9.76	5.40
		Cores 2	6.34	6.50	4.44	4.77	4.31	6.34	5.00
		Average	<b>8.05</b>	<b>6.90</b>	<b>4.62</b>	<b>4.87</b>	<b>4.43</b>	<b>8.05</b>	<b>5.20</b>
		C of V (%)	21.2	6.2	4.1	2.0	2.7	21.2	3.8
	+4 days H	Cores 1	6.55	7.59	6.13	5.88	6.17	6.55	6.44
		Cores 2	8.61	7.77	7.83	8.76	7.18	8.61	7.89
		Average	<b>7.58</b>	<b>7.68</b>	<b>6.98</b>	<b>7.32</b>	<b>6.67</b>	<b>7.58</b>	<b>7.16</b>
		C of V (%)	13.6	1.2	12.2	19.7	7.6	13.6	10.1
	+6 days H	Cores 1	9.16	6.64	9.00	4.70	10.26	9.16	7.65
		Cores 2	6.05	5.77	4.96	6.02	5.19	6.05	5.48
		Average	<b>7.61</b>	<b>6.21</b>	<b>6.98</b>	<b>5.36</b>	<b>7.72</b>	<b>7.61</b>	<b>6.57</b>
		C of V (%)	20.4	7.0	29.0	12.3	32.8	20.4	16.5
West	No Cure	Cores 1	9.70	4.55	3.10	6.19	4.74	9.70	4.64
		Cores 2	5.33	4.61	5.37	4.76	5.48	5.33	5.05
		Average	<b>7.51</b>	<b>4.58</b>	<b>4.23</b>	<b>5.47</b>	<b>5.11</b>	<b>7.51</b>	<b>4.85</b>
		C of V (%)	29.0	0.6	26.8	13.0	7.2	29.0	4.2
	+2 days H	Cores 1	4.95	3.99	2.96	2.88	3.65	4.95	3.37
		Cores 2	3.72	3.51	2.59	5.84	3.96	3.72	3.97
		Average	<b>4.34</b>	<b>3.75</b>	<b>2.78</b>	<b>4.36</b>	<b>3.81</b>	<b>4.34</b>	<b>3.67</b>
		C of V (%)	14.2	6.4	6.7	33.9	4.0	14.2	8.2
	+4 days H	Cores 1	5.34	3.85	4.33	2.65	5.65	5.34	4.12
		Cores 2	5.30	4.39	3.58	6.85	3.82	5.30	4.66
		Average	<b>5.32</b>	<b>4.12</b>	<b>3.95</b>	<b>4.75</b>	<b>4.73</b>	<b>5.32</b>	<b>4.39</b>
		C of V (%)	0.4	6.6	9.5	44.2	19.3	0.4	6.2
	+6 days H	Cores 1	6.35	5.94	6.00	4.43	4.54	6.35	5.23
		Cores 2	5.84	5.27	4.81	4.25	6.23	5.84	5.14
		Average	<b>6.09</b>	<b>5.60</b>	<b>5.40</b>	<b>4.34</b>	<b>5.38</b>	<b>6.09</b>	<b>5.18</b>
		C of V (%)	4.2	6.0	11.0	2.1	15.7	4.2	0.8

Key: +X days H= X days hessian plus 1 day in mould; Average= average of cores 1 and 2; C of V= coefficient of variation (%); Sub-surface (20-50mm)= average k value from 20 to 50mm from surface; Bold value= plotted value (usually average)

Table A1.1(b). Coefficient of air permeability k (m<sup>2</sup> x 10<sup>-16</sup>) for the 30 MPa OPC concrete (top/bottom) - 3 months winter series

Orientation	Curing regime		Average depth from outer surface (mm)					Surface (10mm)	Sub-surface (20-50mm)
			10	20	30	40	50		
Top	No Cure	Cores 1	2.62	1.90	1.68	2.37	2.18	2.62	2.04
		Cores 2	2.31	3.13	2.53	2.92	3.35	2.31	2.98
		Average	<b>2.46</b>	<b>2.51</b>	<b>2.11</b>	<b>2.65</b>	<b>2.77</b>	<b>2.46</b>	<b>2.51</b>
		C of V (%)	6.3	24.4	20.0	10.4	21.0	6.3	18.9
	+2 days H	Cores 1	3.27	3.34	2.35	4.76	3.02	3.27	3.37
		Cores 2	5.98	4.92	4.92	4.84	5.45	5.98	5.03
		Average	<b>4.62</b>	<b>4.13</b>	<b>3.64</b>	<b>4.80</b>	<b>4.24</b>	<b>4.62</b>	<b>4.20</b>
		C of V (%)	29.3	16.1	26.1	0.8	22.3	29.3	19.8
	+4 days H	Cores 1	4.12	2.94	2.72	3.51	3.85	4.12	3.26
		Cores 2	2.86	5.36	2.48	5.66	3.04	2.86	4.13
		Average	<b>3.49</b>	<b>4.15</b>	<b>2.60</b>	<b>4.58</b>	<b>3.45</b>	<b>3.49</b>	<b>3.70</b>
		C of V (%)	18.0	29.1	4.6	23.5	11.7	18.0	11.9
	+6 days H	Cores 1	1.87	2.99	2.83	2.99	2.73	1.87	2.88
		Cores 2	3.60	3.53	4.18	4.25	5.63	3.60	4.40
		Average	<b>2.73</b>	<b>3.26</b>	<b>3.51</b>	<b>3.62</b>	<b>4.18</b>	<b>2.73</b>	<b>3.64</b>
		C of V (%)	31.7	8.2	19.3	17.4	34.8	31.7	20.8
Bottom	No Cure	Cores 1	6.03	1.67	2.34	2.12	1.90	6.03	2.01
		Cores 2	5.62	4.51	4.34	5.01	4.26	5.62	4.53
		Average	<b>5.82</b>	<b>3.09</b>	<b>3.34</b>	<b>3.56</b>	<b>3.08</b>	<b>5.82</b>	<b>3.27</b>
		C of V (%)	3.5	45.9	29.9	40.5	38.5	3.5	38.6
	+2 days H	Cores 1	4.58	4.93	2.42	4.22	3.22	4.58	3.70
		Cores 2	13.84	7.80	7.40	7.08	8.09	13.84	7.59
		Average	<b>9.21</b>	<b>6.36</b>	<b>4.91</b>	<b>5.65</b>	<b>5.66</b>	<b>9.21</b>	<b>5.64</b>
		C of V (%)	50.2	22.5	50.7	25.3	43.1	50.2	34.5
	+4 days H	Cores 1	5.42	5.62	6.02	3.77	3.67	5.42	4.77
		Cores 2	8.36	5.93	5.69	5.36	5.58	8.36	5.64
		Average	<b>6.89</b>	<b>5.77</b>	<b>5.85</b>	<b>4.57</b>	<b>4.63</b>	<b>6.89</b>	<b>5.20</b>
		C of V (%)	21.3	2.7	2.8	17.3	20.6	21.3	8.3
	+6 days H	Cores 1	4.79	1.61	4.06	2.39	2.33	4.79	2.60
		Cores 2	4.66	3.85	3.12	4.20	3.96	4.66	3.78
		Average	<b>4.73</b>	<b>2.73</b>	<b>3.59</b>	<b>3.29</b>	<b>3.14</b>	<b>4.73</b>	<b>3.19</b>
		C of V (%)	1.4	41.0	13.1	27.5	26.0	1.4	18.6

Key: +X days H= X days hessian plus 1 day in mould; Average= average of cores 1 and 2; C of V= coefficient of variation (%); Sub-surface (20-50mm)= average k value from 20 to 50mm from surface; Bold value= plotted value (usually average)

Table A1.2 (a). Coefficient of air permeability k (m<sup>2</sup>x 10<sup>-16</sup>) for the 30 MPa OPC concrete (east/west) - 12 months winter series

Orientation	Curnig regime		Average depth from outer surface (mm)					Surface (10mm)	Sub-surface (20-40mm)
			5	10	20	30	40		
East	No Cure	Cores 1	4.41	6.11	3.30	2.47	2.99	6.11	2.92
		Cores 2	4.41	6.11	3.88	4.14	5.41	6.11	4.48
		Average	<b>4.41</b>	<b>6.11</b>	<b>3.59</b>	<b>3.30</b>	<b>4.20</b>	<b>6.11</b>	<b>3.70</b>
		C of V (%)	0.0	0.0	8.0	25.2	28.8	0.0	21.0
	+2 days H	Cores 1	6.63	6.61	2.16	4.12	2.12	6.61	2.80
		Cores 2	6.63	4.00	2.49	1.95	2.16	4.00	2.20
		Average	<b>6.63</b>	<b>5.30</b>	<b>2.33</b>	<b>3.03</b>	<b>2.14</b>	<b>5.30</b>	<b>2.50</b>
		C of V (%)	0.0	32.5	6.5	55.7	0.8	32.5	12.1
	+4 days H	Cores 1	4.11	6.75	4.23	5.30	3.76	6.75	4.43
		Cores 2	4.11	3.31	4.83	2.53	3.16	3.31	3.50
		Average	<b>4.11</b>	<b>5.03</b>	<b>4.53</b>	<b>3.92</b>	<b>3.46</b>	<b>5.03</b>	<b>3.97</b>
		C of V (%)	0.0	34.3	6.6	35.4	8.8	34.3	11.7
	+6 days H	Cores 1	3.09	5.34	6.87	5.30	4.60	5.34	5.59
		Cores 2	5.30	4.41	3.77	2.92	3.38	4.41	3.36
		Average	<b>4.20</b>	<b>4.88</b>	<b>5.32</b>	<b>4.11</b>	<b>3.99</b>	<b>4.88</b>	<b>4.47</b>
		C of V (%)	26.3	9.5	29.2	29.0	15.2	9.5	25.0
West	No Cure	Cores 1	3.06	3.39	1.93	2.87	1.48	3.39	2.09
		Cores 2	3.06	3.15	3.29	3.36	3.68	3.15	3.44
		Average	<b>3.06</b>	<b>3.27</b>	<b>2.61</b>	<b>3.11</b>	<b>2.58</b>	<b>3.27</b>	<b>2.77</b>
		C of V (%)	0.0	3.7	26.0	7.8	42.7	3.7	24.4
	+2 days H	Cores 1	3.58	2.55	1.85	2.44	1.40	2.55	1.90
		Cores 2	3.58	2.04	1.47	1.52	1.38	2.04	1.46
		Average	<b>3.58</b>	<b>2.29</b>	<b>1.66</b>	<b>1.98</b>	<b>1.39</b>	<b>2.29</b>	<b>1.68</b>
		C of V (%)	0.0	11.2	11.6	23.2	0.6	11.2	13.1
	+4 days H	Cores 1	2.85	4.37	3.05	2.43	2.61	4.37	2.70
		Cores 2	1.71	2.47	2.46	2.18	2.49	2.47	2.38
		Average	<b>2.28</b>	<b>3.42</b>	<b>2.76</b>	<b>2.30</b>	<b>2.55</b>	<b>3.42</b>	<b>2.54</b>
		C of V (%)	25.2	27.8	10.9	5.3	2.5	27.8	6.4
	+6 days H	Cores 1	3.05	2.45	3.08	2.51	3.65	2.45	3.08
		Cores 2	3.89	2.94	4.04	3.35	4.15	2.94	3.84
		Average	<b>3.47</b>	<b>2.69</b>	<b>3.56</b>	<b>2.93</b>	<b>3.90</b>	<b>2.69</b>	<b>3.46</b>
		C of V (%)	12.1	9.2	13.5	14.4	6.3	9.2	11.1

Key: +X days H= X days hessian plus 1 day in mould; Average= average of cores 1 and 2; C of V= coefficient of variation (%); Sub-surface (10-40mm)= average k value from 10 to 40mm from surface; Bold value= plotted value (usually average)

Table A1.2 (b). Coefficient of air permeability k (m<sup>2</sup>x 10<sup>-16</sup>) for the 30 MPa OPC concrete (top/bottom) - 12 months winter series

Orientation	Curing regime	Average depth from outer surface (mm)					Surface (10mm)	Sub-surface (20-40mm)	
		5	10	20	30	40			
Top	No Cure	Cores 1	2.52	0.80	1.54	0.94	1.15	0.80	1.21
		Cores 2	2.52	0.93	1.37	1.02	1.33	0.93	1.24
		Average	<b>2.52</b>	<b>0.86</b>	<b>1.45</b>	<b>0.98</b>	<b>1.24</b>	<b>0.86</b>	<b>1.23</b>
		C of V (%)	0.0	7.5	5.9	4.1	7.4	7.5	1.3
	+2 days H	Cores 1	0.98	1.09	0.95	0.98	1.75	1.09	1.23
		Cores 2	0.98	1.71	1.13	1.21	1.61	1.71	1.32
		Average	<b>0.98</b>	<b>1.40</b>	<b>1.04</b>	<b>1.09</b>	<b>1.68</b>	<b>1.40</b>	<b>1.27</b>
		C of V (%)	0.0	18.1	8.0	9.7	4.5	18.1	3.6
	+4 days H	Cores 1	0.67	1.13	1.60	1.42	1.18	1.13	1.40
		Cores 2	0.96	1.18	1.42	1.26	1.49	1.18	1.39
		Average	<b>0.82</b>	<b>1.15</b>	<b>1.51</b>	<b>1.34</b>	<b>1.33</b>	<b>1.15</b>	<b>1.39</b>
		C of V (%)	18.0	2.2	5.8	5.9	11.3	2.2	0.4
	+6 days H	Cores 1	0.97	1.25	1.17	1.23	1.25	1.25	1.22
		Cores 2	0.81	1.14	1.10	1.19	1.35	1.14	1.22
		Average	<b>0.89</b>	<b>1.19</b>	<b>1.14</b>	<b>1.21</b>	<b>1.30</b>	<b>1.19</b>	<b>1.22</b>
		C of V (%)	9.0	4.7	2.7	1.6	4.0	4.7	0.0
Bottom	No Cure	Cores 1	2.80	1.79	1.78	1.97	1.86	1.79	1.87
		Cores 2	2.80	2.61	2.28	1.29	2.05	2.61	1.87
		Average	<b>2.80</b>	<b>2.20</b>	<b>2.03</b>	<b>1.63</b>	<b>1.95</b>	<b>2.20</b>	<b>1.87</b>
		C of V (%)	0.0	18.7	12.3	20.9	4.9	18.7	0.1
	+2 days H	Cores 1	2.34	1.81	2.20	1.63	1.77	1.81	1.87
		Cores 2	2.34	2.51	2.05	1.52	1.59	2.51	1.72
		Average	<b>2.34</b>	<b>2.16</b>	<b>2.13</b>	<b>1.58</b>	<b>1.68</b>	<b>2.16</b>	<b>1.79</b>
		C of V (%)	0.0	16.2	3.5	3.6	5.2	16.2	4.1
	+4 days H	Cores 1	1.09	1.71	1.21	1.25	1.17	1.71	1.21
		Cores 2	1.82	1.33	2.18	1.26	1.77	1.33	1.74
		Average	<b>1.45</b>	<b>1.52</b>	<b>1.70</b>	<b>1.26</b>	<b>1.47</b>	<b>1.52</b>	<b>1.47</b>
		C of V (%)	25.0	12.7	28.7	0.3	20.6	12.7	17.9
	+6 days H	Cores 1	0.96	1.29	1.26	1.28	1.44	1.29	1.33
		Cores 2	0.96	2.32	1.48	1.45	1.34	2.32	1.42
		Average	<b>0.96</b>	<b>1.80</b>	<b>1.37</b>	<b>1.36</b>	<b>1.39</b>	<b>1.80</b>	<b>1.38</b>
		C of V (%)	0.0	28.6	8.0	6.3	3.7	28.6	3.5

Key: +X days H= X days hessian plus 1 day in mould; Average= average of cores 1 and 2; C of V= coefficient of variation (%); Sub-surface (10-40mm)= average k value from 10 to 40mm from surface; Bold value= plotted value (usually average)

**Table A1.3(a).** Coefficient of air permeability  $k$  ( $m^2 \times 10^{-16}$ ) for the 50 MPa OPC concrete (east/west) - 3 months winter series

Orientation	Curnig regime	Average depth from outer surface (mm)					Surface (10mm)	Sub-surface (20-50mm)	
		10	20	30	40	50			
East	No Cure	Cores 1	1.04	1.00	1.06	0.93	0.78	1.04	0.94
		Cores 2	1.01	0.67	0.95	0.68	0.75	1.01	0.76
		Average	<b>1.02</b>	<b>0.84</b>	<b>1.01</b>	<b>0.80</b>	<b>0.76</b>	<b>1.02</b>	<b>0.85</b>
		C of V (%)	1.5	19.8	5.8	15.9	1.6	1.5	10.7
	+2 days H	Cores 1	0.91	0.98	0.85	0.91	1.03	0.91	0.94
		Cores 2	0.85	1.02	0.75	0.99	0.92	0.85	0.92
		Average	<b>0.88</b>	<b>1.00</b>	<b>0.80</b>	<b>0.95</b>	<b>0.98</b>	<b>0.88</b>	<b>0.93</b>
		C of V (%)	3.3	1.9	6.6	4.2	5.8	3.3	1.1
	+4 days H	Cores 1	3.22	2.01	2.31	1.43	2.29	3.22	2.01
		Cores 2	1.77	2.01	1.65	1.62	1.86	1.77	1.79
		Average	<b>2.49</b>	<b>2.01</b>	<b>1.98</b>	<b>1.53</b>	<b>2.07</b>	<b>2.49</b>	<b>1.90</b>
		C of V (%)	29.0	0.1	16.6	6.3	10.4	29.0	5.9
	+6 days H	Cores 1	1.01	1.26	1.05	1.72	1.07	1.01	1.28
		Cores 2	1.61	1.46	2.19	1.67	1.96	1.61	1.82
		Average	<b>1.31</b>	<b>1.36</b>	<b>1.62</b>	<b>1.69</b>	<b>1.51</b>	<b>1.31</b>	<b>1.55</b>
		C of V (%)	22.6	7.0	35.3	1.6	29.4	22.6	17.5
West	No Cure	Cores 1	1.02	0.99	0.85	0.85	1.13	1.02	0.96
		Cores 2	1.04	0.96	0.89	0.86	1.15	1.04	0.96
		Average	<b>1.03</b>	<b>0.98</b>	<b>0.87</b>	<b>0.85</b>	<b>1.14</b>	<b>1.03</b>	<b>0.96</b>
		C of V (%)	1.3	2.0	2.1	0.8	0.8	1.3	0.4
	+2 days H	Cores 1	1.24	1.20	1.29	1.08	1.12	1.24	1.17
		Cores 2	1.18	1.17	1.30	1.01	0.99	1.18	1.12
		Average	<b>1.21</b>	<b>1.19</b>	<b>1.29</b>	<b>1.04</b>	<b>1.06</b>	<b>1.21</b>	<b>1.14</b>
		C of V (%)	2.3	1.6	0.4	3.5	6.3	2.3	2.5
	+4 days H	Cores 1	1.51	1.16	1.74	1.64	1.97	1.51	1.63
		Cores 2	1.27	1.75	1.48	1.54	1.62	1.27	1.60
		Average	<b>1.39</b>	<b>1.46</b>	<b>1.61</b>	<b>1.59</b>	<b>1.80</b>	<b>1.39</b>	<b>1.61</b>
		C of V (%)	8.6	20.4	8.1	3.0	9.9	8.6	0.9
	+6 days H	Cores 1	1.84	1.01	1.68	1.38	1.62	1.84	1.42
		Cores 2	2.72	1.79	1.80	1.77	2.15	2.72	1.88
		Average	<b>2.28</b>	<b>1.40</b>	<b>1.74</b>	<b>1.58</b>	<b>1.89</b>	<b>2.28</b>	<b>1.65</b>
		C of V (%)	19.3	27.9	3.2	12.7	14.2	19.3	13.8

Key: +X days H= X days hessian plus 1 day in mould; Average= average of cores 1 and 2; C of V= coefficient of variation (%); Sub-surface (20-50mm)= average k value from 20 to 50mm from surface; Bold value= plotted value (usually average)

Table A1.3(b). Coefficient of air permeability k (m<sup>2</sup> x 10<sup>-16</sup>) for the 50 MPa OPC concrete (top/bottom) - 3 months winter series

Orientation	Curing regime	Average depth from outer surface (mm)					Surface (10mm)	Sub-surface (20-50mm)	
		10	20	30	40	50			
Top	No Cure	Cores 1	0.40	0.60	0.63	0.85	0.87	0.40	0.74
		Cores 2	0.45	0.45	0.50	0.76	0.96	0.45	0.67
		Average	<b>0.43</b>	<b>0.53</b>	<b>0.56</b>	<b>0.81</b>	<b>0.91</b>	<b>0.43</b>	<b>0.70</b>
		C of V (%)	6.4	13.5	10.8	5.5	5.1	6.4	4.6
	+2 days H	Cores 1	0.28	0.76	0.35	0.80	0.52	0.28	0.61
		Cores 2	0.37	0.39	0.42	0.49	0.48	0.37	0.44
		Average	<b>0.32</b>	<b>0.58</b>	<b>0.39</b>	<b>0.65</b>	<b>0.50</b>	<b>0.32</b>	<b>0.53</b>
		C of V (%)	13.6	48.9	8.4	32.9	3.6	13.6	15.7
	+4 days H	Cores 1	0.59	0.70	0.68	0.83	0.66	0.59	0.72
		Cores 2	0.56	1.24	1.20	1.17	1.21	0.56	1.21
		Average	<b>0.58</b>	<b>0.97</b>	<b>0.94</b>	<b>1.00</b>	<b>0.94</b>	<b>0.58</b>	<b>0.96</b>
		C of V (%)	2.1	28.1	27.7	17.3	29.5	2.1	25.5
	+6 days H	Cores 1	0.51	0.99	0.96	1.06	0.96	0.51	0.99
		Cores 2	0.90	1.26	1.04	1.36	0.91	0.90	1.14
		Average	<b>0.70</b>	<b>1.12</b>	<b>1.00</b>	<b>1.21</b>	<b>0.93</b>	<b>0.70</b>	<b>1.07</b>
		C of V (%)	27.6	11.7	3.9	12.4	2.7	27.6	6.9
Bottom	No Cure	Cores 1	0.60	0.77	0.54	0.85	0.80	0.60	0.74
		Cores 2	0.55	0.50	0.70	0.65	0.80	0.55	0.66
		Average	<b>0.57</b>	<b>0.63</b>	<b>0.62</b>	<b>0.75</b>	<b>0.80</b>	<b>0.57</b>	<b>0.70</b>
		C of V (%)	4.8	20.9	13.6	13.5	0.5	4.8	5.5
	+2 days H	Cores 1	0.78	0.83	0.57	0.76	0.74	0.78	0.72
		Cores 2	1.22	0.69	0.85	0.51	0.76	1.22	0.70
		Average	<b>1.00</b>	<b>0.76</b>	<b>0.71</b>	<b>0.64</b>	<b>0.75</b>	<b>1.00</b>	<b>0.71</b>
		C of V (%)	21.9	9.0	19.8	19.4	1.3	21.9	1.5
	+4 days H	Cores 1	0.59	0.99	0.86	0.83	0.96	0.59	0.91
		Cores 2	0.95	1.60	0.97	1.38	1.09	0.95	1.26
		Average	<b>0.77</b>	<b>1.30</b>	<b>0.92</b>	<b>1.10</b>	<b>1.03</b>	<b>0.77</b>	<b>1.09</b>
		C of V (%)	23.7	23.4	6.0	25.0	5.9	23.7	16.0
	+6 days H	Cores 1	0.66	1.29	0.96	1.00	0.86	0.66	1.03
		Cores 2	1.22	2.07	1.15	1.47	1.03	1.22	1.43
		Average	<b>0.94</b>	<b>1.68</b>	<b>1.05</b>	<b>1.24</b>	<b>0.95</b>	<b>0.94</b>	<b>1.23</b>
		C of V (%)	29.6	23.3	9.3	19.0	8.9	29.6	16.4

Key: +X days H= X days hessian plus 1 day in mould; Average= average of cores 1 and 2; C of V= coefficient of variation (%); Sub-surface (20-50mm)= average k value from 20 to 50mm from surface; Bold value= plotted value (usually average)

**Table A.1.4 (a).** Coefficient of air permeability  $k$  ( $m^2 \times 10^{-16}$ ) for the 50 MPa OPC concrete (east/west) - 12 months winter series

Orientation	Curnig regime	Average depth from outer surface (mm)					Surface (10mm)	Sub-surface (20-40mm)	
		5	10	20	30	40			
East	No Cure	Cores 1	0.63	0.63	0.62	0.54	0.42	0.63	0.53
		Cores 2	0.67	0.57	0.39	0.43	0.35	0.57	0.39
		Average	<b>0.65</b>	<b>0.60</b>	<b>0.51</b>	<b>0.49</b>	<b>0.39</b>	<b>0.60</b>	<b>0.46</b>
		C of V (%)	2.8	5.0	22.4	10.9	9.0	5.0	14.6
	+2 days H	Cores 1	0.64	0.28	0.39	0.37	0.33	0.28	0.36
		Cores 2	0.49	0.40	0.39	0.43	0.38	0.40	0.40
		Average	<b>0.57</b>	<b>0.34</b>	<b>0.39</b>	<b>0.40</b>	<b>0.35</b>	<b>0.34</b>	<b>0.38</b>
		C of V (%)	13.0	14.9	0.1	7.4	5.9	14.9	4.7
	+4 days H	Cores 1	0.44	0.66	0.49	0.64	0.51	0.66	0.55
		Cores 2	0.44	0.54	0.54	0.53	0.47	0.54	0.51
		Average	<b>0.44</b>	<b>0.60</b>	<b>0.51</b>	<b>0.59</b>	<b>0.49</b>	<b>0.60</b>	<b>0.53</b>
		C of V (%)	0.0	9.6	4.6	9.6	4.2	9.6	3.4
	+6 days H	Cores 1	0.32	0.47	0.38	0.69	0.49	0.47	0.52
		Cores 2	0.72	0.40	0.59	0.47	0.56	0.40	0.54
		Average	<b>0.52</b>	<b>0.43</b>	<b>0.49</b>	<b>0.58</b>	<b>0.52</b>	<b>0.43</b>	<b>0.53</b>
		C of V (%)	38.3	8.6	21.0	18.7	6.1	8.6	1.6
West	No Cure	Cores 1	0.26	0.28	0.33	0.38	0.33	0.28	0.35
		Cores 2	0.39	0.33	0.29	0.30	0.23	0.33	0.27
		Average	<b>0.33</b>	<b>0.30</b>	<b>0.31</b>	<b>0.34</b>	<b>0.28</b>	<b>0.30</b>	<b>0.31</b>
		C of V (%)	19.7	8.5	7.3	12.3	19.3	8.5	12.8
	+2 days H	Cores 1	0.22	0.34	0.27	0.38	0.30	0.34	0.32
		Cores 2	0.41	0.27	0.32	0.33	0.36	0.27	0.34
		Average	<b>0.31</b>	<b>0.31</b>	<b>0.30</b>	<b>0.36</b>	<b>0.33</b>	<b>0.31</b>	<b>0.33</b>
		C of V (%)	29.2	11.4	9.1	7.7	8.7	11.4	2.9
	+4 days H	Cores 1	0.29	0.39	0.38	0.54	0.45	0.39	0.46
		Cores 2	0.26	0.29	0.47	0.44	0.46	0.29	0.46
		Average	<b>0.27</b>	<b>0.34</b>	<b>0.43</b>	<b>0.49</b>	<b>0.45</b>	<b>0.34</b>	<b>0.46</b>
		C of V (%)	5.7	13.9	10.6	9.6	0.8	13.9	0.1
	+6 days H	Cores 1	0.21	0.32	0.44	0.49	0.38	0.32	0.44
		Cores 2	0.23	0.65	0.41	0.42	0.50	0.65	0.44
		Average	<b>0.22</b>	<b>0.48</b>	<b>0.42</b>	<b>0.45</b>	<b>0.44</b>	<b>0.48</b>	<b>0.44</b>
		C of V (%)	4.7	34.7	4.3	7.6	14.4	34.7	0.8

Key: +X days H= X days hessian plus 1 day in mould; Average= average of cores 1 and 2; C of V= coefficient of variation (%); Sub-surface (10-40mm)= average k value from 10 to 40mm from surface; Bold value= plotted value (usually average)

Table A1.4 (b). Coefficient of air permeability k (m<sup>2</sup> x 10<sup>-16</sup>) for the 50 MPa OPC concrete (top/bottom) - 12 months winter series

Orientation	Curing regime	Average depth from outer surface (mm)					Surface (10mm)	Sub-surface (20-40mm)	
		5	10	20	30	40			
Top	No Cure	Cores 1	0.16	0.12	0.21	0.22	0.29	0.12	0.24
		Cores 2	0.15	0.19	0.23	0.37	0.32	0.19	0.31
		Average	<b>0.16</b>	<b>0.16</b>	<b>0.22</b>	<b>0.29</b>	<b>0.31</b>	<b>0.16</b>	<b>0.27</b>
		C of V (%)	2.8	22.7	5.6	25.8	6.0	22.7	12.9
	+2 days H	Cores 1	0.16	0.19	0.24	0.26	0.27	0.19	0.26
		Cores 2	0.43	0.22	0.30	0.29	0.46	0.22	0.35
		Average	<b>0.29</b>	<b>0.21</b>	<b>0.27</b>	<b>0.27</b>	<b>0.36</b>	<b>0.21</b>	<b>0.30</b>
		C of V (%)	46.3	7.4	8.5	4.8	20.6	7.4	10.3
	+4 days H	Cores 1	0.28	0.33	0.40	0.42	0.45	0.33	0.42
		Cores 2	0.23	0.26	0.39	0.46	0.47	0.26	0.44
		Average	<b>0.26</b>	<b>0.30</b>	<b>0.39</b>	<b>0.44</b>	<b>0.46</b>	<b>0.30</b>	<b>0.43</b>
		C of V (%)	8.7	10.3	0.7	4.0	1.6	10.3	1.7
	+6 days H	Cores 1	0.23	0.27	0.42	0.39	0.45	0.27	0.42
		Cores 2	0.28	0.27	0.40	0.45	0.47	0.27	0.44
		Average	<b>0.25</b>	<b>0.27</b>	<b>0.41</b>	<b>0.42</b>	<b>0.46</b>	<b>0.27</b>	<b>0.43</b>
		C of V (%)	9.9	0.8	2.9	8.0	1.9	0.8	2.4
Bottom	No Cure	Cores 1	0.25	0.50	0.34	0.37	0.34	0.50	0.35
		Cores 2	0.46	0.65	0.36	0.39	0.38	0.65	0.38
		Average	<b>0.36</b>	<b>0.57</b>	<b>0.35</b>	<b>0.38</b>	<b>0.36</b>	<b>0.57</b>	<b>0.36</b>
		C of V (%)	29.7	13.3	2.3	3.3	6.5	13.3	4.0
	+2 days H	Cores 1	0.38	0.41	0.38	0.35	0.27	0.41	0.34
		Cores 2	0.27	1.20	0.34	0.40	0.52	1.20	0.42
		Average	<b>0.33</b>	<b>0.80</b>	<b>0.36</b>	<b>0.38</b>	<b>0.39</b>	<b>0.80</b>	<b>0.38</b>
		C of V (%)	16.5	49.1	6.2	5.9	31.0	49.1	10.8
	+4 days H	Cores 1	0.43	0.47	0.48	0.63	0.66	0.47	0.59
		Cores 2	0.62	0.74	0.77	1.31	0.56	0.74	0.88
		Average	<b>0.52</b>	<b>0.60</b>	<b>0.63</b>	<b>0.97</b>	<b>0.61</b>	<b>0.60</b>	<b>0.73</b>
		C of V (%)	18.1	23.1	23.2	35.5	7.8	23.1	20.0
	+6 days H	Cores 1	0.49	0.59	0.52	0.63	0.45	0.59	0.53
		Cores 2	0.55	0.84	0.76	0.53	0.55	0.84	0.61
		Average	<b>0.52</b>	<b>0.72</b>	<b>0.64</b>	<b>0.58</b>	<b>0.50</b>	<b>0.72</b>	<b>0.57</b>
		C of V (%)	6.0	17.4	18.7	9.0	10.2	17.4	6.9

Key: +X days H= X days hessian plus 1 day in mould; Average= average of cores 1 and 2; C of V= coefficient of variation (%); Sub-surface (10-40mm)= average k value from 10 to 40mm from surface; Bold value= plotted value (usually average)

Table A1.5 (a). Coefficient of air permeability  $k$  ( $m^2 \times 10^{-16}$ ) for the 30 MPa OPC/GGBS concrete - 3 months winter series (east/west)

Orientation	Curnig regime	Average depth from outer surface (mm)					Surface (10mm)	Sub-surface (20-50mm)	
		10	20	30	40	50			
East	No Cure	Cores 1	6.30	7.29	6.27	7.16	6.26	6.30	6.75
		Cores 2	7.46	7.72	7.68	7.76	8.38	7.46	7.88
		Average	<b>6.88</b>	<b>7.51</b>	<b>6.98</b>	<b>7.46</b>	<b>7.32</b>	<b>6.88</b>	<b>7.32</b>
		C of V (%)	8.5	2.8	10.2	4.0	14.4	8.5	7.8
	+2 days H	Cores 1	11.27	9.33	6.61	10.94	6.47	11.27	8.34
		Cores 2	10.42	7.00	6.93	10.85	6.09	10.42	7.72
		Average	<b>10.84</b>	<b>8.16</b>	<b>6.77</b>	<b>10.89</b>	<b>6.28</b>	<b>10.84</b>	<b>8.03</b>
		C of V (%)	3.9	16.7	2.3	0.4	3.1	3.9	3.9
	+4 days H	Cores 1	7.00	5.96	6.47	5.96	5.84	7.00	6.06
		Cores 2	9.33	4.93	8.75	6.76	6.45	9.33	6.72
		Average	<b>8.16</b>	<b>5.45</b>	<b>7.61</b>	<b>6.36</b>	<b>6.15</b>	<b>8.16</b>	<b>6.39</b>
		C of V (%)	14.3	9.5	15.0	6.2	5.0	14.3	5.2
	+6 days H	Cores 1	9.33	8.78	8.96	7.63	8.55	9.33	8.48
		Cores 2	9.79	7.68	7.87	7.74	7.35	9.79	7.66
		Average	<b>9.56</b>	<b>8.23</b>	<b>8.42</b>	<b>7.69</b>	<b>7.95</b>	<b>9.56</b>	<b>8.07</b>
		C of V (%)	2.4	6.6	6.5	0.7	7.5	2.4	5.1
West	No Cure	Cores 1	9.05	6.58	6.50	10.30	6.49	9.05	7.47
		Cores 2	12.06	7.68	7.63	7.32	8.60	12.06	7.81
		Average	<b>10.56</b>	<b>7.13</b>	<b>7.06</b>	<b>8.81</b>	<b>7.55</b>	<b>10.56</b>	<b>7.64</b>
		C of V (%)	14.3	7.8	8.0	16.9	14.0	14.3	2.2
	+2 days H	Cores 1	9.93	7.35	5.54	6.07	3.95	9.93	5.73
		Cores 2	9.81	6.64	4.83	4.77	4.76	9.81	5.25
		Average	<b>9.87</b>	<b>7.00</b>	<b>5.19</b>	<b>5.42</b>	<b>4.36</b>	<b>9.87</b>	<b>5.49</b>
		C of V (%)	0.6	5.1	6.8	12.0	9.3	0.6	4.4
	+4 days H	Cores 1	11.03	4.21	6.99	5.98	6.08	11.03	5.81
		Cores 2	11.47	9.40	8.20	7.79	6.98	11.47	8.09
		Average	<b>11.25</b>	<b>6.81</b>	<b>7.59</b>	<b>6.88</b>	<b>6.53</b>	<b>11.25</b>	<b>6.95</b>
		C of V (%)	2.0	38.1	8.0	13.1	6.9	2.0	16.4
	+6 days H	Cores 1	11.28	5.12	6.88	6.07	6.05	11.28	6.03
		Cores 2	10.13	7.58	7.12	7.97	7.79	10.13	7.62
		Average	<b>10.70</b>	<b>6.35</b>	<b>7.00</b>	<b>7.02</b>	<b>6.92</b>	<b>10.70</b>	<b>6.82</b>
		C of V (%)	5.3	19.4	1.8	13.5	12.6	5.3	11.6

Key: +X days H= X days hessian plus 1 day in mould; Average= average of cores 1 and 2; C of V= coefficient of variation (%); Sub-surface (20-50mm)= average k value from 20 to 50mm from surface; Bold value= plotted value (usually average)

Table A1.5 (b). Coefficient of air permeability  $k$  ( $m^2 \times 10^{-16}$ ) for the 30 MPa OPC/GGBS concrete - 3 months winter series (top/bottom)

Orientation	Curing regime	Average depth from outer surface (mm)					Surface (10mm)	Sub-surface (20-50mm)	
		10	20	30	40	50			
Top	No Cure	Cores 1	5.45	3.55	3.90	3.53	5.57	5.45	4.14
		Cores 2	10.96	4.53	4.39	5.24	3.61	10.96	4.44
		Average	<b>8.21</b>	<b>4.04</b>	<b>4.14</b>	<b>4.39</b>	<b>4.59</b>	<b>8.21</b>	<b>4.29</b>
		C of V (%)	33.5	12.1	5.9	19.6	21.4	33.5	3.5
	+2 days H	Cores 1	5.96	5.16	3.33	4.18	4.25	5.96	4.23
		Cores 2	8.13	8.52	8.46	8.77	7.34	8.13	8.27
		Average	<b>7.04</b>	<b>6.84</b>	<b>5.89</b>	<b>6.47</b>	<b>5.79</b>	<b>7.04</b>	<b>6.25</b>
		C of V (%)	15.4	19.7	30.3	26.2	21.1	15.4	32.3
	+4 days H	Cores 1	11.92	6.10	5.53	4.92	6.72	11.92	5.82
		Cores 2	8.80	7.06	4.78	5.54	4.95	8.80	5.58
		Average	<b>10.36</b>	<b>6.58</b>	<b>5.15</b>	<b>5.23</b>	<b>5.84</b>	<b>10.36</b>	<b>5.70</b>
		C of V (%)	15.1	7.2	7.3	5.9	15.1	15.1	2.1
	+6 days H	Cores 1	8.42	7.69	6.30	9.45	6.49	8.42	7.48
		Cores 2	9.55	7.57	6.42	6.85	9.51	9.55	7.59
		Average	<b>8.98</b>	<b>7.63</b>	<b>6.36</b>	<b>8.15</b>	<b>8.00</b>	<b>8.98</b>	<b>7.53</b>
		C of V (%)	6.3	0.8	1.0	16.0	18.9	6.3	0.7
Bottom	No Cure	Cores 1	8.07	2.87	7.83	6.83	7.68	8.07	6.30
		Cores 2	9.14	6.02	4.62	5.75	7.21	9.14	5.90
		Average	<b>8.61</b>	<b>4.45</b>	<b>6.22</b>	<b>6.29</b>	<b>7.44</b>	<b>8.61</b>	<b>6.10</b>
		C of V (%)	6.2	35.5	25.8	8.5	3.2	6.2	3.3
	+2 days H	Cores 1	7.91	4.28	5.82	5.85	5.24	7.91	5.30
		Cores 2	5.47	7.31	3.22	12.17	7.58	5.47	7.57
		Average	<b>6.69</b>	<b>5.80</b>	<b>4.52</b>	<b>9.01</b>	<b>6.41</b>	<b>6.69</b>	<b>6.43</b>
		C of V (%)	18.3	26.2	28.7	35.1	18.3	18.3	17.7
	+4 days H	Cores 1	5.61	7.64	6.53	7.05	6.63	5.61	6.96
		Cores 2	9.64	8.32	6.17	7.80	7.19	9.64	7.37
		Average	<b>7.62</b>	<b>7.98</b>	<b>6.35</b>	<b>7.43</b>	<b>6.91</b>	<b>7.62</b>	<b>7.17</b>
		C of V (%)	26.4	4.3	2.8	5.1	4.0	26.4	2.8
	+6 days H	Cores 1	6.50	7.44	8.11	9.09	8.11	6.50	8.19
		Cores 2	7.25	7.62	7.41	9.21	7.20	7.25	7.86
		Average	<b>6.87</b>	<b>7.53</b>	<b>7.76</b>	<b>9.15</b>	<b>7.66</b>	<b>6.87</b>	<b>8.02</b>
		C of V (%)	5.5	1.2	4.5	0.6	5.9	5.5	2.1

Key: +X days H= X days hessian plus 1 day in mould; Average= average of cores 1 and 2; C of V= coefficient of variation (%); Sub-surface (20-50mm)= average  $k$  value from 20 to 50mm from surface; Bold value= plotted value (usually average)

**Table A1.6 (b).** Coefficient of air permeability  $k$  ( $m^2 \times 10^{-16}$ ) for the 30 MPa OPC/GGBS concrete (top/bottom) - 12 months winter series

Orientation	Curing regime	Average depth from outer surface (mm)					Surface (10mm)	Sub-surface (20-40mm)	
		5	10	20	30	40			
Top	No Cure	Cores 1	9.95	4.40	3.57	2.83	3.88	4.40	3.43
		Cores 2	8.52	5.89	4.34	2.87	3.75	5.89	3.65
		Average	<b>9.24</b>	<b>5.15</b>	<b>3.95</b>	<b>2.85</b>	<b>3.81</b>	<b>5.15</b>	<b>3.54</b>
		C of V (%)	7.7	14.4	9.6	0.6	1.7	14.4	3.1
	+2 days H	Cores 1	3.88	4.28	0.89	2.13	1.02	4.28	1.35
		Cores 2	3.88	6.02	3.78	3.52	3.42	6.02	3.58
		Average	<b>3.88</b>	<b>5.15</b>	<b>2.33</b>	<b>2.83</b>	<b>2.22</b>	<b>5.15</b>	<b>2.46</b>
		C of V (%)	0.0	14.4	38.3	19.8	35.1	14.4	45.3
	+4 days H	Cores 1	9.32	4.82	1.78	2.18	1.85	4.82	1.94
		Cores 2	9.32	4.82	2.98	2.29	1.72	4.82	2.33
		Average	<b>9.32</b>	<b>4.82</b>	<b>2.38</b>	<b>2.23</b>	<b>1.79</b>	<b>4.82</b>	<b>2.13</b>
		C of V (%)	0.0	0.0	25.2	2.4	3.5	0.0	9.2
	+6 days H	Cores 1	8.12	7.00	1.51	1.71	2.21	7.00	1.81
		Cores 2	8.12	7.00	2.75	2.31	2.27	7.00	2.44
		Average	<b>8.12</b>	<b>7.00</b>	<b>2.13</b>	<b>2.01</b>	<b>2.24</b>	<b>7.00</b>	<b>2.13</b>
		C of V (%)	0.0	0.0	29.2	15.0	1.3	0.0	14.9
Bottom	No Cure	Cores 1	9.24	5.18	5.56	5.16	4.65	5.18	5.12
		Cores 2	9.24	5.18	4.50	3.73	4.86	5.18	4.36
		Average	<b>9.24</b>	<b>5.18</b>	<b>5.03</b>	<b>4.44</b>	<b>4.76</b>	<b>5.18</b>	<b>4.74</b>
		C of V (%)	0.0	0.0	10.6	16.1	2.2	0.0	8.0
	+2 days H	Cores 1	5.70	4.40	1.57	2.68	1.60	4.40	1.95
		Cores 2	5.70	6.30	3.62	4.78	4.29	6.30	4.23
		Average	<b>5.70</b>	<b>5.35</b>	<b>2.60</b>	<b>3.73</b>	<b>2.95</b>	<b>5.35</b>	<b>3.09</b>
		C of V (%)	0.0	17.8	39.5	28.2	45.5	17.8	36.9
	+4 days H	Cores 1	11.05	6.11	2.88	2.79	2.72	6.11	2.80
		Cores 2	11.05	6.53	4.75	2.35	3.48	6.53	3.52
		Average	<b>11.05</b>	<b>6.32</b>	<b>3.82</b>	<b>2.57</b>	<b>3.10</b>	<b>6.32</b>	<b>3.16</b>
		C of V (%)	0.0	3.3	24.4	8.6	12.3	3.3	11.5
	+6 days H	Cores 1	12.59	9.80	2.83	3.79	3.13	9.80	3.25
		Cores 2	12.59	9.80	3.72	3.36	3.32	9.80	3.47
		Average	<b>12.59</b>	<b>9.80</b>	<b>3.27</b>	<b>3.58</b>	<b>3.23</b>	<b>9.80</b>	<b>3.36</b>
		C of V (%)	0.0	0.0	13.5	5.9	3.1	0.0	3.3

Key: +X days H= X days hessian plus 1 day in mould; Average= average of cores 1 and 2; C of V= coefficient of variation (%); Sub-surface (10-40mm)= average  $k$  value from 10 to 40mm from surface; Bold value= plotted value (usually average)

Table A1.6 (a). Coefficient of air permeability k (m<sup>2</sup> x 10<sup>-16</sup>) for the 30 MPa OPC/GGBS concrete (east/west) - 12 months winter series

Orientation	Curnig regime	Average depth from outer surface (mm)					Surface (10mm)	Sub-surface (20-40mm)	
		5	10	20	30	40			
East	No Cure	Cores 1	8.40	13.48	9.16	6.35	7.25	13.48	7.59
		Cores 2	8.40	7.61	7.41	6.13	5.11	7.61	6.22
		Average	<b>8.40</b>	<b>10.55</b>	<b>8.29</b>	<b>6.24</b>	<b>6.18</b>	<b>10.55</b>	<b>6.90</b>
		C of V (%)	0.0	27.8	10.5	1.8	17.3	27.8	9.9
	+2 days H	Cores 1	11.19	11.43	6.83	5.00	6.28	11.43	6.04
		Cores 2	11.19	7.72	4.48	4.31	3.94	7.72	5.11
		Average	<b>11.19</b>	<b>9.57</b>	<b>5.65</b>	<b>4.65</b>	<b>5.11</b>	<b>9.57</b>	<b>5.57</b>
		C of V (%)	0.0	24.0	26.3	7.9	29.6	24.0	8.3
	+4 days H	Cores 1	16.51	15.81	6.43	7.79	8.29	15.81	7.50
		Cores 2	16.51	15.81	6.50	6.72	8.45	15.81	7.22
		Average	<b>16.51</b>	<b>15.81</b>	<b>6.47</b>	<b>7.25</b>	<b>8.37</b>	<b>15.81</b>	<b>7.36</b>
		C of V (%)	0.0	0.0	0.5	7.4	1.0	0.0	1.9
	+6 days H	Cores 1	16.79	15.74	7.95	7.71	7.25	15.74	7.64
		Cores 2	16.79	14.81	8.13	6.77	7.91	14.81	7.60
		Average	<b>16.79</b>	<b>15.27</b>	<b>8.04</b>	<b>7.24</b>	<b>7.58</b>	<b>15.27</b>	<b>7.62</b>
		C of V (%)	0.0	3.1	1.1	6.5	4.4	3.1	0.2
West	No Cure	Cores 1	9.50	7.13	21.34	4.63	4.25	7.13	10.07
		Cores 2	11.73	10.78	5.01	4.62	5.77	10.78	5.13
		Average	<b>10.61</b>	<b>8.96</b>	<b>13.17</b>	<b>4.63</b>	<b>5.01</b>	<b>8.96</b>	<b>7.60</b>
		C of V (%)	10.5	20.4	62.0	0.1	15.1	20.4	32.5
	+2 days H	Cores 1	10.32	8.82	5.33	5.16	3.34	8.82	4.61
		Cores 2	8.25	5.91	4.59	3.76	4.23	5.91	4.19
		Average	<b>9.29</b>	<b>7.37</b>	<b>4.96</b>	<b>4.46</b>	<b>3.79</b>	<b>7.37</b>	<b>4.40</b>
		C of V (%)	11.1	19.7	7.5	15.7	11.7	19.7	4.8
	+4 days H	Cores 1	8.68	9.33	6.14	7.96	8.37	9.33	7.49
		Cores 2	8.68	7.94	7.10	7.83	6.73	7.94	7.22
		Average	<b>8.68</b>	<b>8.63</b>	<b>6.62</b>	<b>7.89</b>	<b>7.55</b>	<b>8.63</b>	<b>7.36</b>
		C of V (%)	0.0	8.1	7.2	0.8	10.8	8.1	1.8
	+6 days H	Cores 1	10.35	10.61	7.02	7.52	8.24	10.61	7.59
		Cores 2	10.35	9.64	7.17	8.54	7.99	9.64	7.90
		Average	<b>10.35</b>	<b>10.12</b>	<b>7.09</b>	<b>8.03</b>	<b>8.12</b>	<b>10.12</b>	<b>8.34</b>
		C of V (%)	0.0	4.8	1.1	6.4	1.6	4.8	1.8

Key: +X days H= X days hessian plus 1 day in mould; Average= average of cores 1 and 2; C of V= coefficient of variation (%); Sub-surface (10-40mm)= average k value from 10 to 40mm from surface; Bold value= plotted value (usually average)

**Table A1.7 (a).** Sorptivity S (mm/min<sup>0.5</sup>) for the 30 MPa OPC concrete (east/west) - 3 months winter series

Orientation	Curnig regime		Average depth from outer surface (mm)					Surface (10mm)	Sub-surface (20-50mm)
			10	20	30	40	50		
East	No Cure	Cores 1	0.204	0.186	0.173	0.172	0.202	0.204	0.183
		Cores 2	0.203	0.184	0.176	0.161	0.167	0.203	0.172
		Average	<b>0.204</b>	<b>0.185</b>	<b>0.175</b>	<b>0.167</b>	<b>0.184</b>	<b>0.204</b>	<b>0.178</b>
		C of V (%)	0.2	0.6	0.8	3.2	9.7	0.2	3.2
	+2 days H	Cores 1	0.244	0.180	0.168	0.218	0.166	0.244	0.183
		Cores 2	0.247	0.207	0.212	0.198	0.180	0.247	0.199
		Average	<b>0.245</b>	<b>0.193</b>	<b>0.190</b>	<b>0.208</b>	<b>0.173</b>	<b>0.245</b>	<b>0.191</b>
		C of V (%)	0.7	6.8	11.5	4.6	4.2	0.7	4.3
	+4 days H	Cores 1	0.194	0.184	0.166	0.156	0.152	0.194	0.165
		Cores 2	0.156	0.134	0.146	0.144	0.142	0.156	0.141
		Average	<b>0.175</b>	<b>0.159</b>	<b>0.156</b>	<b>0.150</b>	<b>0.147</b>	<b>0.175</b>	<b>0.153</b>
		C of V (%)	10.9	15.8	6.5	4.0	3.4	10.9	7.6
	+6 days H	Cores 1	0.135	0.132	0.140	0.129	0.134	0.135	0.134
		Cores 2	0.161	0.147	0.164	0.167	0.143	0.161	0.155
		Average	<b>0.148</b>	<b>0.139</b>	<b>0.152</b>	<b>0.148</b>	<b>0.138</b>	<b>0.148</b>	<b>0.144</b>
		C of V (%)	8.8	5.3	7.9	12.6	3.3	8.8	7.4
West	No Cure	Cores 1	0.211	0.175	0.162	0.177	0.155	0.211	0.167
		Cores 2	0.152	0.175	0.174	0.191	0.172	0.152	0.178
		Average	<b>0.181</b>	<b>0.175</b>	<b>0.168</b>	<b>0.184</b>	<b>0.163</b>	<b>0.181</b>	<b>0.173</b>
		C of V (%)	16.2	0.2	3.6	3.9	5.3	16.2	3.2
	+2 days H	Cores 1	0.158	0.155	0.145	0.156	0.217	0.158	0.168
		Cores 2	0.151	0.174	0.193	0.212	0.173	0.151	0.188
		Average	<b>0.154</b>	<b>0.164</b>	<b>0.169</b>	<b>0.184</b>	<b>0.195</b>	<b>0.154</b>	<b>0.178</b>
		C of V (%)	2.3	6.0	14.2	15.1	11.3	2.3	5.6
	+4 days H	Cores 1	0.154	0.152	0.170	0.157	0.167	0.154	0.161
		Cores 2	0.136	0.139	0.133	0.132	0.137	0.136	0.135
		Average	<b>0.145</b>	<b>0.146</b>	<b>0.151</b>	<b>0.145</b>	<b>0.152</b>	<b>0.145</b>	<b>0.148</b>
		C of V (%)	6.4	4.6	12.3	8.5	9.7	6.4	8.8
	+6 days H	Cores 1	0.138	0.143	0.149	0.120	0.141	0.138	0.138
		Cores 2	0.153	0.164	0.146	0.154	0.148	0.153	0.153
		Average	<b>0.145</b>	<b>0.153</b>	<b>0.148</b>	<b>0.137</b>	<b>0.145</b>	<b>0.145</b>	<b>0.146</b>
		C of V (%)	4.9	6.9	1.1	12.7	2.1	4.9	5.0

Key: +X days H= X days hessian plus 1 day in mould; Average= average of cores 1 and 2; C of V= coefficient of variation (%); Sub-surface (20-50mm)= average k value from 20 to 50mm from surface; Bold value= plotted value (usually average)

Table A1.7 (b). Sorptivity S (mm/min<sup>0.5</sup>) for the 30 MPa OPC concrete (top/bottom) - 3 months winter series

Orientation	Curing regime		Average depth from outer surface (mm)					Surface (10mm)	Sub-surface (20-50mm)
			10	20	30	40	50		
Top	No Cure	Cores 1	0.176	0.157	0.147	0.185	0.166	0.176	0.164
		Cores 2	0.196	0.178	0.158	0.171	0.176	0.196	0.171
		Average	<b>0.186</b>	<b>0.167</b>	<b>0.153</b>	<b>0.178</b>	<b>0.171</b>	<b>0.186</b>	<b>0.167</b>
		C of V (%)	5.5	6.4	3.6	3.9	3.1	5.5	2.2
	+2 days H	Cores 1	0.156	0.153	0.151	0.151	0.165	0.156	0.155
		Cores 2	0.162	0.154	0.170	0.171	0.149	0.162	0.161
		Average	<b>0.159</b>	<b>0.153</b>	<b>0.161</b>	<b>0.161</b>	<b>0.157</b>	<b>0.159</b>	<b>0.158</b>
		C of V (%)	1.6	0.4	5.9	6.2	5.1	1.6	1.9
	+4 days H	Cores 1	0.136	0.186	0.172	0.184	0.172	0.136	0.178
		Cores 2	0.149	0.195	0.167	0.192	0.154	0.149	0.177
		Average	<b>0.142</b>	<b>0.191</b>	<b>0.170</b>	<b>0.188</b>	<b>0.163</b>	<b>0.142</b>	<b>0.178</b>
		C of V (%)	4.4	2.5	1.4	2.1	5.5	4.4	0.4
	+6 days H	Cores 1	0.158	0.156	0.198	0.169	0.172	0.158	0.174
		Cores 2	0.159	0.141	0.189	0.168	0.182	0.159	0.170
		Average	<b>0.158</b>	<b>0.149</b>	<b>0.194</b>	<b>0.169</b>	<b>0.177</b>	<b>0.158</b>	<b>0.172</b>
		C of V (%)	0.3	5.1	2.4	0.4	2.6	0.3	1.2
Bottom	No Cure	Cores 1	0.148	0.145	0.163	0.136	0.172	0.148	0.154
		Cores 2	0.207	0.161	0.192	0.162	0.169	0.207	0.171
		Average	<b>0.177</b>	<b>0.153</b>	<b>0.178</b>	<b>0.149</b>	<b>0.170</b>	<b>0.177</b>	<b>0.162</b>
		C of V (%)	16.5	5.1	8.1	8.6	0.9	16.5	5.1
	+2 days H	Cores 1	0.135	0.166	0.144	0.166	0.151	0.135	0.157
		Cores 2	0.195	0.158	0.180	0.174	0.185	0.195	0.174
		Average	<b>0.165</b>	<b>0.162</b>	<b>0.162</b>	<b>0.170</b>	<b>0.168</b>	<b>0.165</b>	<b>0.165</b>
		C of V (%)	18.1	2.6	11.1	2.1	10.4	18.1	5.3
	+4 days H	Cores 1	0.230	0.219	0.214	0.205	0.183	0.230	0.205
		Cores 2	0.234	0.204	0.200	0.196	0.182	0.234	0.196
		Average	<b>0.232</b>	<b>0.212</b>	<b>0.207</b>	<b>0.200</b>	<b>0.183</b>	<b>0.232</b>	<b>0.200</b>
		C of V (%)	0.8	3.6	3.3	2.2	0.3	0.8	2.4
	+6 days H	Cores 1	0.242	0.167	0.211	0.178	0.179	0.242	0.184
		Cores 2	0.215	0.168	0.197	0.177	0.176	0.215	0.180
		Average	<b>0.229</b>	<b>0.168</b>	<b>0.204</b>	<b>0.178</b>	<b>0.177</b>	<b>0.229</b>	<b>0.182</b>
		C of V (%)	6.0	0.4	3.3	0.3	0.7	6.0	1.1

Key: +X days H= X days hessian plus 1 day in mould; Average= average of cores 1 and 2; C of V= coefficient of variation (%); Sub-surface (20-50mm)= average k value from 20 to 50mm from surface; Bold value= plotted value (usually average)

Table A1.8 (a). Sorptivity S (mm/min<sup>0.5</sup>) for the 30 MPa OPC concrete - (east/west) 12 months winter series

Orientation	Curnig regime	Average depth from outer surface (mm)					Surface (10mm)	Sub-surface (20-40mm)	
		5	10	20	30	40			
East	No Cure	Cores 1	0.133	0.171	0.205	0.205	0.201	0.171	0.204
		Cores 2	0.131	0.169	0.194	0.215	0.196	0.169	0.202
		Average	<b>0.132</b>	<b>0.170</b>	<b>0.199</b>	<b>0.210</b>	<b>0.199</b>	<b>0.170</b>	<b>0.203</b>
		C of V (%)	0.9	0.6	2.7	2.5	1.2	0.6	0.4
	+2 days H	Cores 1	0.173	0.214	0.202	0.234	0.196	0.214	0.210
		Cores 2	0.162	0.180	0.196	0.173	0.157	0.180	0.175
		Average	<b>0.167</b>	<b>0.197</b>	<b>0.199</b>	<b>0.203</b>	<b>0.176</b>	<b>0.197</b>	<b>0.193</b>
		C of V (%)	3.2	8.4	1.5	14.9	11.0	8.4	9.1
	+4 days H	Cores 1	0.120	0.136	0.185	0.225	0.186	0.136	0.199
		Cores 2	0.114	0.120	0.196	0.153	0.165	0.120	0.171
		Average	<b>0.117</b>	<b>0.128</b>	<b>0.190</b>	<b>0.189</b>	<b>0.175</b>	<b>0.128</b>	<b>0.185</b>
		C of V (%)	2.5	6.0	2.9	19.0	6.2	6.0	7.4
	+6 days H	Cores 1	0.126	0.187	0.221	0.216	0.203	0.187	0.213
		Cores 2	0.140	0.145	0.176	0.175	0.165	0.145	0.172
		Average	<b>0.133</b>	<b>0.166</b>	<b>0.199</b>	<b>0.196</b>	<b>0.184</b>	<b>0.166</b>	<b>0.193</b>
		C of V (%)	5.4	12.4	11.4	10.5	10.4	12.4	10.8
West	No Cure	Cores 1	0.128	0.147	0.217	0.221	0.187	0.147	0.208
		Cores 2	0.119	0.113	0.188	0.218	0.186	0.113	0.198
		Average	<b>0.124</b>	<b>0.130</b>	<b>0.202</b>	<b>0.220</b>	<b>0.186</b>	<b>0.130</b>	<b>0.203</b>
		C of V (%)	3.8	13.1	7.1	0.6	0.1	13.1	2.6
	+2 days H	Cores 1	0.138	0.171	0.195	0.224	0.167	0.171	0.195
		Cores 2	0.131	0.118	0.167	0.170	0.152	0.118	0.163
		Average	<b>0.135</b>	<b>0.145</b>	<b>0.181</b>	<b>0.197</b>	<b>0.160</b>	<b>0.145</b>	<b>0.179</b>
		C of V (%)	2.4	18.4	7.7	13.7	4.7	18.4	9.0
	+4 days H	Cores 1	0.088	0.108	0.166	0.152	0.162	0.108	0.160
		Cores 2	0.077	0.117	0.145	0.150	0.159	0.117	0.151
		Average	<b>0.083</b>	<b>0.113</b>	<b>0.155</b>	<b>0.151</b>	<b>0.161</b>	<b>0.113</b>	<b>0.156</b>
		C of V (%)	6.5	3.9	6.8	0.4	0.8	3.9	2.7
	+6 days H	Cores 1	0.100	0.090	0.156	0.154	0.160	0.090	0.156
		Cores 2	0.086	0.102	0.175	0.170	0.179	0.102	0.175
		Average	<b>0.093</b>	<b>0.096</b>	<b>0.165</b>	<b>0.162</b>	<b>0.169</b>	<b>0.096</b>	<b>0.165</b>
		C of V (%)	7.3	6.2	5.9	5.1	5.7	6.2	5.6

Key: +X days H= X days hessian plus 1 day in mould; Average= average of cores 1 and 2; C of V= coefficient of variation (%); Sub-surface (10-40mm)= average k value from 10 to 40mm from surface; Bold value= plotted value (usually average)

Table A1.8 (b). Sorptivity S (mm/min<sup>0.5</sup>) for the 30 MPa OPC concrete (top/bottom) - 12 months winter series

Orientation	Curing regime	Average depth from outer surface (mm)					Surface (10mm)	Sub-surface (20-40mm)	
		5	10	20	30	40			
Top	No Cure	Cores 1	0.098	0.094	0.158	0.151	0.110	0.094	0.140
		Cores 2	0.068	0.064	0.153	0.130	0.143	0.064	0.142
		Average	<b>0.083</b>	<b>0.079</b>	<b>0.156</b>	<b>0.140</b>	<b>0.126</b>	<b>0.079</b>	<b>0.141</b>
		C of V (%)	17.8	19.4	1.7	7.7	13.2	19.4	0.8
	+2 days H	Cores 1	0.095	0.098	0.136	0.156	0.175	0.098	0.156
		Cores 2	0.058	0.086	0.140	0.140	0.146	0.086	0.142
		Average	<b>0.076</b>	<b>0.092</b>	<b>0.138</b>	<b>0.148</b>	<b>0.160</b>	<b>0.092</b>	<b>0.149</b>
		C of V (%)	24.4	6.6	1.5	5.4	9.0	6.6	4.6
	+4 days H	Cores 1	0.057	0.076	0.152	0.151	0.157	0.076	0.153
		Cores 2	0.072	0.070	0.121	0.145	0.149	0.070	0.138
		Average	<b>0.064</b>	<b>0.073</b>	<b>0.136</b>	<b>0.148</b>	<b>0.153</b>	<b>0.073</b>	<b>0.146</b>
		C of V (%)	12.0	3.9	11.5	2.1	2.5	3.9	5.2
	+6 days H	Cores 1	0.069	0.088	0.130	0.142	0.134	0.088	0.135
		Cores 2	0.066	0.081	0.123	0.141	0.130	0.081	0.131
		Average	<b>0.068</b>	<b>0.084</b>	<b>0.127</b>	<b>0.141</b>	<b>0.132</b>	<b>0.084</b>	<b>0.133</b>
		C of V (%)	2.4	4.4	2.7	0.4	1.6	4.4	1.5
Bottom	No Cure	Cores 1	0.087	0.103	0.179	0.209	0.175	0.103	0.188
		Cores 2	0.094	0.119	0.193	0.147	0.170	0.119	0.170
		Average	<b>0.091</b>	<b>0.111</b>	<b>0.186</b>	<b>0.178</b>	<b>0.173</b>	<b>0.111</b>	<b>0.179</b>
		C of V (%)	3.7	7.2	3.8	17.3	1.4	7.2	4.9
	+2 days H	Cores 1	0.034	0.100	0.209	0.173	0.176	0.100	0.186
		Cores 2	0.101	0.112	0.191	0.159	0.156	0.112	0.168
		Average	<b>0.068</b>	<b>0.106</b>	<b>0.200</b>	<b>0.166</b>	<b>0.166</b>	<b>0.106</b>	<b>0.177</b>
		C of V (%)	49.7	5.7	4.6	4.1	6.0	5.7	4.9
	+4 days H	Cores 1	0.076	0.087	0.144	0.147	0.136	0.087	0.142
		Cores 2	0.114	0.069	0.155	0.150	0.161	0.069	0.155
		Average	<b>0.095</b>	<b>0.078</b>	<b>0.149</b>	<b>0.149</b>	<b>0.149</b>	<b>0.078</b>	<b>0.149</b>
		C of V (%)	20.0	11.6	3.5	1.0	8.6	11.6	4.4
	+6 days H	Cores 1	0.073	0.067	0.140	0.150	0.150	0.067	0.146
		Cores 2	0.063	0.123	0.129	0.152	0.135	0.123	0.139
		Average	<b>0.068</b>	<b>0.095</b>	<b>0.134</b>	<b>0.151</b>	<b>0.142</b>	<b>0.095</b>	<b>0.142</b>
		C of V (%)	7.3	29.6	3.8	0.6	5.3	29.6	2.8

Key: +X days H= X days hessian plus 1 day in mould; Average= average of cores 1 and 2; C of V= coefficient of variation (%); Sub-surface (10-40mm)= average k value from 10 to 40mm from surface; Bold value= plotted value (usually average)

**Table A1.9 (a). Sorptivity S (mm/min<sup>0.5</sup>) for the 50 MPa OPC concrete (east/west) - 3 months winter series**

Orientation	Curnig regime		Average depth from outer surface (mm)					Surface (10mm)	Sub-surface (20-50mm)
			10	20	30	40	50		
East	No Cure	Cores 1	0.132	0.143	0.138	0.148	0.127	0.132	0.139
		Cores 2	0.120	0.129	0.137	0.132	0.127	0.120	0.131
		Average	<b>0.126</b>	<b>0.136</b>	<b>0.137</b>	<b>0.140</b>	<b>0.127</b>	<b>0.126</b>	<b>0.135</b>
		C of V (%)	4.7	5.2	0.5	5.7	0.3	4.7	2.8
	+2 days H	Cores 1	0.134	0.148	0.141	0.149	0.136	0.134	0.143
		Cores 2	0.137	0.142	0.145	0.142	0.136	0.137	0.141
		Average	<b>0.136</b>	<b>0.145</b>	<b>0.143</b>	<b>0.145</b>	<b>0.136</b>	<b>0.136</b>	<b>0.142</b>
		C of V (%)	1.4	2.0	1.2	2.6	0.2	1.4	0.8
	+4 days H	Cores 1	0.194	0.184	0.188	0.157	0.152	0.194	0.170
		Cores 2	0.155	0.134	0.146	0.144	0.142	0.155	0.141
		Average	<b>0.175</b>	<b>0.159</b>	<b>0.167</b>	<b>0.151</b>	<b>0.147</b>	<b>0.175</b>	<b>0.156</b>
		C of V (%)	11.2	15.8	12.7	4.2	3.4	11.2	9.2
	+6 days H	Cores 1	0.135	0.132	0.140	0.129	0.134	0.135	0.134
		Cores 2	0.161	0.147	0.164	0.167	0.143	0.161	0.155
		Average	<b>0.148</b>	<b>0.139</b>	<b>0.152</b>	<b>0.148</b>	<b>0.138</b>	<b>0.148</b>	<b>0.144</b>
		C of V (%)	8.8	5.3	7.9	12.6	3.3	8.8	7.4
West	No Cure	Cores 1	0.136	0.121	0.130	0.136	0.128	0.136	0.129
		Cores 2	0.157	0.144	0.142	0.131	0.137	0.157	0.139
		Average	<b>0.146</b>	<b>0.133</b>	<b>0.136</b>	<b>0.133</b>	<b>0.132</b>	<b>0.146</b>	<b>0.134</b>
		C of V (%)	7.0	8.6	4.5	1.8	3.5	7.0	3.7
	+2 days H	Cores 1	0.156	0.139	0.154	0.153	0.151	0.156	0.149
		Cores 2	0.151	0.156	0.165	0.151	0.154	0.151	0.157
		Average	<b>0.153</b>	<b>0.148</b>	<b>0.160</b>	<b>0.152</b>	<b>0.153</b>	<b>0.153</b>	<b>0.153</b>
		C of V (%)	1.9	5.7	3.4	0.4	0.9	1.9	2.4
	+4 days H	Cores 1	0.154	0.152	0.170	0.157	0.167	0.154	0.161
		Cores 2	0.136	0.139	0.133	0.132	0.138	0.136	0.135
		Average	<b>0.145</b>	<b>0.146</b>	<b>0.151</b>	<b>0.145</b>	<b>0.152</b>	<b>0.145</b>	<b>0.148</b>
		C of V (%)	6.4	4.6	12.3	8.5	9.5	6.4	8.8
	+6 days H	Cores 1	0.138	0.143	0.149	0.120	0.141	0.138	0.138
		Cores 2	0.153	0.164	0.146	0.154	0.148	0.153	0.153
		Average	<b>0.145</b>	<b>0.153</b>	<b>0.148</b>	<b>0.137</b>	<b>0.145</b>	<b>0.145</b>	<b>0.146</b>
		C of V (%)	4.9	6.9	1.1	12.7	2.1	4.9	5.0

Key: +X days H= X days hessian plus 1 day in mould; Average= average of cores 1 and 2; C of V= coefficient of variation (%); Sub-surface (20-50mm)= average k value from 20 to 50mm from surface; Bold value= plotted value (usually average)

Table A1.9 (b). Sorptivity S (mm/min<sup>0.5</sup>) for the 50 MPa OPC concrete (top/bottom) - 3 months winter series

Orientation	Curing regime		Average depth from outer surface (mm)					Surface (10mm)	Sub-surface (20-50mm)
			10	20	30	40	50		
Top	No Cure	Cores 1	0.119	0.126	0.121	0.147	0.136	0.119	0.132
		Cores 2	0.134	0.105	0.115	0.125	0.121	0.134	0.116
		Average	<b>0.126</b>	<b>0.116</b>	<b>0.118</b>	<b>0.136</b>	<b>0.128</b>	<b>0.126</b>	<b>0.124</b>
		C of V (%)	6.0	9.1	2.8	7.8	6.0	6.0	6.5
	+2 days H	Cores 1	0.130	0.121	0.124	0.131	0.129	0.130	0.126
		Cores 2	0.127	0.113	0.150	0.130	0.126	0.127	0.130
		Average	<b>0.128</b>	<b>0.117</b>	<b>0.137</b>	<b>0.131</b>	<b>0.127</b>	<b>0.128</b>	<b>0.128</b>
		C of V (%)	1.4	3.4	9.6	0.1	1.3	1.4	1.4
	+4 days H	Cores 1	0.124	0.122	0.090	0.134	0.133	0.124	0.120
		Cores 2	0.121	0.132	0.127	0.149	0.126	0.121	0.133
		Average	<b>0.122</b>	<b>0.127</b>	<b>0.109</b>	<b>0.141</b>	<b>0.130</b>	<b>0.122</b>	<b>0.127</b>
		C of V (%)	1.4	3.8	17.1	5.3	2.8	1.4	5.4
	+6 days H	Cores 1	0.138	0.134	0.130	0.143	0.134	0.138	0.136
		Cores 2	0.128	0.133	0.131	0.141	0.125	0.128	0.132
		Average	<b>0.133</b>	<b>0.133</b>	<b>0.131</b>	<b>0.142</b>	<b>0.130</b>	<b>0.133</b>	<b>0.134</b>
		C of V (%)	3.8	0.6	0.3	0.8	3.5	3.8	1.1
Bottom	No Cure	Cores 1	0.140	0.128	0.126	0.142	0.131	0.140	0.132
		Cores 2	0.114	0.098	0.126	0.117	0.104	0.114	0.111
		Average	<b>0.127</b>	<b>0.113</b>	<b>0.126</b>	<b>0.129</b>	<b>0.117</b>	<b>0.127</b>	<b>0.121</b>
		C of V (%)	10.4	13.2	0.1	9.5	11.6	10.4	8.4
	+2 days H	Cores 1	0.145	0.118	0.145	0.137	0.128	0.145	0.132
		Cores 2	0.160	0.157	0.150	0.132	0.137	0.160	0.144
		Average	<b>0.153</b>	<b>0.137</b>	<b>0.148</b>	<b>0.135</b>	<b>0.133</b>	<b>0.153</b>	<b>0.138</b>
		C of V (%)	4.7	14.3	1.6	1.8	3.4	4.7	4.4
	+4 days H	Cores 1	0.139	0.119	0.140	0.134	0.133	0.139	0.131
		Cores 2	0.156	0.150	0.130	0.131	0.122	0.156	0.133
		Average	<b>0.148</b>	<b>0.134</b>	<b>0.135</b>	<b>0.133</b>	<b>0.127</b>	<b>0.148</b>	<b>0.132</b>
		C of V (%)	5.8	11.6	3.6	1.1	4.4	5.8	0.7
	+6 days H	Cores 1	0.141	0.150	0.140	0.133	0.132	0.141	0.139
		Cores 2	0.156	0.147	0.138	0.148	0.128	0.156	0.140
		Average	<b>0.149</b>	<b>0.148</b>	<b>0.139</b>	<b>0.140</b>	<b>0.130</b>	<b>0.149</b>	<b>0.139</b>
		C of V (%)	4.8	1.1	1.0	5.2	1.8	4.8	0.3

Key: +X days H= X days hessian plus 1 day in mould; Average= average of cores 1 and 2; C of V= coefficient of variation (%); Sub-surface (20-50mm)= average k value from 20 to 50mm from surface; Bold value= plotted value (usually average)

Table A1.10 (a) Sorptivity S (mm/min<sup>0.5</sup>) for the 50 MPa OPC concrete (east/west) - 12 months winter series

Orientation	Curnig regime		Average depth from outer surface (mm)					Surface (10mm)	Sub-surface (20-40mm)
			5	10	20	30	40		
East	No Cure	Cores 1	0.093	0.093	0.128	0.122	0.114	0.093	0.121
		Cores 2	0.091	0.087	0.114	0.128	0.104	0.087	0.115
		Average	<b>0.092</b>	<b>0.090</b>	<b>0.121</b>	<b>0.125</b>	<b>0.109</b>	<b>0.090</b>	<b>0.118</b>
		C of V (%)	1.0	3.0	5.9	2.2	4.6	3.0	2.6
	+2 days H	Cores 1	0.079	0.056	0.103	0.104	0.113	0.056	0.107
		Cores 2	0.067	0.074	0.100	0.120	0.121	0.074	0.114
		Average	<b>0.073</b>	<b>0.065</b>	<b>0.101</b>	<b>0.112</b>	<b>0.117</b>	<b>0.065</b>	<b>0.110</b>
		C of V (%)	8.4	13.8	1.5	7.3	3.2	13.8	3.1
	+4 days H	Cores 1	0.061	0.072	0.115	0.125	0.096	0.072	0.112
		Cores 2	0.055	0.076	0.111	0.121	0.104	0.076	0.112
		Average	<b>0.058</b>	<b>0.074</b>	<b>0.113</b>	<b>0.123</b>	<b>0.100</b>	<b>0.074</b>	<b>0.112</b>
		C of V (%)	4.6	3.1	1.9	1.5	4.5	3.1	0.1
	+6 days H	Cores 1	0.067	0.065	0.107	0.115	0.099	0.065	0.107
		Cores 2	0.060	0.063	0.116	0.113	0.110	0.063	0.113
		Average	<b>0.064</b>	<b>0.064</b>	<b>0.112</b>	<b>0.114</b>	<b>0.105</b>	<b>0.064</b>	<b>0.110</b>
		C of V (%)	5.5	1.6	4.3	0.8	5.4	1.6	2.9
West	No Cure	Cores 1	0.061	0.059	0.102	0.127	0.108	0.059	0.112
		Cores 2	0.040	0.044	0.095	0.102	0.102	0.044	0.100
		Average	<b>0.051</b>	<b>0.051</b>	<b>0.098</b>	<b>0.114</b>	<b>0.105</b>	<b>0.051</b>	<b>0.106</b>
		C of V (%)	21.0	14.5	3.3	11.0	2.9	14.5	5.9
	+2 days H	Cores 1	0.053	0.058	0.106	0.108	0.106	0.058	0.106
		Cores 2	0.048	0.039	0.097	0.105	0.106	0.039	0.102
		Average	<b>0.051</b>	<b>0.049</b>	<b>0.101</b>	<b>0.106</b>	<b>0.106</b>	<b>0.049</b>	<b>0.104</b>
		C of V (%)	4.8	18.9	4.4	1.4	0.1	18.9	1.9
	+4 days H	Cores 1	0.042	0.060	0.095	0.106	0.107	0.060	0.102
		Cores 2	0.047	0.052	0.113	0.100	0.102	0.052	0.105
		Average	<b>0.044</b>	<b>0.056</b>	<b>0.104</b>	<b>0.103</b>	<b>0.104</b>	<b>0.056</b>	<b>0.104</b>
		C of V (%)	6.0	7.2	8.7	2.7	2.5	7.2	1.1
	+6 days H	Cores 1	0.050	0.048	0.101	0.117	0.097	0.048	0.105
		Cores 2	0.054	0.065	0.100	0.103	0.101	0.065	0.101
		Average	<b>0.052</b>	<b>0.057</b>	<b>0.100</b>	<b>0.110</b>	<b>0.099</b>	<b>0.057</b>	<b>0.103</b>
		C of V (%)	3.8	15.6	0.3	6.5	1.8	15.6	1.9

Key: +X days H= X days hessian plus 1 day in mould; Average= average of cores 1 and 2; C of V= coefficient of variation (%); Sub-surface (10-40mm)= average k value from 10 to 40mm from surface; Bold value= plotted value (usually average)

**Table A1.10 (b) Sorptivity S (mm/min<sup>0.5</sup>) for the 50 MPa OPC Concrete (top/bottom) - 12 months winter series**

Orientation	Curing regime		Average depth from outer surface (mm)					Surface (10mm)	Sub-surface (20-40mm)
			5	10	20	30	40		
Top	No Cure	Cores 1	0.045	0.048	0.102	0.106	0.096	0.048	0.101
		Cores 2	0.038	0.052	0.086	0.112	0.105	0.052	0.101
		Average	<b>0.041</b>	<b>0.050</b>	<b>0.094</b>	<b>0.109</b>	<b>0.100</b>	<b>0.050</b>	<b>0.101</b>
		C of V (%)	8.4	3.7	8.7	2.7	4.6	3.7	0.2
	+2 days H	Cores 1	0.043	0.050	0.052	0.089	0.099	0.050	0.080
		Cores 2	0.044	0.102	0.047	0.103	0.112	0.102	0.088
		Average	<b>0.043</b>	<b>0.076</b>	<b>0.050</b>	<b>0.096</b>	<b>0.106</b>	<b>0.076</b>	<b>0.084</b>
		C of V (%)	1.4	33.6	4.7	7.4	6.1	33.6	4.5
	+4 days H	Cores 1	0.052	0.064	0.105	0.103	0.104	0.064	0.104
		Cores 2	0.046	0.065	0.104	0.114	0.101	0.065	0.106
		Average	<b>0.049</b>	<b>0.064</b>	<b>0.104</b>	<b>0.109</b>	<b>0.103</b>	<b>0.064</b>	<b>0.105</b>
		C of V (%)	5.9	0.5	0.2	5.0	1.7	0.5	1.1
	+6 days H	Cores 1	0.054	0.056	0.105	0.111	0.104	0.056	0.107
		Cores 2	0.048	0.052	0.105	0.106	0.105	0.052	0.105
		Average	<b>0.051</b>	<b>0.054</b>	<b>0.105</b>	<b>0.108</b>	<b>0.104</b>	<b>0.054</b>	<b>0.106</b>
		C of V (%)	5.6	4.1	0.0	2.3	0.5	4.1	0.6
Bottom	No Cure	Cores 1	0.049	0.061	0.106	0.116	0.107	0.061	0.109
		Cores 2	0.055	0.079	0.105	0.121	0.098	0.079	0.108
		Average	<b>0.052</b>	<b>0.070</b>	<b>0.105</b>	<b>0.119</b>	<b>0.103</b>	<b>0.070</b>	<b>0.109</b>
		C of V (%)	6.4	12.8	0.3	2.4	4.1	12.8	0.6
	+2 days H	Cores 1	0.059	0.051	0.096	0.114	0.105	0.051	0.105
		Cores 2	0.040	0.105	0.096	0.121	0.113	0.105	0.110
		Average	<b>0.050</b>	<b>0.078</b>	<b>0.096</b>	<b>0.117</b>	<b>0.109</b>	<b>0.078</b>	<b>0.107</b>
		C of V (%)	19.2	34.9	0.3	2.9	3.7	34.9	2.4
	+4 days H	Cores 1	0.064	0.064	0.100	0.115	0.107	0.064	0.107
		Cores 2	0.082	0.065	0.130	0.125	0.122	0.065	0.126
		Average	<b>0.073</b>	<b>0.064</b>	<b>0.115</b>	<b>0.120</b>	<b>0.114</b>	<b>0.064</b>	<b>0.116</b>
		C of V (%)	12.0	0.9	13.1	4.2	6.6	0.9	7.9
	+6 days H	Cores 1	0.067	0.067	0.116	0.132	0.118	0.067	0.122
		Cores 2	0.070	0.074	0.136	0.124	0.113	0.074	0.125
		Average	<b>0.068</b>	<b>0.071</b>	<b>0.126</b>	<b>0.128</b>	<b>0.116</b>	<b>0.071</b>	<b>0.123</b>
		C of V (%)	2.3	5.0	8.1	3.0	2.0	5.0	1.1

**Key:** +X days H= X days hessian plus 1 day in mould; Average= average of cores 1 and 2; C of V= coefficient of variation (%); Sub-surface (10-40mm)= average k value from 10 to 40mm from surface; Bold value= plotted value (usually average)

**Table A1.11 (a).** Sorptivity S (mm/min<sup>0.5</sup>) for the 30 MPa OPC/GGBS concrete (east/west) - 3 months winter series

Orientation	Curnig regime		Average depth from outer surface (mm)					Surface (10mm)	Sub-surface (20-50mm)
			10	20	30	40	50		
East	No Cure	Cores 1	0.202	0.179	0.171	0.177	0.162	0.202	0.172
		Cores 2	0.203	0.184	0.176	0.161	0.167	0.203	0.172
		Average	<b>0.202</b>	<b>0.181</b>	<b>0.173</b>	<b>0.169</b>	<b>0.164</b>	<b>0.202</b>	<b>0.172</b>
		C of V (%)	0.4	1.4	1.4	4.7	1.5	0.4	0.1
	+2 days H	Cores 1	0.257	0.287	0.200	0.224	0.204	0.257	0.229
		Cores 2	0.247	0.207	0.212	0.198	0.180	0.247	0.199
		Average	<b>0.252</b>	<b>0.247</b>	<b>0.206</b>	<b>0.211</b>	<b>0.192</b>	<b>0.252</b>	<b>0.214</b>
		C of V (%)	1.9	16.4	2.9	6.1	6.2	1.9	6.9
	+4 days H	Cores 1	0.146	0.139	0.142	0.150	0.147	0.146	0.145
		Cores 2	0.205	0.124	0.158	0.177	0.149	0.205	0.152
		Average	<b>0.176</b>	<b>0.132</b>	<b>0.150</b>	<b>0.163</b>	<b>0.148</b>	<b>0.176</b>	<b>0.148</b>
		C of V (%)	16.7	5.7	5.1	8.4	0.5	16.7	2.5
	+6 days H	Cores 1	0.230	0.154	0.181	0.170	0.172	0.230	0.169
		Cores 2	0.230	0.161	0.163	0.174	0.149	0.230	0.162
		Average	<b>0.230</b>	<b>0.158</b>	<b>0.172</b>	<b>0.172</b>	<b>0.160</b>	<b>0.230</b>	<b>0.165</b>
		C of V (%)	0.1	2.3	5.1	0.9	7.0	0.1	2.2
West	No Cure	Cores 1	0.171	0.189	0.199	0.214	0.187	0.171	0.197
		Cores 2	0.152	0.175	0.174	0.191	0.172	0.152	0.178
		Average	<b>0.161</b>	<b>0.182</b>	<b>0.187</b>	<b>0.203</b>	<b>0.179</b>	<b>0.161</b>	<b>0.188</b>
		C of V (%)	6.0	3.8	6.6	5.7	4.1	6.0	5.1
	+2 days H	Cores 1	0.167	0.165	0.198	0.215	0.201	0.167	0.195
		Cores 2	0.151	0.174	0.193	0.212	0.173	0.151	0.188
		Average	<b>0.159</b>	<b>0.170</b>	<b>0.195</b>	<b>0.214</b>	<b>0.187</b>	<b>0.159</b>	<b>0.191</b>
		C of V (%)	5.2	2.7	1.4	0.8	7.5	5.2	1.8
	+4 days H	Cores 1	0.183	0.164	0.177	0.173	0.165	0.183	0.170
		Cores 2	0.189	0.160	0.163	0.155	0.153	0.189	0.158
		Average	<b>0.186</b>	<b>0.162</b>	<b>0.170</b>	<b>0.164</b>	<b>0.159</b>	<b>0.186</b>	<b>0.164</b>
		C of V (%)	1.5	1.2	4.0	5.7	3.6	1.5	3.6
	+6 days H	Cores 1	0.204	0.170	0.200	0.186	0.165	0.204	0.180
		Cores 2	0.178	0.145	0.176	0.159	0.152	0.178	0.158
		Average	<b>0.191</b>	<b>0.158</b>	<b>0.188</b>	<b>0.172</b>	<b>0.158</b>	<b>0.191</b>	<b>0.169</b>
		C of V (%)	6.9	7.9	6.2	7.7	3.9	6.9	6.5

Key: +X days H= X days hessian plus 1 day in mould; Average= average of cores 1 and 2; C of V= coefficient of variation (%); Sub-surface (20-50mm)= average k value from 20 to 50mm from surface; Bold value= plotted value (usually average)

Table A1.11 (b). Sorptivity S (mm/min<sup>0.5</sup>) for the 30 MPa OPC/GGBS concrete (top/bottom) - 3 months winter series

Orientation	Curing regime	Average depth from outer surface (mm)					Surface (10mm)	Sub-surface (20-50mm)	
		10	20	30	40	50			
Top	No Cure	Cores 1	0.135	0.142	0.149	0.165	0.144	0.135	0.150
		Cores 2	0.153	0.142	0.163	0.148	0.138	0.153	0.147
		Average	<b>0.144</b>	<b>0.142</b>	<b>0.156</b>	<b>0.156</b>	<b>0.141</b>	<b>0.144</b>	<b>0.149</b>
		C of V (%)	6.4	0.0	4.4	5.6	2.0	6.4	0.8
	+2 days H	Cores 1	0.155	0.154	0.162	0.146	0.143	0.155	0.151
		Cores 2	0.135	0.170	0.151	0.194	0.186	0.135	0.175
		Average	<b>0.145</b>	<b>0.162</b>	<b>0.157</b>	<b>0.170</b>	<b>0.165</b>	<b>0.145</b>	<b>0.163</b>
		C of V (%)	6.7	5.0	3.5	14.2	12.9	6.7	7.3
	+4 days H	Cores 1	0.147	0.127	0.150	0.144	0.133	0.147	0.138
		Cores 2	0.144	0.130	0.128	0.147	0.125	0.144	0.132
		Average	<b>0.145</b>	<b>0.129</b>	<b>0.139</b>	<b>0.145</b>	<b>0.129</b>	<b>0.145</b>	<b>0.135</b>
		C of V (%)	1.3	0.9	7.7	1.2	3.0	1.3	2.2
	+6 days H	Cores 1	0.142	0.143	0.155	0.154	0.157	0.142	0.152
		Cores 2	0.131	0.120	0.117	0.137	0.135	0.131	0.127
		Average	<b>0.136</b>	<b>0.132</b>	<b>0.136</b>	<b>0.145</b>	<b>0.146</b>	<b>0.136</b>	<b>0.140</b>
		C of V (%)	4.1	8.8	13.9	6.0	7.6	4.1	9.0
Bottom	No Cure	Cores 1	0.163	0.161	0.188	0.174	0.174	0.163	0.174
		Cores 2	0.160	0.176	0.158	0.179	0.160	0.160	0.168
		Average	<b>0.161</b>	<b>0.168</b>	<b>0.173</b>	<b>0.177</b>	<b>0.167</b>	<b>0.161</b>	<b>0.171</b>
		C of V (%)	0.7	4.3	8.6	1.3	4.1	0.7	1.8
	+2 days H	Cores 1	0.184	0.159	0.193	0.228	0.170	0.184	0.188
		Cores 2	0.165	0.162	0.156	0.220	0.166	0.165	0.176
		Average	<b>0.175</b>	<b>0.160</b>	<b>0.175</b>	<b>0.224</b>	<b>0.168</b>	<b>0.175</b>	<b>0.182</b>
		C of V (%)	5.5	0.8	10.6	1.8	1.2	5.5	3.2
	+4 days H	Cores 1	0.132	0.165	0.145	0.152	0.148	0.132	0.153
		Cores 2	0.153	0.138	0.128	0.153	0.152	0.153	0.143
		Average	<b>0.143</b>	<b>0.152</b>	<b>0.136</b>	<b>0.153</b>	<b>0.150</b>	<b>0.143</b>	<b>0.148</b>
		C of V (%)	7.3	8.7	6.5	0.6	1.1	7.3	3.3
	+6 days H	Cores 1	0.128	0.162	0.165	0.172	0.148	0.128	0.162
		Cores 2	0.153	0.144	0.142	0.155	0.140	0.153	0.145
		Average	<b>0.140</b>	<b>0.153</b>	<b>0.153</b>	<b>0.163</b>	<b>0.144</b>	<b>0.140</b>	<b>0.153</b>
		C of V (%)	9.0	5.8	7.5	5.4	2.8	9.0	5.4

Key: +X days H= X days hessian plus 1 day in mould; Average= average of cores 1 and 2; C of V= coefficient of variation (%); Sub-surface (20-50mm)= average k value from 20 to 50mm from surface; Bold value= plotted value (usually average)

Table A1.12 (a) Sorptivity S (mm/min<sup>0.5</sup>) for the 30 MPa OPC/GGBS concrete (east/west) - 12 months winter series

Orientation	Curnig regime	Average depth from outer surface (mm)					Surface (10mm)	Sub-surface (20-40mm)	
		5	10	20	30	40			
East	No Cure	Cores 1	0.135	0.205	0.166	0.144	0.144	0.205	0.152
		Cores 2	0.106	0.152	0.120	0.120	0.129	0.152	0.123
		Average	<b>0.120</b>	<b>0.178</b>	<b>0.143</b>	<b>0.132</b>	<b>0.137</b>	<b>0.178</b>	<b>0.137</b>
		C of V (%)	12.1	14.9	16.2	9.4	5.5	14.9	10.5
	+2 days H	Cores 1	0.175	0.195	0.149	0.142	0.133	0.195	0.141
		Cores 2	0.171	0.174	0.119	0.123	0.106	0.174	0.116
		Average	<b>0.173</b>	<b>0.185</b>	<b>0.134</b>	<b>0.132</b>	<b>0.119</b>	<b>0.185</b>	<b>0.129</b>
		C of V (%)	1.2	5.7	11.5	7.3	11.4	5.7	10.0
	+4 days H	Cores 1	0.144	0.186	0.119	0.124	0.139	0.186	0.127
		Cores 2	0.131	0.154	0.108	0.111	0.118	0.154	0.112
		Average	<b>0.137</b>	<b>0.170</b>	<b>0.113</b>	<b>0.117</b>	<b>0.129</b>	<b>0.170</b>	<b>0.120</b>
		C of V (%)	4.7	9.3	4.9	5.7	8.2	9.3	6.3
	+6 days H	Cores 1	0.158	0.206	0.142	0.132	0.104	0.206	0.126
		Cores 2	0.175	0.135	0.122	0.102	0.117	0.135	0.114
		Average	<b>0.166</b>	<b>0.170</b>	<b>0.132</b>	<b>0.117</b>	<b>0.110</b>	<b>0.170</b>	<b>0.120</b>
		C of V (%)	5.3	20.9	7.4	13.1	6.0	20.9	5.1
West	No Cure	Cores 1	0.100	0.118	0.082	0.115	0.110	0.118	0.102
		Cores 2	0.120	0.127	0.109	0.106	0.117	0.127	0.111
		Average	<b>0.110</b>	<b>0.123</b>	<b>0.095</b>	<b>0.111</b>	<b>0.113</b>	<b>0.123</b>	<b>0.107</b>
		C of V (%)	9.1	3.5	14.4	4.3	3.2	3.5	3.9
	+2 days H	Cores 1	0.114	0.116	0.123	0.121	0.106	0.116	0.117
		Cores 2	0.100	0.101	0.110	0.108	0.119	0.101	0.112
		Average	<b>0.107</b>	<b>0.108</b>	<b>0.116</b>	<b>0.114</b>	<b>0.113</b>	<b>0.108</b>	<b>0.114</b>
		C of V (%)	6.6	6.9	5.9	5.9	5.6	6.9	2.1
	+4 days H	Cores 1	0.149	0.140	0.117	0.131	0.139	0.140	0.129
		Cores 2	0.130	0.154	0.129	0.136	0.124	0.154	0.130
		Average	<b>0.139</b>	<b>0.147</b>	<b>0.123</b>	<b>0.133</b>	<b>0.132</b>	<b>0.147</b>	<b>0.129</b>
		C of V (%)	6.7	4.7	4.9	2.1	5.9	4.7	0.3
	+6 days H	Cores 1	0.181	0.143	0.118	0.139	0.122	0.143	0.126
		Cores 2	0.157	0.117	0.112	0.113	0.126	0.117	0.117
		Average	<b>0.169</b>	<b>0.130</b>	<b>0.115</b>	<b>0.126</b>	<b>0.124</b>	<b>0.130</b>	<b>0.122</b>
		C of V (%)	7.0	10.1	2.8	10.4	1.6	10.1	3.9

Key: +X days H= X days hessian plus 1 day in mould; Average= average of cores 1 and 2; C of V= coefficient of variation (%); Sub-surface (10-40mm)= average k value from 10 to 40mm from surface; Bold value= plotted value (usually average)

Table A1.12 (b) Sorptivity S (mm/min<sup>0.5</sup>) for the 30 MPa OPC/GGBS concrete (top/bottom) - 12 months winter series

Orientation	Curing regime		Average depth from outer surface (mm)					Surface (10mm)	Sub-surface (20-40mm)
			5	10	20	30	40		
Top	No Cure	Cores 1	0.093	0.078	0.093	0.076	0.073	0.078	0.081
		Cores 2	0.094	0.118	0.095	0.092	0.095	0.118	0.094
		Average	<b>0.094</b>	<b>0.098</b>	<b>0.094</b>	<b>0.084</b>	<b>0.084</b>	<b>0.098</b>	<b>0.087</b>
		C of V (%)	0.5	20.7	1.1	9.8	12.6	20.7	7.6
	+2 days H	Cores 1	0.068	0.077	0.060	0.078	0.059	0.077	0.066
		Cores 2	0.092	0.098	0.105	0.112	0.080	0.098	0.099
		Average	<b>0.080</b>	<b>0.087</b>	<b>0.083</b>	<b>0.095</b>	<b>0.070</b>	<b>0.087</b>	<b>0.083</b>
		C of V (%)	15.0	11.8	27.3	18.1	15.2	11.8	20.4
	+4 days H	Cores 1	0.114	0.110	0.091	0.073	0.075	0.110	0.079
		Cores 2	0.109	0.110	0.092	0.090	0.151	0.110	0.111
		Average	<b>0.111</b>	<b>0.110</b>	<b>0.091</b>	<b>0.081</b>	<b>0.113</b>	<b>0.110</b>	<b>0.095</b>
		C of V (%)	2.3	0.0	0.7	10.3	33.7	0.0	16.5
	+6 days H	Cores 1	0.102	0.131	0.046	0.072	0.064	0.131	0.061
		Cores 2	0.093	0.103	0.086	0.075	0.076	0.103	0.079
		Average	<b>0.097</b>	<b>0.117</b>	<b>0.066</b>	<b>0.073</b>	<b>0.070</b>	<b>0.117</b>	<b>0.070</b>
		C of V (%)	4.3	11.7	30.1	1.6	8.9	11.7	13.0
Bottom	No Cure	Cores 1	0.135	0.129	0.128	0.117	0.096	0.129	0.114
		Cores 2	0.112	0.131	0.105	0.118	0.110	0.131	0.111
		Average	<b>0.124</b>	<b>0.130</b>	<b>0.117</b>	<b>0.118</b>	<b>0.103</b>	<b>0.130</b>	<b>0.112</b>
		C of V (%)	9.1	0.9	9.9	0.6	6.9	0.9	1.1
	+2 days H	Cores 1	0.098	0.103	0.077	0.097	0.070	0.103	0.081
		Cores 2	0.118	0.125	0.104	0.116	0.097	0.125	0.106
		Average	<b>0.108</b>	<b>0.114</b>	<b>0.090</b>	<b>0.107</b>	<b>0.084</b>	<b>0.114</b>	<b>0.093</b>
		C of V (%)	9.5	9.6	14.9	8.7	16.3	9.6	13.0
	+4 days H	Cores 1	0.127	0.104	0.095	0.085	0.078	0.104	0.086
		Cores 2	0.101	0.115	0.115	0.079	0.124	0.115	0.106
		Average	<b>0.114</b>	<b>0.109</b>	<b>0.105</b>	<b>0.082</b>	<b>0.101</b>	<b>0.109</b>	<b>0.096</b>
		C of V (%)	11.8	5.2	9.4	3.4	22.8	5.2	10.4
	+6 days H	Cores 1	0.113	0.112	0.088	0.105	0.093	0.112	0.095
		Cores 2	0.101	0.108	0.091	0.085	0.085	0.108	0.087
		Average	<b>0.107</b>	<b>0.110</b>	<b>0.090</b>	<b>0.095</b>	<b>0.089</b>	<b>0.110</b>	<b>0.091</b>
		C of V (%)	5.8	2.0	1.9	10.3	4.7	2.0	4.5

Key: +X days H= X days hessian plus 1 day in mould; Average= average of cores 1 and 2; C of V= coefficient of variation (%); Sub-surface (10-40mm)= average k value from 10 to 40mm from surface; Bold value= plotted value (usually average)

**Table A1.13 (a)** Carbonation depth (mm) for the 30 and 50 MPa OPC concrete - 6 months winter series

Microclimate	Reference	30 MPa OPC concrete				50 MPa OPC concrete			
		Average depth of carbonation (mm)				Average depth of carbonation (mm)			
		No cure	+2days H	+4 days H	+ 6 days H	No cure	+2 days H	+4 days H	+6 days H
East	Cores 1	4.0	4.0	3.0	2.0	-	-	-	-
	Cores 2	2.5	4.0	3.0	1.0	-	-	-	-
	Average	3.3	4.0	3.0	1.5	-	-	-	-
	C of V (%)	23.1	0.0	0.0	33.3	-	-	-	-
West	Cores 1	4.0	5.0	3.0	3.0	-	-	-	-
	Cores 2	3.5	3.0	3.5	2.5	-	-	-	-
	Average	3.8	4.0	3.3	2.8	-	-	-	-
	C of V (%)	6.7	25.0	7.7	9.1	-	-	-	-
Top	Cores 1	3.0	1.5	3.5	2.0	-	-	-	-
	Cores 2	1.5	1.5	3.5	2.0	-	-	-	-
	Average	2.3	1.5	3.5	2.0	-	-	-	-
	C of V (%)	33.3	0.0	0.0	0.0	-	-	-	-
Bottom	Cores 1	1.5	1.0	4.0	2.5	-	-	-	-
	Cores 2	2.5	1.0	3.0	4.0	-	-	-	-
	Average	2.0	1.0	3.5	3.3	-	-	-	-
	C of V (%)	25.0	0.0	14.3	23.1	-	-	-	-

**Table A1.13 (b)** Carbonation depth (mm) for the 30 MPa OPC/GGBS concrete - 6 months winter series

Microclimate	Reference	30 MPa OPC/GGBS concrete			
		Average depth of carbonation (mm)			
		No cure	+2 days H	+4 days H	+ 6 days H
East	Cores 1	6.5	4.0	6.0	3.0
	Cores 2	6.0	3.5	6.0	3.0
	Average	6.3	3.8	6.0	3.0
	C of V (%)	4.0	6.7	0.0	0.0
West	Cores 1	6.0	5.0	5.0	3.0
	Cores 2	6.5	7.0	4.5	2.0
	Average	6.3	6.0	4.8	2.5
	C of V (%)	4.0	16.7	5.3	20.0
Top	Cores 1	5.0	4.5	5.0	4.0
	Cores 2	7.0	4.0	5.0	4.5
	Average	6.0	4.3	5.0	4.3
	C of V (%)	16.7	5.9	0.0	5.9
Bottom	Cores 1	4.5	6.0	6.0	2.0
	Cores 2	5.0	5.5	5.0	2.0
	Average	4.8	5.8	5.5	2.0
	C of V (%)	5.3	4.3	9.1	0.0

**Key:** +2 days H = 2 days hessian plus 1 day in mould; Average = average of cores 1 and 2; C of V = coefficient of variation (%); Bold value = plotted value (usually average)

**Table A1.14 (a)** Carbonation depth (mm) for the 30 and 50 MPa OPC concrete - 12 months winter series

Microclimate	Reference	30 MPa OPC concrete				50 MPa OPC concrete			
		Average depth of carbonation (mm)				Average depth of carbonation (mm)			
		No cure	+2days H	+4 days H	+ 6 days H	No cure	+2 days H	+4 days H	+6 days H
East	Cores 1	5.0	7.0	5.8	6.5	2.0	1.0	2.3	1.8
	Cores 2	5.0	6.3	5.8	7.3	1.8	1.0	2.0	1.3
	Average	5.0	6.7	5.8	6.9	1.9	1.0	2.1	1.5
	C of V (%)	0.0	5.3	0.0	5.5	5.3	0.0	5.9	16.7
West	Cores 1	5.3	5.0	4.0	5.3	1.0	1.0	2.3	1.7
	Cores 2	5.0	6.0	5.0	6.0	1.0	1.0	0.8	1.0
	Average	5.2	5.5	4.5	5.6	1.0	1.0	1.5	1.3
	C of V (%)	2.9	9.1	11.1	6.7	0.0	0.0	50.0	25.1
Top	Cores 1	2.7	2.5	3.8	3.5	0.0	0.0	1.5	0.0
	Cores 2	2.0	5.0	4.0	2.8	0.0	0.0	1.0	0.0
	Average	2.4	3.8	3.9	3.1	0.0	0.0	1.3	0.0
	C of V (%)	14.9	33.3	2.6	12.0	0.0	0.0	20.0	0.0
Bottom	Cores 1	7.8	5.0	5.0	5.0	2.0	2.0	2.0	2.0
	Cores 2	5.0	7.5	4.0	8.0	2.5	3.3	2.3	2.0
	Average	6.4	6.3	4.5	6.5	2.3	2.6	2.1	2.0
	C of V (%)	21.6	20.0	11.1	23.1	11.1	23.8	5.9	0.0

**Table A1.14 (b)** Carbonation depth (mm) for the 30 MPa OPC/GGBS concrete - 12 months winter series

Microclimate	Reference	30 MPa OPC/GGBS concrete			
		Average depth of carbonation (mm)			
		No cure	+2 days H	+4 days H	+ 6 days H
East	Cores 1	13.0	13.0	15.0	15.0
	Cores 2	13.0	13.0	13.8	12.0
	Average	13.0	13.0	14.4	13.5
	C of V (%)	0.0	0.0	4.3	11.1
West	Cores 1	10.0	11.0	11.0	11.0
	Cores 2	10.0	9.0	10.0	11.0
	Average	10.0	10.0	10.5	11.0
	C of V (%)	0.0	10.0	4.8	0.0
Top	Cores 1	5.5	6.0	7.5	9.0
	Cores 2	7.5	9.0	7.5	9.0
	Average	6.5	7.5	7.5	9.0
	C of V (%)	15.4	20.0	0.0	0.0
Bottom	Cores 1	8.0	6.5	7.0	9.5
	Cores 2	8.0	8.3	7.5	8.0
	Average	8.0	7.4	7.3	8.8
	C of V (%)	0.0	11.9	3.4	8.6

Key: +2 days H = 2 days hessian plus 1 day in mould; Average = average of cores 1 and 2; C of V = coefficient of variation (%); Bold value = plotted value (usually average)

**A1.15 Areas under DTG curves - weight loss (%) (A1 to A5 according to Figure 5.29)**

Concrete	Curing	Depth	A1	A2	A3	A4	A5	(A1+A2)	A3	(A4+A5)
30 MPa OPC Concrete	no cure	5	1.20	1.93	0.48	1.94	5.10	3.13	0.48	7.04
		10	1.68	2.16	1.40	3.18	6.42	3.84	1.4	9.6
		20	1.7	2.39	1.82	3.38	4.2	4.09	1.82	7.57
	+2 days	5	1.62	2.07	1.43	3.10	6.30	3.68	1.43	9.4
		10	2.36	3.10	2.04	2.62	4.46	5.10	2.04	7.08
		20	1.50	2.44	1.67	3.13	4.92	3.94	1.67	8.04
	+4 days	5	1.17	1.91	0.55	2.29	6.17	3.07	0.55	8.46
		10	2.15	3.21	2.82	2.14	2.39	5.36	2.82	4.53
		20	2.23	2.72	2.19	2.00	2.19	4.94	2.19	4.19
	+6 days	5	1.19	2.28	0.58	2.30	5.61	3.48	0.58	7.90
		10	2.40	3.28	2.91	2.05	1.95	5.68	2.91	4.00
		20	2.28	3.24	2.86	2.09	2.12	5.52	2.86	4.21
50 MPa OPC Concrete	no cure	5	1.58	2.71	0.73	2.79	6.67	4.29	0.73	9.46
		10	1.82	1.88	1.16	3.54	6.41	3.69	1.16	9.94
		20	2.64	2.21	1.96	3.73	5.57	4.84	2.21	9.30
	+2 days	5	2.25	1.88	1.18	3.66	4.74	4.13	1.18	8.41
		10	2.23	2.72	2.19	2.00	2.19	4.94	2.19	4.19
		20	2.73	3.45	3.14	2.54	1.66	6.18	3.14	4.20
30 MPa GGBS Concrete	no cure	5	2.53	3.20	0.98	1.61	2.49	5.73	0.98	4.10
		10	3.84	3.71	1.14	1.37	2.49	7.55	1.14	3.87
		20	4.28	3.88	1.20	1.32	2.22	8.16	1.20	3.55
	+2 days	5	3.52	4.13	1.32	1.34	1.58	7.62	1.32	2.92
		10	1.29	3.53	1.15	1.8	1.48	4.82	1.15	3.27
		20	2.01	3.64	1.20	1.64	1.52	5.64	1.20	3.17
	+4 days	5	1.29	3.53	1.15	1.80	1.48	4.82	1.15	3.27
		10	1.81	3.26	1.14	1.98	1.11	5.07	1.14	3.09
		20	1.58	3.11	0.91	1.77	1.83	4.69	0.91	3.10
+6 days	5	1.77	3.44	1.09	1.48	1.36	5.21	1.09	2.84	
	10	1.75	3.11	0.92	1.80	1.55	4.86	0.92	3.35	
	20	1.63	2.88	0.89	1.88	1.41	4.51	0.89	3.29	

# Appendix B

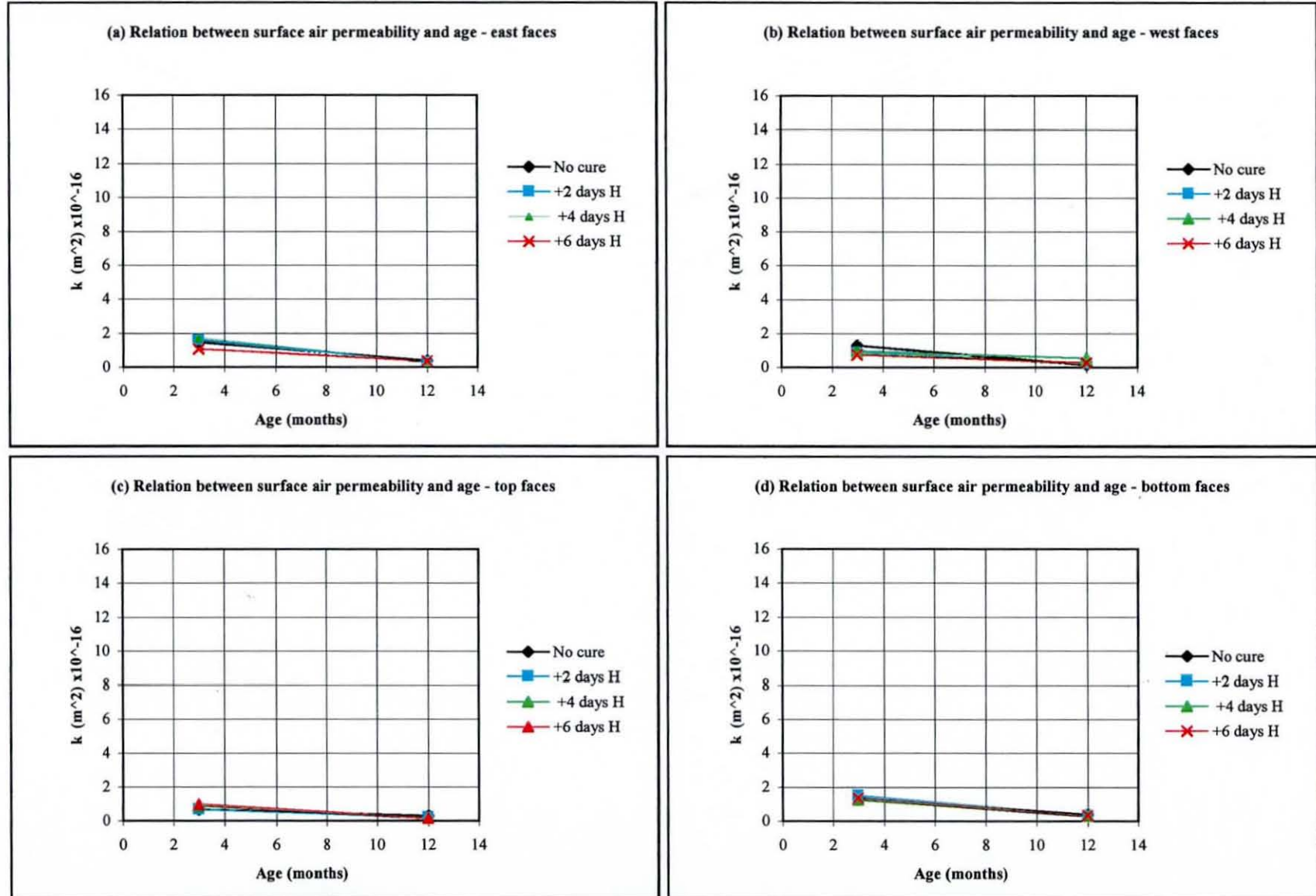


Fig. B1.1 Relationship between surface air permeability and age of the 50 MPa OPC concrete - UK summer

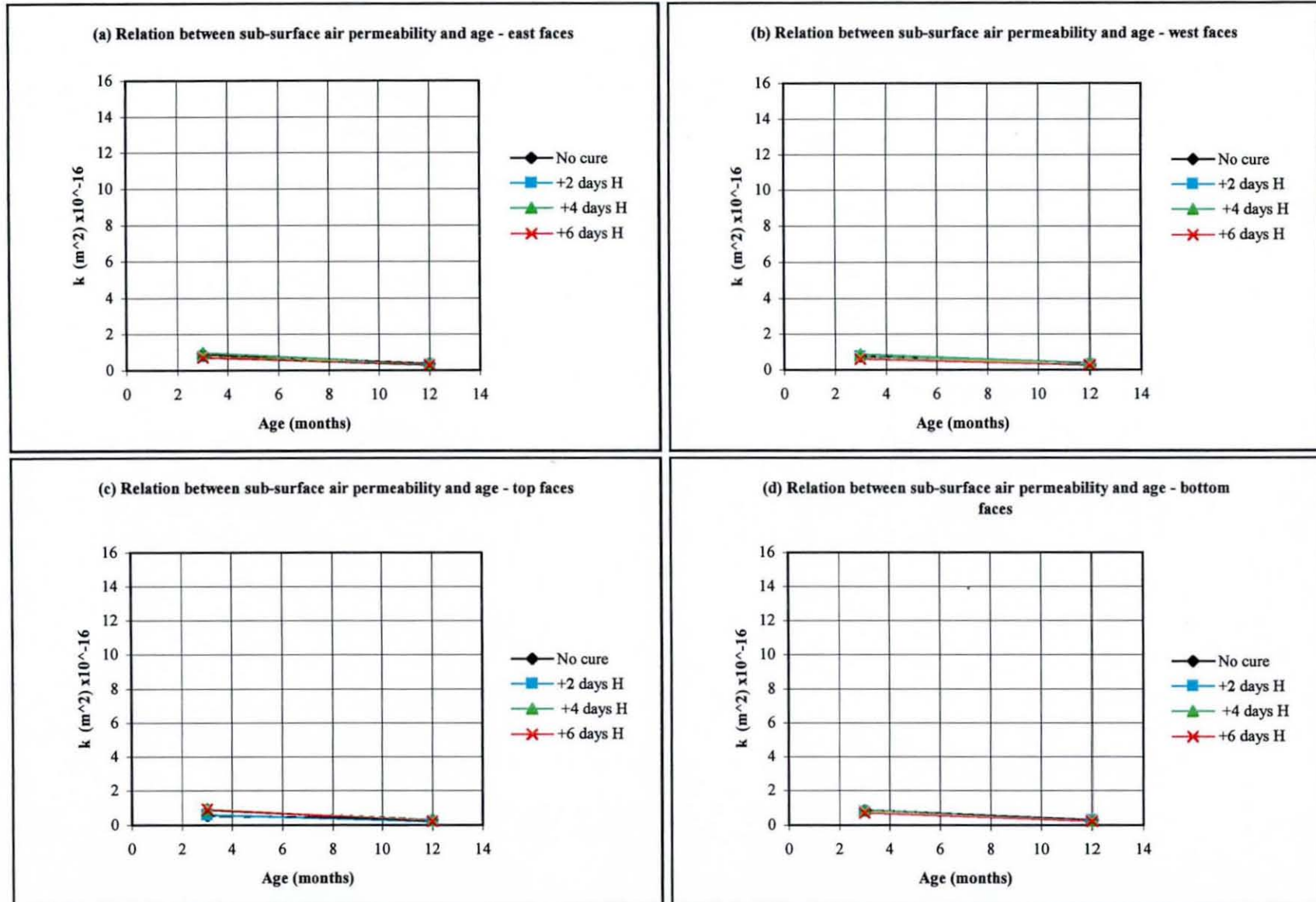
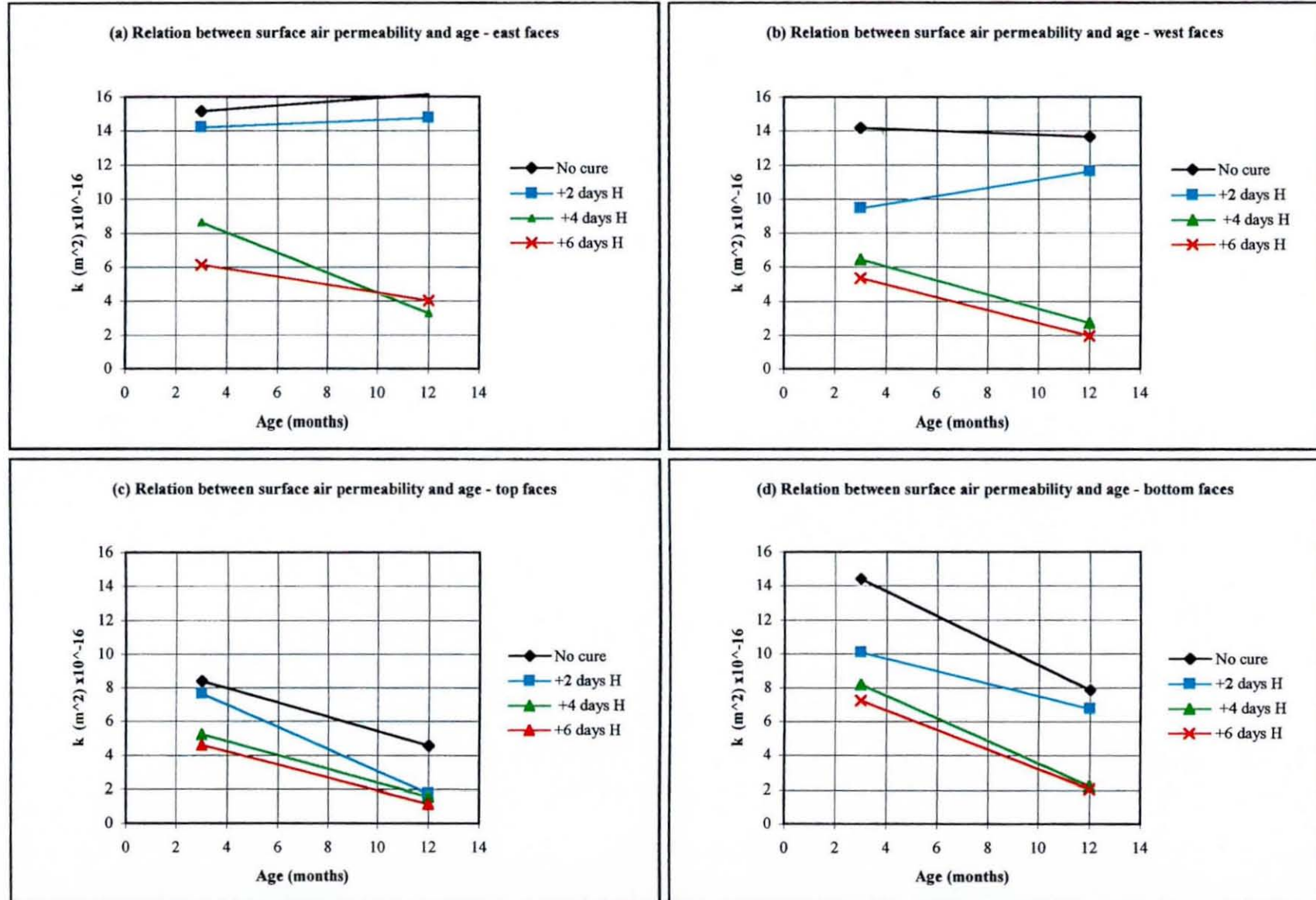


Fig. B1.2 Relationship between sub-surface air permeability and age of the 50 MPa OPC concrete - UK summer



**Fig. B1.3** Relationship between surface air permeability and age of the 30 MPa OPC/GGBS concrete - UK summer

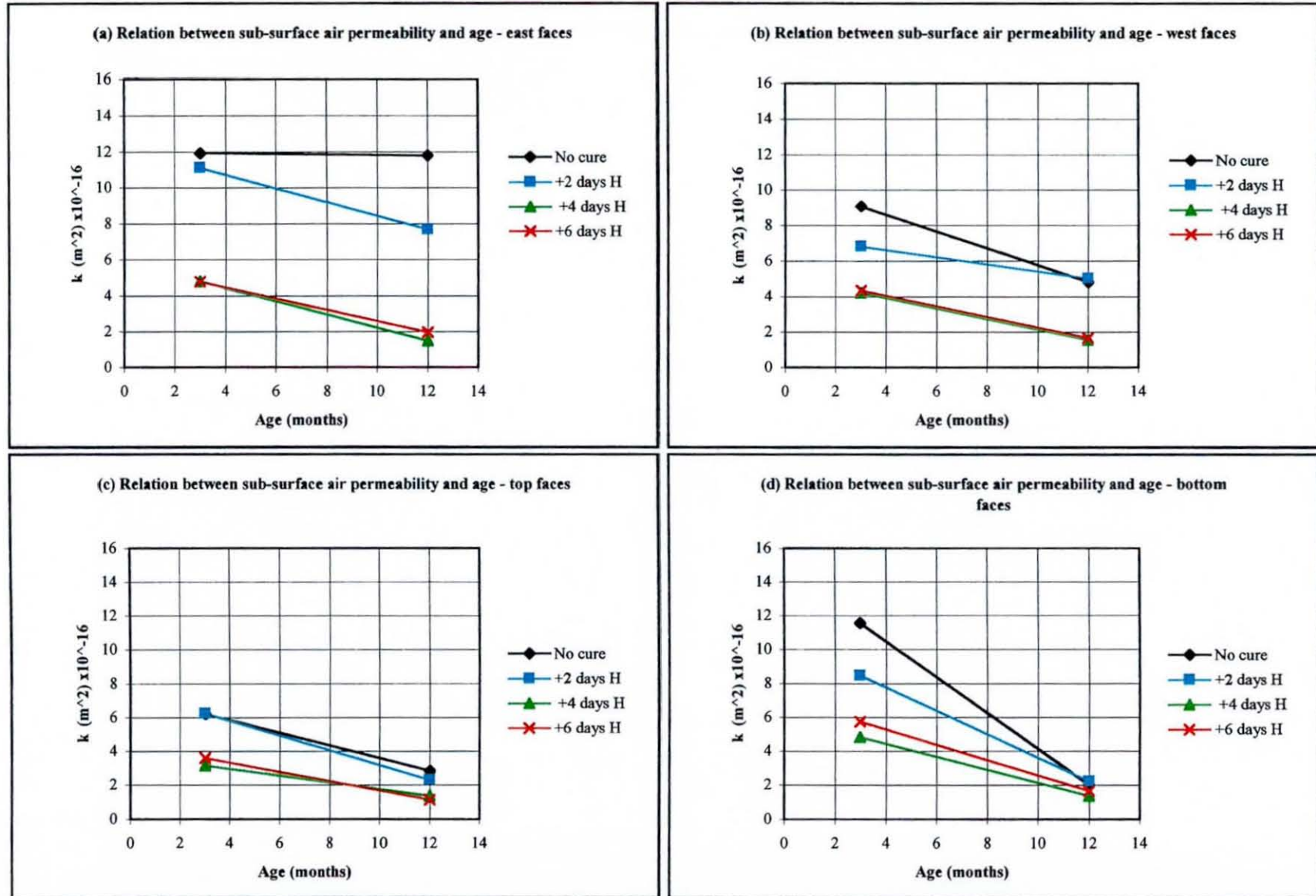
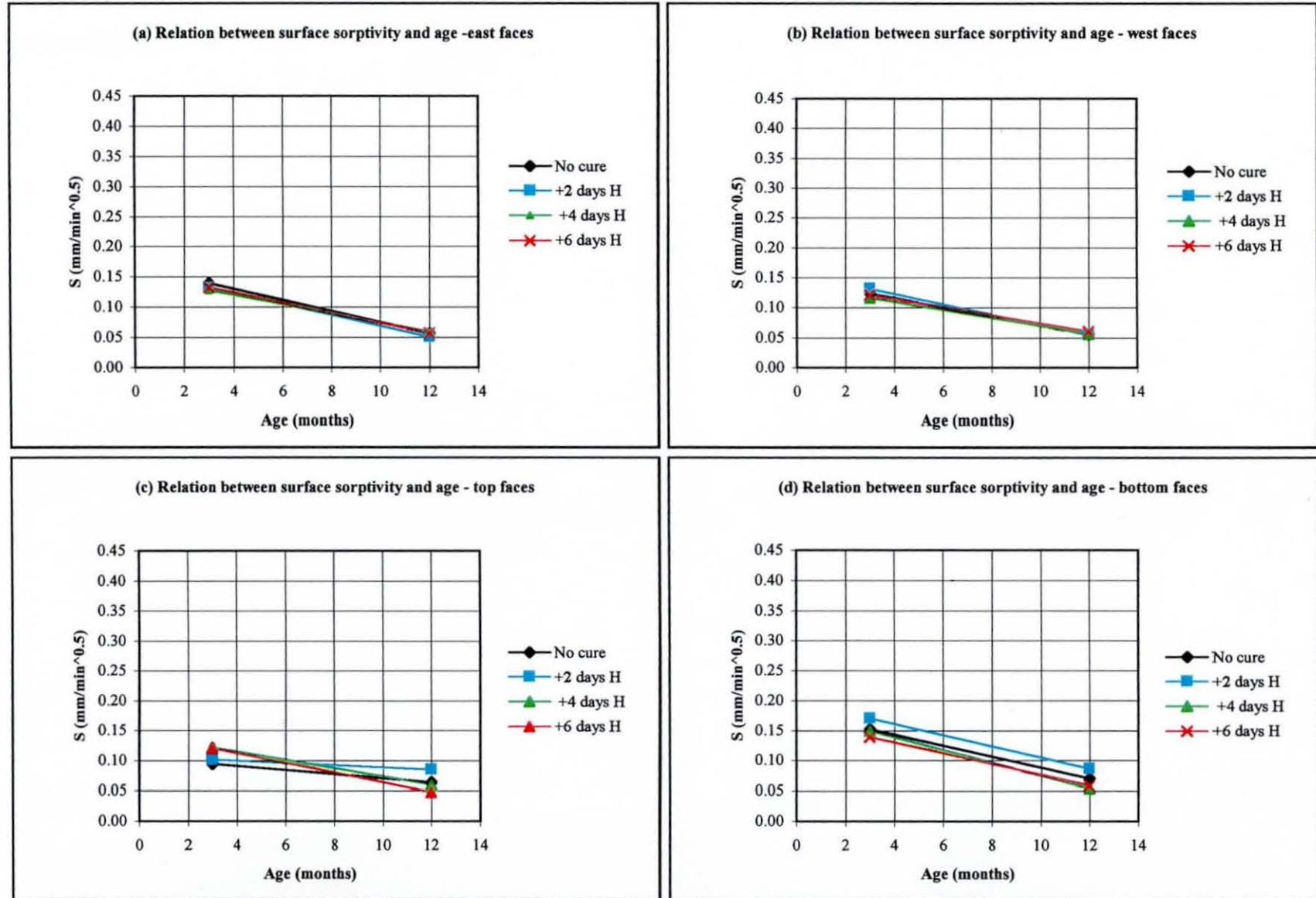


Fig. B1.4 Relationship between sub-surface air permeability and age of the 30 MPa OPC/GGBS concrete - UK summer



**Fig. B1.5** Relationship between surface sorptivity and age of the 50 MPa OPC concrete - UK summer

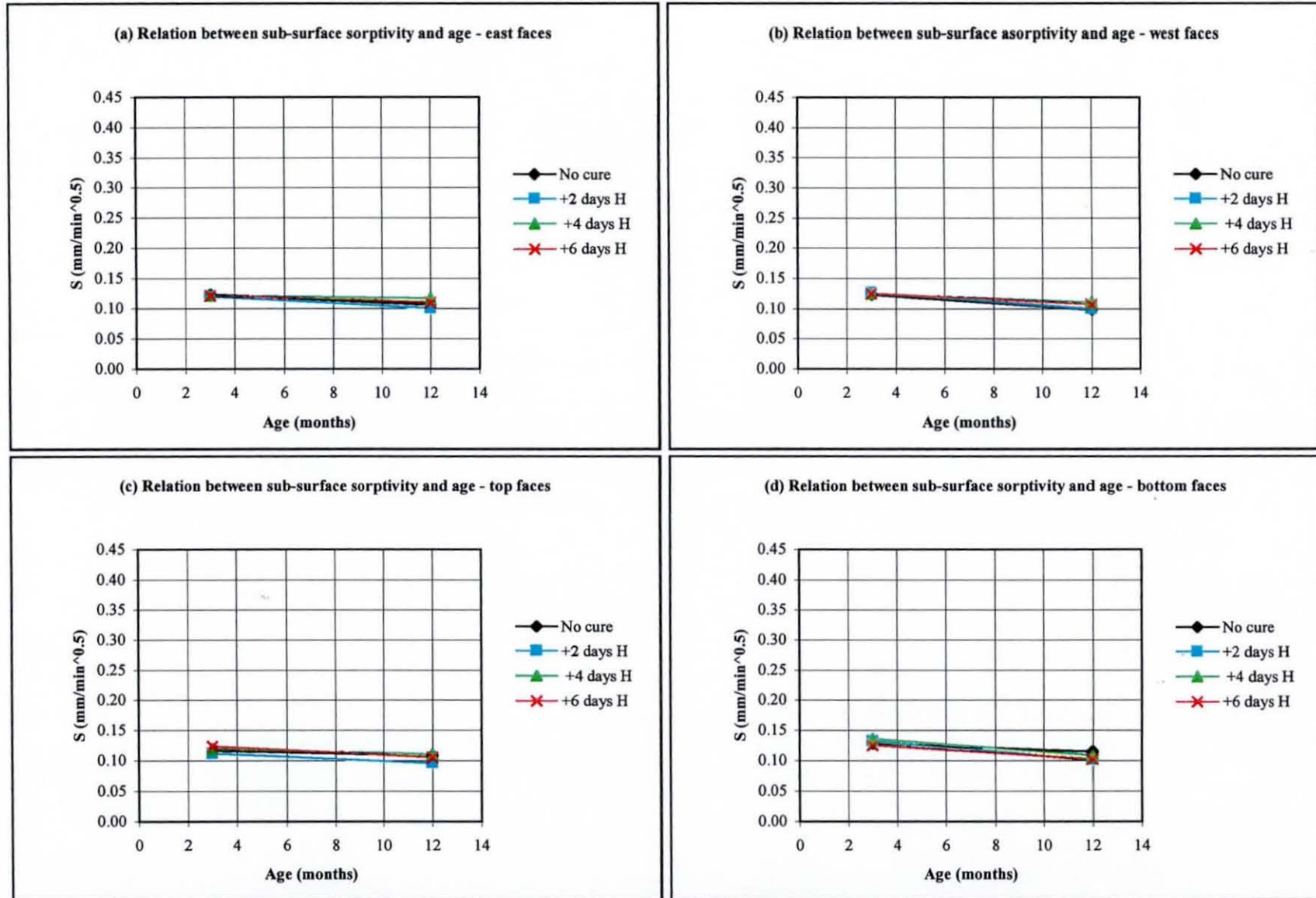


Fig. B1.6 Relationship between sub-surface sorptivity and age of the 50 MPa OPC concrete - UK summer

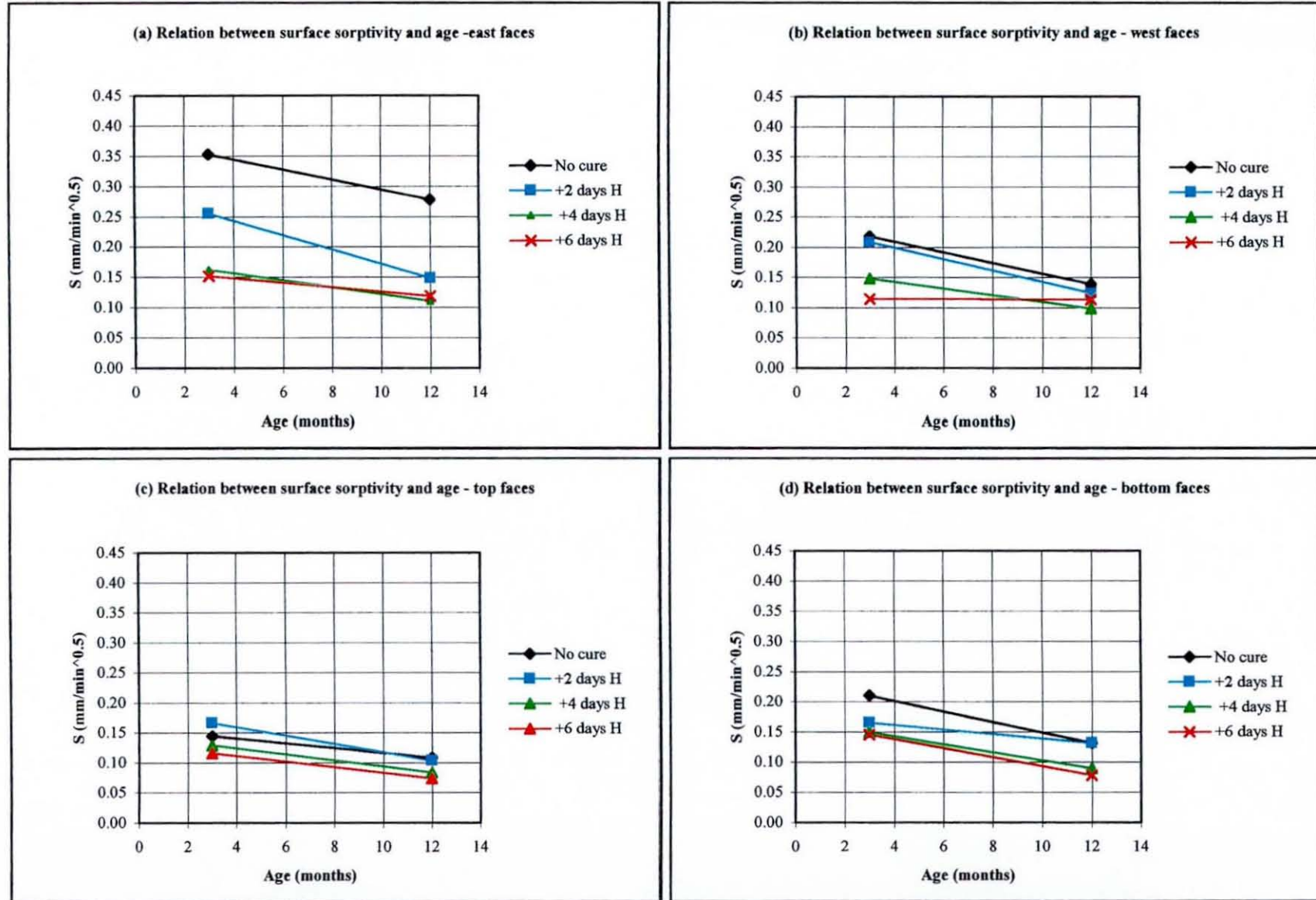


Fig. B1.7 Relationship between surface sorptivity and age of the 30 MPa OPC/GGBS concrete - UK summer

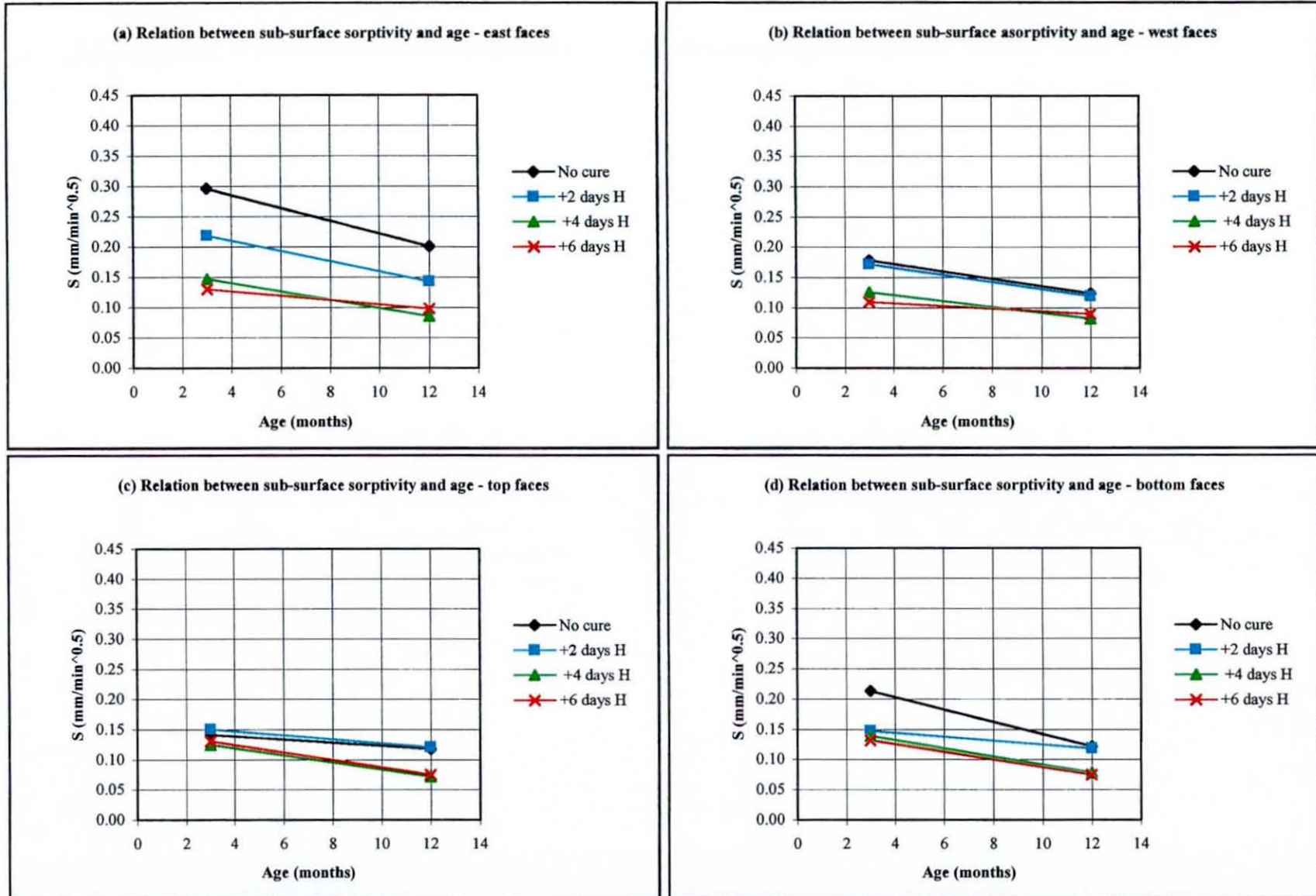
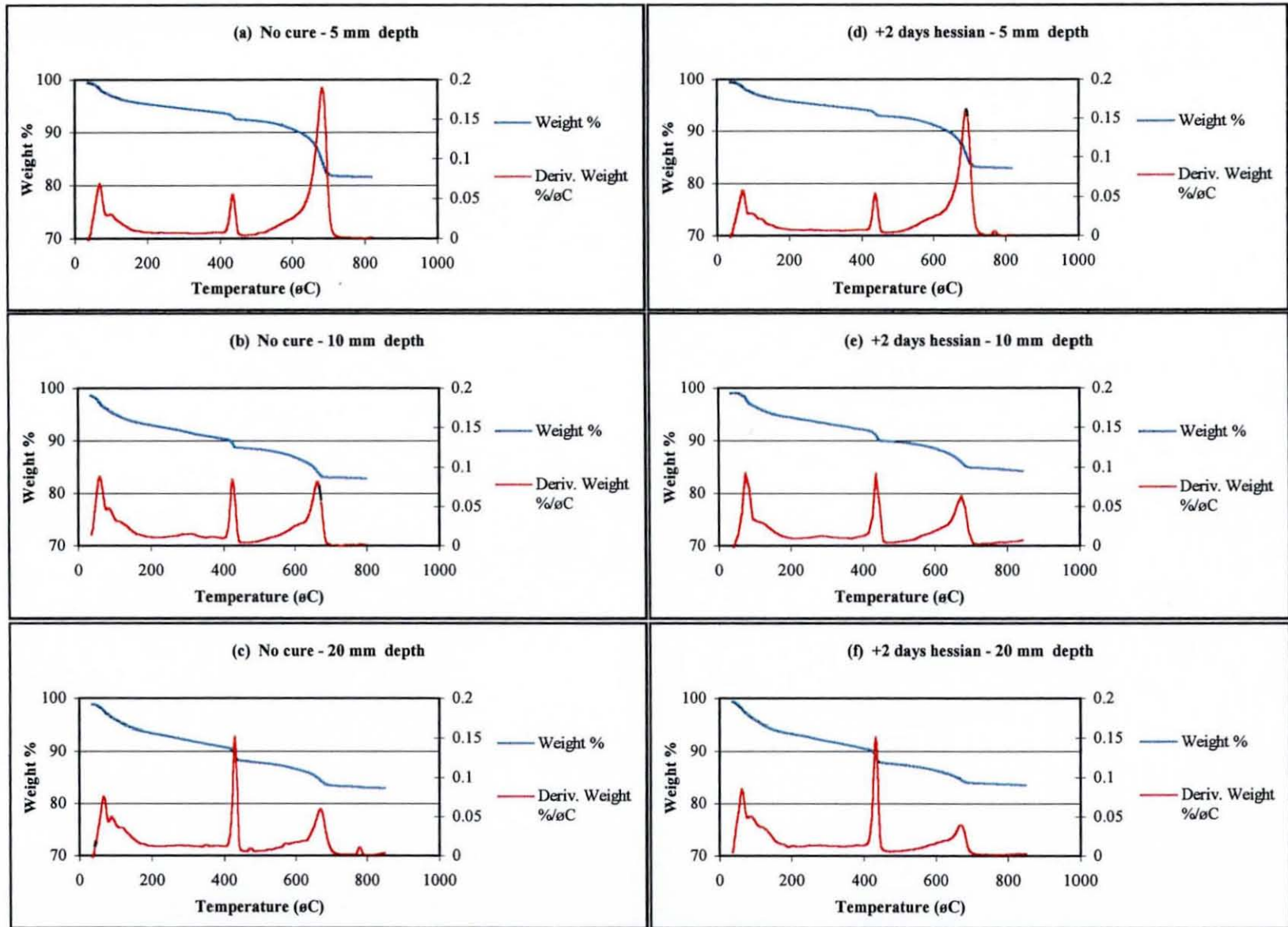


Fig. B1.8 Relationship between sub-surface sorptivity and age of the 30 MPa OPC/GGBS concrete - UK summer



**Fig. B1.9** TG and DTG curves of 30 MPa OPC mortar samples at various depths from exposed surface - 12 months summer series

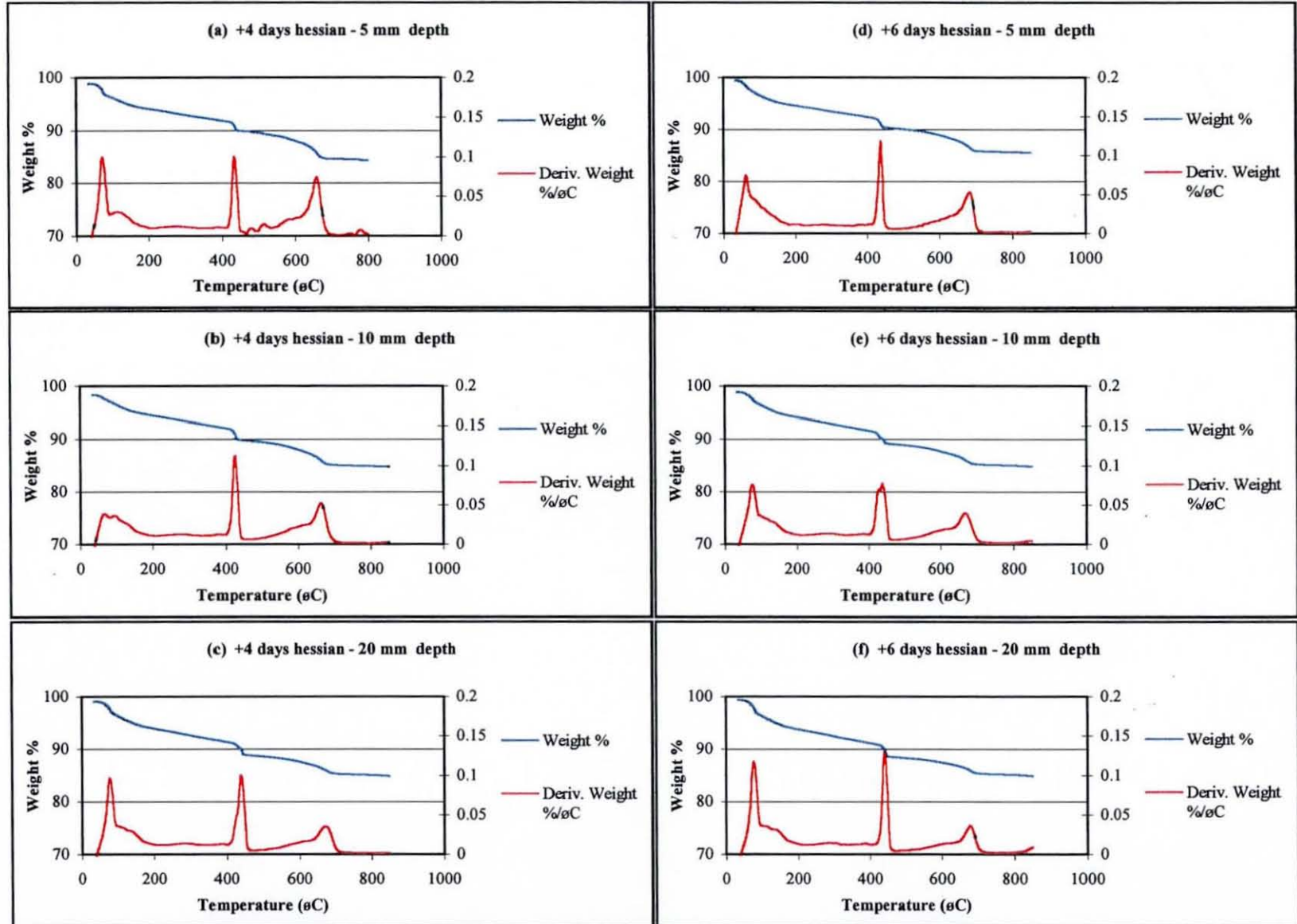


Fig. B1.10 TG and DTG curves of 30 MPa OPC mortar samples at various depths from exposed surface - 12 months summer series

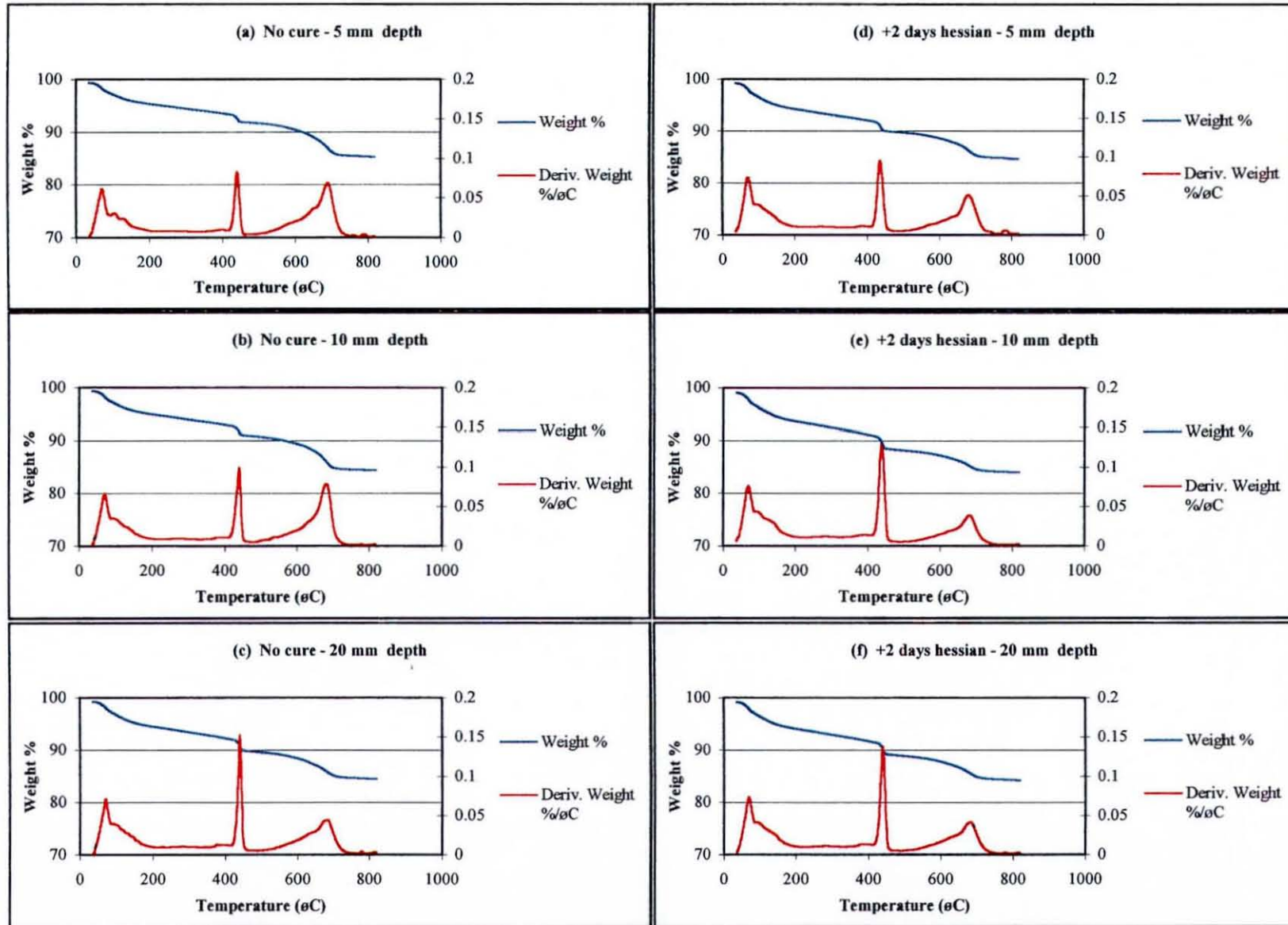


Fig. B1.11 TG and DTG curves of 50 MPa OPC mortar samples at various depths from exposed surface - 12 months summer series

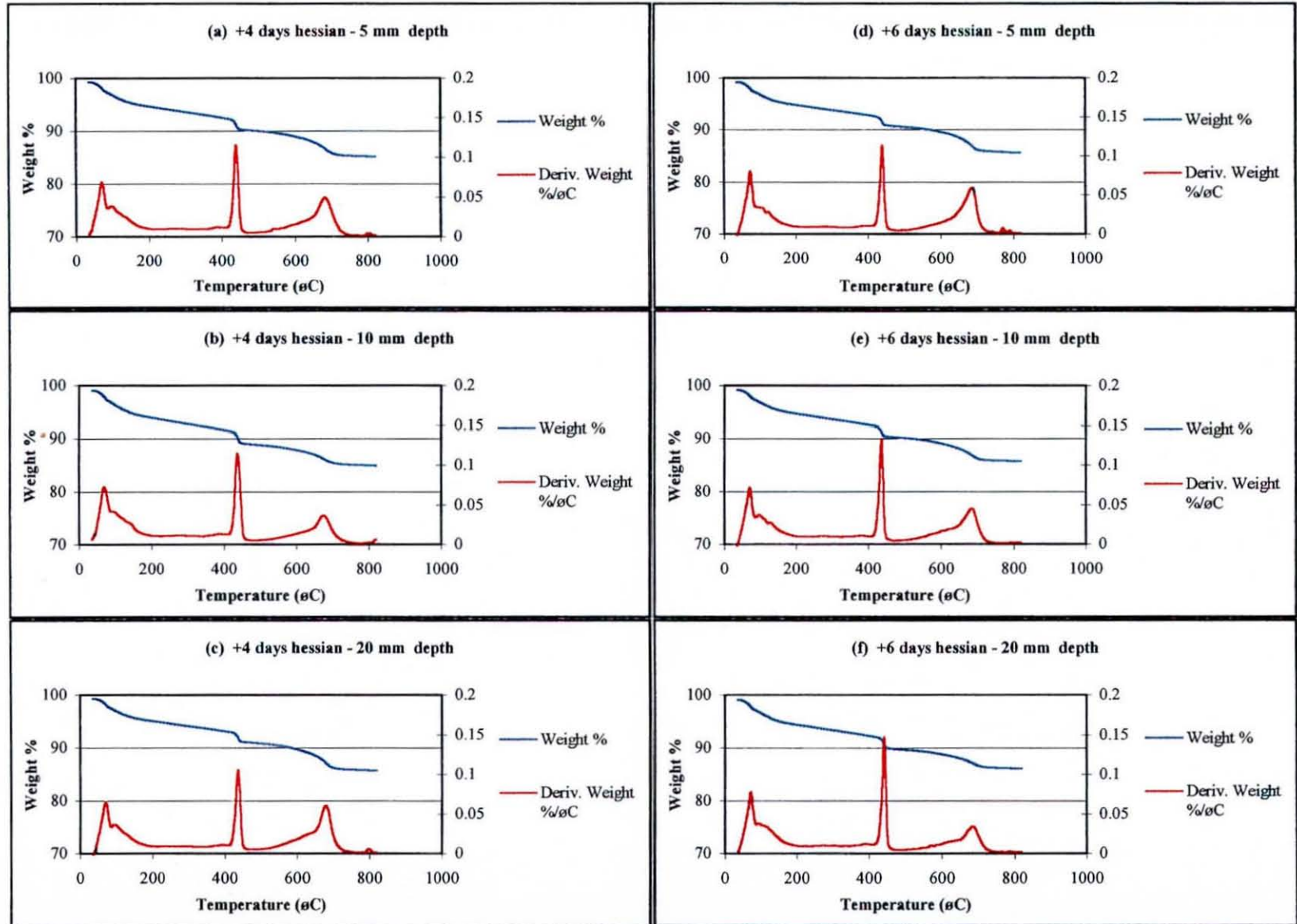


Fig. B1.12 TG and DTG curves of 50 MPa OPC mortar samples at various depths from exposed surface - 12 months summer series

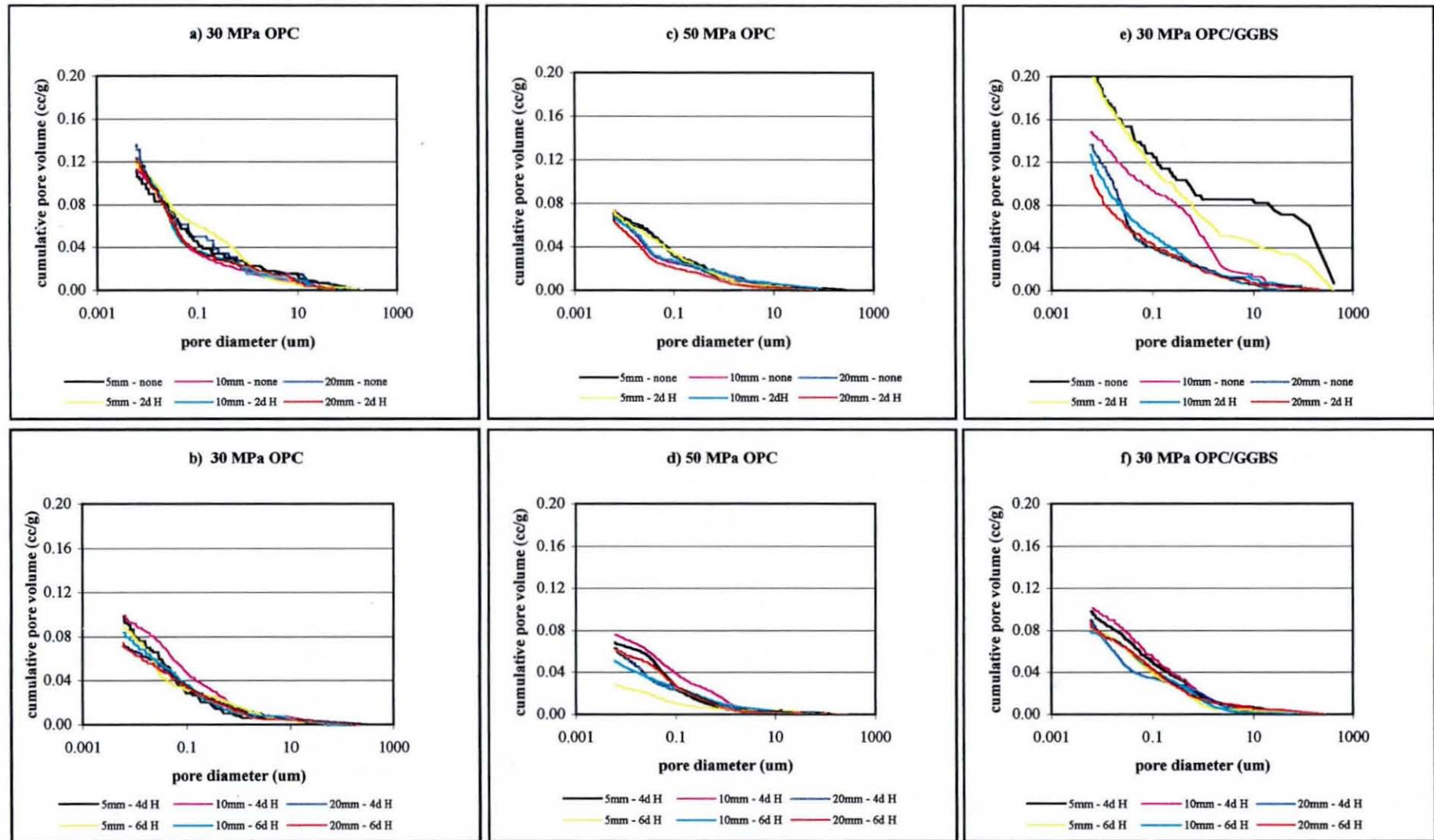


Fig. B1.13 Effect of curing and depth on the cumulative pore volume of the mortar samples - 12 months summer series

**Table B1.1 (a)** Coefficient of air permeability  $k$  ( $m^2 \times 10^{-16}$ ) for the 30 MPa OPC concrete (east/west) - 3 months summer series

Orientation	Curnig regime		Average depth from outer surface (mm)					Surface (10mm)	Sub-surface (20-50mm)
			10	20	30	40	50		
East	No Cure	Cores 1	14.18	6.76	6.74	4.71	4.37	14.18	5.65
		Cores 2	12.28	6.86	6.29	4.75	3.97	12.28	5.47
		Average	<b>13.23</b>	<b>6.81</b>	<b>6.52</b>	<b>4.73</b>	<b>4.17</b>	<b>13.23</b>	<b>5.56</b>
		C of V (%)	7.2	0.7	3.5	0.4	4.8	7.2	1.6
	+2 days H	Cores 1	11.26	6.23	5.60	5.85	9.10	11.26	6.69
		Cores 2	11.43	6.40	4.88	4.67	7.52	11.43	5.87
		Average	<b>11.34</b>	<b>6.32</b>	<b>5.24</b>	<b>5.26</b>	<b>8.31</b>	<b>11.34</b>	<b>6.28</b>
		C of V (%)	0.7	1.3	7.4	12.6	10.5	0.7	6.6
	+4 days H	Cores 1	9.45	3.56	5.38	2.82	3.90	9.45	3.91
		Cores 2	8.67	4.96	3.85	2.47	1.99	8.67	3.32
		Average	<b>9.06</b>	<b>4.26</b>	<b>4.61</b>	<b>2.65</b>	<b>2.95</b>	<b>9.06</b>	<b>3.62</b>
		C of V (%)	4.3	16.5	16.6	6.6	32.3	4.3	8.2
	+6 days H	Cores 1	6.64	3.19	2.32	2.79	2.22	6.64	2.63
		Cores 2	6.03	3.45	2.39	2.94	1.79	6.03	2.64
		Average	<b>6.33</b>	<b>3.32</b>	<b>2.36</b>	<b>2.86</b>	<b>2.01</b>	<b>6.33</b>	<b>2.64</b>
		C of V (%)	4.8	3.9	1.6	2.5	10.8	4.8	0.2
West	No Cure	Cores 1	6.12	3.25	3.23	2.66	3.34	6.12	3.12
		Cores 2	7.55	3.46	3.17	2.89	2.76	7.55	3.07
		Average	<b>6.83</b>	<b>3.36</b>	<b>3.20</b>	<b>2.78</b>	<b>3.05</b>	<b>6.83</b>	<b>3.10</b>
		C of V (%)	10.5	3.2	1.0	4.2	9.5	10.5	0.8
	+2 days H	Cores 1	7.51	3.57	4.01	4.27	3.85	7.51	3.93
		Cores 2	6.91	4.97	3.99	3.96	3.53	6.91	4.11
		Average	<b>7.21</b>	<b>4.27</b>	<b>4.00</b>	<b>4.12</b>	<b>3.69</b>	<b>7.21</b>	<b>4.02</b>
		C of V (%)	4.2	16.4	0.3	3.7	4.4	4.2	2.3
	+4 days H	Cores 1	7.26	3.43	2.23	3.50	3.46	7.26	3.15
		Cores 2	6.13	4.40	2.49	2.35	1.81	6.13	2.76
		Average	<b>6.69</b>	<b>3.91</b>	<b>2.36</b>	<b>2.92</b>	<b>2.64</b>	<b>6.69</b>	<b>2.96</b>
		C of V (%)	8.4	12.4	5.4	19.7	31.2	8.4	6.7
	+6 days H	Cores 1	4.12	2.35	2.74	2.97	3.22	4.12	2.82
		Cores 2	5.85	3.49	2.21	1.79	2.31	5.85	2.45
		Average	<b>4.99</b>	<b>2.92</b>	<b>2.47</b>	<b>2.38</b>	<b>2.76</b>	<b>4.99</b>	<b>2.63</b>
		C of V (%)	17.4	19.5	10.8	24.8	16.5	17.4	7.1

Key: +X days H= X days hessian plus 1 day in mould; Average= average of cores 1 and 2; C of V= coefficient of variation (%); Sub-surface (20-50mm)= average k value from 20 to 50mm from surface; Bold value= plotted value (usually average)

Table B1.1 (b) Coefficient of air permeability  $k$  ( $m^2 \times 10^{-16}$ ) for the 30 MPa OPC concrete (top/bottom) - 3 months summer series

Orientation	Curing regime		Average depth from outer surface (mm)					Surface (10mm)	Sub-surface (20-50mm)
			10	20	30	40	50		
Top	No Cure	Cores 1	4.79	1.92	2.80	2.81	3.87	4.79	2.85
		Cores 2	4.23	1.85	2.92	2.78	3.56	4.23	2.78
		Average	<b>4.51</b>	<b>1.88</b>	<b>2.86</b>	<b>2.79</b>	<b>3.71</b>	<b>4.51</b>	<b>2.81</b>
		C of V (%)	6.2	2.0	2.2	0.4	4.2	6.2	1.2
	+2 days H	Cores 1	3.49	1.51	2.27	1.81	2.26	3.49	1.96
		Cores 2	2.98	2.01	2.26	1.81	1.75	2.98	1.96
		Average	<b>3.24</b>	<b>1.76</b>	<b>2.26</b>	<b>1.81</b>	<b>2.00</b>	<b>3.24</b>	<b>1.96</b>
		C of V (%)	7.9	12.5	0.3	0.0	14.4	7.9	0.1
	+4 days H	Cores 1	3.38	2.46	2.28	2.16	2.67	3.38	2.39
		Cores 2	4.20	2.78	2.69	2.88	1.81	4.20	2.54
		Average	<b>3.79</b>	<b>2.62</b>	<b>2.48</b>	<b>2.52</b>	<b>2.24</b>	<b>3.79</b>	<b>2.47</b>
		C of V (%)	10.8	6.1	8.2	14.4	19.1	10.8	3.0
	+6 days H	Cores 1	3.29	2.19	2.65	2.12	2.62	3.29	2.39
		Cores 2	3.83	2.65	2.85	2.14	2.79	3.83	2.61
		Average	<b>3.56</b>	<b>2.42</b>	<b>2.75</b>	<b>2.13</b>	<b>2.70</b>	<b>3.56</b>	<b>2.50</b>
		C of V (%)	7.6	9.5	3.6	0.4	3.3	7.6	4.3
Bottom	No Cure	Cores 1	10.06	5.93	3.18	5.97	2.64	10.06	4.43
		Cores 2	15.06	6.65	3.83	4.57	2.51	15.06	4.39
		Average	<b>12.56</b>	<b>6.29</b>	<b>3.50</b>	<b>5.27</b>	<b>2.58</b>	<b>12.56</b>	<b>4.41</b>
		C of V (%)	19.9	5.7	9.2	13.3	2.4	19.9	0.4
	+2 days H	Cores 1	10.54	1.51	2.33	2.93	3.11	10.54	2.47
		Cores 2	11.39	8.10	4.58	3.47	3.06	11.39	4.81
		Average	<b>10.97</b>	<b>4.81</b>	<b>3.46</b>	<b>3.20</b>	<b>3.09</b>	<b>10.97</b>	<b>3.64</b>
		C of V (%)	3.8	68.6	32.5	8.5	0.8	3.8	32.1
	+4 days H	Cores 1	12.95	4.87	4.31	3.34	2.62	12.95	3.79
		Cores 2	8.63	5.13	3.55	3.16	3.41	8.63	3.82
		Average	<b>10.79</b>	<b>5.00</b>	<b>3.93</b>	<b>3.25</b>	<b>3.02</b>	<b>10.79</b>	<b>3.80</b>
		C of V (%)	20.0	2.7	9.7	2.8	13.1	20.0	0.4
	+6 days H	Cores 1	8.64	5.16	5.34	3.45	3.27	8.64	4.31
		Cores 2	9.20	5.54	4.14	3.14	2.70	9.20	3.88
		Average	<b>8.92</b>	<b>5.35</b>	<b>4.74</b>	<b>3.29</b>	<b>2.98</b>	<b>8.92</b>	<b>4.09</b>
		C of V (%)	3.2	3.5	12.6	4.7	9.5	3.2	5.2

Key: +X days H= X days hessian plus 1 day in mould; Average= average of cores 1 and 2; C of V= coefficient of variation (%); Sub-surface (20-50mm)= average k value from 20 to 50mm from surface; Bold value= plotted value (usually average)

Table B1.2 (a). Coefficient of air permeability k (m<sup>2</sup> x 10<sup>-16</sup>) for the 30 MPa OPC concrete (east/west) - 12 months summer series

Orientation	Curnig regime		Average depth from outer surface (mm)					Surface (10mm)	Sub-surface (20-40mm)
			5	10	20	30	40		
East	No Cure	Cores 1	4.05	4.26	4.76	4.35	3.74	4.26	4.28
		Cores 2	1.92	7.15	5.24	12.83	3.93	7.15	7.33
		Average	<b>2.98</b>	<b>5.70</b>	<b>5.00</b>	<b>8.59</b>	<b>3.84</b>	<b>5.70</b>	<b>5.81</b>
		C of V (%)	35.6	25.3	4.7	49.4	2.5	25.3	26.2
	+2 days H	Cores 1	6.06	5.26	10.15	3.62	5.82	5.26	6.53
		Cores 2	5.49	6.01	4.66	12.68	5.11	6.01	7.12
		Average	<b>5.78</b>	<b>5.63</b>	<b>7.41</b>	<b>8.15</b>	<b>5.46</b>	<b>5.63</b>	<b>6.82</b>
		C of V (%)	5.0	6.3	58.9	35.7	6.9	6.3	4.3
	+4 days H	Cores 1	2.66	2.64	2.47	3.06	1.95	2.64	2.50
		Cores 2	6.06	3.15	4.11	2.49	4.03	3.15	3.54
		Average	<b>4.36</b>	<b>2.90</b>	<b>3.29</b>	<b>2.78</b>	<b>2.99</b>	<b>2.90</b>	<b>3.02</b>
		C of V (%)	39.0	8.8	24.9	10.3	34.7	8.8	17.3
	+6 days H	Cores 1	2.50	3.85	4.07	3.70	2.87	3.85	3.55
		Cores 2	3.77	3.07	3.34	2.02	1.67	3.07	2.34
		Average	<b>3.14</b>	<b>3.46</b>	<b>3.71</b>	<b>2.86</b>	<b>2.27</b>	<b>3.46</b>	<b>2.95</b>
		C of V (%)	20.2	11.2	9.9	29.4	26.3	11.2	20.4
West	No Cure	Cores 1	1.51	1.69	3.38	3.48	3.32	1.69	3.40
		Cores 2	1.04	2.59	2.46	3.28	2.81	2.59	2.85
		Average	<b>1.28</b>	<b>2.14</b>	<b>2.92</b>	<b>3.38</b>	<b>3.07</b>	<b>2.14</b>	<b>3.12</b>
		C of V (%)	18.6	21.0	15.8	3.0	8.4	21.0	8.8
	+2 days H	Cores 1	2.37	2.04	3.49	4.58	5.88	2.04	4.65
		Cores 2	2.37	3.35	4.63	5.21	4.52	3.35	4.79
		Average	<b>2.37</b>	<b>2.70</b>	<b>4.06</b>	<b>4.90</b>	<b>5.20</b>	<b>2.70</b>	<b>4.72</b>
		C of V (%)	0.0	24.3	14.0	6.5	13.1	24.3	1.5
	+4 days H	Cores 1	1.37	4.75	2.15	3.53	2.01	4.75	2.57
		Cores 2	1.51	1.87	1.83	1.72	2.81	1.87	2.12
		Average	<b>1.44</b>	<b>3.31</b>	<b>1.99</b>	<b>2.63</b>	<b>2.41</b>	<b>3.31</b>	<b>2.34</b>
		C of V (%)	4.8	43.6	8.2	34.5	16.6	43.6	9.5
	+6 days H	Cores 1	2.43	3.45	2.25	1.92	2.07	3.45	2.08
		Cores 2	6.30	3.61	3.42	2.48	2.57	3.61	2.83
		Average	<b>4.37</b>	<b>3.53</b>	<b>2.83</b>	<b>2.20</b>	<b>2.32</b>	<b>3.53</b>	<b>2.72</b>
		C of V (%)	44.3	2.3	20.7	12.7	10.9	2.3	13.7

Key: +X days H= X days hessian plus 1 day in mould; Average= average of cores 1 and 2; C of V= coefficient of variation (%); Sub-surface (10-40mm)= average k value from 10 to 40mm from surface; Bold value= plotted value (usually average)

**Table B1.2 (b).** Coefficient of air permeability  $k$  ( $m^2 \times 10^{-16}$ ) for the 30 MPa OPC concrete (top/bottom) - 12 months summer series

Orientation	Curing regime		Average depth from outer surface (mm)					Surface (10mm)	Sub-surface (20-40mm)
			5	10	20	30	40		
Top	No Cure	Cores 1	1.32	2.14	1.49	1.89	2.00	2.14	1.79
		Cores 2	1.24	1.83	2.11	3.15	2.26	1.83	2.51
		Average	<b>1.28</b>	<b>1.98</b>	<b>1.80</b>	<b>2.52</b>	<b>2.13</b>	<b>1.98</b>	<b>2.15</b>
		C of V (%)	3.3	7.7	17.1	25.0	6.2	7.7	16.6
	+2 days H	Cores 1	1.22	1.50	1.56	2.74	2.06	1.50	2.12
		Cores 2	1.18	1.31	1.86	1.40	1.84	1.31	1.70
		Average	<b>1.20</b>	<b>1.40</b>	<b>1.71</b>	<b>2.07</b>	<b>1.95</b>	<b>1.40</b>	<b>1.91</b>
		C of V (%)	1.5	6.9	7.9	47.5	6.0	6.9	11.0
	+4 days H	Cores 1	1.77	1.25	1.33	1.21	1.36	1.25	1.30
		Cores 2	1.44	1.11	1.25	1.31	1.11	1.11	1.22
		Average	<b>1.60</b>	<b>1.18</b>	<b>1.29</b>	<b>1.26</b>	<b>1.24</b>	<b>1.18</b>	<b>1.26</b>
		C of V (%)	10.3	5.8	3.3	4.1	10.3	5.8	3.1
	+6 days H	Cores 1	2.76	1.16	1.38	0.89	1.22	1.16	1.16
		Cores 2	1.13	1.14	1.19	1.09	0.71	1.14	1.00
		Average	<b>1.95</b>	<b>1.15</b>	<b>1.28</b>	<b>0.99</b>	<b>0.97</b>	<b>1.15</b>	<b>1.08</b>
		C of V (%)	41.7	0.7	7.4	10.0	26.3	0.7	7.7
Bottom	No Cure	Cores 1	2.01	2.21	2.28	2.23	2.08	2.21	2.20
		Cores 2	2.57	3.14	2.84	1.68	2.49	3.14	2.33
		Average	<b>2.29</b>	<b>2.68</b>	<b>2.56</b>	<b>1.95</b>	<b>2.28</b>	<b>2.68</b>	<b>2.27</b>
		C of V (%)	12.3	17.2	10.8	14.1	9.0	17.2	3.0
	+2 days H	Cores 1	2.92	3.11	1.38	2.14	1.82	3.11	1.78
		Cores 2	2.12	2.00	1.21	2.57	2.18	2.00	1.99
		Average	<b>2.52</b>	<b>2.56</b>	<b>1.30</b>	<b>2.36</b>	<b>2.00</b>	<b>2.56</b>	<b>1.88</b>
		C of V (%)	15.9	21.8	6.7	9.2	9.1	21.8	5.5
	+4 days H	Cores 1	1.97	2.97	1.59	1.38	1.37	2.97	1.45
		Cores 2	2.79	3.15	2.36	1.61	1.80	3.15	1.92
		Average	<b>2.38</b>	<b>3.06</b>	<b>1.98</b>	<b>1.50</b>	<b>1.58</b>	<b>3.06</b>	<b>1.69</b>
		C of V (%)	17.3	2.9	19.3	7.9	13.6	2.9	14.1
	+6 days H	Cores 1	5.13	2.88	3.08	2.12	1.88	2.88	2.36
		Cores 2	5.13	3.80	2.31	2.23	1.16	3.80	1.90
		Average	<b>5.13</b>	<b>3.34</b>	<b>2.69</b>	<b>2.18</b>	<b>1.52</b>	<b>3.34</b>	<b>2.13</b>
		C of V (%)	0.0	13.8	14.2	2.7	23.8	13.8	10.7

Key: +X days H= X days hessian plus 1 day in mould; Average= average of cores 1 and 2; C of V= coefficient of variation (%); Sub-surface (10-40mm)= average  $k$  value from 10 to 40mm from surface; Bold value= plotted value (usually average)

Table B1.3 (a). Coefficient of air permeability k (m<sup>2</sup> x 10<sup>-16</sup>) for the 50 MPa OPC concrete (east/west) - 3 months summer series

Orientation	Curnig regime		Average depth from outer surface (mm)					Surface (10mm)	Sub-surface (20-50mm)
			10	20	30	40	50		
East	No Cure	Cores 1	1.59	1.62	0.81	0.92	0.50	1.59	0.96
		Cores 2	1.39	1.17	0.95	0.90	0.70	1.39	0.93
		Average	<b>1.49</b>	<b>1.39</b>	<b>0.88</b>	<b>0.91</b>	<b>0.60</b>	<b>1.49</b>	<b>0.95</b>
		C of V (%)	6.8	16.2	7.9	1.3	16.3	6.8	1.8
	+2 days H	Cores 1	1.87	0.86	0.76	0.65	0.67	1.87	0.74
		Cores 2	1.34	1.16	0.73	0.70	0.64	1.34	0.81
		Average	<b>1.61</b>	<b>1.01</b>	<b>0.75</b>	<b>0.68</b>	<b>0.65</b>	<b>1.61</b>	<b>0.77</b>
		C of V (%)	16.4	13.0	2.6	3.0	2.8	16.4	4.4
	+4 days H	Cores 1	1.66	1.20	1.00	0.96	0.87	1.66	1.01
		Cores 2	1.80	1.26	0.91	0.90	0.79	1.80	0.96
		Average	<b>1.73</b>	<b>1.23</b>	<b>0.95</b>	<b>0.93</b>	<b>0.83</b>	<b>1.73</b>	<b>0.99</b>
		C of V (%)	4.1	2.6	4.9	3.1	4.8	4.1	2.1
	+6 days H	Cores 1	1.10	0.88	0.64	0.65	0.72	1.10	0.72
		Cores 2	1.06	1.00	0.85	0.69	0.70	1.06	0.81
		Average	<b>1.08</b>	<b>0.94</b>	<b>0.75</b>	<b>0.67</b>	<b>0.71</b>	<b>1.08</b>	<b>0.77</b>
		C of V (%)	2.1	6.3	14.3	3.2	1.0	2.1	5.9
West	No Cure	Cores 1	1.25	0.72	0.86	0.68	0.71	1.25	0.74
		Cores 2	1.39	0.86	0.90	0.70	0.78	1.39	0.81
		Average	<b>1.32</b>	<b>0.79</b>	<b>0.88</b>	<b>0.69</b>	<b>0.74</b>	<b>1.32</b>	<b>0.78</b>
		C of V (%)	5.3	9.1	2.1	1.7	4.3	5.3	4.3
	+2 days H	Cores 1	0.79	0.73	0.67	0.66	0.64	0.79	0.68
		Cores 2	1.00	0.79	0.99	0.87	0.73	1.00	0.84
		Average	<b>0.90</b>	<b>0.76</b>	<b>0.83</b>	<b>0.77</b>	<b>0.68</b>	<b>0.90</b>	<b>0.76</b>
		C of V (%)	11.7	3.8	19.0	13.6	6.2	11.7	11.0
	+4 days H	Cores 1	0.88	0.99	1.00	0.87	0.84	0.88	0.93
		Cores 2	1.03	0.93	0.87	0.89	0.77	1.03	0.87
		Average	<b>0.95</b>	<b>0.96</b>	<b>0.94</b>	<b>0.88</b>	<b>0.81</b>	<b>0.95</b>	<b>0.90</b>
		C of V (%)	7.5	3.1	6.7	0.7	4.2	7.5	3.3
	+6 days H	Cores 1	0.62	0.74	0.61	0.71	0.53	0.62	0.65
		Cores 2	0.90	0.88	0.66	0.69	0.47	0.90	0.68
		Average	<b>0.76</b>	<b>0.81</b>	<b>0.63</b>	<b>0.70</b>	<b>0.50</b>	<b>0.76</b>	<b>0.66</b>
		C of V (%)	18.1	8.9	4.1	0.8	6.2	18.1	2.3

Key: +X days H= X days hessian plus 1 day in mould; Average= average of cores 1 and 2; C of V= coefficient of variation (%); Sub-surface (20-50mm)= average k value from 20 to 50mm from surface; Bold value= plotted value (usually average)

Table B1.3 (b). Coefficient of air permeability k (m<sup>2</sup> x 10<sup>-16</sup>) for the 50 MPa OPC concrete (top/bottom) - 3 months summer series

Orientation	Curing regime	Average depth from outer surface (mm)					Surface (10mm)	Sub-surface (20-50mm)	
		10	20	30	40	50			
Top	No Cure	Cores 1	0.70	0.67	0.63	0.82	0.74	0.70	0.72
		Cores 2	0.63	0.50	0.55	0.43	0.36	0.63	0.46
		Average	<b>0.67</b>	<b>0.59</b>	<b>0.59</b>	<b>0.62</b>	<b>0.55</b>	<b>0.67</b>	<b>0.59</b>
		C of V (%)	4.8	14.9	6.4	31.7	34.9	4.8	21.9
	+2 days H	Cores 1	0.68	0.68	0.70	0.62	0.58	0.68	0.64
		Cores 2	0.69	0.69	0.62	0.51	0.47	0.69	0.57
		Average	<b>0.68</b>	<b>0.69</b>	<b>0.66</b>	<b>0.56</b>	<b>0.52</b>	<b>0.68</b>	<b>0.61</b>
		C of V (%)	1.3	0.6	6.0	11.3	11.5	1.3	5.9
	+4 days H	Cores 1	1.04	1.03	1.08	1.14	0.95	1.04	1.05
		Cores 2	0.77	0.92	0.88	0.92	0.70	0.77	0.86
		Average	<b>0.91</b>	<b>0.97</b>	<b>0.98</b>	<b>1.03</b>	<b>0.82</b>	<b>0.91</b>	<b>0.95</b>
		C of V (%)	14.4	5.7	9.9	10.5	15.0	14.4	10.1
	+6 days H	Cores 1	1.05	1.20	0.93	1.18	0.92	1.05	1.06
		Cores 2	0.93	1.24	0.73	0.91	0.63	0.93	0.88
		Average	<b>0.99</b>	<b>1.22</b>	<b>0.83</b>	<b>1.04</b>	<b>0.78</b>	<b>0.99</b>	<b>0.97</b>
		C of V (%)	6.0	1.7	12.1	12.6	18.6	6.0	9.2
Bottom	No Cure	Cores 1	1.69	1.40	1.26	1.05	0.91	1.69	1.15
		Cores 2	1.06	0.83	0.66	0.68	0.56	1.06	0.68
		Average	<b>1.38</b>	<b>1.11</b>	<b>0.96</b>	<b>0.86</b>	<b>0.74</b>	<b>1.38</b>	<b>0.92</b>
		C of V (%)	22.7	25.6	30.8	21.3	23.7	22.7	25.6
	+2 days H	Cores 1	1.59	0.90	1.05	0.64	0.67	1.59	0.81
		Cores 2	1.39	1.06	0.87	0.58	0.51	1.39	0.75
		Average	<b>1.49</b>	<b>0.98</b>	<b>0.96</b>	<b>0.61</b>	<b>0.59</b>	<b>1.49</b>	<b>0.78</b>
		C of V (%)	6.6	8.1	9.5	5.6	13.2	6.6	3.9
	+4 days H	Cores 1	1.43	1.40	1.07	0.94	0.72	1.43	1.03
		Cores 2	1.11	0.93	0.84	0.76	0.68	1.11	0.81
		Average	<b>1.27</b>	<b>1.16</b>	<b>0.96</b>	<b>0.85</b>	<b>0.70</b>	<b>1.27</b>	<b>0.92</b>
		C of V (%)	12.8	20.2	11.9	10.5	2.3	12.8	12.4
	+6 days H	Cores 1	1.48	1.04	0.75	0.94	0.74	1.48	0.87
		Cores 2	1.26	0.84	0.66	0.63	0.74	1.26	0.72
		Average	<b>1.37</b>	<b>0.94</b>	<b>0.70</b>	<b>0.79</b>	<b>0.74</b>	<b>1.37</b>	<b>0.79</b>
		C of V (%)	8.0	10.8	6.8	19.5	0.6	8.0	9.4

Key: +X days H= X days hessian plus 1 day in mould; Average= average of cores 1 and 2; C of V= coefficient of variation (%); Sub-surface (20-50mm)= average k value from 20 to 50mm from surface; Bold value= plotted value (usually average)

Table B1.4 (a). Coefficient of air permeability k (m<sup>2</sup> x 10<sup>-16</sup>) for the 50 MPa OPC Concrete (east/west) - 12 months summer series

Orientation	Curnig regime	Average depth from outer surface (mm)					Surface (10mm)	Sub-surface (20-40mm)	
		5	10	20	30	40			
East	No Cure	Cores 1	0.55	0.43	0.39	0.31	0.44	0.43	0.38
		Cores 2	0.82	0.37	0.39	0.41	0.38	0.37	0.39
		Average	<b>0.69</b>	<b>0.40</b>	<b>0.39</b>	<b>0.36</b>	<b>0.41</b>	<b>0.40</b>	<b>0.39</b>
		C of V (%)	19.2	7.1	0.4	14.3	6.9	7.1	1.9
	+2 days H	Cores 1	0.30	0.27	0.25	0.35	0.35	0.27	0.32
		Cores 2	0.32	0.39	0.32	0.35	0.32	0.39	0.35
		Average	<b>0.31</b>	<b>0.33</b>	<b>0.29</b>	<b>0.35</b>	<b>0.33</b>	<b>0.33</b>	<b>0.33</b>
		C of V (%)	4.0	14.5	10.8	0.1	4.2	14.5	4.3
	+4 days H	Cores 1	0.45	0.32	0.32	0.42	0.33	0.32	0.36
		Cores 2	0.45	0.32	0.32	0.42	0.33	0.32	0.36
		Average	<b>0.45</b>	<b>0.32</b>	<b>0.32</b>	<b>0.42</b>	<b>0.33</b>	<b>0.32</b>	<b>0.36</b>
		C of V (%)	0.0	0.0	0.0	0.0	0.0	0.0	0.0
	+6 days H	Cores 1	0.34	0.35	0.33	0.36	0.31	0.35	0.34
		Cores 2	0.37	0.40	0.37	0.39	0.38	0.40	0.38
		Average	<b>0.36</b>	<b>0.37</b>	<b>0.35</b>	<b>0.37</b>	<b>0.35</b>	<b>0.37</b>	<b>0.36</b>
		C of V (%)	3.8	6.4	5.0	3.2	9.8	6.4	6.0
West	No Cure	Cores 1	0.30	0.18	0.30	0.24	0.37	0.18	0.30
		Cores 2	0.25	0.19	0.26	0.31	0.34	0.19	0.30
		Average	<b>0.28</b>	<b>0.19</b>	<b>0.28</b>	<b>0.27</b>	<b>0.36</b>	<b>0.19</b>	<b>0.30</b>
		C of V (%)	9.1	4.0	7.7	12.8	3.7	4.0	0.1
	+2 days H	Cores 1	0.25	0.28	0.30	0.33	0.33	0.28	0.32
		Cores 2	0.24	0.20	0.24	0.30	0.29	0.20	0.28
		Average	<b>0.24</b>	<b>0.24</b>	<b>0.27</b>	<b>0.32</b>	<b>0.31</b>	<b>0.24</b>	<b>0.30</b>
		C of V (%)	2.8	16.7	10.3	4.5	7.8	16.7	7.4
	+4 days H	Cores 1	0.54	0.54	0.35	0.48	0.35	0.54	0.39
		Cores 2	0.54	0.54	0.35	0.48	0.35	0.54	0.39
		Average	<b>0.54</b>	<b>0.54</b>	<b>0.35</b>	<b>0.48</b>	<b>0.35</b>	<b>0.54</b>	<b>0.39</b>
		C of V (%)	0.0	0.0	0.0	0.0	0.0	0.0	0.0
	+6 days H	Cores 1	0.29	0.30	0.35	0.30	0.34	0.30	0.33
		Cores 2	0.29	0.31	0.39	0.30	0.36	0.31	0.35
		Average	<b>0.29</b>	<b>0.30</b>	<b>0.37</b>	<b>0.30</b>	<b>0.35</b>	<b>0.30</b>	<b>0.33</b>
		C of V (%)	0.0	0.6	6.0	0.5	4.0	0.6	3.5

Key: +X days H= X days hessian plus 1 day in mould; Average= average of cores 1 and 2; C of V= coefficient of variation (%); Sub-surface (20-40mm)= average k value from 10 to 40mm from surface; Bold value= plotted value (usually average)

Table B1.4 (b). Coefficient of air permeability k (m<sup>2</sup> x 10<sup>-16</sup>) for the 50 MPa OPC Concrete (top/bottom) - 12 months summer series

Orientation	Curing regime	Average depth from outer surface (mm)					Surface (10mm)	Sub-surface (20-40mm)	
		5	10	20	30	40			
Top	No Cure	Cores 1	0.42	0.34	0.32	0.42	0.38	0.34	0.37
		Cores 2	0.55	0.31	0.24	0.28	0.27	0.31	0.27
		Average	<b>0.48</b>	<b>0.32</b>	<b>0.28</b>	<b>0.35</b>	<b>0.33</b>	<b>0.32</b>	<b>0.32</b>
		C of V (%)	13.8	4.5	14.4	19.2	16.6	4.5	16.9
	+2 days H	Cores 1	0.29	0.20	0.20	0.15	0.25	0.20	0.20
		Cores 2	0.26	0.22	0.19	0.33	0.31	0.22	0.28
		Average	<b>0.27</b>	<b>0.21</b>	<b>0.19</b>	<b>0.24</b>	<b>0.28</b>	<b>0.21</b>	<b>0.24</b>
		C of V (%)	5.4	5.0	2.9	27.7	8.9	5.0	15.9
	+4 days H	Cores 1	0.20	0.20	0.32	0.28	0.33	0.20	0.31
		Cores 2	0.18	0.19	0.38	0.28	0.32	0.19	0.33
		Average	<b>0.19</b>	<b>0.20</b>	<b>0.35</b>	<b>0.28</b>	<b>0.33</b>	<b>0.20</b>	<b>0.32</b>
		C of V (%)	6.0	3.0	7.3	1.0	1.6	3.0	2.4
	+6 days H	Cores 1	0.17	0.13	0.28	0.28	0.28	0.13	0.28
		Cores 2	0.20	0.22	0.30	0.36	0.31	0.22	0.32
		Average	<b>0.18</b>	<b>0.17</b>	<b>0.29</b>	<b>0.32</b>	<b>0.29</b>	<b>0.17</b>	<b>0.30</b>
		C of V (%)	6.9	25.7	2.1	12.9	5.1	25.7	6.9
Bottom	No Cure	Cores 1	0.43	0.39	0.34	0.33	0.36	0.39	0.35
		Cores 2	0.35	0.42	0.34	0.31	0.31	0.42	0.32
		Average	<b>0.39</b>	<b>0.41</b>	<b>0.34</b>	<b>0.32</b>	<b>0.34</b>	<b>0.41</b>	<b>0.33</b>
		C of V (%)	9.7	3.3	1.2	3.1	8.0	3.3	4.1
	+2 days H	Cores 1	0.39	0.25	0.25	0.23	0.26	0.25	0.25
		Cores 2	0.56	0.38	0.35	0.34	0.36	0.38	0.35
		Average	<b>0.47</b>	<b>0.32</b>	<b>0.30</b>	<b>0.29</b>	<b>0.31</b>	<b>0.32</b>	<b>0.30</b>
		C of V (%)	17.1	20.8	17.2	19.9	16.7	20.8	17.9
	+4 days H	Cores 1	0.33	0.32	0.40	0.23	0.18	0.32	0.27
		Cores 2	0.28	0.32	0.30	0.31	0.29	0.32	0.30
		Average	<b>0.31</b>	<b>0.32</b>	<b>0.35</b>	<b>0.27</b>	<b>0.24</b>	<b>0.32</b>	<b>0.28</b>
		C of V (%)	8.6	0.0	14.6	13.3	22.1	0.0	4.4
	+6 days H	Cores 1	0.25	0.34	0.27	0.29	0.28	0.34	0.28
		Cores 2	0.39	0.36	0.28	0.35	0.26	0.36	0.30
		Average	<b>0.32</b>	<b>0.35</b>	<b>0.28</b>	<b>0.32</b>	<b>0.27</b>	<b>0.35</b>	<b>0.29</b>
		C of V (%)	20.9	3.3	2.0	9.9	2.7	3.3	3.5

Key: +X days H= X days hessian plus 1 day in mould; Average= average of cores 1 and 2; C of V= coefficient of variation (%); Sub-surface (20-40mm)= average k value from 10 to 40mm from surface; Bold value= plotted value (usually average)

**Table B1.5 (a).** Coefficient of air permeability k (m<sup>2</sup> x 10<sup>-16</sup>) for the 30 MPa OPC/GGBS concrete (east/west) - 3 months summer series

Orientation	Curnig regime		Average depth from outer surface (mm)					Surface (10mm)	Sub-surface (20-50mm)
			10	20	30	40	50		
East	No Cure	Cores 1	14.56	13.53	11.66	12.59	9.33	14.56	11.78
		Cores 2	15.77	14.24	11.93	12.88	9.28	15.77	12.08
		Average	<b>15.17</b>	<b>13.88</b>	<b>11.79</b>	<b>12.74</b>	<b>9.30</b>	<b>15.17</b>	<b>11.93</b>
		C of V (%)	4.0	2.6	1.1	1.1	0.3	4.0	1.3
	+2 days H	Cores 1	13.99	13.06	9.33	11.66	10.26	13.99	11.08
		Cores 2	14.48	13.28	9.49	11.73	10.20	14.48	11.17
		Average	<b>14.23</b>	<b>13.17</b>	<b>9.41</b>	<b>11.69</b>	<b>10.23</b>	<b>14.23</b>	<b>11.13</b>
		C of V (%)	1.7	0.8	0.8	0.3	0.3	1.7	0.4
	+4 days H	Cores 1	8.37	6.94	4.16	4.83	3.68	8.37	4.90
		Cores 2	8.94	6.91	4.21	4.65	3.16	8.94	4.73
		Average	<b>8.65</b>	<b>6.92</b>	<b>4.18</b>	<b>4.74</b>	<b>3.42</b>	<b>8.65</b>	<b>4.82</b>
		C of V (%)	3.3	0.2	0.7	1.9	7.6	3.3	1.7
	+6 days H	Cores 1	6.52	5.48	6.61	4.30	4.29	6.52	5.17
		Cores 2	5.79	6.29	4.72	3.38	3.16	5.79	4.39
		Average	<b>6.16</b>	<b>5.88</b>	<b>5.66</b>	<b>3.84</b>	<b>3.73</b>	<b>6.16</b>	<b>4.78</b>
		C of V (%)	5.9	6.9	16.7	12.0	15.2	5.9	8.2
West	No Cure	Cores 1	13.99	11.66	7.00	8.40	8.86	13.99	8.98
		Cores 2	14.39	12.27	7.16	8.59	8.81	14.39	9.21
		Average	<b>14.19</b>	<b>11.97</b>	<b>7.08</b>	<b>8.49</b>	<b>8.84</b>	<b>14.19</b>	<b>9.09</b>
		C of V (%)	1.4	2.6	1.1	1.1	0.3	1.4	1.3
	+2 days H	Cores 1	9.33	7.23	7.00	7.46	5.60	9.33	6.82
		Cores 2	9.65	7.31	7.00	7.50	5.57	9.65	6.84
		Average	<b>9.49</b>	<b>7.27</b>	<b>7.00</b>	<b>7.48</b>	<b>5.58</b>	<b>9.49</b>	<b>6.83</b>
		C of V (%)	1.7	0.6	0.0	0.3	0.3	1.7	0.2
	+4 days H	Cores 1	6.07	3.62	3.92	5.89	5.26	6.07	4.68
		Cores 2	6.88	3.96	3.48	4.22	3.59	6.88	3.81
		Average	<b>6.47</b>	<b>3.79</b>	<b>3.70</b>	<b>5.06</b>	<b>4.43</b>	<b>6.47</b>	<b>4.24</b>
		C of V (%)	6.3	4.4	5.9	16.6	18.9	6.3	10.2
	+6 days H	Cores 1	4.43	4.17	5.06	4.36	5.37	4.43	4.74
		Cores 2	6.29	4.22	4.05	3.42	4.16	6.29	3.96
		Average	<b>5.36</b>	<b>4.20</b>	<b>4.55</b>	<b>3.89</b>	<b>4.76</b>	<b>5.36</b>	<b>4.35</b>
		C of V (%)	17.3	0.5	11.1	12.1	12.7	17.3	9.0

Key: +X days H= X days hessian plus 1 day in mould; Average= average of cores 1 and 2; C of V= coefficient of variation (%); Sub-surface (20-50mm)= average k value from 20 to 50mm from surface; Bold value= plotted value (usually average)

Table B1.5 (b) Coefficient of air permeability  $k$  ( $m^2 \times 10^{-16}$ ) for the 30 MPa OPC/GGBS concrete (top/bottom) - 3 months summer series

Orientation	Curing regime	Average depth from outer surface (mm)					Surface (10mm)	Sub-surface (20-50mm)	
		10	20	30	40	50			
Top	No Cure	Cores 1	8.40	6.53	5.60	7.46	6.31	8.40	6.48
		Cores 2	8.44	6.57	5.82	5.87	5.69	8.44	5.99
		Average	<b>8.42</b>	<b>6.55</b>	<b>5.71</b>	<b>6.66</b>	<b>6.00</b>	<b>8.42</b>	<b>6.23</b>
		C of V (%)	0.3	0.3	2.0	12.0	5.2	0.3	3.9
	+2 days H	Cores 1	7.70	7.00	6.06	6.01	5.81	7.70	6.22
		Cores 2	7.65	7.04	6.10	5.96	6.10	7.65	6.30
		Average	<b>7.68</b>	<b>7.02</b>	<b>6.08</b>	<b>5.99</b>	<b>5.96</b>	<b>7.68</b>	<b>6.26</b>
		C of V (%)	0.3	0.3	0.3	0.4	2.4	0.3	0.6
	+4 days H	Cores 1	5.03	3.95	3.55	3.13	2.62	5.03	3.31
		Cores 2	5.55	3.75	3.13	2.87	2.40	5.55	3.04
		Average	<b>5.29</b>	<b>3.85</b>	<b>3.34</b>	<b>3.00</b>	<b>2.51</b>	<b>5.29</b>	<b>3.17</b>
		C of V (%)	4.9	2.6	6.3	4.3	4.3	4.9	4.3
	+6 days H	Cores 1	4.37	4.67	5.25	2.97	3.77	4.37	4.16
		Cores 2	4.92	3.83	3.49	2.52	2.44	4.92	3.07
		Average	<b>4.64</b>	<b>4.25</b>	<b>4.37</b>	<b>2.75</b>	<b>3.10</b>	<b>4.64</b>	<b>3.62</b>
		C of V (%)	5.9	9.8	20.1	8.3	21.3	5.9	15.1
Bottom	No Cure	Cores 1	14.26	13.99	12.13	12.59	7.93	14.26	11.66
		Cores 2	14.60	13.84	11.93	12.25	7.84	14.60	11.47
		Average	<b>14.43</b>	<b>13.92</b>	<b>12.03</b>	<b>12.42</b>	<b>7.89</b>	<b>14.43</b>	<b>11.56</b>
		C of V (%)	1.2	0.6	0.8	1.4	0.6	1.2	0.8
	+2 days H	Cores 1	7.46	9.33	8.40	11.19	7.93	7.46	9.21
		Cores 2	12.79	9.18	8.08	6.72	6.96	12.79	7.73
		Average	<b>10.13</b>	<b>9.25</b>	<b>8.24</b>	<b>8.96</b>	<b>7.45</b>	<b>10.13</b>	<b>8.47</b>
		C of V (%)	26.3	0.8	1.9	25.0	6.5	26.3	8.7
	+4 days H	Cores 1	7.56	5.88	5.25	6.16	5.24	7.56	5.63
		Cores 2	8.88	4.73	4.10	3.55	3.90	8.88	4.07
		Average	<b>8.22</b>	<b>5.30</b>	<b>4.67</b>	<b>4.86</b>	<b>4.57</b>	<b>8.22</b>	<b>4.85</b>
		C of V (%)	8.0	10.9	12.3	26.9	14.6	8.0	16.1
	+6 days H	Cores 1	7.43	6.27	6.45	5.64	7.04	7.43	6.35
		Cores 2	7.05	7.28	4.64	4.15	4.53	7.05	5.15
		Average	<b>7.24</b>	<b>6.77</b>	<b>5.54</b>	<b>4.89</b>	<b>5.79</b>	<b>7.24</b>	<b>5.75</b>
		C of V (%)	2.6	7.4	16.3	15.1	21.6	2.6	10.4

Key: +X days H= X days hessian plus 1 day in mould; Average= average of cores 1 and 2; C of V= coefficient of variation (%); Sub-surface (20-50mm)= average k value from 20 to 50mm from surface; Bold value= plotted value (usually average)

Table B1.6 (b). Coefficient of air permeability  $k$  ( $m^2 \times 10^{-16}$ ) for the 30 MPa OPC/GGBS concrete (top/bottom) - 12 months summer series

Orientation	Curing regime		Average depth from outer surface (mm)					Surface (10mm)	Sub-surface (20-40mm)
			5	10	20	30	40		
Top	No Cure	Cores 1	5.29	3.27	0.96	1.66	3.49	3.27	2.04
		Cores 2	6.97	5.89	1.19	1.67	8.08	5.89	3.65
		Average	<b>6.13</b>	<b>4.58</b>	<b>1.08</b>	<b>1.67</b>	<b>5.79</b>	<b>4.58</b>	<b>2.84</b>
		C of V (%)	13.8	28.6	11.0	0.2	39.6	28.6	28.3
	+2 days H	Cores 1	5.49	1.50	0.99	2.94	3.97	1.50	2.64
		Cores 2	2.60	2.10	1.13	1.59	3.35	2.10	2.03
		Average	<b>4.05</b>	<b>1.80</b>	<b>1.06</b>	<b>2.27</b>	<b>3.66</b>	<b>1.80</b>	<b>2.33</b>
		C of V (%)	35.8	14.2	6.1	42.2	9.3	14.2	13.1
	+4 days H	Cores 1	2.79	1.80	1.15	1.24	1.84	1.80	1.41
		Cores 2	2.21	1.40	0.92	1.12	1.98	1.40	1.34
		Average	<b>2.50</b>	<b>1.60</b>	<b>1.04</b>	<b>1.18</b>	<b>1.91</b>	<b>1.60</b>	<b>1.38</b>
		C of V (%)	11.7	12.2	11.0	5.3	3.7	12.2	2.6
	+6 days H	Cores 1	2.63	1.28	0.79	1.17	1.34	1.28	1.10
		Cores 2	2.20	1.09	1.12	1.04	1.35	1.09	1.17
		Average	<b>2.42</b>	<b>1.18</b>	<b>0.96</b>	<b>1.11</b>	<b>1.35</b>	<b>1.18</b>	<b>1.14</b>
		C of V (%)	8.9	7.8	17.2	5.7	0.0	7.8	3.0
Bottom	No Cure	Cores 1	9.07	7.16	2.25	1.71	2.00	7.16	1.99
		Cores 2	8.41	8.57	2.35	1.49	2.19	8.57	2.01
		Average	<b>8.74</b>	<b>7.87</b>	<b>2.30</b>	<b>1.60</b>	<b>2.10</b>	<b>7.87</b>	<b>2.00</b>
		C of V (%)	3.7	9.0	2.1	7.0	4.5	9.0	0.5
	+2 days H	Cores 1	7.09	7.54	1.80	1.78	3.25	7.54	2.27
		Cores 2	5.34	6.04	2.00	1.47	3.04	6.04	2.17
		Average	<b>6.22</b>	<b>6.79</b>	<b>1.90</b>	<b>1.62</b>	<b>3.15</b>	<b>6.79</b>	<b>2.22</b>
		C of V (%)	14.1	11.1	5.3	9.4	3.2	11.1	2.3
	+4 days H	Cores 1	2.25	2.32	1.41	0.98	1.18	2.32	1.19
		Cores 2	3.87	2.18	1.83	1.70	1.21	2.18	1.58
		Average	<b>3.06</b>	<b>2.25</b>	<b>1.62</b>	<b>1.34</b>	<b>1.19</b>	<b>2.25</b>	<b>1.39</b>
		C of V (%)	26.5	3.3	12.9	26.8	1.2	3.3	14.0
	+6 days H	Cores 1	4.41	1.85	1.34	2.10	1.21	1.85	1.55
		Cores 2	3.48	2.33	1.74	1.72	1.90	2.33	1.79
		Average	<b>3.95</b>	<b>2.09</b>	<b>1.54</b>	<b>1.91</b>	<b>1.55</b>	<b>2.09</b>	<b>1.67</b>
		C of V (%)	11.8	11.4	13.1	10.0	22.3	11.4	7.1

Key: +X days H= X days hessian plus 1 day in mould; Average= average of cores 1 and 2; C of V= coefficient of variation (%); Sub-surface (20-40mm)= average  $k$  value from 10 to 40mm from surface; Bold value= plotted value (usually average)

**Table B1.6 (a).** Coefficient of air permeability  $k$  ( $m^2 \times 10^{-16}$ ) for the 30 MPa OPC/GGBS concrete (east/west) - 12 months summer series

Orientation	Curnig regime		Average depth from outer surface (mm)					Surface (10mm)	Sub-surface (20-40mm)
			5	10	20	30	40		
East	No Cure	Cores 1	11.45	17.06	15.39	12.73	7.93	17.06	12.02
		Cores 2	16.79	15.28	15.23	11.23	8.21	15.28	11.55
		Average	<b>14.12</b>	<b>16.17</b>	<b>15.31</b>	<b>11.98</b>	<b>8.07</b>	<b>16.17</b>	<b>11.79</b>
		C of V (%)	18.9	5.5	0.5	6.3	1.7	5.5	2.0
	+2 days H	Cores 1	10.49	13.26	4.07	4.68	3.93	13.26	4.23
		Cores 2	10.49	16.37	7.87	8.47	12.04	16.37	11.19
		Average	<b>10.49</b>	<b>14.82</b>	<b>5.97</b>	<b>6.57</b>	<b>7.99</b>	<b>14.82</b>	<b>7.71</b>
		C of V (%)	0.0	9.5	24.1	22.3	33.7	9.5	45.1
	+4 days H	Cores 1	4.16	1.96	1.36	1.30	1.24	1.96	1.30
		Cores 2	4.01	4.66	1.39	2.22	1.64	4.66	1.75
		Average	<b>4.08</b>	<b>3.31</b>	<b>1.37</b>	<b>1.76</b>	<b>1.44</b>	<b>3.31</b>	<b>1.52</b>
		C of V (%)	1.9	40.7	0.8	26.2	13.9	40.7	14.7
	+6 days H	Cores 1	9.03	4.44	2.02	1.79	1.83	4.44	1.88
		Cores 2	7.38	3.61	2.18	2.50	1.56	3.61	2.08
		Average	<b>8.20</b>	<b>4.03</b>	<b>2.10</b>	<b>2.14</b>	<b>1.69</b>	<b>4.03</b>	<b>1.98</b>
		C of V (%)	10.1	10.3	3.8	16.6	8.1	10.3	5.0
West	No Cure	Cores 1	13.00	14.67	5.49	3.97	4.32	14.67	4.59
		Cores 2	13.72	12.62	2.67	3.72	8.74	12.62	5.04
		Average	<b>13.36</b>	<b>13.64</b>	<b>4.08</b>	<b>3.84</b>	<b>6.53</b>	<b>13.64</b>	<b>4.82</b>
		C of V (%)	2.7	7.5	34.6	3.2	33.8	7.5	4.7
	+2 days H	Cores 1	12.88	16.14	3.56	5.69	8.24	16.14	5.83
		Cores 2	6.17	7.18	3.76	3.80	5.10	7.18	4.22
		Average	<b>9.52</b>	<b>11.66</b>	<b>3.66</b>	<b>4.75</b>	<b>6.67</b>	<b>11.66</b>	<b>5.03</b>
		C of V (%)	35.2	38.4	2.8	19.9	23.5	38.4	16.0
	+4 days H	Cores 1	3.77	2.26	1.32	2.06	1.01	2.26	1.46
		Cores 2	4.30	3.24	1.84	1.26	2.10	3.24	1.73
		Average	<b>4.04</b>	<b>2.75</b>	<b>1.58</b>	<b>1.66</b>	<b>1.56</b>	<b>2.75</b>	<b>1.60</b>
		C of V (%)	6.6	17.9	16.4	24.1	35.3	17.9	8.5
	+6 days H	Cores 1	6.50	1.93	1.35	2.30	1.22	1.93	1.63
		Cores 2	6.81	1.98	1.63	1.38	1.56	1.98	1.53
		Average	<b>6.66</b>	<b>1.95</b>	<b>1.49</b>	<b>1.84</b>	<b>1.39</b>	<b>1.95</b>	<b>1.67</b>
		C of V (%)	2.4	1.2	9.3	25.0	12.2	1.2	3.0

Key: +X days H= X days hessian plus 1 day in mould; Average= average of cores 1 and 2; C of V= coefficient of variation (%); Sub-surface (20-40mm)= average k value from 10 to 40mm from surface; Bold value= plotted value (usually average)

Table B1.7 (a). Coefficient of air permeability  $k$  ( $m^2 \times 10^{-16}$ ) for the 30 MPa OPC/GGBS concrete (east/west) - 3 months summer series

Orientation	Curnig regime		Average depth from outer surface (mm)					Surface (10mm)	Sub-surface (20-50mm)
			10	20	30	40	50		
East	No Cure	Cores 1	14.56	13.53	11.66	12.59	9.33	14.56	11.78
		Cores 2	15.77	14.24	11.93	12.88	9.28	15.77	12.08
		Average	<b>15.17</b>	<b>13.88</b>	<b>11.79</b>	<b>12.74</b>	<b>9.30</b>	<b>15.17</b>	<b>11.93</b>
		C of V (%)	4.0	2.6	1.1	1.1	0.3	4.0	1.3
	+2 days H	Cores 1	13.99	13.06	9.33	11.66	10.26	13.99	11.08
		Cores 2	14.48	13.28	9.49	11.73	10.20	14.48	11.17
		Average	<b>14.23</b>	<b>13.17</b>	<b>9.41</b>	<b>11.69</b>	<b>10.23</b>	<b>14.23</b>	<b>11.13</b>
		C of V (%)	1.7	0.8	0.8	0.3	0.3	1.7	0.4
	None (CPF)	Cores 1	14.03	13.99	15.59	12.00	10.62	14.03	13.05
		Cores 2	1.38	19.36	16.52	13.68	10.40	1.38	14.99
		Average	<b>7.70</b>	<b>16.68</b>	<b>16.06</b>	<b>12.84</b>	<b>10.51</b>	<b>7.70</b>	<b>14.02</b>
		C of V (%)	82.1	16.1	2.9	6.5	1.0	82.1	6.9
	+2 days (CPF)	Cores 1	10.71	11.62	11.33	9.40	7.23	10.71	9.90
		Cores 2	9.33	10.09	9.39	11.00	9.72	9.33	10.05
		Average	<b>10.02</b>	<b>10.85</b>	<b>10.36</b>	<b>10.20</b>	<b>8.48</b>	<b>10.02</b>	<b>9.97</b>
		C of V (%)	6.9	7.0	9.4	7.8	14.7	6.9	0.8
West	No Cure	Cores 1	13.99	11.66	7.00	8.40	8.86	13.99	8.98
		Cores 2	14.39	12.27	7.16	8.59	8.81	14.39	9.21
		Average	<b>14.19</b>	<b>11.97</b>	<b>7.08</b>	<b>8.49</b>	<b>8.84</b>	<b>14.19</b>	<b>9.09</b>
		C of V (%)	1.4	2.6	1.1	1.1	0.3	1.4	1.3
	+2 days H	Cores 1	9.33	7.23	7.00	7.46	5.60	9.33	6.82
		Cores 2	9.65	7.31	7.00	7.50	5.57	9.65	6.84
		Average	<b>9.49</b>	<b>7.27</b>	<b>7.00</b>	<b>7.48</b>	<b>5.58</b>	<b>9.49</b>	<b>6.83</b>
		C of V (%)	1.7	0.6	0.0	0.3	0.3	1.7	0.2
	None (CPF)	Cores 1	6.83	13.54	18.08	13.88	11.81	6.83	14.33
		Cores 2	1.24	16.64	14.81	19.99	10.45	1.24	15.47
		Average	<b>4.03</b>	<b>15.09</b>	<b>16.44</b>	<b>16.94</b>	<b>11.13</b>	<b>4.03</b>	<b>14.90</b>
		C of V (%)	69.4	10.3	9.9	18.0	6.1	69.4	3.8
	+2 days (CPF)	Cores 1	7.48	11.94	14.43	9.38	7.94	7.48	10.92
		Cores 2	4.96	15.13	16.36	11.70	8.49	4.96	12.92
		Average	<b>6.22</b>	<b>13.53</b>	<b>15.40</b>	<b>10.54</b>	<b>8.21</b>	<b>6.22</b>	<b>11.92</b>
		C of V (%)	20.3	11.8	6.3	11.0	3.4	20.3	8.4

Key: +X days H= X days hessian plus 1 day in mould; Average= average of cores 1 and 2; C of V= coefficient of variation (%); Sub-surface (20-50mm)= average k value from surface; Bold value= plotted value (usually average); CPF= controlled permeability formwork

**Table B1.7 (b).** Coefficient of air permeability  $k$  ( $m^2 \times 10^{-16}$ ) for the 30 MPa OPC/GGBS concrete (top/bottom) - 3 months summer series

Orientation	Curing regime		Average depth from outer surface (mm)					Surface (10mm)	Sub-surface (20-50mm)
			10	20	30	40	50		
Top	No Cure	Cores 1	8.40	6.53	5.60	7.46	6.31	8.40	6.48
		Cores 2	8.44	6.57	5.82	5.87	5.69	8.44	5.99
		Average	<b>8.42</b>	<b>6.55</b>	<b>5.71</b>	<b>6.66</b>	<b>6.00</b>	<b>8.42</b>	<b>6.23</b>
		C of V (%)	0.3	0.3	2.0	12.0	5.2	0.3	3.9
	+2 days H	Cores 1	7.70	7.00	6.06	6.01	5.81	7.70	6.22
		Cores 2	7.65	7.04	6.10	5.96	6.10	7.65	6.30
		Average	<b>7.68</b>	<b>7.02</b>	<b>6.08</b>	<b>5.99</b>	<b>5.96</b>	<b>7.68</b>	<b>6.26</b>
		C of V (%)	0.3	0.3	0.3	0.4	2.4	0.3	0.6
	None (CPF)	Cores 1	0.37	14.68	12.06	15.81	11.22	0.37	13.44
		Cores 2	0.37	6.48	10.20	9.66	10.38	0.37	9.18
		Average	<b>0.37</b>	<b>10.58</b>	<b>11.13</b>	<b>12.73</b>	<b>10.80</b>	<b>0.37</b>	<b>11.31</b>
		C of V (%)	0.1	38.7	8.4	24.2	3.9	0.1	18.8
	+2 days (CPF)	Cores 1	0.22	5.21	13.33	9.59	8.30	0.22	9.11
		Cores 2	0.32	4.22	12.77	12.50	12.78	0.32	10.57
		Average	<b>0.27</b>	<b>4.71</b>	<b>13.05</b>	<b>11.04</b>	<b>10.54</b>	<b>0.27</b>	<b>9.84</b>
		C of V (%)	18.7	10.5	2.1	13.2	21.2	18.7	7.4
Bottom	No Cure	Cores 1	14.26	13.99	12.13	12.59	7.93	14.26	11.66
		Cores 2	14.60	13.84	11.93	12.25	7.84	14.60	11.47
		Average	<b>14.43</b>	<b>13.92</b>	<b>12.03</b>	<b>12.42</b>	<b>7.89</b>	<b>14.43</b>	<b>11.56</b>
		C of V (%)	1.2	0.6	0.8	1.4	0.6	1.2	0.8
	+2 days H	Cores 1	7.46	9.33	8.40	11.19	7.93	7.46	9.21
		Cores 2	12.79	9.18	8.08	6.72	6.96	12.79	7.73
		Average	<b>10.13</b>	<b>9.25</b>	<b>8.24</b>	<b>8.96</b>	<b>7.45</b>	<b>10.13</b>	<b>8.47</b>
		C of V (%)	26.3	0.8	1.9	25.0	6.5	26.3	8.7
	None (CPF)	Cores 1	0.29	15.36	12.15	10.63	9.62	0.29	11.94
		Cores 2	0.28	8.13	9.30	9.99	9.10	0.28	9.13
		Average	<b>0.29</b>	<b>11.75</b>	<b>10.72</b>	<b>10.31</b>	<b>9.36</b>	<b>0.29</b>	<b>10.53</b>
		C of V (%)	1.7	30.8	13.3	3.1	2.8	1.7	13.3
	+2 days (CPF)	Cores 1	1.04	8.08	13.98	10.11	7.67	1.04	9.96
		Cores 2	0.33	7.91	9.39	11.00	9.72	0.33	9.50
		Average	<b>0.68</b>	<b>7.99</b>	<b>11.68</b>	<b>10.56</b>	<b>8.70</b>	<b>0.68</b>	<b>9.73</b>
		C of V (%)	52.2	1.0	19.7	4.2	11.8	52.2	2.3

Key: +X days H= X days hessian plus 1 day in mould; Average= average of cores 1 and 2; C of V= coefficient of variation (%); Sub-surface (20-50mm)= average k value from rface; Bold value= plotted value (usually average); CPF= controlled permeability formwork

**Table B1.8 (a).** Coefficient of air permeability  $k$  ( $m^2 \times 10^{-16}$ ) for the 30 MPa OPC/GGBS concrete (east/west) - 12 months summer series

Orientation	Curnig regime	Average depth from outer surface (mm)					Surface (10mm)	Sub-surface (20-40mm)	
		5	10	20	30	40			
East	No Cure	Cores 1	11.45	17.06	15.39	12.73	7.93	17.06	12.02
		Cores 2	16.79	15.28	15.23	11.23	8.21	15.28	11.55
		Average	<b>14.12</b>	<b>16.17</b>	<b>15.31</b>	<b>11.98</b>	<b>8.07</b>	<b>16.17</b>	<b>11.79</b>
		C of V (%)	18.9	5.5	0.5	6.3	1.7	5.5	2.0
	+2 days H	Cores 1	10.49	13.26	4.07	4.68	3.93	13.26	4.23
		Cores 2	10.49	16.37	7.87	8.47	12.04	16.37	11.19
		Average	<b>10.49</b>	<b>14.82</b>	<b>5.97</b>	<b>6.57</b>	<b>7.99</b>	<b>14.82</b>	<b>7.71</b>
		C of V (%)	0.0	9.5	24.1	22.3	33.7	9.5	45.1
	None (CPF)	Cores 1	0.33	<b>0.60</b>	2.00	3.24	3.10	0.60	2.78
		Cores 2	0.31	0.26	3.03	3.03	3.80	0.26	3.29
		Average	<b>0.32</b>	<b>0.43</b>	<b>2.51</b>	<b>3.13</b>	<b>3.45</b>	<b>0.43</b>	<b>3.03</b>
		C of V (%)	3.0	40.1	20.6	3.5	10.2	40.1	8.4
	+2 days (CPF)	Cores 1	0.37	0.44	3.28	2.22	2.87	0.44	2.79
		Cores 2	0.28	0.25	1.67	2.61	2.72	0.25	2.33
		Average	<b>0.33</b>	<b>0.34</b>	<b>2.48</b>	<b>2.41</b>	<b>2.80</b>	<b>0.34</b>	<b>2.56</b>
		C of V (%)	14.7	28.7	32.7	8.0	2.7	28.7	9.0
West	No Cure	Cores 1	13.00	14.67	5.49	3.97	4.32	14.67	4.59
		Cores 2	13.72	12.62	2.67	3.72	8.74	12.62	5.04
		Average	<b>13.36</b>	<b>13.64</b>	<b>4.08</b>	<b>3.84</b>	<b>6.53</b>	<b>13.64</b>	<b>4.82</b>
		C of V (%)	2.7	7.5	34.6	3.2	33.8	7.5	4.7
	+2 days H	Cores 1	12.88	16.14	3.56	5.69	8.24	16.14	5.83
		Cores 2	6.17	7.18	3.76	3.80	5.10	7.18	4.22
		Average	<b>9.52</b>	<b>11.66</b>	<b>3.66</b>	<b>4.75</b>	<b>6.67</b>	<b>11.66</b>	<b>5.03</b>
		C of V (%)	35.2	38.4	2.8	19.9	23.5	38.4	16.0
	None (CPF)	Cores 1	0.29	0.14	1.80	2.88	3.36	0.14	2.68
		Cores 2	0.44	0.27	3.30	2.85	3.42	0.27	3.19
		Average	<b>0.37</b>	<b>0.21</b>	<b>2.55</b>	<b>2.86</b>	<b>3.39</b>	<b>0.21</b>	<b>2.93</b>
		C of V (%)	20.1	30.3	29.3	0.4	1.0	30.3	8.7
	+2 days (CPF)	Cores 1	0.42	0.32	3.08	2.19	2.70	0.32	2.66
		Cores 2	0.19	0.25	1.90	2.34	2.51	0.25	2.25
		Average	<b>0.30</b>	<b>0.29</b>	<b>2.49</b>	<b>2.27</b>	<b>2.61</b>	<b>0.29</b>	<b>1.91</b>
		C of V (%)	37.5	11.3	23.5	3.3	3.7	11.3	10.6

Key: +X days H= X days hessian plus 1 day in mould; Average= average of cores 1 and 2; C of V= coefficient of variation (%); Sub-surface (20-40mm)= average k value from surface; Bold value= plotted value (usually average); CPF= controlled permeability formwork

**Table B1.8 (b).** Coefficient of air permeability  $k$  ( $m^2 \times 10^{-16}$ ) for the 30 MPa OPC/GGBS concrete (top/bottom) - 12 months summer series

Orientation	Curing regime	Average depth from outer surface (mm)					Surface (10mm)	Sub-surface (20-40mm)	
		5	10	20	30	40			
Top	No Cure	Cores 1	5.29	3.27	0.96	1.66	3.49	3.27	2.04
		Cores 2	6.97	5.89	1.19	1.67	8.08	5.89	3.65
		Average	<b>6.13</b>	<b>4.58</b>	<b>1.08</b>	<b>1.67</b>	<b>5.79</b>	<b>4.58</b>	<b>2.84</b>
		C of V (%)	13.8	28.6	11.0	0.2	39.6	28.6	28.3
	+2 days H	Cores 1	5.49	1.50	0.99	2.94	3.97	1.50	2.64
		Cores 2	2.60	2.10	1.13	1.59	3.35	2.10	2.03
		Average	<b>4.05</b>	<b>1.80</b>	<b>1.06</b>	<b>2.27</b>	<b>3.66</b>	<b>1.80</b>	<b>2.33</b>
		C of V (%)	35.8	14.2	6.1	42.2	9.3	14.2	13.1
	None (CPF)	Cores 1	1.42	2.33	3.58	3.68	3.50	2.33	3.59
		Cores 2	2.07	2.42	3.35	2.77	3.19	2.42	3.11
		Average	<b>1.75</b>	<b>2.37</b>	<b>3.47</b>	<b>3.23</b>	<b>3.35</b>	<b>2.37</b>	<b>3.35</b>
		C of V (%)	18.6	1.9	3.4	14.1	4.5	1.9	7.2
	+2 days (CPF)	Cores 1	1.52	2.64	3.00	2.48	2.63	2.64	2.70
		Cores 2	1.52	2.26	4.21	2.93	2.15	2.26	3.10
		Average	<b>1.52</b>	<b>2.45</b>	<b>3.61</b>	<b>2.70</b>	<b>2.39</b>	<b>2.45</b>	<b>2.90</b>
		C of V (%)	0.1	7.9	16.8	8.4	9.9	7.9	6.9
Bottom	No Cure	Cores 1	9.07	7.16	2.25	1.71	2.00	7.16	1.99
		Cores 2	8.41	8.57	2.35	1.49	2.19	8.57	2.01
		Average	<b>8.74</b>	<b>7.87</b>	<b>2.30</b>	<b>1.60</b>	<b>2.10</b>	<b>7.87</b>	<b>2.00</b>
		C of V (%)	3.7	9.0	2.1	7.0	4.5	9.0	0.5
	+2 days H	Cores 1	7.09	7.54	1.80	1.78	3.25	7.54	2.27
		Cores 2	5.34	6.04	2.00	1.47	3.04	6.04	2.17
		Average	<b>6.22</b>	<b>6.79</b>	<b>1.90</b>	<b>1.62</b>	<b>3.15</b>	<b>6.79</b>	<b>2.22</b>
		C of V (%)	14.1	11.1	5.3	9.4	3.2	11.1	2.3
	None (CPF)	Cores 1	1.55	3.88	2.50	3.10	2.97	3.88	2.86
		Cores 2	1.92	3.32	2.73	3.38	2.18	3.32	2.76
		Average	<b>1.74</b>	<b>3.60</b>	<b>2.61</b>	<b>3.24</b>	<b>2.58</b>	<b>3.60</b>	<b>2.81</b>
		C of V (%)	10.5	7.7	4.3	4.3	15.5	7.7	1.7
	+2 days (CPF)	Cores 1	1.98	2.20	2.73	2.21	2.41	2.20	2.45
		Cores 2	1.77	2.81	3.59	2.97	2.87	2.81	3.15
		Average	<b>1.88</b>	<b>2.50</b>	<b>3.16</b>	<b>2.59</b>	<b>2.64</b>	<b>2.50</b>	<b>2.80</b>
		C of V (%)	5.5	12.2	13.5	14.6	8.7	12.2	12.3

Key: +X days H= X days hessian plus 1 day in mould; Average= average of cores 1 and 2; C of V= coefficient of variation (%); Sub-surface (20-40mm)= average k value from rface; Bold value= plotted value (usually average); CPF= controlled permeability formwork

**Table B1.9 (b) Coefficient of air permeability  $k$  ( $m^2 \times 10^{-16}$ ) for the 30 MPa OPC/GGBS concrete (top/bottom) - 3 months summer series**

Orientation	Curing regime		Average depth from outer surface (mm)					Surface (10mm)	Sub-surface (20-50mm)
			10	20	30	40	50		
Top	+ 6 days P	Cores 1	5.59	5.09	5.10	5.00	4.94	5.59	5.03
		Cores 2	4.10	4.72	3.67	3.60	6.85	4.10	4.71
		Average	4.84	4.91	4.38	4.30	5.89	4.84	4.87
		C of V (%)	15.4	3.8	16.3	16.3	16.2	15.4	3.3
	C/M	Cores 1	12.18	9.30	7.76	6.80	8.11	12.18	7.99
		Cores 2	8.80	8.80	5.44	4.47	7.18	8.80	6.47
		Average	10.49	9.05	6.60	5.63	7.64	10.49	7.23
		C of V (%)	16.1	2.8	21.4	26.0	6.5	16.1	10.5
	+6 days P (CPF)	Cores 1	0.71	5.55	3.40	2.49	5.23	0.71	4.17
		Cores 2	1.18	7.46	6.38	8.57	3.04	1.18	6.36
		Average	0.95	6.51	4.89	5.53	4.13	0.95	5.27
		C of V (%)	24.6	14.7	30.5	55.0	26.4	24.6	20.9
	C/M (CPF)	Cores 1	1.73	12.54	6.68	9.41	8.15	1.73	9.19
		Cores 2	3.34	12.21	10.40	8.52	6.68	3.34	9.45
		Average	2.54	12.37	8.54	8.96	7.42	2.54	9.32
		C of V (%)	31.9	1.3	21.8	5.0	9.9	31.9	1.4
Bottom	+ 6 days P	Cores 1	10.45	9.02	7.89	9.21	7.76	10.45	8.47
		Cores 2	12.44	5.70	8.19	7.23	7.10	12.44	7.06
		Average	11.45	7.36	8.04	8.22	7.43	11.45	7.76
		C of V (%)	8.7	22.5	1.9	12.0	4.4	8.7	9.1
	C/M	Cores 1	12.36	9.50	8.21	9.49	10.39	12.36	9.40
		Cores 2	12.36	10.18	9.49	8.18	6.95	12.36	8.70
		Average	12.36	9.84	8.85	8.84	8.67	12.36	9.05
		C of V (%)	0.0	3.5	7.2	7.4	19.9	0.0	3.9
	+6 days P (CPF)	Cores 1	1.35	8.47	7.04	5.23	6.32	1.35	6.77
		Cores 2	1.70	12.48	5.37	8.48	3.91	1.70	7.56
		Average	1.52	10.47	6.21	6.85	5.12	1.52	7.16
		C of V (%)	11.7	19.1	13.5	23.7	23.5	11.7	5.5
	C/M (CPF)	Cores 1	1.87	11.95	10.76	8.13	7.77	1.87	9.65
		Cores 2	2.04	12.44	13.27	11.06	9.02	2.04	11.45
		Average	1.96	12.19	12.02	9.59	8.39	1.96	10.55
		C of V (%)	4.1	2.0	10.4	15.3	7.5	4.1	8.5

Key: +X days H= X days hessian plus 1 day in mould; Average= average of cores 1 and 2; C of V= coefficient of variation (%); Sub-surface (20-50mm)= average k value from slotted value (usually average); P= polythene; C/M= curing membrane; CPF= controlled permeability formwork

Table B1.9 (a). Coefficient of air permeability  $k$  ( $m^2 \times 10^{-16}$ ) for the 30 MPa OPC/GGBS concrete (east/west) - 3 months summer series

Orientation	Curnig regime		Average depth from outer surface (mm)					Surface (10mm)	Sub-surface (20-50mm)
			10	20	30	40	50		
East	+6 days P	Cores 1	14.84	12.23	12.08	8.78	11.28	14.84	11.09
		Cores 2	8.54	9.26	7.36	10.20	7.14	8.54	8.49
		Average	11.69	10.75	9.72	9.49	9.21	11.69	9.79
		C of V (%)	26.9	13.8	24.3	7.5	22.4	26.9	13.3
	C/M	Cores 1	15.16	16.54	14.29	12.51	10.63	15.16	13.49
		Cores 2	15.16	12.49	12.19	11.60	11.90	15.16	12.04
		Average	15.16	14.51	13.24	12.05	11.27	15.16	12.77
		C of V (%)	0.0	16.2	8.6	3.9	5.4	0.0	5.7
	+6 days P (CPF)	Cores 1	2.14	8.45	8.12	7.73	5.90	2.14	7.55
		Cores 2	2.69	6.75	9.83	9.67	8.88	2.69	8.78
		Average	2.42	7.60	8.98	8.70	7.39	2.42	8.17
		C of V (%)	11.5	11.2	9.5	11.2	20.1	11.5	7.6
	C/M (CPF)	Cores 1	3.37	19.99	9.96	9.80	4.54	3.37	11.07
		Cores 2	2.14	9.51	11.41	14.85	6.68	2.14	10.61
		Average	2.75	14.75	10.69	12.32	5.61	2.75	10.84
		C of V (%)	22.4	35.5	6.8	20.5	19.1	22.4	2.1
West	+ 6 days P	Cores 1	9.22	7.34	5.65	6.50	4.64	9.22	6.03
		Cores 2	6.44	6.05	6.94	5.70	4.17	6.44	5.72
		Average	7.83	6.70	6.29	6.10	4.40	7.83	5.87
		C of V (%)	17.7	9.6	10.3	6.6	5.3	17.7	2.7
	C/M	Cores 1	16.54	10.25	8.94	9.28	8.12	16.54	9.15
		Cores 2	14.59	9.72	13.02	11.80	12.05	14.59	11.64
		Average	15.56	9.98	10.98	10.54	10.08	15.56	10.40
		C of V (%)	6.3	2.7	18.6	11.9	19.5	6.3	12.0
	+6 days P (CPF)	Cores 1	1.38	5.05	4.89	7.09	5.66	1.38	5.67
		Cores 2	1.43	5.64	17.25	6.25	7.52	1.43	9.17
		Average	1.40	5.35	11.07	6.67	6.59	1.40	7.42
		C of V (%)	1.9	5.5	55.9	6.3	14.1	1.9	23.5
	C/M (CPF)	Cores 1	2.53	17.49	11.49	9.56	12.63	2.53	12.79
		Cores 2	0.92	12.43	11.74	10.57	8.00	0.92	10.69
		Average	1.73	14.96	11.61	10.07	10.32	1.73	11.74
		C of V (%)	46.5	16.9	1.1	5.0	22.4	46.5	9.0

Key: +X days H= X days hessian plus 1 day in mould; Average= average of cores 1 and 2; C of V= coefficient of variation (%); Sub-surface (20-50mm)= average k value from slotted value (usually average); P= polythene; C/M= curing membrane; CPF= controlled permeability formwork

**Table B1.10 (a).** Coefficient of air permeability  $k$  ( $m^2 \times 10^{-16}$ ) for the 30 MPa OPC/GGBS concrete (east/west) - 12 months summer series

Orientation	Curnig regime		Average depth from outer surface (mm)					Surface (10mm)	Sub-surface (20-40mm)
			5	10	20	30	40		
East	+6 days P	Cores 1	12.59	10.10	2.18	1.70	1.74	10.10	1.87
		Cores 2	6.86	8.33	1.63	2.62	4.40	8.33	2.88
		Average	9.72	9.22	1.90	2.16	3.07	9.22	2.38
		C of V (%)	29.5	9.6	14.5	21.2	43.3	9.6	21.2
	C/M	Cores 1	13.08	15.96	8.50	4.71	7.31	15.96	6.84
		Cores 2	14.76	12.01	3.72	7.09	6.25	12.01	7.27
		Average	13.92	13.98	6.11	5.90	6.78	13.98	7.05
		C of V (%)	6.0	16.4	64.2	16.8	8.5	16.4	3.0
	+6 days P (CPF)	Cores 1	0.16	0.85	1.27	2.93	2.86	0.85	2.35
		Cores 2	0.68	0.19	1.38	1.46	2.65	0.19	1.83
		Average	0.42	0.52	1.33	2.20	2.75	0.52	2.09
		C of V (%)	61.4	64.1	4.0	33.3	3.8	64.1	12.5
	C/M (CPF)	Cores 1	0.32	0.26	2.52	2.24	2.73	0.26	2.50
		Cores 2	0.16	0.35	0.91	2.25	2.37	0.35	1.84
		Average	0.24	0.31	1.72	2.24	2.55	0.31	2.17
		C of V (%)	48.6	20.7	66.4	0.2	10.1	20.7	15.1
West	+ 6 days P	Cores 1	4.34	2.52	2.51	3.84	4.44	2.52	3.60
		Cores 2	5.64	4.66	3.30	4.53	6.07	4.66	4.63
		Average	4.99	3.59	2.91	4.19	5.26	3.59	4.12
		C of V (%)	13.1	29.9	13.4	8.2	15.5	29.9	12.6
	C/M	Cores 1	10.10	6.03	5.59	6.53	7.45	6.03	6.52
		Cores 2	9.18	10.06	2.98	3.00	7.63	10.06	4.54
		Average	9.64	8.05	4.29	4.76	7.54	8.05	5.53
		C of V (%)	4.8	25.0	30.5	37.1	1.2	25.0	18.0
	+6 days P (CPF)	Cores 1	0.32	0.41	0.93	2.97	2.75	0.41	2.22
		Cores 2	0.16	0.32	1.11	2.45	2.36	0.32	1.97
		Average	0.24	0.37	1.02	2.71	2.56	0.37	2.09
		C of V (%)	34.5	12.3	8.7	9.7	7.6	12.3	5.9
	C/M (CPF)	Cores 1	0.60	0.27	2.25	1.91	2.63	0.27	2.26
		Cores 2	0.26	0.17	1.06	1.78	2.01	0.17	1.62
		Average	0.43	0.22	1.65	1.84	2.32	0.22	1.51
		C of V (%)	39.0	23.9	36.0	3.6	13.2	23.9	21.3

Key: +X days H= X days hessian plus 1 day in mould; Average= average of cores 1 and 2; C of V= coefficient of variation (%); Sub-surface (20-40mm)= average k value from slotted value (usually average); P= polythene; C/M= curing membrane; CPF= controlled permeability formwork

**Table B1.10 (b). Coefficient of air permeability k (m<sup>2</sup> x 10<sup>-16</sup>) for the 30 MPa OPC/GGBS concrete (top/bottom) - 12 months summer series**

Orientation	Curing regime	Average depth from outer surface (mm)					Surface (10mm)	Sub-surface (20-40mm)	
		5	10	20	30	40			
Top	+ 6 days P	Cores 1	3.35	2.25	0.90	1.87	2.29	2.25	1.68
		Cores 2	3.26	1.73	1.57	1.45	1.56	1.73	1.53
		Average	3.31	1.99	1.23	1.66	1.93	1.99	1.61
		C of V (%)	1.3	13.0	27.1	12.5	18.7	13.0	4.9
	C/M	Cores 1	3.65	2.58	1.45	1.40	2.58	2.58	1.81
		Cores 2	2.85	1.93	1.45	1.92	1.39	1.93	1.58
		Average	3.25	2.26	1.45	1.66	1.98	2.26	1.70
		C of V (%)	12.4	16.9	0.2	13.4	43.1	16.9	6.7
	+6 days P (CPF)	Cores 1	0.54	0.16	1.55	2.35	2.17	0.16	2.02
		Cores 2	0.19	0.22	0.81	2.00	2.33	0.22	1.72
		Average	0.37	0.19	1.18	2.18	2.25	0.19	1.87
		C of V (%)	47.3	15.3	31.0	8.0	3.7	15.3	8.2
	C/M (CPF)	Cores 1	0.28	0.26	1.55	2.16	2.41	0.26	2.04
		Cores 2	0.28	1.31	1.97	3.04	2.69	1.31	2.56
		Average	0.28	0.78	1.76	2.60	2.55	0.78	2.30
		C of V (%)	0.3	66.9	12.0	16.9	5.6	66.9	11.5
Bottom	+ 6 days P	Cores 1	6.81	3.37	1.99	3.36	3.00	3.37	2.78
		Cores 2	5.29	3.27	2.11	3.60	4.47	3.27	3.40
		Average	6.05	3.32	2.05	3.48	3.74	3.32	3.09
		C of V (%)	12.6	1.5	3.0	3.6	19.8	1.5	10.0
	C/M	Cores 1	3.87	3.80	0.89	1.43	2.52	3.80	1.61
		Cores 2	3.87	4.14	0.91	1.57	3.56	4.14	2.01
		Average	3.87	3.97	0.90	1.50	3.04	3.97	1.81
		C of V (%)	0.0	4.4	1.1	4.6	17.1	4.4	11.1
	+6 days P (CPF)	Cores 1	1.11	0.19	2.30	1.75	2.27	0.19	2.11
		Cores 2	0.33	0.22	0.99	1.84	2.98	0.22	1.94
		Average	0.72	0.21	1.64	1.80	2.63	0.21	2.02
		C of V (%)	54.2	7.1	39.8	2.5	13.5	7.1	4.2
	C/M (CPF)	Cores 1	0.10	0.18	1.08	1.95	2.55	0.18	1.86
		Cores 2	0.20	1.71	1.58	2.97	3.30	1.71	2.62
		Average	0.15	0.94	1.33	2.46	2.92	0.94	2.24
		C of V (%)	34.6	81.3	19.2	20.9	12.8	81.3	17.0

Key: +X days H= X days hessian plus 1 day in mould; Average= average of cores 1 and 2; C of V= coefficient of variation (%); Sub-surface (20-40mm)= average k value from slotted value (usually average); P= polythene; C/M= curing membrane; CPF= controlled permeability formwork

Table B1.11 (a) Sorptivity S (mm/min<sup>0.5</sup>) for the 30 MPa OPC concrete (east/west) - 3 months summer series

Orientation	Curnig regime		Average depth from outer surface (mm)					Surface (10mm)	Sub-surface (20-50mm)
			10	20	30	40	50		
East	No Cure	Cores 1	0.263	0.185	0.163	0.150	0.159	0.263	0.164
		Cores 2	0.272	0.176	0.155	0.152	0.150	0.272	0.158
		Average	<b>0.267</b>	<b>0.180</b>	<b>0.159</b>	<b>0.151</b>	<b>0.154</b>	<b>0.267</b>	<b>0.161</b>
		C of V (%)	1.7	2.6	2.6	0.6	2.9	1.7	1.9
	+2 days H	Cores 1	0.267	0.171	0.149	0.177	0.161	0.267	0.164
		Cores 2	0.276	0.185	0.152	0.169	0.159	0.276	0.166
		Average	<b>0.271</b>	<b>0.178</b>	<b>0.150</b>	<b>0.173</b>	<b>0.160</b>	<b>0.271</b>	<b>0.165</b>
		C of V (%)	1.7	3.8	1.2	2.3	0.8	1.7	0.5
	+4 days H	Cores 1	0.216	0.184	0.192	0.170	0.180	0.216	0.181
		Cores 2	0.224	0.175	0.166	0.150	0.145	0.224	0.159
		Average	<b>0.220</b>	<b>0.180</b>	<b>0.179</b>	<b>0.160</b>	<b>0.162</b>	<b>0.220</b>	<b>0.170</b>
		C of V (%)	1.8	2.6	7.2	6.3	10.7	1.8	6.6
	+6 days H	Cores 1	0.217	0.160	0.155	0.145	0.145	0.217	0.151
		Cores 2	0.201	0.168	0.152	0.159	0.142	0.201	0.155
		Average	<b>0.209</b>	<b>0.164</b>	<b>0.153</b>	<b>0.152</b>	<b>0.144</b>	<b>0.209</b>	<b>0.153</b>
		C of V (%)	3.9	2.6	0.7	4.6	1.0	3.9	1.4
West	No Cure	Cores 1	0.228	0.138	0.137	0.148	0.150	0.228	0.143
		Cores 2	0.218	0.150	0.149	0.154	0.143	0.218	0.149
		Average	<b>0.223</b>	<b>0.144</b>	<b>0.143</b>	<b>0.151</b>	<b>0.146</b>	<b>0.223</b>	<b>0.146</b>
		C of V (%)	2.2	4.1	4.0	2.2	2.3	2.2	2.0
	+2 days H	Cores 1	0.238	0.142	0.139	0.159	0.167	0.238	0.152
		Cores 2	0.230	0.155	0.149	0.155	0.156	0.230	0.154
		Average	<b>0.234</b>	<b>0.149</b>	<b>0.144</b>	<b>0.157</b>	<b>0.162</b>	<b>0.234</b>	<b>0.153</b>
		C of V (%)	1.7	4.2	3.3	1.3	3.5	1.7	0.5
	+4 days H	Cores 1	0.185	0.190	0.172	0.191	0.184	0.185	0.184
		Cores 2	0.210	0.174	0.154	0.131	0.135	0.210	0.149
		Average	<b>0.198</b>	<b>0.182</b>	<b>0.163</b>	<b>0.161</b>	<b>0.160</b>	<b>0.198</b>	<b>0.166</b>
		C of V (%)	6.4	4.5	5.3	18.5	15.1	6.4	10.7
	+6 days H	Cores 1	0.162	0.145	0.153	0.136	0.158	0.162	0.148
		Cores 2	0.173	0.150	0.142	0.139	0.139	0.173	0.142
		Average	<b>0.167</b>	<b>0.148</b>	<b>0.148</b>	<b>0.137</b>	<b>0.149</b>	<b>0.167</b>	<b>0.145</b>
		C of V (%)	3.4	1.7	3.6	1.2	6.6	3.4	1.9

Key: +X days H= X days hessian plus 1 day in mould; Average= average of cores 1 and 2; C of V= coefficient of variation (%); Sub-surface (20-50mm)= average k value from 20 to 50mm from surface; Bold value= plotted value (usually average)

Table B1.11 (b) Sorptivity  $s$  (mm/min<sup>0.5</sup>) for the 30 MPa OPC concrete (top/bottom) - 3 months summer series

Orientation	Curing regime	Average depth from outer surface (mm)					Surface (10mm)	Sub-surface (20-50mm)	
		10	20	30	40	50			
Top	No Cure	Cores 1	0.185	0.124	0.147	0.154	0.155	0.185	0.145
		Cores 2	0.199	0.144	0.154	0.122	0.121	0.199	0.135
		Average	<b>0.192</b>	<b>0.134</b>	<b>0.151</b>	<b>0.138</b>	<b>0.138</b>	<b>0.192</b>	<b>0.140</b>
		C of V (%)	3.6	7.3	2.2	11.4	12.4	3.6	3.5
	+2 days H	Cores 1	0.159	0.125	0.126	0.114	0.142	0.159	0.127
		Cores 2	0.180	0.141	0.136	0.131	0.123	0.180	0.133
		Average	<b>0.169</b>	<b>0.133</b>	<b>0.131</b>	<b>0.122</b>	<b>0.133</b>	<b>0.169</b>	<b>0.130</b>
		C of V (%)	6.2	6.1	3.7	7.1	7.3	6.2	2.3
	+4 days H	Cores 1	0.116	0.152	0.159	0.150	0.162	0.116	0.155
		Cores 2	0.175	0.132	0.131	0.119	0.102	0.175	0.121
		Average	<b>0.146</b>	<b>0.142</b>	<b>0.145</b>	<b>0.134</b>	<b>0.132</b>	<b>0.146</b>	<b>0.138</b>
		C of V (%)	20.4	6.9	9.4	11.5	22.8	20.4	12.5
	+6 days H	Cores 1	0.134	0.147	0.155	0.144	0.162	0.134	0.152
		Cores 2	0.158	0.133	0.115	0.121	0.109	0.158	0.119
		Average	<b>0.146</b>	<b>0.140</b>	<b>0.135</b>	<b>0.132</b>	<b>0.135</b>	<b>0.146</b>	<b>0.136</b>
		C of V (%)	8.2	5.2	14.8	8.5	19.7	8.2	12.0
Bottom	No Cure	Cores 1	0.247	0.189	0.175	0.192	0.158	0.247	0.178
		Cores 2	0.252	0.212	0.186	0.176	0.165	0.252	0.185
		Average	<b>0.250</b>	<b>0.200</b>	<b>0.181</b>	<b>0.184</b>	<b>0.162</b>	<b>0.250</b>	<b>0.182</b>
		C of V (%)	1.2	5.8	2.9	4.3	2.3	1.2	1.7
	+2 days H	Cores 1	0.261	0.157	0.168	0.144	0.151	0.261	0.155
		Cores 2	0.257	0.154	0.144	0.140	0.130	0.257	0.142
		Average	<b>0.259</b>	<b>0.156</b>	<b>0.156</b>	<b>0.142</b>	<b>0.141</b>	<b>0.259</b>	<b>0.149</b>
		C of V (%)	0.7	0.9	7.5	1.2	7.4	0.7	4.2
	+4 days H	Cores 1	0.127	0.191	0.190	0.177	0.177	0.127	0.184
		Cores 2	0.145	0.132	0.121	0.125	0.116	0.145	0.124
		Average	<b>0.136</b>	<b>0.161</b>	<b>0.155</b>	<b>0.151</b>	<b>0.146</b>	<b>0.136</b>	<b>0.154</b>
		C of V (%)	6.7	18.2	22.0	17.1	20.8	6.7	19.5
	+6 days H	Cores 1	0.211	0.184	0.192	0.145	0.174	0.211	0.174
		Cores 2	0.224	0.166	0.152	0.121	0.101	0.224	0.135
		Average	<b>0.218</b>	<b>0.175</b>	<b>0.172</b>	<b>0.133</b>	<b>0.137</b>	<b>0.218</b>	<b>0.154</b>
		C of V (%)	3.1	5.2	11.6	9.2	26.4	3.1	12.5

Key: +X days H= X days hessian plus 1 day in mould; Average= average of cores 1 and 2; C of V= coefficient of variation (%); Sub-surface (20-50mm)= average k value from 20 to 50mm from surface; Bold value= plotted value (usually average)

Table B1.12 (a) Sorptivity S (mm/min<sup>0.5</sup>) for the 30 MPa OPC concrete (east/west) - 12 months summer series

Orientation	Curnig regime		Average depth from outer surface (mm)					Surface (10mm)	Sub-surface (20-40mm)
			5	10	20	30	40		
East	No Cure	Cores 1	0.103	0.112	0.191	0.177	0.155	0.112	0.174
		Cores 2	0.069	0.110	0.153	0.211	0.176	0.110	0.180
		Average	<b>0.086</b>	<b>0.111</b>	<b>0.172</b>	<b>0.194</b>	<b>0.166</b>	<b>0.111</b>	<b>0.177</b>
		C of V (%)	19.5	1.0	11.0	8.6	6.3	1.0	1.6
	+2 days H	Cores 1	0.124	0.124	0.215	0.195	0.174	0.124	0.195
		Cores 2	0.078	0.086	0.168	0.196	0.176	0.086	0.180
		Average	<b>0.101</b>	<b>0.105</b>	<b>0.192</b>	<b>0.195</b>	<b>0.175</b>	<b>0.105</b>	<b>0.187</b>
		C of V (%)	22.7	18.3	12.2	0.1	0.4	18.3	4.0
	+4 days H	Cores 1	0.090	0.104	0.176	0.185	0.170	0.104	0.177
		Cores 2	0.096	0.109	0.171	0.184	0.190	0.109	0.182
		Average	<b>0.093</b>	<b>0.107</b>	<b>0.173</b>	<b>0.184</b>	<b>0.180</b>	<b>0.107</b>	<b>0.179</b>
		C of V (%)	3.5	2.1	1.6	0.3	5.4	2.1	1.2
	+6 days H	Cores 1	0.126	0.124	0.198	0.198	0.188	0.124	0.194
		Cores 2	0.106	0.096	0.179	0.183	0.172	0.096	0.178
		Average	<b>0.116</b>	<b>0.110</b>	<b>0.188</b>	<b>0.190</b>	<b>0.180</b>	<b>0.110</b>	<b>0.186</b>
		C of V (%)	8.6	13.1	5.0	3.9	4.4	13.1	4.4
West	No Cure	Cores 1	0.073	0.075	0.110	0.193	0.176	0.075	0.159
		Cores 2	0.062	0.062	0.155	0.180	0.167	0.062	0.167
		Average	<b>0.067</b>	<b>0.068</b>	<b>0.133</b>	<b>0.186</b>	<b>0.171</b>	<b>0.068</b>	<b>0.163</b>
		C of V (%)	7.7	9.6	17.3	3.4	2.4	9.6	2.5
	+2 days H	Cores 1	0.086	0.083	0.176	0.178	0.190	0.083	0.182
		Cores 2	0.086	0.096	0.174	0.186	0.181	0.096	0.181
		Average	<b>0.086</b>	<b>0.090</b>	<b>0.175</b>	<b>0.182</b>	<b>0.186</b>	<b>0.090</b>	<b>0.181</b>
		C of V (%)	0.1	7.1	0.5	2.2	2.5	7.1	0.3
	+4 days H	Cores 1	0.087	0.117	0.162	0.205	0.181	0.117	0.183
		Cores 2	0.073	0.081	0.145	0.168	0.187	0.081	0.167
		Average	<b>0.080</b>	<b>0.099</b>	<b>0.154</b>	<b>0.187</b>	<b>0.184</b>	<b>0.099</b>	<b>0.175</b>
		C of V (%)	9.1	18.6	5.5	10.0	1.6	18.6	4.6
	+6 days H	Cores 1	0.101	0.105	0.180	0.181	0.177	0.105	0.179
		Cores 2	0.086	0.104	0.189	0.181	0.180	0.104	0.183
		Average	<b>0.093</b>	<b>0.105</b>	<b>0.184</b>	<b>0.181</b>	<b>0.178</b>	<b>0.105</b>	<b>0.181</b>
		C of V (%)	7.7	0.5	2.5	0.2	0.9	0.5	1.0

Key: +X days H= X days hessian plus 1 day in mould; Average= average of cores 1 and 2; C of V= coefficient of variation (%); Sub-surface (10-40mm)= average k value from 10 to 40mm from surface; Bold value= plotted value (usually average)

Table B1.12 (b) Sorptivity S (mm/min<sup>0.5</sup>) for the 30 MPa OPC concrete (top/bottom) - 12 months summer series

Orientation	Curing regime	Average depth from outer surface (mm)					Surface (10mm)	Sub-surface (20-40mm)	
		5	10	20	30	40			
Top	No Cure	Cores 1	0.059	0.086	0.147	0.154	0.153	0.086	0.151
		Cores 2	0.063	0.070	0.172	0.166	0.166	0.070	0.168
		Average	<b>0.061</b>	<b>0.078</b>	<b>0.159</b>	<b>0.160</b>	<b>0.160</b>	<b>0.078</b>	<b>0.160</b>
		C of V (%)	3.3	10.4	7.8	3.7	4.0	10.4	5.2
	+2 days H	Cores 1	0.063	0.066	0.141	0.131	0.142	0.066	0.138
		Cores 2	0.056	0.059	0.143	0.149	0.157	0.059	0.150
		Average	<b>0.059</b>	<b>0.063</b>	<b>0.142</b>	<b>0.140</b>	<b>0.150</b>	<b>0.063</b>	<b>0.144</b>
		C of V (%)	5.8	5.1	0.9	6.3	5.2	5.1	4.2
	+4 days H	Cores 1	0.075	0.078	0.134	0.145	0.163	0.078	0.147
		Cores 2	0.104	0.064	0.171	0.167	0.155	0.064	0.164
		Average	<b>0.090</b>	<b>0.071</b>	<b>0.153</b>	<b>0.156</b>	<b>0.159</b>	<b>0.071</b>	<b>0.156</b>
		C of V (%)	16.5	9.7	12.2	7.0	2.4	9.7	5.5
	+6 days H	Cores 1	0.154	0.088	0.145	0.158	0.139	0.088	0.148
		Cores 2	0.086	0.092	0.170	0.164	0.148	0.092	0.161
		Average	<b>0.120</b>	<b>0.090</b>	<b>0.158</b>	<b>0.161</b>	<b>0.144</b>	<b>0.090</b>	<b>0.154</b>
		C of V (%)	28.3	2.4	7.9	2.0	3.1	2.4	4.3
Bottom	No Cure	Cores 1	0.073	0.082	0.152	0.155	0.157	0.082	0.155
		Cores 2	0.083	0.097	0.180	0.155	0.181	0.097	0.172
		Average	<b>0.078</b>	<b>0.089</b>	<b>0.166</b>	<b>0.155</b>	<b>0.169</b>	<b>0.089</b>	<b>0.163</b>
		C of V (%)	6.6	8.7	8.6	0.1	7.0	8.7	5.4
	+2 days H	Cores 1	0.089	0.115	0.122	0.174	0.140	0.115	0.145
		Cores 2	0.089	0.085	0.135	0.159	0.160	0.085	0.151
		Average	<b>0.089</b>	<b>0.100</b>	<b>0.129</b>	<b>0.167</b>	<b>0.150</b>	<b>0.100</b>	<b>0.148</b>
		C of V (%)	0.1	15.1	5.0	4.6	6.8	15.1	2.0
	+4 days H	Cores 1	0.080	0.070	0.155	0.145	0.149	0.070	0.150
		Cores 2	0.105	0.074	0.176	0.178	0.180	0.074	0.178
		Average	<b>0.092</b>	<b>0.072</b>	<b>0.165</b>	<b>0.162</b>	<b>0.165</b>	<b>0.072</b>	<b>0.164</b>
		C of V (%)	13.6	3.0	6.2	10.5	9.5	3.0	8.7
	+6 days H	Cores 1	0.120	0.086	0.176	0.159	0.175	0.086	0.170
		Cores 2	0.087	0.078	0.176	0.199	0.167	0.078	0.181
		Average	<b>0.104</b>	<b>0.082</b>	<b>0.176</b>	<b>0.179</b>	<b>0.171</b>	<b>0.082</b>	<b>0.175</b>
		C of V (%)	16.2	4.7	0.2	11.2	2.1	4.7	3.2

Key: +X days H= X days hessian plus 1 day in mould; Average= average of cores 1 and 2; C of V= coefficient of variation (%); Sub-surface (10-40mm)= average k value from 10 to 40mm from surface; Bold value= plotted value (usually average)

**Table B1.13 (a) Sorptivity S (mm/min<sup>0.5</sup>) for the 50 MPa OPC concrete (east/west) - 3 months summer series**

Orientation	Curnig regime		Average depth from outer surface (mm)					Surface (10mm)	Sub-surface (20-50mm)
			10	20	30	40	50		
East	No Cure	Cores 1	0.131	0.149	0.116	0.115	0.110	0.131	0.123
		Cores 2	0.150	0.126	0.132	0.126	0.120	0.150	0.126
		Average	<b>0.140</b>	<b>0.137</b>	<b>0.124</b>	<b>0.120</b>	<b>0.115</b>	<b>0.140</b>	<b>0.124</b>
		C of V (%)	6.6	8.4	6.6	4.2	4.6	6.6	1.4
	+2 days H	Cores 1	0.124	0.112	0.117	0.124	0.121	0.124	0.119
		Cores 2	0.142	0.133	0.124	0.118	0.110	0.142	0.121
		Average	<b>0.133</b>	<b>0.122</b>	<b>0.121</b>	<b>0.121</b>	<b>0.115</b>	<b>0.133</b>	<b>0.120</b>
		C of V (%)	6.8	8.6	2.9	2.7	4.4	6.8	1.2
	+4 days H	Cores 1	0.131	0.144	0.139	0.126	0.148	0.131	0.139
		Cores 2	0.126	0.111	0.100	0.105	0.101	0.126	0.104
		Average	<b>0.128</b>	<b>0.127</b>	<b>0.120</b>	<b>0.116</b>	<b>0.124</b>	<b>0.128</b>	<b>0.122</b>
		C of V (%)	2.1	12.7	16.2	9.0	19.0	2.1	14.3
	+6 days H	Cores 1	0.127	0.134	0.142	0.119	0.129	0.127	0.131
		Cores 2	0.140	0.120	0.101	0.122	0.111	0.140	0.114
		Average	<b>0.134</b>	<b>0.127</b>	<b>0.122</b>	<b>0.121</b>	<b>0.120</b>	<b>0.134</b>	<b>0.122</b>
		C of V (%)	4.9	5.5	16.9	1.3	7.7	4.9	7.2
West	No Cure	Cores 1	0.112	0.109	0.134	0.115	0.126	0.112	0.121
		Cores 2	0.137	0.133	0.121	0.125	0.127	0.137	0.127
		Average	<b>0.124</b>	<b>0.121</b>	<b>0.128</b>	<b>0.120</b>	<b>0.127</b>	<b>0.124</b>	<b>0.124</b>
		C of V (%)	9.8	9.8	5.1	4.2	0.2	9.8	2.1
	+2 days H	Cores 1	0.098	0.131	0.127	0.129	0.142	0.098	0.132
		Cores 2	0.165	0.129	0.128	0.120	0.101	0.165	0.119
		Average	<b>0.131</b>	<b>0.130</b>	<b>0.127</b>	<b>0.125</b>	<b>0.122</b>	<b>0.131</b>	<b>0.126</b>
		C of V (%)	25.7	0.7	0.2	3.6	16.8	25.7	5.1
	+4 days H	Cores 1	0.085	0.137	0.140	0.137	0.142	0.085	0.139
		Cores 2	0.149	0.133	0.108	0.103	0.100	0.149	0.111
		Average	<b>0.117</b>	<b>0.135</b>	<b>0.124</b>	<b>0.120</b>	<b>0.121</b>	<b>0.117</b>	<b>0.125</b>
		C of V (%)	27.1	1.6	13.0	14.5	17.1	27.1	11.3
	+6 days H	Cores 1	0.087	0.147	0.144	0.136	0.135	0.087	0.141
		Cores 2	0.159	0.120	0.113	0.112	0.101	0.159	0.112
		Average	<b>0.123</b>	<b>0.133</b>	<b>0.129</b>	<b>0.124</b>	<b>0.118</b>	<b>0.123</b>	<b>0.126</b>
		C of V (%)	29.2	10.0	12.1	9.6	14.3	29.2	11.4

Key: +X days H= X days hessian plus 1 day in mould; Average= average of cores 1 and 2; C of V= coefficient of variation (%); Sub-surface (20-50mm)= average k value from 20 to 50mm from surface; Bold value= plotted value (usually average)

Table B1.13 (b) Sorptivity  $S$  (mm/min<sup>0.5</sup>) for the 50 MPa OPC concrete (top/bottom) - 3 months summer series

Orientation	Curing regime	Average depth from outer surface (mm)					Surface (10mm)	Sub-surface (20-50mm)	
		10	20	30	40	50			
Top	No Cure	Cores 1	0.063	0.127	0.125	0.125	0.125	0.063	0.125
		Cores 2	0.128	0.122	0.112	0.101	0.100	0.128	0.109
		Average	<b>0.095</b>	<b>0.124</b>	<b>0.118</b>	<b>0.113</b>	<b>0.112</b>	<b>0.095</b>	<b>0.117</b>
		C of V (%)	34.3	2.2	5.3	10.9	11.0	34.3	7.2
	+2 days H	Cores 1	0.083	0.112	0.122	0.123	0.116	0.083	0.118
		Cores 2	0.121	0.118	0.111	0.098	0.091	0.121	0.105
		Average	<b>0.102</b>	<b>0.115</b>	<b>0.116</b>	<b>0.111</b>	<b>0.103</b>	<b>0.102</b>	<b>0.111</b>
		C of V (%)	18.9	2.6	4.5	11.0	12.2	18.9	6.1
	+4 days H	Cores 1	0.090	0.127	0.145	0.134	0.139	0.090	0.136
		Cores 2	0.155	0.118	0.100	0.098	0.092	0.155	0.102
		Average	<b>0.122</b>	<b>0.123</b>	<b>0.123</b>	<b>0.116</b>	<b>0.116</b>	<b>0.122</b>	<b>0.119</b>
		C of V (%)	26.4	3.5	18.1	15.4	20.3	26.4	14.2
	+6 days H	Cores 1	0.099	0.143	0.127	0.135	0.128	0.099	0.133
		Cores 2	0.143	0.122	0.124	0.111	0.105	0.143	0.116
		Average	<b>0.121</b>	<b>0.132</b>	<b>0.125</b>	<b>0.123</b>	<b>0.117</b>	<b>0.121</b>	<b>0.124</b>
		C of V (%)	18.1	7.9	1.4	9.6	9.8	18.1	7.1
Bottom	No Cure	Cores 1	0.151	0.128	0.160	0.131	0.141	0.151	0.140
		Cores 2	0.155	0.144	0.112	0.114	0.101	0.155	0.118
		Average	<b>0.153</b>	<b>0.136</b>	<b>0.136</b>	<b>0.122</b>	<b>0.121</b>	<b>0.153</b>	<b>0.129</b>
		C of V (%)	1.6	6.0	17.6	6.9	16.4	1.6	8.5
	+2 days H	Cores 1	0.162	0.139	0.133	0.122	0.124	0.162	0.130
		Cores 2	0.179	0.146	0.138	0.129	0.122	0.179	0.134
		Average	<b>0.170</b>	<b>0.143</b>	<b>0.136</b>	<b>0.126</b>	<b>0.123</b>	<b>0.170</b>	<b>0.132</b>
		C of V (%)	4.9	2.5	2.1	2.6	1.1	4.9	1.6
	+4 days H	Cores 1	0.145	0.139	0.137	0.138	0.146	0.145	0.140
		Cores 2	0.155	0.143	0.132	0.131	0.120	0.155	0.132
		Average	<b>0.150</b>	<b>0.141</b>	<b>0.135</b>	<b>0.134</b>	<b>0.133</b>	<b>0.150</b>	<b>0.136</b>
		C of V (%)	3.4	1.1	1.8	2.5	9.7	3.4	3.1
	+6 days H	Cores 1	0.137	0.135	0.126	0.139	0.138	0.137	0.135
		Cores 2	0.142	0.131	0.122	0.112	0.102	0.142	0.117
		Average	<b>0.140</b>	<b>0.133</b>	<b>0.124</b>	<b>0.126</b>	<b>0.120</b>	<b>0.140</b>	<b>0.126</b>
		C of V (%)	1.8	1.4	2.0	10.6	14.9	1.8	7.1

Key: +X days H= X days hessian plus 1 day in mould; Average= average of cores 1 and 2; C of V= coefficient of variation (%); Sub-surface (20-50mm)= average k value from 20 to 50mm from surface; Bold value= plotted value (usually average)

Table B1.14 (a) Sorptivity S (mm/min<sup>0.5</sup>) for the 50 MPa OPC concrete (east/west) - 12 months summer series

Orientation	Curnig regime		Average depth from outer surface (mm)					Surface (10mm)	Sub-surface (20-40mm)
			5	10	20	30	40		
East	No Cure	Cores 1	0.057	0.055	0.107	0.101	0.103	0.055	0.104
		Cores 2	0.054	0.060	0.108	0.106	0.115	0.060	0.109
		Average	<b>0.056</b>	<b>0.057</b>	<b>0.107</b>	<b>0.104</b>	<b>0.109</b>	<b>0.057</b>	<b>0.107</b>
		C of V (%)	3.0	3.7	0.6	2.3	5.2	3.7	2.7
	+2 days H	Cores 1	0.044	0.051	0.095	0.100	0.098	0.051	0.098
		Cores 2	0.052	0.051	0.098	0.108	0.103	0.051	0.103
		Average	<b>0.048</b>	<b>0.051</b>	<b>0.096</b>	<b>0.104</b>	<b>0.100</b>	<b>0.051</b>	<b>0.100</b>
		C of V (%)	8.2	0.7	2.0	3.7	2.4	0.7	2.7
	+4 days H	Cores 1	0.053	0.060	0.112	0.124	0.117	0.060	0.118
		Cores 2	0.053	0.060	0.112	0.124	0.117	0.060	0.118
		Average	<b>0.053</b>	<b>0.060</b>	<b>0.112</b>	<b>0.124</b>	<b>0.117</b>	<b>0.060</b>	<b>0.118</b>
		C of V (%)	0.0	0.0	0.0	0.0	0.0	0.0	0.0
	+6 days H	Cores 1	0.047	0.056	0.107	0.110	0.104	0.056	0.107
		Cores 2	0.039	0.061	0.112	0.119	0.115	0.061	0.116
		Average	<b>0.043</b>	<b>0.058</b>	<b>0.110</b>	<b>0.115</b>	<b>0.110</b>	<b>0.058</b>	<b>0.111</b>
		C of V (%)	9.4	4.6	2.4	4.1	5.0	4.6	3.8
West	No Cure	Cores 1	0.055	0.051	0.099	0.055	0.113	0.051	0.089
		Cores 2	0.054	0.060	0.108	0.106	0.115	0.060	0.109
		Average	<b>0.054</b>	<b>0.055</b>	<b>0.104</b>	<b>0.080</b>	<b>0.114</b>	<b>0.055</b>	<b>0.099</b>
		C of V (%)	0.7	7.3	4.3	31.8	0.8	7.3	10.4
	+2 days H	Cores 1	0.045	0.047	0.096	0.098	0.099	0.047	0.098
		Cores 2	0.058	0.062	0.100	0.113	0.093	0.062	0.102
		Average	<b>0.051</b>	<b>0.054</b>	<b>0.098</b>	<b>0.105</b>	<b>0.096</b>	<b>0.054</b>	<b>0.100</b>
		C of V (%)	12.5	13.1	2.4	6.8	3.2	13.1	2.1
	+4 days H	Cores 1	0.060	0.057	0.108	0.119	0.104	0.057	0.110
		Cores 2	0.060	0.057	0.108	0.119	0.104	0.057	0.110
		Average	<b>0.060</b>	<b>0.057</b>	<b>0.108</b>	<b>0.119</b>	<b>0.104</b>	<b>0.057</b>	<b>0.110</b>
		C of V (%)	0.0	0.0	0.0	0.0	0.0	0.0	0.0
	+6 days H	Cores 1	0.050	0.063	0.112	0.099	0.103	0.063	0.104
		Cores 2	0.045	0.060	0.116	0.104	0.112	0.060	0.111
		Average	<b>0.047</b>	<b>0.062</b>	<b>0.114</b>	<b>0.101</b>	<b>0.107</b>	<b>0.062</b>	<b>0.108</b>
		C of V (%)	4.9	2.6	2.0	2.7	4.3	2.6	3.0

Key: +X days H= X days hessian plus 1 day in mould; Average= average of cores 1 and 2; C of V= coefficient of variation (%); Sub-surface (10-40mm)= average k value from 10 to 40mm from surface; Bold value= plotted value (usually average)

**Table B1.14 (b) Sorptivity S (mm/min<sup>0.5</sup>) for the 50 MPa OPC concrete (top/bottom) - 12 months summer series**

Orientation	Curing regime		Average depth from outer surface (mm)					Surface (10mm)	Sub-surface (20-40mm)
			5	10	20	30	40		
Top	No Cure	Cores 1	0.060	0.069	0.102	0.117	0.110	0.069	0.109
		Cores 2	0.067	0.060	0.104	0.114	0.108	0.060	0.109
		Average	<b>0.063</b>	<b>0.065</b>	<b>0.103</b>	<b>0.115</b>	<b>0.109</b>	<b>0.065</b>	<b>0.109</b>
		C of V (%)	5.0	7.0	1.1	1.3	0.6	7.0	0.3
	+2 days H	Cores 1	0.068	0.060	0.104	0.089	0.104	0.060	0.099
		Cores 2	0.054	0.110	0.057	0.113	0.105	0.110	0.092
		Average	<b>0.061</b>	<b>0.085</b>	<b>0.081</b>	<b>0.101</b>	<b>0.105</b>	<b>0.085</b>	<b>0.095</b>
		C of V (%)	11.7	29.6	29.4	11.8	0.3	29.6	4.0
	+4 days H	Cores 1	0.062	0.060	0.116	0.111	0.112	0.060	0.113
		Cores 2	0.057	0.061	0.109	0.106	0.107	0.061	0.107
		Average	<b>0.059</b>	<b>0.060</b>	<b>0.112</b>	<b>0.108</b>	<b>0.109</b>	<b>0.060</b>	<b>0.110</b>
		C of V (%)	3.8	0.5	3.1	2.1	2.3	0.5	2.5
	+6 days H	Cores 1	0.045	0.049	0.115	0.114	0.109	0.049	0.113
		Cores 2	0.049	0.049	0.103	0.097	0.103	0.049	0.101
		Average	<b>0.047</b>	<b>0.049</b>	<b>0.109</b>	<b>0.105</b>	<b>0.106</b>	<b>0.049</b>	<b>0.107</b>
		C of V (%)	4.7	0.3	5.3	8.2	3.2	0.3	5.6
Bottom	No Cure	Cores 1	0.077	0.076	0.120	0.111	0.109	0.076	0.113
		Cores 2	0.055	0.065	0.121	0.108	0.121	0.065	0.117
		Average	<b>0.066</b>	<b>0.070</b>	<b>0.120</b>	<b>0.110</b>	<b>0.115</b>	<b>0.070</b>	<b>0.115</b>
		C of V (%)	16.1	7.9	0.3	1.3	4.9	7.9	1.3
	+2 days H	Cores 1	0.059	0.063	0.099	0.101	0.105	0.063	0.102
		Cores 2	0.065	0.109	0.068	0.117	0.118	0.109	0.101
		Average	<b>0.062</b>	<b>0.086</b>	<b>0.084</b>	<b>0.109</b>	<b>0.112</b>	<b>0.086</b>	<b>0.101</b>
		C of V (%)	5.0	27.0	18.1	7.5	5.9	27.0	0.1
	+4 days H	Cores 1	0.055	0.059	0.113	0.117	0.124	0.059	0.118
		Cores 2	0.045	0.050	0.103	0.099	0.095	0.050	0.099
		Average	<b>0.050</b>	<b>0.055</b>	<b>0.108</b>	<b>0.108</b>	<b>0.109</b>	<b>0.055</b>	<b>0.109</b>
		C of V (%)	9.8	8.8	4.7	8.4	13.5	8.8	8.9
	+6 days H	Cores 1	0.056	0.068	0.105	0.115	0.111	0.068	0.110
		Cores 2	0.048	0.050	0.098	0.098	0.092	0.050	0.096
		Average	<b>0.052</b>	<b>0.059</b>	<b>0.102</b>	<b>0.107</b>	<b>0.101</b>	<b>0.059</b>	<b>0.103</b>
		C of V (%)	7.1	15.2	3.4	7.8	9.4	15.2	6.9

Key: +X days H= X days hessian plus 1 day in mould; Average= average of cores 1 and 2; C of V= coefficient of variation (%); Sub-surface (10-40mm)= average k value from 10 to 40mm from surface; Bold value= plotted value (usually average)

**Table B1.15 (a) Sorptivity S (mm/min<sup>0.5</sup>) for the 30 MPa OPC/GGBS concrete (east/west) - 3 months summer series**

Orientation	Curnig regime		Average depth from outer surface (mm)					Surface (10mm)	Sub-surface (20-50mm)
			10	20	30	40	50		
East	No Cure	Cores 1	0.350	0.323	0.320	0.289	0.253	0.350	0.296
		Cores 2	0.355	0.327	0.326	0.275	0.263	0.355	0.298
		Average	<b>0.353</b>	<b>0.325</b>	<b>0.323</b>	<b>0.282</b>	<b>0.258</b>	<b>0.353</b>	<b>0.297</b>
		C of V (%)	0.8	0.6	0.8	2.4	1.8	0.8	0.2
	+2 days H	Cores 1	0.235	0.276	0.249	0.253	0.215	0.235	0.248
		Cores 2	0.275	0.211	0.200	0.179	0.166	0.275	0.189
		Average	<b>0.255</b>	<b>0.244</b>	<b>0.224</b>	<b>0.216</b>	<b>0.191</b>	<b>0.255</b>	<b>0.219</b>
		C of V (%)	7.9	13.3	10.8	17.2	12.9	7.9	13.5
	+4 days H	Cores 1	0.168	0.170	0.177	0.146	0.157	0.168	0.162
		Cores 2	0.157	0.145	0.134	0.126	0.123	0.157	0.132
		Average	<b>0.163</b>	<b>0.157</b>	<b>0.155</b>	<b>0.136</b>	<b>0.140</b>	<b>0.163</b>	<b>0.147</b>
		C of V (%)	3.5	7.7	13.6	7.6	11.9	3.5	10.2
	+6 days H	Cores 1	0.156	0.135	0.148	0.131	0.130	0.156	0.136
		Cores 2	0.149	0.141	0.124	0.121	0.120	0.149	0.127
		Average	<b>0.152</b>	<b>0.138</b>	<b>0.136</b>	<b>0.126</b>	<b>0.125</b>	<b>0.152</b>	<b>0.131</b>
		C of V (%)	2.4	2.3	8.6	4.0	3.8	2.4	3.5
West	No Cure	Cores 1	0.216	0.193	0.200	0.180	0.203	0.216	0.194
		Cores 2	0.221	0.185	0.171	0.167	0.130	0.221	0.163
		Average	<b>0.219</b>	<b>0.189</b>	<b>0.185</b>	<b>0.174</b>	<b>0.167</b>	<b>0.219</b>	<b>0.178</b>
		C of V (%)	1.1	2.1	7.7	4.0	21.9	1.1	8.6
	+2 days H	Cores 1	0.206	0.186	0.178	0.161	0.188	0.206	0.178
		Cores 2	0.211	0.183	0.176	0.176	0.131	0.211	0.167
		Average	<b>0.209</b>	<b>0.185</b>	<b>0.177</b>	<b>0.168</b>	<b>0.160</b>	<b>0.209</b>	<b>0.172</b>
		C of V (%)	1.2	0.6	0.5	4.4	17.8	1.2	3.3
	+4 days H	Cores 1	0.128	0.135	0.147	0.167	0.157	0.128	0.151
		Cores 2	0.169	0.126	0.111	0.078	0.087	0.169	0.100
		Average	<b>0.149</b>	<b>0.130</b>	<b>0.129</b>	<b>0.123</b>	<b>0.122</b>	<b>0.149</b>	<b>0.126</b>
		C of V (%)	13.9	3.5	14.1	36.4	28.5	13.9	20.3
	+6 days H	Cores 1	0.106	0.110	0.134	0.126	0.134	0.106	0.126
		Cores 2	0.125	0.108	0.090	0.090	0.094	0.125	0.095
		Average	<b>0.116</b>	<b>0.109</b>	<b>0.112</b>	<b>0.108</b>	<b>0.114</b>	<b>0.116</b>	<b>0.111</b>
		C of V (%)	8.5	1.0	19.6	16.7	17.5	8.5	13.8

**Key:** +X days H= X days hessian plus 1 day in mould; Average= average of cores 1 and 2; C of V= coefficient of variation (%); Sub-surface (20-50mm)= average k value from 20 to 50mm from surface; Bold value= plotted value (usually average)

**Table B1.15 (b) Sorptivity S (mm/min<sup>0.5</sup>) for the 30 MPa OPC/GGBS Concrete (top/bottom) - 3 months summer series**

Orientation	Curing regime		Average depth from outer surface (mm)					Surface (10mm)	Sub-surface (20-50mm)
			10	20	30	40	50		
Top	No Cure	Cores 1	0.131	0.141	0.176	0.177	0.175	0.131	0.167
		Cores 2	0.160	0.147	0.110	0.101	0.110	0.160	0.117
		Average	<b>0.145</b>	<b>0.144</b>	<b>0.143</b>	<b>0.139</b>	<b>0.142</b>	<b>0.145</b>	<b>0.142</b>
		C of V (%)	10.2	1.9	23.1	27.2	22.7	10.2	17.7
	+2 days H	Cores 1	0.136	0.149	0.138	0.190	0.195	0.136	0.168
		Cores 2	0.198	0.146	0.137	0.130	0.120	0.198	0.133
		Average	<b>0.167</b>	<b>0.147</b>	<b>0.138</b>	<b>0.160</b>	<b>0.157</b>	<b>0.167</b>	<b>0.151</b>
		C of V (%)	18.7	1.2	0.6	18.6	23.7	18.7	11.6
	+4 days H	Cores 1	0.122	0.121	0.129	0.151	0.158	0.122	0.140
		Cores 2	0.136	0.133	0.121	0.100	0.092	0.136	0.112
		Average	<b>0.129</b>	<b>0.127</b>	<b>0.125</b>	<b>0.125</b>	<b>0.125</b>	<b>0.129</b>	<b>0.126</b>
		C of V (%)	5.4	4.9	3.2	20.3	26.3	5.4	11.2
	+6 days H	Cores 1	0.090	0.129	0.144	0.177	0.160	0.090	0.152
		Cores 2	0.146	0.118	0.112	0.102	0.114	0.146	0.111
		Average	<b>0.118</b>	<b>0.123</b>	<b>0.128</b>	<b>0.139</b>	<b>0.137</b>	<b>0.118</b>	<b>0.132</b>
		C of V (%)	23.8	4.7	12.4	26.8	16.9	23.8	15.6
Bottom	No Cure	Cores 1	0.133	0.270	0.178	0.226	0.188	0.133	0.215
		Cores 2	0.290	0.224	0.241	0.201	0.186	0.290	0.213
		Average	<b>0.211</b>	<b>0.247</b>	<b>0.209</b>	<b>0.213</b>	<b>0.187</b>	<b>0.211</b>	<b>0.214</b>
		C of V (%)	37.1	9.4	15.1	5.8	0.3	37.1	0.5
	+2 days H	Cores 1	0.119	0.167	0.186	0.192	0.184	0.119	0.182
		Cores 2	0.214	0.136	0.110	0.100	0.112	0.214	0.114
		Average	<b>0.166</b>	<b>0.152</b>	<b>0.148</b>	<b>0.146</b>	<b>0.148</b>	<b>0.166</b>	<b>0.148</b>
		C of V (%)	28.7	10.2	25.7	31.5	24.3	28.7	22.8
	+4 days H	Cores 1	0.139	0.148	0.147	0.150	0.157	0.139	0.150
		Cores 2	0.162	0.143	0.133	0.121	0.122	0.162	0.130
		Average	<b>0.151</b>	<b>0.146</b>	<b>0.140</b>	<b>0.136</b>	<b>0.139</b>	<b>0.151</b>	<b>0.140</b>
		C of V (%)	7.8	1.6	5.2	10.7	12.5	7.8	7.4
	+6 days H	Cores 1	0.131	0.157	0.160	0.138	0.140	0.131	0.149
		Cores 2	0.163	0.126	0.112	0.113	0.121	0.163	0.118
		Average	<b>0.147</b>	<b>0.141</b>	<b>0.136</b>	<b>0.125</b>	<b>0.130</b>	<b>0.147</b>	<b>0.133</b>
		C of V (%)	10.9	11.2	17.7	9.8	7.1	10.9	11.5

Key: +X days H= X days hessian plus 1 day in mould; Average= average of cores 1 and 2; C of V= coefficient of variation (%); Sub-surface (20-50mm)= average k value from 20 to 50mm from surface; Bold value= plotted value (usually average)

Table B1.16 (a) Sorptivity S (mm/min<sup>0.5</sup>) for the 30 MPa OPC/GGBS concrete (east/west) - 12 months summer series

Orientation	Curnig regime		Average depth from outer surface (mm)					Surface (10mm)	Sub-surface (20-40mm)
			5	10	20	30	40		
East	No Cure	Cores 1	0.111	0.289	0.224	0.180	0.169	0.289	0.191
		Cores 2	0.111	0.268	0.262	0.200	0.177	0.268	0.213
		Average	<b>0.111</b>	<b>0.278</b>	<b>0.243</b>	<b>0.190</b>	<b>0.173</b>	<b>0.278</b>	<b>0.202</b>
		C of V (%)	0.0	3.8	7.7	5.5	2.3	3.8	5.5
	+2 days H	Cores 1	0.115	0.140	0.115	0.116	0.143	0.140	0.125
		Cores 2	0.106	0.156	0.152	0.172	0.163	0.156	0.162
		Average	<b>0.110</b>	<b>0.148</b>	<b>0.134</b>	<b>0.144</b>	<b>0.153</b>	<b>0.148</b>	<b>0.144</b>
		C of V (%)	4.0	5.4	14.0	19.6	6.3	5.4	13.1
	+4 days H	Cores 1	0.113	0.098	0.083	0.092	0.084	0.098	0.086
		Cores 2	0.104	0.124	0.080	0.090	0.087	0.124	0.086
		Average	<b>0.108</b>	<b>0.111</b>	<b>0.082</b>	<b>0.091</b>	<b>0.085</b>	<b>0.111</b>	<b>0.086</b>
		C of V (%)	4.1	11.7	2.0	0.8	1.8	11.7	0.3
	+6 days H	Cores 1	0.125	0.126	0.101	0.102	0.092	0.126	0.098
		Cores 2	0.120	0.114	0.099	0.105	0.098	0.114	0.101
		Average	<b>0.122</b>	<b>0.120</b>	<b>0.100</b>	<b>0.104</b>	<b>0.095</b>	<b>0.120</b>	<b>0.100</b>
		C of V (%)	2.2	5.0	1.0	1.8	3.0	5.0	1.2
West	No Cure	Cores 1	0.081	0.130	0.105	0.103	0.150	0.130	0.119
		Cores 2	0.081	0.149	0.129	0.128	0.130	0.149	0.129
		Average	<b>0.081</b>	<b>0.139</b>	<b>0.117</b>	<b>0.115</b>	<b>0.140</b>	<b>0.139</b>	<b>0.124</b>
		C of V (%)	0.0	6.9	10.4	11.0	7.2	6.9	3.9
	+2 days H	Cores 1	0.081	0.141	0.120	0.111	0.114	0.141	0.115
		Cores 2	0.099	0.109	0.105	0.135	0.132	0.109	0.124
		Average	<b>0.090</b>	<b>0.125</b>	<b>0.113</b>	<b>0.123</b>	<b>0.123</b>	<b>0.125</b>	<b>0.120</b>
		C of V (%)	9.7	12.8	6.5	9.5	7.5	12.8	3.8
	+4 days H	Cores 1	0.092	0.097	0.078	0.088	0.076	0.097	0.081
		Cores 2	0.091	0.101	0.084	0.077	0.090	0.101	0.084
		Average	<b>0.092</b>	<b>0.099</b>	<b>0.081</b>	<b>0.083</b>	<b>0.083</b>	<b>0.099</b>	<b>0.082</b>
		C of V (%)	0.4	2.0	3.9	6.7	8.9	2.0	2.0
	+6 days H	Cores 1	0.113	0.131	0.095	0.092	0.100	0.131	0.095
		Cores 2	0.099	0.098	0.078	0.091	0.089	0.098	0.086
		Average	<b>0.106</b>	<b>0.114</b>	<b>0.086</b>	<b>0.091</b>	<b>0.095</b>	<b>0.114</b>	<b>0.091</b>
		C of V (%)	6.6	14.1	9.7	0.2	5.9	14.1	5.2

Key: +X days H= X days hessian plus 1 day in mould; Average= average of cores 1 and 2; C of V= coefficient of variation (%); Sub-surface (10-40mm)= average k value from 10 to 40mm from surface; Bold value= plotted value (usually average)

Table B1.16 (b) Sorptivity  $s$  (mm/min<sup>0.5</sup>) for the 30 MPa OPC/GGBS Concrete (top/bottom) - 12 months summer series

Orientation	Curing regime		Average depth from outer surface (mm)					Surface (10mm)	Sub-surface (20-40mm)
			5	10	20	30	40		
Top	No Cure	Cores 1	0.104	0.107	0.112	0.102	0.136	0.107	0.117
		Cores 2	0.103	0.112	0.116	0.120	0.125	0.112	0.120
		Average	<b>0.104</b>	<b>0.109</b>	<b>0.114</b>	<b>0.111</b>	<b>0.130</b>	<b>0.109</b>	<b>0.118</b>
		C of V (%)	0.4	2.4	2.0	8.3	4.6	2.4	1.6
	+2 days H	Cores 1	0.092	0.099	0.088	0.103	0.150	0.099	0.114
		Cores 2	0.093	0.108	0.108	0.112	0.164	0.108	0.128
		Average	<b>0.092</b>	<b>0.104</b>	<b>0.098</b>	<b>0.108</b>	<b>0.157</b>	<b>0.104</b>	<b>0.121</b>
		C of V (%)	0.6	4.5	10.0	4.2	4.5	4.5	5.9
	+4 days H	Cores 1	0.076	0.094	0.054	0.074	0.086	0.094	0.071
		Cores 2	0.068	0.075	0.065	0.070	0.085	0.075	0.073
		Average	<b>0.072</b>	<b>0.085</b>	<b>0.060</b>	<b>0.072</b>	<b>0.085</b>	<b>0.085</b>	<b>0.072</b>
		C of V (%)	5.3	11.5	9.5	2.6	1.1	11.5	1.3
	+6 days H	Cores 1	0.091	0.077	0.072	0.077	0.080	0.077	0.076
		Cores 2	0.076	0.074	0.075	0.072	0.085	0.074	0.077
		Average	<b>0.083</b>	<b>0.075</b>	<b>0.073</b>	<b>0.075</b>	<b>0.083</b>	<b>0.075</b>	<b>0.077</b>
		C of V (%)	9.3	1.8	2.0	3.4	3.3	1.8	0.7
Bottom	No Cure	Cores 1	0.105	0.131	0.116	0.108	0.150	0.131	0.124
		Cores 2	0.123	0.134	0.122	0.124	0.118	0.134	0.121
		Average	<b>0.114</b>	<b>0.132</b>	<b>0.119</b>	<b>0.116</b>	<b>0.134</b>	<b>0.132</b>	<b>0.123</b>
		C of V (%)	7.9	0.9	2.5	6.7	12.0	0.9	1.4
	+2 days H	Cores 1	0.134	0.128	0.103	0.112	0.120	0.128	0.111
		Cores 2	0.115	0.137	0.110	0.120	0.150	0.137	0.127
		Average	<b>0.124</b>	<b>0.132</b>	<b>0.106</b>	<b>0.116</b>	<b>0.135</b>	<b>0.132</b>	<b>0.119</b>
		C of V (%)	7.4	3.1	3.3	3.8	11.0	3.1	6.4
	+4 days H	Cores 1	0.084	0.096	0.073	0.075	0.085	0.096	0.077
		Cores 2	0.092	0.085	0.082	0.082	0.077	0.085	0.080
		Average	<b>0.088</b>	<b>0.091</b>	<b>0.078</b>	<b>0.078</b>	<b>0.081</b>	<b>0.091</b>	<b>0.079</b>
		C of V (%)	4.6	6.2	5.6	4.9	4.6	6.2	1.9
	+6 days H	Cores 1	0.090	0.070	0.072	0.073	0.070	0.070	0.072
		Cores 2	0.089	0.090	0.077	0.081	0.087	0.090	0.082
		Average	<b>0.090</b>	<b>0.080</b>	<b>0.075</b>	<b>0.077</b>	<b>0.078</b>	<b>0.080</b>	<b>0.077</b>
		C of V (%)	0.9	12.4	3.2	5.6	10.7	12.4	6.5

Key: +X days H= X days hessian plus 1 day in mould; Average= average of cores 1 and 2; C of V= coefficient of variation (%); Sub-surface (10-40mm)= average k value from 10 to 40mm from surface; Bold value= plotted value (usually average)

**Table B1.17 (a) Sorptivity S (mm/min<sup>0.5</sup>) for the 30 MPa OPC/GGBS concrete (east/west) - 3 months summer series**

Orientation	Curnig regime		Average depth from outer surface (mm)					Surface (10mm)	Sub-surface (20-50mm)
			10	20	30	40	50		
East	No Cure	Cores 1	0.350	0.323	0.320	0.289	0.253	0.350	0.296
		Cores 2	0.355	0.327	0.326	0.275	0.263	0.355	0.298
		Average	<b>0.353</b>	<b>0.325</b>	<b>0.323</b>	<b>0.282</b>	<b>0.258</b>	<b>0.353</b>	<b>0.297</b>
		C of V (%)	0.8	0.6	0.8	2.4	1.8	0.8	0.2
	+2 days H	Cores 1	0.235	0.276	0.249	0.253	0.215	0.235	0.248
		Cores 2	0.275	0.211	0.200	0.179	0.166	0.275	0.189
		Average	<b>0.255</b>	<b>0.244</b>	<b>0.224</b>	<b>0.216</b>	<b>0.191</b>	<b>0.255</b>	<b>0.219</b>
		C of V (%)	7.9	13.3	10.8	17.2	12.9	7.9	13.5
	None (CPF)	Cores 1	0.109	0.178	0.175	0.160	0.150	0.109	0.166
		Cores 2	0.050	0.167	0.176	0.189	0.164	0.050	0.174
		Average	<b>0.079</b>	<b>0.172</b>	<b>0.176</b>	<b>0.175</b>	<b>0.157</b>	<b>0.079</b>	<b>0.170</b>
		C of V (%)	37.2	3.1	0.3	8.2	4.3	37.2	2.4
	+2 days H (CPF)	Cores 1	0.097	0.112	0.122	0.111	0.098	0.097	0.111
		Cores 2	0.111	0.127	0.122	0.111	0.098	0.111	0.114
		Average	<b>0.104</b>	<b>0.119</b>	<b>0.122</b>	<b>0.111</b>	<b>0.098</b>	<b>0.104</b>	<b>0.113</b>
		C of V (%)	6.7	6.3	0.0	0.0	0.0	6.7	1.7
West	No Cure	Cores 1	0.216	0.193	0.200	0.180	0.203	0.216	0.194
		Cores 2	0.221	0.185	0.171	0.167	0.130	0.221	0.163
		Average	<b>0.219</b>	<b>0.189</b>	<b>0.185</b>	<b>0.174</b>	<b>0.167</b>	<b>0.219</b>	<b>0.178</b>
		C of V (%)	1.1	2.1	7.7	4.0	21.9	1.1	8.6
	+2 days H	Cores 1	0.206	0.186	0.178	0.161	0.188	0.206	0.178
		Cores 2	0.211	0.183	0.176	0.176	0.131	0.211	0.167
		Average	<b>0.209</b>	<b>0.185</b>	<b>0.177</b>	<b>0.168</b>	<b>0.160</b>	<b>0.209</b>	<b>0.172</b>
		C of V (%)	1.2	0.6	0.5	4.4	17.8	1.2	3.3
	None (CPF)	Cores 1	0.089	0.118	0.162	0.159	0.147	0.089	0.146
		Cores 2	0.045	0.140	0.183	0.187	0.173	0.045	0.171
		Average	<b>0.067</b>	<b>0.129</b>	<b>0.172</b>	<b>0.173</b>	<b>0.160</b>	<b>0.067</b>	<b>0.158</b>
		C of V (%)	32.3	8.5	6.1	8.1	8.2	32.3	7.6
	+2 days H (CPF)	Cores 1	0.074	0.107	0.124	0.112	0.104	0.074	0.112
		Cores 2	0.088	0.134	0.127	0.150	0.159	0.088	0.143
		Average	<b>0.081</b>	<b>0.121</b>	<b>0.126</b>	<b>0.131</b>	<b>0.131</b>	<b>0.081</b>	<b>0.127</b>
		C of V (%)	8.6	11.2	1.2	14.7	20.9	8.6	12.1

Key: +X days H= X days hessian plus 1 day in mould; Average= average of cores 1 and 2; C of V= coefficient of variation (%); Sub-surface (20-50mm)= average k value from rface; Bold value= plotted value (usually average); CPF= controlled permeability formwork

**Table B1.17 (b) Sorptivity S (mm/min<sup>0.5</sup>) for the 30 MPa OPC/GGBS concrete (top/bottom) - 3 months summer series**

Orientation	Curing regime		Average depth from outer surface (mm)					Surface (10mm)	Sub-surface (20-50mm)
			10	20	30	40	50		
Top	No Cure	Cores 1	0.131	0.141	0.176	0.177	0.175	0.131	0.167
		Cores 2	0.160	0.147	0.110	0.101	0.110	0.160	0.117
		Average	<b>0.145</b>	<b>0.144</b>	<b>0.143</b>	<b>0.139</b>	<b>0.142</b>	<b>0.145</b>	<b>0.142</b>
		C of V (%)	10.2	1.9	23.1	27.2	22.7	10.2	17.7
	+2 days H	Cores 1	0.136	0.149	0.138	0.190	0.195	0.136	0.168
		Cores 2	0.198	0.146	0.137	0.130	0.120	0.198	0.133
		Average	<b>0.167</b>	<b>0.147</b>	<b>0.138</b>	<b>0.160</b>	<b>0.157</b>	<b>0.167</b>	<b>0.151</b>
		C of V (%)	18.7	1.2	0.6	18.6	23.7	18.7	11.6
	None (CPF)	Cores 1	0.011	0.133	0.161	0.197	0.146	0.011	0.159
		Cores 2	0.018	0.097	0.152	0.140	0.158	0.018	0.137
		Average	<b>0.015</b>	<b>0.115</b>	<b>0.156</b>	<b>0.168</b>	<b>0.152</b>	<b>0.015</b>	<b>0.148</b>
		C of V (%)	24.5	15.7	2.9	17.0	3.7	24.5	7.7
	+2 days H (CPF)	Cores 1	0.015	0.094	0.136	0.144	0.153	0.015	0.132
		Cores 2	0.026	0.103	0.163	0.188	0.166	0.026	0.155
		Average	<b>0.020</b>	<b>0.099</b>	<b>0.150</b>	<b>0.166</b>	<b>0.159</b>	<b>0.020</b>	<b>0.143</b>
		C of V (%)	25.3	4.9	8.9	13.2	3.9	25.3	8.1
Bottom	No Cure	Cores 1	0.133	0.270	0.178	0.226	0.188	0.133	0.215
		Cores 2	0.290	0.224	0.241	0.201	0.186	0.290	0.213
		Average	<b>0.211</b>	<b>0.247</b>	<b>0.209</b>	<b>0.213</b>	<b>0.187</b>	<b>0.211</b>	<b>0.214</b>
		C of V (%)	37.1	9.4	15.1	5.8	0.3	37.1	0.5
	+2 days H	Cores 1	0.119	0.167	0.186	0.192	0.184	0.119	0.182
		Cores 2	0.214	0.136	0.110	0.100	0.112	0.214	0.114
		Average	<b>0.166</b>	<b>0.152</b>	<b>0.148</b>	<b>0.146</b>	<b>0.148</b>	<b>0.166</b>	<b>0.148</b>
		C of V (%)	28.7	10.2	25.7	31.5	24.3	28.7	22.8
	None (CPF)	Cores 1	0.015	0.132	0.148	0.201	0.160	0.015	0.160
		Cores 2	0.024	0.116	0.162	0.171	0.158	0.024	0.152
		Average	<b>0.019</b>	<b>0.124</b>	<b>0.155</b>	<b>0.186</b>	<b>0.159</b>	<b>0.019</b>	<b>0.156</b>
		C of V (%)	23.5	6.1	4.4	8.1	0.5	23.5	2.7
	+2 days H (CPF)	Cores 1	0.038	0.127	0.148	0.144	0.149	0.038	0.142
		Cores 2	0.046	0.129	0.156	0.175	0.151	0.046	0.153
		Average	<b>0.042</b>	<b>0.128</b>	<b>0.152</b>	<b>0.159</b>	<b>0.150</b>	<b>0.042</b>	<b>0.147</b>
		C of V (%)	9.8	0.7	2.5	9.7	0.5	9.8	3.6

Key: +X days H= X days hessian plus 1 day in mould; Average= average of cores 1 and 2; C of V= coefficient of variation (%); Sub-surface (20-50mm)= average k value from surface; Bold value= plotted value (usually average); CPF= controlled permeability formwork

**Table B1.18 (a) Sorptivity S (mm/min<sup>0.5</sup>) for the 30 MPa OPC/GGBS concrete (east/west) - 12 months summer series**

Orientation	Curnig regime		Average depth from outer surface (mm)					Surface (10mm)	Sub-surface (20-40mm)
			5	10	20	30	40		
East	No Cure	Cores 1	0.111	0.289	0.224	0.180	0.169	0.289	0.191
		Cores 2	0.111	0.268	0.262	0.200	0.177	0.268	0.213
		Average	<b>0.111</b>	<b>0.278</b>	<b>0.243</b>	<b>0.190</b>	<b>0.173</b>	<b>0.278</b>	<b>0.202</b>
		C of V (%)	0.0	3.8	7.7	5.5	2.3	3.8	5.5
	+2 days H	Cores 1	0.115	0.140	0.115	0.116	0.143	0.140	0.125
		Cores 2	0.106	0.156	0.152	0.172	0.163	0.156	0.162
		Average	<b>0.110</b>	<b>0.148</b>	<b>0.134</b>	<b>0.144</b>	<b>0.153</b>	<b>0.148</b>	<b>0.144</b>
		C of V (%)	4.0	5.4	14.0	19.6	6.3	5.4	13.1
	None (CPF)	Cores 1	0.048	0.039	0.103	0.142	0.188	0.039	0.144
		Cores 2	0.045	0.037	0.152	0.150	0.175	0.037	0.159
		Average	<b>0.046</b>	<b>0.038</b>	<b>0.127</b>	<b>0.146</b>	<b>0.181</b>	<b>0.038</b>	<b>0.152</b>
		C of V (%)	3.7	2.2	19.1	2.6	3.5	2.2	4.8
	+2 days H (CPF)	Cores 1	0.056	0.055	0.124	0.116	0.132	0.055	0.124
		Cores 2	0.053	0.052	0.090	0.159	0.143	0.052	0.131
		Average	<b>0.055</b>	<b>0.054</b>	<b>0.107</b>	<b>0.137</b>	<b>0.138</b>	<b>0.054</b>	<b>0.127</b>
		C of V (%)	2.9	2.6	15.7	15.9	3.8	2.6	2.7
West	No Cure	Cores 1	0.081	0.130	0.105	0.103	0.150	0.130	0.119
		Cores 2	0.081	0.149	0.129	0.128	0.130	0.149	0.129
		Average	<b>0.081</b>	<b>0.139</b>	<b>0.117</b>	<b>0.116</b>	<b>0.140</b>	<b>0.139</b>	<b>0.124</b>
		C of V (%)	0.1	6.8	10.2	10.9	7.2	6.8	3.8
	+2 days H	Cores 1	0.081	0.141	0.120	0.111	0.114	0.141	0.115
		Cores 2	0.099	0.109	0.105	0.135	0.132	0.109	0.124
		Average	<b>0.090</b>	<b>0.125</b>	<b>0.113</b>	<b>0.123</b>	<b>0.123</b>	<b>0.125</b>	<b>0.120</b>
		C of V (%)	9.7	12.8	6.5	9.5	7.5	12.8	3.8
	None (CPF)	Cores 1	0.043	0.038	0.105	0.153	0.180	0.038	0.146
		Cores 2	0.050	0.051	0.158	0.167	0.164	0.051	0.163
		Average	<b>0.046</b>	<b>0.044</b>	<b>0.131</b>	<b>0.160</b>	<b>0.172</b>	<b>0.044</b>	<b>0.154</b>
		C of V (%)	7.3	14.5	20.1	4.4	4.7	14.5	5.5
	+2 days H (CPF)	Cores 1	0.032	0.037	0.112	0.117	0.150	0.037	0.126
		Cores 2	0.042	0.040	0.107	0.131	0.140	0.040	0.126
		Average	<b>0.037</b>	<b>0.039</b>	<b>0.110</b>	<b>0.124</b>	<b>0.145</b>	<b>0.039</b>	<b>0.126</b>
		C of V (%)	14.7	3.7	2.3	5.6	3.5	3.7	0.2

Key: +X days H= X days hessian plus 1 day in mould; Average= average of cores 1 and 2; C of V= coefficient of variation (%); Sub-surface (20-40mm)= average k value from rface; Bold value= plotted value (usually average); CPF= controlled permeability formwork

Table B1.18 (b) Sorptivity S (mm/min<sup>0.5</sup>) for the 30 MPa OPC/GGBS concrete (top/bottom) - 12 months summer series

Orientation	Curing regime		Average depth from outer surface (mm)					Surface (10mm)	Sub-surface (20-40mm)
			5	10	20	30	40		
Top	No Cure	Cores 1	0.104	0.107	0.112	0.102	0.136	0.107	0.117
		Cores 2	0.103	0.112	0.116	0.120	0.125	0.112	0.120
		Average	<b>0.104</b>	<b>0.109</b>	<b>0.114</b>	<b>0.111</b>	<b>0.130</b>	<b>0.109</b>	<b>0.118</b>
		C of V (%)	0.4	2.4	2.0	8.3	4.6	2.4	1.6
	+2 days H	Cores 1	0.092	0.099	0.088	0.103	0.150	0.099	0.114
		Cores 2	0.093	0.108	0.108	0.112	0.164	0.108	0.128
		Average	<b>0.092</b>	<b>0.104</b>	<b>0.098</b>	<b>0.108</b>	<b>0.157</b>	<b>0.104</b>	<b>0.121</b>
		C of V (%)	0.6	4.5	10.0	4.2	4.5	4.5	5.9
	None (CPF)	Cores 1	0.062	0.085	0.115	0.119	0.146	0.085	0.127
		Cores 2	0.090	0.094	0.124	0.120	0.130	0.094	0.125
		Average	<b>0.076</b>	<b>0.089</b>	<b>0.119</b>	<b>0.120</b>	<b>0.138</b>	<b>0.089</b>	<b>0.126</b>
		C of V (%)	18.2	5.3	3.4	0.5	5.7	5.3	0.8
	+2 days H (CPF)	Cores 1	0.060	0.099	0.101	0.117	0.121	0.099	0.113
		Cores 2	0.078	0.092	0.114	0.117	0.116	0.092	0.116
		Average	<b>0.069</b>	<b>0.096</b>	<b>0.107</b>	<b>0.117</b>	<b>0.119</b>	<b>0.096</b>	<b>0.114</b>
		C of V (%)	12.9	3.9	5.6	0.0	2.0	3.9	1.0
Bottom	No Cure	Cores 1	0.105	0.131	0.116	0.108	0.150	0.131	0.124
		Cores 2	0.123	0.134	0.122	0.124	0.118	0.134	0.121
		Average	<b>0.114</b>	<b>0.132</b>	<b>0.119</b>	<b>0.116</b>	<b>0.134</b>	<b>0.132</b>	<b>0.123</b>
		C of V (%)	7.9	0.9	2.5	6.7	12.0	0.9	1.4
	+2 days H	Cores 1	0.134	0.128	0.103	0.112	0.120	0.128	0.111
		Cores 2	0.115	0.137	0.110	0.120	0.150	0.137	0.127
		Average	<b>0.124</b>	<b>0.132</b>	<b>0.106</b>	<b>0.116</b>	<b>0.135</b>	<b>0.132</b>	<b>0.119</b>
		C of V (%)	7.4	3.1	3.3	3.8	11.0	3.1	6.4
	None (CPF)	Cores 1	0.077	0.091	0.108	0.132	0.129	0.091	0.123
		Cores 2	0.091	0.091	0.104	0.133	0.127	0.091	0.121
		Average	<b>0.084</b>	<b>0.091</b>	<b>0.106</b>	<b>0.133</b>	<b>0.128</b>	<b>0.091</b>	<b>0.122</b>
		C of V (%)	8.4	0.4	2.2	0.4	0.6	0.4	0.7
	+2 days H (CPF)	Cores 1	0.086	0.103	0.089	0.105	0.106	0.103	0.100
		Cores 2	0.095	0.100	0.120	0.113	0.118	0.100	0.117
		Average	<b>0.091</b>	<b>0.102</b>	<b>0.104</b>	<b>0.109</b>	<b>0.112</b>	<b>0.102</b>	<b>0.108</b>
		C of V (%)	4.9	1.2	14.6	3.6	5.1	1.2	7.7

Key: +X days H= X days hessian plus 1 day in mould; Average= average of cores 1 and 2; C of V= coefficient of variation (%); Sub-surface (20-40mm)= average k value from surface; Bold value= plotted value (usually average); CPF= controlled permeability formwork

**Table B1.19 (a) Sorptivity S (mm/min<sup>0.5</sup>) for the 30 MPa OPC/GGBS concrete (east/west) - 3 months summer series**

Orientation	Curnig regime		Average depth from outer surface (mm)					Surface (10mm)	Sub-surface (20-50mm)
			10	20	30	40	50		
East	+6 days P	Cores 1	0.152	0.158	0.178	0.175	0.169	0.152	0.170
		Cores 2	0.123	0.153	0.169	0.191	0.187	0.123	0.175
		Average	<b>0.138</b>	<b>0.155</b>	<b>0.174</b>	<b>0.183</b>	<b>0.178</b>	<b>0.138</b>	<b>0.173</b>
		C of V (%)	10.4	1.6	2.6	4.5	5.0	10.4	1.5
	C/M	Cores 1	0.245	0.201	0.191	0.183	0.175	0.245	0.188
		Cores 2	0.261	0.217	0.193	0.201	0.192	0.261	0.201
		Average	<b>0.253</b>	<b>0.209</b>	<b>0.192</b>	<b>0.192</b>	<b>0.184</b>	<b>0.253</b>	<b>0.194</b>
		C of V (%)	3.1	3.8	0.4	4.9	4.6	3.1	3.4
	+6 days P (CPF)	Cores 1	0.154	0.144	0.163	0.169	0.151	0.154	0.157
		Cores 2	0.171	0.137	0.163	0.204	0.148	0.171	0.163
		Average	<b>0.163</b>	<b>0.141</b>	<b>0.163</b>	<b>0.187</b>	<b>0.149</b>	<b>0.163</b>	<b>0.160</b>
		C of V (%)	5.4	2.5	0.1	9.5	1.0	5.4	2.0
	C/M (CPF)	Cores 1	0.209	0.250	0.167	0.194	0.134	0.209	0.186
		Cores 2	0.184	0.167	0.196	0.156	0.160	0.184	0.170
		Average	<b>0.197</b>	<b>0.209</b>	<b>0.181</b>	<b>0.175</b>	<b>0.147</b>	<b>0.197</b>	<b>0.178</b>
		C of V (%)	6.5	19.9	8.0	10.9	8.6	6.5	4.7
West	+6 days P	Cores 1	0.114	0.143	0.136	0.160	0.168	0.114	0.152
		Cores 2	0.120	0.130	0.135	0.167	0.184	0.120	0.154
		Average	<b>0.117</b>	<b>0.137</b>	<b>0.136</b>	<b>0.164</b>	<b>0.176</b>	<b>0.117</b>	<b>0.153</b>
		C of V (%)	2.5	4.7	0.4	2.1	4.5	2.5	0.7
	C/M	Cores 1	0.105	0.149	0.141	0.173	0.139	0.105	0.151
		Cores 2	0.170	0.158	0.164	0.183	0.169	0.170	0.169
		Average	<b>0.138</b>	<b>0.154</b>	<b>0.152</b>	<b>0.178</b>	<b>0.154</b>	<b>0.138</b>	<b>0.160</b>
		C of V (%)	23.9	2.9	7.4	2.7	9.8	23.9	5.6
	+6 days P (CPF)	Cores 1	0.105	0.116	0.122	0.181	0.152	0.105	0.143
		Cores 2	0.117	0.145	0.149	0.150	0.162	0.117	0.151
		Average	<b>0.111</b>	<b>0.130</b>	<b>0.135</b>	<b>0.166</b>	<b>0.157</b>	<b>0.111</b>	<b>0.147</b>
		C of V (%)	5.0	11.0	10.2	9.4	3.0	5.0	2.9
	C/M (CPF)	Cores 1	0.130	0.198	0.142	0.184	0.131	0.130	0.164
		Cores 2	0.105	0.147	0.179	0.186	0.177	0.105	0.172
		Average	<b>0.117</b>	<b>0.172</b>	<b>0.161</b>	<b>0.185</b>	<b>0.154</b>	<b>0.117</b>	<b>0.168</b>
		C of V (%)	10.9	14.9	11.4	0.7	14.8	10.9	2.5

Key: +X days H= X days hessian plus 1 day in mould; Average= average of cores 1 and 2; C of V= coefficient of variation (%); Sub-surface (20-50mm)= average k value from dotted value (usually average); P=polythene; C/M= curing membrane; CPF= controlled permeability formwork;

**Table B1.19 (b) Sorptivity S (mm/min<sup>0.5</sup>) for the 30 MPa OPC and OPC/GGBS concrete (top/bottom) - 3 months summer series**

Orientation	Curing regime		Average depth from outer surface (mm)					Surface (10mm)	Sub-surface (20-50mm)
			10	20	30	40	50		
Top	+6 days P	Cores 1	0.080	0.131	0.133	0.138	0.122	0.080	0.131
		Cores 2	0.078	0.133	0.128	0.139	0.146	0.078	0.136
		Average	0.079	0.132	0.130	0.138	0.134	0.079	0.133
		C of V (%)	0.9	0.8	1.8	0.3	8.9	0.9	2.1
	C/M	Cores 1	0.099	0.108	0.117	0.115	0.113	0.099	0.113
		Cores 2	0.094	0.116	0.145	0.113	0.125	0.094	0.125
		Average	0.097	0.112	0.131	0.114	0.119	0.097	0.119
		C of V (%)	2.8	3.7	10.7	1.0	4.7	2.8	4.8
	+6 days P (CPF)	Cores 1	0.073	0.114	0.117	0.120	0.136	0.073	0.122
		Cores 2	0.091	0.130	0.120	0.182	0.117	0.091	0.137
		Average	0.082	0.122	0.118	0.151	0.127	0.082	0.129
		C of V (%)	10.8	6.6	1.4	20.6	7.2	10.8	6.1
	C/M (CPF)	Cores 1	0.116	0.171	0.154	0.179	0.148	0.116	0.163
		Cores 2	0.148	0.137	0.142	0.160	0.144	0.148	0.146
		Average	0.132	0.154	0.148	0.170	0.146	0.132	0.154
		C of V (%)	12.3	11.0	4.2	5.5	1.3	12.3	5.6
Bottom	+ 6 days P	Cores 1	0.100	0.188	0.139	0.154	0.140	0.100	0.155
		Cores 2	0.130	0.144	0.172	0.142	0.152	0.130	0.153
		Average	0.115	0.166	0.156	0.148	0.146	0.115	0.154
		C of V (%)	13.1	13.1	10.5	3.8	4.2	13.1	0.8
	C/M	Cores 1	0.188	0.116	0.154	0.123	0.123	0.188	0.129
		Cores 2	0.201	0.144	0.156	0.132	0.159	0.201	0.148
		Average	0.195	0.130	0.155	0.127	0.141	0.195	0.138
		C of V (%)	3.4	11.0	0.7	3.7	12.6	3.4	6.8
	+6 days P (CPF)	Cores 1	0.093	0.141	0.161	0.150	0.138	0.093	0.147
		Cores 2	0.086	0.155	0.119	0.147	0.112	0.086	0.133
		Average	0.089	0.148	0.140	0.148	0.125	0.089	0.140
		C of V (%)	3.5	4.6	14.8	1.1	10.4	3.5	5.1
	C/M (CPF)	Cores 1	0.120	0.169	0.166	0.164	0.150	0.120	0.162
		Cores 2	0.117	0.156	0.154	0.156	0.147	0.117	0.153
		Average	0.118	0.162	0.160	0.160	0.148	0.118	0.158
		C of V (%)	1.3	3.9	3.7	2.5	1.1	1.3	2.8

Key: +X days H= X days hessian plus 1 day in mould; Average= average of cores 1 and 2; C of V= coefficient of variation (%); Sub-surface (20-50mm)= average k value from dotted value (usually average); P=polythene; C/M= curing membrane; CPF= controlled permeability formwork;

**Table B1.20 (a) Sorptivity S (mm/min<sup>0.5</sup>) for the 30 MPa OPC/GGBS concrete (east/west) - 12 months summer series**

Orientation	Curing regime		Average depth from outer surface (mm)					Surface (10mm)	Sub-surface (20-40mm)
			5	10	20	30	40		
East	+6 days P	Cores 1	0.115	0.118	0.100	0.091	0.084	0.118	0.092
		Cores 2	0.109	0.115	0.076	0.094	0.117	0.115	0.096
		Average	0.112	0.117	0.088	0.092	0.101	0.117	0.094
		C of V (%)	2.3	1.2	13.4	1.5	16.3	1.2	2.2
	C/M	Cores 1	0.164	0.233	0.155	0.134	0.163	0.233	0.151
		Cores 2	0.164	0.169	0.098	0.083	0.155	0.169	0.112
		Average	0.164	0.201	0.127	0.108	0.159	0.201	0.131
		C of V (%)	0.1	15.8	22.5	23.4	2.4	15.8	14.6
	+6 days P (CPF)	Cores 1	0.036	0.039	0.060	0.149	0.124	0.039	0.111
		Cores 2	0.046	0.032	0.080	0.091	0.125	0.032	0.099
		Average	0.041	0.035	0.070	0.120	0.125	0.035	0.105
		C of V (%)	11.8	9.7	14.3	24.3	0.4	9.7	6.0
	C/M (CPF)	Cores 1	0.035	0.036	0.105	0.094	0.136	0.036	0.112
		Cores 2	0.041	0.046	0.064	0.119	0.122	0.046	0.102
		Average	0.038	0.041	0.085	0.107	0.129	0.041	0.107
		C of V (%)	8.4	11.8	24.1	11.7	5.4	11.8	4.6
West	+6 days P	Cores 1	0.089	0.076	0.077	0.112	0.126	0.076	0.105
		Cores 2	0.104	0.101	0.097	0.117	0.134	0.101	0.116
		Average	0.097	0.089	0.087	0.114	0.130	0.089	0.110
		C of V (%)	7.8	13.8	11.7	2.1	3.1	13.8	5.0
	C/M	Cores 1	0.116	0.124	0.160	0.160	0.171	0.124	0.164
		Cores 2	0.123	0.144	0.084	0.093	0.137	0.144	0.105
		Average	0.119	0.134	0.122	0.126	0.154	0.134	0.134
		C of V (%)	2.8	7.5	31.2	26.7	11.1	7.5	22.1
	+6 days P (CPF)	Cores 1	0.032	0.033	0.059	0.139	0.125	0.033	0.108
		Cores 2	0.032	0.046	0.072	0.130	0.123	0.046	0.108
		Average	0.032	0.040	0.065	0.135	0.124	0.040	0.108
		C of V (%)	0.5	16.6	10.0	3.4	0.8	16.6	0.3
	C/M (CPF)	Cores 1	0.031	0.039	0.090	0.100	0.141	0.039	0.110
		Cores 2	0.026	0.037	0.077	0.111	0.116	0.037	0.101
		Average	0.028	0.038	0.084	0.105	0.129	0.038	0.106
		C of V (%)	8.8	2.4	8.0	5.1	9.8	2.4	4.4

Key: +X days H= X days hessian plus 1 day in mould; Average= average of cores 1 and 2; C of V= coefficient of variation (%); Sub-surface (20-40mm)= average k value from lotted value (usually average); P=polythene; C/M= curing membrane; CPF= controlled permeability formwork;

**Table B1.20 (b) Sorptivity S (mm/min<sup>0.5</sup>) for the 30 MPa OPC and OPC/GGBS concrete (top/bottom) - 12 months summer series**

Orientation	Curing regime		Average depth from outer surface (mm)					Surface (10mm)	Sub-surface (20-40mm)
			5	10	20	30	40		
Top	+6 days P	Cores 1	0.069	0.081	0.075	0.080	0.098	0.081	0.084
		Cores 2	0.088	0.071	0.085	0.075	0.089	0.071	0.083
		Average	<b>0.078</b>	<b>0.076</b>	<b>0.080</b>	<b>0.077</b>	<b>0.094</b>	<b>0.076</b>	<b>0.084</b>
		C of V (%)	12.0	6.4	6.1	2.7	4.8	6.4	0.7
	C/M	Cores 1	0.087	0.116	0.089	0.088	0.106	0.116	0.094
		Cores 2	0.103	0.088	0.077	0.085	0.096	0.088	0.086
		Average	<b>0.095</b>	<b>0.102</b>	<b>0.083</b>	<b>0.087</b>	<b>0.101</b>	<b>0.102</b>	<b>0.090</b>
		C of V (%)	8.5	13.8	7.5	1.5	5.0	13.8	4.7
	+6 days P (CPF)	Cores 1	0.029	0.019	0.082	0.080	0.110	0.019	0.090
		Cores 2	0.021	0.023	0.061	0.085	0.113	0.023	0.086
		Average	<b>0.025</b>	<b>0.021</b>	<b>0.071</b>	<b>0.083</b>	<b>0.111</b>	<b>0.021</b>	<b>0.088</b>
		C of V (%)	16.2	9.1	14.7	3.0	1.3	9.1	2.5
	C/M (CPF)	Cores 1	0.017	0.017	0.064	0.092	0.109	0.017	0.088
		Cores 2	0.018	0.049	0.088	0.117	0.121	0.049	0.109
		Average	<b>0.018</b>	<b>0.033</b>	<b>0.076</b>	<b>0.105</b>	<b>0.115</b>	<b>0.033</b>	<b>0.099</b>
		C of V (%)	4.5	48.0	15.7	12.1	5.3	48.0	10.4
Bottom	+ 6 days P	Cores 1	0.094	0.072	0.086	0.096	0.100	0.072	0.094
		Cores 2	0.106	0.084	0.083	0.078	0.116	0.084	0.092
		Average	<b>0.100</b>	<b>0.078</b>	<b>0.084</b>	<b>0.087</b>	<b>0.108</b>	<b>0.078</b>	<b>0.093</b>
		C of V (%)	5.6	7.8	1.7	10.2	7.6	7.8	0.8
	C/M	Cores 1	0.095	0.133	0.080	0.086	0.117	0.133	0.094
		Cores 2	0.087	0.078	0.073	0.081	0.105	0.078	0.086
		Average	<b>0.091</b>	<b>0.105</b>	<b>0.076</b>	<b>0.084</b>	<b>0.111</b>	<b>0.105</b>	<b>0.090</b>
		C of V (%)	4.6	25.8	4.5	3.1	5.1	25.8	4.3
	+6 days P (CPF)	Cores 1	0.090	0.026	0.102	0.079	0.093	0.026	0.091
		Cores 2	0.022	0.026	0.062	0.094	0.117	0.026	0.091
		Average	<b>0.056</b>	<b>0.026</b>	<b>0.082</b>	<b>0.087</b>	<b>0.105</b>	<b>0.026</b>	<b>0.091</b>
		C of V (%)	60.0	0.2	24.1	8.7	11.3	0.2	0.1
	C/M (CPF)	Cores 1	0.023	0.027	0.060	0.090	0.112	0.027	0.087
		Cores 2	0.033	0.089	0.077	0.134	0.148	0.089	0.120
		Average	<b>0.028</b>	<b>0.058</b>	<b>0.068</b>	<b>0.112</b>	<b>0.130</b>	<b>0.058</b>	<b>0.103</b>
		C of V (%)	18.0	53.5	12.3	19.8	14.0	53.5	15.7

Key: +X days H= X days hessian plus 1 day in mould; Average= average of cores 1 and 2; C of V= coefficient of variation (%); Sub-surface (20-40mm)= average k value from dotted value (usually average); P=polythene; C/M= curing membrane; CPF= controlled permeability formwork;

**Table B1.21 (a)** Carbonation depth (mm) for the 30 and 50 MPa OPC concrete - 6 months summer series

Microclimate	Reference	30 MPa OPC concrete				50 MPa OPC concrete			
		Average depth of carbonation (mm)				Average depth of carbonation (mm)			
		No cure	+2days H	+4 days H	+ 6 days H	No cure	+2 days H	+4 days H	+6 days H
East	Cores 1	6.0	5.8	3.5	3.5	3.0	2.5	1.5	0.5
	Cores 2	6.0	6.0	4.0	3.5	3.0	2.5	1.0	1.0
	Average	<b>6.0</b>	<b>5.9</b>	<b>3.8</b>	<b>3.5</b>	<b>3.0</b>	<b>2.5</b>	<b>1.3</b>	<b>0.8</b>
	C of V (%)	0.0	2.1	6.7	0.0	0.0	0.0	20.0	33.3
West	Cores 1	5.0	4.5	4.0	3.5	2.5	1.0	0.0	0.0
	Cores 2	6.0	4.3	4.0	4.0	2.5	1.0	0.0	0.0
	Average	<b>5.5</b>	<b>4.4</b>	<b>4.0</b>	<b>3.8</b>	<b>2.5</b>	<b>1.0</b>	<b>0.0</b>	<b>0.0</b>
	C of V (%)	9.1	2.9	0.0	6.7	0.0	0.0	0.0	0.0
Top	Cores 1	4.0	4.0	3.5	3.0	1.0	2.0	0.8	0.5
	Cores 2	4.0	4.0	2.5	3.5	1.0	1.0	0.5	0.5
	Average	<b>4.0</b>	<b>4.0</b>	<b>3.0</b>	<b>3.3</b>	<b>1.0</b>	<b>1.5</b>	<b>0.6</b>	<b>0.5</b>
	C of V (%)	0.0	0.0	16.7	7.7	0.0	33.3	20.0	0.0
Bottom	Cores 1	6.0	5.3	6.0	6.0	2.5	3.0	1.0	0.5
	Cores 2	7.0	4.5	5.0	4.0	2.5	3.0	1.0	0.5
	Average	<b>6.5</b>	<b>4.9</b>	<b>5.5</b>	<b>5.0</b>	<b>2.5</b>	<b>3.0</b>	<b>1.0</b>	<b>0.5</b>
	C of V (%)	7.7	7.7	9.1	20.0	0.0	0.0	0.0	0.0

**Table B1.21 (b)** Carbonation depth (mm) for the 30 MPa OPC/GGBS concrete - 6 months summer series

Microclimate	Reference	Average depth of carbonation (mm)									
		Conventional formwork						Controlled permeability formwork			
		No cure	+2 days H	+4 days H	+6 days H	+6 days P	C/M	No cure	+2 days H	+6 days P	C/M
East	Cores 1	8.0	8.5	7.0	5.5	4.0	4.0	0.0	0.0	0.0	4.0
	Cores 2	8.0	6.5	6.0	4.0	3.0	5.0	2.0	5.0	3.0	3.0
	Average	<b>8.0</b>	<b>7.5</b>	<b>6.5</b>	<b>4.8</b>	<b>3.5</b>	<b>4.5</b>	<b>1.0</b>	<b>2.5</b>	<b>1.5</b>	<b>3.5</b>
	C of V (%)	0.0	13.3	7.7	15.8	14.3	11.1	100.0	100.0	100.0	14.3
West	Cores 1	6.5	6.5	3.5	3.0	2.0	5.0	0.5	0.5	3.0	3.0
	Cores 2	6.5	7.5	4.5	3.0	3.5	4.0	0.5	0.5	0.0	4.0
	Average	<b>6.5</b>	<b>7.0</b>	<b>4.0</b>	<b>3.0</b>	<b>2.8</b>	<b>4.5</b>	<b>0.5</b>	<b>0.5</b>	<b>1.5</b>	<b>3.5</b>
	C of V (%)	0.0	7.1	12.5	0.0	27.3	11.1	0.0	0.0	100.0	14.3
Top	Cores 1	6.0	4.0	4.0	2.5	2.0	2.5	0.1	0.0	0.0	4.0
	Cores 2	7.0	8.0	3.0	2.5	2.0	3.5	0.1	0.0	4.5	2.0
	Average	<b>6.5</b>	<b>6.0</b>	<b>3.5</b>	<b>2.5</b>	<b>2.0</b>	<b>3.0</b>	<b>0.1</b>	<b>0.0</b>	<b>2.3</b>	<b>3.0</b>
	C of V (%)	7.7	33.3	14.3	0.0	0.0	16.7	0.0	0.0	100.0	33.3
Bottom	Cores 1	6.0	7.0	5.0	5.0	2.0	6.0	0.0	0.5	2.0	0.0
	Cores 2	5.0	7.0	5.0	3.5	1.0	5.0	0.5	0.0	1.0	3.0
	Average	<b>5.5</b>	<b>7.0</b>	<b>5.0</b>	<b>4.3</b>	<b>1.5</b>	<b>5.5</b>	<b>0.3</b>	<b>0.3</b>	<b>1.5</b>	<b>1.5</b>
	C of V (%)	9.1	0.0	0.0	17.6	33.3	9.1	100.0	100.0	33.3	100.0

Key: +2 days H= 2 days hessian plus 1 day in mould; Average= average of cores 1 and 2; C of V= coefficient of variation (%); Bold value= plotted value (usually average); P= polythene; C/M= curing membrane; CPF= controlled permeability formwork

**Table B1.22 (a)** Carbonation depth (mm) for the 30 and 50 MPa OPC concrete -12 months summer series

Microclimate	Reference	30 MPa OPC concrete				50 MPa OPC concrete			
		Average depth of carbonation (mm)				Average depth of carbonation (mm)			
		No cure	+2days H	+4 days H	+ 6 days H	No cure	+2 days H	+4 days H	+6 days H
East	Cores 1	7.5	7.7	4.5	4.0	3.8	3.0	2.0	1.8
	Cores 2	8.5	7.5	5.8	4.0	4.3	3.0	2.0	2.2
	<b>Average</b>	<b>8.0</b>	<b>7.6</b>	<b>5.1</b>	<b>4.0</b>	<b>4.1</b>	<b>3.0</b>	<b>2.0</b>	<b>2.0</b>
	C of V (%)	6.3	1.3	12.2	0.0	6.2	0.0	0.0	11.4
West	Cores 1	6.0	5.9	6.0	5.0	2.5	1.0	2.0	1.8
	Cores 2	6.0	5.0	4.5	3.3	2.5	1.0	1.5	1.0
	<b>Average</b>	<b>6.0</b>	<b>5.5</b>	<b>5.3</b>	<b>4.1</b>	<b>2.5</b>	<b>1.0</b>	<b>1.8</b>	<b>1.4</b>
	C of V (%)	0.0	8.3	14.3	21.2	0.0	0.0	14.3	27.3
Top	Cores 1	5.0	4.0	2.0	5.5	3.0	2.0	1.0	0.0
	Cores 2	5.0	4.5	5.0	4.0	3.0	2.0	1.0	1.0
	<b>Average</b>	<b>5.0</b>	<b>4.3</b>	<b>3.5</b>	<b>4.8</b>	<b>3.0</b>	<b>2.0</b>	<b>1.0</b>	<b>0.5</b>
	C of V (%)	0.0	5.9	42.9	15.8	0.0	0.0	0.0	100.0
Bottom	Cores 1	7.0	6.3	7.3	6.5	5.0	4.0	1.5	2.3
	Cores 2	7.0	5.0	5.0	4.5	3.8	2.0	2.0	2.3
	<b>Average</b>	<b>7.0</b>	<b>5.6</b>	<b>6.1</b>	<b>5.5</b>	<b>4.4</b>	<b>3.0</b>	<b>1.8</b>	<b>2.3</b>
	C of V (%)	0.0	11.1	18.4	18.2	14.3	33.3	14.3	0.0

**Table B1.22 (b)** Carbonation depth (mm) for the 30 MPa OPC/GGBS concrete - 12 months summer series

Microclimate	Reference	Average depth of carbonation (mm)									
		Conventional formwork						Controlled permeability formwork			
		No cure	+2 days H	+4 days H	+6 days H	+6 days P	C/M	No cure	+2 days H	+6 days P	C/M
East	Cores 1	12.0	11.3	9.8	9.0	11.0	9.0	3.8	3.0	2.3	5.0
	Cores 2	14.0	9.5	6.3	7.0	10.0	8.5	2.8	3.0	1.0	3.0
	<b>Average</b>	<b>13.0</b>	<b>10.4</b>	<b>8.0</b>	<b>8.0</b>	<b>10.5</b>	<b>8.8</b>	<b>3.3</b>	<b>3.0</b>	<b>1.6</b>	<b>4.0</b>
	C of V (%)	7.7	8.4	21.9	12.5	4.8	2.9	16.0	0.0	38.5	25.0
West	Cores 1	11.5	11.5	7.8	7.0	9.0	7.6	2.0	1.4	2.0	4.0
	Cores 2	10.0	12.0	7.0	5.3	7.0	9.3	1.0	1.4	2.0	4.0
	<b>Average</b>	<b>10.8</b>	<b>11.8</b>	<b>7.4</b>	<b>6.1</b>	<b>8.0</b>	<b>8.5</b>	<b>1.5</b>	<b>1.4</b>	<b>2.0</b>	<b>4.0</b>
	C of V (%)	7.0	2.1	5.1	14.3	12.5	10.1	33.3	0.0	0.0	0.0
Top	Cores 1	8.0	7.0	4.0	4.3	4.5	6.8	2.5	4.6	2.0	4.0
	Cores 2	7.5	7.0	6.5	4.5	5.4	6.0	7.0	4.0	4.0	4.0
	<b>Average</b>	<b>7.8</b>	<b>7.0</b>	<b>5.3</b>	<b>4.4</b>	<b>5.0</b>	<b>6.4</b>	<b>4.8</b>	<b>4.3</b>	<b>3.0</b>	<b>4.0</b>
	C of V (%)	3.2	0.0	23.8	2.9	9.1	5.9	47.4	7.0	33.3	0.0
Bottom	Cores 1	11.3	10.0	5.5	4.0	5.0	7.5	6.0	6.3	3.0	2.0
	Cores 2	12.0	11.3	7.0	6.5	5.8	7.5	4.5	5.5	0.0	2.0
	<b>Average</b>	<b>11.6</b>	<b>10.6</b>	<b>6.3</b>	<b>5.3</b>	<b>5.4</b>	<b>7.5</b>	<b>5.3</b>	<b>5.9</b>	<b>1.5</b>	<b>2.0</b>
	C of V (%)	3.2	5.9	12.0	23.8	7.0	0.0	14.3	6.4	100.0	0.0

Key: +2 days H= 2 days hessian plus 1 day in mould; Average= average of cores 1 and 2; C of V= coefficient of variation (%); Bold value= plotted value (usually average); P= polythene; C/M= curing membrane; CPF= controlled permeability formwork.

e B1.23 Areas under DTG curves – weight loss (%) (A1 to A5 according to Figure 5.29)

Concrete	Curing	Depth	A1	A2	A3	A4	A5	(A1+A2)	A3	(A4+A5)
30 MPa OPC Concrete	no cure	5	1.91	2.12	1.36	3.36	6.95	4.03	1.36	10.31
		10	2.84	2.82	1.89	3.01	1.37	5.66	1.89	4.37
		20	2.15	3.21	2.82	2.14	2.39	5.36	2.82	4.53
	+2 days	5	1.57	2.11	1.33	2.92	6.53	3.69	1.33	9.46
		10	2.43	2.47	2.43	2.93	2.13	4.90	2.43	5.06
		20	2.65	3.34	2.99	1.95	1.60	5.99	2.99	3.55
	+4 days	5	2.17	2.63	2.08	2.94	0.83	4.80	2.08	3.77
		10	1.25	2.64	2.47	2.57	1.73	3.89	2.47	4.30
		20	2.06	3.18	2.71	1.72	1.62	5.25	2.71	3.33
	+6 days	5	2.23	2.72	2.19	2.00	2.19	4.94	2.19	4.19
		10	1.79	3.00	2.63	2.00	1.66	4.79	2.63	3.66
		20	2.33	3.37	2.79	1.43	1.58	5.70	2.79	3.01
50 MPa OPC Concrete	no cure	5	1.68	2.34	1.77	2.47	3.65	4.02	1.77	6.12
		10	1.86	2.57	2.07	2.58	3.47	4.43	2.07	6.05
		20	1.90	2.89	2.54	2.27	2.58	4.79	2.54	4.85
	+2 days	5	2.03	2.99	2.27	1.97	2.83	5.02	2.27	4.80
		10	2.18	3.25	2.91	1.75	2.19	5.42	2.91	3.95
		20	2.04	3.07	2.72	2.01	2.39	5.10	2.72	4.40
	+4 days	5	1.86	2.80	2.40	1.91	2.71	4.66	2.40	4.62
		10	2.12	3.09	2.65	1.65	1.99	5.21	2.65	3.64
		20	1.72	2.50	2.17	2.16	2.73	4.22	2.17	4.89
	+6 days	5	1.84	2.59	2.12	1.85	2.91	4.43	2.12	4.76
		10	1.81	2.71	2.31	1.86	2.34	4.52	2.31	4.20
		20	1.92	2.81	2.51	1.44	1.92	4.73	2.51	3.36

**Table B1.24** Total porosity and fraction of pore volume in selected sizes of OPC and OPC/GGBS concrete at various depths from the exposed surface (east faces)

Concrete mix		30 MPa OPC concrete			50 MPa OPC concrete			30 MPa OPC/GGBS concrete		
Curing regime	Depth (mm)	5	10	20	5	10	20	5	10	20
	Pore diameter (µm)	fraction of volume in pores (cc/g) x 10 <sup>-2</sup>			fraction of volume in pores (cc/g) x 10 <sup>-2</sup>			fraction of volume in pores (cc/g) x 10 <sup>-2</sup>		
No cure	> 0.1	4.17	3.40	5.05	3.30	2.51	2.98	17.96	7.37	4.05
	0.1 - 0.006	6.95	7.92	9.15	3.98	5.23	3.87	10.45	8.93	9.63
	Total porosity	11.12	11.32	14.20	7.28	7.74	6.85	28.41	16.30	13.68
+2 days H	> 0.1	5.93	3.70	3.57	3.30	2.70	2.02	11.40	5.11	4.31
	0.1 - 0.006	5.82	8.74	8.74	4.42	4.05	4.38	9.41	7.66	6.46
	Total porosity	11.75	12.44	12.31	7.72	6.75	6.40	20.81	12.77	10.77
+4 days H	> 0.1	2.89	4.58	3.05	2.52	3.81	2.39	4.80	5.31	3.48
	0.1 - 0.006	7.07	5.37	5.65	4.75	3.81	3.95	5.13	5.06	5.54
	Total porosity	9.96	9.95	8.70	7.27	7.62	6.34	9.93	10.37	9.02
+6 days H	> 0.1	3.16	3.65	3.30	1.03	2.54	2.60	3.88	4.25	4.31
	0.1 - 0.006	5.75	4.78	4.43	2.04	2.62	3.65	4.52	3.66	4.02
	Total porosity	8.91	8.43	7.73	3.07	5.16	6.25	8.40	7.91	8.33

Key: +2 days H = 2 days hessian cured plus one days in the mould

# Appendix C

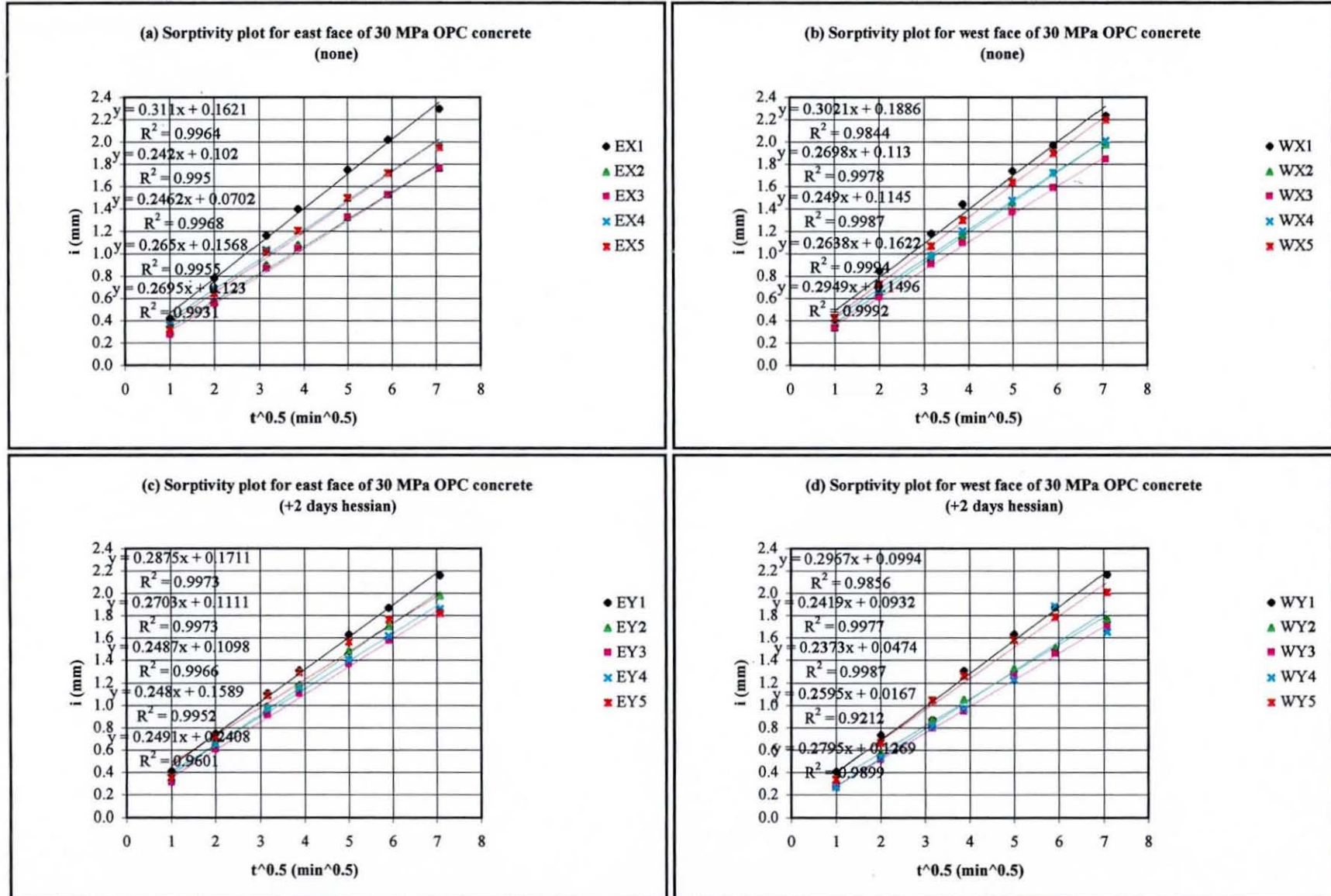


Fig. C1.1 Sorptivity plot for the 30 MPa OPC concrete - 12 months Muscat summer series

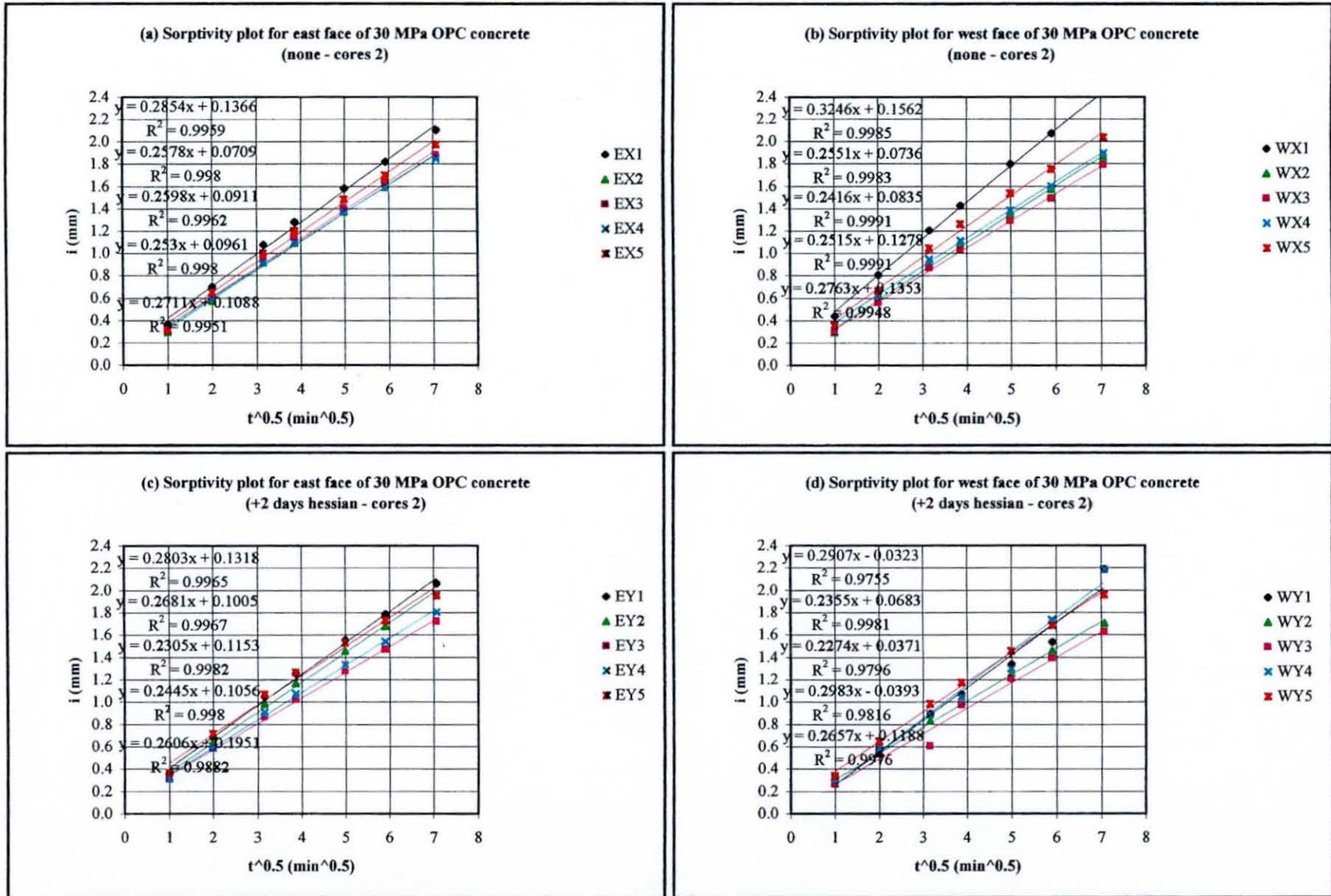


Fig. C1.2 Sorptivity plot for the 30 MPa OPC concrete (reproducibility - compare with Fig. C1.1) - 12 months Muscat summer series

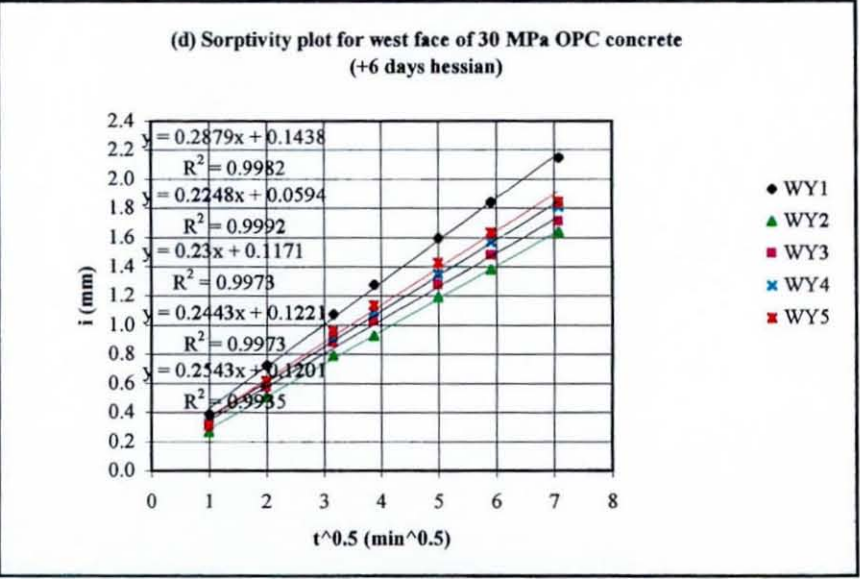
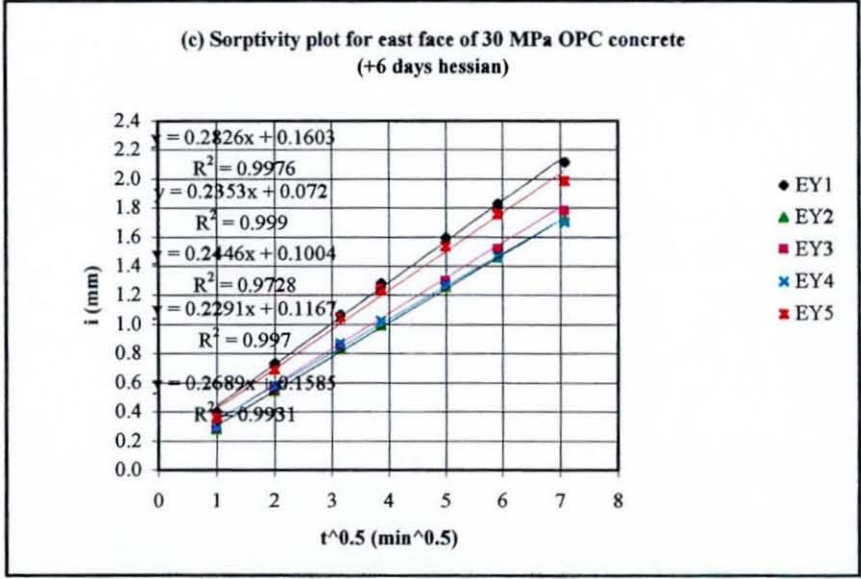
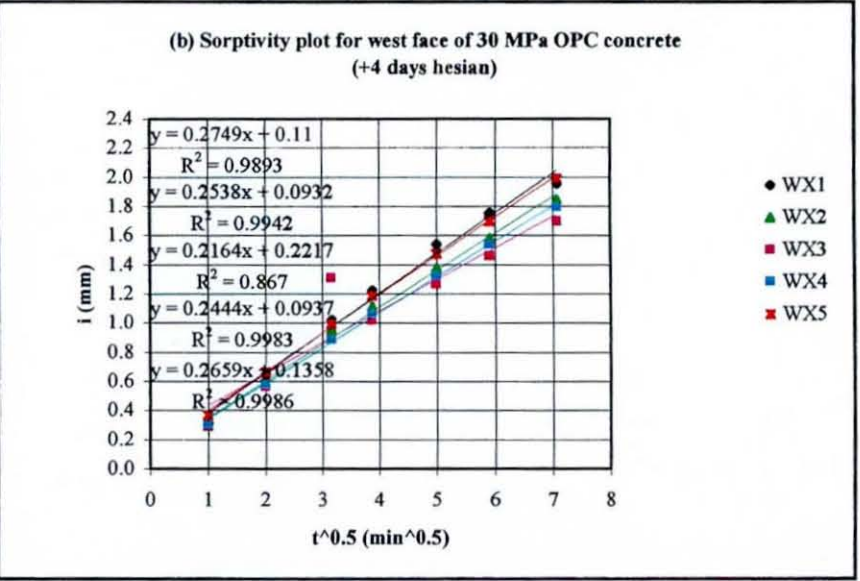
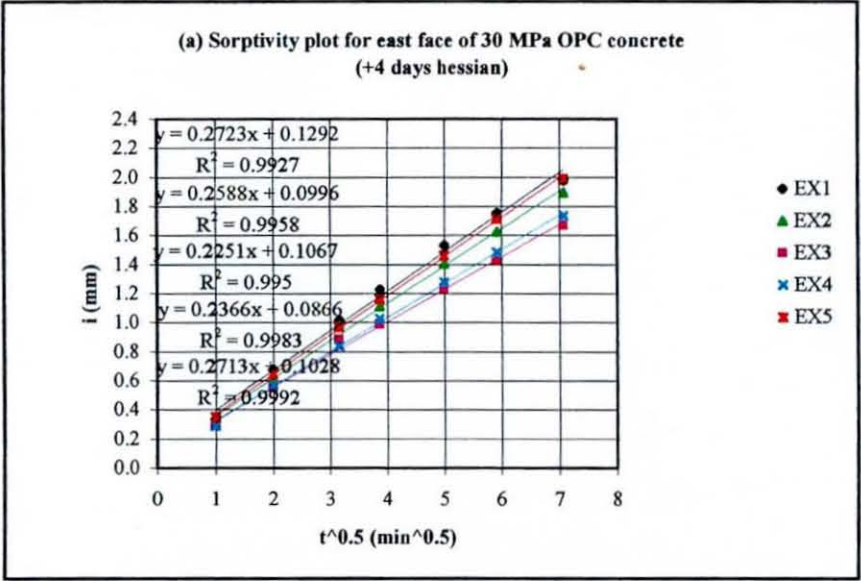


Fig. C1.3 Sorptivity plot for the 30 MPa OPC concrete - 12 months Muscat summer series

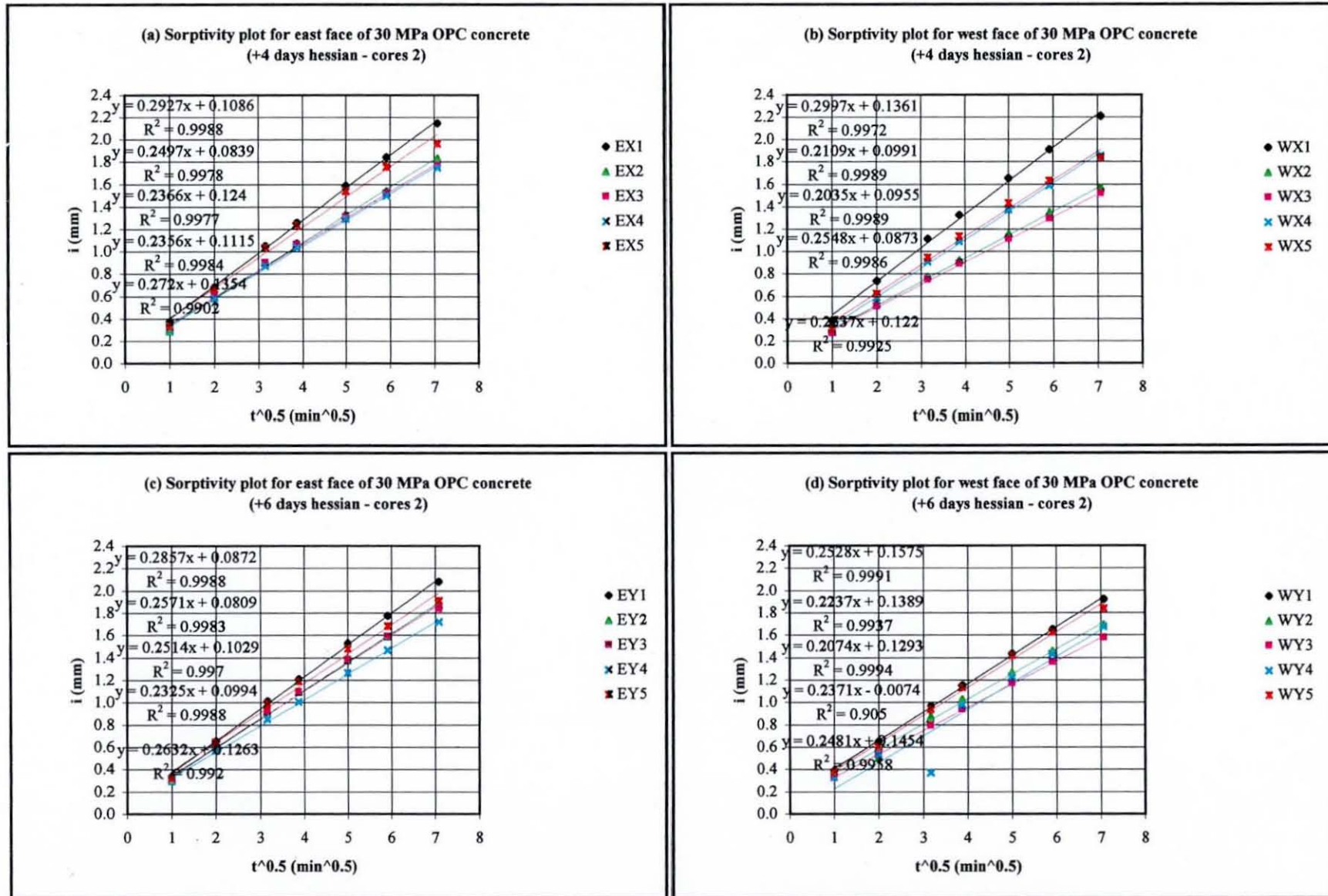


Fig. C1.4 Sorptivity plot for the 30 MPa OPC concrete (reproducibility - compare with Fig. C1.3) - 12 months Muscat summer series

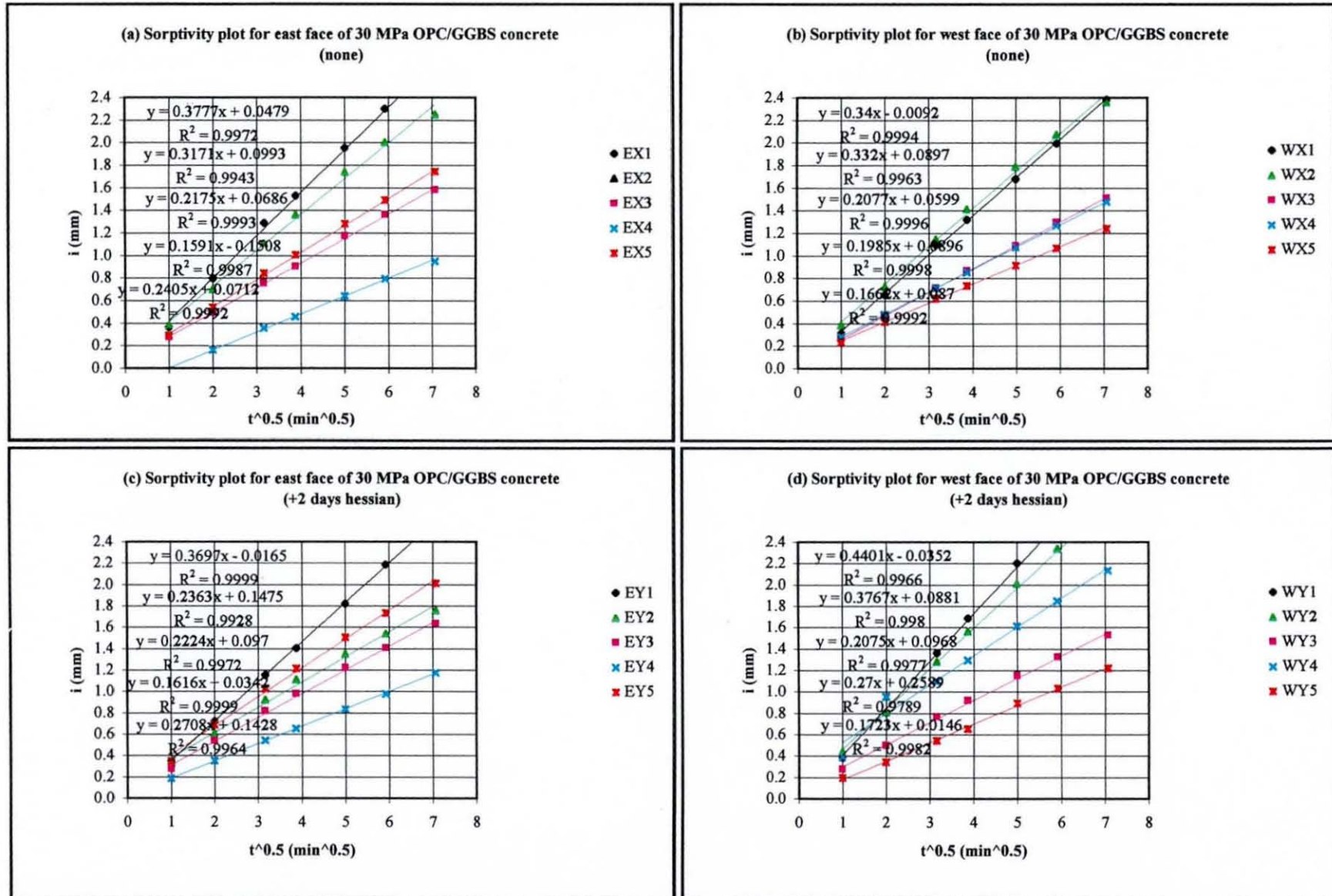


Fig. C1.5 Sorptivity plot for the 30 MPa OPC/GGBS concrete - 12 months Muscat summer series

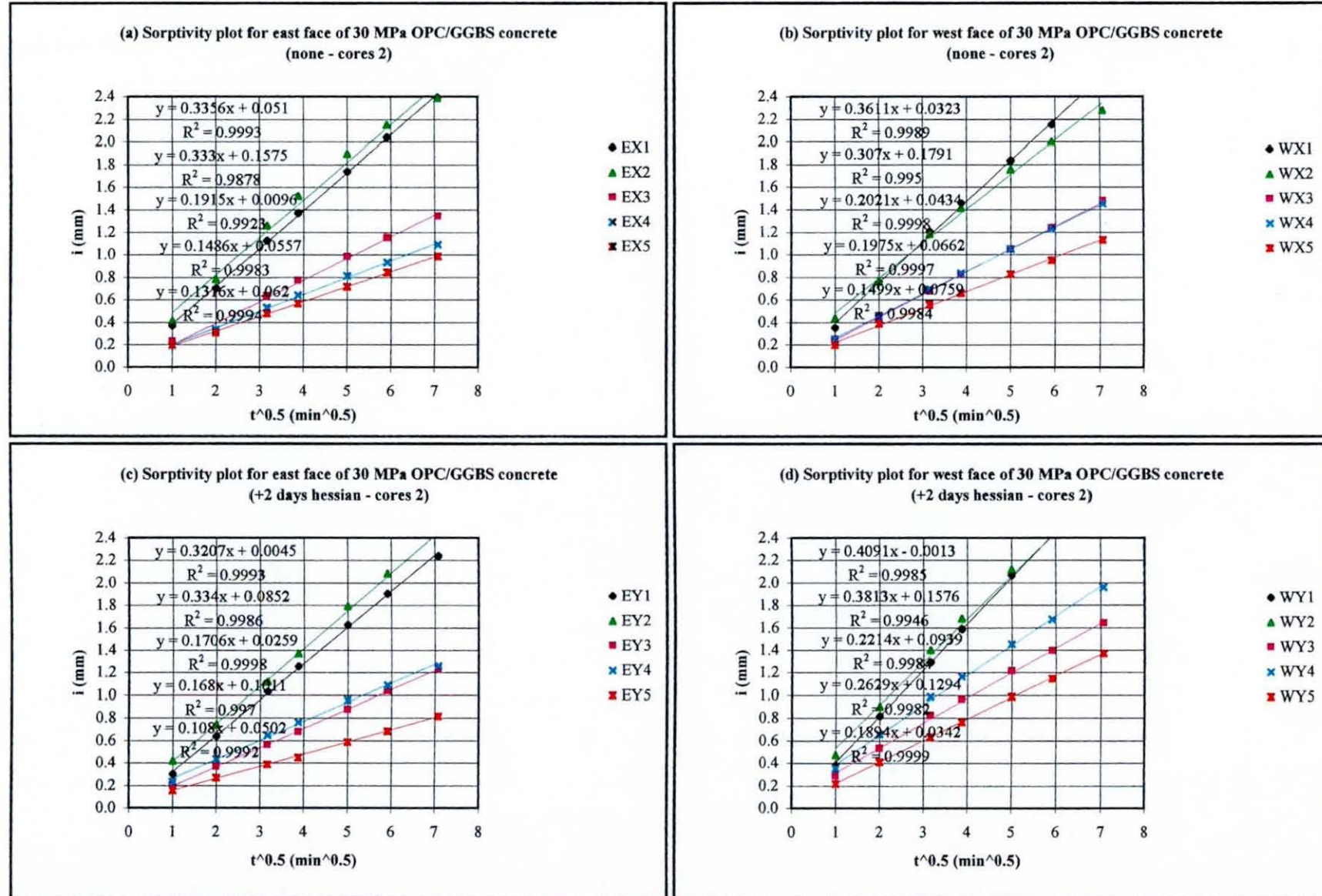


Fig. C1.6 Sorptivity plot for the 30 MPa OPC/GGBS concrete (reproducibility - compare with Fig. C1.5) - 12 months Muscat summer series

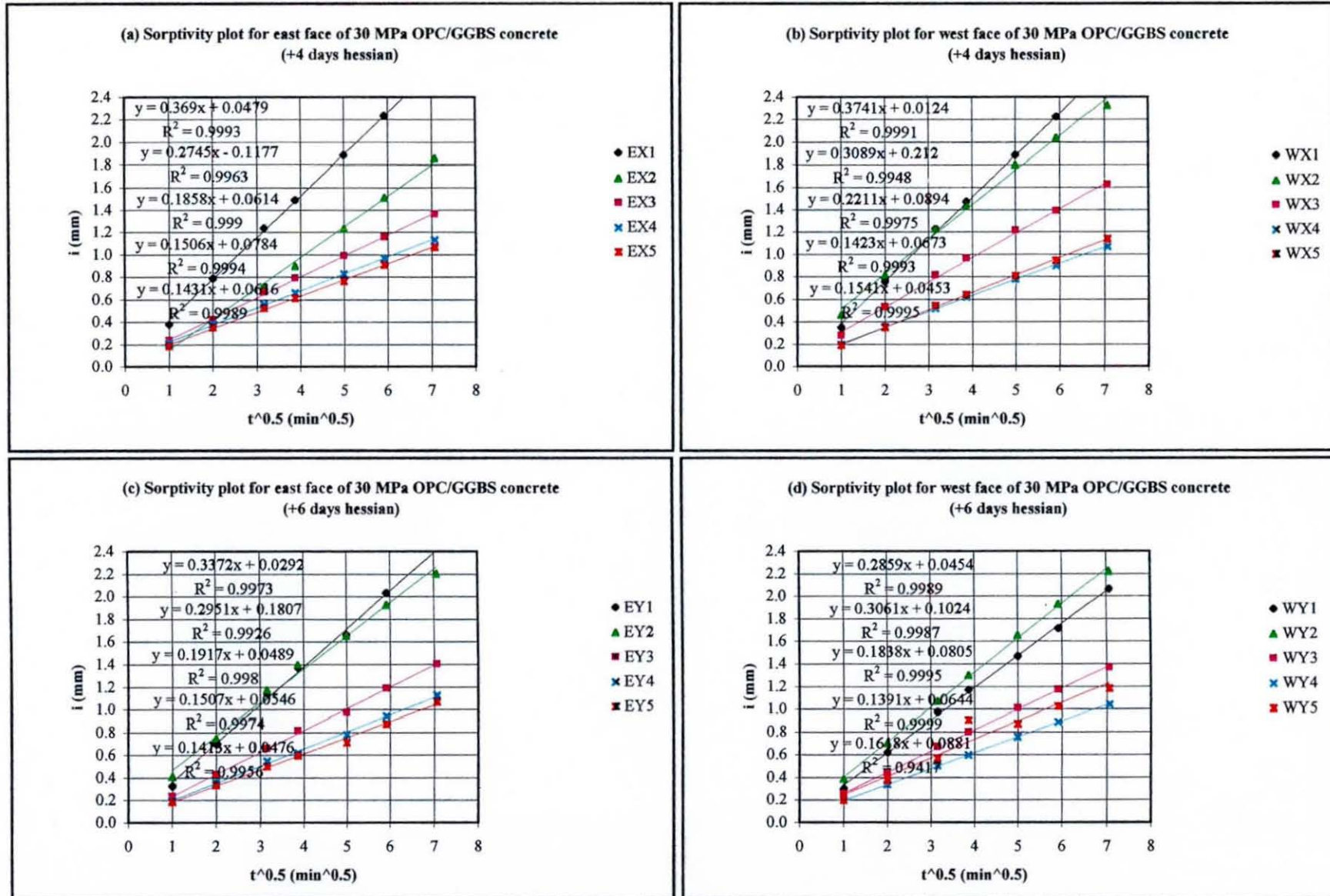


Fig. C1.7 Sorptivity plot for the 30 MPa OPC/GGBS concrete - 12 months Muscat summer series

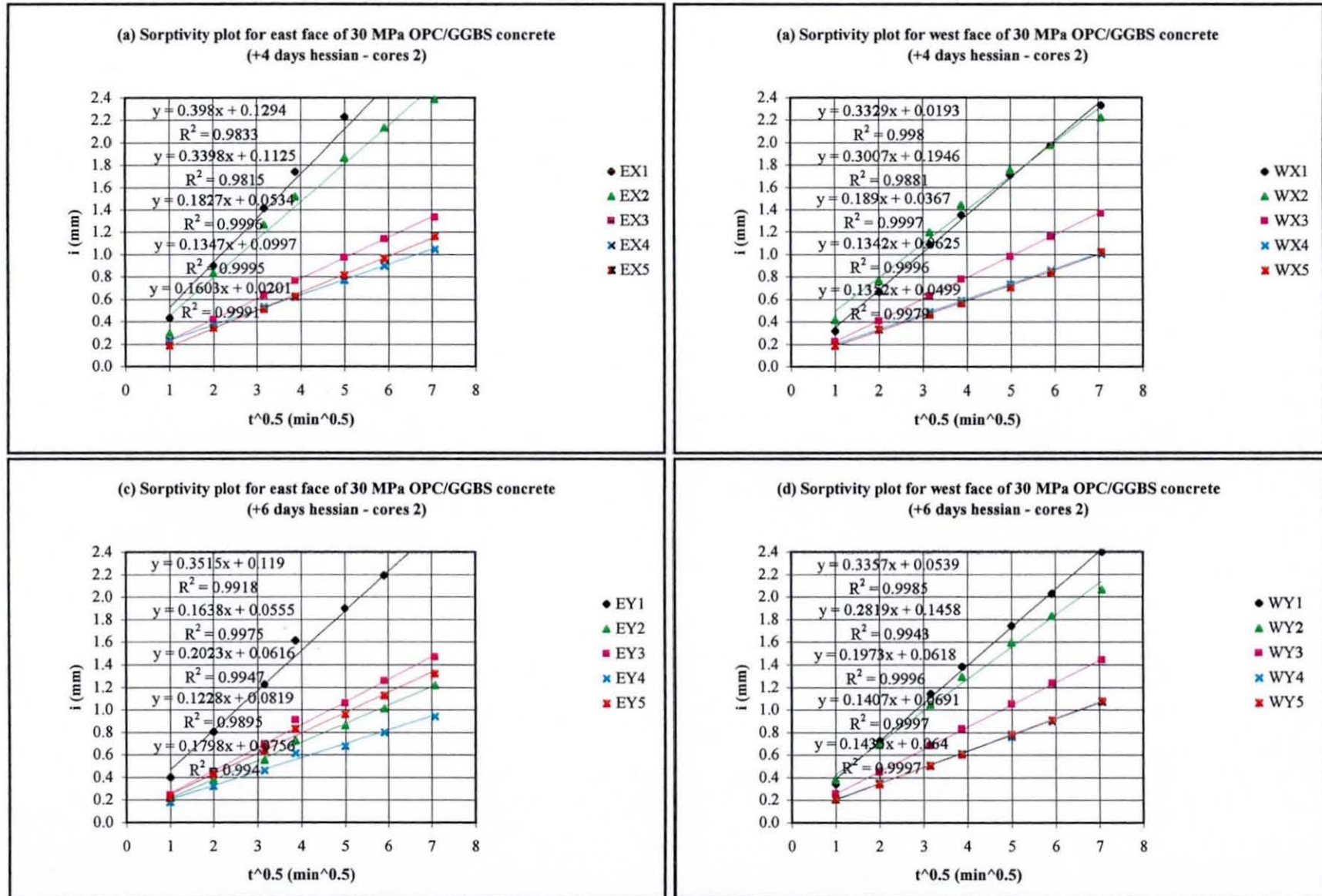
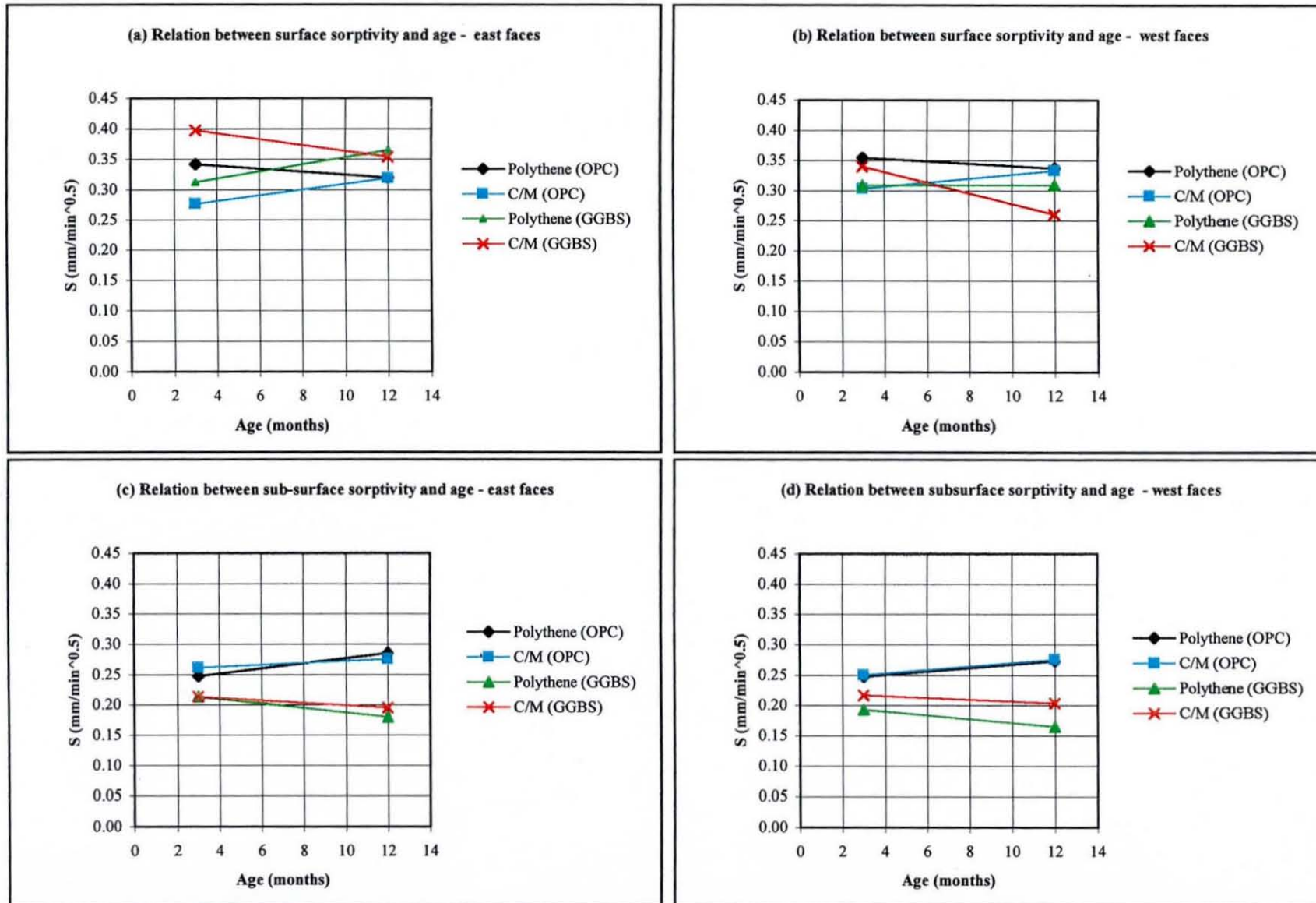


Fig. C1.8 Sorptivity plot for the 30 MPa OPC/GGBS concrete (reproducibility - compare with Fig. C1.7) - 12 months Muscat summer series



**Fig. C1.9** Relation between surface and sub-surface sorptivity with age of the 30 MPa OPC and OPC/GGBS concrete - Oman summer

Table C1.1 Sorptivity S (mm/min<sup>0.5</sup>) for the 30 MPa OPC concrete (east/west) - 3 months Muscat summer series

Orientation	Curnig regime		Average depth from outer surface (mm)					Surface (10mm)	Sub-surface (20-50mm)
			10	20	30	40	50		
East	No Cure	Cores 1	0.331	0.271	0.245	0.240	0.284	0.331	0.260
		Cores 2	0.214	0.282	0.246	0.228	0.249	0.214	0.251
		Average	<b>0.273</b>	<b>0.277</b>	<b>0.246</b>	<b>0.234</b>	<b>0.266</b>	<b>0.273</b>	<b>0.256</b>
		C of V (%)	21.5	1.8	0.2	2.7	6.5	21.5	1.8
	+2 days H	Cores 1	0.326	0.266	0.267	0.257	0.267	0.326	0.264
		Cores 2	0.342	0.244	0.244	0.196	0.216	0.342	0.225
		Average	<b>0.334</b>	<b>0.255</b>	<b>0.256</b>	<b>0.227</b>	<b>0.242</b>	<b>0.334</b>	<b>0.245</b>
		C of V (%)	2.4	4.3	4.6	13.5	10.6	2.4	8.1
	+4 days H	Cores 1	0.298	0.276	0.217	0.215	0.200	0.298	0.227
		Cores 2	0.366	0.241	0.283	0.214	0.237	0.366	0.244
		Average	<b>0.332</b>	<b>0.258</b>	<b>0.250</b>	<b>0.215</b>	<b>0.218</b>	<b>0.332</b>	<b>0.235</b>
		C of V (%)	10.1	6.8	13.3	0.2	8.6	10.1	3.6
	+6 days H	Cores 1	0.303	0.249	0.248	0.225	0.256	0.303	0.244
		Cores 2	0.324	0.250	0.223	0.183	0.206	0.324	0.216
		Average	<b>0.313</b>	<b>0.249</b>	<b>0.236</b>	<b>0.204</b>	<b>0.231</b>	<b>0.313</b>	<b>0.230</b>
		C of V (%)	3.5	0.3	5.4	10.3	10.7	3.5	6.3
West	No Cure	Cores 1	0.336	0.285	0.274	0.261	0.251	0.336	0.268
		Cores 2	0.367	0.267	0.262	0.261	0.218	0.367	0.252
		Average	<b>0.352</b>	<b>0.276</b>	<b>0.268</b>	<b>0.261</b>	<b>0.235</b>	<b>0.352</b>	<b>0.260</b>
		C of V (%)	4.5	3.3	2.3	0.0	6.9	4.5	3.0
	+2 days H	Cores 1	0.309	0.267	0.225	0.240	0.220	0.309	0.238
		Cores 2	0.307	0.230	0.228	0.270	0.231	0.307	0.240
		Average	<b>0.308</b>	<b>0.249</b>	<b>0.226</b>	<b>0.255</b>	<b>0.225</b>	<b>0.308</b>	<b>0.239</b>
		C of V (%)	0.3	7.5	0.6	5.8	2.5	0.3	0.3
	+4 days H	Cores 1	0.247	0.262	0.217	0.217	0.198	0.247	0.224
		Cores 2	0.359	0.247	0.260	0.215	0.240	0.359	0.240
		Average	<b>0.303</b>	<b>0.255</b>	<b>0.239</b>	<b>0.216</b>	<b>0.219</b>	<b>0.303</b>	<b>0.232</b>
		C of V (%)	18.4	3.1	8.9	0.5	9.6	18.4	3.6
	+6 days H	Cores 1	0.317	0.247	0.226	0.216	0.223	0.317	0.228
		Cores 2	0.292	0.240	0.236	0.207	0.203	0.292	0.222
		Average	<b>0.304</b>	<b>0.243</b>	<b>0.231</b>	<b>0.212</b>	<b>0.213</b>	<b>0.304</b>	<b>0.225</b>
		C of V (%)	4.1	1.5	2.2	2.1	4.7	4.1	1.4

Key: +X days H= X days hessian plus 1 day in mould; Average= average of cores 1 and 2; C of V= coefficient of variation (%); Sub-surface (20-50mm)= average k value from 20 to 50mm from surface; Bold value= plotted value (usually average)

Table C1.2 Sorptivity S (mm/min<sup>0.5</sup>) for the 30 MPa OPC concrete (east/west) - 12 months Muscat summer series

Orientation	Curnig regime		Average depth from outer surface (mm)					Surface (10mm)	Sub-surface (20-50mm)
			10	20	30	40	50		
East	No Cure	Cores 1	0.311	0.242	0.246	0.265	0.270	0.311	0.256
		Cores 2	0.285	0.258	0.260	0.253	0.271	0.285	0.260
		Average	<b>0.298</b>	<b>0.250</b>	<b>0.253</b>	<b>0.259</b>	<b>0.270</b>	<b>0.298</b>	<b>0.258</b>
		C of V (%)	4.3	3.2	2.7	2.3	0.3	4.3	0.9
	+2 days H	Cores 1	0.288	0.270	0.249	0.248	0.249	0.288	0.254
		Cores 2	0.280	0.268	0.231	0.245	0.261	0.280	0.251
		Average	<b>0.284</b>	<b>0.269</b>	<b>0.240</b>	<b>0.246</b>	<b>0.255</b>	<b>0.284</b>	<b>0.252</b>
		C of V (%)	1.3	0.4	3.8	0.7	2.3	1.3	0.6
	+4 days H	Cores 1	0.272	0.259	0.225	0.237	0.271	0.272	0.248
		Cores 2	0.293	0.250	0.237	0.236	0.272	0.293	0.248
		Average	<b>0.283</b>	<b>0.254</b>	<b>0.231</b>	<b>0.236</b>	<b>0.272</b>	<b>0.283</b>	<b>0.248</b>
		C of V (%)	3.6	1.8	2.5	0.2	0.1	3.6	0.1
	+6 days H	Cores 1	0.283	0.235	0.245	0.229	0.269	0.283	0.244
		Cores 2	0.286	0.257	0.251	0.233	0.263	0.286	0.251
		Average	<b>0.284</b>	<b>0.246</b>	<b>0.248</b>	<b>0.231</b>	<b>0.266</b>	<b>0.284</b>	<b>0.248</b>
		C of V (%)	0.5	4.4	1.4	0.7	1.1	0.5	1.3
West	No Cure	Cores 1	0.302	0.270	0.249	0.264	0.295	0.302	0.269
		Cores 2	0.325	0.255	0.242	0.252	0.276	0.325	0.256
		Average	<b>0.313</b>	<b>0.262</b>	<b>0.245</b>	<b>0.258</b>	<b>0.286</b>	<b>0.313</b>	<b>0.263</b>
		C of V (%)	3.6	2.8	1.5	2.4	3.3	3.6	2.5
	+2 days H	Cores 1	0.297	0.242	0.237	0.260	0.280	0.297	0.255
		Cores 2	0.291	0.286	0.227	0.298	0.266	0.291	0.269
		Average	<b>0.294</b>	<b>0.264</b>	<b>0.232</b>	<b>0.279</b>	<b>0.273</b>	<b>0.294</b>	<b>0.262</b>
		C of V (%)	1.0	8.3	2.1	7.0	2.5	1.0	2.8
	+4 days H	Cores 1	0.275	0.254	0.216	0.244	0.266	0.275	0.245
		Cores 2	0.300	0.211	0.204	0.255	0.254	0.300	0.231
		Average	<b>0.287</b>	<b>0.232</b>	<b>0.210</b>	<b>0.250</b>	<b>0.260</b>	<b>0.287</b>	<b>0.238</b>
		C of V (%)	4.3	9.2	3.1	2.1	2.3	4.3	3.0
	+6 days H	Cores 1	0.288	0.225	0.230	0.244	0.254	0.288	0.238
		Cores 2	0.253	0.224	0.207	0.237	0.248	0.253	0.229
		Average	<b>0.270</b>	<b>0.224</b>	<b>0.219</b>	<b>0.241</b>	<b>0.251</b>	<b>0.270</b>	<b>0.234</b>
		C of V (%)	6.5	0.2	5.2	1.5	1.2	6.5	2.0

Key: +X days H= X days hessian plus 1 day in mould; Average= average of cores 1 and 2; C of V= coefficient of variation (%); Sub-surface (20-50mm)= average k value from 20 to 50mm from surface; Bold value= plotted value (usually average)

Table C1.3 Sorptivity S (mm/min<sup>0.5</sup>) for the 30 MPa OPC and OPC/GGBS concrete - 3 months Muscat summer series (east/west)

Orientation	Curnig regime		Average depth from outer surface (mm)					Surface (10mm)	Sub-surface (20-50mm)
			10	20	30	40	50		
East	+6 days P (OPC)	Cores 1	0.328	0.321	0.246	0.232	0.223	0.328	0.255
		Cores 2	0.357	0.258	0.271	0.214	0.218	0.357	0.240
		Average	<b>0.342</b>	<b>0.289</b>	<b>0.258</b>	<b>0.223</b>	<b>0.221</b>	<b>0.342</b>	<b>0.248</b>
		C of V (%)	4.3	11.0	4.8	4.0	1.0	4.3	3.1
	C/M (OPC)	Cores 1	0.266	0.279	0.243	0.206	0.230	0.266	0.239
		Cores 2	0.287	0.301	0.292	0.302	0.247	0.287	0.286
		Average	<b>0.276</b>	<b>0.290</b>	<b>0.268</b>	<b>0.254</b>	<b>0.238</b>	<b>0.276</b>	<b>0.262</b>
		C of V (%)	3.9	3.8	9.2	19.1	3.6	3.9	8.8
	+6 days P (GGBS)	Cores 1	0.340	0.293	0.242	0.192	0.194	0.340	0.230
		Cores 2	0.286	0.287	0.199	0.154	0.156	0.286	0.199
		Average	<b>0.313</b>	<b>0.290</b>	<b>0.221</b>	<b>0.173</b>	<b>0.175</b>	<b>0.313</b>	<b>0.215</b>
		C of V (%)	8.6	1.0	9.6	11.1	10.7	8.6	7.2
	C/M (GGBS)	Cores 1	0.402	0.300	0.205	0.188	0.197	0.402	0.223
		Cores 2	0.395	0.260	0.217	0.189	0.156	0.395	0.205
		Average	<b>0.399</b>	<b>0.280</b>	<b>0.211</b>	<b>0.189</b>	<b>0.177</b>	<b>0.399</b>	<b>0.214</b>
		C of V (%)	0.9	7.3	3.0	0.2	11.7	0.9	4.0
West	+6 days P (OPC)	Cores 1	0.357	0.258	0.271	0.214	0.218	0.357	0.240
		Cores 2	0.353	0.287	0.258	0.243	0.237	0.353	0.256
		Average	<b>0.355</b>	<b>0.273</b>	<b>0.264</b>	<b>0.229</b>	<b>0.228</b>	<b>0.355</b>	<b>0.248</b>
		C of V (%)	0.6	5.4	2.5	6.3	4.1	0.6	3.2
	C/M (OPC)	Cores 1	0.281	0.280	0.241	0.206	0.240	0.281	0.242
		Cores 2	0.327	0.297	0.260	0.231	0.252	0.327	0.260
		Average	<b>0.304</b>	<b>0.289</b>	<b>0.250</b>	<b>0.218</b>	<b>0.246</b>	<b>0.304</b>	<b>0.251</b>
		C of V (%)	7.6	2.9	3.6	5.5	2.4	7.6	3.5
	+6 days P (GGBS)	Cores 1	0.321	0.283	0.168	0.198	0.175	0.321	0.206
		Cores 2	0.299	0.249	0.145	0.176	0.156	0.299	0.181
		Average	<b>0.310</b>	<b>0.266</b>	<b>0.156</b>	<b>0.187</b>	<b>0.165</b>	<b>0.310</b>	<b>0.194</b>
		C of V (%)	3.5	6.4	7.3	5.8	5.9	3.5	6.3
	C/M (GGBS)	Cores 1	0.376	0.266	0.260	0.197	0.212	0.376	0.234
		Cores 2	0.307	0.245	0.210	0.198	0.153	0.307	0.201
		Average	<b>0.341</b>	<b>0.256</b>	<b>0.235</b>	<b>0.198</b>	<b>0.182</b>	<b>0.341</b>	<b>0.218</b>
		C of V (%)	10.1	4.1	10.8	0.2	16.1	10.1	7.5

Key: +X days H= X days hessian plus 1 day in mould; Average= average of cores 1 and 2; C of V= coefficient of variation (%); Sub-surface (20-50mm)= average k value from 20 to 50mm from surface; Bold value= plotted value (usually average)

**Table C1.4 Sorptivity S (mm/min<sup>0.5</sup>) for the 30 MPa OPC and OPC/GGBS concrete (east/west) - 12 months Muscat summer series**

Orientation	Curing regime		Average depth from outer surface (mm)					Surface (10mm)	Sub-surface (20-50mm)
			10	20	30	40	50		
East	+6 days P (OPC)	Cores 1	0.322	0.294	0.252	0.266	0.294	0.322	0.277
		Cores 2	0.318	0.321	0.290	0.277	0.292	0.318	0.295
		Average	<b>0.320</b>	<b>0.308</b>	<b>0.271</b>	<b>0.272</b>	<b>0.293</b>	<b>0.320</b>	<b>0.286</b>
		C of V (%)	0.7	4.4	6.8	2.0	0.3	0.7	3.2
	C/M (OPC)	Cores 1	0.314	0.284	0.259	0.260	0.286	0.314	0.272
		Cores 2	0.326	0.305	0.274	0.278	0.261	0.326	0.279
		Average	<b>0.320</b>	<b>0.294</b>	<b>0.267</b>	<b>0.269</b>	<b>0.274</b>	<b>0.320</b>	<b>0.276</b>
		C of V (%)	1.8	3.4	2.8	3.3	4.6	1.8	1.3
	+6 days P (GGBS)	Cores 1	0.358	0.186	0.149	0.130	0.294	0.358	0.190
		Cores 2	0.374	0.141	0.106	0.298	0.141	0.374	0.171
		Average	<b>0.366</b>	<b>0.163</b>	<b>0.128</b>	<b>0.214</b>	<b>0.218</b>	<b>0.366</b>	<b>0.181</b>
		C of V (%)	2.1	13.9	16.8	39.1	35.0	2.1	5.0
	C/M (GGBS)	Cores 1	0.361	0.123	0.179	0.142	0.317	0.361	0.190
		Cores 2	0.348	0.180	0.160	0.303	0.169	0.348	0.203
		Average	<b>0.355</b>	<b>0.151</b>	<b>0.169</b>	<b>0.222</b>	<b>0.243</b>	<b>0.355</b>	<b>0.197</b>
		C of V (%)	1.9	18.7	5.9	36.2	30.5	1.9	3.1
West	+6 days P (OPC)	Cores 1	0.336	0.293	0.260	0.301	0.252	0.336	0.276
		Cores 2	0.339	0.287	0.267	0.277	0.255	0.339	0.271
		Average	<b>0.337</b>	<b>0.290</b>	<b>0.263</b>	<b>0.289</b>	<b>0.253</b>	<b>0.337</b>	<b>0.274</b>
		C of V (%)	0.4	1.0	1.2	4.0	0.5	0.4	0.9
	C/M (OPC)	Cores 1	0.335	0.304	0.260	0.293	0.270	0.335	0.282
		Cores 2	0.333	0.277	0.248	0.295	0.262	0.333	0.270
		Average	<b>0.334</b>	<b>0.291</b>	<b>0.254</b>	<b>0.294</b>	<b>0.266</b>	<b>0.334</b>	<b>0.276</b>
		C of V (%)	0.3	4.7	2.4	0.4	1.5	0.3	2.0
	+6 days P (GGBS)	Cores 1	0.322	0.120	0.161	0.124	0.316	0.322	0.180
		Cores 2	0.297	0.145	0.171	0.119	0.170	0.297	0.151
		Average	<b>0.310</b>	<b>0.132</b>	<b>0.166</b>	<b>0.122</b>	<b>0.243</b>	<b>0.310</b>	<b>0.166</b>
		C of V (%)	4.1	9.6	2.8	2.1	30.2	4.1	8.8
	C/M (GGBS)	Cores 1	0.297	0.234	0.187	0.223	0.161	0.297	0.201
		Cores 2	0.225	0.184	0.176	0.133	0.334	0.225	0.207
		Average	<b>0.261</b>	<b>0.209</b>	<b>0.181</b>	<b>0.178</b>	<b>0.248</b>	<b>0.261</b>	<b>0.204</b>
		C of V (%)	13.8	12.0	2.8	25.3	34.9	13.8	1.4

Key: +X days H= X days hessian plus 1 day in mould; Average= average of cores 1 and 2; C of V= coefficient of variation (%); Sub-surface (20-50mm)= average k value from 20 to 50mm from surface; Bold value= plotted value (usually average)

**Table C1.5 Sorptivity S (mm/min<sup>0.5</sup>) for the 30 MPa OPC/GGBS concrete (east/west) - 3 months Muscat summer series**

Orientation	Curing regime		Average depth from outer surface (mm)					Surface (10mm)	Sub-surface (20-50mm)
			10	20	30	40	50		
East	No Cure	Cores 1	0.343	0.266	0.224	0.143	0.188	0.343	0.205
		Cores 2	0.293	0.200	0.159	0.126	0.149	0.293	0.158
		Average	<b>0.318</b>	<b>0.233</b>	<b>0.192</b>	<b>0.134</b>	<b>0.168</b>	<b>0.318</b>	<b>0.182</b>
		C of V (%)	7.8	14.2	17.0	6.4	11.8	7.8	12.9
	+2 days H	Cores 1	0.315	0.227	0.165	0.148	0.120	0.315	0.165
		Cores 2	0.264	0.182	0.134	0.147	0.126	0.264	0.147
		Average	<b>0.289</b>	<b>0.204</b>	<b>0.150</b>	<b>0.148</b>	<b>0.123</b>	<b>0.289</b>	<b>0.156</b>
		C of V (%)	8.9	11.0	10.4	0.4	2.7	8.9	5.6
	+4 days H	Cores 1	0.302	0.238	0.121	0.180	0.127	0.302	0.167
		Cores 2	0.271	0.286	0.142	0.214	0.125	0.271	0.192
		Average	<b>0.286</b>	<b>0.262</b>	<b>0.132</b>	<b>0.197</b>	<b>0.126</b>	<b>0.286</b>	<b>0.179</b>
		C of V (%)	5.5	9.1	8.1	8.7	0.9	5.5	7.0
	+6 days H	Cores 1	0.254	0.175	0.106	0.116	0.108	0.254	0.126
		Cores 2	0.293	0.196	0.140	0.136	0.131	0.293	0.151
		Average	<b>0.274</b>	<b>0.186</b>	<b>0.123</b>	<b>0.126</b>	<b>0.120</b>	<b>0.274</b>	<b>0.139</b>
		C of V (%)	7.1	5.6	13.9	8.0	9.6	7.1	8.9
West	No Cure	Cores 1	0.381	0.246	0.190	0.173	0.188	0.381	0.199
		Cores 2	0.319	0.295	0.198	0.191	0.174	0.319	0.214
		Average	<b>0.350</b>	<b>0.271</b>	<b>0.194</b>	<b>0.182</b>	<b>0.181</b>	<b>0.350</b>	<b>0.207</b>
		C of V (%)	8.8	9.1	2.1	4.9	3.9	8.8	3.7
	+2 days H	Cores 1	0.282	0.197	0.142	0.124	0.121	0.282	0.146
		Cores 2	0.310	0.202	0.192	0.173	0.154	0.310	0.180
		Average	<b>0.296</b>	<b>0.199</b>	<b>0.167</b>	<b>0.148</b>	<b>0.138</b>	<b>0.296</b>	<b>0.163</b>
		C of V (%)	4.6	1.2	14.9	16.2	12.1	4.6	10.4
	+4 days H	Cores 1	0.323	0.171	0.195	0.140	0.132	0.323	0.159
		Cores 2	0.278	0.140	0.127	0.106	0.118	0.278	0.123
		Average	<b>0.301</b>	<b>0.155</b>	<b>0.161</b>	<b>0.123</b>	<b>0.125</b>	<b>0.301</b>	<b>0.141</b>
		C of V (%)	7.5	9.9	21.0	13.7	5.4	7.5	12.9
	+6 days H	Cores 1	0.222	0.201	0.129	0.105	0.112	0.222	0.137
		Cores 2	0.252	0.180	0.121	0.139	0.126	0.252	0.142
		Average	<b>0.237</b>	<b>0.191</b>	<b>0.125</b>	<b>0.122</b>	<b>0.119</b>	<b>0.237</b>	<b>0.139</b>
		C of V (%)	6.5	5.5	3.3	14.1	5.9	6.5	1.7

Key: +X days H= X days hessian plus 1 day in mould; Average= average of cores 1 and 2; C of V= coefficient of variation (%); Sub-surface (20-50mm)= average k value from 20 to 50mm from surface; Bold value= plotted value (usually average)

**Table C1.6 Sorptivity  $s$  (mm/min<sup>0.5</sup>) for the 30 MPa OPC/GGBS concrete (east/west) - 12 months Muscat summer series**

Orientation	Curing regime		Average depth from outer surface (mm)					Surface (10mm)	Sub-surface (20-50mm)
			10	20	30	40	50		
East	No Cure	Cores 1	0.378	0.317	0.218	0.159	0.241	0.378	0.234
		Cores 2	0.336	0.333	0.192	0.149	0.132	0.336	0.201
		Average	<b>0.357</b>	<b>0.325</b>	<b>0.205</b>	<b>0.154</b>	<b>0.186</b>	<b>0.357</b>	<b>0.217</b>
		C of V (%)	5.9	2.4	6.4	3.4	29.3	5.9	7.4
	+2 days H	Cores 1	0.370	0.236	0.222	0.162	0.271	0.370	0.223
		Cores 2	0.321	0.334	0.171	0.168	0.108	0.321	0.195
		Average	<b>0.345</b>	<b>0.285</b>	<b>0.197</b>	<b>0.165</b>	<b>0.189</b>	<b>0.345</b>	<b>0.209</b>
		C of V (%)	7.1	17.1	13.2	1.9	43.0	7.1	6.6
	+4 days H	Cores 1	0.369	0.275	0.186	0.151	0.143	0.359	0.189
		Cores 2	0.398	0.340	0.183	0.135	0.160	0.398	0.204
		Average	<b>0.384</b>	<b>0.307</b>	<b>0.184</b>	<b>0.143</b>	<b>0.152</b>	<b>0.379</b>	<b>0.196</b>
		C of V (%)	3.8	10.6	0.8	5.6	5.7	5.2	4.0
	+6 days H	Cores 1	0.337	0.295	0.192	0.151	0.141	0.337	0.195
		Cores 2	0.352	0.164	0.202	0.123	0.180	0.352	0.167
		Average	<b>0.344</b>	<b>0.229</b>	<b>0.197</b>	<b>0.137</b>	<b>0.161</b>	<b>0.344</b>	<b>0.181</b>
		C of V (%)	2.1	28.6	2.7	10.2	12.0	2.1	7.6
West	No Cure	Cores 1	0.340	0.332	0.208	0.199	0.166	0.340	0.226
		Cores 2	0.361	0.307	0.202	0.198	0.150	0.361	0.214
		Average	<b>0.351</b>	<b>0.320</b>	<b>0.205</b>	<b>0.198</b>	<b>0.158</b>	<b>0.351</b>	<b>0.220</b>
		C of V (%)	3.0	3.9	1.4	0.3	5.2	3.0	2.7
	+2 days H	Cores 1	0.440	0.377	0.208	0.270	0.172	0.440	0.257
		Cores 2	0.409	0.381	0.221	0.263	0.189	0.409	0.264
		Average	<b>0.425</b>	<b>0.379</b>	<b>0.214</b>	<b>0.266</b>	<b>0.181</b>	<b>0.425</b>	<b>0.260</b>
		C of V (%)	3.7	0.6	3.2	1.3	4.7	3.7	1.4
	+4 days H	Cores 1	0.374	0.309	0.221	0.142	0.154	0.374	0.207
		Cores 2	0.333	0.301	0.189	0.134	0.135	0.339	0.190
		Average	<b>0.354</b>	<b>0.305</b>	<b>0.205</b>	<b>0.138</b>	<b>0.145</b>	<b>0.357</b>	<b>0.198</b>
		C of V (%)	5.8	1.3	7.8	2.9	6.5	4.9	4.2
	+6 days H	Cores 1	0.286	0.306	0.184	0.139	0.162	0.286	0.198
		Cores 2	0.336	0.282	0.197	0.141	0.144	0.336	0.191
		Average	<b>0.311</b>	<b>0.294</b>	<b>0.191</b>	<b>0.140</b>	<b>0.153</b>	<b>0.311</b>	<b>0.194</b>
		C of V (%)	8.0	4.1	3.5	0.6	6.0	8.0	1.8

Key: +X days H= X days hessian plus 1 day in mould; Average= average of cores 1 and 2; C of V= coefficient of variation (%); Sub-surface (20-50mm)= average k value from 20 to 50mm from surface; Bold value= plotted value (usually average)

